NOTE TO USERS

The original manuscript received by UMI contains indistinct, slanted and or light print. All efforts were made to acquire the highest quality manuscript from the author or school. Microfilmed as received.

This reproduction is the best copy available

UMI

University of Alberta

CoA Transferase: Folding, Assembly, and Catalysis

by

Jean-Christophe Rochet ©

A thesis submitted to the Faculty of Graduate Studies and Research in partial
fulfillment of the requirements for the degree of Doctor of Philosophy

Department of Biochemistry

Edmonton, Alberta

Spring, 1998

National Library
of Canada

Acquisitions and
Bibliographic Services

395 Wellington Street
Ottawa ON K1A 0N4
Canada

Bibliothèque nationale
du Canada

Acquisitions et
services bibliographiques

395, rue Wellington
Ottawa ON K1A 0N4
Canada

Your file Votre référence

Our file Notre référence

The author has granted a non-exclusive licence allowing the National Library of Canada to reproduce, loan, distribute or sell copies of this thesis in microform, paper or electronic formats.

L'auteur a accordé une licence non exclusive permettant à la Bibliothèque nationale du Canada de reproduire, prêter, distribuer ou vendre des copies de cette thèse sous la forme de microfiche/film, de reproduction sur papier ou sur format électronique.

The author retains ownership of the copyright in this thesis. Neither the thesis nor substantial extracts from it may be printed or otherwise reproduced without the author's permission.

L'auteur conserve la propriété du droit d'auteur qui protège cette thèse. Ni la thèse ni des extraits substantiels de celle-ci ne doivent être imprimés ou autrement reproduits sans son autorisation.

0-612-29099-9

Canadä

University of Alberta

Faculty of Graduate Studies and Research

The undersigned certify that they have read, and recommend to the Faculty of Graduate Studies and Research for acceptance, a thesis entitled *CoA Transferase: Folding, Assembly, and Catalysis* submitted by Jean-Christophe Rochet in partial fulfillment of the requirements for the degree of Doctor of Philosophy.

W.T Wolodko
W. T. Wolodko

W. A. Bridger

M. J. Ellison

Charles F B Holmes
C. F. B. Holmes

J. C. Vederas

Thomas O. Baldwin
T. O. Baldwin

Date: 4th December, 1997

Abstract

CoA Transferase: Folding, Assembly, and Catalysis

Succinyl-CoA:3-ketoacid CoA transferase [EC 2.8.3.5] catalyzes the transfer of CoA from succinyl-CoA to acetoacetate, which is an essential step in the metabolism of ketone bodies. Each subunit of the homodimeric CoA transferase from pig heart consists of two interacting domains (the N- and C-domains) connected by a hydrophilic bridge.

Noncovalent interactions that play critical roles at different points along the CoA transferase folding pathway have been identified. First, each "native-like" N-domain interacts with its counterpart on the opposite subunit before associating with the partially folded C-domains. Assembly leads to the stabilization and compaction of the N- and C-domains, and ultimately to the formation of active enzyme. Second, early intermediates along the CoA transferase folding pathway are susceptible to aggregation, due to nonproductive interactions involving mainly the C-domain. Chaperonins such as GroEL may increase the yield of active enzyme during refolding *in vitro* by protecting partially folded species from aggregation. Third, CoA transferase can exist in two oligomeric forms: a homodimer and a homotetrameric variant. These two conformers are identical with respect to specific activity, secondary and tertiary structure, and refolding ability. However, their interconversion is very slow due to a large kinetic barrier. An intact hydrophilic linker is essential for the formation and stability of the homotetramer.

The layout of the active site of CoA transferase has also been studied. Glutamate 344 has been identified as the amino acid residue which undergoes thiolesterification during catalysis. The replacement of this residue with an alanine or an aspartate residue abolishes the activity of the enzyme, but the E344Q mutant gains enzymatic activity during the course of its incubation with the substrate acetoacetyl-CoA. In addition, the replacement of cysteine 67 with a serine residue protects the enzyme-CoA intermediate

from rapid inactivation by DTNB. The specific activity of the C67S mutant is only 0.3 times that of the wild-type enzyme. Finally, from the results of subunit hybridization studies, it is concluded that each active site of the CoA transferase homodimer is shared between the domains of a single monomer, rather than between two monomers.

Acknowledgements

I am very grateful to both of my supervisors for their assistance during the course of my graduate studies. Dr. Bridger (Bill) was very supportive of my pursuing several avenues of research in an independent manner. Dr. Wolodko (Willie) offered critical advice, and I owe much of my learning in the fields of enzymology and x-ray crystallography to his careful instruction. I am also appreciative of the friendship and understanding shown to me by both Bill and Willie.

I am indebted to the members of my laboratory:

Marie Fraser, for her assistance with the x-ray crystallography work;
Edward Brownie, for his advice with the purification of proteins;
Fellow graduate students Michael Joyce, David Ryan, and Darrin Bailey, for helpful discussions and their assistance with techniques in molecular biology; and
Tracy Morton, for his work on mutants of CoA transferase, and Ziya Skaper, for her time spent crystallizing the wild-type enzyme.

I must also thank other people who have contributed to my work as a graduate student:

Members of my supervisory committee, Dr. Michael Ellison, Dr. Charles Holmes, and Dr. Michael James, for their helpful advice and direction during my graduate studies;
Dr. Cyril Kay, Kimio Oikawa, and Leslie Hicks, for their interest in collaborating and carrying out biophysical studies on CoA transferase;
Dr. Raymond Turner, for providing numerous useful plasmids, and for stimulating discussions;
Dr. Thomas Baldwin, Dr. Heman Chao, Dr. Pierre Lavigne, and Dr. Bruce Malcolm, for their selfless exchange of ideas;
Paul Semchuk, Therese Hutton, Anne Maisey, and Brian Tripet, for their technical assistance with mass spectral analyses;
Mike Carpenter, for the amino acid analyses, and Jack Moore, for the N-terminal sequencing of proteins;
Perry d'Obrenan, for oligonucleotide syntheses and nucleotide sequencing; and
Roger Bradley, for his very careful, thorough photography work.

My research was supported by studentships from the Natural Sciences and Engineering Research Council of Canada (NSERC), the Medical Research Council of Canada (MRC), and the Alberta Heritage Foundation for Medical Research (AHFMR).

Finally, I am extremely grateful to my family and friends, and especially to Joanne, for their encouragement and understanding during the past six years. Their support has gone a long way towards helping me remain optimistic even during the difficult times.

Table of Contents

Page

CHAPTER 1: Introduction 1

Part A: The Biochemistry of CoA and the CoA Transferases 1
- The structure of coenzyme A 1
- The chemistry of the thiolester 4
- CoA in metabolism 6
- The energetics of acyl-CoA formation 10
- CoA transferases in fermentative metabolism 11
- CoA transferase and ketone body metabolism 13

Part B: Structural Organization of the Prokaryotic and Mammalian CoA Transferases 19
- Subunit and domain organization of the mammalian CoA transferases ... 19
- Subunit organization of the prokaryotic CoA transferases 26

Part C: The Enzymology of Porcine CoA Transferase 36
- Substrate specificity of succinyl-CoA:3-ketoacid CoA transferase 36
- Kinetic mechanism of succinyl-CoA:3-ketoacid CoA transferase 39
- Chemical mechanism of CoA transferase 43
- The acidic nucleophile of succinyl-CoA:3-ketoacid CoA transferase 48
- A reactive cysteine residue in the active site of succinyl-CoA:3-ketoacid CoA transferase 51
- A binding site for the carboxylate substrates 56
- Noncovalent interactions and catalysis: general considerations 57
- Noncovalent interactions at the active site of succinyl-CoA:3-ketoacid CoA transferase 59
- Accounting for catalysis by succinyl-CoA:3-ketoacid CoA transferase .. 63
- The importance of a conformational change 66

Part D: The Objectives of the Thesis 67

Endnotes 70

References 71

CHAPTER 2: Productive Interactions Between the Two Domains of CoA Transferase During Folding and Assembly 76

Introduction 76

Experimental Procedures 77
  Materials 77
  Subcloning and mutagenesis 77
  Gene expression 80
  Protein purification 81
  Measurement of enzyme activity 84
  Preparation of N- and C-domain mixtures 84
  Amino acid analysis, Edman degradation sequencing, and mass spectrometry 85
  Circular dichroism and fluorescence studies 85
  Equilibrium unfolding studies 86
  Calculation of the apparent free energy of unfolding in the absence of denaturant 87
  Crosslinking studies 88
  Sedimentation equilibrium analyses 88
  Light scattering procedures 90
  Refolding studies *in vitro* 90
  Kinetic data analysis 91

Results 91
  Synthesis of CoA transferase forms in *E. coli* 91
  Mixtures of the purified N- and C-domains 94
  Conformational changes in the N- and C-domains upon assembly to the active enzyme form 104
  Stabilities of CoA transferase forms in denaturant 120
  Refolding of CoA transferase from denaturant 126

Discussion 129
    Folding and assembly of the N- and C-domains 129
    Structural rearrangements concomitant with assembly to the active enzyme form 133
    Equilibrium unfolding transitions 135
    Implications for the folding pathway of CoA transferase 137

Endnotes 139

References 140

CHAPTER 3: The Aggregation of CoA Transferase Folding Intermediates 143

Introduction 143

Experimental Procedures 149
    Materials 149
    Gene expression and protein purification 150
    Measurement of enzyme activity 152
    Preparation of N- and C-domain mixtures 152
    Radioactive labeling experiments 153
    Refolding studies *in vitro* 154
    Kinetic data analysis 155

Results 155
    Aggregation of the N- and C-domains *in vitro* 155
    Aggregation of wild-type CoA transferase during refolding *in vitro* 159
    Effect of temperature on aggregation *in vivo* 162
    Aggregation of the individual N- and C-domains *in vivo* 168
    Depletion of recombinant protein from the cell lysate 170
    Effects of GroEL and GroES on the refolding of CoA transferase 174

Discussion 181
    The aggregation of the N- and C-domains *in vitro* 181

The aggregation of CoA transferase refolding intermediates *in vitro* 184
The thermal instability of CoA transferase *in vivo* 186
The relative solubilities of the N- and C-domains 187
The disappearance of recombinant protein from the soluble fraction 188
Assembly versus aggregation: the role of the C-domain 190
Chaperonins and the aggregation of wild-type CoA transferase 191
Chaperonins and the aggregation of the hinge-mutant 195

Endnotes 197

References 198

CHAPTER 4: Alternative Oligomeric Forms of CoA Transferase 203

Introduction 203

Experimental Procedures 205
Materials 205
Gene expression and protein purification 206
Measurement of enzyme activity 207
Non-denaturing PAGE analysis 207
Mass spectrometry 207
Circular dichroism and fluorescence studies 207
Equilibrium unfolding studies 208
Calculation of $[\Delta G_u^{H_2O}]_{app}$ 208
Sedimentation velocity analyses 208
Sedimentation equilibrium analyses 209
Determination of molecular weights by gel filtration analysis 209
Refolding studies *in vitro* 210
Proteolysis experiments 210
X-ray crystallography studies 211

Results 212
Major and minor forms of wild-type CoA transferase 212
Molecular weights of the two forms of CoA transferase 217

Structural properties of the two forms of CoA transferase 220
Stabilities of the small and large conformers in denaturant 222
A kinetic barrier between the homodimer and the homotetramer 227
Role of the hinge region in the formation of the homotetramer 233
Crystallization of CoA transferase 236

Discussion 243
Two oligomeric forms of wild-type CoA transferase 243
Structural features of the homodimer and homotetramer 244
Thermodynamic stabilities of the small and large conformers 245
Interconversion of the homodimer and homotetramer 246
Intermolecular interactions involving the hydrophilic linker segment 248
Models for the formation of the homotetramer 250
Crystallization studies 252

Endnotes 253

References 254

CHAPTER 5: Identification of Glutamate 344 as the Catalytic Nucleophile in the Active Site of CoA Transferase 258

Introduction 258

Experimental Procedures 261
Materials 261
Protein purification 261
Measurement of enzyme activity 261
Autolytic fragmentation 262
Tricine SDS-PAGE 262
RP-HPLC 262
Mass spectrometry 262

Results 263
SDS-PAGE analysis of autolytically fragmented CoA transferase ... 263

Autolysis of proteolytically nicked CoA transferase 266
RP-HPLC and electrospray mass spectrometry 270

Discussion 276
Conditions suitable for autolysis 276
Identification of Glu 344 as the catalytic nucleophile by ESI-MS 276
Related studies and applications 278
A conserved sequence motif 279

Endnotes 282

References 283

CHAPTER 6: Site-Directed Mutagenesis at the Active Site of CoA Transferase 285

Introduction 285

Experimental Procedures 289
Materials 289
Site-directed mutagenesis 289
Gene expression and protein purification 292
Measurement of enzyme activity 293
Enzyme kinetics 294
Autolytic fragmentation 296
Activation of E344Q 296
Active site titration experiments 296
Circular dichroism and fluorescence studies 297
Equilibrium unfolding studies 297
Calculation of $[\Delta G_u^{H_2O}]_{app}$ 297
Inactivation of CoA transferase by DTNB 298
Active site complementation 299
Kinetic data analysis 299

Results 299
Effects of replacing glutamate 344 with alanine or aspartate 299

Effects of replacement of glutamate 344 with glutamine 306
Activation of E344Q — effects of acyl-CoA substrates 308
Activation of E344Q — effects of carboxylate substrates 310
Active site titration of E344Q 316
Thiol inactivation of C67S and C235S 320
Subunit hybridization of E344A and C67S 328

Discussion 330
The E344A and E344D mutants 330
The E344Q mutant 334
The identification of an essential cysteine residue 340
Active site complementation 343

Endnotes 346

References 347

CHAPTER 7: Conclusions and Final Discussion 351

Part A: Summary 351

Part B: Significance and Future Perspectives 354
Assembly of the N- and C-domains of CoA transferase 354
Refolding versus aggregation *in vitro* 361
Effects of chaperonins on folding and refolding 364
Two multimeric forms of CoA transferase 369
The active site of CoA transferase 372
The importance of x-ray crystallography 377
Final remarks 378

Endnotes 379

References 380

APPENDICES 384

Appendix 1: Enzyme Commission Numbers for some CoA Transferases ... 385
Appendix 2: Fundamental Constants and Conversion Factors 386
Appendix 3: Oligonucleotides used for PCR and/or Mutagenesis 387
Appendix 4: Plasmids and RF-DNA 388
Appendix 5: Strains of *E. coli* 389
Appendix 6: Buffers and Media 390
Appendix 7: Calculation of the Percentage of Activity in E344Q Attributable to Wild-Type CoA Transferase 391

List of Tables

Page

Table 1-1: Reactions of Acyl-CoA Thiolesters in Metabolism 7

Table 1-2: Metabolic Roles of the Prokaryotic CoA Transferases 12

Table 1-3: Molecular Properties of the Prokaryotic CoA Transferases 33

Table 1-4: Kinetic Constants of Succinyl-CoA:3-Ketoacid CoA Transferase of Porcine Heart 40

Table 1-5: Energetic Contribution of Noncovalent Binding Interactions to Catalysis by Succinyl-CoA:3-ketoacid CoA Transferase 60

Table 2-1: Electrospray Mass Spectral Analysis of the N- and C-domains 101

Table 2-2: Fluorescence Properties of Engineered CoA Transferase Proteins 108

Table 2-3: Quaternary Structures of Engineered CoA Transferase Proteins 110

Table 2-4: Denaturation of CoA Transferase Proteins with GuHCl 124

Table 3-1: Growth Times of Bacterial Cultures Analyzed by Immunoblotting 151

Table 4-1: Preliminary Characterization of the Major and Minor Forms of CoA Transferase 215

Table 4-2: Electrospray Mass Spectral Analysis of the Small and Large Forms of CoA Transferase 225

Table 4-3: Denaturation of the Small and Large Molecules of CoA Transferase with GuHCl 228

Table 4-4: Conditions Tested for the Growth of Crystals of Wild-Type CoA Transferase by Microdialysis 239

Table 4-5: Crystallographic Data for Crystals of CoA Transferase 241

Table 5-1: Predicted Molecular Masses for Fragment P 269

Table 5-2: Summary of Significant Components Detected by Electrospray Mass Spectrometry 275

Table 6-1: Specific Enzyme Activities of Wild-Type and Mutant Forms of CoA Transferase 301

Table 6-2: Fluorescence Properties of Wild-Type and Mutant Forms of CoA Transferase 304

Table 6-3: Denaturation of Wild-type and Mutant Forms of CoA Transferase with GuHCl 305

Table 6-4: Kinetic Constants of Wild-type and Mutant Forms of Pig Heart CoA Transferase 307

List of Figures

Page

Figure 1-1: Schematic representation of coenzyme A 2

Figure 1-2: Metabolism of coenzyme A 3

Figure 1-3: Reactions involving acyl-CoA thiolesters 9

Figure 1-4: Map of metabolism within the hydrogenosome of *Trichomonas vaginalis* and *Tritrichomonas foetus* 14

Figure 1-5: Pathways of ketone body metabolism 16

Figure 1-6: Amino acid sequence of succinyl-CoA:3-ketoacid CoA transferase from porcine heart 22

Figure 1-7: Hydrophilicity plot of the amino acid sequence of the porcine CoA transferase monomer 23

Figure 1-8: Analyses of the secondary structure of succinyl-CoA:3-ketoacid CoA transferase from porcine heart 25

Figure 1-9: Alignment of the amino acid sequences of the eukaryotic and $\alpha_2\beta_2$-type prokaryotic CoA transferases 28

Figure 1-10: Schematic representation of coenzyme A and of truncated analogues of CoA discussed in the text 38

Figure 1-11: Chemical mechanisms proposed for the half-reaction between ECoA and the carboxylate substrate 44

Figure 1-12: Evidence for a stepwise CoA transferase half-reaction from non-enzymatic models 49

Figure 1-13: Mechanism proposed for the autolytic fragmentation of CoA transferase 52

Figure 1-14: Modification of an essential cysteine residue in the active site of pig heart CoA transferase 54

Figure 1-15: The use of the intrinsic binding energy of the substrates to achieve catalysis 58

Figure 1-16: The use of the intrinsic binding energy of the nonreacting portion of CoA at specific points along the reaction coordinate 65

Figure 2-1: Construction of expression vectors encoding CoA transferase polypeptides 78

Figure 2-2: Production of soluble CoA transferase polypeptides in *E. coli* 92

Figure 2-3: Purification of intact CoA transferase 95

Figure 2-4: Purification of the hinge-mutant 96

Figure 2-5: Purity of isolated CoA transferase polypeptides 98

Figure 2-6: Identification of the N- and C-domains by ESI-MS 100

Figure 2-7: Kinetics of the formation of active CoA transferase in equimolar mixtures of the N- and C-domains 103

Figure 2-8: Analysis of the assembly of the N- and C-domains by far-UV CD 106

Figure 2-9: Molecular weight determinations for the N- and C-domains by sedimentation equilibrium 109

Figure 2-10: Molecular weight determination of the C-domain by light-scattering 112

Figure 2-11: N-domain sedimentation equilibrium data fit to a single-species model 114

Figure 2-12: Molecular weight determination of the hinge-mutant by light-scattering 116

Figure 2-13: Molecular weight determinations by crosslinking with BS^3 118

Figure 2-14: Molecular weight determinations by crosslinking with DTSSP 119

Figure 2-15: Kinetics of assembly of the N_2C_2-domain complex in an equimolar mixture of the N- and C-domains 122

Figure 2-16: Equilibrium unfolding of CoA transferase 125

Figure 2-17: Refolding of CoA transferase *in vitro* 128

Figure 2-18: Model describing the folding properties of CoA transferase 132

Figure 3-1: Folding *in vivo* versus refolding *in vitro* 145

Figure 3-2: Major features of the mitochondrial protein import pathway 148

Figure 3-3: Commitment to aggregation *in vitro* of the isolated N- and C-domains 157

Figure 3-4: Effect of concentration on the rate of commitment to aggregation *in vitro* of the isolated N- and C-domains 158

Figure 3-5: Effect of temperature and protein concentration on the refolding of CoA transferase *in vitro* 160

Figure 3-6: Commitment to aggregation *in vitro* of CoA transferase upon refolding 161

Figure 3-7: Aggregation of wild-type CoA transferase and the hinge-mutant *in vivo*, as measured by autoradiography 163

Figure 3-8: Quantification of the results from Figure 3-7 by phosphorimagery 164

Figure 3-9: Total radioactivity associated with the N- and C-domains in cells of BL-Hng 165

Figure 3-10: Kinetics of the appearance of CoA transferase activity in *E. coli* 167

Figure 3-11: Aggregation of wild-type CoA transferase and the hinge-mutant *in vivo*, as measured by immunoreactivity 169

Figure 3-12: Aggregation of the N- and C-domains *in vivo* 171

Figure 3-13: Depletion of recombinant protein from *E. coli* cell lysates 172

Figure 3-14: Quantification of the results from Figure 3-13 by phosphorimagery 173

Figure 3-15: Kinetics of refolding of CoA transferase at 22 °C 176

Figure 3-16: Effect of GroEL and GroES on the yield of refolded CoA transferase or citrate synthase at 22 °C 178

Figure 3-17: Inhibition of CoA transferase refolding by GroEL in the absence of ATP 180

Figure 3-18: Proposed pathways for the aggregation of CoA transferase 183

Figure 4-1: Separation of two forms of wild-type CoA transferase 214

Figure 4-2: Distinct electrophoretic behavior of three forms of CoA transferase under non-denaturing conditions 216

Figure 4-3: Determination of the molecular weights of the two components of wild-type CoA transferase by sedimentation equilibrium 218

Figure 4-4: Sedimentation equilibrium data of the small conformer fit to a monomer-dimer model 219

Figure 4-5: Molecular weight determinations for the two components of wild-type CoA transferase by gel filtration 221

Figure 4-6: Analysis of the two oligomeric forms of CoA transferase by ESI-MS 224

Figure 4-7: Analysis of the two oligomeric forms of CoA transferase by far-UV CD 226

Figure 4-8: Lack of detectable dissociation of homotetrameric CoA transferase in dilute protein solutions 230

Figure 4-9: Lack of detectable dissociation of homotetrameric CoA transferase in dilute protein solutions at elevated temperatures 231

Figure 4-10: Non-denaturing PAGE analysis of the homotetramer and the homodimer after unfolding and renaturation 234

Figure 4-11: Effect of limited tryptic digestion on the stability of homotetrameric CoA transferase 235

Figure 4-12: Analysis of the hinge-mutant by gel filtration chromatography 237

Figure 4-13: Crystals of wild-type CoA transferase 240

Figure 4-14: X-ray diffraction by crystals of CoA transferase 242

Figure 4-15: Models for the assembly of two homodimers to the homotetrameric form 251

Figure 5-1: Primary structure of pig heart CoA transferase in the vicinity of the active site glutamate residue 260

Figure 5-2: SDS-PAGE analysis of autolytically fragmented CoA transferase 265

Figure 5-3: Effect of succinyl-CoA concentration on the autolysis of CoA transferase 267

Figure 5-4: Schematic representation of the nicked form of CoA transferase, both prior and subsequent to autolysis 268

Figure 5-5: Analysis of nicked, autolytically fragmented CoA transferase by tricine SDS-PAGE 271

Figure 5-6: Elution profiles for RP-HPLC of CoA transferase 272

Figure 5-7: Electrospray mass spectrum of peptide Z 274

Figure 5-8: Conservation of the "ENG" sequence motif 280

Figure 6-1: The identification of shared active sites of a homodimeric enzyme by subunit hybridization 288

Figure 6-2: Mutagenesis at position 344 of CoA transferase by overlap extension 290

Figure 6-3: Inability of E344A and E344D to undergo autolysis 302

Figure 6-4: Analysis of mutant forms of CoA transferase by far-UV CD (part 1) 303

Figure 6-5: Activation of E344Q in the presence of acetoacetyl-CoA 309

Figure 6-6: Kinetics of activation of E344Q at various temperatures 311

Figure 6-7: Autolytic fragmentation of E344Q 312

Figure 6-8: Effect of acetoacetate on the activation of E344Q 313

Figure 6-9: Effect of succinate on the activation of E344Q 315

Figure 6-10: Effect of acetoacetate on the succinate-dependent inhibition of the activation of E344Q 317

Figure 6-11: Titration of functional active sites within the sample of E344Q........ 319

Figure 6-12: Autolytic fragmentation of C67S and C235S........ 322

Figure 6-13: Analysis of mutant forms of CoA transferase by far-UV CD (part 2)........ 323

Figure 6-14: Kinetics of inactivation by DTNB........ 325

Figure 6-15: Effect of DTT on the rapid inactivation of ECoA by DTNB........ 326

Figure 6-16: Effect of DTT on the inactivation of C67S by DTNB........ 327

Figure 6-17: Models for the hybridization of CoA transferase subunits........ 329

Figure 6-18: Active site complementation analyses of CoA transferase........ 331

Figure 6-19: Non-denaturing PAGE analysis of C67S and E344A after unfolding and renaturation........ 332

Figure 6-20: Mechanism for the activation of E344Q to wild-type CoA transferase via the formation of ECoA........ 337

Figure 6-21: Mechanism for the activation of E344Q to wild-type CoA transferase via cyclization........ 339

Figure 6-22: Models proposed for the evolution of homodimeric enzymes with two-domain subunits........ 345

Figure 7-1: Model describing the folding and assembly of wild-type CoA transferase to the active enzyme form........ 353

List of Abbreviations and Symbols

A_{278}	absorbance at 278 nm
AHA	acetohydroxamic acid
ADP	adenosine-5'-diphosphate
AMP	adenosine-5'-monophosphate
ATP	adenosine-5'-triphosphate
β_{lg}	Brønsted value for leaving-group ability
β_{nuc}	Brønsted value for nucleophilicity
BS^3	bis(sulfosuccinimidyl) suberate
cDNA	complementary deoxyribonucleic acid
CoA	coenzyme A (A refers to "acetylation")
Da	Dalton
$\Delta G^{\circ\prime}$	standard Gibbs free energy
$\Delta G_u^{H_2O}$	free energy of unfolding in the absence of denaturant
$\Delta G^{\ddagger}$	Gibbs free energy of activation
$\Delta H^{\ddagger}$	enthalpy of activation
$\Delta S^{\ddagger}$	entropy of activation
$\Delta\psi$	electrochemical gradient
DTNB	5, 5'-dithiobis(2-nitrobenzoic) acid
DTSSP	3,3'-dithio bis(sulfosuccinimidylpropionate)
DTT	dithiothreitol
ε_{278}	molar extinction coefficient at 278 nm
E_a	activation energy
ECoA	enzyme-CoA intermediate
EDTA	ethylene diamine tetraacetic acid
ESI-MS	electrospray ionization mass spectrometry
ESI-MS/MS	electrospray ionization tandem mass spectrometry
far-UV CD	far-ultraviolet circular dichroism
g	force due to gravity
GDP	guanosine-5'-diphosphate
GTP	guanosine-5'-triphosphate
GuHCl	guanidine hydrochloride
$[GuHCl]_{1/2}$	concentration of GuHCl resulting in half-maximal denaturation

HEPES	*N*-2-hydroxyethylpiperazine-*N'*-2-ethanesulfonic acid
HMG-CoA	3-hydroxy-3-methylglutaryl-CoA
Hsp	heat shock protein
IM	inner membrane
IPTG	isopropylthiogalactoside
kb	kilobase
k_{cat}	enzymatic turnover number
K_M	Michaelis constant
$K_{S\text{-}V}$	Stern-Volmer constant
$\lambda_{max,em}$	wavelength of maximal fluorescence emission
LB	Luria broth
LDH	lactate dehydrogenase
MCS	multiple cloning site
2ME	2-mercaptoethanol
MIR	multiple isomorphous replacement
MMP	methyl mercaptopropionate
MPP	matrix-processing peptidase
MSF	mitochondrial import stimulating factor
MWCO	molecular weight cutoff
NAA	N-acetylaletheine
NAC	N-acetylcysteamine
NADH	nicotinamide adenine dinucleotide (reduced form)
NEM	N-ethylmaleimide
NMR	nuclear magnetic resonance
NTCB	2-nitro-5-(thiocyanato)-benzoate
NTP	nucleoside-5'-triphosphate
OM	outer membrane
PAGE	polyacrylamide gel electrophoresis
PCR	polymerase chain reaction
PDH	pyruvate dehydrogenase complex
PEG	polyethylene glycol
pI	isoelectric point
PIP	di-μ-iodobis(ethylenediamine)diplatinum(II) nitrate
pK_a	negative logarithm of the acid dissociation constant
PMSF	phenylmethylsulfonyl fluoride
RF	replicative form

RP-HPLC	reversed-phase high performance liquid chromatography
rpm	revolutions per minute
$s_{20,w}$	sedimentation coefficient (standard solvent and temperature)
S	Svedberg unit
SCS	succinyl-CoA synthetase
SDS	sodium dodecyl sulphate
SHA	succinomonohydroxamic acid
TCA	tricarboxylic acid
TFA	trifluoroacetic acid
Θ	ellipticity
Tim	transport across the inner membrane
Tom	transport across the outer membrane
TPP	thiamine pyrophosphate
Tris-HCl	tris(hydroxymethyl)aminomethane hydrochloride

Chapter 1. Introduction

Part A: The Biochemistry of CoA and the CoA Transferases

The structure of coenzyme A

Coenzyme A (CoA) is a small molecular cofactor which plays a key role in biosynthetic and biodegradative processes in organisms as diverse as bacteria, plants, and mammals. It was first characterized in tissue homogenates as a heat-stable component necessary for the acetylation of compounds such as sulfanilamide and choline (Lipmann, 1945; Lipmann & Kaplan, 1946). The importance of this cofactor in such reactions is emphasized by the "A" portion of coenzyme A, which signifies "acetylation."

Early studies on the structure of CoA were designed to characterize its constituents, which could be released by acid hydrolysis or enzymatic degradation. In this manner, pantothenic acid (or vitamin B_5) was identified as the central component of the CoA molecule (Lipmann et al., 1947). Further work based on this approach (Baddiley et al., 1953; Novelli et al., 1954) led to the complete description of the CoA structure, consisting of adenosine 3'-monophosphate, 5'-diphosphate and 2-mercaptoethylamine in addition to pantothenic acid. The pantothenic acid "core" of CoA is linked at its carboxyl end to 2-mercaptoethylamine via an amide bond, and at its 4'-hydroxyl end to the 5'-pyrophosphate group of adenosine 3'-monophosphate, 5'-diphosphate (Figure 1-1). These three components of CoA are assembled by a pathway (Figure 1-2A) which uses adenosine triphosphate (ATP), pantothenic acid, and cysteine as starting metabolites (reviewed in [Robishaw & Neely, 1985]). The pathway by which CoA is degraded (Figure 1-2B) is nearly the reverse of the CoA biosynthetic pathway, yielding inorganic phosphate, pantothenic acid, and hypotaurine as the final products (reviewed in [Robishaw & Neely, 1985]).

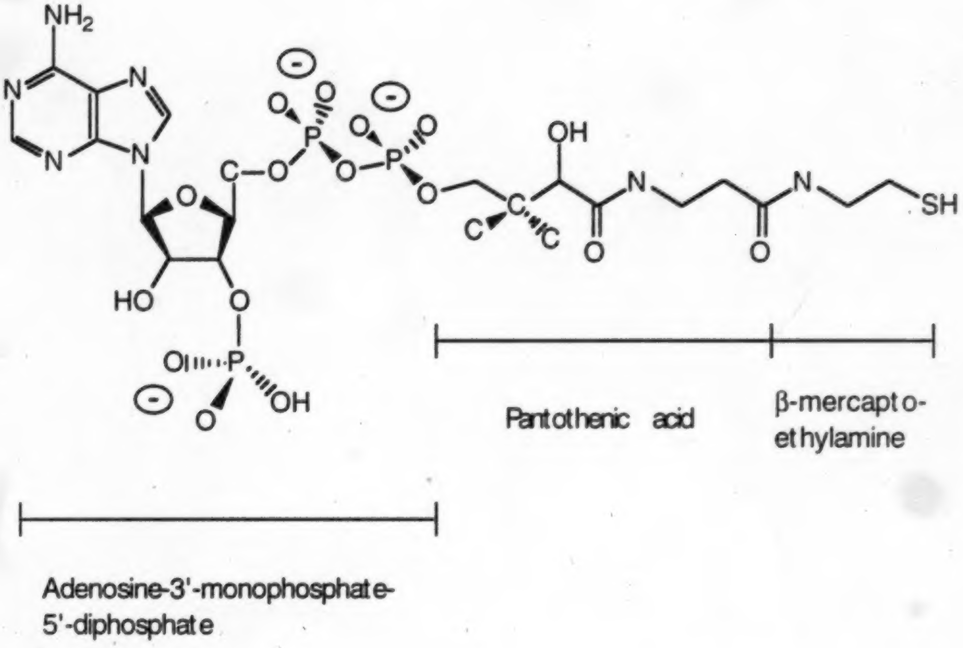
NH2
N
N
N
N
O
C
O
HO
O
O
P
OH
O
O
P
O
O
O
P
O
O
OH
C
C
C
N
O
N
O
SH
Pantothenic acid
β-mercapto-ethylamine
Adenosine-3'-monophosphate-5'-diphosphate

Figure 1-1: Schematic representation of coenzyme A. The three structural components described in the text are indicated. (Adapted from [Engel & Wierenga, 1996]).

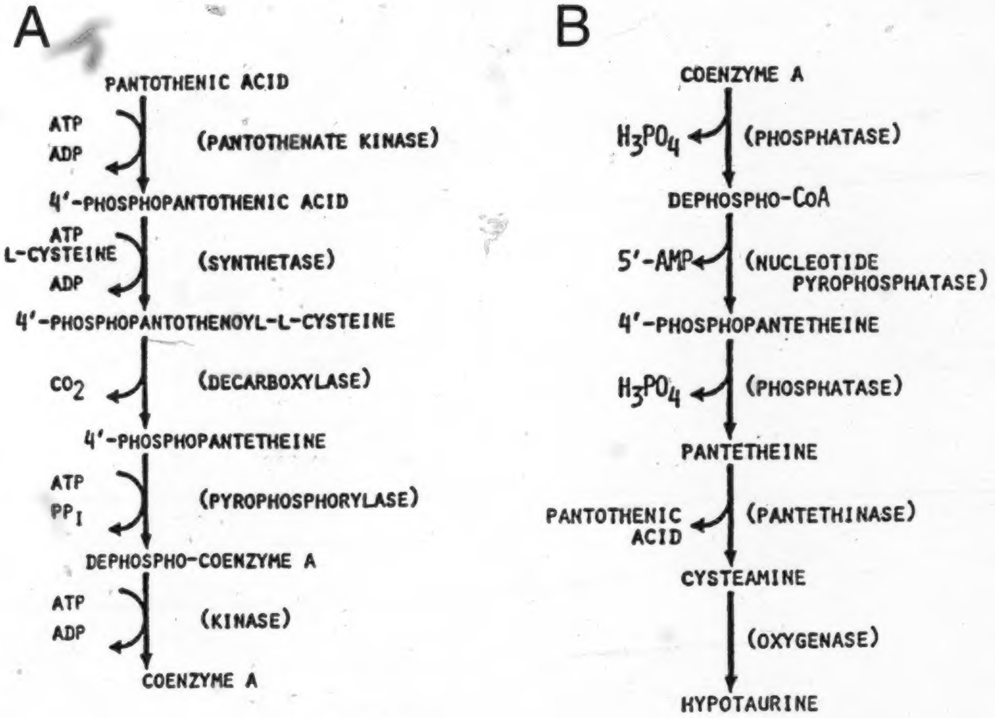
A
PANTOTHENIC ACID
ATP
ADP
(PANTOTHENATE KINASE)
4'-PHOSPHOPANTOTHENIC ACID
ATP
L-CYSTEINE
ADP
(SYNTHETASE)
4'-PHOSPHOPANTOTHENOYL-L-CYSTEINE
CO2
(DECARBOXYLASE)
4'-PHOSPHOPANTETHEINE
ATP
PPI
(PYROPHOSPHORYLASE)
DEPHOSPHO-COENZYME A
ATP
ADP
(KINASE)
COENZYME A
B
COENZYME A
H3PO4
(PHOSPHATASE)
DEPHOSPHO-CoA
5'-AMP
(NUCLEOTIDE PYROPHOSPHATASE)
4'-PHOSPHOPANTETHEINE
H3PO4
(PHOSPHATASE)
PANTETHEINE
PANTOTHENIC ACID
(PANTETHINASE)
CYSTEAMINE
(OXYGENASE)
HYPOTAURINE

Figure 1-2: Metabolism of coenzyme A. (A) Pathway of CoA synthesis. (B) Pathway of CoA degradation. (Reprinted from [Robishaw & Neely, 1985], with the permission of the American Physiological Society).

CoA exists either as a free thiol or as an acyl-CoA thiolester. The importance of acyl-CoA in the metabolic pathways of these organisms can be attributed to the chemical properties which distinguish thiolesters from oxyesters.

The chemistry of the thiolester

Thiolesters play a prominent role in metabolism because they are more reactive than oxyesters with respect to essential chemical transformations such as acylation and Claisen-type reactions (Solomons, 1984; Kyte, 1995). The enhanced reactivity of the thiolester is due in part to poor overlap (and thus to poor electron delocalization) between the 3*p* atomic orbitals of the sulfur atom and the π molecular orbital system of the adjacent carbonyl group. In contrast, since the orbital overlap is much greater in an oxyester, electrons are shared between the 2*p* atomic orbitals of an oxygen atom and the adjacent π molecular orbital system (Solomons, 1984; Kyte, 1995). As a result, the resonance forms which stabilize the oxyester and the thiolester differ markedly. A resonance structure in which the carbonyl carbon atom is linked to the bridging oxygen atom by a double bond stabilizes the oxyester, whereas the analogous conformer does not contribute significantly to the structure of the thiolester:

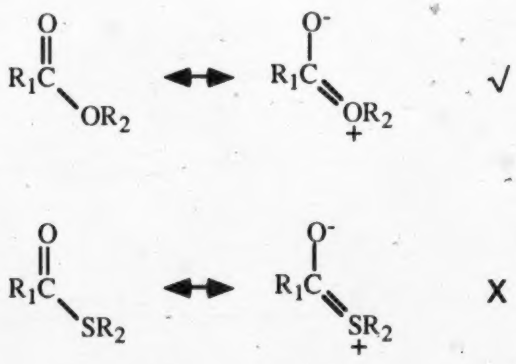

In contrast, the thiolester is stabilized by a resonance form in which a positive and a negative charge exist on the carbonyl carbon and oxygen atoms, respectively:

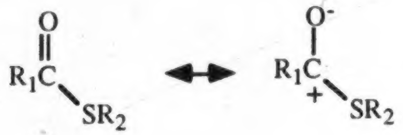

√

Thus, the carbonyl group of the thiolester, which is similar to that of a ketone, is much more electrophilic than the carbonyl moiety of the oxyester (Solomons, 1984; Kyte, 1995).

These differences in resonance stabilization also account for the 40- to 100-fold greater acidity of the thiolester relative to the oxyester (Bruice & Benkovic, 1966; Solomons, 1984; Kyte, 1995). In both cases, deprotonation at the α-position produces a carbanion with a negative charge on the α-carbon atom. This excess electron density on the thiolester carbanion is partially dissipated by the formation of a double bond between the α-carbon atom and the adjacent carbonyl carbon atom, which is relatively electrophilic:

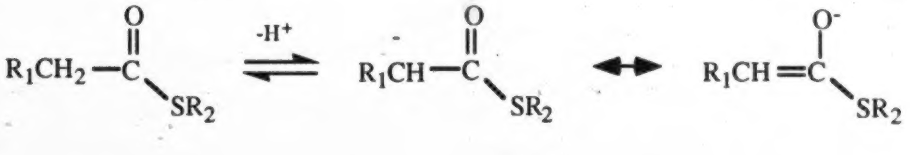

√

In contrast, the oxyester carbanion is stabilized to a lesser degree by an analogous resonance structure since its carbonyl carbon atom is much less electrophilic:

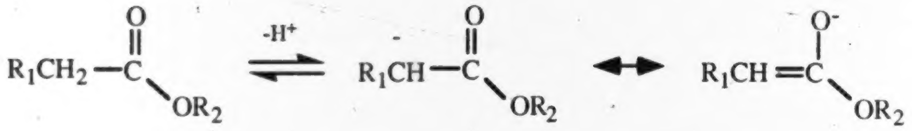

X

Thus, deprotonation at the α-carbon atom is more favorable for the thiolester than for the oxyester.

Finally, the thiol of a thiolester is a much better leaving group than the alcohol of an oxyester. This can be explained by the relative weakness of the carbon-sulfur bond of the thiolester, which lacks the double-bond character of the linkage between the carbonyl carbon atom and the bridging oxygen atom of the oxyester (Solomons, 1984). Given that the leaving group ability increases with acidity, the difference in the transfer potential of the thiol and alcohol anions is reflected in their pK_a values. For example, a pK_a value of 10.5 has been reported for ethanethiol, compared to 15.9 for ethanol (Danehy & Noel, 1960; Ballinger & Long, 1960).

CoA in metabolism

Acyl-CoA thiolesters are ubiquitous metabolic intermediates which undergo a broad range of biochemical transformations in prokaryotes and eukaryotes (Table 1-1). The reactivity of these compounds can be attributed to the electronic properties described above for thiolesters in general. For example, many of the reactions of acyl-CoA thiolesters involve a nucleophilic attack at the carbonyl group, leading to the transfer of the acyl moiety of the thiolester to an acyl-acceptor. This process is favored by the electrophilicity of the carbonyl carbon atom and the relatively good leaving ability of the thiol anion (Table 1-1A; Figure 1-3A). Other reactions (including Claisen-type reactions) involve the transient formation of a carbanion, and are thus also favored by the electrophilicity of the carbonyl carbon atom (Table 1-1B; Figure 1-3B). Due to their chemical versatility, acyl-CoA intermediates play seminal roles in a large number of

Table 1-1: Reactions of Acyl-CoA Thiolesters in Metabolism[a]

Part A: Reactions facilitated by the electrophilicity of the thiolester carbonyl moiety

Reaction type	Metabolic role	Enzyme involved in catalysis
N-acetylation	Ornithine, arginine biosynthesis[b]	*N*-acetylglutamate synthase[b]
O-acetylation	Cysteine biosynthesis[b]	Serine acetyltransferase[b]
N-succinylation	Lysine biosynthesis[b]	*N*-succinyl-2-amino-6-ketopimelate synthase[b]
O-succinylation	Methionine biosynthesis[b]	Homoserine acyltransferase[b]
N-acylation	Sphingolipid biosynthesis[c]	Sphinganine acyltransferase[c]
O-acylation	Triacylglycerol biosynthesis Phospholipid biosynthesis Cholesterol esterification	Acyl-CoA-dependent acyltransferases
C-acylation	Sphingolipid biosynthesis[c]	3-Ketosphinganine synthase[c]
Reduction	Cholesterol biosynthesis	HMG-CoA reductase[d]
Hydrolysis, coupled to NTP synthesis	TCA cycle	Succinyl-CoA synthetase
CoA transfer	Ketone body degradation[c]	Succinyl-CoA:3-ketoacid CoA transferase[c]
	Glutamate fermentation[b]	Glutaconate CoA transferase[b]

[a] Adapted from: Moat & Foster, 1988; Mack et al., 1994; Voet & Voet, 1995.

[b] Specific to non-mammalian metabolic pathways.

[c] Specific to mammalian metabolic pathways.

[d] HMG-CoA, β-hydroxy-β-methylglutaryl-CoA.

Table 1-1: Reactions of Acyl-CoA Thiolesters in Metabolism[a]

Part B: Reactions facilitated by the stabilization of an anionic intermediate

Reaction type	Metabolic pathway	Enzyme involved in catalysis
Mixed aldol-Claisen ester condensation	TCA cycle	Citrate synthase
	Glyoxylate pathway[b]	Malate synthase[b]
	Ketogenesis[c] Cholesterol biosynthesis Lysine degradation	HMG-CoA synthase[d]
	Leucine biosynthesis[b]	α-Isopropylmalate synthase[b]
Mixed aldol-Claisen ester cleavage	Ketogenesis[c] Leucine, lysine, tryptophan degradation	HMG-CoA lyase[d]
Claisen ester condensation	Ketogenesis[c] Cholesterol biosynthesis	Thiolase
Claisen ester cleavage	Fatty acid oxidation Ketone body degradation[c]	Thiolase
Racemization	Odd-chain fatty acid oxidation Isoleucine, methionine, valine degradation	Methylmalonyl-CoA racemase
Carboxylation	Leucine degradation	β-Methylcrotonyl-CoA carboxylase
Decarboxylation	Lysine, tryptophan degradation	Glutaconyl-CoA decarboxylase

[a] Adapted from: Moat & Foster, 1988; Voet & Voet, 1995.

[b] Specific to non-mammalian metabolic pathways.

[c] Specific to mammalian metabolic pathways.

[d] HMG-CoA, β-hydroxy-β-methylglutaryl-CoA.

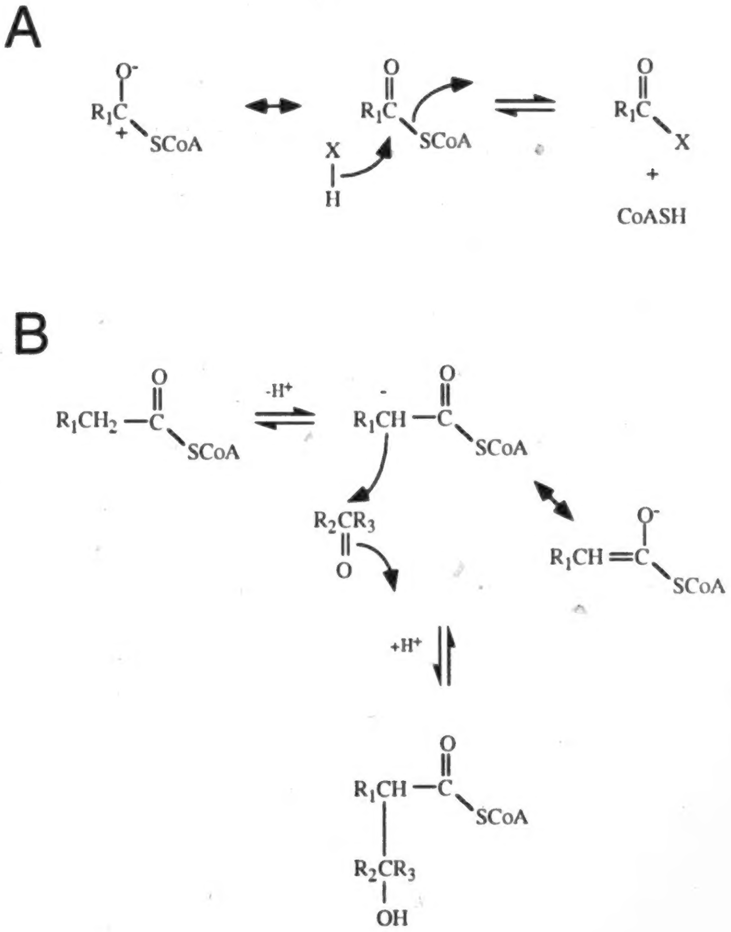
A
B
-H+
+H+
SCoA
CoASH
X
H

Figure 1-3: Reactions involving acyl-CoA thiolesters. (A) Transfer of the acyl moiety to a nucleophile "X". (B) Claisen ester condensation.

metabolic pathways, including the biosynthesis and/or catabolism of carbohydrates, lipids, ketone bodies, sterols, and amino acids (Table 1-1).

The energetics of acyl-CoA formation

The formation of acyl-CoA thiolesters is energetically expensive, due to the instability of the thiolester relative to its products of hydrolysis. The standard Gibbs free energy ($\Delta G°'$) for the hydrolysis of acetyl-CoA is -31.5 kJ/mol, which is similar to the value of -30.5 kJ/mol reported for the hydrolysis of the "energy-rich" phosphoanhydride bond linking the β- and γ-phosphates of ATP (Voet & Voet, 1995). This large, negative free energy change can be attributed to: (1) the equal distribution of electron density between both oxygen atoms of the carboxylate ion; and (2) a more favorable total energy of solvation of the carboxylate and thiol anions, relative to the thiolester alone.

The large activation energy associated with the formation of acyl-CoA can be overcome in several ways. First, the ligation of a CoA molecule to an α-keto group can involve the transient formation of an "active aldehyde" moiety. As an integral step in the synthesis of acetyl-CoA by the pyruvate dehydrogenase (PDH) complex, this reaction is driven by the exergonic decarboxylation of pyruvate linked to thiamine pyrophosphate (TPP). Second, CoA can be attached to an "activated" carboxylate moiety rather than to a keto group. For example, the thiolesterification of a fatty acid to yield acyl-CoA proceeds through an acyl-adenosine-5'-monophosphate (acyl-AMP) intermediate, in which the acyl moiety is "primed" for transfer to CoA. This reaction is driven bioenergetically by the hydrolysis of the two "energy-rich" bonds of ATP. Similarly, the formation of succinyl-CoA, catalyzed by succinyl-CoA synthetase (SCS), involves the preliminary conversion of succinate to succinyl-phosphate, once again at the expense of a "high-energy" phosphoanhydride bond of ATP or GTP. In these reactions, AMP and phosphate facilitate thiolesterification by extracting an oxygen atom from the carboxylate ion (Hersh & Jencks, 1967a).

In contrast to the previous two examples, the CoA transferase reaction does not involve free CoA and a separate activating agent (Table 1-1). Instead, CoA is transferred from an acyl-CoA thiolester to a carboxylate ion such that the energy of the products and reactants is identical:

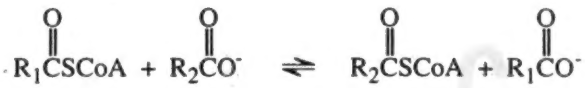

$$R_1\overset{\overset{O}{\|}}{C}SCoA + R_2\overset{\overset{O}{\|}}{C}O^- \rightleftharpoons R_2\overset{\overset{O}{\|}}{C}SCoA + R_1\overset{\overset{O}{\|}}{C}O^-$$

This reaction is unique in that the initial thiolester is both the donor of the thiol group and the "activating" agent responsible for dehydration of the carboxylate ion (Jencks, 1973).

CoA transferases in fermentative metabolism

The CoA transferases constitute an extremely diverse class of enzymes. They exist in many different types of organisms and display various substrate specificities that satisfy numerous metabolic requirements.

The growth of gram-negative and gram-positive eubacteria on a broad range of carbon sources (including aromatic compounds, amino acids, and mono- and dicarboxylic acids) is dependent on the activity of specific CoA transferases (Table 1-2). These enzymes catalyze the activation of organic acids to acyl-CoA thiolesters, which are further oxidized to more useful intermediates such as acetyl-CoA and succinyl-CoA. In addition, metabolic pathways which utilize CoA transferases also have industrial and ecological uses. For instance, acetone produced by *Clostridium acetobutylicum* is a useful solvent, and the concomitant biodegradation of complex organic molecules prevents the accumulation of chemicals which are toxic to other lifeforms (Stanier & Ornston, 1973).

CoA transferases are also essential for the complete, anaerobic fermentation of sugars in lower eukaryotes, including the protozoan parasites *Trichomonas vaginalis* and *Tritrichomonas foetus* (Müller, 1989), and the fungus *Neocallimastix sp. L2* (Marvin-

Table 1-2: Metabolic Roles of the Prokaryotic CoA Transferases

Substrate pair	Role in metabolism	Organism(s)	Reference(s)
acetoacetyl-CoA; acetate/butyrate	solventogenic fermentation	*Clostridium acetobutylicum*	Fischer et al., 1993 Petersen et al., 1993
butyryl-CoA; acetoacetate	lysine degradation	*Clostridium SB4*	Barker et al., 1978
acetyl-CoA; acetoacetate	C_3-C_6 fatty acid degradation	*Escherichia coli*	Sramek & Frerman, 1975a
acetyl-CoA; glutaconate	glutamate degradation	*Acidaminococcus fermentans*	Buckel et al., 1981
acetyl-CoA; 4-hydroxybutyrate	4-aminobutyrate fermentation	*Clostridium aminobutyricum*	Scherf & Buckel, 1991
acetyl-CoA; 5-hydroxyvalerate	5-aminovalerate fermentation	*Clostridium aminovalericum*	Eikmanns & Buckel, 1990
acetyl-CoA; succinate	ethanol-succinate fermentation	*Clostridium kluyveri*	Söhling & Gottschalk, 1996
formyl-CoA; oxalate/succinate	oxalate degradation	*Oxalobacter formigenes*	Baetz & Allison, 1990
3-hydroxypropionyl-CoA; acrylate butyryl-CoA; acetate	C_2-C_6 fatty acid degradation	*Peptostreptococcus elsdenii*	Tung & Wood, 1975 Schulman & Valentino, 1976
propionyl-CoA; succinate	propionic acid fermentation	*Propionibacterium sherwinii*	Allen et al., 1964.
succinyl-CoA; β-ketoadipate	benzoate/ hydroxybenzoate degradation	*Pseudomonas putida* *Acinetobacter calcoaceticus* *Agrobacterium tumefaciens*	Stanier & Ornston, 1973 *Ibid.* Parke, 1995

Sikkema et al., 1993). These organisms harbor rudimentary energy-converting organelles known as hydrogenosomes instead of the mitochondria typical of higher eukaryotes (Steinbüchel & Müller, 1986; Müller, 1988; Müller, 1989; Müller, 1993). As implied by their name, hydrogenosomes produce molecular hydrogen, along with acetate, malate, and carbon dioxide, during the course of pyruvate fermentation under anaerobic conditions (Figure 1-4). Given their lack of a functional tricarboxylic acid (TCA) cycle, hydrogenosomes must catabolize acetyl-CoA by an alternative pathway. This involves two steps: (1) the reaction of acetyl-CoA and succinate, catalyzed by a specific CoA transferase, to yield acetate and succinyl-CoA; and (2) the hydrolysis of succinyl-CoA and the concomitant substrate-level phosphorylation of ADP, catalyzed by SCS. Due to the combined activities of acetate:succinate CoA transferase and SCS in the hydrogenosome, the energy of oxidation of one mole of pyruvate is conserved as one mole of ATP. This is a significant contribution to the overall energy yield of the organism, given that two moles of ATP per mole of hexose are derived from glycolysis, the only other energy-yielding pathway (Müller, 1993).

CoA transferase and ketone body metabolism

The mammalian CoA transferases play a key role in the catabolism of ketone bodies, which are carriers of acetyl-CoA prepared by the liver and secreted into the bloodstream. These metabolic intermediates are essential fuels for the heart and kidney under normal circumstances, and for the brain under conditions of starvation, exercise, or diabetes (Voet & Voet, 1995).

Ketogenesis, which occurs in the mitochondrial matrix of hepatocytes (Figure 1-5A), involves the successive ligations of three acetyl-CoA molecules to produce β-hydroxy-β-methylglutaryl-CoA (HMG-CoA). This intermediate is subsequently cleaved to form acetoacetate and acetyl-CoA. Acetoacetate and its reduced equivalent, β-hydroxybutyrate, are the two major ketone bodies distributed to peripheral tissues via the

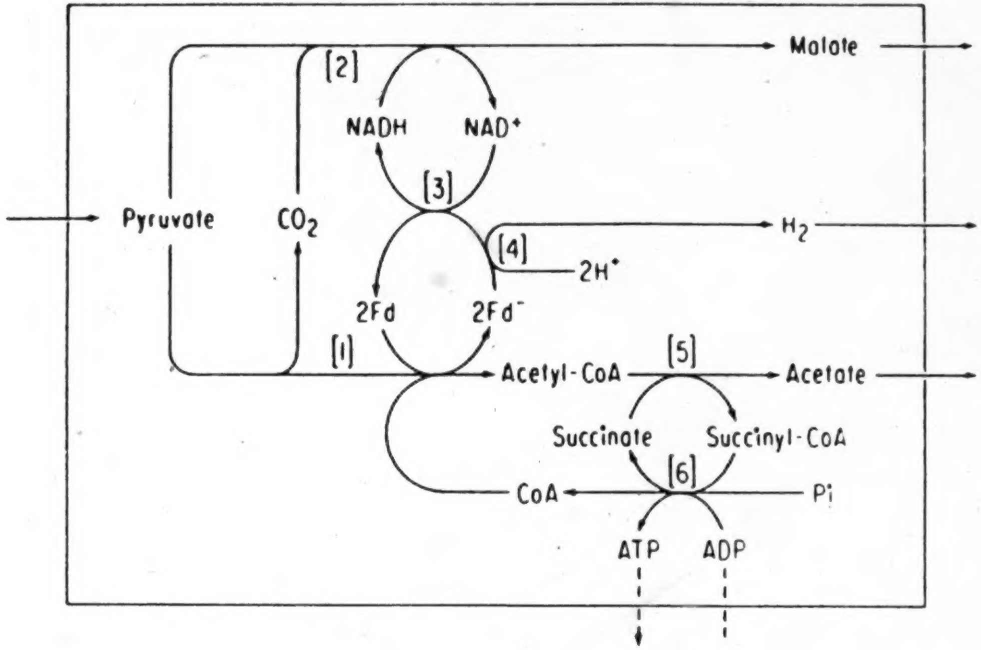

Malate
[2]
NADH
NAD⁺
[3]
Pyruvate
CO2
H2
[4]
2H⁺
2Fd
2Fd⁻
[1]
Acetyl-CoA
[5]
Acetate
Succinate
Succinyl-CoA
[6]
CoA
Pi
ATP
ADP

Figure 1-4: Map of metabolism within the hydrogenosome of *Trichomonas vaginalis* and *Tritrichomonas foetus*. Acetate/succinate CoA-transferase (5) catalyzes the formation of succinyl-CoA, which is then broken down to yield succinate, CoA, and ATP by the action of succinyl-CoA synthetase (6). Other enzymes shown are: pyruvate/ferredoxin oxidoreductase (1); malate dehydrogenase, decarboxylating, NAD (2); NAD/ferredoxin oxidoreductase (3); and H_2/ferredoxin oxidoreductase (4). (Reprinted from [Steinbüchel & Müller, 1986], with the permission of Elsevier Science).

Figure 1-5: Pathways of ketone body metabolism. (A) Acetoacetate and β-hydroxybutyrate are produced in the mitochondrial matrix of hepatocytes and distributed to extrahepatic tissues via the bloodstream. Alternatively, acetoacetate is delivered to the cytosol and subsequently converted to acetoacetyl-CoA by the action of acetoacetyl-CoA synthetase (5). Other enzymes shown are citrate synthase (1), ATP-citrate lyase (2), acetoacetyl-CoA thiolase (3), β-hydroxybutyrate dehydrogenase (4), and hydroxymethyl-glutaryl-CoA synthase (6). (Reprinted from [Endemann et al., 1982], with the permission of the American Society for Biochemistry and Microbiology). (B) Breakdown of ketone bodies in the mitochondrial matrix of extrahepatic cells. Succinyl-CoA:3-ketoacid CoA transferase catalyzes the transfer of CoA from succinyl-CoA to acetoacetate to form acetoacetyl-CoA, which is then catabolized to acetyl-CoA. (Reprinted from [Rochet & Bridger, 1994], with the permission of Cambridge University Press).

A

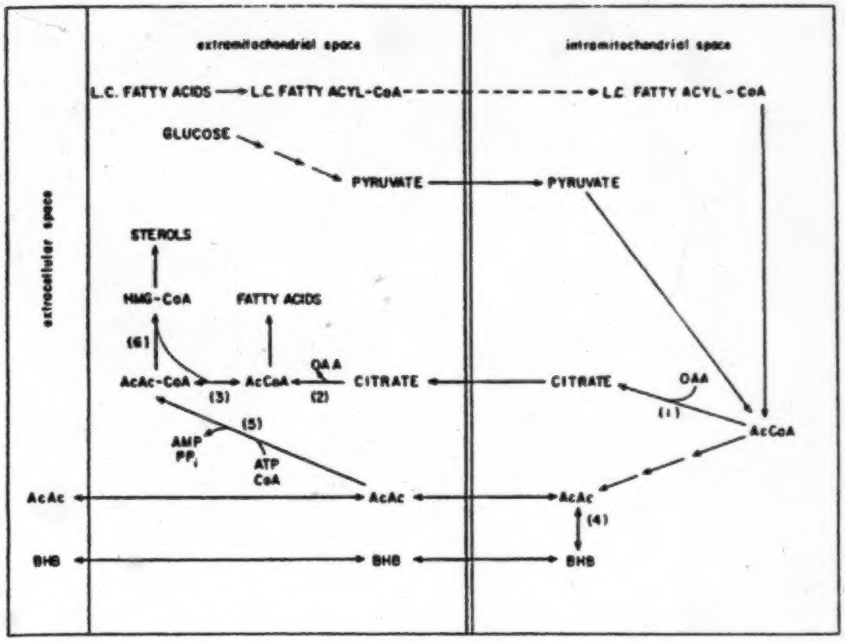
extracellular space
extramitochondrial space
intramitochondrial space
L.C. FATTY ACIDS
L.C. FATTY ACYL-CoA
L.C. FATTY ACYL - CoA
GLUCOSE
PYRUVATE
PYRUVATE
STEROLS
HMG-CoA
FATTY ACIDS
(6)
AcAc-CoA
(3)
AcCoA
OAA
(2)
CITRATE
CITRATE
OAA
(1)
AcCoA
(5)
AMP
PP$_i$
ATP
CoA
AcAc
AcAc
AcAc
(4)
BHB
BHB
BHB

B

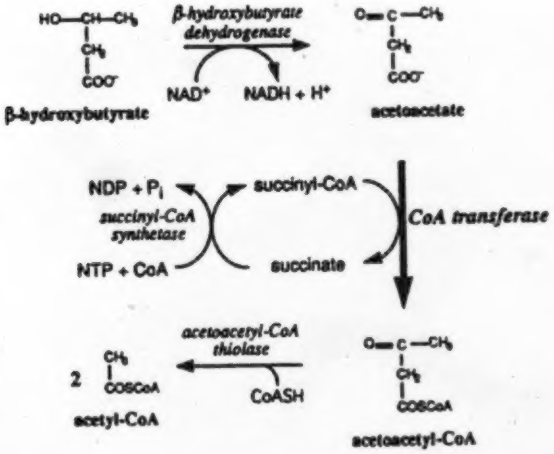
HO—CH—CH$_3$
CH$_2$
COO$^-$
β-hydroxybutyrate
β-hydroxybutyrate dehydrogenase
NAD$^+$
NADH + H$^+$
O═C—CH$_3$
CH$_2$
COO$^-$
acetoacetate
NDP + P$_i$
succinyl-CoA synthetase
NTP + CoA
succinyl-CoA
succinate
CoA transferase
acetoacetyl-CoA thiolase
CoASH
2
CH$_3$
COSCoA
acetyl-CoA
O═C—CH$_3$
CH$_2$
COSCoA
acetoacetyl-CoA

circulatory system (Figure 1-5A). Under conditions of severe ketoacidosis, resulting from diabetes or starvation, acetoacetate may also be decarboxylated to acetone (Voet & Voet, 1995).

Once assimilated in the cells of extrahepatic tissues, ketone bodies are processed in the mitochondrial matrix (Figure 1-5B). The first step of this degradative pathway is the activation of acetoacetate to acetoacetyl-CoA. Thus, β-hydroxybutyrate can only be catabolized following its oxidation to acetoacetate, catalyzed by β-hydroxybutyrate dehydrogenase. The formation of acetoacetyl-CoA, involving the transfer of CoA from succinyl-CoA to acetoacetate, is catalyzed by succinyl-CoA:3-ketoacid CoA transferase. The K_M of the myocardial enzyme for acetoacetate is 10 times less than that of the enzyme from skeletal muscle, consistent with the proposed role of ketone body catabolism in each of these tissues (Blair, 1969). Although ketone bodies are an important fuel for heart muscle under normal physiological conditions, this is only true for skeletal muscle during ketonemia, when the concentration of acetoacetate in the blood is much higher. Following the activation of acetoacetate, succinyl-CoA is regenerated from succinate, CoA, and GTP by a specific SCS isoenzyme (McClellan & Ottaway, 1980; Jenkins & Weitzman, 1986). Given that the ratio of GTP to GDP in the mitochondrial matrix is on the order of 100 to 1, use of a GTP-specific form of SCS ensures that the levels of succinyl-CoA remain above a threshold necessary for continued ketone body catabolism (McClellan & Ottaway, 1980; Ottaway et al., 1981; Jenkins & Weitzman, 1986).[1] Finally, acetoacetyl-CoA undergoes thiolysis, releasing two molecules of acetyl-CoA.

Depending on the metabolic status of the cell, several possible fates exist for acetyl-CoA produced from the mitochondrial breakdown of ketone bodies (reviewed in [Williamson, 1979]). If the cellular ATP levels are low, acetyl-CoA may be fully oxidized to carbon dioxide by the TCA cycle in the mitochondrion. Alternatively, if the energy load is high, acetyl-CoA may be shuttled to the cytosol in the form of citrate, reformed from citrate by the action of ATP-citrate lyase, and incorporated into fatty acids or cholesterol (Figure 1-5A). In lipogenic tissues such as brain, liver, lactating mammary gland, and adipose tissue, however, the conversion of ketone bodies to fatty acids or sterols may bypass the mitochondrion altogether (Buckley & Williamson, 1973; Buckley & Williamson, 1975; Ito et al., 1986). In this case, acetoacetyl-CoA is formed from acetoacetate, CoA, and ATP directly in the cytosol, in a reaction catalyzed by acetoacetyl-CoA synthetase (Figure 1-5A). Cytosolic acetoacetyl-CoA is then converted to acetyl-CoA for fatty acid synthesis, or to HMG-CoA for cholesterol biogenesis (Endemann et al., 1982; Bergstrom et al., 1984). This pathway yields one additional mole of cytosolic acetyl-CoA per mole of ATP consumed, compared to the mitochondrial route (reviewed in [Williamson, 1979]).

In summary, succinyl-CoA:3-ketoacid CoA transferase is essential for the oxidative degradation of ketone bodies in the mitochondrion. It is absent from the liver, which produces ketone bodies for distribution rather than for catabolism. Although the mitochondrial breakdown of ketone bodies may also supply a pool of acetyl-CoA for lipogenesis, this function is satisfied more efficiently by the cytosolic enzyme, acetoacetyl-CoA synthetase.

Human disorders caused by a deficiency in succinyl-CoA:3-ketoacid CoA transferase are rare but have been reported (Tildon & Cornblath, 1972; Spence et al., 1973; Middleton et al., 1987; Saudubray et al., 1987; Pérez-Cerdá et al., 1992; Sakazaki et al., 1995; Kassovska-Bratinova et al., 1996; Pretorius et al., 1996). The clinical symptoms for this condition include permanent hyperketonemia and ketonuria along with recurring episodes of ketoacidosis, with normal levels of blood glucose and lactate (Pérez-Cerdá et al., 1992). In cases where the syndrome is severe and ultimately fatal, levels of CoA transferase activity are less than 5% of normal (Tildon & Cornblath, 1972; Spence et al., 1973). Residual enzyme activity, ranging from 10% to 20% of normal values, is generally associated with milder forms of the disease (Middleton et al., 1987;

Saudubray et al., 1987; Pérez-Cerdá et al., 1992; Sakazaki et al., 1995; Pretorius et al., 1996). These observations underscore the essential role of succinyl-CoA:3-ketoacid CoA transferase in the catabolism of ketone bodies.

Part B: Structural Organization of the Prokaryotic and Mammalian CoA Transferases

As described above, the CoA transferases display diverse substrate specificities and metabolic functions. Fundamentally, however, each member of this class of enzymes achieves the same chemical result: CoA is transferred from an acyl-CoA thiolester to a carboxylate ion. In the absence of a three-dimensional molecular model for any of the CoA transferases, the structural features which account for this catalytic function remain unclear. Nevertheless, many of these enzymes have been successfully purified, and cDNA molecules encoding several CoA transferases have been isolated. From the characterization of the primary and quaternary structures of these enzymes, it is clear that a number of mammalian and prokaryotic CoA transferases have a similar architecture.

Subunit and domain organization of the mammalian CoA transferases

Succinyl-CoA:3-ketoacid CoA transferase has been purified to homogeneity from mammalian tissues such as pig heart (Hersh & Jencks, 1967a; Edwards et al., 1973; White & Jencks, 1976b), sheep kidney (Sharp & Edwards, 1978), and rat brain (Russell & Patel, 1982). Molecular weights reported for these enzymes range from 7.8×10^4 to 1.13×10^5 (Hersh & Jencks, 1967a; Edwards et al., 1973; White & Jencks, 1976b; Sharp & Edwards, 1978; Russell & Patel, 1982).[2] In addition, molecular weights determined under denaturing conditions range from 4.56×10^4 to 6.3×10^4 (Edwards et al., 1973; White & Jencks, 1976b; Sharp & Edwards, 1978; Russell & Patel, 1982).[3] Based on these measurements, it is assumed that under benign conditions mammalian CoA transferase is a homodimer.

Preparations of succinyl-CoA:3-ketoacid CoA transferase from sheep kidney (Sharp & Edwards, 1978) and pig heart (Moore & Jencks, 1982c; Lin & Bridger, 1992), purified in the absence of proteinase inhibitors, consist of two polypeptides of 2.8×10^4 and 2.4×10^4. The sum of these molecular weights is consistent with the values estimated for the intact subunit, suggesting that two fragments are released from the CoA transferase monomer by proteolysis. Importantly, this cleavage of the enzyme to a "nicked" form does not abolish catalytic function. Thus, each mammalian subunit consists of two interacting domains linked by a segment which is exposed to the action of proteinases (Sharp & Edwards, 1978; Moore & Jencks, 1982c; Lin & Bridger, 1992).

The primary structure of succinyl-CoA:3-ketoacid CoA transferase provides a rationale for the enzyme's sensitivity to limited proteolysis. The amino acid sequence of the porcine monomer (Figure 1-6) was deduced from a cDNA insert encoding the cytoplasmic precursor of the enzyme (Lin & Bridger, 1992). The first 39 residues comprise a signal peptide for targeting the enzyme to the mitochondrial matrix. The molecular weight of the mature monomer, which consists of the remaining 481 residues, is 52 197 (Lin & Bridger, 1992), in agreement with previous estimates. A hydrophilicity plot for this subunit (Figure 1-7) suggests a structure of two relatively hydrophobic regions, connected by a sequence of hydrophilic residues referred to as a "hinge" or "linker" segment (Lin & Bridger, 1992). From the distribution of acidic and basic residues in this segment, it is conceivable that the hinge adopts an α-helical structure, with positive and negative charges clustering on opposite faces (Lin & Bridger 1992). Moreover, a helix-turn-helix motif (Figure 1-8) is predicted for this region, based on the secondary-structural preferences calculated for the 20 amino acid residues (Chou & Fasman, 1978; Levitt, 1978; Deléage & Roux, 1987). Interestingly, the site of proteolysis in the "nicked" enzyme coincides with the loop of the proposed helix-turn-helix linker.

Figure 1-6: Amino acid sequence of succinyl-CoA:3-ketoacid CoA transferase from porcine heart, shown below the nucleotide sequence of the corresponding cDNA. Numbers in plain text refer to the nucleotide sequence, while numbers in italics correspond to the amino acid sequence. Amino acid residues 1 to 30 (dotted underline) constitute the proposed mitochondrial presequence. Residues 40 to 80 and 295 to 305 (boxed) correspond to the sequences determined by Edman degradation analysis of the N-terminal and C-terminal fragments of the nicked enzyme, respectively. (Reprinted from [Lin & Bridger, 1992], with the permission of the American Society for Biochemistry and Microbiology).

```
 1                                                                                     81
 GAATTCCGACCGGTCCCGGCGGAGCAGTTGACACACTGAGAGGCGCTCCAACCCCGGCCTGCGCCCGCCGCCCTCCCGACC

ATGGCGGCTCTCACACTCCTCTCCTCCCGCCTGCGCCTCTGCGCCTCCGCCTACCGCTCCGGGGGCGCCTGGTCCCAGGGATGTGCTGGC
MetAlaAlaLeuThrLeuLeuSerSerArgLeuArgLeuCysAlaSerAlaTyrArgSerGlyGlyAlaTrpSerGlnGlyCysAlaGly 30

TACTTTTCAACTAGCACGCGTCGTCATACCAAATTTTATACGGATGCAGTGGAAGCTGTAAAAGACATCCCTAATGGTGCAACAGTGCTG
TyrPheSerThrSerThrArgArgHisThrLysPheTyrThrAspAlaValGluAlaValLysAspIleProAsnGlyAlaThrValLeu 60

GTTGGTGGTTTTGGGTTATGTGGAATTCCGGAGAATCTTATAGGAGCTTTGCTAAAGACTGGAGTAAAAGAACTTACTGCAGTCAGCAAC
ValGlyGlyPheGlyLeuCysGlyIleProGluAsnLeuIleGlyAlaLeuLeuLysThrGlyValLysGluLeuThrAlaValSerAsn 90

AATGCAGGGGTTGACAACTTTGGTTTGGGCCTTTTACTTCAATCCAAGCAGATAAAACGCATGATCTCTTCATACGTGGGAGAAAATGCA
AsnAlaGlyValAspAsnPheGlyLeuGlyLeuLeuLeuGlnSerLysGlnIleLysArgMetIleSerSerTyrValGlyGluAsnAla 120

GAATTTGAACGACAGTACTTAGCTGGTGAATTAGAAGTAGAGCTGACACCTCAGGGCACCCTGGCAGAGAGGATCCGTGCAGGTGGGGCA
GluPheGluArgGlnTyrLeuAlaGlyGluLeuGluValGluLeuThrProGlnGlyThrLeuAlaGluArgIleArgAlaGlyGlyAla 150

GGTGTTCCTGCGTTTTACACCAGCACAGGGTATGGCACCCTGGTGCAAGAAGGAGGGTCCCCGATCAAATACAACAAAGACGGCAGCATT
GlyValProAlaPheTyrThrSerThrGlyTyrGlyThrLeuValGlnGluGlyGlySerProIleLysTyrAsnLysAspGlySerIle 180

GCCATTGCCAGTAAACCGAGAGAGGTGAGGGAATTTAATGGTCAGCACTTTATTTTGGAGGAAGCAATCAGAGGGGATTTTGCTTTGGTG
AlaIleAlaSerLysProArgGluValArgGluPheAsnGlyGlnHisPheIleLeuGluGluAlaIleArgGlyAspPheAlaLeuVal 210

AAAGCCTGGAAGGCAGACCAAGCTGGAAACGTGACTTTCAGGAAAAGTGCAAGAAATTTCAACCTGCCGATGTGCAAAGCTGCAGAAACC
LysAlaTrpLysAlaAspGlnAlaGlyAsnValThrPheArgLysSerAlaArgAsnPheAsnLeuProMetCysLysAlaAlaGluThr 240

ACAGTGGTGGAGGTTGAAGAAATTGTGGATATTGGATCATTTGCCCCAGAGGACATTCATATTCCTAAGATTTATGTACATCGCCTTGTA
ThrValValGluValGluGluIleValAspIleGlySerPheAlaProGluAspIleHisIleProLysIleTyrValHisArgLeuVal 270

AAGGGAGAAAAATATGAGAAAAGAATTGAGCGTTTATCAGTCCGGAAAGAGGAAGATGTAAAAACCAGATCTGGTAAACTTGGAGATAAT
LysGlyGluLysTyrGluLysArgIleGluArgLeuSerValArgLysGluGluAspValLysThrArgSerGlyLysLeuGlyAspAsn 300

GTAAGAGAACGGATCATCAAGCGGGCGGCTCTTGAATTTGAGGATGGCATGTATGCTAATTTGGGCATAGGAATCCCACTTCTGGCCAGC
ValArgGluArgIleIleLysArgAlaAlaLeuGluPheGluAspGlyMetTyrAlaAsnLeuGlyIleGlyIleProLeuLeuAlaSer 330

AACTTTATCAGCCCAAATATGACTGTCCACCTGCAAAGTGAAAATGGAATCCTGGGTTTGGGTCCATATCCTTTACAAAATGAAGTTGAT
AsnPheIleSerProAsnMetThrValHisLeuGlnSerGluAsnGlyIleLeuGlyLeuGlyProTyrProLeuGlnAsnGluValAsp 360

GCAGATCTAATCAATGCAGGCAAGGAAACAGTTACTGTTCTTCCAGGAGCCTCTTACTTCTCCAGCGATGAATCATTTGCAATGATTAGA
AlaAspLeuIleAsnAlaGlyLysGluThrValThrValLeuProGlyAlaSerTyrPheSerSerAspGluSerPheAlaMetIleArg 390

GGGGGACATGTCAATCTAACAATGCTAGGAGCCATGCAGGTTTCCAAATATGGTGACCTGGCTAACTGGATGATACCTGGGAAGCTGGTG
GlyGlyHisValAsnLeuThrMetLeuGlyAlaMetGlnValSerLysTyrGlyAspLeuAlaAsnTrpMetIleProGlyLysLeuVal 420

AAAGGAATGGGAGGGGCTATGGATCTAGTGTCCAGTGCCAAAACCAAAGTGGTGGTCACCATGGAGCATTCTGCAAAGGGAAATGCACAT
LysGlyMetGlyGlyAlaMetAspLeuValSerSerAlaLysThrLysValValValThrMetGluHisSerAlaLysGlyAsnAlaHis 450

AAAATCATGGAGAAATGTACATTACCACTGACGGGAAAGCAATGTGTCAACCGCATCATTACTGAAAAGGCAGTGTTTGATGTGGACAGA
LysIleMetGluLysCysThrLeuProLeuThrGlyLysGlnCysValAsnArgIleIleThrGluLysAlaValPheAspValAspArg 480

AAGAAAGGTCTGACTCTGATTGAACTCTGGGAAGGCCTGACAGTGGATGACATAAAAAAGAGCACTGGGTGTGATTTTGCTGTTTCACCA
LysLysGlyLeuThrLeuIleGluLeuTrpGluGlyLeuThrValAspAspIleLysLysSerThrGlyCysAspPheAlaValSerPro 510

AAACTGATACCAATGCAGCAGGTCACAACT
LysLeuIleProMetGlnGlnValThrThr 520
1642
TGAAATGTGGAACAGATATTTGTCCCAAGCTGTGTGCTTTTCATTTTAGCCACATAGGATTTTATTGAAAAGACATCAGTAATTGTAATT

GTATTCAAACAAGTAGTTTTTGACTCGTTTTCTTCTAGTGTCTTATGCTTTATACAGCCATATAGACTTTGTTCTCTCAGATGTACTCTG

                           1851
ACATTTCAAGGAAAAACAAAAAAAAAAAGG
```

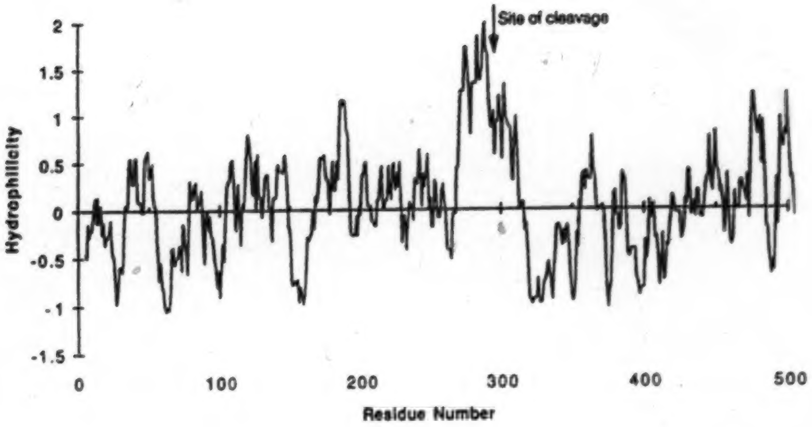

Figure 1-7: Hydrophilicity plot of the amino acid sequence of the porcine CoA transferase monomer. (Reprinted from [Lin & Bridger, 1992], with the permission of the American Society for Biochemistry & Molecular Biology).

Figure 1-8: Analyses of the secondary structure of succinyl-CoA:3-ketoacid CoA transferase from porcine heart. The probabilities of formation of α-helix (A) and β-turn (B) are plotted against the amino acid sequence number of the mature enzyme form. The site of proteolysis (residue 295) coincides with a minimum on the α-helix plot and a maximum on the β-turn plot. The probabilities were calculated using a nine-residue window, based on the secondary-structural preferences determined by Chou and Fasman (1978). The plots were generated using the program ProtScale on the ExPASy Molecular Biology Server, courtesy of the Geneva University Hospital and the University of Geneva (Geneva, Switzerland; Appel et al., 1994).

A

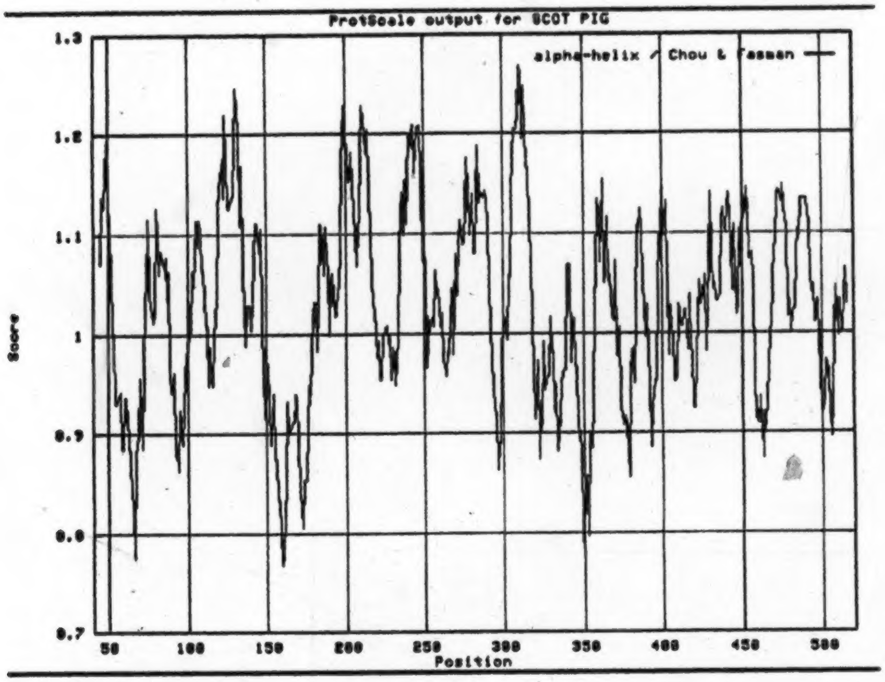
ProtScale output for SCOT PIG
alpha-helix / Chou & Fasman
Score
1.3
1.2
1.1
1
0.9
0.8
0.7
50
100
150
200
250
300
350
400
450
500
Position

B

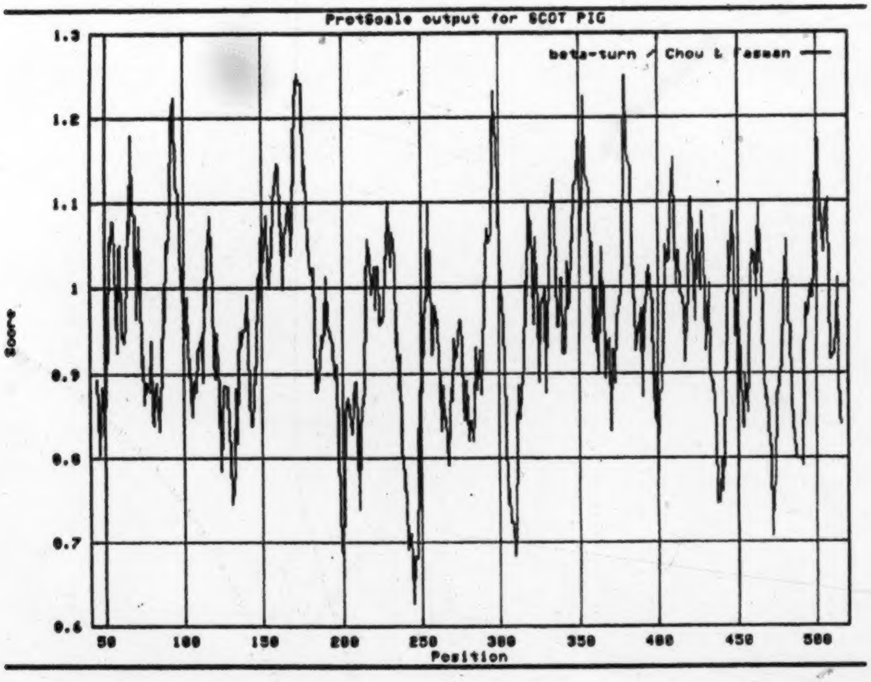
ProtScale output for SCOT PIG
beta-turn / Chou & Fasman
Score
1.3
1.2
1.1
1
0.9
0.8
0.7
0.6
50
100
150
200
250
300
350
400
450
500
Position

Cleavage in this segment generates amino-terminal (N-domain) and carboxyl-terminal (C-domain) fragments of 27 906 and 24 308, respectively (Lin & Bridger, 1992).

On the basis of amino acid sequence identity, it is likely that the subunits of other eukaryotic CoA transferases also consist of two domains linked by a flexible hinge region. For example, the primary structures of the human CoA transferase (Kassovska-Bratinova et al., 1996) and the porcine enzyme are 90% identical (Figure 1-9).[4] Thus, the subunits of different mammalian CoA transferases adopt a common fold. In addition, the primary structures of the succinyl-CoA:3-ketoacid CoA transferases of *Caenorhabditis elegans* (Kassovska-Bratinova et al., 1996) and pig heart are 66% identical (Figure 1-9).[5] From this example, similar structures can be predicted for the CoA transferases of organisms as diverse as mammals and lower eukaryotes.

In summary, succinyl-CoA:3-ketoacid CoA transferase consists of two identical subunits. ~~Each of~~ these is organized as two compact domains linked by a hydrophilic, helical hinge. This fold accounts for the susceptibility of the mammalian monomer to proteolysis at a defined location in its sequence.

Subunit organization of the prokaryotic CoA transferases

The subunit composition of the prokaryotic CoA transferases (Table 1-3) is much more variable than that of their mammalian equivalents. Some of the bacterial enzymes consist of only one type of subunit, designated α, and are homotetramers (α_4), homodimers (α_2), or monomers (α). The majority of known prokaryotic CoA transferases consist of two separate polypeptides (referred to as α and β), which are organized as $\alpha_2\beta$ trimers, $\alpha_2\beta_2$ tetramers, or $\alpha_4\beta_4$ octamers (Table 1-3).

Genomic DNA fragments encoding heterotetrameric ($\alpha_2\beta_2$) CoA transferases have been isolated from gram-negative and gram-positive eubacteria, including *Pseudomonas putida* (Parales & Harwood, 1992), *Clostridium acetobutylicum* (Fischer et al., 1993; Peterson et al., 1993), *Acinetobacter calcoaceticus* (Kowalchuk et al., 1994;

Figure 1-9: Alignment of the amino acid sequences of the eukaryotic and $\alpha_2\beta_2$-type prokaryotic CoA transferases. Fully conserved amino acid residues are depicted in bold lettering, and the glycine cluster is enclosed within a box. The numbers adjacent to the sequences of the eukaryotic enzymes refer to the precursor forms. The abbreviations are: *C. eleg.*, *Caenorhabditis elegans*; *C. acet.*, *Clostridium acetobutylicum*; *A. calc.*, *Acinetobacter calcoaceticus*; *P. puti.*, *Pseudomonas putida*; *A. tume.*, *Agrobacter tumefaciens*; *B. subt.*, *Bacillus subtilis*; *M. tube.*, *Mycobacterium tuberculosis*; *H. infl.*, *Haemophilus influenzae*; and *E. coli*, *Escherichia coli*. Deletions with respect to the mammalian CoA transferases are indicated by a dash (-). Insertions with respect to the mammalian CoA transferases are as follows: Thr-Glu in the CoA transferase of *C. elegans*, between residues 176 and 177 of the mammalian enzymes; Arg-Gln in the CoA transferases of *A. calcoaceticus* and *P. Putida*, between residues 116 and 117 of the mammalian enzymes; and Asp or Gly in the CoA transferase of *A. calcoaceticus* or *P. Putida* (respectively), between residues 418 and 419 of the mammalian enzymes (Kassovska-Bratinova et al., 1996). Only partial amino acid sequences are available for the enzymes of *A. tumefaciens* and *M. tuberculosis*. The identity of the gene encoding the CoA transferase of *M. tuberculosis* is inferred, based on the apparent amino acid sequence similarity between this enzyme and the CoA transferase of *B. subtilis*. The sequence alignment was generated using the program BLAST (Altschul et al., 1990) and the SwissProt database on the ExPASy Molecular Biology Server, courtesy of the Geneva University Hospital and the University of Geneva (Geneva, Switzerland; Appel et al., 1994).

```
Pig                 MAALTLLSSR LRLCASAYRS GGAWSQGCAG YFSTSTRRHT  40
Human               MAALKLLSSG LRLCASARGS GATWYKGCVC SFSTSAHRHT  40
C. eleg.            MPILSKIWAA -PAAGILRKT PRNAHQMRLI SMTSS--MKA  37
C. acet. (Ctf A)                                             MN   2
A. calc. (Cat I)                                            MID   3
P. puti.  (Pca I)                                           MIN   3
A. tume. (Pca I)
B. subt. (Pca I)                                             MG   2
M. tube. (Pca I?)                                            MD   2
H. infl. (Ato D)                                             MT   2
E. coli (Ato D)                                              MK   2

Pig                 KFYTDAVEAV KDIPNGATVL VGGFGLCGIP ENLIGALLKT  80
Human               KFYTDPVEAV KDIPDGATVL VGGFGLCGIP ENLIDALLKT  80
C. eleg.            KVFNSAEEAV KDIPDNAKLL VGGFGLCGIP ENLIQAITKT  77
C. acet. (Ctf A)    SKIIRFENLR SFFKDGMTIM IGGFLNCGTP TKLIDFLVNL  42
A. calc. (Cat I)    KSAATLTEAL SQIHDGATIL IGGFGTAGQP AELIDGLIEL  43
P. puti.  (Pca I)   KTYESIASAV EGITDGSTIM VGGFGTAGMP SELIDGLIAT  43
A. tume. (Pca I)
B. subt. (Pca I)    KVLSSSKEAA KLIHDGDTLI AGGFGLCGIP EQLILSIRDQ  42
M. tube. (Pca I?)   KVVATAAEAV ADIANGSSLA VGGFGLCGIP EALIAALVDS  42
H. infl. (Ato D)    QKHLKLNNLN QHLHDGMSIM FGGFMGIGTP AKLVQQILDS  42
E. coli (Ato D)     TKLMTLQDAT GFFRDGMTIM VGGFMGIGTP SRLVEALLES  42

Pig                 GVKELTAVSN NAGVDNFGLG LLLQSKQIKR MISSYVGENA 120
Human               GVKGLTAVSN NAGVDNFGLG LLLRSKQIKR MVSSYVGENA 120
C. eleg.            GQKGLTCVSN NAGVDNWGLG LLLQTRQIKK MISSYVGENA 117
C. acet. (Ctf A)    NIKNLTIISN DTCYPNTGIG KLISNNQVKK LIASYIGSNP  82
A. calc. (Cat I)    GRKNLTIVSN NAGNGDYGLA KLLKTGAVKK IICSFPADSY  85
P. puti.  (Pca I)   GARDLTIISN NAGNGEIGLA ALLMAGSVRK VVCSFPSDSY  85
A. tume. (Pca I)
B. subt. (Pca I)    GVKDLTVVSN NCGVDDWGLG LLLANKQIKK MIASYVGENK  82
M. tube. (Pca I?)   GVTDLETVSN NCGIDGVGLG LLLQHKRIRR TVSSYVGENK  82
H. infl. (Ato D)    GVKDLTLIGN DTAFIDTGVG PLIVNNRVKR LITSHIGTNP  82
E. coli (Ato D)     GVRDLTLIAN DTAFVDTGIG PLIVNGRVRK VIASHIGTNP  82
```

Pig	EFERQYLAGE	LEVELTPQGT	LAERIRAGGA	GVPAFYTSTG	160
Human	EFERQYLSGE	LEVELTPQGT	LAERIRAGGA	GVPAFYTPTG	160
C. eleg.	EFARQYLSGE	LEVEFTPQGT	LAERIRAGGA	GVPAFYTPTG	157
C. acet. (CtfA)	DTGKKLFNNE	LEVELSPQGT	LVERIRAGGS	GLGGVLTKTG	122
A. calc. (Cat I)	VFDELYRAGK	IELEIVPQGN	LACRIQAAGM	GLGPIYTPTG	125
P. puti. (Pca I)	VFDELYRAGK	IELEVVPQGN	LAERIAAAGS	GIGAFFSPTG	125
A. tume. (Pca I)		IELELVPQGT	LAQRIRAGGA	GIPAFYTPTG	125
B. subt. (Pca I)	IFERQFLSGE	LEVELVPQGT	LAERIRAGGA	GIPGFYTATG	122
M. tube. (Pca I?)	EFARQFLAGE	LEVELTPQGT	LAERLRAGGM	GIPAFYTPAG	122
H. infl. (Ato D)	ETGKKMIAGE	IDVELVPQGT	LAERIRAGGA	GLGGILTPTG	122
E. coli (Ato D)	ETGRRMISGE	MDVVLVPQGT	LIEQIRCGGA	GLGGFLTPTG	122
Pig	YGTLVQEGGS	PIKYNKDGSI	AIASKPREVR	EFNGQHFILE	200
Human	YGTLVQEGGS	PIKYNKDGSV	AIASKPREVR	EFNGQHFILE	200
C. eleg.	YGTQIQEGGA	PIKYSKKGKI	EVASKAKETR	QFNGINYVME	199
C. acet. (CtfA)	LGTLIEKG--	----------	------KKKI	SINGTEYLLE	144
A. calc. (Cat I)	FGTLLAEG--	----------	------KPTL	NFDGKDYVLE	147
P. puti. (Pca I)	YGTLLAEG--	----------	------KETR	EIDGRMYVLE	147
A. tume. (Pca I)	FGTELANG--	----------	------KVIA	EF	139
B. subt. (Pca I)	VGTSIAEG--	----------	------KEHK	TFGGRTYVLE	144
M. tube. (Pca I?)	VGTQVADGGL	PWRYDASGGV	AVVSPAKETR	EFDGVTYVLE	162
H. infl. (Ato D)	VGTVVEEG--	----------	------KQKI	QIDGREYLLE	144
E. coli (Ato D)	VGTVVEEG--	----------	------KQTL	TLDGKTWLLE	144
Pig	EAIRGDFALV	KAWKADQAGN	VTFRKSARNF	NLPMCKAAET	240
Human	EAITGDFALV	KAWKADRAGN	VIFRKSARNF	NLPMCKAAET	240
C. eleg.	EAIWGDFALI	KAWRADTLGN	IQFRHAAGNF	NNPMCKASKC	239
C. acet. (CtfA)	LPLTADVALI	KGSIVDEAGN	TFYKGTTKNF	NPYMAMAAKT	184
A. calc. (Cat I)	NPIKADFALI	KAYKGDRWGN	LVYRKSARNF	GPIMAMAANV	187
P. puti. (Pca I)	MPLHADFALI	KAHKGDRWGN	LTYRKAARNF	GPIMAMAAKT	187
A. tume. (Pca I)					
B. subt. (Pca I)	RGITGDVAIV	KAWKADTMGN	LIFRKTARNF	NPIAAMAGKI	184
M. tube. (Pca I?)	RGIRTDFALV	HAWQGDRHGN	LMYRHAAANF	NPECASAGRI	202
H. infl. (Ato D)	LPLKADIAII	HAQKGDMNGN	LAYELSARNF	NPLVALAAKT	184
E. coli (Ato D)	RPLRADLALI	RAHRCDTLGN	LTYQLSARNF	NPLIALAADI	184

Pig	TVVEVEEIVD	IGSFAPEDIH	IPKIYVHRLV	KGEKYEKRIE	280
Human	TVVEVEEIVD	IGAFAPEDIH	IPQIYVHRLI	KGEKYEKRIE	280
C. eleg.	TIVEVEEIVE	PGVIAPNDVH	IPSIYCHRLV	LGKNYKKPIE	279
C. acet. (CtfA)	VIVEAENLVS	CEKLEKEKAM	TPGVLINYIV	KEPA	218
A. calc. (Cat I)	TIAQVSEVVA	LGELDPENVV	TPGIFVQHVV	PVQSTPASAA	227
P. puti. (Pca I)	AIAQVDQVVE	LGELDPEHII	TPGIFVQRVV	AVSGAAASSI	227
A. tume. (Pca I)					
B. subt. (Pca I)	TIAEAEEIVE	AGELDPDHIH	TPGIYVQHVV	LGASQEKRIE	224
M. tube. (Pca I?)	TIAEVEHLVE	PGEIDPATVH			222
H. infl. (Ato D)	VIAQVDNLLE	VGQLPPDEVI	TPAALIDYIV	CSE	217
E. coli (Ato D)	TLVEPDELVE	TGELQPDHIV	TPGAVIDHII	VSQESK	220

Pig	RLSVRKEEDV	KTRSGKLGDN	VRERIIK**R**AA	LEFED**G**MYA**N**	320
Human	RLSIRKEGDG	EAKSAKPGDD	VRERIIK**R**AA	LEFED**G**MYA**N**	320
C. eleg.	RPMFAHEGPI	KPSTSAAGKS	-REIIAA**R**AA	LEFTD**G**MYA**N**	318
C. acet. (CtfB)		MINDKNL	AKEIIAK**R**VA	RELKN**G**QLV**N**	27
A. calc. (Cat I/J)	P	MSYHKL	TRDQIAQ**R**VA	QDIPE**G**SYV**N**	26
P. puti. (Pca I/J)	AKAI	MTITKKL	SRTEMAQ**R**VA	ADIQE**G**AYV**N**	27
A. tume. (Pca J)					
B. subt. (Pca I/J)	KRTVQQASGK	GEAK MKE	ARKRMVK**R**AV	QEIKD**G**MNV**N**	23
M. tube. (Pca J?)			SRDEMAA**R**VA	AEFED**G**QYV**N**	26
H. infl. (Ato A)		MN	AKELIAR**R**IA	MELHD**G**DIV**N**	22
E. coli. (Ato A)		MD	AKQRIAR**R**VA	QELRD**G**DIV**N**	22

Pig	**LG**IGI**P**LLAS	NFISPNMTVH	LQS**ENG**ILGL	GPYPLQNEVD	360
Human	**LG**IGI**P**LLAS	NFISPNITVH	LQS**ENG**VLGL	GPYPRQHEAD	360
C. eleg.	**LG**IGI**P**TLAP	NYIPNGFTVH	LQS**ENG**IIGV	GPYPRKGTED	358
C. acet. (CtfB)	**LG**VGL**P**TMVA	DYIPKNFKIT	FQS**ENG**IVGM	GASPKINEAD	67
A. calc. (Cat J)	**LG**IGL**P**TKIA	SYLPADKDVF	LHS**ENG**LLAF	GPPPAAGEED	66
P. puti. (Pca J)	**LG**IGA**P**TLVA	NYL-GDKEVF	LHS**ENG**LLGM	GPSPAPGEED	66
A. tume. (Pca J)			HT**ENG**ILNF	GEAPPEGEED	66
B. subt. (Pca J)	**LG**IGM**P**TLVA	NEIPDGVHVM	LQS**ENG**LLGI	GPYPLEGTED	63
M. tube. (Pca J?)	**LG**IGM**P**TLIP	NHIPDGVHVV	LHS**ENG**ILGV	GPYPRREDVD	66
H. infl. (Ato A)	**LG**IGL**P**TQVV	NYLPDNVNIT	LQS**ENG**FLGL	TAFDPENANS	62
E. coli. (Ato A)	**LG**IGL**P**TMVA	NYLPEGIHIT	LQS**ENG**FLGL	GPVT--TAHP	60

Pig	ADLI**NAG**KET	VTVLPGASYF	SSDE**S**FAMI**R**	**G**GHVNLTM**LG**	400
Human	ADLI**NAG**KET	VTILPGASFF	SSDE**S**FAMI**R**	**G**GHVDLTM**LG**	400
C. eleg.	ADLI**NAG**KEP	ITLLKGASIV	GSDE**S**FAMI**R**	**G**SHMDITV**LG**	398
C. acet. (*Ctf B*)	KDVV**NAG**GDY	TTVLPDGTFF	DSSV**S**FSLI**R**	**G**GHVDVTV**LG**	107
A. calc. (*Cat J*)	PELI**NAG**KEY	VTMLEGGCFF	HHGD**S**FAMM**R**	**G**GHLDICV**LG**	106
P. puti. (*Pca J*)	DDLI**NAG**KQH	VTLLTGGAFF	HHAD**S**FSMM**R**	**G**GHLDIAV**LG**	106
A. tume. (*Pca J*)	WNLI**NAG**KKA	VTLKPGAAFF	HHAD**S**FAM		94
B. subt. (*Pca J*)	ADLI**NAG**KET	ITEVTGASYF	DSAE**S**FAMI**R**	**G**GHIDLAI**LG**	103
M. tube. (*Pca J?*)	ADLI**NAG**KET	VTTLPGAAFF	SSST**S**FGII**R**	**G**GHLDVAV**LG**	106
H. infl. (*Ato A*)	-NLV**NAG**GQP	CGIKKGGSTF	DSAF**S**FALI**R**	**G**GHVDACV**LG**	101
E. coli. (*Ato A*)	-DLV**NAG**GQP	CGVLPGAAMF	DSAM**S**FALI**R**	**G**GHIDACV**LG**	99

Pig	AMQVSKYGDL	**ANW**MIPGKLV	KGM**GGAMD**LV	SSAKTKVVVT	440
Human	AMQVSKYGDL	**ANW**MIPGKMV	KGM**GGAMD**LV	SSAKTKVVVT	440
C. eleg.	ALQCSQFGDL	**ANW**MIPGKLV	KGM**GGAMD**LV	SAPGARVIVV	438
C. acet. (*Ctf B*)	ALQVDEKGNI	**ANW**IVPGKML	SGM**GGAMD**LV	NGAK-KVIIA	146
A. calc. (*Cat J*)	AFQIAANGDL	**ANW**HTGAPAI	PSV**GGAMD**LA	VGAK-KVFVT	146
P. puti. (*Pca J*)	AFQVSVKGDL	**ANW**HTGAESI	PAV**GGAMD**LA	TGAR-QVFVM	146
A. tume. (*Pca J*)					
B. subt. (*Pca J*)	GMEVSEQGDL	**ANW**MIPGKMV	KGM**GGAMD**LV	NGAK-RIVVI	142
M. tube. (*Pca J?*)	AMQVSVTGDL	**ANW**MIPGKMV	KGM**GGAMD**LV	HGAR-KVIVM	145
H. infl. (*Ato A*)	GLEVDQEANL	**ANW**MVPGKMV	PGM**GGAMD**LV	TGAK-KVIIG	140
E. coli. (*Ato A*)	GLQVDEEANL	**ANW**VVPGKMV	PGM**GGAMD**LV	TGSR-KVIIA	138

Pig	**M**E**H**SAKGNAH	**K**IMEKCTLPL	**T**GKQCVNRII	**T**EKAVFDVDR	480
Human	**M**E**H**SAKGNAH	**K**IMEKCTLPL	**T**GKQCVNRII	**T**EKAVFDVDK	480
C. eleg.	**M**E**H**VSKNGEP	**K**ILEHCELPL	**T**GKGVISRII	**T**DMAVFDVDT	478
C. acet. (*Ctf B*)	**M**R**H**TNKGQP-	**K**ILKKCTLPL	**T**AKSQANLIV	**T**ELGVIEVI-	184
A. calc. (*Cat J*)	TD**H**VTKKGEP	**K**IVAELTYPA	**T**GQKCVDRIY	**T**DLCIIDVVP	186
P. puti. (*Pca J*)	**M**D**H**LTKTGES	**K**LVPECTYPL	**T**GIACVSRIY	**T**DLAVLEVTP	186
A. tume. (*Pca J*)					
B. subt. (*Pca J*)	**M**E**H**VNKHGES	**K**VKKTCSLPL	**T**GQKVVHRLI	**T**DLAVFDFVN	182
M. tube. (*Pca J?*)	**M**E**H**TAKDGSP	**K**ILERCTLPL	**T**GVGCVDRIV	**T**ELAVIDVCA	185
H. infl. (*Ato A*)	**M**E**H**CAKSGSS	**K**ILKKCTLPL	**T**ASKKVAMVV	**T**ELAVFNFIE	180
E. coli. (*Ato A*)	**M**E**H**CAKDGSA	**K**ILRRCTMPL	**T**AQHAVHMLV	**T**ELAVFRFID	178

Pig	KKGLTLIELW	EGLTVDDIKK	STGCDFAVSP	KLIPMQQVTT	520
Human	KKGLTLIELW	EGLTVDDVQK	STGCDFAVSP	KLMPMQQIAN	520
C. eleg.	KNGLTLIEVR	KDLTVDDIKK	LTACKFEISE	NLKPMGQAPL	518
C. acet. (Ctf B)	NDGLLLTEIN	KNTTIDEIRS	LTAADLLISN	ELRPMAV	221
A. calc. (Cat J)	-EGLKVIEKV	EGLSFEELQR	LTGATLIDAT	QG	217
P. puti. (Pca J)	-EGLKVVEIC	ADIDFDELQK	LSGVPLIK		213
A. tume. (Pca J)					
B. subt. (Pca J)	-GRMTLTELQ	DGVTIEEVYE	KTEADFAVSQ	SVLNS	216
M. tube. (Pca J?)	-DGLHLVQTA	PGVSVDEVVA	KTQPPL-VLR	DLATQ	218
H. infl. (Ato A)	-GRLVLKEHA	PHVDLETIKA	KTEADFIVAD	DFKEMQISQK	219
E. coli. (Ato A)	-GKMWLTEIA	DGCDLATVRA	KTEARFEVAA	DLNTQRGDL	216

Pig		
Human		
C. eleg.	NQG	521
C. acet. (Ctf B)		
A. calc. (Cat J)		
P. puti. (Pca J)		
A. tume. (Pca J)		
B. subt. (Pca J)		
M. tube. (Pca J?)		
H. infl. (Ato A)	GLEL	223
E. coli. (Ato A)		

Table 1-3: Molecular Properties of the Prokaryotic CoA Transferases

Part A: Enzymes homologous to porcine CoA transferase[a]

Substrate pair	Organism(s)	Quaternary structure	Subunit molecular weight(s)[b]	Comparison with amino acid sequence of porcine CoA transferase (% identical; % similar)	Reference(s)
succinyl-CoA; β-ketoadipate	*Pseudomonas putida*	$\alpha_2\beta_2$	$\alpha = 24\,234$ $\beta = 22\,420$	α: 42; 63 β: 42; 63	Yeh & Ornston, 1981 Parales & Harwood, 1992
	Acinetobacter calcoaceticus	$\alpha_2\beta_2$	$\alpha = 24\,073$ $\beta = 23\,296$	α: 41; 61 β: 42; 61	Yeh & Ornston, 1981 Kowalchuk et al., 1994 Shanley et al., 1994
	Bacillus subtilis	$[\alpha_2\beta_2]$[c]	$\alpha = 25\,399$ $\beta = 23\,331$	α: 57; 71 β: 57; 75	Swiss-Prot database[d]
acetoacetyl-CoA; acetate/butyrate	*Clostridium acetobutylicum*	$\alpha_2\beta_2$	$\alpha = 23\,640$ $\beta = 23\,623$	α: 37; 56 β: 47; 67	Wiesenborn et al., 1989 Fischer et al., 1993 Petersen et al., 1993
acetyl-CoA; acetoacetate	*Escherichia coli*	$\alpha_2\beta_2$	$\alpha = 23\,526$ $\beta = 22\,959$	α: 40; 65 β: 44; 65	Sramek & Frerman, 1975a Swiss-Prot database[d]
	Haemophilus influenzae	$[\alpha_2\beta_2]$[c]	$\alpha = 23\,090$ $\beta = 23\,749$	α: 36; 61 β: 44; 62	Swiss-Prot database[d]
(unknown)	*Mycobacterium tuberculosis*	$[\alpha_2\beta_2]$[c]	$\alpha = 26\,300$ $\beta = 22\,900$	α: 56, 71 β: 57, 70	Swiss-Prot database[d]

[a] Enzymes with amino acid sequences at least 35% identical and 55% similar to the porcine enzyme sequence are considered homologous. Homologous enzymes for which the full-length amino acid sequence is available are listed. The β-ketoadipate:succinyl-CoA transferase of *Agrobacterium tumefaciens* (Parke, 1995) is not included, since only a portion of its amino acid sequence is known (Figure 1-9).

[b] Molecular weights calculated from deduced amino acid sequences are from the Swiss-Prot database.

[c] Quaternary structures of enzymes not yet purified are inferred from homologous CoA transferases.

[d] The amino acid sequences of these enzymes are currently unpublished.

Table 1-3: Molecular Properties of the Prokaryotic CoA Transferases

Part B: Enzymes of weak or unknown homology to porcine CoA transferase[a]

Substrate pair	Organism(s)	Quaternary structure	Subunit molecular weight(s)[b]	Amino acid sequence available?	Reference(s)
butyryl-CoA; acetoacetate	*Clostridium SB4*	$\alpha_2\beta_2$	$\alpha \sim 2.3 \times 10^4$ $\beta \sim 2.5 \times 10^4$	No	Barker et al., 1978
acetyl-CoA; glutaconate	*Acidaminococcus fermentans*	$\alpha_4\beta_4$	$\alpha = 35\ 725$ $\beta = 29\ 168$	Yes	Buckel et al., 1981 Mack et al., 1994
acetyl-CoA; 4-hydroxybutyrate	*Clostridium aminobutyricum*	α_2	$\alpha \sim 5.4 \times 10^4$	No	Scherf & Buckel, 1991
	Clostridium kluyveri	α_n	$\alpha = 47\ 071$	Yes	Swiss-Prot database[c]
acetyl-CoA; 5-hydroxyvalerate	*Clostridium aminovalericum*	α_4	$\alpha \sim 4.7 \times 10^4$	No	Eikmanns & Buckel, 1990
acetyl-CoA; succinate	*Clostridium kluyveri*	α_n	$\alpha = 58\ 852$	Yes	Söhling & Gottschalk, 1996
formyl-CoA; oxalate/succinate	*Oxalobacter formigenes*	α	$\alpha \sim 4.4 \times 10^4$	Yes	Baetz & Allison, 1990
3-hydroxypropionyl-CoA; acrylate butyryl-CoA; acetate	*Peptostreptococcus elsdenii*	α_2 (or $\alpha_2\beta$)[d]	$\alpha \sim 6.4 \times 10^4$ ($\beta \sim 5.0 \times 10^4$)[d]	No	Tung & Wood, 1975 Schulman & Valentino, 1976

[a] Enzymes with amino acid sequences less than 35% identical or 55% similar to the porcine enzyme sequence are considered weakly homologous. "Unknown" homology refers to enzymes for which the amino acid sequence is unavailable.

[b] Molecular weights estimated by SDS-PAGE analysis (denoted by "~") are approximate. Molecular weights calculated from deduced amino acid sequences (denoted by "=") are from the Swiss-Prot database.

[c] The amino acid sequence of this enzyme is currently unpublished.

[d] Two alternative quaternary structures have been proposed for the short-chain acyl-CoA transferase of *P. elsdenii*.

Shanley et al., 1994), *Agrobacterium tumefaciens* (Parke, 1995), *Mycobacterium tuberculosis*, *Haemophilus influenzae*, *Bacillus subtilis*, and *Escherichia coli*.[6] The coding sequences for the α- and β-subunits of each of these enzymes are contained within an operon. Alignment of this operon with the cDNA inserts encoding the porcine, human, and nematode CoA transferases reveals substantial similarity in the resulting amino acid sequence (Figure 1-9). The prokaryotic α- and β-polypeptides align with the N- and C-domains of the eukaryotic monomer, respectively (Parales & Harwood, 1992; Kassovska-Bratinova et al., 1996). In general, the molecular weight of the α-subunit is slightly greater than that of the β-subunit, just as the molecular weight of the N-domain exceeds that of the C-domain (Table 1-3A).[7] Finally, a gap in the coding sequence of the prokaryotic operon (Figure 1-9) exists in a region that corresponds to the hinge segment of the mammalian enzyme (Parales & Harwood, 1992; Kassovska-Bratinova et al., 1996). These observations suggest that the cDNA encoding the eukaryotic CoA transferase monomer may be the product of a fusion between two ancestral genes (Parales & Harwood, 1992).

Genes encoding prokaryotic CoA transferases with little amino acid sequence similarity to the eukaryotic enzymes have also been isolated. The CoA transferases encoded by these genes are not heterotetrameric (Table 1-3B). For example, the 4-hydroxybutyrate CoA transferase of *Clostridium aminobutyricum* (Scherf & Buckel, 1991) and the succinyl-CoA:CoA transferase of *Clostridium kluyveri* (Söhling & Gottschalk, 1996) consist of a single type of subunit. The glutaconate CoA transferase of *Acidaminococcus fermentans*, which is assembled from two non-identical polypeptide chains, is an $\alpha_4\beta_4$ octamer rather than an $\alpha_2\beta_2$ dimer (Buckel et al., 1981; Mack et al., 1994).

In summary, the bacterial CoA transferases are extremely diverse. Based on current information, they can be divided into two families: (1) the $\alpha_2\beta_2$-type enzymes, similar in amino acid sequence to the eukaryotic CoA transferases; and (2) the enzymes which lack both an $\alpha_2\beta_2$-fold and significant amino acid sequence similarity to the eukaryotic CoA transferases. Based on this classification, it is tempting to speculate that prokaryotic CoA transferases which lack an $\alpha_2\beta_2$-fold are less closely related to the eukaryotic enzymes than the $\alpha_2\beta_2$-type enzymes. However, a precise delineation of the evolutionary relationships between the CoA transferases will require the purification of additional enzymes and the isolation of their corresponding genes.

Part C: The Enzymology of Porcine CoA Transferase

The catalytic properties of the CoA transferases have been studied extensively over the past four decades. As a result, our current knowledge of the mechanism of rate acceleration by these enzymes is extremely sophisticated. This level of understanding has been achieved primarily by work on the CoA transferase of pig heart, carried out by Jencks and his coworkers. Their contributions are reviewed below, with reference (where appropriate) to parallel investigations of related CoA transferases.

Substrate specificity of succinyl-CoA:3-keto-acid CoA transferase

Acetoacetate and succinate are the preferred carboxylate substrates of succinyl-CoA:3-keto-acid CoA transferase from pig heart. However, other β-keto acids such as malonic semialdehyde, β-ketovalerate, and β-ketocaproate, and the dicarboxylic acid malonate, are also significantly reactive (Stern et al., 1956; Menon et al., 1960). Thus, some variation in the chain-length of the carboxylate substrate is accomodated at the active site. Given that the *s-cis* unsaturated dicarboxylic acid maleate is a much better substrate than its *s-trans* isomer fumarate, succinate most likely assumes an *s-cis* conformation upon binding (White & Jencks, 1976a). In addition, β-keto acids with α-methyl substituents react poorly compared to their unbranched equivalents. In contrast, branched dicarboxylic acids are reasonable substrates, presumably because they bind with their substituents oriented in the β-position relative to the reactive carboxylate moiety (White & Jencks, 1976a). From these observations, it can be concluded that: (1) branched α-keto acids and long-chain dicarboxylic acids bind poorly due to steric hindrance at the active site; and (2) short-chain acids are poor substrates because they lack groups which normally participate in key noncovalent interactions with the enzyme.

Succinyl-CoA:3-ketoacid CoA transferase is also very specific with respect to the molecular structure of the acyl-CoA substrates, as demonstrated by the fact that acyl thiolesters consisting of truncated analogs of CoA (Figure 1-10) react very poorly. For example, the enzyme is 10^6 times less active with acetoacetyl-pantetheine than with acetoacetyl-CoA in the presence of succinate (Fierke & Jencks, 1986). Half-reactions are undetectable between the enzyme and acyl thiolesters consisting of even shorter analogs of CoA, including methyl mercaptopropionate (MMP), N-acetylcysteamine (NAC), and N-acetylaletheine (NAA) (White & Jencks, 1976a; Moore & Jencks, 1982c; Whitty et al., 1995). Thus, binding of the nonreacting portion of CoA is essential for the CoA transferase reaction (see below).

The prokaryotic CoA transferases also display well-defined substrate specificities. For example, the short-chain fatty acid CoA transferase of *Peptostreptococcus elsdenii* reacts preferentially with saturated or α-hydroxy "C_2-C_6" carboxylic acids, or with β-hydroxy "C_3-C_4" carboxylic acids (Tung & Wood, 1975). In addition, the glutaconate CoA transferase of *Acidaminococcus fermentans* exchanges CoA most efficiently between acetate or propionate, and glutaconate, glutarate, or (*R*)-2-hydroxyglutarate (Buckel et al., 1981). The acetyl-pantetheine or acetyl-4'-phosphopantetheine is not a substrate for the short-chain fatty acid CoA transferase or glutaconate CoA transferase, respectively (Tung & Wood, 1975; Buckel et al., 1981).

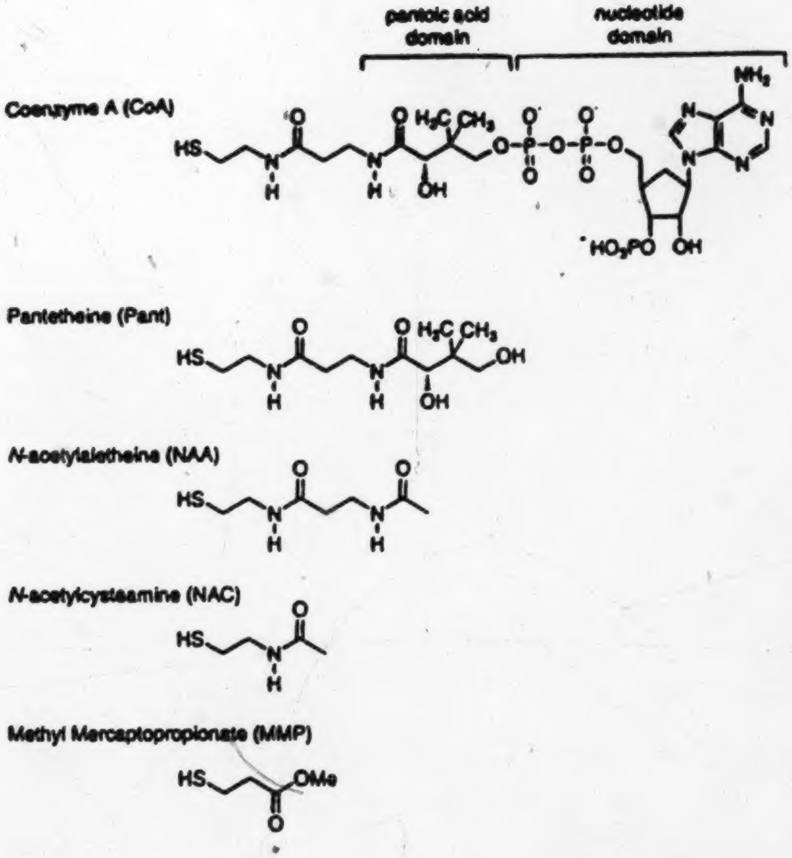
pantoic acid domain
nucleotide domain
Coenzyme A (CoA)
Pantetheine (Pant)
N-acetylaletheine (NAA)
N-acetylcysteamine (NAC)
Methyl Mercaptopropionate (MMP)

Figure 1-10: Schematic representation of coenzyme A and of truncated analogues of CoA discussed in the text. (Reprinted from [Whitty et al., 1995], with the permission of the American Chemical Society).

Kinetic mechanism of succinyl-CoA:3-keto-acid CoA transferase

Succinyl-CoA:3-keto-acid CoA transferase catalyzes the reversible exchange of CoA between carboxylate substrates with kinetics referred to as "ping-pong bi-bi" (Hersh & Jencks, 1967a). The complete enzymatic process can be thought of as two half-reactions. First, acyl-CoA reacts with the free enzyme, yielding an enzyme-CoA intermediate (ECoA) and a free carboxylate ion that diffuses from the active site. Second, ECoA reacts with an acyl group to yield free enzyme and a new acyl-CoA product. This kinetic scheme has been shown to be valid according to numerous criteria.

First, reciprocal plots of the initial velocity of the enzymatic reaction as a function of the concentration of acyl-CoA thiolester result in parallel lines, each of which corresponds to a different concentration of carboxylate substrate (Hersh & Jencks, 1967a; White & Jencks, 1976a; Moore & Jencks, 1982c). These kinetic relationships are equally evident for the transfer of CoA from succinyl-CoA to acetoacetate and from acetoacetyl-CoA to succinate. Lineweaver-Burk plots of this type are characteristic of "ping-pong" kinetics, as they reflect the inability of a saturating amount of one substrate to increase the rate of the overall enzymatic reaction past a limiting value, in the presence of a less than saturating amount of the second substrate (Hersh & Jencks, 1967a). The kinetic parameters derived from these plots are listed in Table 1-4.

Second, each carboxylate product inhibits the CoA transferase reaction leading to its formation. This product inhibition is competitive between the carboxylate product and the carboxylate substrate, and non-competitive between the carboxylate product and the acyl-CoA substrate (Hersh & Jencks, 1967a). For example, in the direction of acetoacetyl-CoA formation, succinate inhibits competitively with respect to acetoacetate and non-competitively with respect to succinyl-CoA:

$$\text{succinyl-CoA} + \text{acetoacetate} \rightleftharpoons \text{succinate} + \text{acetoacetyl-CoA}$$

Table 1-4: Kinetic Constants of Succinyl-CoA:3-Ketoacid CoA Transferase of Porcine Heart[a]

Kinetic parameter	Data of Hersh & Jencks (1967a)	Data of White & Jencks (1976a)	Data of Moore & Jencks (1982c)
$k_{\text{cat[forward]}}$ ($\times 10^4$ min^{-1})[b]	13.2[c]	7.9[c]	7.5
acetoacetyl-CoA			
K_M (mM)	0.93	0.19	0.20
K_I (mM)	0.17	0.033	-
succinate			
K_M (mM)	36	23	20
K_I (mM)	1.0	0.54	-
$k_{\text{cat[reverse]}}$ ($\times 10^3$ min^{-1})[d]	4.1[c]	5.7[c]	5.9
succinyl-CoA			
K_M (mM)	4.2	4.2	6.5
K_I (mM)	1.9	2.4	-
acetoacetate			
K_M (mM)	0.20	0.16	0.10
K_I (mM)	0.78	0.29	-

[a] Based on the molarity of active sites, assuming $M_r = 4.6 \times 10^4$ and $\varepsilon_{280} = 0.962$ mL/mg (White & Jencks, 1976a,b).

[b] Forward direction: [acetoacetyl-CoA + succinate $\rightarrow$ succinyl-CoA + acetoacetate].

[c] Corrected by a factor of 3.15, to account for the lower specific enzyme activity of this preparation relative to that of Moore & Jencks (1982c).

[d] Reverse direction: [succinyl-CoA + acetoacetate $\rightarrow$ acetoacetyl-CoA + succinate].

Product inhibition by succinate can be interpreted as a depletion of ECoA available for reaction with acetoacetate, and is alleviated by increasing the concentration of acetoacetate but not of succinyl-CoA (Hersh & Jencks, 1967a). This effect, also observed for the reaction in the reverse direction, is consistent with the "ping-pong" kinetic mechanism proposed for the overall enzymatic process. The inhibition constants determined for each substrate are listed in Table 1-4.

Third, the kinetics of acetoacetate and acetoacetyl-CoA exchange are consistent with the formation of ECoA as part of a "ping-pong" kinetic mechanism. The maximal rate of exchange between radioactively labeled acetoacetate and acetoacyl-CoA in the absence of succinate is equal to the maximal rate of enzyme turnover in the presence of succinate (Hersh & Jencks, 1967a). Furthermore, at saturating levels of succinate, the degree of product inhibition by acetoacetate is equal to the amount of exchange of acetoacetate into acetoacetyl-CoA. At low levels of succinate, the rate of formation of ECoA is no longer rate-determining. Under these conditions, the reaction between acetoacetate and ECoA has very little effect on the rate-limiting formation of succinyl-CoA, and the extent of product inhibition by acetoacetate is less than the amount of exchange (Hersh & Jencks, 1967a). These results provide strong evidence for a "ping-pong" kinetic mechanism, since they prove that ECoA exists and is kinetically competent with respect to the overall CoA transferase reaction (Jencks, 1973).

Fourth, isotopically labeled oxygen (^{18}O) is transferred from succinate to the enzyme in the presence of succinyl-CoA or acetoacetyl-CoA (Benson & Boyer, 1969). The subsequent transfer of labeled oxygen from the enzyme to acetoacetate occurs during a second turnover (Jencks, 1973). Assuming that the sidechain of an acidic residue plays the role of nucleophile at the active site, these events can be rationalized as follows (Jencks, 1973):

1st turnover:

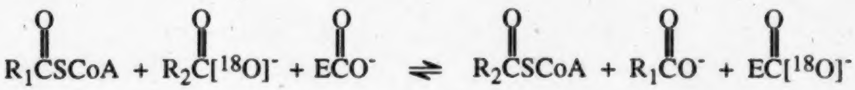

$$R_1\overset{O}{\overset{\|}{C}}SCoA + R_2\overset{O}{\overset{\|}{C}}[^{18}O]^- + E\overset{O}{\overset{\|}{C}}O^- \rightleftharpoons R_2\overset{O}{\overset{\|}{C}}SCoA + R_1\overset{O}{\overset{\|}{C}}O^- + E\overset{O}{\overset{\|}{C}}[^{18}O]^-$$

(a) $R_1COSCoA + ECOO^- \rightleftharpoons ECOSCoA + R_1COO^-$

(b) $ECOSCoA + R_2COO[^{18}O]^- \rightleftharpoons R_2COSCoA + ECO[^{18}O]^-$

2nd turnover:

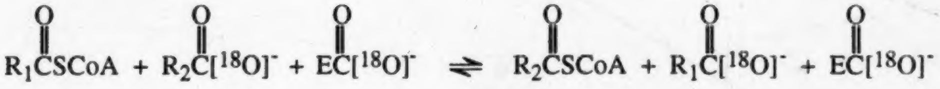

$$R_1\overset{O}{\overset{\|}{C}}SCoA + R_2\overset{O}{\overset{\|}{C}}[^{18}O]^- + E\overset{O}{\overset{\|}{C}}[^{18}O]^- \rightleftharpoons R_2\overset{O}{\overset{\|}{C}}SCoA + R_1\overset{O}{\overset{\|}{C}}[^{18}O]^- + E\overset{O}{\overset{\|}{C}}[^{18}O]^-$$

(a) $R_1COSCoA + ECO[^{18}O]^- \rightleftharpoons ECOSCoA + R_1CO[^{18}O]^-$

(b) $ECOSCoA + R_2CO[^{18}O]^- \rightleftharpoons R_2COSCoA + ECO[^{18}O]^-$

where

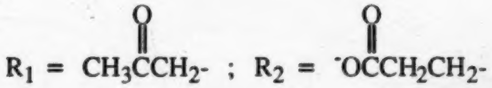

$R_1 = CH_3\overset{O}{\overset{\|}{C}}CH_2\text{-}$; $R_2 = {}^-O\overset{O}{\overset{\|}{C}}CH_2CH_2\text{-}$

Thus, the transfer of labeled oxygen can only be explained in terms of the participation of ECoA, which is consistent with the "ping-pong" kinetic mechanism proposed for the CoA transferase reaction.

Fifth, incubation of the enzyme with succinyl-CoA or acetoacetyl-CoA, but not CoA alone, leads to the formation of ECoA (Hersh & Jencks, 1967b). This intermediate can be isolated by gel filtration, is unstable at high pH, and consists of CoA rather than acyl-CoA. Furthermore, reduction of the ECoA thiolester with tritiated borohydride leads to the incorporation of radioactive label in the enzyme. Given that thiolesters are sensitive to base and susceptible to reduction by borohydride (Hersh & Jencks, 1967b), these results suggest that CoA is covalently linked to an acidic residue in ECoA. Finally, this intermediate reacts with succinate to yield succinyl-CoA, and is thus catalytically competent. In short, the properties of the complex formed upon incubation of the enzyme with either acyl-CoA substrate are identical to those predicted for the intermediate of a "ping-pong" kinetic mechanism.

From these results, it is clear that succinyl-CoA:3-ketoacid CoA transferase catalyzes the transfer of CoA with "ping-pong" kinetics, involving two half-reactions and the formation of ECoA. The energy of the thiolester bond of this intermediate is equivalent to that of succinyl-CoA or acetoacetyl-CoA. Importantly, each half-reaction requires the immobilization of only one reacting group, since the other is already fixed at the active site by a covalent linkage to the enzyme. Thus, the formation of ECoA may provide an entropic advantage to the overall reaction, compared to a mechanism in which two substrates must be bound simultaneously. This kinetic behavior has also been confirmed for the CoA transferases of other mammals (Blair, 1969; Russell & Patel, 1982) and of prokaryotes (Sramek & Frerman, 1975b; Tung & Wood, 1975; Schulman & Valentino, 1976; Barker et al., 1978; Buckel et al., 1981; Wiesenborn et al., 1989; Eikmanns & Buckel, 1990).

Chemical mechanism of CoA transferase

Although it has been established that the overall reaction catalyzed by CoA transferase proceeds with ping-pong kinetics, the chemical details underlying this process remain uncertain. Each of the two half-reactions can proceed in a stepwise or concerted manner (Jencks, 1973; White & Jencks, 1976a). The stepwise reaction (Figure 1-11A) involves a nucleophilic attack by a carboxylate oxygen, which displaces CoA from the carbonyl moiety of the thiolester to generate an anhydride intermediate. A subsequent nucleophilic attack by CoA on the opposite carbonyl group of this anhydride yields a new

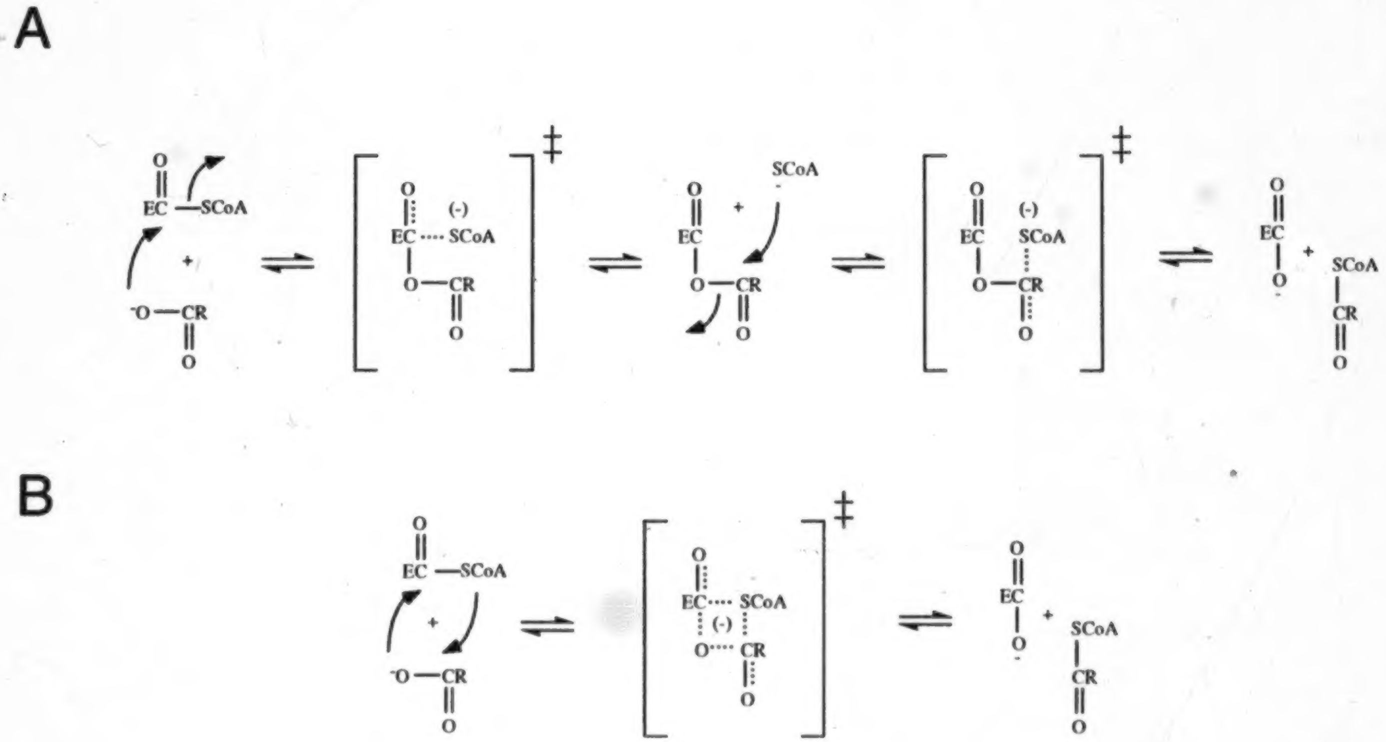

Figure 1-11: Chemical mechanisms proposed for the half-reaction between ECoA and the carboxylate substrate. (A) Stepwise pathway, involving an anhydride intermediate (center) and two possible transition states (labeled "‡"). (B) Concerted pathway, involving a four-center transition state in which all of the reacting bonds are formed and broken simultaneously. (Adapted from [White & Jencks, 1976a]).

carboxylate ion and a new thiolester as products. This mechanism is thermodynamically unfavorable in aqueous solution, given that acetic anhydride is less stable than acetyl-CoA by 14 kcal/mol (Moore & Jencks, 1982a,b). Furthermore, anhydride formation proceeds very slowly in aqueous solution, and would require a 10^6-fold rate acceleration to account for the observed rate of formation of ECoA (Fedor & Bruice, 1965; White & Jencks, 1976a; Moore & Jencks, 1982a). Thus, if the CoA transferase half-reaction occurs by stepwise chemistry, then significant thermodynamic and kinetic difficulties inherent with anhydride formation must be overcome. Nevertheless, such barriers are surmountable. For example, succinate and amino acids are converted to mixed anhydrides by SCS and the aminoacyl-tRNA synthetases, respectively (reviewed in [Bridger, 1974], and [Delarue, 1995]). The concerted pathway (Figure 1-11B) involves a four-center transition state rather than a high-energy intermediate, and is thus more thermodynamically acceptable than the stepwise reaction. Nevertheless, the concerted chemistry lacks an obvious driving force, and there are no convenient methods for proving or disproving its existence (White & Jencks, 1976a). A hypothetical four-center transition state has been proposed for several non-enzymatic reactions, including the intramolecular O-N and S-N acyl-transfer reactions of isoimides and *S*-benzoylisothioureas, respectively (Curtin & Miller, 1967; Pratt & Bruice, 1972). However, it is not known if these reactions proceed by concerted chemistry. Reactions of ylids, which also involve a four-center transition state, occur in a stepwise manner (Johnson & Wong, 1962).

At present, neither of the two chemical schemes proposed for the CoA transferase half-reaction has been established conclusively. Attempts to trap the proposed anhydride intermediate have been unsuccessful (Benson & Boyer, 1969), although this may merely reflect its extremely short lifetime. Furthermore, [^{3}H]CoA does not exchange into acyl-CoA substrates bound to the enzyme, as predicted for a stepwise chemical pathway (White & Jencks, 1976a). However, this result may simply indicate that the rate of nucleophilic attack by CoA on the anhydride intermediate exceeds the rate at which CoA is liberated from the active site. Finally, no evidence exists to support or contradict the concerted chemistry involving a four-center transition state.

Although the stepwise pathway has not been formally proven, results from several experiments provide indirect evidence for the formation of an anhydride intermediate. First, electron-donating substituents which increase the basicity of carboxylate substrates also enhance the reactivity of these substrates with ECoA. In quantitative terms, the Brønsted value, β_{nuc}, which relates the logarithm of k_{cat} or k_{cat}/K_M to the pK_a of the substrate, is equal to 1.0 (White & Jencks, 1976a). Thus, the change in the electrostatic environment incurred by the polar substituent as the enzymatic half-reaction proceeds to the transition state reflects that which occurs as the carboxylate ion loses its negative charge upon protonation (White & Jencks, 1976a). Any hypothetical transition state proposed for the CoA transferase half-reaction must account for this loss of a negative charge. The stepwise pathway may proceed through one of two transition states (Figure 1-11A), given that the possible rate-limiting steps are: (1) the initial release of CoA, or (2) the subsequent nucleophilic attack by CoA on the anhydride intermediate (White & Jencks, 1976a).[8] In each of these transition states, the anionic character of the carboxylate nucleophile is completely lost due to the formation of a covalent bond with the carbonyl carbon atom of ECoA (Figure 1-11A). In contrast, the four-center transition state, in which all bonds are formed and broken simultaneously, involves no net alteration of charge relative to the ground state (Figure 1-11B). Thus, the observed reactivity of substituted, carboxylate substrates with ECoA is consistent with the formation of an anhydride intermediate.

Second, the formation of mixed anhydrides from ECoA and hydroxamic acids also supports the stepwise pathway (Pickart & Jencks, 1979). Notably, the mixed anhydrides are similar to the "true" anhydride intermediate proposed for the CoA transferase half-reaction.

Formation of a mixed anhydride:

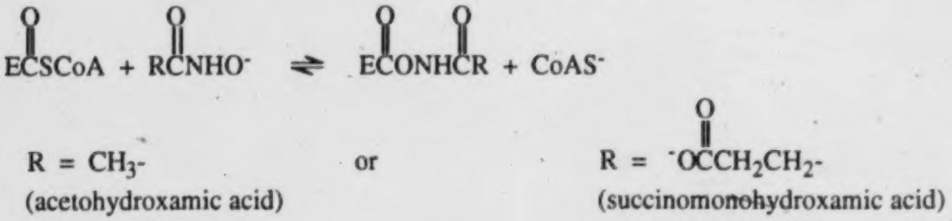

$$\mathrm{E\overset{O}{\overset{\|}{C}}SCoA + R\overset{O}{\overset{\|}{C}}NHO^- \rightleftharpoons E\overset{O}{\overset{\|}{C}}ONH\overset{O}{\overset{\|}{C}}R + CoAS^-}$$

$\mathrm{R = CH_3\text{-}}$ (acetohydroxamic acid) or $\mathrm{R = {}^-O\overset{O}{\overset{\|}{C}}CH_2CH_2\text{-}}$ (succinomonohydroxamic acid)

Formation of a "true" anhydride:

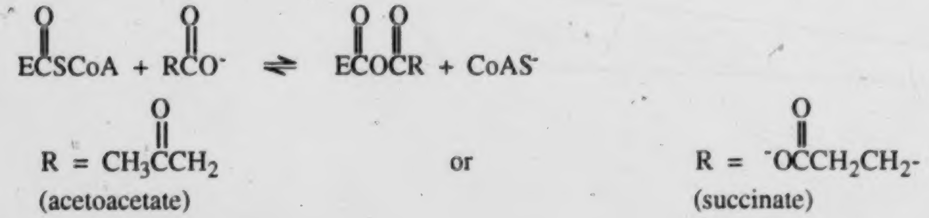

$$\mathrm{E\overset{O}{\overset{\|}{C}}SCoA + R\overset{O}{\overset{\|}{C}}O^- \rightleftharpoons E\overset{O}{\overset{\|}{C}}O\overset{O}{\overset{\|}{C}}R + CoAS^-}$$

$\mathrm{R = CH_3\overset{O}{\overset{\|}{C}}CH_2}$ (acetoacetate) or $\mathrm{R = {}^-O\overset{O}{\overset{\|}{C}}CH_2CH_2\text{-}}$ (succinate)

The mixed anhydride is much more resistant to nucleophilic attack by CoA than the "true" anhydride intermediate. This stability can be attributed in part to the poor electrophilicity of the carbonyl moiety provided by the hydroxamic acid. In addition, this carbonyl group is most likely displaced from its ideal position in the active site, due to the presence of the "intervening" nitrogen atom of the hydroxamic acid (Pickart & Jencks, 1979). The equilibrium constant for mixed anhydride formation from acetohydroxamic acid (AHA) and ECoA is nearly 100-fold greater than that for the nonenzymatic reaction between AHA and acetyl-CoA (Pickart & Jencks, 1979). Furthermore, the mixed anhydride produced from ECoA and succinomonohydroxamic acid (SHA) is even more stable than the enzyme-AHA intermediate, presumably because the succinate moiety of the enzyme-SHA mixed anhydride interacts more specifically with the enzyme (Pickart & Jencks, 1979). These results imply that the formation of a "true" anhydride intermediate at the active site of CoA transferase is favored thermodynamically compared to the equivalent reaction in free solution. The stabilization of this intermediate as part of a stepwise chemical mechanism could be crucial for catalysis (Pickart & Jencks, 1979).

Third, the results of studies of nonenzymatic reactions also provide evidence for the stepwise reaction. Specifically, it has been demonstrated that anhydride formation is accelerated by the release of a good leaving group and by intramolecular nucleophilic attack (Moore & Jencks, 1982a,b). For example, succinic anhydride is readily formed from succinyl-phosphate at lower pH (Figure 1-12A) due to the improved leaving potential conferred upon the phosphate group by protonation (Moore & Jencks, 1982a). Furthermore, the formation of succinic anhydride from *p*-nitrophenyl thiosuccinate occurs 10^5 times more rapidly than the rate of formation of acetic anhydride from *p*-nitrophenyl thioacetate in acetate buffer (Moore & Jencks, 1982b). This acceleration is due to the entropic advantage of the intramolecular reaction, which requires a loss of fewer degrees of freedom than the corresponding intermolecular reaction (Figure 1-12B). Each of these nonenzymatic processes involves the formation of an anhydride (Figure 1-12), and can therefore be considered a "model" for the CoA transferase half-reaction (Moore & Jencks, 1982a,b). It is reasonable to assume that anhydride formation at the active site of CoA transferase is accelerated by factors similar to those described above for the "model" reactions. For instance, the leaving ability of CoA may be improved by protonation or by an alteration of its effective pK_a. In addition, the enzyme may bind the reacting carboxylate and thiolester moieties tightly and in proximity, achieving the equivalent of an intramolecular reaction (Moore & Jencks, 1982b).

The acidic nucleophile of succinyl-CoA:3-ketoacid CoA transferase

As mentioned previously, the reactivity of the ECoA thiolester with nucleophilic agents such as hydroxide or borohydride is consistent with a covalent linkage between CoA and the sidechain of an acidic residue in the active site (Hersh & Jencks, 1967b).

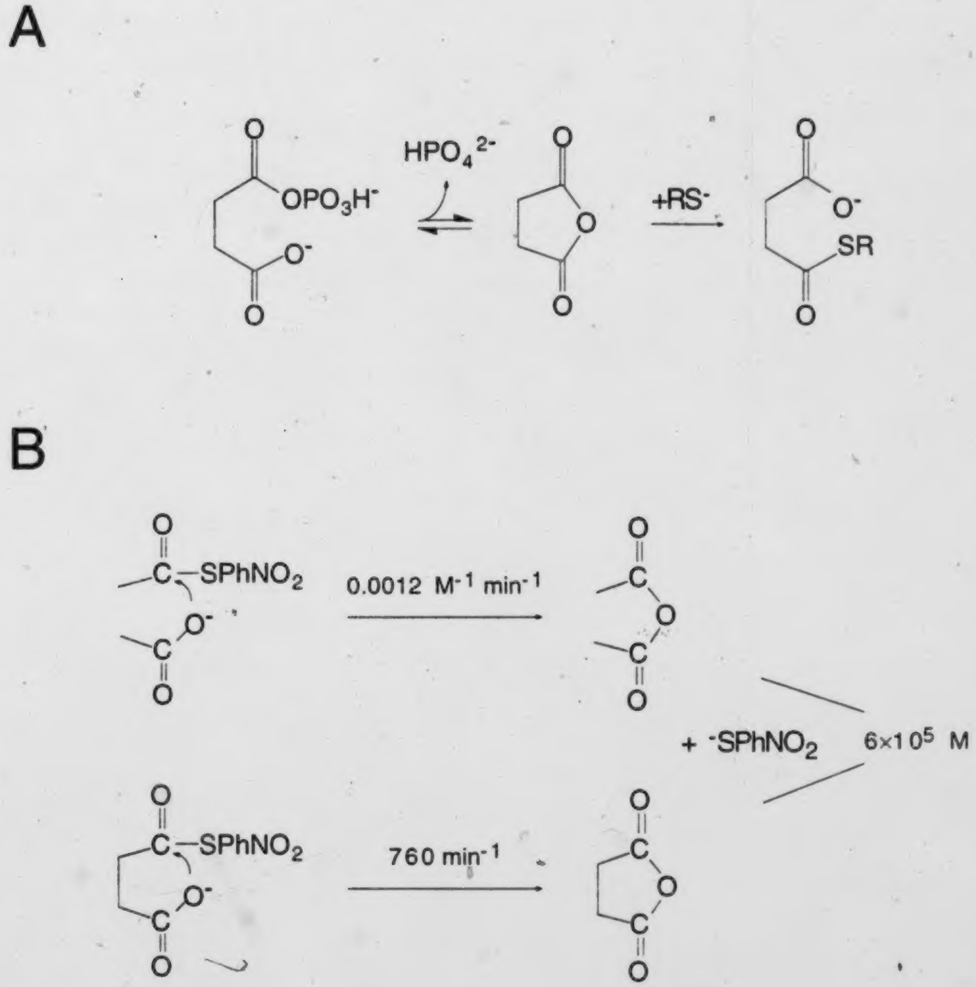
A
HPO$_4^{2-}$
OPO$_3$H$^-$
O$^-$
+RS$^-$
SR
B
SPhNO$_2$
0.0012 M^{-1} min^{-1}
760 min^{-1}
+ $^-$SPhNO$_2$
6×10^5 M

Figure 1-12: Evidence for a stepwise CoA transferase half-reaction from non-enzymatic models. (A) The reaction of succinyl-phosphate with a thiol anion involves the formation of succinic anhydride. (Adapted from [Moore & Jencks, 1982a]). (B) The formation of anhydride from *p*-nitrophenyl thiolesters. The intramolecular reaction (lower pathway) is accelerated by a factor of 6×10^5 compared to the intermolecular reaction (upper pathway). (Reproduced from [Jencks, 1987], with the permission of Cold Spring Harbor Laboratory Press).

This residue can be radioactively labeled by inactivating the enzyme with tritiated borohydride (Hersh & Jencks, 1967b; Solomon & Jencks, 1969). The major tritiated product released from the labeled enzyme by acid hydrolysis is α-amino-δ-hydroxyvaleric acid, the reduced form of glutamate (Solomon & Jencks, 1969). Tritiated homoserine, predicted if CoA were thiolesterified to an aspartate residue, is absent from the acid hydrolysate.

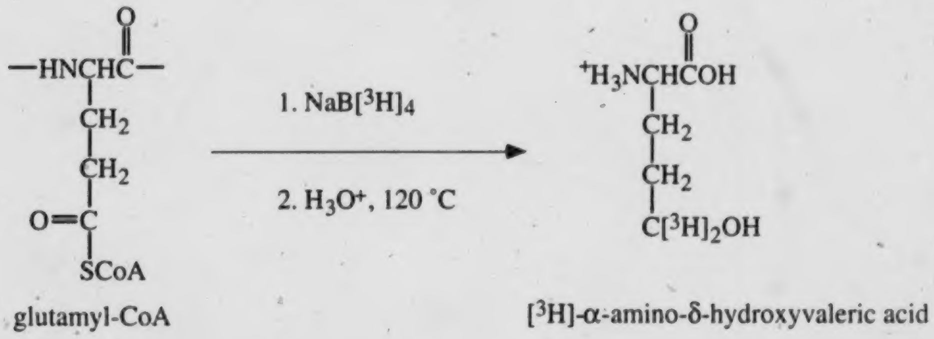
1. NaB[³H]₄
2. H₃O⁺, 120 °C
glutamyl-CoA
[³H]-α-amino-δ-hydroxyvaleric acid

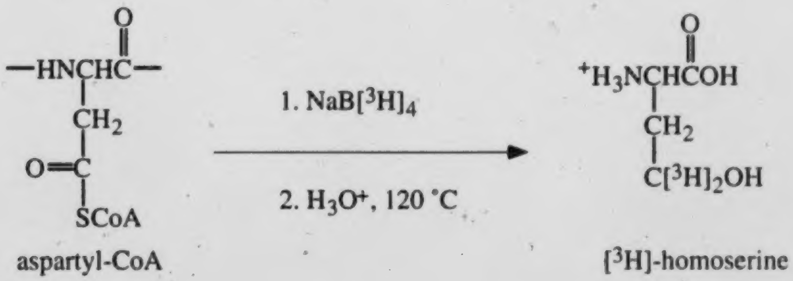
1. NaB[³H]₄
2. H₃O⁺, 120 °C
aspartyl-CoA
[³H]-homoserine

Thus, CoA is covalently linked to the γ-carboxyl group of a nucleophilic glutamate residue in ECoA (Solomon & Jencks, 1969). Similar experiments have identified a catalytic glutamate residue in the CoA transferases of *Escherichia coli* (Sramek & Frerman, 1975b) and *Acidaminococcus fermentans* (Mack et al., 1994).

The position of the nucleophilic glutamate residue in the polypeptide sequence of succinyl-CoA:3-ketoacid CoA transferase has been suggested by studies of a unique autolytic fragmentation reaction (Howard et al., 1986). This cleavage was first observed for plasma proteins containing a glutamate residue that is activated by an internal thiolester linkage (Howard et al., 1986). In CoA transferase, autolysis occurs at the active site of ECoA upon heating the enzyme solution to 70 °C (Howard et al., 1986). The mechanism proposed for the autolytic fragmentation (Figure 1-13) involves the cyclization of the activated glutamate residue to form an oxyproline derivative, followed by the hydrolysis of the peptide bond N-terminal to the glutamate residue (Khan & Erickson, 1984; Howard et al., 1986). From the size of the autolytic products, the catalytic glutamate residue of CoA transferase must be located approximately two-thirds of the distance from the N-terminus of the enzyme (Howard et al., 1986). Three glutamate residues, numbered 344, 358, and 369 based on the precursor form of the enzyme, are located in this vicinity of the CoA transferase primary structure (Figure 1-9). Of these three residues, only glutamate 344 is strictly conserved among all CoA transferases of known amino acid sequence (Figure 1-9).

A reactive cysteine residue in the active site of succinyl-CoA:3-ketoacid CoA transferase

The treatment of succinyl-CoA:3-ketoacid CoA transferase with 5, 5'-dithiobis(2-nitrobenzoic) acid (DTNB) or N-ethylmaleimide (NEM) results in the progressive loss of enzyme activity, due to the covalent attachment of a bulky group to the sidechain of a cysteine residue (White et al., 1976). Inactivation by DTNB occurs 100 times less rapidly for free CoA transferase than for ECoA. In turn, ECoA is inactivated with a second-order rate constant only 12 times less than that for the reaction of 2-mercaptoethanol (2ME) with DTNB. Furthermore, the rapid inactivation of ECoA occurs with a stoichiometry of 1.9 moles of DTNB per mole of CoA transferase homodimer. These results suggest that a

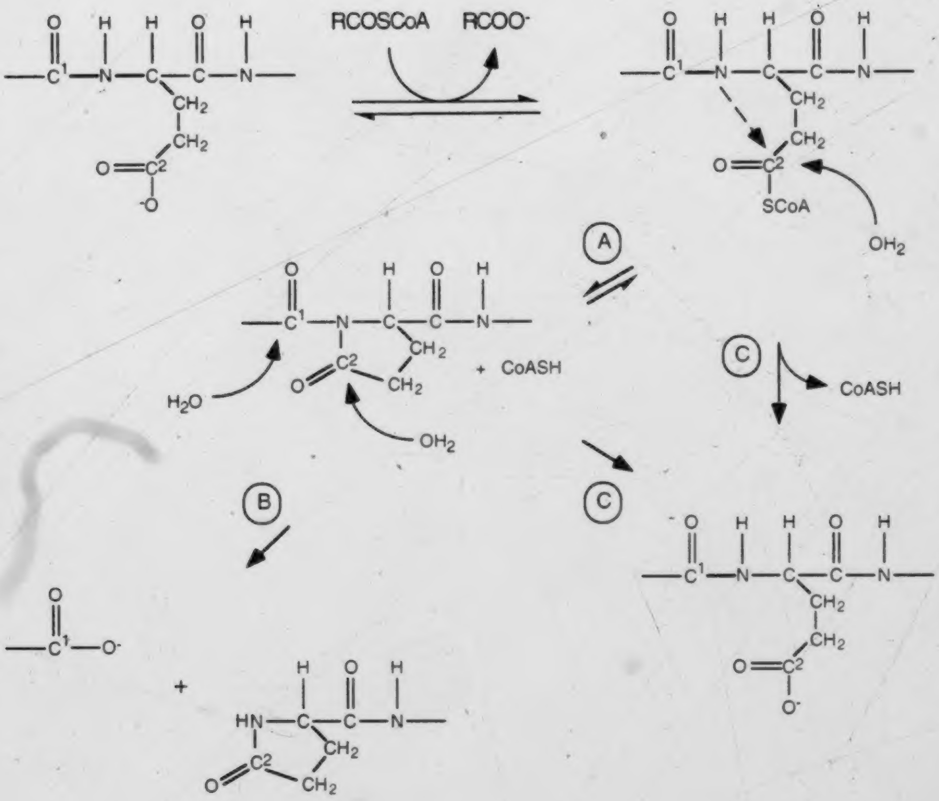

Figure 1-13: Mechanism proposed for the autolytic fragmentation of CoA transferase. (A) The main chain amide nitrogen of the catalytic glutamate residue carries out a nucleophilic attack on the ECoA thiolester linkage to form an oxyproline intermediate. (B) At 70 °C, hydrolysis at carbon 1 (C^1) generates an N-terminal fragment and a C-terminal fragment blocked at its N-terminus by a pyroglutamate moiety. (C) Competing hydrolysis side-reactions at the ECoA thiolester linkage or at carbon 2 (C^2) of the oxyproline intermediate lead to a decrease in the yield of autolysis. (Adapted from [Howard et al., 1986]).

single, reactive cysteine residue becomes more susceptible to modification by thiol reagents upon the formation of ECoA, which presumably exists in a more "open" conformation than the free enzyme (Figure 1-14A; White et al., 1976).

Importantly, a maximal rate of inactivation by DTNB is observed for samples of ECoA prepared by treating the enzyme with an equimolar amount of acyl-CoA substrate, relative to the number of active sites. In the presence of saturating amounts of the acyl-CoA and carboxylate substrates, the rate of inactivation of the enzyme is equal only to the rate observed for free CoA transferase (White et al., 1976). Under these conditions, the enzyme exists primarily as two rapidly exchanging Michaelis complexes:

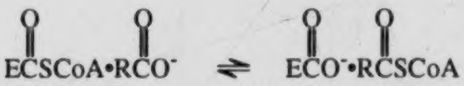

$$E\overset{O}{\overset{\|}{C}}SCoA\bullet R\overset{O}{\overset{\|}{C}}O^{-} \rightleftharpoons E\overset{O}{\overset{\|}{C}}O^{-}\bullet R\overset{O}{\overset{\|}{C}}SCoA$$

Within these complexes, the reactive cysteine residue is apparently masked and less reactive, which suggests that it is located near the substrate binding pocket (Figure 1-14A).

The loss of enzyme activity can be attributed either to the disruption of an essential catalytic function of the reactive cysteine residue or merely to steric hindrance at the active site. These possibilities are distinguishable by treating the enzyme with a thiol reagent which transfers a relatively small group to the reactive cysteine residue. The thiol reagent 2-nitro-5-(thiocyanato)benzoic acid (NTCB) modifies the cysteine residue by one of two mechanisms (Figure 1-14B): (1) disulfide bond formation with a thionitrobenzoate group, or (2) the transfer of a much smaller cyanide group (Kindman & Jencks, 1981). Although 70% of the initial enzyme population is inactivated following a lengthy incubation with NTCB, the remaining 30% is both functionally intact and resistant to further inactivation by thiol reagents (Kindman & Jencks, 1981). Presumably, the portion of the enzyme which is inactivated reacts with NTCB by the first mechanism, while the pool of enzyme which remains active is modified by the second pathway. Given that the

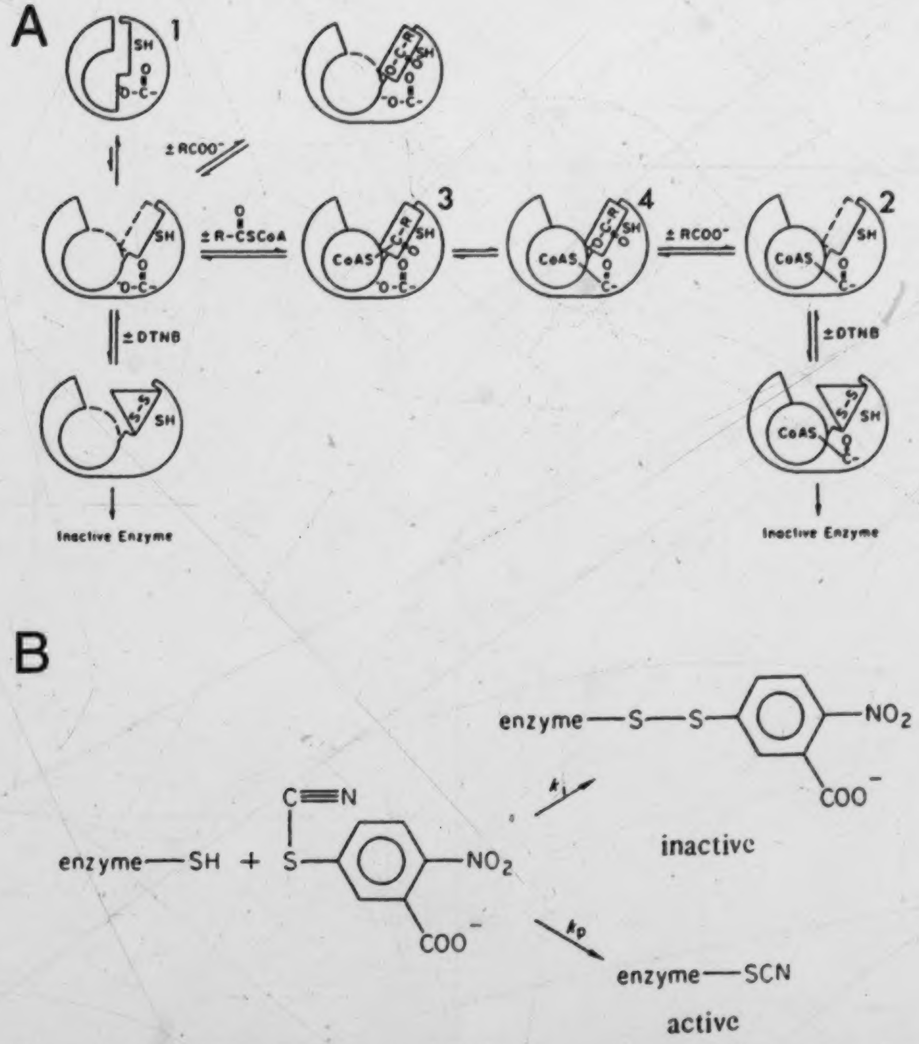
A
1
SH
O
-O-C-
± RCOO⁻
± R-CSCoA
3
4
2
CoAS
± DTNB
Inactive Enzyme
Inactive Enzyme
B
enzyme—S—S—
NO₂
COO⁻
inactive
C≡N
S
enzyme—SH +
k_i
k_p
enzyme—SCN
active

Figure 1-14: Modification of an essential cysteine residue in the active site of pig heart CoA transferase. (A) Model for the inactivation of the enzyme by DTNB. In the absence of the acyl-CoA substrate, the enzyme exists predominantly in a "closed" conformation (1), and the reactive cysteine residue is relatively resistant to modification by DTNB. In the presence of an equimolar amount of the acyl-CoA substrate the enzyme is converted to ECoA, which adopts an "open" conformation (2). Under these conditions, the essential cysteine residue reacts rapidly with DTNB. In the presence of saturating amounts of the acyl-CoA and carboxylate substrates the enzyme exists as rapidly exchanging Michaelis complexes (3 and 4), within which the reactive cysteine residue is protected from modification by DTNB. (Reprinted from [White et al., 1976], with the permission of the American Society for Biochemistry and Microbiology). (B) Two modes of reaction between the enzyme and NTCB, leading to the covalent attachment of a thionitrobenzoate group (top) or a cyanide moiety (bottom) to the essential cysteine residue. (Reprinted from [Kindman & Jencks, 1981], with the permission of the American Chemical Society).

activity of the enzyme is not altered by the covalent attachment of the cyanide group to the active site cysteine residue, the latter must not participate in the chemistry of the CoA transferase reaction.

The CoA transferases of *Escherichia coli* (Sramek & Frerman, 1975a; Sramek et al., 1977), *Acidaminococcus fermentans* (Buckel et al., 1981), *Acinetobacter calcoaceticus* (Yeh & Ornston, 1984), and *Pseudomonas putida* (Yeh & Ornston, 1984) are also inactivated by thiol reagents. In addition, a substantial increase in the rate of inactivation of the enzyme of *Escherichia coli* is observed upon the formation of ECoA (Sramek & Frerman, 1975a; Sramek et al., 1977). Although these results suggest that a reactive cysteine residue is common to the active sites of the prokaryotic and eukaryotic CoA transferases (Yeh & Ornston, 1984), none of the five cysteine residues of the porcine enzyme is strictly conserved (Figure 1-9). Cysteine 67, however, is located in the conserved sequence motif [Gly-Gly-Phe-(Xxx)-(Xxx)-(Xxx)-Gly]. This "glycine cluster" is similar to a sequence associated with the ADP-binding $\beta\alpha\beta$ fold of other proteins, and may play a role in the binding of the nucleotide portion of CoA (Wierenga et al., 1986; Williams, 1990; Parales & Harwood, 1992).

Finally, the sensitivity of succinyl-CoA:3-ketoacid CoA transferase to thiol reagents has been used to evaluate the thermodynamic and kinetic parameters of the enzyme. The inactivation of a mixture of ECoA and free enzyme by DTNB involves two distinct phases: a rapid phase corresponding to the inactivation of ECoA, and a slow phase corresponding to the inactivation of free CoA transferase (White et al., 1976). By assessing the relative contribution of each of these two phases to the overall rate of inactivation, the concentrations of ECoA and free enzyme in a sample of CoA transferase can be determined. Using this method, Jencks and his coworkers have estimated that ECoA is hydrolyzed with a first-order rate constant of 0.10 min^{-1} at pH 8.1, which is 10^3-fold greater than the rate constant for the hydrolysis of acetyl-CoA (White et al., 1976). Thus, the thiolester of ECoA is poised to react with non-specific reagents (Moore &

Jencks, 1982c), as further described below. In addition, the equilibrium constants for the two half-reactions of CoA transferase have been determined (White et al., 1976):

$$\text{acetoacetyl-CoA} + \text{E} \overset{K_{eq} = 9}{\rightleftharpoons} \text{acetoacetate} + \text{E-CoA}$$

$$\text{succinyl-CoA} + \text{E} \overset{K_{eq} = 0.2}{\rightleftharpoons} \text{succinate} + \text{E-CoA}$$

Based on these half-reaction equilibria, the overall equilibrium constant for the transfer of CoA from succinyl-CoA to acetoacetate is 0.026 (White et al., 1976).

A binding site for the carboxylate substrates

Results from several experiments suggest that a cationic group in the active site of succinyl-CoA:3-ketoacid CoA transferase is necessary for the binding of the carboxylate substrates. First, monovalent anions inhibit the CoA transferase reaction to an extent which correlates with the Hofmeister series (Hersh & Jencks, 1967a; Jencks, 1973). The inhibition by chloride ion is competitive with respect to acetoacetate and succinate. Second, CoA transferase is irreversibly inactivated by the acylation of a deprotonated group at alkaline pH (Hersh & Jencks, 1967a). At pH 7.0, this group is protonated, and thus no longer sensitive to acylation. Examples of acylating agents which inactivate the enzyme include acetoacetyl-CoA (in the presence of divalent metal ions and in the absence of succinate), acetic anhydride, and 2,4-nitrophenyl acetate. The enzyme is not inactivated in the presence of chloride ion, implying that the group which undergoes acylation is the same as that which binds monovalent anions. Third, at low levels of succinate, the rate of the enzymatic reaction between acetoacetyl-CoA and succinate is dependent on the protonation of a group with an apparent pK_a of 8.4 (Jencks, 1973). Since the half-reaction of ECoA with succinate is rate-limiting under these conditions, the protonated group may be responsible for the binding of succinate. Together, these observations suggest that the carboxylate substrates interact electrostatically with a cationic moiety in the active site of CoA transferase. Based on its apparent pK_a, this group is most likely the protonated sidechain of a lysine residue at neutral pH (Jencks, 1973).

The CoA transferase of *Escherichia coli* is inactivated upon incubation with acetyl-CoA in the absence of metal ion chelators (Sramek & Frerman, 1975a). The loss of activity is prevented by cysteine but not by 2ME, which suggests that acetyl-CoA inactivates by *N*-acetylation rather than by *S*-acetylation. By analogy with the CoA transferase of porcine heart, the enzyme of *Escherichia coli* also makes use of a protonated lysine residue for the binding of its carboxylate substrates (Sramek & Frerman, 1975a).

Noncovalent interactions and catalysis: general considerations

Noncovalent binding interactions between an enzyme and a substrate contribute to catalysis by two mechanisms (Moore & Jencks, 1982b). First, the binding of a substrate to the active site increases the effective concentration of the substrate above that of the reactant in solution. The magnitude of this increase, relative to a standard state of 1 M, is equal to the reciprocal of the K_M for the substrate (Moore & Jencks, 1982b; Jencks, 1987). Second, much of the intrinsic binding energy of the substrate is utilized by the enzyme to achieve a decrease in the free energy of activation of the reaction. This decrease involves the loss of entropy in the ground state, the destabilization of the ground state, or the stabilization of the transition state (Moore & Jencks, 1982c; Whitty et al., 1995).[9] This ability of the enzyme to use the intrinsic binding energy of a substrate at specific points along the reaction coordinate is essential for catalysis (Figure 1-15). If the ground state were stabilized to the same degree as the transition state, then the enzyme would derive no benefit from noncovalent binding interactions with the substrate (Jencks, 1987; Whitty et al., 1995).

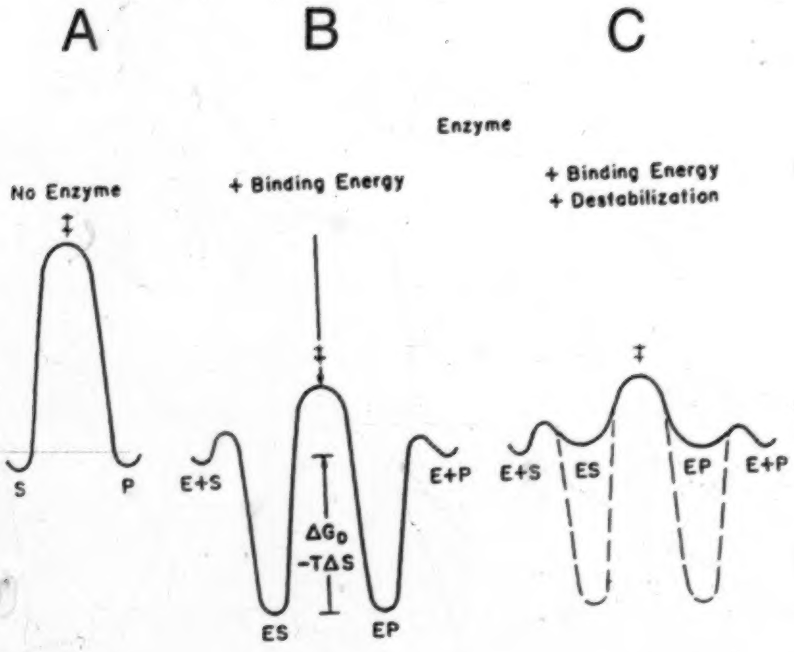
A
B
C
Enzyme
No Enzyme
+ Binding Energy
+ Binding Energy
+ Destabilization
‡
‡
‡
S
P
E+S
E+P
ΔG_D
-TΔS
ES
EP
E+S
ES
EP
E+P

Figure 1-15: The use of the intrinsic binding energy of the substrates to achieve catalysis. If the transition state (‡) and the Michaelis complex (ES or EP) are stabilized to equal extents, then the enzymatic and uncatalyzed reactions proceed with identical activation energies (compare panels "A" and "B"). However, if the transition state is stabilized but the Michaelis complex is destabilized, then the activation energy is substantially less for the enzymatic reaction than for the uncatalyzed reaction (compare panels "A" and "C"). (Reprinted from [Jencks, 1987], with the permission of Cold Spring Harbor Laboratory Press).

The decrease in the free energy of activation occurs at the expense of intrinsic energy available to the substrate for binding interactions with the enzyme. The amount of binding energy which remains is the "observed" binding energy, reflected by the K_M for the substrate. Thus, the utilization of the intrinsic binding energy of the substrate involves a compromise: a large proportion is consumed to lower the free energy of activation, but a minimal amount must remain as observed binding energy to allow the initial formation of the Michaelis complex.

Noncovalent interactions at the active site of succinyl-CoA:3-ketoacid CoA transferase

Acetoacetate is the preferred 3-ketoacid substrate for succinyl-CoA:3-ketoacid CoA transferase. The second-order rate constant (k_{cat}/K_M) for the reaction of ECoA with acetoacetate is 4.5×10^4 fold greater than that for the reaction of ECoA with butyrate, suggesting that the 3-keto group of acetoacetate interacts more favorably with the enzyme than a methylene group at the same position (White & Jencks, 1976a). This rate enhancement reflects a decrease of 27 kJ/mol in the free energy of activation relative to unbound substrates (Table 1-5A). Acetoacetate is also more reactive than acetate by a factor of 2×10^5, indicating that noncovalent interactions which involve the CH_3CO-moiety of acetoacetate result in a decrease of 30 kJ/mol in the free energy of activation relative to unbound substrates (White & Jencks, 1976a; Table 1-5A). Given that the K_M for acetoacetate is only 10^2-fold less than the K_M for butyrate or acetate (White & Jencks, 1976a), the greater part of these rate accelerations can be attributed to an increase in k_{cat} rather than a decrease in K_M. Thus, much of the intrinsic binding energy of the nonreacting portion of acetoacetate is used to lower the free energy of activation. The remainder (about 11 kJ/mol) is used as observed binding energy (Table 1-5A).

Succinyl-CoA:3-ketoacid CoA transferase also reacts specifically with succinate. The transfer of CoA from ECoA to succinate is accelerated by a factor of 6×10^3 compared to the equivalent reaction with acetate (White & Jencks, 1976a; Moore &

Table 1-5: Energetic Contribution of Noncovalent Binding Interactions to Catalysis by Succinyl-CoA:3-ketoacid CoA Transferase

Part A: Half-reaction between ECoA and the carboxylate substrates

Reacting group	Decrease in E_a relative to unbound substrates[a] (kJ/mol)	Observed binding energy (kJ/mol)	Decrease in E_a relative to the Michaelis complex[b] (kJ/mol)
Acetoacetate[c]			
3-keto group	27	11	16
CH_3CO— group	30	11	19
Succinate[d]			
—CH_2COO^- group	21	0	21
CoA[e]			
nucleotide group	6	N/A[f]	6
pantoic acid group[g]	40	N/A[f]	40

[a] E_a is an abbreviation for "activation energy".

[b] Each value in this column is calculated as the difference between the decrease in E_a relative to unbound substrates and the observed binding energy.

[c] Data are from White & Jencks (1976a).

[d] Data are from White & Jencks (1976a) and Moore & Jencks (1982c).

[e] Data are from Whitty et al. (1995).

[f] "Observed binding energy" is not applicable in this case, since CoA is covalently bound to the enzyme in the ECoA complex.

[g] The decrease in E_a due to the pantoic acid group of CoA results from destabilizing interactions in the ECoA ground state and stabilizing interactions in the transition state (see text for details).

Table 1-5: Energetic Contribution of Noncovalent Binding Interactions to Catalysis by Succinyl-CoA:3-ketoacid CoA Transferase

Part B: Half-reaction between the free enzyme and succinyl-CoA

Reacting group	Decrease in E_a relative to unbound substrates[a] (kJ/mol)	Observed binding energy (kJ/mol)	Decrease in E_a relative to the Michaelis complex[b] (kJ/mol)
CoA[c]			
nucleotide group	35	9	26
pantoic acid group	21	8	13

[a] E_a is an abbreviation for "activation energy".

[b] Each value in this column is calculated as the difference between the decrease in E_a relative to unbound substrates and the observed binding energy.

[c] Data are from Whitty et al. (1995).

Jencks, 1982c). This rate enhancement implies that noncovalent interactions involving the -CH_2COO^- moiety of succinate result in a decrease in the free energy of activation of 21 kJ/mol (Table 1-5A). Interestingly, the K_M for succinate (23 mM) is similar to the K_M for acetate (White & Jencks, 1976a). Thus, most of the intrinsic binding energy of the nonreacting portion of succinate is used to decrease the free energy of activation. Very little of this intrinsic binding energy remains as observed binding energy.

The binding of the nonreacting portion of CoA to the enzyme contributes substantially to catalysis, and has been characterized in detail by the study of thiolesters derived from truncated analogs of CoA (Figure 1-10). For example, succinate is 3×10^8 times more reactive with ECoA than with EMMP, corresponding to a decrease of 48 kJ/mol in the free energy of activation relative to unbound substrates (Moore & Jencks, 1982c; Whitty et al., 1995).[10] Most of this decrease is due to interactions between the enzyme and the pantoic acid portion of CoA (Table 1-5A). Furthermore, the enzyme reacts with succinyl-CoA 2×10^{12} fold more rapidly than with succinyl-MMP, which represents a decrease of 70 kJ/mol in the free energy of activation relative to unbound substrates (Moore & Jencks, 1982c; Whitty et al., 1995).[11] This decrease is attributed largely to interactions involving both the nucleotide and pantoic acid portions of CoA (Table 1-5B). Interestingly, the observed binding energy of CoA at the active site is relatively weak. Acetoacetyl-CoA and succinyl-CoA react with K_M values of 0.2 mM and 5 mM (respectively), and CoA itself only inhibits the turnover of substrates with a K_I of 1.7 mM (White & Jencks, 1976a; Moore & Jencks, 1982c; Whitty et al., 1995).[12] Thus, much of the intrinsic binding energy of the nonreacting portion of CoA is used to lower the free energy of activation for each of the two CoA transferase half-reactions.

In conclusion, the catalytic potential of succinyl-CoA:3-ketoacid CoA transferase is derived largely from noncovalent interactions at the active site. Specifically, the enzyme utilizes much of the intrinsic binding energy of the nonreacting portions of acetoacetate, succinate, and CoA to achieve substantial rate accelerations, at the expense of the observed binding of each of these components (White & Jencks, 1976a; Moore & Jencks, 1982c). This ability to use binding energy selectively is the critical feature of an enzyme which distinguishes it from a nonenzymatic catalyst (Jencks, 1987).

Accounting for catalysis by succinyl-CoA:3-ketoacid CoA transferase

From the above discussion, it is clear that a decrease in the Gibbs free energy of activation occurs at the expense of the intrinsic binding energy of the substrates. However, it is more difficult to ascertain the relative importance of the specific mechanisms by which the free energy of activation is lowered. To achieve catalysis, succinyl-CoA:3-ketoacid CoA transferase makes use of the loss of entropy in the ground state, the destabilization of the ground state (due to unfavorable binding interactions), and the stabilization of the transition state (due to favorable binding interactions).

The complete CoA transferase reaction consists of two ground states: the Michaelis complex of enzyme and acyl-CoA for the first-half reaction, and the Michaelis complex of ECoA and carboxylate substrate for the second half-reaction. If the reactive groups are held in precise conformations in the ground state, then the transition state can be reached with little additional entropy loss. This effect, referred to as "induced intramolecularity" by Moore & Jencks (1982b), likely plays a key role in the catalysis of CoA transfer. It is estimated from studies of model reactions that the loss of entropy in the ground state could accelerate either of the CoA transferase half-reactions by a factor of 6×10^5, if the carboxylate and thiolester moieties are held together as effectively as they are in a monothiolester of succinate (Moore & Jencks, 1982b).

The Gibbs free energy of each Michaelis complex is also increased by destabilization. For example, the thiolester group of ECoA is activated to react with non-specific substrates such as water, borohydride, or MMP, relative to acetyl-CoA or EMMP (White et al., 1976; Moore & Jencks, 1982c). Assuming that the intrinsic chemical reactivities of acetyl-CoA and the active site glutamyl-CoA are similar, it can be inferred that unfavorable interactions between the nonreacting portion of CoA and the enzyme increase the Gibbs free energy of the ECoA ground state (Moore & Jencks, 1982c). As further discussed below, the pantoic acid "domain"[13] of CoA accounts for most of these unfavorable interactions (Fierke & Jencks, 1986; Whitty et al., 1995). The destabilization of ECoA may result from the disruption of hydrogen bonding and/or the distortion of the planar thiolester linkage to a configuration resembling the tetrahedral geometry of the transition state (Moore & Jencks, 1982c).

Finally, the transition state for each half-reaction is stabilized relative to the ground state by favorable interactions between the enzyme and the nonreacting portion of CoA. The magnitude of this effect is well understood for the half-reaction of free enzyme with succinyl-CoA. Specifically, the nucleotide and pantoic acid domains of CoA stabilize the transition state for this half-reaction, relative to the Michaelis complex, by 26 kJ/mol and 13 kJ/mol, respectively (Fierke & Jencks, 1986; Whitty et al., 1995; Table 1-5B).[14] In total, this stabilization accounts for more than half of the decrease in the free energy of activation of the first half-reaction due to the nonreacting portion of CoA, relative to unbound substrates (Moore & Jencks, 1982c; Whitty et al., 1995; Table 1-5B). In addition, the pantoic acid domain stabilizes the transition state for the second half-reaction by 22 kJ/mol (Whitty et al., 1995).[15]

The nucleotide and pantoic acid domains of CoA play opposing roles with respect to the ECoA ground state (Fierke & Jencks, 1986; Whitty et al., 1995). Whereas the binding of the nucleotide portion of CoA to the enzyme *stabilizes* ECoA by 30 kJ/mol, the binding of the pantoic acid domain *destabilizes* ECoA by 20 kJ/mol (Whitty et al., 1995). The terminal acetamide moiety accounts for 25% of this destabilization energy (Whitty et al., 1995). The destabilization of ECoA due to the pantoic acid domain effectively lowers the free energy of activation (Figure 1-16), and is hence essential for catalysis (Whitty et al., 1995). Significantly, the binding of the pantoic acid domain of CoA differs dramatically between the ECoA ground state and the two transition states.

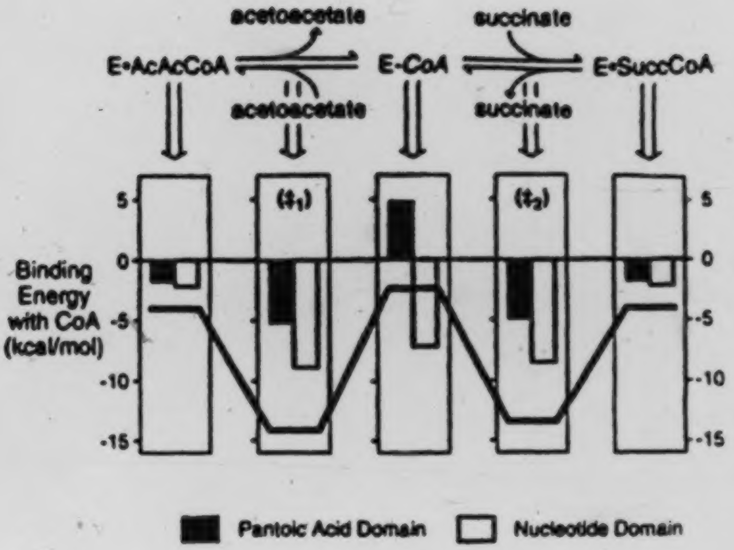

Figure 1-16: The use of the intrinsic binding energy of the nonreacting portion of CoA at specific points along the reaction coordinate. (Top) Scheme for the reaction between acetoacetyl-CoA and succinate, catalyzed by CoA transferase. (Bottom) Histograms representing the binding energies of the ground states and the transition states. These binding energies are derived from interactions between the enzyme and the pantoic acid domain (black bar) or the nucleotide domain (white bar) of CoA. The net noncovalent binding energy, derived from the sum of both types of interactions, is represented by the solid black line. (Reprinted from [Whitty et al., 1995], with the permission of the American Chemical Society).

The importance of a conformational change

As described previously, ECoA exists in a more "open" state than the free enzyme (White et al., 1976). The conformational change associated with the formation of ECoA consumes at least 24 kJ/mol of the intrinsic binding energy of the acyl-CoA substrate (Moore & Jencks, 1982c). However, this cost in Gibbs free energy is partially offset by the net stabilization of the ECoA thiolester, resulting from the compromise between favorable and unfavorable binding of the nucleotide and pantoic acid domains of CoA, respectively (Moore & Jencks, 1982c; Whitty et al., 1995). Thus, the energetically expensive conversion of the enzyme to its "open" form is driven thermodynamically by stabilizing forces at the active site of ECoA.

The conformational change is thought to be necessary for the acceleration of the half-reaction between ECoA and the carboxylate substrates. First, the "open" conformer may immobilize the reacting groups more fully than the "closed" conformer. This "clamping" effect may increase the loss of entropy in the ground state beyond that which occurs solely at the expense of intrinsic binding energy (Moore & Jencks, 1982c). Second, the conformational change may be necessary for the destabilization of the pantoic acid domain, which accounts largely for the reactivity of ECoA with specific and nonspecific reagents (Moore & Jencks, 1982c; Whitty et al., 1995). Third, the affinity of succinate and acetoacetate is greater for the "open" form of the enzyme, suggesting that the conformational change leads to the formation of an optimal binding pocket for the carboxylate substrates (Moore & Jencks, 1982c; Whitty et al., 1995). Thus, the conversion of the enzyme from a "closed" to an "open" state likely facilitates several mechanisms used by the enzyme to achieve catalysis.

Part D: The Objectives of the Thesis

It is evident that in certain areas, the current knowledge of the CoA transferases is extensive. These enzymes are particularly well understood in terms of their metabolic roles and their interactions with substrates. In addition, the primary and quaternary structures of several CoA transferases have been characterized. Nevertheless, many of the molecular details underlying the function of these enzymes remain uncertain. For example, the structural determinants which influence the folding, assembly, and aggregation of the CoA transferases have not been investigated. Furthermore, specific residues located in the active sites of these enzymes have not been identified. The experiments described in this thesis were performed on the succinyl-CoA:3-ketoacid CoA transferase of porcine heart to gain insight in these areas. Specifically, seven areas have been addressed:

(1) Is the hydrophilic linker segment necessary for the folding of the mammalian CoA transferase? Although not required for catalytic function, the hinge region may facilitate the assembly of the N- and C-domains to the active enzyme form. This question was addressed by assessing whether or not a "hinge-mutant" of CoA transferase, in which the N- and C-domains exist as separate polypeptides, is correctly assembled *in vivo* and *in vitro*.

(2) Do the N- and C-domains fold independently of each other prior to their association? If so, then the assembly of these domains to the active enzyme form may be a simple docking event. If not, then the N- and C-domains must complete their folding through productive interactions as part of an assembly intermediate. To address this question, the secondary, tertiary, and quaternary structures of the purified N- and C-domains have been compared with those of the intact enzyme.

(3) To what extent are different intermediates along the folding pathway of CoA transferase susceptible to aggregation *in vivo* and *in vitro*? Can structural features of the enzyme which account for incorrect self-association be identified? Are such non-productive interactions influenced by chaperonins? These questions were addressed by evaluating the yield of soluble, active CoA transferase following induction in *E. coli*, or upon (re)folding *in vitro* in the presence or absence of GroEL and GroES.

(4) Do the correctly folded subunits of CoA transferase assemble to more than one oligomeric state? If so, are certain structural features of the enzyme necessary for these interactions? To address these questions, the secondary, tertiary, and quaternary structures of the homodimeric wild-type enzyme have been compared with those of a "large" version of the wild-type enzyme, and with those of the hinge-mutant. In addition, crystals of CoA transferase were obtained as a first step towards solving the three-dimensional structure of the enzyme.

(5) Which of the three proposed glutamate residues is the nucleophile in the active site of CoA transferase? This question was addressed by identifying the precise location of the autolytic fragmentation. In addition, mutants in which the catalytic glutamate residue is replaced with alanine, aspartate, or glutamine have been characterized with respect to specific enzyme activity.

(6) Is cysteine 67 of the glycine cluster the reactive cysteine residue located in the active site of ECoA? To address this question, a mutant in which cysteine 67 is replaced with a serine residue has been characterized with respect to specific enzyme activity and reactivity with DTNB.

(7) Is the active site of CoA transferase shared between two subunits or between two domains of the same subunit? This question was addressed by performing active site complementation experiments *in vitro*.

These studies will prove to be of general importance. First, by investigating the folding, assembly, and aggregation of the mammalian CoA transferase, we improve our knowledge of how proteins adopt active conformations while avoiding competing, nonproductive interactions. This "protein folding problem" (Creighton, 1994) is far from being solved, particularly for large, multimeric proteins. Second, a detailed investigation of the quaternary structure of CoA transferase will provide clues as to why many proteins are multimers, and why homologous enzymes of prokaryotes and eukaryotes adopt different oligomeric states. Third, given the uniqueness of the CoA transferase reaction, a description of the active site will contribute to our understanding of the diversity of enzyme catalysts in biology. Finally, a three-dimensional model for the structure of CoA transferase would provide the basis to rationalize how enzymes makes use of noncovalent binding interactions to achieve large rate accelerations.

ENDNOTES

[1] In contrast, a different isoenzyme, specific for adenine rather than guanine nucleotides, is thought to catalyze the reverse reaction in the TCA cycle (Jenkins & Weitzman, 1986; Jenkins et al., 1988). In this case, the hydrolysis of succinyl-CoA, coupled with the formation of ATP, is driven by the progress of the TCA cycle rather than by the mitochondrial ratio of ATP to ADP, which is approximately equal to 1 (Ottaway et al., 1981; Jenkins & Weitzman, 1986; Jenkins et al., 1988).

[2] These values were estimated by gel filtration, sedimentation-equilibrium, and PAGE under non-denaturing conditions, or by crosslinking followed by SDS-PAGE.

[3] These values were estimated by sedimentation-equilibrium analyses of protein denatured in 6 M GuHCl, or by SDS-PAGE.

[4] The amino acid sequence of the human CoA transferase was deduced from a cDNA sequence.

[5] The amino acid sequence of the *C. elegans* CoA transferase was deduced from a genomic DNA sequence (Kassovska-Bratinova et al., 1996).

[6] The coding sequences for the CoA transferases from *M. tuberculosis*, *H. influenzae*, *B. subtilis*, and *E. coli* have not been published. The deduced amino acid sequences for the α- and β-subunits of these enzymes were retrieved from the Swiss-Prot database. Only a portion of the coding sequence for the CoA transferase from *A. tumefaciens* has been published (Parke, 1995).

[7] The subunits of the *Haemophilus influenzae* CoA transferase are an exception.

[8] The rate of the nonenzymatic reaction between a thiolester and a substituted carboxylate ion increases with the acidity of the thiol leaving group ($\beta_{lg} = -0.99$), suggesting that the expulsion of the thiol anion is rate-determining. By analogy, the release of CoA may be the rate-limiting step in the enzymatic half-reaction (Moore & Jencks, 1982b).

[9] Although the loss of entropy may be seen as a form of destabilization, the terminology used here is the same as that used by Jencks and coworkers. Thus, destabilization refers to an increase in the free energy of the reactants by means other than the loss of entropy (for instance, desolvation or bond strain).

[10] These contributions are attributed specifically to the stabilization of the transition state (Whitty et al., 1995), as discussed below.

[11] Whitty et al. (1995) attribute these contributions specifically to the stabilization of the transition state, as described further in the following section.

[12] Millimolar values for K_M suggest relatively weak substrate binding. By comparison, K_M values ranging from 10 μM to 10 mM are reported for the substrates of some glycolytic enzymes (see p. 328 in [Fersht, 1985]).

[13] The term "domain," adapted from Whitty et al. (1995), is used here to describe a portion of the CoA molecule.

[14] The contributions from the nucleotide and pantoic acid domains of CoA are evaluated by comparing the reactivities of: (1) succinyl-CoA and succinyl-pantetheine with free CoA transferase; and (2) succinyl-pantetheine and succinyl-NAC with free enzyme (Fierke & Jencks, 1986; Whitty et al., 1995).

[15] The contribution from the pantoic acid domain of CoA is evaluated by comparing the reactivities of E-pantetheine and E-NAC with succinate (Fierke & Jencks, 1986; Whitty et al., 1995).

REFERENCES

Allen, S. H. G., Kellmeyer, R. W., Stjernholn, R. L., & Wood, H. G. (1964) *J. Bacteriol. 87*, 171-187.

Altschul, S. F., Gish, W., Miller, W., Myers, E. W., & Lipman, D. J. (1990) *J. Mol. Biol. 215*, 403-410.

Appel, R. D., Bairoch, A., & Hochstrasser, D. F. (1994) *Trends Biochem. Sci. 19*, 258-260.

Baddiley, J., Thain, E., Novelli, G., & Lipmann, F. (1953) *Nature 171*, 76.

Baetz, A. L., & Allison, M. J. (1990) *J. Bacteriol. 172*, 3537-3540.

Ballinger, P., & Long, F. A. (1960) *J. Am. Chem. Soc. 82*, 795-798.

Barker, H. A., Jeng, I.-M., Neff, N., Robertson, J. M., Tam, F. K., & Hosaka, S. (1978) *J. Biol. Chem. 253*, 1219-1225.

Benson, R. W., & Boyer, P. D. (1969) *J. Biol. Chem. 244*, 2366-2371.

Bergstrom, J. D., Wong, G. A., Edwards, P. A., & Edmond, J. (1984) *J. Biol. Chem. 259*, 14548-14553.

Blair, J. B. (1969) *J. Biol. Chem. 244*, 951-954.

Bridger, W. A. (1974) in *The Enzymes*, 3rd ed. (Boyer, P. D., Ed.) Vol. X, pp. 581-606, Academic Press, Inc., New York.

Bruice, T. C., & Benkovic, S. J. (1966) in *Bioorganic Mechanisms*, Vol. I, pp. 259-297, W. A. Benjamin, Inc., New York.

Buckel, W., Dorn, U., & Semmler, R. (1981) *Eur. J. Biochem. 118*, 315-321.

Buckley, B. M., & Williamson, D. H. (1973) *Biochem. J. 132*, 653-656.

Buckley, B. M., & Williamson, D. H. (1975) *FEBS Lett. 60*, 7-10.

Chou, P. Y., & Fasman, G. D. (1978) *Adv. Enzymol. 47*, 45-148.

Creighton, T. E. (1994) in *Mechanisms of Protein Folding* (Pain, R. H., Ed.) pp. 1-25, IRL Press, Oxford, U. K.

Curtin, D. Y., & Miller, L. L. (1967) *J. Am. Chem. Soc. 89*, 637-645.

Danehy, J. P., & Noel, C. J. (1960) *J. Am. Chem. Soc. 82*, 2511-2515.

Delarue, M. (1995) *Curr. Opin. Struct. Biol. 5*, 48-55.

Deléage, G., & Roux, B. (1987) *Protein Eng. 1*, 289-294.

Edwards, M. R., Singh, M., & Tubbs, P. K. (1973) *FEBS Lett. 37*, 155-158.

Eikmanns, U., & Buckel, W. (1990) *Biol. Chem. Hoppe-Seyler 371*, 1077-1082.

Endemann, G., Goetz, P. G., Edmond, J., & Brunengraber, H. (1982) *J. Biol. Chem. 257*, 3434-3440.

Engel, C., & Wierenga, R. (1996) *Curr. Opin. Struct. Biol. 6*, 790-797.

Fedor, L. R., & Bruice, T. C. (1965) *J. Am. Chem. Soc. 87*, 4138-4147.

Fersht, A. (1985) *Enzyme Structure and Mechanism*, 2nd ed. W. H. Freeman & Co., New York.

Fierke, C. A., & Jencks, W. P. (1986) *J. Biol. Chem. 261*, 7603-7606.

Fischer, R. J., Helms, J., & Dürre, P. (1993) *J. Bacteriol. 175*, 6959-6969.

Hersh, L. B., & Jencks, W. P. (1967a) *J. Biol. Chem. 242*, 3468-3480.

Hersh, L. B., & Jencks, W. P. (1967b) *J. Biol. Chem. 242*, 3481-3486.

Howard, J. B., Zieske, L., Clarkson, J., & Rathe, L. (1986) *J. Biol. Chem. 261*, 60-65.

Ito, M., Fukui, T., Saito, T., & Tomita, K. (1986) *Biochim. Biophys. Acta 876*, 280-287.

Jencks, W. P. (1973) in *The Enzymes*, 3rd ed. (Boyer, P. D., Ed.) Vol. IX, pp. 483-496. Academic Press, Inc., New York.

Jencks, W. P. (1987) *Cold Spring Harbor Symp. Quant. Biol. 52*, 65-73.

Jenkins, T. M., & Weitzman, P. D. J. (1986) *FEBS Lett. 205*, 215-218.

Jenkins, T. M., Eisenthal, R., & Weitzman, P. D. J. (1988) *Biochem. Biophys. Res. Commun. 151*, 257-261.

Johnson, A. W., & Wong, S. C. K. (1962) *J. Org. Chem. 37*, 1850-1853.

Kassovska-Bratinova, S., Fukao, T., Song, X.-Q., Duncan, A. M. V., Chen, H. S., Robert, M.-F., Pérez-Cerdá, C., Ugarte, M., Chartrand, C., Vobecky, S., Kondo, N., & Mitchell, G. A. (1996) *Am. J. Hum. Genet. 59*, 519-528.

Khan, S. A., & Erickson, B. W. (1984) *J. Am. Chem. Soc. 106*, 798-799.

Kindman, L. A., & Jencks, W. P. (1981) *Biochemistry 20*, 5183-5187.

Kowalchuk, G. A., Hartnett, G. B., Benson, A., & Houghton, J. E., Ngai, K.-L., & Ornston, L. N. (1994) *Gene 146*, 23-30.

Kyte, J. (1995) in *Mechanism in Protein Chemistry*, pp. 38-48, Garland Publishing, Inc., New York.

Levitt, M. (1978) *Biochemistry 17*, 4277-4285.

Lin, T., & Bridger, W. A. (1992) *J. Biol. Chem. 267*, 975-978.

Lipmann, F. (1945) *J. Biol. Chem. 160*, 173-190.

Lipmann, F., & Kaplan, N. (1946) *J. Biol. Chem. 162*, 743-744.

Lipmann, F., Kaplan, N., Novelli, G., Tuttle, L., & Guirard, B. (1947) *J. Biol. Chem. 167*, 869-870.

McClellan, J. A., & Ottaway, J. H. (1980) *Comp. Biochem. Physiol. 67B*, 679-684.

Mack, M., Bendrat, K., Zelder, O., Eckel, E., Linder, D., & Buckel, W. (1994) *Eur. J. Biochem. 226*, 41-51.

Marvin-Sikkema, F. D., Pedro Gomes, T. M., Grivet, J. P., Gottschal, J. C., & Prins, R. A. (1993) *Arch. Microbiol. 160*, 388-396.

Menon, G. K. K., Stern, J. R., Kupiecki, F. P., & Coon, M. J. (1960) *Biochim. Biophys. Acta 44*, 602-604.

Middleton, B., Day, R., Lombes, A., & Saudubray, J. M. (1987) *J. Inher. Metab. Dis. 10*, 273-275.

Moat, A. G., & Foster, J. W. (1988) *Microbial Physiology*, 2nd ed. John Wiley & Sons, Inc., New York.

Moore, S. A., & Jencks, W. P. (1982a) *J. Biol. Chem. 257*, 10874-10881.

Moore, S. A., & Jencks, W. P. (1982b) *J. Biol. Chem. 257*, 10882-10892.

Moore, S. A., & Jencks, W. P. (1982c) *J. Biol. Chem. 257*, 10893-10907.

Müller, M. (1988) *Annu. Rev. Microbiol. 42*, 465-488.

Müller, M. (1989) in *Trichomonads Parasitic in Humans* (Honigberg, B. M., Ed.) pp. 53-83, Springer, New York.

Müller, M. (1993) *J. Gen. Microbiol. 139*, 2879-2889.

Novelli, G., Schmetz, F., & Kaplan, N. (1954) *J. Biol. Chem. 206*, 533-545.

Ottaway, J. H., McClellan, J. A., & Saunderson, C. L. (1981) *Int. J. Biochem. 13*, 401-410.

Parales, R. E., & Harwood, C. S. (1992) *J. Bacteriol. 174*, 4657-4666.

Parke, D. (1995) *J. Bacteriol. 177*, 3808-3817.

Pérez-Cerdá, C., Merinero, B., Sanz, P., Jiménez, A., Hernández, C., Garciá, M. J., & Ugarte, M. (1992) *J. Inher. Metab. Dis. 15*, 371-373.

Petersen, D. J., Cary, J. W., Vanderleyden, J., & Bennett, G. N. (1993) *Gene 123*, 93-97.

Pickart, C. M., & Jencks, W. P. (1979) *J. Biol. Chem. 254*, 9120-9129.

Pratt, R. F., & Bruice, T. C. (1972) *J. Am. Chem. Soc. 94*, 2823-2837.

Pretorius, C. J., Loy Son, G. G., Bonnici, F., & Harley, E. H. (1996) *J. Inher. Metab. Dis. 19*, 296-300.

Robishaw, J. D., & Neely, J. R. (1985) *Am J. Physiol. 248 (Endocrinol. Metab. 11)*, E1-E9.

Rochet, J.-C., & Bridger, W. A. (1994) *Protein Sci. 3*, 975-981.

Russell, J. J., & Patel, M. S. (1982) *J. Neurochem. 38*, 1446-1452.

Sakazaki, H., Hirayama, K., Murakami, S., Yonezawa, S., Shintaku, H., Sawada, Y., Fukao, T., Watanabe, H., Orii, T., & Isshiki, G. (1995) *J. Inher. Metab. Dis. 18*, 323-325.

Saudubray, J. M., Specola, N., Middleton, B., Lombes, A., Bonnefont, J. P., Jakobs, C., Vassault, A., Charpentier, C., & Day, R. (1987) *Enzyme 38*, 80-90.

Scherf, U., & Buckel, W. (1991) *Appl. Environ. Microbiol. 57*, 2699-2702.

Schulman, M., & Valentino, D. (1976) *J. Bacteriol. 128*, 372-381.

Shanley, M. S., Harrison, A., Parales, R. E., Kowalchuk, G., Mitchell, D. J., & Ornston, L. N. (1994) *Gene 138*, 59-65.

Sharp, J. A., & Edwards, M. R. (1978) *Biochem. J. 173*, 759-765.

Söhling, B., & Gottschalk, G. (1996) *J. Bacteriol. 178*, 871-880.

Solomon, F., & Jencks, W. P. (1969) *J. Biol. Chem. 244*, 1079-1081.

Solomons, T. W. G. (1984) *Organic Chemistry*, 3rd ed. John Wiley & Sons, Inc., New York.

Spence, M. W., Murphy, M. G., Cook, H. W., Ripley, B. A., & Embil, J. A. (1973) *Pediatr. Res. Suppl. 7*, 394.

Sramek, S. J., & Frerman, F. E. (1975a) *Arch. Biochem. Biophys. 171*, 14-26.

Sramek, S. J., & Frerman, F. E. (1975b) *Arch. Biochem. Biophys. 171*, 27-35.

Sramek, S. J., Frerman, F. E., & Adams, M. B. (1977) *Arch. Biochem. Biophys. 181*, 516-524.

Stanier, R. Y., & Ornston, L. N. (1973) *Adv. Microb. Physiol. 9*, 89-151.

Steinbüchel, A., & Müller, M. (1986) *Mol. Biochem. Parasitol. 20*, 57-65.

Stern, J. R., Coon, M. J., del Campillo, A., & Schneider, M. C. (1956) *J. Biol. Chem. 221*, 15-31.

Tildon, J. T., & Cornblath, M. (1972) *J. Clin. Invest. 51*, 493-498.

Tung, K. K., & Wood, W. A. (1975) *J. Bacteriol. 124*, 1462-1474.

Voet, D., & Voet, J. G. (1995) *Biochemistry*, 2nd ed. John Wiley & Sons, Inc., New York.

White, H., & Jencks, W. P. (1976a) *J. Biol. Chem. 251*, 1688-1699.

White, H., & Jencks, W. P. (1976b) *J. Biol. Chem. 251*, 1708-1711.

White, H., Solomon, F., & Jencks, W. P. (1976) *J. Biol. Chem. 251*, 1700-1707.

Whitty, A., Fierke, C. A., & Jencks, W. P. (1995) *Biochemistry 34*, 11678-11689.

Wierenga, R. K., Terpstra, P., & Hol, W. G. J. (1986) *J. Mol. Biol. 187*, 101-107.

Wiesenborn, D. P., Rudolph, F. B., & Papoutsakis, E. T. (1989) *Appl. Environ. Microbiol. 55*, 323-329.

Williams, W. A. (1990) Ph. D. thesis, University of Minnesota, Minneapolis.

Williamson, D. H. (1979) *Biochem. Soc. Trans. 7*, 1313-1321.

Yeh, W.-K., & Ornston, L. N. (1981) *J. Biol. Chem. 256*, 1565-1569.

Yeh, W.-K., & Ornston, L. N. (1984) *Arch. Microbiol. 138*, 102-105.

Chapter 2. Productive Interactions Between the Two Domains of CoA Transferase During Folding and Assembly[1]

INTRODUCTION

From the substantial amino acid sequence identity observed between correspondingly the α- and β-subunits of the $\alpha_2\beta_2$-type prokaryotic CoA transferases and the N- and C-domains of the eukaryotic monomer, Parales & Harwood (1992) proposed that the cDNA encoding the mammalian enzyme is the product of a fusion between two ancestral genes (Chapter 1). The evolutionary advantage of such a fusion event is unclear, however, given that an intact hinge connecting the N- and C-domains of the mammalian enzyme is not necessary to maintain a conformation with full catalytic activity. The linker segment may instead facilitate an essential interaction between the two domains of CoA transferase during the folding and assembly of the enzyme, prior to the achievement of its active configuration.

To test this hypothesis, a number of studies were carried out to determine whether or not the N- and C-domains of pig heart CoA transferase fold independently of each other under different conditions. Initially, the production of the wild-type, recombinant enzyme in *Escherichia coli* was compared to that of a "hinge-mutant" form in which the N- and C-domains are assembled as separate polypeptides. Subsequently, each domain fragment was characterized according to its far-ultraviolet circular dichroism (far-UV CD), fluorescence, and ultracentrifugation properties, and its stability in guanidine hydrochloride (GuHCl). These properties were also monitored, in parallel with the appearance of enzyme activity, in a mixture of the two domains incubated at various temperatures. Finally, wild-type CoA transferase and the hinge-mutant were compared in terms of their ability to refold upon dilution from denaturant.

EXPERIMENTAL PROCEDURES[2]

Materials. The restriction endonucleases and T4 DNA ligase were purchased from New England Biolabs, Inc. or as Gibco BRL products from Life Technologies, with no obvious differences. Acrylamide and *Taq* DNA polymerase were also obtained as Gibco BRL products from Life Technologies. The deoxynucleotide triphosphates, DEAE Sephacel, Superose 12, Sephadex G-50, and Sephacryl S-200 were purchased from Pharmacia Biotech. The Sequenase was supplied by the United States Biochemical Corporation. The T4 DNA polymerase and the Lumi-Phos 530 were obtained from Boehringer Mannheim. The plasmid pT7-7 was a gift from Dr. Stanley Tabor, while pMS119EH and pKIXX were generously provided by Dr. Raymond Turner. The column matrices Affi-Gel Blue and hydroxyapatite were purchased from Bio-Rad Laboratories, Ltd. The substrates acetoacetate and succinyl-CoA were obtained from Sigma Chemical Company. Purified protein preparations were concentrated using Amicon brand Centriprep-10 concentrators (MWCO = 1.0×10^4). Dialyses were carried out using Spectra/Por membranes supplied by Spectrum. Finally, the GuHCl was provided by ICN Biomedicals, Inc.

Subcloning and mutagenesis. A flow diagram of these procedures is presented in Figure 2-1. A 1.5 kb segment of the λT6 cDNA clone (Lin & Bridger, 1992) encoding the mature form of CoA transferase was amplified by the polymerase chain reaction (PCR), using the primers NDE and HIND (Appendix 3). An expression plasmid for the production of wild-type enzyme (pT7-WT) was then created in two steps. First, the amplified DNA was subcloned as an *Nde*I-*Hin*dIII fragment into the multiple cloning site (MCS) of pT7-7. Second, to ensure that most of the cDNA insert from this initial recombinant plasmid was free of mutations due to misincorporation by Taq polymerase, a 1.3 kb *Eco*RI-*Stu*I segment was cleaved and replaced with the equivalent region excised from the λT6 cDNA. M13-WT was then prepared for subsequent mutagenesis

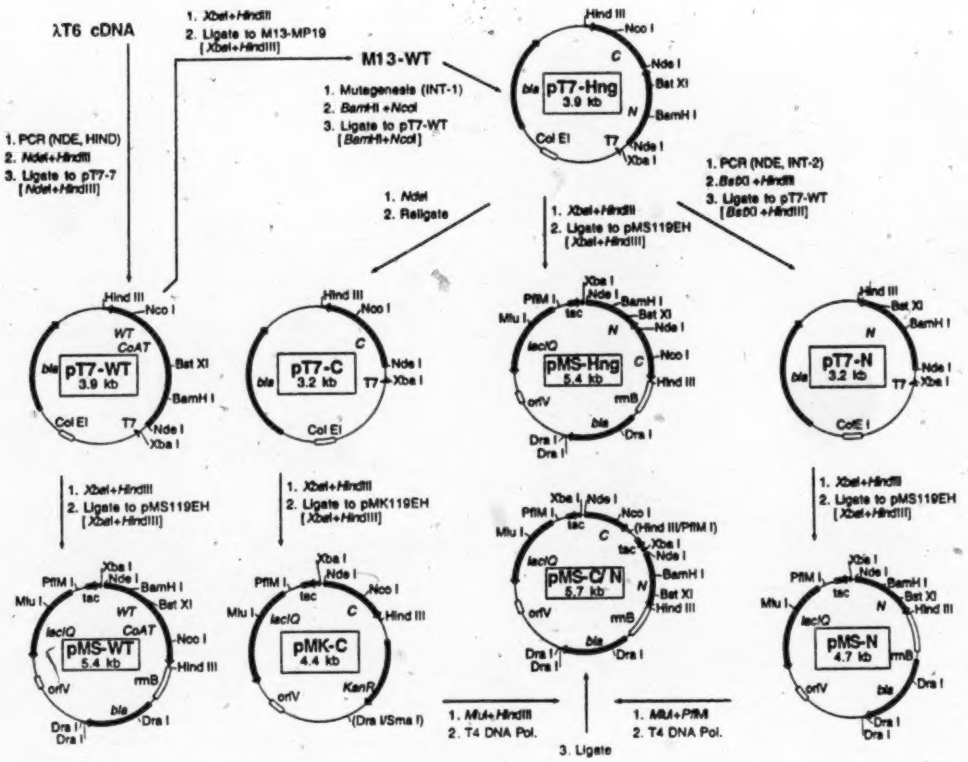
λT6 cDNA
1. XbaI+HindIII
2. Ligate to M13-MP19
[XbaI+HindIII]
M13-WT
1. Mutagenesis (INT-1)
2. BamHI+NcoI
3. Ligate to pT7-WT
[BamHI+NcoI]
1. PCR (NDE, HIND)
2. NdeI+HindIII
3. Ligate to pT7-7
[NdeI+HindIII]
pT7-Hng
3.9 kb
1. NdeI
2. Religate
1. XbaI+HindIII
2. Ligate to pMS119EH
[XbaI+HindIII]
1. PCR (NDE, INT-2)
2. BstXI+HindIII
3. Ligate to pT7-WT
[BstXI+HindIII]
pT7-WT
3.9 kb
WT CoAT
pT7-C
3.2 kb
pMS-Hng
5.4 kb
pT7-N
3.2 kb
1. XbaI+HindIII
2. Ligate to pMS119EH
[XbaI+HindIII]
1. XbaI+HindIII
2. Ligate to pMK119EH
[XbaI+HindIII]
1. XbaI+HindIII
2. Ligate to pMS119EH
[XbaI+HindIII]
pMS-WT
5.4 kb
pMK-C
4.4 kb
pMS-C/N
5.7 kb
pMS-N
4.7 kb
(Hind III/PflM I)
(Dra I/Sma I)
1. MluI+HindIII
2. T4 DNA Pol.
1. MluI+PflMI
2. T4 DNA Pol.
3. Ligate
Hind III
Nco I
Nde I
Bst XI
BamH I
Xba I
PflM I
Mlu I
Dra I
Col EI
T7
tac
lacIQ
oriV
rrnB
bla
KanR
C
N

Figure 2-1: Construction of expression vectors encoding CoA transferase polypeptides. The primers used for PCR were NDE, HIND, and INT-2 (Appendix 3). The vector pT7-Hng was created by site-directed mutagenesis using single-stranded M13-WT as the template and INT-1 (Appendix 3) as the mutagenic primer (Kunkel, 1985). ColE1 and oriV designate origins of DNA replication, while T7 and *tac* refer to promoter sequences. *KanR* and *bla* designate genes conferring resistance to kanamycin and ampicillin, respectively. Other encoded proteins are identified as follows: *lacI*^{Q}, lac repressor; *WT CoAT*, wild-type CoA transferase; *Hng*, hinge-mutant; *N*, N-domain; *C*, C-domain. (*Hin*dIII/*Pfl*MI) and (*Dra*I/*Sma*I) refer to restriction sites destroyed as a result of blunt-end ligation. "T4 DNA Pol." is an abbreviation for T4 DNA polymerase.

experiments by transferring the 1.5 kb *Xba*I-*Hin*dIII segment of pT7-WT into the MCS of M13-mp19 replicative form (RF) DNA.

An M13 vector containing a gene to encode the hinge-mutant form of CoA transferase (M13-Hng) was generated by site-directed mutagenesis according to previously described methods (Kunkel, 1985), using M13-WT DNA as the single-stranded template and INT-1 as the mutagenic primer (Appendix 3). This primer included a stop codon and a reinitiation site in the region of the DNA encoding the hydrophilic linker segment. Due to the design of this primer, the hinge-mutant form of CoA transferase lacked residues 249 to 254, which are normally present in the linker segment of the wild-type enzyme. (Thus, the predicted molecular weight of the N-domain of the hinge-mutant was 2.7×10^4.) The 0.9 kb *Bam*HI-*Nco*I segment cleaved from M13-Hng RF DNA was subcloned into pT7-WT, yielding pT7-Hng.

An expression vector for the production of the C-domain of CoA transferase was prepared by digestion of pT7-Hng with *Nde*I and subsequent religation, yielding the vector pT7-C. (The predicted molecular weight of the C-domain of the hinge-mutant was 2.4×10^4.) In addition, a DNA insert encoding the N-domain of CoA transferase was amplified from pT7-Hng by the PCR, using the primers NDE and INT-2 (Appendix 3). The latter was designed such that a stop codon associated with a *Hin*dIII restriction site was incorporated in the region of the DNA insert encoding the hydrophilic linker segment. An expression plasmid for the production of the N-domain was then prepared by subcloning the amplified DNA as a 0.16 kb *Bst*XI-*Hin*dIII fragment into pT7-WT, yielding pT7-7-N.

A parallel series of expression plasmids was generated by transferring an *Xba*I-*Hin*dIII segment from each pT7-7-derived vector into the MCS of pMS119EH or its kanamycin-resistant variant, pMK119EH. The latter was constructed by replacing the 0.7 kb *Dra*I fragment of pMS119EH (which included most of the gene encoding β-lactamase) with the 1.2 kb *Sma*I fragment of pKIXX (which encoded a marker for resistance to kanamycin).

The vector pMS-C/N, in which the genes encoding the N- and C-domains of CoA transferase are incorporated within two separate transcription units, was derived from pMS-N and pMK-C. Specifically, the 1.4 kb *Mlu*I-*Hin*dIII insert of pMK-C was attached in two steps to the 4.4 kb fragment cleaved from pMS-N with *Mlu*I and *Pfl*MI: (1) ligation of the complementary *Mlu*I sites on the two fragments; and (2) repair of the *Hind*III site on the small fragment and the *Pfl*MI site on the large fragment with T4 DNA polymerase, followed by ligation of the resulting blunt ends.

The absence of possible mutations due to misincorporation by *Taq* DNA polymerase or Sequenase during the *in vitro* DNA synthesis reactions was confirmed by automated sequence determinations using previously described methods (Sanger et al., 1977) and an Applied Biosystems (ABI) 373A DNA sequencer.

Electrocompetent BL21(DE3) cells (*hsdS gal* [*λc*I*ts*857 *ind*1 *S*am7 *nin*5 *lac*UV5-T7 gene*1*]) were electroporated with vectors of the pT7-7 series, yielding the new strains BL-WT, BL-Hng, BL-N, and BL-C. Similarly, electrocompetent HB101 cells (*supE*44 *hsdS*20[$r_B^- m_B^-$] *recA*13 *ara*-14 *proA*2 *lacY*1 *galK*2 *rpsL*20 *xyl*-5 *mtl*-1) were electroporated with vectors of the pMS119-EH series, yielding the new strains HB-WT, HB-Hng, HB-N, HB-C, HB-N+C, and HB-C/N.

Gene expression. Saturated liquid cultures *E. coli* BL21(DE3) or HB101 were diluted 1:100 with Luria Broth (LB) supplemented with ampicillin (final concentration, 0.10 mg/mL). Culture volumes were generally 1-10 mL (small scale cultures) or 2-4 L (large-scale cultures). Following growth of the cells at 37 °C to the mid-log phase (OD_{600} = 0.5-0.6), gene expression was induced by the addition of isopropylthiogalactoside (IPTG) to a final concentration of 0.1 mM for BL21 cells or 1 mM for HB101 cells. HB101 cells containing two plasmids, one derived from pMS119 and the second derived from pMK119, were grown in the presence of 0.10 mg/mL ampicillin and 0.040 mg/mL kanamycin. Following growth at 25 °C for 8 to 12 h, the cells were harvested by centrifugation (10 min, 4.2×10^3 g, 4 °C), and the cell pellets were resuspended in buffer S (0.05 M K[phosphate], 0.5 mM EDTA, 10 mM 2ME, pH 7.4). The volumes of buffer S used were 0.5-1.0 mL (small-scale preparation) or 0.4-0.5 L (large scale preparation). The resuspended cells were then partially cracked by freezing at -70 °C and thawing at 4 °C. Small scale protein suspensions (0.5-1.0 mL) were sonicated at 4 °C with three twenty-second pulses using a BioSonik III sonicator (Bronwill Scientific), set at an intensity of 30. Large-scale protein suspensions (0.4-0.5 L) were sonicated at 4 °C with four one-minute pulses using a medium-sized (yellow-coded) probe attached to a Braun-Sonic 200 sonicator, set at an intensity of 350. The cell debris were separated from the cell lysate by centrifugation (10 min, 4.2×10^3 g). Generally, the protein concentration of the cell lysate prepared in this manner was 0.5 to 1 mg/mL. The relative amounts of CoA transferase protein present in the pellet and soluble fractions were determined by immunoblot analysis using the Lumi-Phos chemiluminescent detection system.

Protein purification. All protein purification procedures were carried out at 4 °C. The lysate recovered from a large-scale preparation of *E. coli* cells was treated with $(NH_4)_2SO_4$ (final concentration, 18% [w/v]) for 8 h. The suspension was cleared by centrifugation (10 min, 4.2×10^3 g), and $(NH_4)_2SO_4$ was added to the supernatant to a final concentration of 50% (w/v). After further incubation for 8 h, the precipitate was collected by centrifugation (10 min, 4.2×10^3 g). The pellet was dissolved in 40 mL buffer A (0.01 M K[phosphate], 0.1 mM EDTA, 10 mM 2ME, pH 7.4) or buffer D (0.005 M Tris-HCl, 0.1 mM EDTA, 10 mM 2ME, pH 8.0), depending on the desired ensuing chromatographic separation scheme (see below). The protein solution (3 to 5 mg/mL) was desalted by gel exclusion chromatography on a Sephadex G-50 column (diameter 5 cm, height 60 cm, total volume 1.2 L) prior to further purification. Typically, elution of the protein mixture from this column occurred at 0.32-0.56 L.

Wild-type CoA transferase and the hinge-mutant were purified according to a previously published procedure (Lin & Bridger, 1992). The enzyme was eluted from: (1) a column of DEAE-Sephacel (diameter 2.5 cm, height 60 cm, total volume 0.29 L) at 0.10 to 0.19 M KCl, using a gradient of 0 to 0.50 M KCl in 1.8 L buffer D; (2) a column of Sephacryl S-200 (diameter 2.5 cm, height 100 cm, total volume 0.49 L) at 0.27 to 0.38 L, using buffer A; and (3) a column of Affi-Gel Blue (diameter 2.5 cm, height 20 cm, total volume 0.098 L) at 0.35 to 0.70 M KCl, using a gradient of 0 to 1.5 M KCl in 0.60 L buffer A. After each chromatographic step, fractions containing the wild-type enzyme or hinge-mutant in purest form were identified by SDS-PAGE analysis and subsequently pooled. Optimally, a 2 L culture of BL-WT or BL-Hng yielded 10 mg of pure CoA transferase or 30 mg of pure hinge-mutant, respectively. This yield corresponded to a final recovery of 80 to 90% of the enzyme activity present in the cell lysate.

The N- and C-domains of CoA transferase were purified by two different schemes, both adapted from the chromatographic procedure described above for the wild-type enzyme or hinge-mutant. The N-domain was eluted from: (1) a column of DEAE-Sephacel (diameter 2.5 cm, height 60 cm, total volume 0.29 L), from 0.20 to 0.26 M KCl, using a gradient of 0 to 0.50 M KCl in 1.8 L buffer D; (2) a column of Sephacryl S-200 (diameter 2.5 cm, height 1000 cm, total volume 0.49 L), from 0.32 to 0.50 L, using buffer A; and (3) a column of hydroxyapatite (diameter 2.5 cm, height 20 cm, total volume 0.098 L), from 0.10 to 0.21 M K[phosphate], using a gradient of 0.010 to 0.40 M K[phosphate] (0.60 L). The C-domain was eluted from: (1) a column of Affi-Gel Blue (diameter 2.5 cm, height 20 cm, total volume 0.098 L), from 0.59 to 0.94 M KCl, using a gradient of 0 to 1.5 M KCl in 0.60 L buffer A; (2) a column of Sephacryl S-200 (diameter 2.5 cm, height 1000 cm, total volume 0.49 L), from 0.38 to 0.48 L, using buffer A; and (3) a column of hydroxyapatite (diameter 2.5 cm, height 20 cm, total volume 0.098 L), from 0.19 to 0.29 M K[phosphate], using a gradient of 0.010 to 0.40 M K[phosphate] (0.60 L). After each chromatographic step, fractions containing the N- or C-domain in purest form were identified by SDS-PAGE analysis and subsequently pooled. Optimal yields were 80 mg of pure N-domain or 20 mg of pure C-domain isolated from 2 L cultures of HB-N or HB-C, respectively. Each of these yields corresponded to a final recovery of 60 to 70% of the immunoreactive protein present in the cell lysate.

In general, columns were equilibrated with buffer A or D (2.5 times the column volume) prior to loading a protein sample. Similarly, ion-exchange resins with bound protein were washed with buffer A or D (3 times the column volume) prior to gradient elution. In addition, partially pure protein samples ($\geq$ 0.3 mg/mL) were concentrated by precipitation in $(NH_4)_2SO_4$ (final concentration, 50% [w/v]) prior to gel filtration chromatography on Sephacryl S-200. Alternatively, partially pure protein samples (< 0.3 mg/mL) were concentrated by centrifugation (2×10^3 g) using Centriprep-10 concentrators (MWCO = 1.0×10^4) prior to gel filtration chromatography on Sephacryl S-200. Finally, pure protein solutions were concentrated by centrifugation (2×10^3 g) using Centriprep-10 concentrators (MWCO = 1.0×10^4).

The homogeneity of all protein preparations was confirmed by SDS-PAGE analysis. The protein concentration of each enzyme solution was determined from the absorbance at 278 nm (A_{278}), which was corrected for scatter.[3] The following extinction coefficients (ε_{278}), in units of $(mg/mL)^{-1}$, were used: 0.65 for the wild-type enzyme, 0.66 for the hinge-mutant, 0.63 for the N-domain, and 0.69 for the C-domain. These values were calculated based on the molecular absorbances of the aromatic amino acids, as previously tabulated (Mihalyi, 1968), and were confirmed using the fringe-count method (Babul & Stellwagen, 1969).

The protein concentration of solutions of the purified wild-type enzyme or hinge-mutant used for refolding studies was determined by measuring A_{278} without correcting for scatter. In such cases, an ε_{278} value of 0.75 $(mg/mL)^{-1}$ was used for both forms of CoA transferase. This value was calculated from: (1) the uncorrected A_{278} reading of a solution of wild-type CoA transferase; and (2) the concentration of this solution, which had been determined previously by amino acid analysis. Generally, protein concentrations based on corrected or uncorrected A_{278} readings agreed to within 10%.

Measurement of enzyme activity. CoA transferase activity was determined by monitoring the absorbance increase at 310 nm, representative of the initial rate of appearance of the acetoacetyl-CoA enolate anion from the reaction of succinyl-CoA with acetoacetate (Stern et al., 1956). In the present study, the assay solutions consisted of 50 mM Tris-HCl, 15 mM $MgCl_2$, 0.060 to 0.30 mM succinyl-CoA, and 13 to 67 mM acetoacetate, at pH 9.1. The extinction coefficient for acetoacetyl-CoA at 310 nm (ε_{310}) was taken to be 7.8×10^3 M^{-1} cm^{-1} under these conditions (Howard et al., 1986). Assay solutions used for determining specific enzyme activities contained 0.30 mM succinyl-CoA and 67 mM acetoacetate. All assays were carried out at 22 °C. The specific activities of the purified wild-type enzyme and hinge-mutant ranged typically from 15 to 25 µmol/min/mg.

Preparation of N- and C-domain mixtures. Appropriate amounts of the two domains were initially mixed at 4 °C in preparation for folding studies at higher temperatures. Once the incubation temperature was raised, aliquots were removed at specific times, cooled immediately, and stored at 4 °C. After several days, all aliquots were assayed for CoA transferase activity under standard conditions. Results from control experiments indicated that no increase or decrease in enzyme activity occurred over background levels in mixtures of the domains stored at 4 °C for periods of at least 6 weeks.

A sample of N_2C_2 complex suitable for detailed biophysical analyses (including far-UV CD, fluorescence, ultracentrifugation, and light scattering studies) was generated by incubating an equimolar mixture of the N- and C-domains at 22 °C for 4 h. This sample was subsequently purified by gel filtration chromatography through a Sephacryl S-200 column using buffer A.

Amino acid analysis, Edman degradation sequencing, and mass spectrometry. Amino acid compositional analysis was carried out using standard procedures on a ninhydrin-based Beckmann 6300 instrument. Protein sequence analysis was performed using a 473A pulsed liquid/gas phase microsequencer from Applied Biosystems Incorporated (Foster City, CA). Standard cycles (ABI version 2.00) and Edman degradation chemistry were used. Mass analyses were performed on a Fisons VG Quattro triple quadrupole mass spectrometer (Manchester, UK) fitted with an electrospray ionization source operating in positive ion mode (Fenn et al., 1989; Smith et al., 1990; Mann & Wilm, 1995). Protein samples (10 µL of monomer, 50 pmol/µL in 0.2 M K[phosphate], 0.1 mM EDTA, 10 mM 2ME, pH 7.4) were injected into the electrospray source at a rate of 10 µL/min via a carrier solution of water:acetonitrile (1:1, v/v) containing 0.05% (v/v) trifluoroacetic acid (TFA). The quadrupoles were scanned at 10 s per scan for mass over charge ratios ranging from 600 to 1400. Data were acquired in the MCA mode, and 10 to 15 scans were typically summed to produce the final spectrum. Each molecular mass was determined as the mean value calculated for several multiply charged ions within a coherent series. Predicted molecular masses were average masses, calculated using the program MacProMass.

Circular dichroism and fluorescence studies. Far-UV CD measurements were carried out using a Jasco J-720 spectropolarimeter (Jasco Inc., Easton, MD) interfaced to an Epson Equity 386/25 computer and controlled by Jasco software. The thermostatted cell holder was maintained at 22 °C with a Lauda RMS circulating water bath (Lauda, Westbury, NY). The instrument was routinely calibrated with ammonium *d*-(+)-10-camphorsulfonate at 290.5 nm and 192 nm and with *d*-(-)-pantoyllactone at 219 nm. Each protein sample was diluted to a final concentration of 0.4 to 1 mg/mL in buffer X (0.2 M K[phosphate], 0.1 mM EDTA, 10 mM 2ME, pH 7.4).[4] The data of ten scans, each collected from 255 to 190 nm and measured at 0.025 nm intervals, were averaged. Noise reduction was applied to remove the high frequencies before calculating molar ellipticities. Mean residue ellipticities [Θ], with units of deg·cm^2·dmol^{-1}, were calculated from the following equation (Murray et al., 1969; Woody, 1995):

$$[\Theta] = ([\Theta]_{obs} \times MRW)/(10 \times l \times c),$$

where $[\Theta]_{obs}$ is the ellipticity measured in millidegrees, MRW is the mean residue molecular weight (molecular weight divided by the number of amino acid residues), c is the protein concentration (mg/mL), and l is the optical path length (cm). The voltage of the photomultiplier tube was maintained below 500 V to prevent distortion of the CD spectrum. A cuvette with a calibrated pathlength of 0.02 cm was used for all measurements. The following mean residue weights were used: wild-type enzyme, 108.687; hinge-mutant, 108.526; N-domain, 109.171; C-domain, 107.900; N + C complex (1:1), 108.563.

Fluorescence analyses were performed at 22 °C using a Perkin-Elmer MPF-44B spectrofluorometer linked to a differential corrected spectra unit (DSCU2). A cuvette with a calibrated pathlength of 1.0 cm was used for all measurements. Temperature control was achieved by means of a thermostatted cell holder and a Lauda RMS water bath. Baseline-corrected excitation and emission spectra were recorded using a bandwidth of 8 nm. Protein samples (0.07 to 0.3 mg/mL in buffer X) were excited at 295 nm in order to minimize energy-transfer effects due to proximal tyrosines. Absorbance measurements were performed on a Perkin Elmer Lambda 3 spectrophotometer.

Equilibrium unfolding studies. Equilibrium unfolding transitions were analyzed as outlined by Jaenicke & Rudolph (1986). Proteins were denatured overnight at 4 °C in buffer X containing different concentrations of GuHCl. Measurements of far-UV CD or fluorescence were carried out at 22 °C as described above.

Calculation of the apparent free energy of unfolding in the absence of denaturant. To facilitate the numerical analyses of thermodynamic parameters, a reversible "two-state" transition between the native and denatured forms was assumed throughout these studies (Pace, 1975; Pace, 1986; Shortle, 1989).[5] The apparent free energy of unfolding in the absence of denaturant ($[\Delta G_u^{H_2O}]_{app}$) was estimated for the monomeric C-domain by fitting the data to the following equations (Pace, 1975; Pace, 1986; Shortle, 1989; Milla et al., 1993):

$$y = f_u (y_u + ds[\text{GuHCl}]) + (1 - f_u)(y_n + ns[\text{GuHCl}])$$

$$f_u = K_{d,app}/(1 + K_{d,app})$$

$$K_{d,app} = \exp\{(-[\Delta G_u^{H_2O}]_{app} + m[\text{GuHCl}])/RT\}$$

where y is the observed ellipticity ($[\Theta]_{obs}$) or the maximal wavelength of tryptophan fluorescence ($\lambda_{max.em}$) at a given concentration of GuHCl; y_n and y_u are the extrapolated ordinate-intercept values of $[\Theta]_{obs}$ or $\lambda_{max.em}$ for the native and unfolded protein, respectively; ns and ds are the slopes of the baselines for the native and denatured protein, respectively; f_u is the molar fraction of unfolded protein; $K_{d,app}$ is the apparent equilibrium dissociation constant; R is the universal gas constant (8.31 J/mol·K); T is the absolute temperature (K); and m is a constant proportional to the increase in the solvent-accessible surface area of the protein upon denaturation (Schellman, 1978; Myers et al., 1995).

The wild-type enzyme and N-domain would be expected to undergo concentration-dependent unfolding transitions, given that both are homodimers (see "Results"). Therefore, values of $[\Delta G_u^{H_2O}]_{app}$ were estimated for these molecules by fitting the data to the following equations (De Francesco et al., 1991; Milla et al., 1993):

$$y = f_u (y_u + ds[GuHCl]) + (1-f_u)(y_n + ns[GuHCl])$$

$$f_u = \{-K_{d,app} + ([K_{d,app}]^2 + 8P_t K_{d,app})^{0.5}\}/(4P_t)$$

$$K_{d,app} = \exp\{(-[\Delta G_u^{H_2O}]_{app} + m[GuHCl])/RT\}$$

where P_t is the total concentration of monomeric protein in mol/L.

The data were fit to the appropriate equations using the program TableCurve 2D (Jandel Scientific, San Rafael, CA), with r^2 values generally exceeding 0.98. Errors are reported as the standard errors given by the program. Typically, a reliable estimate of ns could not be obtained from measurements of far-UV CD or fluorescence, due to the small number of points in the pre-transition region of the denaturation curve. In such cases, ns was taken to be equal to zero. This assumption was reasonable, given that the values of y in the pre-transition region did not differ greatly from y_n.

Crosslinking studies. Purified proteins (diluted to 1 mg/mL in 0.15 M NaCl, 1 mM DTT) were incubated for 4-5 h at 4 °C with the crosslinking agents bis(sulfosuccinimidyl) suberate (BS^3) or 3,3'-dithio bis(sulfosuccinimidylpropionate) (DTSSP) at final crosslinker concentrations of 1-2 mM. The reactions were quenched by the addition of Tris-HCl (pH 7.4) to a final concentration of 50 mM. Crosslinked samples were then analyzed by SDS-PAGE under both reducing and non-reducing conditions (DTSSP-crosslinked proteins) or under reducing conditions only (BS^3-crosslinked proteins) and visualized by staining with Coomassie Brilliant Blue.

Sedimentation equilibrium analyses. Molecular weight determinations were made using the conventional sedimentation equilibrium technique (Chervenka, 1970). Prior to centrifugation, protein solutions (1.5 mL, 1 to 2 mg/mL) were dialyzed for 48 h at 4 °C against 1 L of buffer G (50 mM K[phosphate], 0.15 M KCl, 1 mM EDTA, 10 mM 2ME, pH 7.4), using a semi-permeable membrane with a MWCO of 1.2 × 10^4. Protein samples were analyzed at 20 °C except for the C-domain, which was analyzed at 10 °C to avoid complications due to aggregation. Sedimentation equilibrium runs were carried out for 48 h using a Beckman Model E Analytical Ultracentrifuge equipped with Rayleigh interference optics. The initial concentration of the protein solutions was determined by the fringe count method (Babul & Stellwagen, 1969), assuming 4.1 fringes per mg of protein. Apparent weight-average molecular weights were calculated from the slope of ln(y) vs r^2 plots, after fitting the sedimentation equilibrium data to a second-degree polynomial equation using least-squares techniques. The partial specific volume for each sample was calculated based on the corresponding amino acid composition (Cohn & Edsall, 1943).

The combined sedimentation equilibrium data from multiple runs of the N-domain were analyzed using the program NONLIN (Nonlinear Least Squares Analysis of Sedimentation Equilibrium Data) of Johnson et al. (1981). Specifically, the data were fit to the equation:

$$c_{\text{total}} = \delta c + \sum_{i=1}^{n} C_i(r) = \delta c + \sum_{i=1}^{n} K_{1,i}\, C_1(r)^{q(i)}$$

where δc is the concentration offset of the first data point, $C_i(r)$ is the concentration of the ith species at a radial distance r, n is the total number of species present in the model being used for fitting (ranging from 1 for no association to a maximum of 5), and $K_{1,i}$ and $q(i)$ are the association constant and the stoichiometry for the ith associated species, respectively. The term $C_1(r)$ was expanded to:

$$C_1(r) = C_{1,0} \exp[0.5\sigma(r^2 - r_0^2) - 2B \sum_{i=1}^{n} C_i(r)\,]$$

where $C_{1,0}$ is the concentration of monomer at the initial point of the data set, r_0 is the reference radial distance, B is the colligative second virial coefficient, and σ is the reduced molecular weight, defined by: $\sigma = M_1 (1-v\rho)\omega^2/RT$. In the latter equation, M_1 is the monomer molecular weight, v is the partial specific volume, ρ is the solvent density, and ω is the rotor speed in (radians per s). The parameters fitted by the program were δc, ln $C_{1,0}$, $q(i)$, ln $K_{1,i}$, σ, and B, with a confidence interval set at 95%. The convergence of a given variable was considered complete when the fractional change in the variance was less than 1×10^{-6}.

Light scattering procedures. Weight-average molecular weights were determined by light scattering measurements as previously described (Wyatt, 1993), using equipment purchased from Wyatt Technology Corporation (Santa Barbara, CA). Protein samples (1 to 2 mg/mL in buffer G) were injected manually onto a Superose 12 gel filtration column, equipped with vacuum solvent degasser, HPLC pump, pulse dampener, and in-line filters (pore sizes, 0.22 and 0.1 µm). At defined intervals along a peak eluted from the gel filtration column, data were collected for two parameters: (1) the intensity (R_Θ) of light scattered at multiple angles (Θ) relative to the incident beam, using a DAWN-F multi-angle laser light scattering photometer; and (2) the refractive index (n), using a Wyatt Optilab 903 interferometric refractometer. The protein concentration (c) was estimated from n assuming a value of 0.185 for the differential refractive index increment ($\delta n/\delta c$). The molecular weight of the protein at each point along the peak was derived from the ordinate intercept of a plot of $R_\Theta/(K^*c)$ vs $\sin^2[\Theta/2]$, where K^* is a constant for vertically polarized light. The apparent weight-average molecular weight was then calculated as the mean of the values determined across the entire peak.

Refolding studies in vitro. Wild-type CoA transferase (final concentration of the NC monomer, 10 µM) and the hinge-mutant (final concentration of each domain, 10 µM) were denatured in "unfolding" buffer (6.0 M GuHCl, 0.09 M Tris-HCl, 0.045 M KCl, 0.09 mM EDTA, 1 mM DTT, pH 8.0) at 22 °C for a minimum of 5 h. The solutions of the unfolded proteins were then diluted 1:50 (v/v) in "refolding" buffer (0.09 M Tris-HCl, 0.045 M KCl, 0.09 mM EDTA, 1 mM DTT, pH 8.0). Alternatively, the solutions of the unfolded enzymes were placed on a semi-permeable membrane (Millipore VM, pore size 0.05μm) and dialyzed against 600 mL of the same refolding buffer (Marusyk & Sergeant, 1980). In both cases, the samples were incubated for 90 min at 22 °C or 37 °C prior to being assayed for enzyme activity.

Kinetic data analysis. Kinetic data (Figures 2-7, 2-15B) were fit to single- or double-exponential curves using the program TableCurve 2D (Jandel). The data and best-fit curves were subsequently plotted using the program SigmaPlot (also from Jandel).

RESULTS

Synthesis of CoA transferase forms[6] *in E. coli*. To generate the material necessary to examine the folding properties of pig heart CoA transferase *in vivo*, the plasmids pT7-WT and pMS-WT were prepared. Both plasmids encode the wild-type enzyme in its mature form (Figure 2-1). Subsequent transfection of *E. coli* HB101 with pMS-WT yielded the strain HB-WT. Lysates recovered from these cells, grown in the presence of 1 mM IPTG for 8-12 h at 25 °C, typically yielded 0.5 unit (μmol/min) of enzyme activity per mg total protein (Figure 2-2, lane 2).[7] In addition, these lysates were correspondingly enriched with a polypeptide whose apparent molecular weight (estimated by SDS-PAGE) was similar to the value of 5.2×10^4 predicted for mature pig heart CoA transferase (Figure 2-2, lane 2 versus lane 1).

If the hydrophilic segment linking the N- and C-domains of CoA transferase were necessary for the proper folding of the enzyme, then a mutant form of CoA transferase in which the N- and C-domains are physically separated (referred to as the "hinge-mutant") should not be properly assembled *in vivo*. A gene encoding such a hinge-mutant was constructed by incorporation of a stop codon and a reinitiation site in the portion of the DNA corresponding to the hydrophilic linker (see "Experimental Procedures" and Figure 2-1). This mutant gene was subsequently expressed in the strain HB-Hng, grown in the

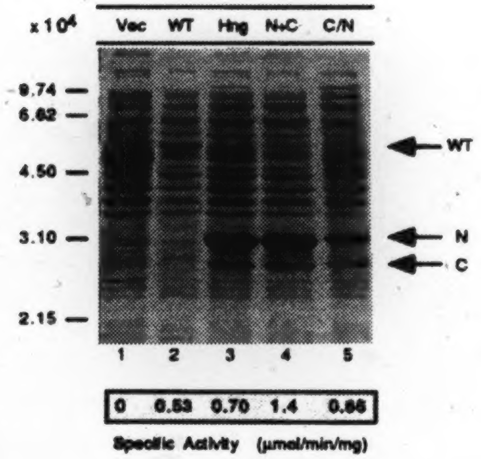
x 10^4
Vec
WT
Hng
N+C
C/N
9.74
6.62
4.50
3.10
2.15
WT
N
C
1
2
3
4
5
0
0.53
0.70
1.4
0.66
Specific Activity (µmol/min/mg)

Figure 2-2: Production of soluble CoA transferase polypeptides in *E. coli*. Lysates from cells grown for 8 h at 25 °C in the presence of 1 mM IPTG were analyzed by SDS-PAGE with Coomassie-Blue staining (top) and enzyme assay (bottom). Lane 1, HB-pMS119EH vector control; lane 2, HB-WT; lane 3, HB-Hng; lane 4, HB-N+C; lane 5, HB-C/N. Each lane was loaded with 30 µg of total cell lysate protein. Bands representing the 5.2×10^4 wild-type subunit (WT), 2.7×10^4 N-domain (N), and 2.4×10^4 C-domain (C) are indicated by appropriately labeled arrows. Enzyme activities were measured with an assay solution of 50 mM Tris-HCl, 15 mM $MgCl_2$, 0.30 mM succinyl-CoA, and 67 mM acetoacetate, at pH 9.1.

presence of 1 mM IPTG for 8-12 h at 25 °C. Two proteins with apparent molecular weights similar to those predicted for the N- and C-domains (2.7×10^4 and 2.4×10^4, respectively) were evident in the lysates prepared from these cells and examined by SDS-PAGE (Figure 2-2, lane 3). The specific enzyme activity measured in these lysates was comparable to that observed in lysates recovered from the strain HB-WT (Figure 2-2, lane 3 versus lane 2). Thus, an intact linker region is not essential for the formation of active CoA transferase produced in *E. coli*.

Next, it was considered that the hinge-mutant may be correctly folded and assembled only upon translation of a polycistronic mRNA, which might permit a crucial interaction between the two nascent polypeptide chains prior to or immediately following the completion of protein synthesis. If this were true, then active enzyme would not be assembled from N- and C-domain proteins encoded within separate transcription units. This hypothesis was first addressed by generating two plasmids (pMS-N and pMK-C), each containing, respectively, the gene for the N- and C-domain of CoA transferase (see "Experimental Procedures" and Figure 2-1). These genes were subsequently co-expressed in a strain of *E. coli* (HB-N+C) which harbored both plasmids. Analysis of the lysates from these cells by SDS-PAGE revealed that the N- and C-domain polypeptides were present at levels similar to those observed in the soluble fraction prepared from HB-Hng cells (Figure 2-2, lane 4). The presence of these proteins in the HB-N+C cell lysates once again correlated with a substantial amount of CoA transferase activity. Finally, due to uncertainties concerning the relative copy-number of the pMS-N and pMK-C vectors in the strain HB-N+C, the plasmid pMS-C/N was designed to carry the genes encoding the N- and C-domains downstream of two separate promoters (see "Experimental Procedures" and Figure 2-1). Results similar to those described above were also observed in cell lysates recovered from the strain HB-C/N (Figure 2-2, lane 5). Thus, the N- and C-domains of the hinge-mutant of CoA transferase need not be synthesized from sequential genes within the same operon in order to assemble correctly and form active enzyme *in vivo*.

Interestingly, a higher level of CoA transferase activity was detected in lysates of cells which produced the hinge-mutant than in lysates recovered from HB-WT (Figure 2-2, lane 3 versus lane 2). This observation was unexpected, given the assumption that the specific activity of the nicked form of CoA transferase is identical to that of the intact enzyme (Chapter 1). It was predicted that the unequal specific enzyme activities measured in lysates of HB-WT and HB-Hng cells reflected differences in the levels of synthesis and/or solubilities of CoA transferase in these strains. To verify this hypothesis, the intact enzyme and the hinge-mutant were purified from cultures of BL-E344A[8] and BL-Hng, respectively. Both forms were separated with equal efficiency from other proteins by successive elutions from columns of DEAE-Sephacel, Sephacryl S-200, and Affi-Gel Blue (Figures 2-3, 2-4). The preparation of the hinge-mutant initially contained more N-domain than C-domain (Figure 2-4A,B), which was consistent with the relative amounts of the two domain polypeptides observed in lysates of HB-Hng cells (Figure 2-2, lane 3). This excess N-domain bound to DEAE-Sephacel more tightly than the hinge-mutant (Figure 2-4A), and was therefore almost completely removed after the initial ion-exchange step. The hinge-mutant was purified from the remaining excess N-domain by gel filtration through a column of Sephacryl S-200 (Figure 2-4B); as discussed below, this separation was possible because the N-domain is smaller than the hinge-mutant. Importantly, the specific activity of the hinge-mutant following purification was equivalent to that of purified wild-type CoA transferase. Thus, the hinge-mutant must be produced more efficiently and/or in more soluble form than the wild-type enzyme in *E. coli*, which would account for the different specific enzyme activities measured in cell lysates of HB-Hng and HB-WT.

Mixtures of the purified N- and C-domains. Given the observation that the N- and C-domains encoded from separate transcription units are properly assembled in *E. coli*, it

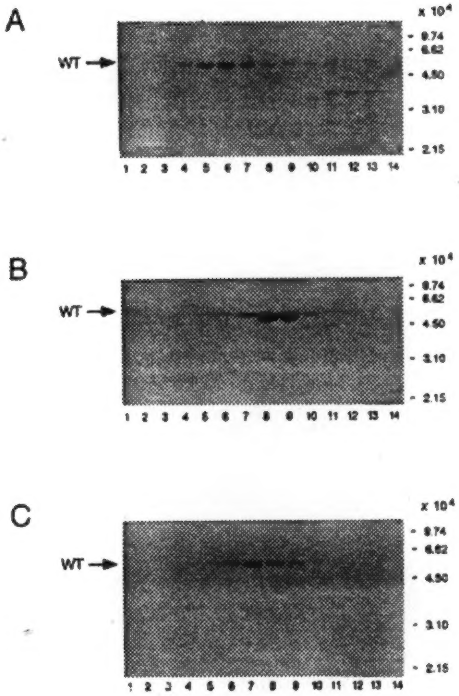

Figure 2-3: Purification of intact CoA transferase. Aliquots of fractions (30 μL) eluted from the three columns were analyzed by SDS-PAGE with Coomassie-Blue staining. (A) Fractions eluted from a column of DEAE Sephacel with buffer D, containing 0.11 to 0.23 M KCl (lanes 1 to 14). The fractions that were pooled eluted at 0.13 to 0.18 M KCl. (B) Fractions eluted from a column of Sephacryl S-200 with buffer A at 0.42 to 0.87 times the column volume (lanes 1 to 14). The fractions that were pooled eluted at 0.54 to 0.75 times the column volume. (C) Fractions eluted from a column of Affi-Gel Blue with buffer A containing 0.26 to 0.83 M KCl (lanes 1 to 14). The fractions that were pooled eluted at 0.42 to 0.76 M KCl. Bands representing the 5.2×10^4 intact subunit (WT) are indicated by appropriately labeled arrows.

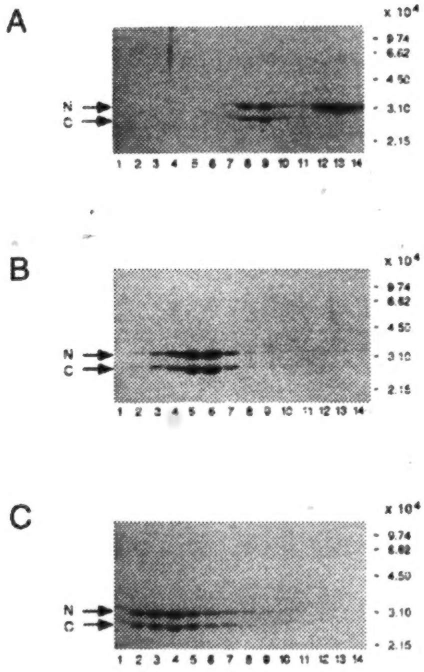
A
x 10⁴
9.74
6.62
4.50
3.10
2.15
N
C
1 2 3 4 5 6 7 8 9 10 11 12 13 14
B
x 10⁴
9.74
6.62
4.50
3.10
2.15
N
C
1 2 3 4 5 6 7 8 9 10 11 12 13 14
C
x 10⁴
9.74
6.62
4.50
3.10
2.15
N
C
1 2 3 4 5 6 7 8 9 10 11 12 13 14

Figure 2-4: Purification of the hinge-mutant. Aliquots of fractions (A: 20 µL; B or C: 30 µL) eluted from the three columns were analyzed by SDS-PAGE with Coomassie-Blue staining. (A) Fractions eluted from a column of DEAE Sephacel with buffer D containing 0.10 to 0.23 M KCl (lanes 1 to 14). The fractions that were pooled eluted at 0.16 to 0.19 M KCl. (B) Fractions eluted from a column of Sephacryl S-200 with buffer A at 0.52 to 0.98 times the column volume (lanes 1 to 14). The fractions that were pooled eluted at 0.55 to 0.75 times the column volume. (C) Fractions eluted from a column of Affi-Gel Blue with buffer A containing 0.38 to 0.84 M KCl (lanes 1 to 14). The fractions that were pooled eluted at 0.35 to 0.70 M KCl. Bands representing the 2.7×10^4 N-domain (N) and 2.4×10^4 C-domain (C) are indicated by appropriately labeled arrows.

was proposed that each domain may fold independently of the other, such that their final association consists of the docking of two polypeptides possessing their native folds. If this were true, then this docking event should be reproduced *in vitro* by mixing the two purified domains, leading to the rapid generation of full CoA transferase activity.

The individual N- and C-domains were isolated from the strains HB-N and HB-C, respectively, using methods similar to those described above for the purification of wild-type CoA transferase and the hinge-mutant. A visual demonstration of the final purity of the N- and C-domains by SDS-PAGE is provided in Figure 2-5A. Each domain was positively identified by Western blot analysis using a polyclonal antiserum raised against CoA transferase (Figure 2-5B). In addition, the first eight residues of each domain were identical to those predicted from the corresponding cDNA (Figure 1-9), assuming that the N-terminal methionine is removed prior to purification. Moreover, molecular masses of 27 050 Da and 24 468 Da (Figure 2-6) were determined for the N- and C-domains, respectively, by electrospray ionization mass spectrometry (ESI-MS). Each of these values corresponded very closely to the molecular weight predicted for the N- or C-domain polypeptide lacking its N-terminal methionine (Table 2-1), thus confirming the absence of additional post-translational modifications.

Next, the appearance of CoA transferase activity in equimolar mixtures of the purified N- and C-domains was examined. Initially, these domains were isolated in the absence of 2ME, given the observation that the recovery of large amounts of wild-type CoA transferase activity is not adversely affected by the omission of this reductant. A mixture of such N- and C-domains yielded no CoA transferase activity, even following a lengthy incubation at 22 °C. In contrast, a progressive increase in enzyme activity with apparent first-order kinetics (Figure 2-7A) was observed upon combining N- and C-domains (final concentration of each, 0.10 mM) that had been isolated in the presence of 2ME. A maximal specific activity of about 85% that of wild-type CoA transferase accumulated after a 2 h incubation at 22 °C. By repeating this experiment at different

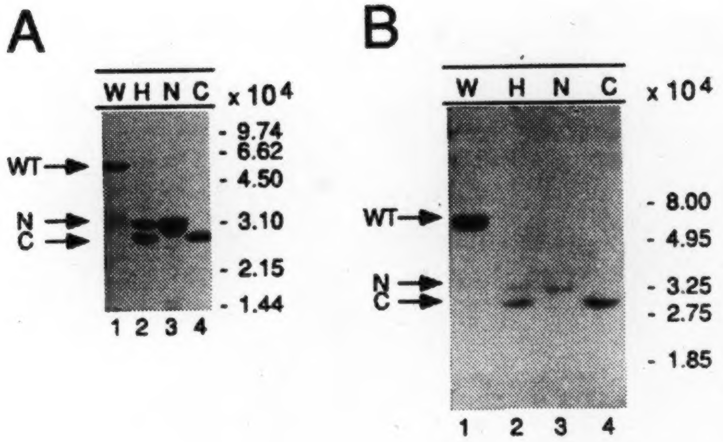
A
W H N C
x 10⁴
- 9.74
- 6.62
- 4.50
- 3.10
- 2.15
- 1.44
WT
N
C
1 2 3 4
B
W H N C
x 10⁴
- 8.00
- 4.95
- 3.25
- 2.75
- 1.85
WT
N
C
1 2 3 4

Figure 2-5: Purity of isolated CoA transferase polypeptides. Proteins were analyzed by SDS-PAGE with Coomassie-Blue staining (A) or Western blotting (B). Lane 1, wild-type CoA transferase (W); lane 2, hinge-mutant (H); lane 3, N-domain (N); lane 4, C-domain (C). Bands representing the 5.2×10^4 wild-type subunit (WT), 2.7×10^4 N-domain (N), and 2.4×10^4 C-domain (C) are indicated by appropriately labeled arrows. Each lane was loaded with approximately 3 μg (A) or 5 μg (B) of purified protein.

Figure 2-6: Identification of the N- and C-domains by ESI-MS. Approximately 500 pmol of the purified C-domain (A) or N-domain (B) were analyzed for molecular mass (see "Experimental Procedures"). Shown beside each peak is the number of protons associated with the corresponding ion.

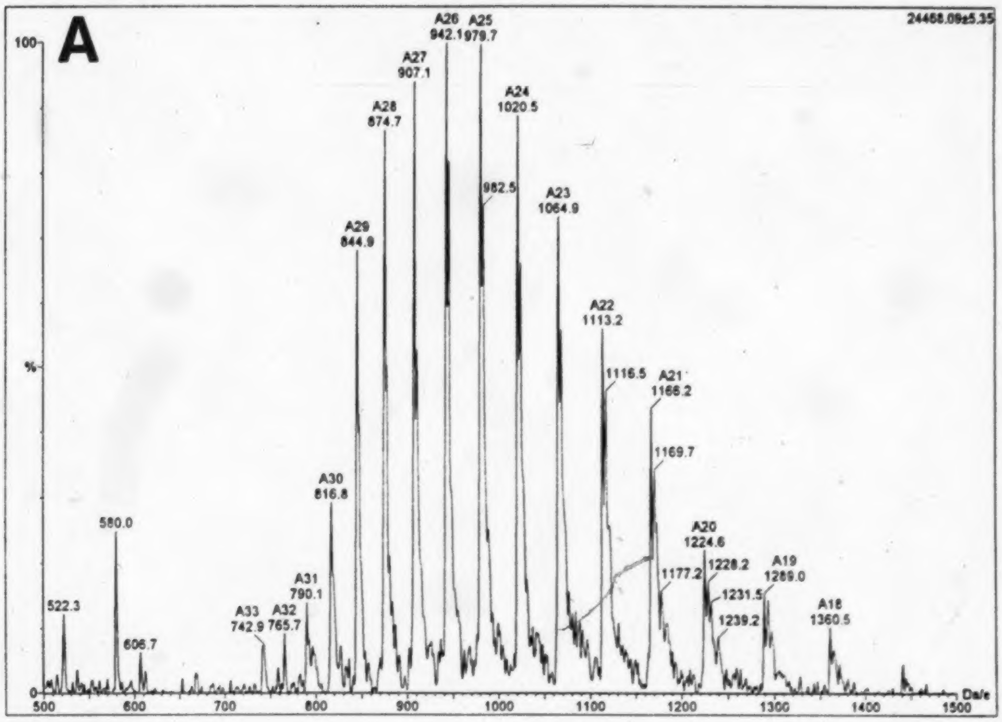
A
24468.09±5.35
100
%
0
A26
942.1
A25
979.7
A27
907.1
A28
874.7
A24
1020.5
982.5
A29
844.9
A23
1064.9
A22
1113.2
1116.5
A21
1166.2
1169.7
A30
816.8
580.0
A20
1224.6
1228.2
1177.2
A19
1289.0
A31
790.1
1231.5
522.3
A33
742.9
A32
765.7
A18
1360.5
1239.2
606.7
500
600
700
800
900
1000
1100
1200
1300
1400
1500
Da/e

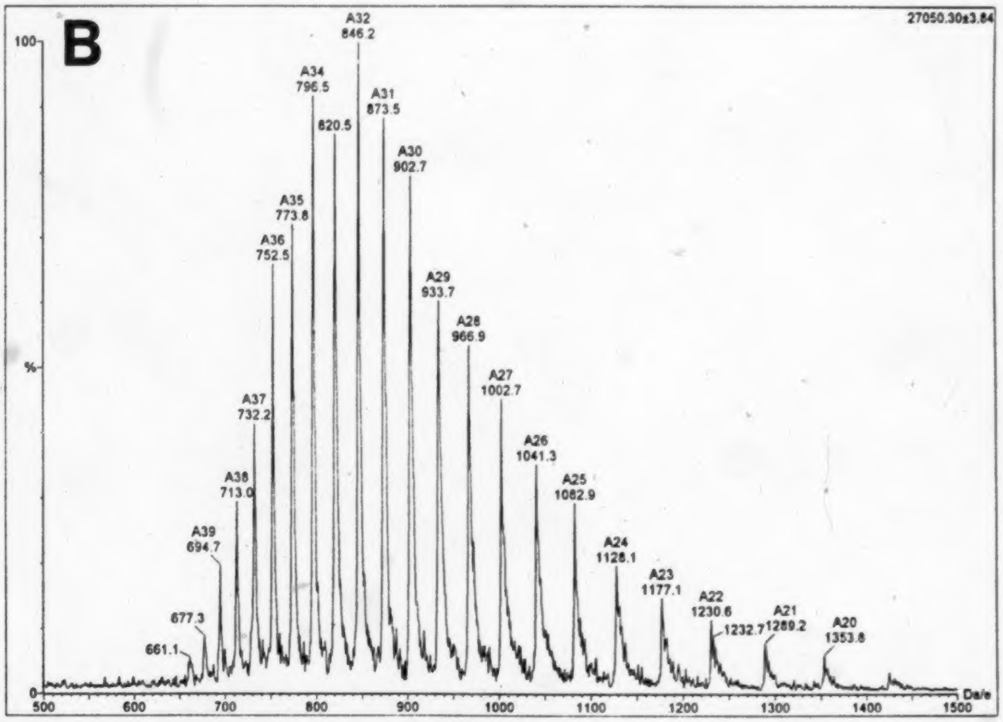
B
27050.30±3.84
100
%
0
A32
846.2
A34
796.5
A31
873.5
820.5
A30
902.7
A35
773.8
A36
752.5
A29
933.7
A28
966.9
A27
1002.7
A37
732.2
A26
1041.3
A38
713.0
A25
1082.9
A39
694.7
A24
1128.1
A23
1177.1
A22
1230.6
677.3
1232.7
A21
1289.2
A20
1353.8
661.1
500
600
700
800
900
1000
1100
1200
1300
1400
1500
Da/e

Table 2-1: Electrospray Mass Spectral Analysis of the N- and C-domains

Polypeptide fragment	Predicted mass ($M+H^+$ [Da])[a]	Experimental mass ($M+H^+$ [Da])	% Difference[b]
N-domain	27 052	27 050 ± 4	0.0074
C-domain	24 470	24 468 ± 5	0.0082

[a] Predicted masses are average masses, calculated using the program MacProMass by assuming the cleavage of the N-terminal methionine residue from each polypeptide produced in *E. coli*. The mass of the corresponding unmodified protein is obtained by adding 131 Da.

[b] Percent differences were calculated from the following equation:

$$\{|\text{Predicted Mass - Experimental Mass}| \div (\text{Predicted Mass})\} \times 100\%.$$

Figure 2-7: Kinetics of the formation of active CoA transferase in equimolar mixtures of the N- and C-domains. (A) Appearance of enzyme activity in mixtures of the purified N- and C-domain polypeptides (100 μM each). The mixtures were incubated at 8 °C (□), 16 °C (●), and 22 °C (○). The apparent first-order rate constants are: 8 °C, $k = 1.6 \times 10^{-6}$ s^{-1} ($r^2 = 0.98$); 16 °C, $k = 9.8 \times 10^{-5}$ s^{-1} ($r^2 = 0.95$); and 22 °C, $k = 5.4 \times 10^{-4}$ s^{-1} ($r^2 = 0.99$). (B) Arrhenius replot of the apparent first-order rate constants in (A), from which an E_a of $2.9 \pm 0.4 \times 10^2$ kJ/mol was calculated ($r^2 = 0.98$). (C) Concentration-dependence of the rate of enzyme formation. Mixtures of the purified N- and C-domain polypeptides, each at 10 μM (■), 20 μM (□), 50 μM (▲), or 100 μM (○), were incubated at 22 °C. The apparent first-order rate constants are: 10 μM, $k = 6.1 \times 10^{-5}$ s^{-1} ($r^2 = 0.98$); 20 μM, $k = 1.1 \times 10^{-4}$ s^{-1} ($r^2 = 0.99$); 50 μM, $k = 2.5 \times 10^{-4}$ s^{-1} ($r^2 = 0.98$); and 100 μM, $k = 5.4 \times 10^{-4}$ s^{-1} ($r^2 = 0.99$). All experiments were performed in duplicate, with an average relative error of ± 3% in (A) and (C). Enzyme activities were measured with an assay solution of 50 mM Tris-HCl, 15 mM $MgCl_2$, 0.060 mM succinyl-CoA, and 13 mM acetoacetate, at pH 9.1.

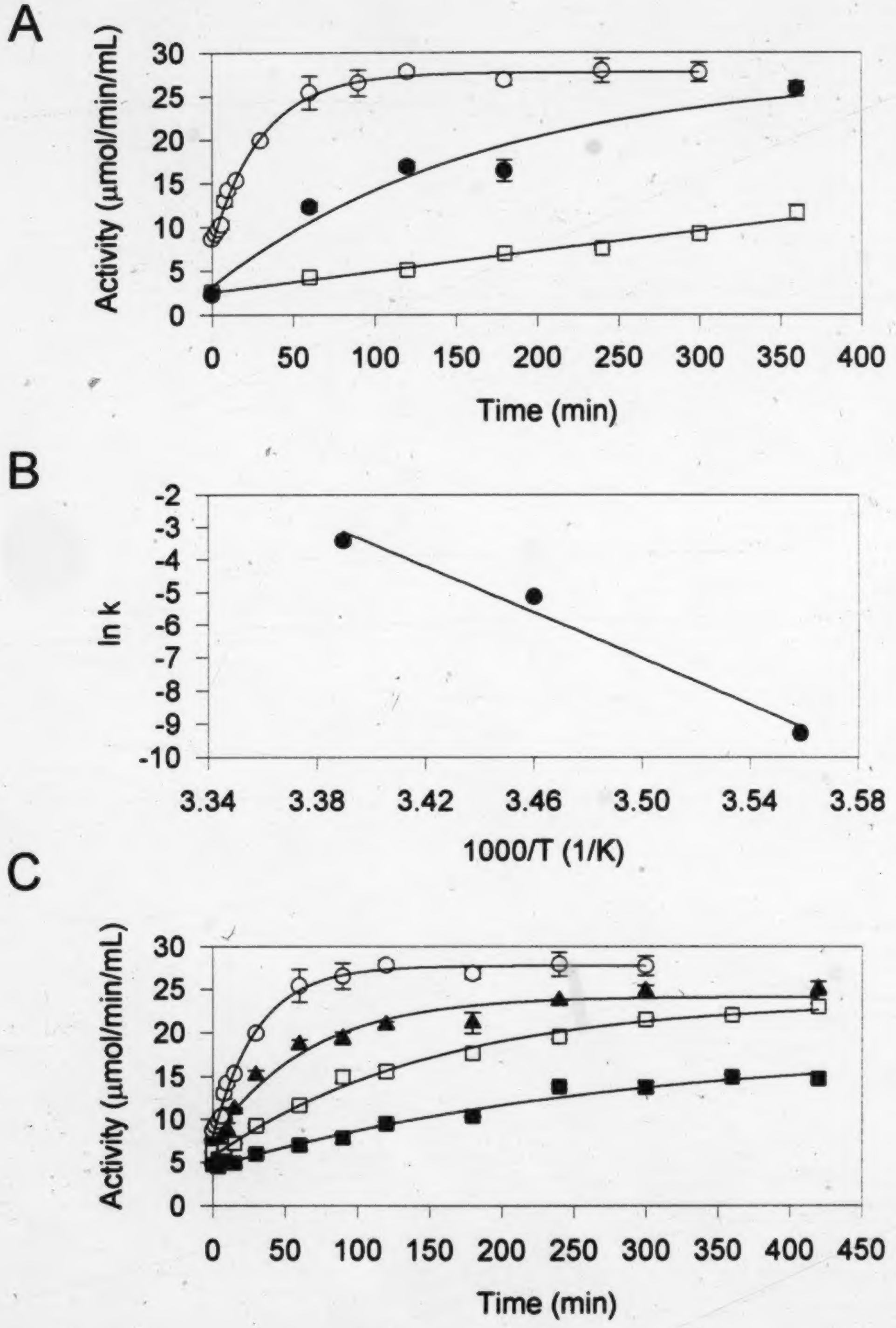
A
Activity (µmol/min/mL)
30
25
20
15
10
5
0
0
50
100
150
200
250
300
350
400
Time (min)
B
ln k
-2
-3
-4
-5
-6
-7
-8
-9
-10
3.34
3.38
3.42
3.46
3.50
3.54
3.58
1000/T (1/K)
C
Activity (µmol/min/mL)
30
25
20
15
10
5
0
0
50
100
150
200
250
300
350
400
450
Time (min)

temperatures, a value of $2.9 \pm 0.4 \times 10^2$ kJ/mol was calculated for the activation energy (E_a) associated with this process (Figure 2-7B). At 37 °C much of the protein became insoluble, and very little activity was recovered. Furthermore, no increase in activity was detected above background levels in mixtures incubated at 4 °C for extended periods.

Finally, the kinetics of assembly of the N- and C-domains to the active enzyme form were investigated. Activity measurements were performed on equimolar mixtures of the domains which had been diluted 1/2, 1/5, and 1/10 prior to their incubation for different lengths of time at 22 °C. Enzyme activity appeared with apparent first-order kinetics in all samples examined (Figure 2-7C). The fact that second-order kinetics were not observed suggested that the incubation required for the generation of active CoA transferase cannot be attributed to the irreversible association of the N- and C-domains already possessing a native fold. Instead, the observed rate of activity production may be limited by a structural rearrangement in the domains following their initial interaction. Pre-incubation of the individual domains at 22 °C did not alter the observed kinetics, indicating that each domain only achieves its native fold in the presence of the other.

Conformational changes in the N- and C-domains upon assembly to the active enzyme form. The folding of a polypeptide to its native state generally involves a progressive compaction due to the formation of secondary, tertiary, and quaternary structures (reviewed in [Jaenicke, 1991]; [Landry & Gierasch, 1994]; [Miranker & Dobson, 1996]). Since preliminary results implied that the purified N- and C-domains initially lack a native fold, conformational rearrangements associated with their assembly to the active enzyme form were probed for. For these studies, a sample of the N_2C_2-domain complex was generated and purified as described in "Experimental Procedures." The specific activity of this purified sample was 17 μmol/min/mg, equivalent to the level of wild-type enzyme.

First, far-UV CD spectra were recorded to estimate the secondary structure of the various engineered forms of CoA transferase. The spectrum recorded for the purified N-domain was characterized by a maximum near 195 nm and a minimum near 215 nm, most likely reflecting significant β-sheet and/or β-turn components (Figure 2-8A). The spectrum recorded for the purified C-domain was characterized by a maximum and minimum displaced to wavelengths lower than those of the N-domain spectrum, reflecting a mixture of random-coil and β-structure (Figure 2-8A). The secondary structure of each purified domain was estimated to be only about 20% α-helix, similar to the value predicted for the wild-type enzyme and the hinge-mutant. Attempts to use the method of trifluoroethanol (TFE) titration to determine the α-helix content more precisely (Chen et al., 1972; Jasanoff & Fersht, 1994) were unsuccessful, due to the propensity of all four proteins to precipitate in buffers containing 10 to 40% (v/v) TFE. The sum of the individual N- and C-domain spectra was clearly distinct from the profile recorded for an equimolar mixture of the two domains following incubation at 22 °C (Figure 2-8B). Moreover, the latter spectrum was very similar to that determined for the wild-type enzyme or the hinge-mutant (Figure 2-8B). The relationships between the observed and summed spectra were emphasized by the corresponding difference spectra, each of which revealed a strong positive signal near 200 nm and a much weaker negative signal near 220 nm (Figure 2-8C). These results were most consistent with the productive assembly of the N- and C-domains being associated with a conversion of random coil to β-structure (Murray et al., 1969; Woody, 1995). Finally, the sum of the spectra recorded for the individual domains was very similar to the profile determined for a mixture of the domains which was preincubated at 4 °C instead of 22 °C. These results suggested that: (1) the two domains do not assemble to form a complex at 4 °C; and (2) they assume an overall secondary structure similar to that of wild-type CoA transferase when they assemble after incubation at a permissive temperature.

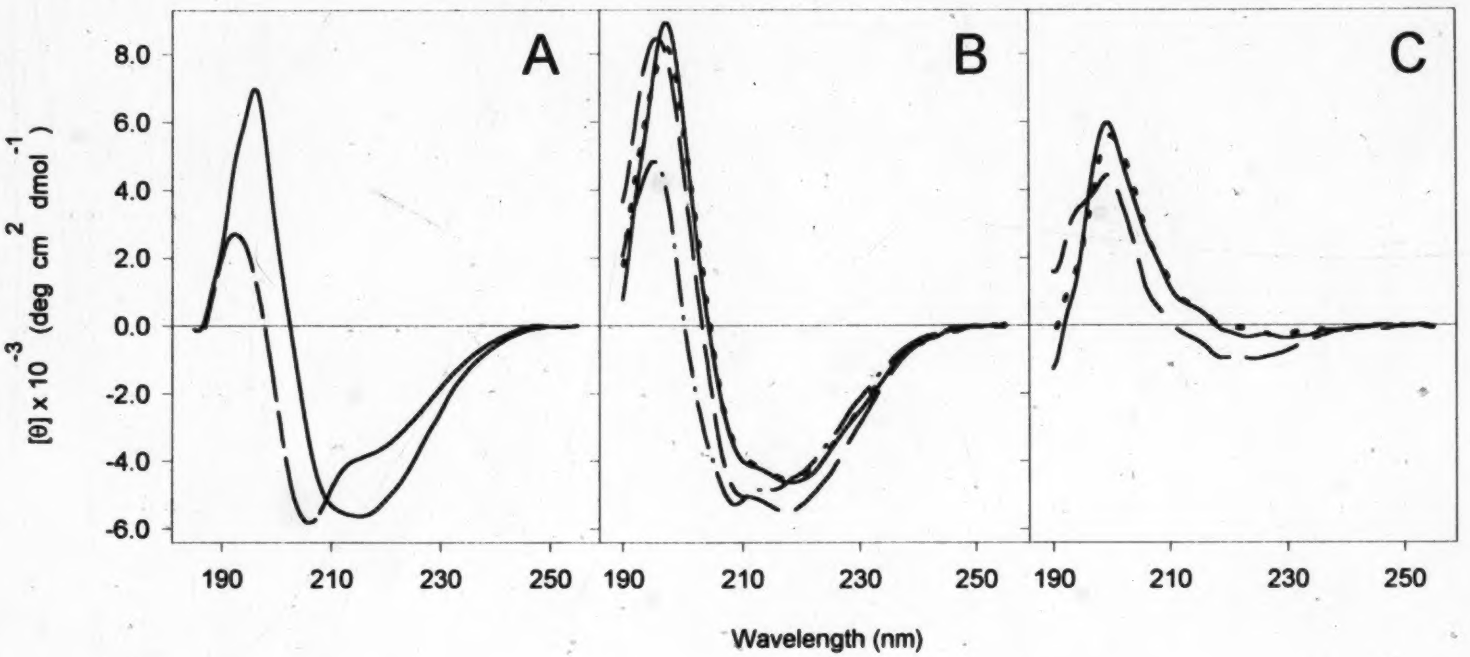

Figure 2-8: Analysis of the assembly of the N- and C-domains by far-UV CD. (A) Spectra representing the N-domain (——) and C-domain (– – –). (B) Spectra representing wild-type CoA transferase (– – –), the hinge-mutant (——), the complex of N- and C-domains formed at 22 °C (· · · ·), and the summed N- and C-domain curves (– · –). (C) Difference spectra derived by subtracting the summed N- and C-domain curves from the curves recorded for wild-type CoA transferase (– – –), the hinge-mutant (——), and the complex of N- and C-domains formed at 22 °C (· · · ·).

Second, given that the N- and C-domains contain one and two tryptophan residues (respectively), measurements of intrinsic fluorescence were carried out in order to study further the conformational rearrangements associated with the assembly of the domains to the active enzyme form (Table 2-2). Excitation at 295 nm produced a wavelength of maximal fluorescence ($\lambda_{max,em}$) of 338 nm with the N-domain and 343 nm with the C-domain. These maxima were significantly red-shifted relative to the $\lambda_{max,em}$ value of 335 nm determined upon the excitation at 295 nm of the wild-type enzyme, hinge-mutant, or pre-assembled N- and C-domains (Table 2-2). Moreover, the $\lambda_{max,em}$ determined for the purified C-domain most closely resembled the $\lambda_{max,em}$ value of 346 nm recorded for each of these proteins in 6.0 M GuHCl (Table 2-2). The intrinsic tryptophan fluorescence of each polypeptide was further assessed by measuring its sensitivity to quenching by acrylamide, a property reflected by the magnitude of K_{S-V}, the Stern-Volmer constant (Martin et al., 1991). The K_{S-V} estimates revealed that the intrinsic fluorescence of the purified N- and C-domains was more sensitive to acrylamide quenching than that of the wild-type enzyme, hinge-mutant, or pre-assembled complex (Table 2-2). Moreover, the K_{S-V} value determined for the C-domain was closest to that calculated for free tryptophan in solution (Table 2-2), consistent with the fluorescence spectra described above. Together, these results indicated that: (1) the tryptophan residue(s) of each purified domain is (are) more exposed to solvent than those of the wild-type enzyme; and (2) the tryptophan residues of the purified C-domain are, on average, more accessible to solvent than that of the N-domain.

Third, the quaternary structures of the two purified domains and the complex produced by their mixing and subsequent incubation were investigated. Sedimentation equilibrium (Figure 2-9) revealed that the individual N- and C-domains are dimeric and monomeric, respectively, in benign buffer (summarized in Table 2-3). The absence of stable oligomers in the C-domain preparation was verified by light-scattering studies (Figure 2-10; Table 2-3). Attempts to calculate a dissociation constant for the N-domain

Table 2-2: Fluorescence Properties of Engineered CoA Transferase Proteins

Sample[a]	$\lambda_{max,em}$[b] (nm)	$K_{S\text{-}V}$ (acrylamide)[c] (M^{-1})
Wild-type		
Native	335.1	3.82 ± 0.22[d]
6M GuHCl	346.2	
Hinge-mutant		
Native	335.4	3.46 ± 0.09[d]
6M GuHCl	346.5	
N-domain		
Native	338.1	8.41 ± 0.30[e]
6M GuHCl	346.0	
C-domain		
Native	342.6	10.30 ± 0.08[e]
6M GuHCl	346.6	
Domain mixture[f]		
Native	335.4	3.64 ± 0.06[e]
6M GuHCl	346.2	
Tryptophan	348.0	19.46 ± 0.18[e]

[a] Protein samples were prepared as 0.07 mg/mL solutions in 0.2 M K[phosphate], 0.1 mM EDTA, 10 mM 2ME (pH 7.4). A standard solution of tryptophan (1.8 mg/mL) was prepared using the same buffer.

[b] Wavelength of maximal tryptophan fluorescence; excitation at 295 nm.

[c] Stern-Volmer constant for quenching by acrylamide, according to the relation:

$$F_0/F = 1 + K_{S\text{-}V}[\text{acrylamide}].$$

Note that the Stern-Volmer plots were linear for acrylamide concentrations ranging from 0 to 0.4 M.

[d] Average of three experiments; error is sample standard deviation.

[e] Average of two experiments; error is deviation from mean.

[f] Equimolar mixture of the N- and C-domains.

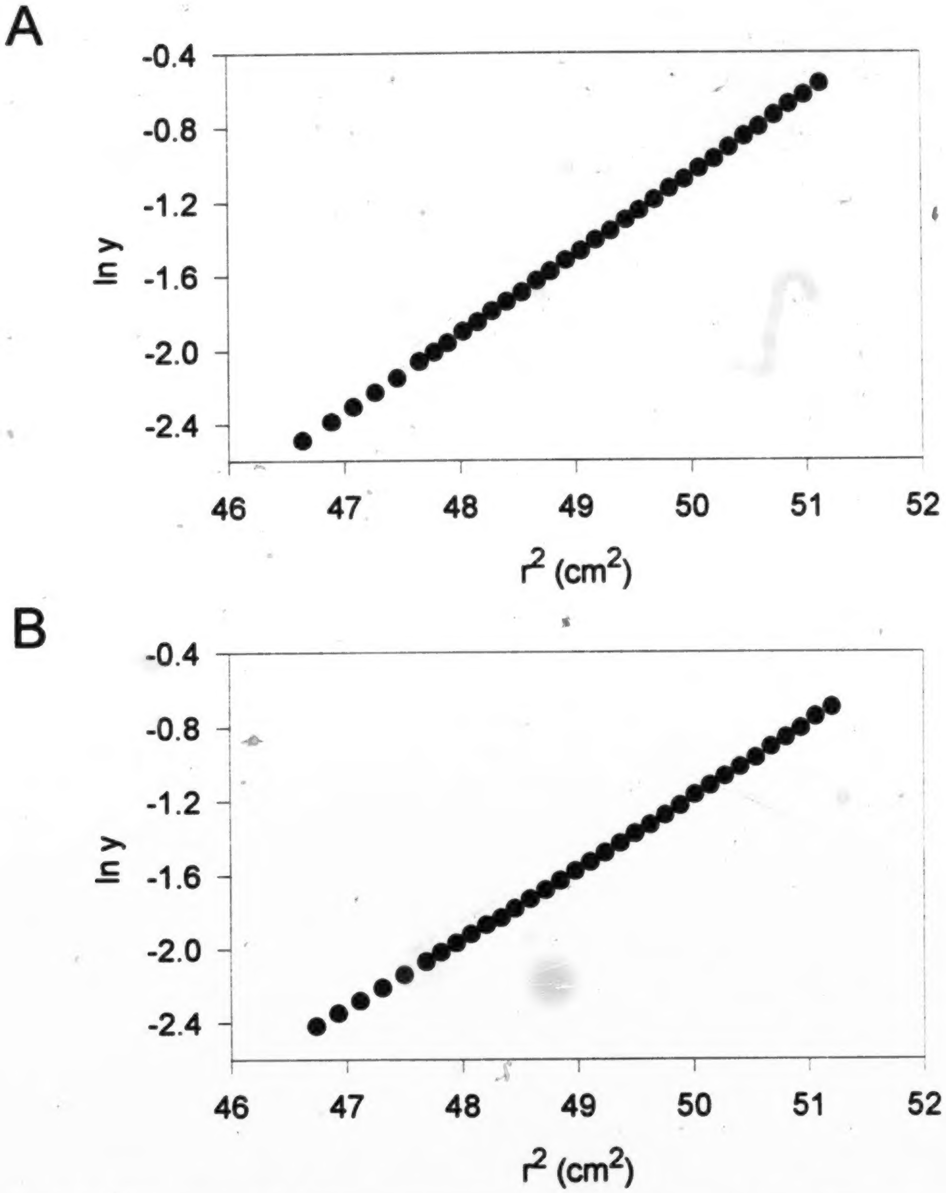

Figure 2-9: Molecular weight determinations for the N- and C-domains by sedimentation equilibrium. Apparent weight-average molecular weights of $5.32 \pm 0.004 \times 10^4$ ($r^2 = 1.0$) for the N-domain (A) and $2.46 \pm 0.01 \times 10^4$ ($r^2 = 1.0$) for the C-domain (B) were determined as described in "Experimental Procedures." Note that both ln y vs r^2 plots are linear, indicating that neither of the two domain polypeptides undergoes association or dissociation at the protein concentrations examined. The errors are the standard errors given by TableCurve 2D.

Table 2-3: Quaternary Structures of Engineered CoA Transferase Proteins

Protein	M_w (x10^4)[a]	M_w (x10^4)[b]	4° Structure[c]
Wild-type[d]	9.15	ND[e]	$(N\sim C)_2$
Hinge-mutant	9.22	11.1	N_2C_2
N-domain	5.32	ND	N_2
C-domain	2.46	2.52	C
Domain mixture[f]	ND	10.2	N_2C_2

[a] Weight-average molecular weight determined by sedimentation equilibrium.
[b] Weight-average molecular weight determined by light scattering.
[c] Quaternary structure: N, N-domain; C, C-domain; and ~, hydrophilic linker.
[d] Data taken from White & Jencks, 1976.
[e] ND, not determined.
[f] Equimolar mixture of the N- and C-domains.

Figure 2-10: Molecular weight determination of the C-domain by light-scattering. A sample of the C-domain eluted from a Superose 12 gel filtration column was analyzed as described in "Experimental Procedures." Top panel: elution curves. Background curves (numbered 9-15) correspond to the intensity of light scattered at angles (Θ) of 64.9°, 77.1°, 90.0°, 102.9°, 115.1°, 126.0°, and 135.5°. The foreground curve, denoted "ri," represents the refractive index relative to the reference solvent. The relative refractive index is proportional to the concentration of the eluted protein. Bottom panel: calculated molecular weights (+) plotted at regular intervals along the elution peak, which is shown as the relative refractive index across a range of volumes. From these molecular weights, an apparent weight-average molecular weight of 2.52×10^4 was determined for the C-domain.

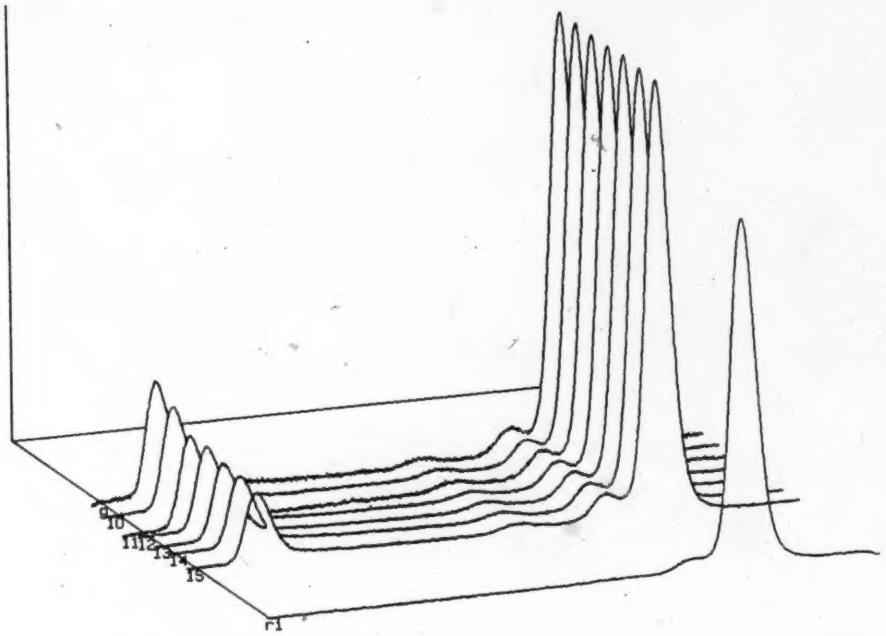
9
10
11
12
13
14
15
r1

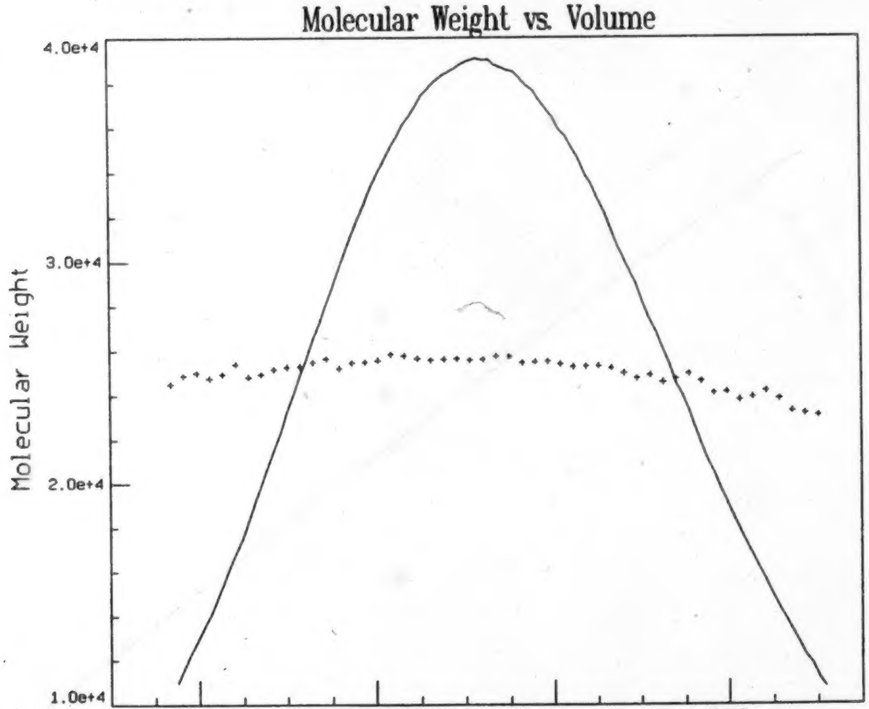
Molecular Weight vs. Volume
Molecular Weight
4.0e+4
3.0e+4
2.0e+4
1.0e+4
13.6
13.8
14.0
14.2
Volume (ml)

homodimer by repeating the sedimentation equilibrium analysis with different initial protein concentrations and rotor speeds were unsuccessful, since the data for each of these experiments were best fit to a single-species model (Figure 2-11). In addition, sedimentation equilibrium and light-scattering studies (Figure 2-12; Table 2-3) indicated that the hinge-mutant and the complex assembled from the isolated domains contain two of each domain (N_2C_2). This result was consistent with previous sedimentation equilibrium analyses of the wild-type enzyme by White & Jencks (1976), who proposed that CoA transferase is a homodimer consisting of two N-domains and two C-domains.

Results consistent with those described above were obtained from SDS-PAGE analysis of the purified polypeptides treated with the bifunctional crosslinking agents BS^3 (Figure 2-13) or DTSSP (Figure 2-14). For all proteins examined, crosslinking with DTSSP was less efficient than with BS^3, and fully reversible in the presence of 2ME (Figure 2-14, panel A versus panel B). Incubation of the N-domain with either reagent led to the formation of a protein product with a molecular weight approximately twice that of the N-domain monomer (Figure 2-13A, lane 2 and 2-14B, lane 2). In contrast, most of the treated C-domain was absent from the polyacrylamide gel (Figure 2-13A, lane 4; Figure 2-14B, lane 3), perhaps due to denaturation and precipitation following the covalent modification of the protein by the crosslinking agent. The crosslinking of the N-domain by BS^3 was not diminished in the presence of a large excess of C-domain (Figure 2-13C), confirming that the interaction between two N-domain monomers was specific and stable. In addition, the crosslinking of an equimolar mixture of the N- and C-domains which had been preincubated at 12 °C for 32 h[9] (Figure 2-13A, lane 6; Figure 2-14B, lane 1) led to the formation of a protein product with a molecular weight approximately equal to 5×10^4. This species, presumably a complex containing one of each domain, was also observed for the purified wild-type enzyme and hinge mutant following their treatment with crosslinking agent (Figure 2-13B; Figure 2-14B, lanes 4 and 5). However, a band corresponding to a protein product of molecular weight 1.0×10^5 was not detected,

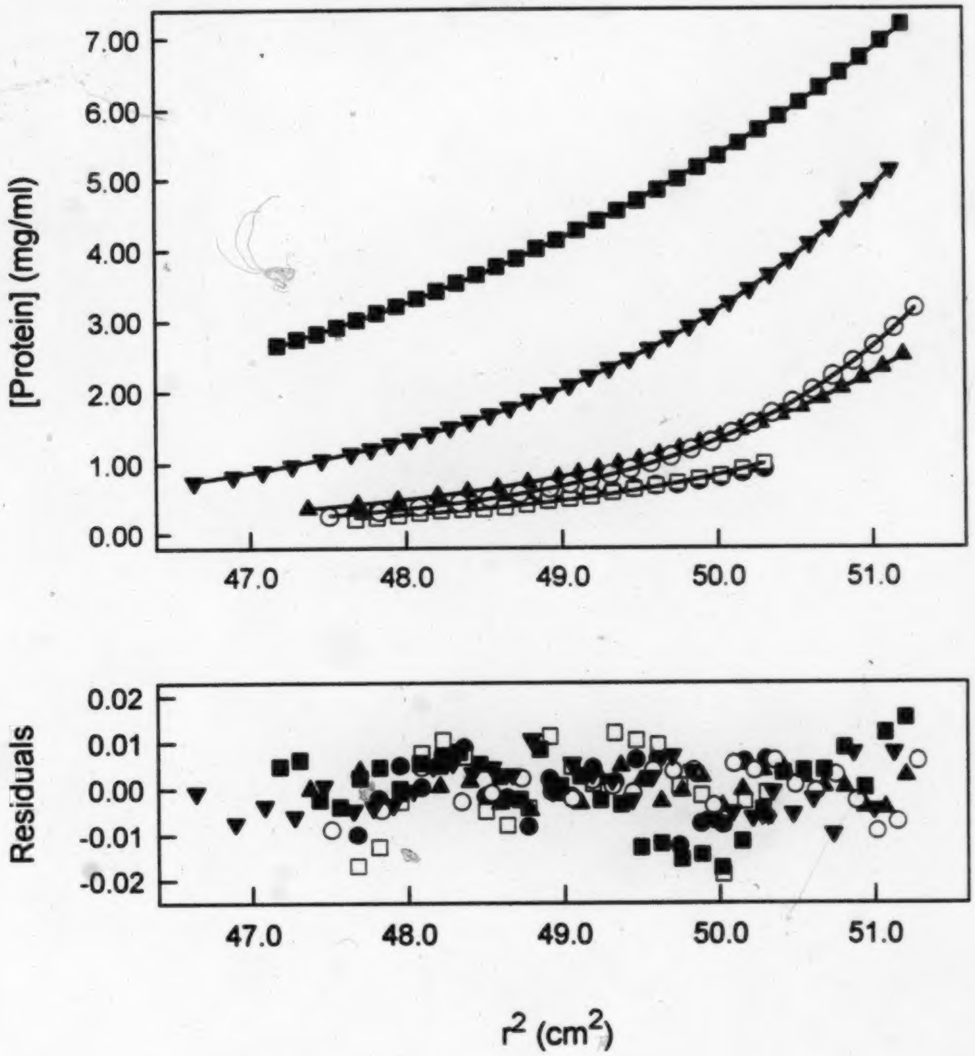

Figure 2-11: N-domain sedimentation equilibrium data fit to a single-species model. The N-domain (in 50 mM K[phosphate], 150 mM KCl, 1 mM EDTA, 10 mM 2ME, pH 7.4) was analyzed by ultracentrifugation for 48 h at 20 °C. Top panel: data from six runs were fit to curves consistent with a single-species model by the program NONLIN. Bottom panel: residuals from the six curves were combined and plotted using the same symbols as in the top panel. The initial loading concentrations and rotor speeds were: 0.69 mg/mL, 1.2×10^4 rpm (●); 0.69 mg/mL, 1.4×10^4 rpm (☐); 1.06 mg/mL, 1.3×10^4 rpm (▲); 1.06 mg/mL, 1.5×10^4 rpm (○); 2.25 mg/mL, 1.2×10^4 rpm (▼); 4.48 mg/mL, 9.0×10^3 rpm (■). The goodness of the fit was apparent from the random scatter in the residual plot and the low magnitude of the square-root of the variance (6.5×10^{-3}).

Figure 2-12: Molecular weight determination of the hinge-mutant by light-scattering. A sample of the hinge-mutant eluted from a Superose 12 gel filtration column was analyzed as described in "Experimental Procedures." Top panel: elution curves. Background curves (numbered 9-14) correspond to the intensity of light scattered at angles (Θ) of 64.9°, 77.1°, 90.0°, 102.9°, 115.1°, and 126.0°. The foreground curve, denoted "ri," represents the refractive index relative to the reference solvent. Bottom panel: calculated molecular weights (+) plotted at regular intervals along the elution peak, which is shown as the relative refractive index across a range of volumes. From these molecular weights, an apparent weight-average molecular weight of 1.11×10^5 was determined for the hinge-mutant.

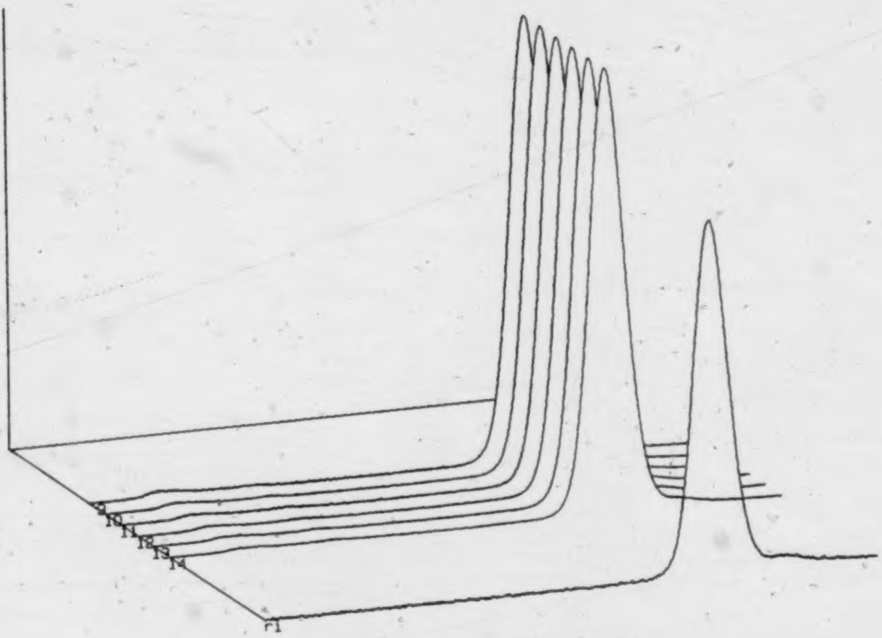
9
10
11
12
13
14
r1

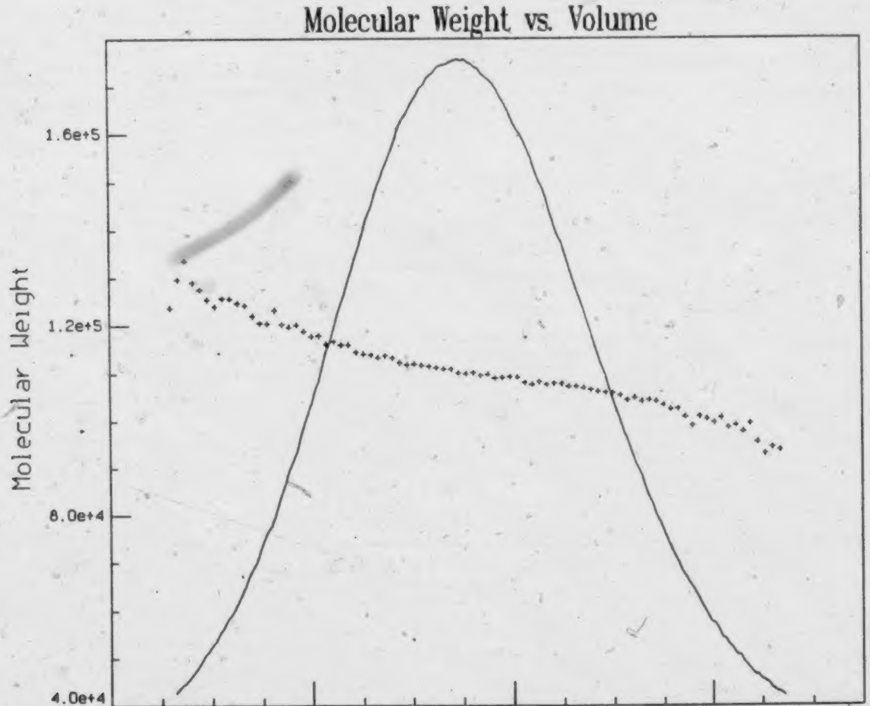
Molecular Weight vs. Volume
Molecular Weight
1.6e+5
1.2e+5
8.0e+4
4.0e+4
11.2
11.6
12.0
12.4
Volume (ml)

Figure 2-13: Molecular weight determinations by crosslinking with BS^3. Proteins were analyzed by SDS-PAGE with Coomassie-Blue staining. (A) The purified N-domain (lanes 1 and 2) and C-domain (lanes 3 and 4), and an equimolar mixture of the N- and C-domains (100 μM each), preincubated at 12 °C for 32 h (lanes 5 and 6), were incubated in the absence (lanes 1, 3, and 5) or presence (lanes 2, 4, and 6) of BS^3 (final concentration 2 mM). (B) Wild-type CoA transferase (lanes 1 and 2) and the hinge-mutant (lanes 3 and 4) were incubated in the absence (lanes 1 and 3) or presence (lanes 2 and 4) of BS^3 (final concentration 2 mM). (C) The purified N-domain was treated with BS^3 (final concentration, 1 mM) in the absence (lanes 1, 3, and 5) or presence (lanes 2, 4, and 6) of the purified C-domain (final concentration, 1 mg/mL). The final concentrations of the N-domain were: 0.05 mg/mL (lanes 1 and 2), 0.10 mg/mL (lanes 3 and 4), and 0.20 mg/mL (lanes 5 and 6). Two control samples, in which the purified C-domain was incubated in the presence (lane 7) or absence (lane 8) of BS^3 (final concentration, 1 mM), were also included. Bands representing the 2.7×10^4 N-domain (N) and 2.4×10^4 C-domain (C) are indicated by appropriately labeled arrows. The unlabeled top arrow represents a crosslinked product of 5×10^4 (panel A, lanes 2 and 6; panel B, lane 4; panel C, lanes 1-6) or the 5.2×10^4 wild-type subunit (panel B, lanes 1 and 2). Each lane in panels (A) and (B) was loaded with approximately 50 μg of protein. The total amounts of protein shown in panel (C) are as follows: 105 μg (lanes 1 and 2), 110 μg (lanes 3 and 4), 120 μg (lanes 5 and 6), and 100 μg (lanes 7 and 8).

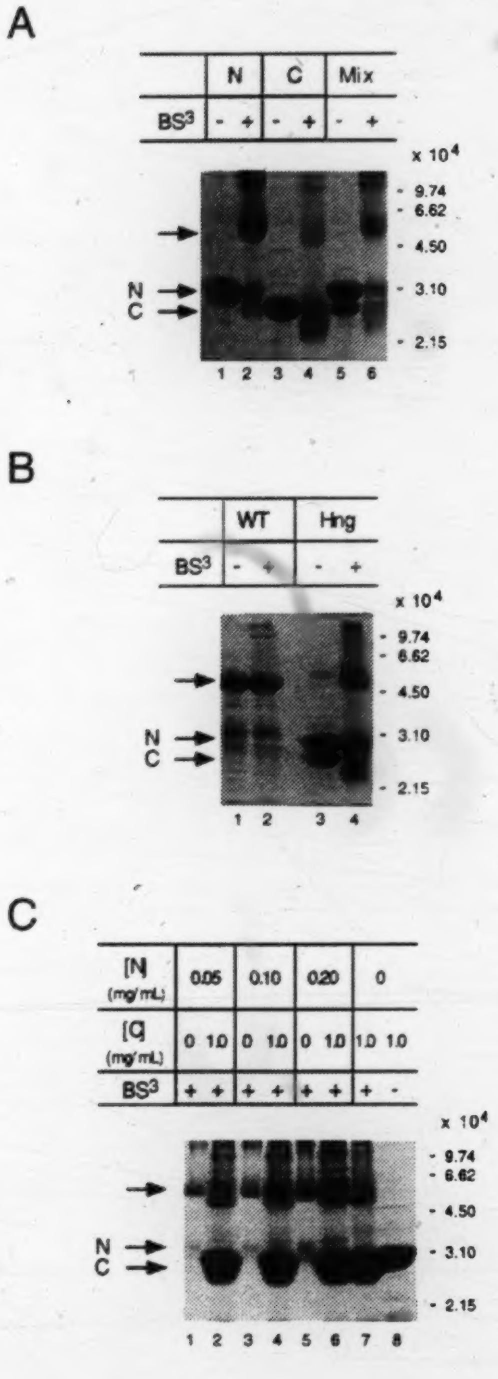
A
N
C
Mix
BS3
- + - + - +
x 10^4
9.74
6.62
4.50
3.10
2.15
N
C
1 2 3 4 5 6
B
WT
Hng
BS3
- + - +
x 10^4
9.74
6.62
4.50
3.10
2.15
N
C
1 2 3 4
C
[N] (mg/mL)
0.05
0.10
0.20
0
[C] (mg/mL)
0 1.0 0 1.0 0 1.0 1.0 1.0
BS3
+ + + + + + + -
x 10^4
9.74
6.62
4.50
3.10
2.15
N
C
1 2 3 4 5 6 7 8

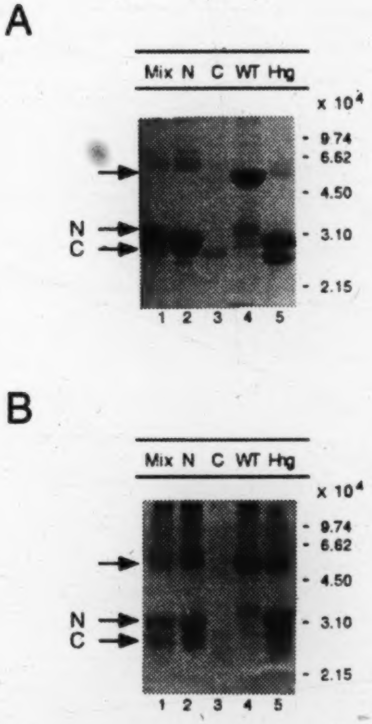

Figure 2-14: Molecular weight determinations by crosslinking with DTSSP. Crosslinked proteins were analyzed by SDS-PAGE with Coomassie-Blue staining, following incubation for 5 min at 95 °C in the presence (A) or absence (B) of 2ME (final concentration, 1% w/v). An equimolar mixture of the N- and C-domains (100 μM each) preincubated at 12 °C for 32 h (lane 1), the purified N-domain (lane 2), the purified C-domain (lane 3), the wild-type enzyme (lane 4), and the hinge-mutant (lane 5) were incubated in the presence of DTSSP (final concentration, 2 mM) prior to electrophoresis. Bands representing the 2.7×10^4 N-domain (N) and 2.4×10^4 C-domain (C) are indicated by appropriately labeled arrows. The unlabeled top arrow represents a crosslinked product of 5×10^4 (panel B, lanes 1, 2, and 5) or the 5.2×10^4 wild-type subunit (panels A and B, lane 4). Each lane was loaded with approximately 50 μg of protein.

indicating that the N_2C_2-domain complex observed by sedimentation equilibrium and/or light scattering was not susceptible to crosslinking.

To further characterize the assembly of the N- and C-domains to the active enzyme form, equimolar mixtures of the domains were incubated at 4 °C, 12 °C, or 22 °C for various times and analyzed by PAGE under non-denaturing conditions (Figure 2-15A). A decrease with time in the intensities of the bands representing the two individual domains at 12 °C coincided with an increase in the intensity of the band corresponding to the N_2C_2-domain complex (Figure 2-15A, lanes 3-11). Furthermore, the CoA transferase activity of the mixture increased with time in a parallel manner (Figure 2-15B). The N_2C_2-heterotetramer, which displayed electrophoretic properties identical to those of the pre-assembled hinge-mutant (Figure 2-15A, lane 14), was the major species in the mixture after 32 h at 12 °C (Figure 2-15A, lane 11) or after 3 h at 22 °C (Figure 2-15A, lane 1). In contrast, the two most intense bands in the mixture at 4 °C corresponded to the individual domains, while the N_2C_2-domain complex was a relatively minor background component (Figure 2-15A, lane 2). Thus, when mixed and incubated at a permissive temperature, one dimeric N-domain complex and two monomeric C-domains associate predominantly to yield an active N_2C_2 species.

Stabilities of CoA transferase forms in denaturant. In general, folded proteins are more stable than nonnative polypeptides or folding intermediates (reviewed in [Pace, 1975]; [Jaenicke, 1991]). This stability arises primarily from the burial of hydrophobic groups within the interior of the protein, associated with the collapse of a polypeptide to its compact, native fold (reviewed in [Dill, 1990]). As discussed above, the assembly of the N- and C-domains to the active enzyme form involved several conformational rearrangements, implying that each domain initially possessed a nonnative structure. Thus, it was predicted that the correctly folded wild-type enzyme should be more resistant to denaturation than the individual N- and C-domains. This hypothesis was verified by studying the equilibrium unfolding transition of each protein. Specifically, the

Figure 2-15. Kinetics of assembly of the N_2C_2-domain complex in an equimolar mixture of the N- and C-domains. (A) Analysis by PAGE under non-denaturing conditions. The purified N- and C-domains (100 μM each) were mixed and incubated at 22 °C for 3 h (lane 1), maintained at 4 °C (lane 2), or incubated at 12 °C for various times (lanes 3-11). The purified N-domain (lane 12), C-domain (lane 13), and hinge-mutant (lane 14) were included as standards. All protein samples were separated by electrophoresis under non-denaturing conditions through a 3% (w/v) stacking gel (pH 6.8) followed by a 6% (w/v) resolving gel (pH 8.8), both of which were subsequently stained with Coomassie-Blue. Bands representing the C-domain (C), N_2C_2 complex (Hng), and dimeric N-domain (N) are indicated by appropriately labeled arrows. The dashed line indicates the interface between the stacking and resolving gels. The amount of protein loaded per lane was: 7.5 μg (lane 1), 20 μg (lanes 2-11), and 10 μg (lanes 12-14). (B) Analysis by measurement of CoA transferase activity. Enzyme activity was assayed at various times in a mixture of the purified N- and C-domains (100 μM each) incubated at 12 °C. The apparent first-order rate constant is $k = 3.7 \times 10^{-5}\ s^{-1}$ ($r^2 = 0.98$). The experiment was performed in duplicate, with an average relative error of ± 5%.

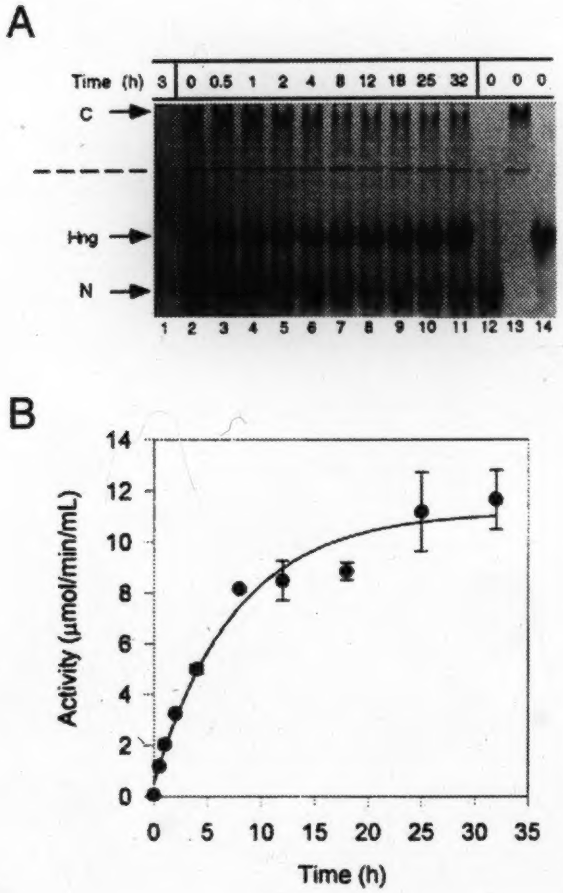
A
Time (h)
3
0 0.5 1 2 4 8 12 18 25 32
0 0 0
C
Hng
N
1 2 3 4 5 6 7 8 9 10 11 12 13 14
B
Activity (µmol/min/mL)
0 2 4 6 8 10 12 14
Time (h)
0 5 10 15 20 25 30 35

observed ellipticity at 222 nm ($[\Theta_{obs,222}]$) or the maximal wavelength of tryptophan fluorescence ($\lambda_{max,em}$) was measured for each polypeptide, following its denaturation in the presence of different concentrations of GuHCl. Subsequently, the apparent Gibbs free energy of unfolding in the absence of denaturant ($[\Delta G_u^{H_2O}]_{app}$) was determined. Knowledge of the quaternary structure of each molecule was necessary to select the appropriate calculation, given that the equilibrium unfolding transition of a multimeric protein depends on the concentration of its subunits, P_t (Jaenicke & Rudolph, 1986; De Francesco et al., 1991). The values of $[\Delta G_u^{H_2O}]_{app}$ calculated for wild-type CoA transferase from far-UV CD and fluorescence measurements were similar to the corresponding values estimated for the N-domain, and significantly greater than those determined for the C-domain (Table 2-4). Thus, it was inferred that the N-domain and the wild-type enzyme are thermodynamically more stable than the C-domain. Furthermore, the *m* values derived from these measurements were greater for the N-domain than for the wild-type enzyme or the C-domain (Table 2-4), reflecting a greater increase in the solvent-accessible surface area of the N-domain upon denaturation compared to the two other proteins (Schellman, 1978; Shortle, 1989; Myers et al., 1995). Finally, the mean concentration of GuHCl which resulted in half-maximal denaturation ($[\mathrm{GuHCl}]_{1/2}$) was approximately 1 M for the wild-type enzyme (1.8 to 9.6 μM of each subunit) or the N-domain (13 to 37 μM of each subunit), and 2 M for the C-domain (Table 2-4).[10] For both the wild-type enzyme and the N-domain, the values determined for $[\Delta G_u^{H_2O}]_{app}$ or *m* by fluorescence methods exceeded those calculated from far-UV CD measurements, while the values of $[\mathrm{GuHCl}]_{1/2}$ determined by both procedures were similar.

The presumably complex equilibrium unfolding transition of the tetrameric hinge-mutant was not analyzed quantitatively. Nevertheless, the $\lambda_{max,em}$ values determined for the hinge-mutant (final concentration of each domain, 4.4 μM) were red-shifted at lower concentrations of GuHCl (Figure 2-16), compared to the corresponding values observed

Table 2-4: Denaturation of CoA Transferase Proteins with GuHCl

Part A: Parameters derived from far-UV CD measurements[a]

Protein	P_t (μM)	$[\Delta G_u^{H_2O}]_{app}$ (kJ/mol)	m (kJ/mol/M)	$[GuHCl]_{1/2}$ (M)
Wild-type	9.6	40 ± 0.8	7.1 ± 0.4	1.7 ± 0.1[b]
Wild-type	1.8	41 ± 1.3	6.7 ± 0.8	1.3 ± 0.2[b]
N-domain	37	40 ± 0.4	16 ± 0.2	0.94 ± 0.01[b]
C-domain	41	9.2 ± 2.1	4.1 ± 0.9	2.3 ± 0.7[c]

Part B: Parameters derived from fluorescence measurements[a]

Protein	P_t (μM)	$[\Delta G_u^{H_2O}]_{app}$ (kJ/mol)	m (kJ/mol/M)	$[GuHCl]_{1/2}$ (M)
Wild-type	4.4	59 ± 0.8	29 ± 0.0	0.97 ± 0.01[b]
N-domain	13	63 ± 0.0	33 ± 0.0	1.0 ± 0.00[b]
C-domain	6.1	10 ± 1.3	6.3 ± 0.8	1.7 ± 0.3[c]

[a] The error shown for each parameter is the standard error due to fitting of the curve, and may therefore be an underestimate. The actual experimental error can be reasonably estimated to be as high as ± 10%.

[b] Calculated from: $[GuHCl]_{1/2} = \{(RT\ln P_t) + [\Delta G_u^{H_2O}]_{app}\} \div m$ (Mok et al., 1996).

[c] Calculated from: $[GuHCl]_{1/2} = [\Delta G_u^{H_2O}]_{app} \div m$.

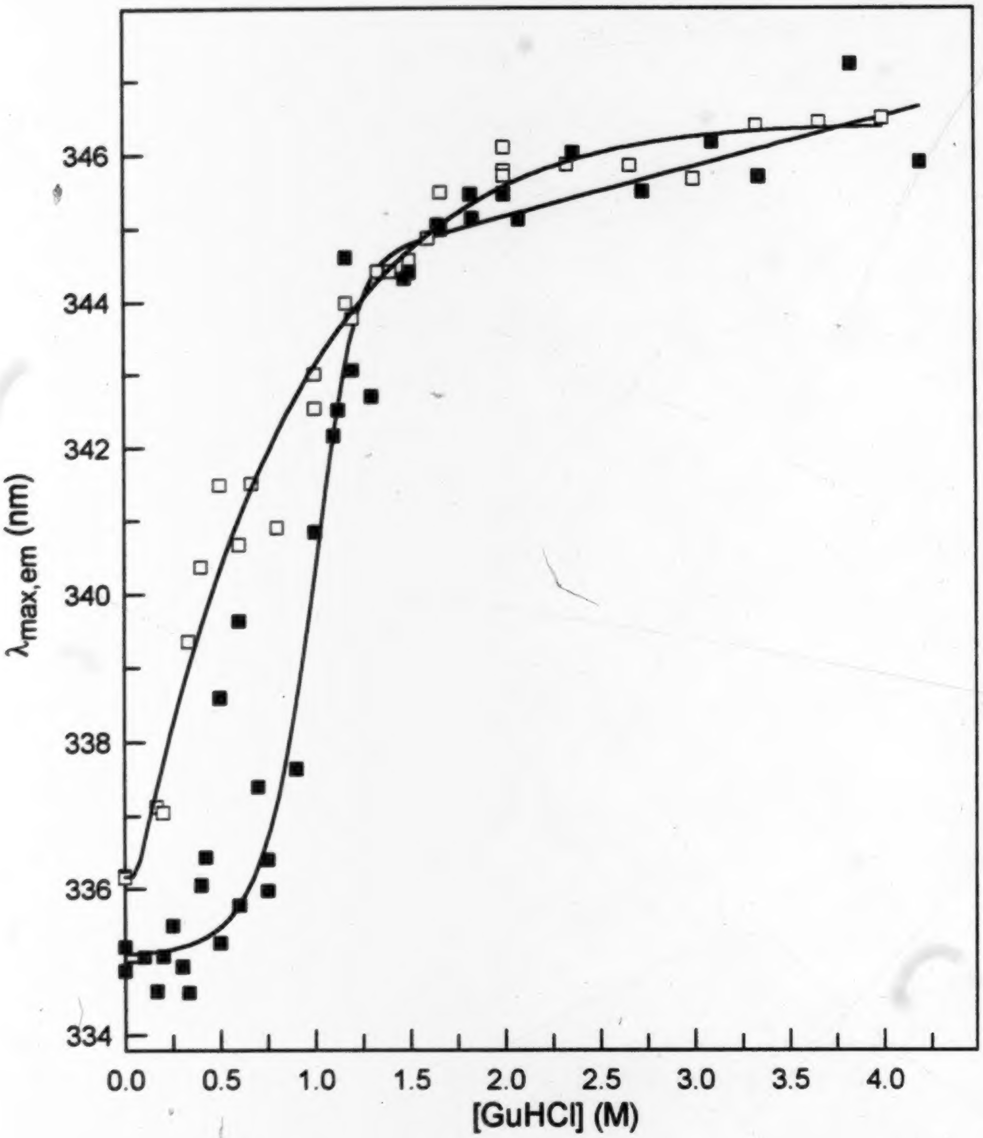

Figure 2-16: Equilibrium unfolding of CoA transferase. The wild-type enzyme (■; final concentration of the NC monomer, 4.4 μM) and the hinge-mutant (□; final concentration of each domain, 4.4 μM) were incubated overnight at 22 °C in buffers containing 0 to 4 M GuHCl. Subsequently, the $\lambda_{max,em}$ value of each denatured protein sample was determined.

for wild-type CoA transferase (final concentration of the NC monomer, 4.4 μM). This observation suggested that the hinge-mutant is less stable than the wild-type enzyme.

Refolding of CoA transferase from denaturant. Since (1) an intact hinge region is not required for the folding of CoA transferase *in vivo*, and (2) the purified N- and C-domains are capable of assembling *in vitro* under benign conditions, then the fully unfolded hinge-mutant form of CoA transferase may also be capable of refolding from denaturant *in vitro*. To test this hypothesis, each of the hinge-mutant and wild-type forms of the enzyme was incubated in a solution containing 6.0 M GuHCl. At this concentration of denaturant, both forms of CoA transferase were equally devoid of secondary and tertiary structure, as proven by far-UV CD and fluorescence measurements (data not shown). Subsequently, the activity recoverable upon the dilution of each unfolded protein was determined. The wild-type enzyme (final concentration of the NC monomer, 0.2 μM) refolded spontaneously at room temperature, with yields of 35% of the initial activity. Conversely, the hinge-mutant was found not to refold under the same conditions (Figure 2-17A). Analysis of the diluted samples by SDS-PAGE revealed that the wild-type polypeptide was partially nicked (Figure 2-17B, bottom panel), implying that the yield of refolded enzyme was most likely an underestimate. Only the diluted wild-type enzyme was detected by PAGE under non-denaturing conditions; the hinge-mutant presumably aggregated following its dilution into refolding buffer (Figure 2-17B, top panel). These results demonstrated that the presence of the hydrophilic linker may facilitate the wild-type enzyme competing more effectively than the hinge-mutant against off-pathway aggregation reactions during its refolding *in vitro*.

Figure 2-17: Refolding of CoA transferase *in vitro*. The wild-type enzyme (WT) and hinge-mutant (Hng) were denatured in 6.0 M GuHCl at 22 °C for 6 h before dilution (50-fold) in refolding buffer. The final protein concentration was 0.2 μM of wild-type monomer or 0.2 μM of each domain of the hinge-mutant in the refolding solution. (A) Yield of active enzyme recovered upon renaturation (expressed as a percentage of the initial activity of non-denatured enzyme). (B) Analysis of diluted wild-type CoA transferase or hinge-mutant by PAGE under non-denaturing conditions (top panel) and SDS-PAGE (bottom panel). Lanes 1 and 2, control samples diluted without prior denaturation; lanes 3 and 4, samples diluted after unfolding in 6.0 M GuHCl. For both gels, 1 μg of control or refolded protein was loaded per lane. Bands representing the wild-type enzyme [$(N{\sim}C)_2$], hinge-mutant (Hng), 5.2 × 10^4 wild-type subunit (WT), 2.7 × 10^4 N-domain (N), and 2.4 × 10^4 C-domain (C) are indicated by appropriately labeled arrows. The gels were stained with $AgNO_3$; the native gel consisted of a 3% (w/v) stacking gel (pH 6.8) and a 9% (w/v) resolving gel (pH 8.8).

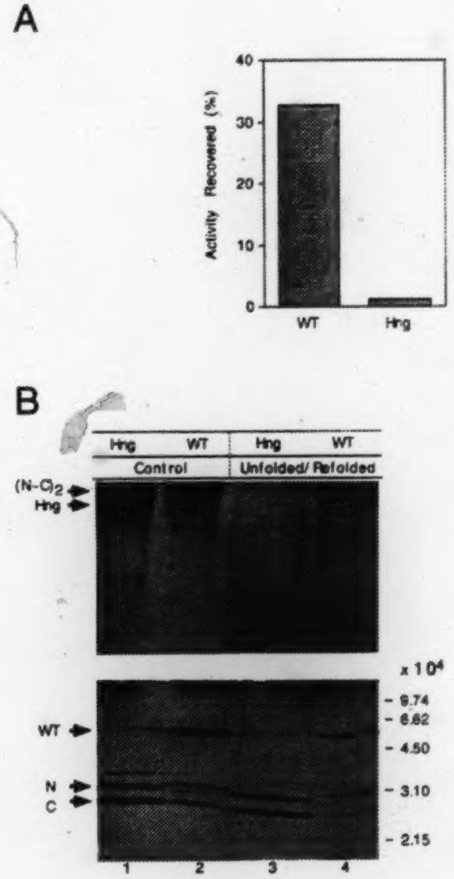
A
Activity Recovered (%)
40
30
20
10
0
WT
Hng
B
Hng
WT
Hng
WT
Control
Unfolded/ Refolded
(N-C)2
Hng
x 10⁴
- 9.74
- 6.62
- 4.50
- 3.10
- 2.15
WT
N
C
1
2
3
4

DISCUSSION

Folding and assembly of the N- and C-domains. To determine whether the N- and C-domains fold independently, the expression of a hinge-mutant of this enzyme was examined. The N-domain was present in large excess over the C-domain in lysates recovered from cells of HB-Hng, grown under inducing conditions (Figure 2-2, lane 3). As demonstrated in Chapter 3, the difference in the levels of the two domain polypeptides is primarily due to inefficient reinitiation of translation along the polycistronic mRNA encoding the hinge-mutant. Despite this inefficiency of protein synthesis, equimolar amounts of the N- and C-domains did associate in the BL-and HB-Hng strains to generate an adduct with levels of enzyme activity and an oligomeric structure equivalent to those of the wild-type enzyme. An active enzyme complex was also observed in lysates recovered from HB-N+C and HB-C/N. Thus, sequestering the genes which encode the N- and C-domains on separate plasmids or downstream of separate promoters on the same plasmid did not preclude the formation of active CoA transferase in *E. coli.* It is inferred from these observations that the two domains of CoA transferase need not be synthesized in proximity to produce a correctly folded enzyme. Comparable results involving the assembly *in vivo* of two complementary fragments derived from trypanosomal ornithine decarboxylase (Osterman et al., 1995) and mitochondrial creatine kinase have recently been reported (Gross et al., 1996).

The purified N- and C-domains assembled to form an active enzyme complex *in vitro* under non-denaturing conditions. This complex could only be generated from domains purified in the presence of 2ME, suggesting that the conformation of one or both domain polypeptides is sensitive to undesirable side reactions involving the oxidation of cysteine or methionine residues. In addition, the initial rate of assembly increased as the incubation temperature was raised to a maximum of 22 °C, above which competing aggregation reactions became significant (further discussed in Chapter 3). Obviously, this increase in the rate of association was partially due to the enhanced rate of diffusion of the two domains. However, the absence of any increase in activity in mixtures maintained at 4 °C suggests that a minimal kinetic energy requirement (implicitly due to a substantial conformational change) may be associated with the assembly of the two domains to the active enzyme form. This conclusion is consistent with the large E_a value ($2.9 \pm 0.4 \times 10^2$ kJ/mol) determined for the production of CoA transferase activity. This high E_a barrier is reasonable when compared with those previously reported for the folding of other enzymes, including 112 kJ/mol for octopine dehydrogenase (Zettlmeissl et al., 1984) and 172 and 240 kJ/mol for the tetrameric lactate dehydrogenase isoenzymes from heart and muscle, respectively (Rudolph et al., 1977). Consistent with the magnitude of these values, it is predicted that structural rearrangements associated with folding should be more complex (and the corresponding E_a barriers greater) for multimeric enzymes such as CoA transferase and lactate dehydrogenase than for smaller, monomeric enzymes such as octopine dehydrogenase. That enzyme activity appeared with apparent first-order kinetics in equimolar mixtures of the domains over a range of protein concentrations (0.01 to 0.1 mM N- or C-domain) supports the hypothesis that a conformational rearrangement is required in addition to domain pairing for the production of an active enzyme complex. Significantly, the rate of accumulation of enzyme activity was directly proportional to the concentration of the domains in each mixture examined. Also, maximal enzyme activity was greatest in the N- and C-domain mixtures of highest protein concentration. These data can be rationalized in the following manner: (1) a rapid equilibrium exists between the separate domains and an initial assembled complex (see Figure 2-18A and below); (2) the rate of formation of this initial complex is predicted to be much less than its rate of dissociation; and (3) this rapid equilibrium is followed by a relatively slow, nearly irreversible conformational change to yield active CoA transferase. A similar mechanism has been described for the reversible association of enzyme with substrate (Fersht, 1985) or slow-binding inhibitor (Morrison & Walsh, 1988).

Figure 2-18: Model describing the folding properties of CoA transferase. (A) Assembly of the N- and C-domains to the active enzyme form. (1) Each of two partially folded, interacting N-domains (I_{N_2*}) associates with an incompletely folded C-domain (I_{C*}). This docking event is fast relative to the ensuing rearrangement in secondary and tertiary structure (2), which converts the initial assembly intermediate ($I_{[N_2C_2]*}$) to the native enzyme ($N_{[N_2C_2]}$) and may involve additional intermediates. (B) Folding and assembly from two initial states. Firstly, the denatured N- and C-domains (U_N and U_C, respectively) isomerize to early intermediate forms (I_N and I_C), which may then associate incorrectly to yield aggregates (A) or correctly to produce an intermediate adduct ($I_{[N_2C_2]}$) followed by the native enzyme form ($N_{[N_2C_2]}$). Aggregation occurs much more rapidly if the domains are not covalently linked. Secondly, each domain achieves a metastable fold when produced in *E. coli*, yielding a second class of intermediates ($I_{N_2}*$ and I_{C*}). Whether or not they are covalently linked to each other, these partially folded N- and C-domains may then assemble to form a second intermediate complex ($I_{[N_2C_2]*}$). Finally, $I_{[N_2C_2]*}$ isomerizes to $N_{[N_2C_2]}$, either directly or indirectly through $I_{[N_2C_2]}$. Regardless of the point at which folding is initiated, productive interactions between the N- and C-domains are essential for stabilizing the native enzyme form ($N_{[N_2C_2]}$).

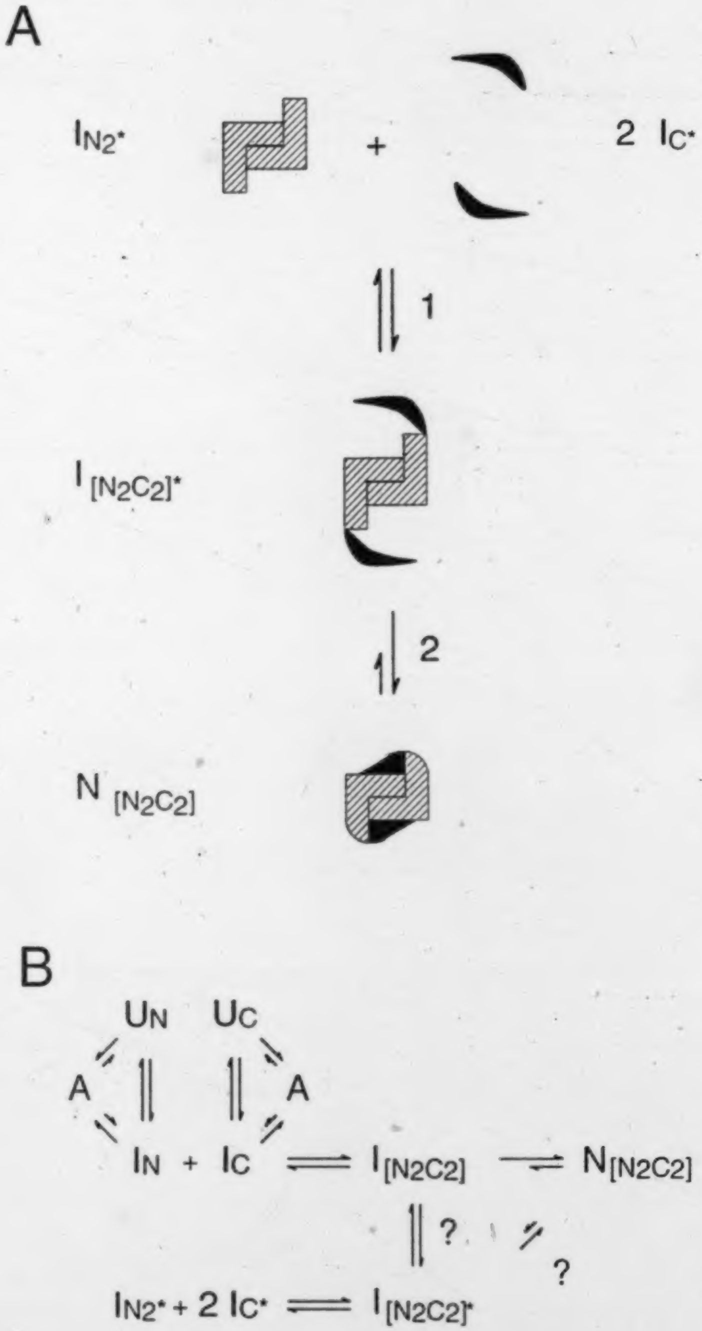
A
IN2*
+
2 IC*
1
I[N2C2]*
2
N[N2C2]
B
UN
UC
A
A
IN + IC
I[N2C2]
N[N2C2]
?
?
IN2* + 2 IC*
I[N2C2]*

Structural rearrangements concomitant with assembly to the active enzyme form. The association *in vitro* of the individual N- and C-domains to form active enzyme involved substantial conformational changes. Far-UV CD analyses indicated a significant amount of β-sheet or β-turn (N-domain) and random coil (C-domain). The overall secondary structures of the two domains were altered following their assembly to the active enzyme form. Although the exact nature of this conformational change could not be assigned from the difference CD profile alone (Figure 2-8C), the presence of a positive signal near 200 nm on this spectrum reflects a reorganization of random-coil upon formation of the active complex. This rearrangement may reasonably be attributed for the most part to the C-domain. The measurements of intrinsic tryptophan fluorescence in the presence and absence of the collisional quencher acrylamide indicated that the tryptophan residues of the N- and C-domains were more buried following the assembly of the domains to produce active CoA transferase. These results suggest, as one possibility, that both domains acquire a more compact structure following their association. Alternatively, the tryptophan residues may be sequestered from solvent in the wild-type enzyme simply by being located at the interface between the N- and C-domains. However, it can be reasonably inferred from the combination of far-UV CD and fluorescence data that at least the C-domain possesses a more open, unfolded structure as a purified polypeptide rather than as a properly assembled component of the wild-type enzyme. Finally, ultracentrifugation, light-scattering, crosslinking, and non-denaturing PAGE showed that the purified N-domain is dimeric (N_2), the purified C-domain is monomeric, and the active enzyme complex consists of two molecules of each domain polypeptide (N_2C_2). The ln(y) versus r^2 plots derived from the sedimentation equilibrium analyses of the N-domain were linear, indicating that no significant association-dissociation equilibria occurred at the protein concentrations examined. Importantly, the appearance of CoA transferase activity in the N- and C-domain mixture at 12 °C did not precede the formation of the N_2C_2-complex, implying that earlier folding intermediates are not enzymatically active. These results can be interpreted according to a simple model (Figure 2-18A) in which each of two partially folded, interacting N-domains associates with an incompletely folded C-domain. This docking event is followed by a much slower conformational change, most likely involving: (1) a rearrangement in secondary and tertiary structure, leading to the stabilization and compaction of both domains; and (2) the exclusion of water and the burial of hydrophobic sidechains at the interface between the N- and C-domains (reviewed in [Jaenicke & Rudolph, 1986]; [Jaenicke, 1987] and [Price, 1994]). Folding steps which follow subunit assembly have also been proposed for the refolding of the β_2 subunit of tryptophan synthase (Blond & Goldberg, 1985) and bacterial luciferase (Ziegler et al., 1993).

However, this model is most likely an oversimplification, given that the dimer interface of the N_2 species may be different from that in the N_2C_2-domain complex. Consistent with this possibility, a crosslinked product of molecular weight 1.0×10^5 was not observed in a sample of wild-type CoA transferase treated with BS^3 or DTSSP. This species should have formed readily if the two N-domains of the wild-type enzyme or hinge-mutant were crosslinked as efficiently as those of the N_2 dimer.[11] Thus, the association of the N-domain in the absence of the C-domain may involve nonnative intermolecular interactions, analogous to those described for cytoplasmic malate dehydrogenase (Rudolph et al., 1986), the homodimeric form of the bacterial luciferase β-subunit (Baldwin et al., 1993; Sinclair et al., 1993; Sinclair et al., 1994), or various mutant, oligomeric forms of the phage P22 coat protein (Teschke & King, 1995). If this were true, then the active complex might be assembled by a more complicated mechanism than that described above, involving perhaps the preliminary dissociation of the N-domains from the N_2 species or a reshuffling of the N_2 interface subsequent to the formation of an early N_2C_2 complex. Such reshuffling could account at least in part for the E_a barrier and the conformational changes described above.

From the results, it is predicted that the purified domains consist of several species at different stages of folding, each possessing a different ability to assemble to yield active enzyme. The presence at "zero" time of minimal background activity recoverable from the N- and C-domain mixtures implies that some conformers are able to associate to yield active CoA transferase almost immediately. In contrast, the yield of CoA transferase activity generated decreases with the lengthy storage of the purified domain preparations, suggesting that yet other conformers which are incapable of productive assembly accumulate with time. Based on this study, it is postulated that the predominant conformers in the N- and C-domain preparations are capable of forming active CoA transferase by an assembly event which also involves significant structural rearrangements. Conformational changes also accompany the assembly of complementary fragments derived from other proteins, including: tryptophan repressor (Tasayco & Carey, 1992; Wu et al., 1994); phosphoglycerate kinase (Pecorari et al., 1993); cytochrome C (Wu et al., 1994); chymotrypsin inhibitor-2 (Prat Gay & Fersht, 1994; Prat Gay et al., 1994a,b; Ruiz-Sanz et al., 1995); barnase (Kippen et al., 1994; Kippen & Fersht, 1995); and creatine kinase (Gross et al., 1996).

Equilibrium unfolding transitions. The denaturation of wild-type CoA transferase and the N- and C-domains in buffers containing different concentrations of GuHCl was studied by measurements of $[\Theta_{obs,222}]$ or $\lambda_{max,em}$. Two parameters were evaluated for each protein: (1) $[\Delta G_u^{H_2O}]_{app}$, which provides an estimate of stability in the absence of denaturant (Pace, 1975; Pace, 1986; Shortle, 1989); and (2) *m*, which is proportional to the increase in solvent-accessible surface area associated with unfolding (Schellman, 1978; Shortle, 1989; Myers et al., 1995). The values of $[\Delta G_u^{H_2O}]_{app}$ observed for the C-domain were significantly less than those determined for the wild-type enzyme or the N-domain, suggesting that the C-domain is the less stable molecular species. Furthermore, the relatively low *m* value observed for the C-domain implies that much of the surface area of this polypeptide is accessible to solvent under benign conditions. Thus, little further increase in exposure of the C-domain surface area occurs upon denaturation, compared to the wild-type enzyme or the N-domain. These results support the hypothesis, based on measurements of far-UV CD and intrinsic tryptophan fluorescence, that the purified C-domain possesses a nonnative fold. Other isolated protein fragments which display low intrinsic stabilities include a truncated, dimeric form of lactate dehydrogenase (Opitz et al., 1987), the N- and C-domains of phosphoglycerate kinase (Missiakas et al., 1990), the N- and C-domains of γB-crystallin (Sharma et al., 1990; Mayr et al., 1994), and the N- and C-domains of troponin C (Fredricksen & Swenson, 1996). These polypeptides are more readily denatured as separate entities than as components of the intact protein because they lack stabilizing interactions associated with the native fold (Jaenicke, 1995).

The values of $[\Delta G_u^{H_2O}]_{app}$ determined for the N-domain were similar to those calculated for the wild-type enzyme, implying that both proteins are equally stable under benign conditions. In contrast, the value of m determined for the N-domain by far-UV CD analysis was significantly greater than the mean value calculated for wild-type CoA transferase, suggesting that the N-domain is more compact than the intact enzyme. Perhaps the interacting N-domains adopt a more open conformation as the N_2-dimer and two C-domains assemble to the enzymatically active, N_2C_2-domain form. Alternatively, the unfolding of the wild-type enzyme may simply represent an average of equilibrium transitions involving the relatively open C-domains and the relatively compact N-domains. Finally, the hinge-mutant was less resistant to denaturation than the intact enzyme, presumably due to stabilizing interactions provided by the hydrophilic linker.

For both the wild-type enzyme and the N-domain, the values of $[\Delta G_u^{H_2O}]_{app}$ or m determined by fluorescence methods were greater than those calculated from far-UV CD measurements, suggesting that the unfolding process was not perfectly concerted. The intrinsic tryptophan fluorescence, presumably determined by a relatively local, buried fold, may be more resistant to denaturation than the observed ellipticity, which reflects the global secondary structure at the protein surface and interior. Nevertheless, the denaturation curves produced by both methods were similar and provided no evidence for well-populated intermediate states. Thus, the assumption of a predominantly "two-state" equilibrium unfolding transition for each of these proteins is acceptable.

Finally, the $[GuHCl]_{1/2}$ values determined for the C-domain exceeded those observed for wild-type CoA transferase or the N-domain, despite the greater apparent stability of the two homodimeric proteins (see above). This anomalous result is attributed to the low cooperativity of the equilibrium unfolding transition observed for the C-domain. This phenomenon has previously been reported for fragments of lactate dehydrogenase (Opitz et al., 1987) and chymotrypsin inhibitor-2 (Prat Gay & Fersht, 1994), and may be characteristic of polypeptides which lack a compact, native fold. Furthermore, the values of $[GuHCl]_{1/2}$ reflect association-dissociation equilibria for the wild-type enzyme and the N-domain, but not for the C-domain. For these reasons, it is argued that $[\Delta G_u^{H_2O}]_{app}$ provides a more meaningful estimate of the relative stabilities of the proteins discussed here.

Implications for the folding pathway of CoA transferase. Complementary fragments derived from bovine serum albumin (Taylor & Silver, 1976) and lactate dehydrogenase (Opitz et al., 1987; Jaenicke, 1991) refold with lower efficiencies than the corresponding native protein. Similarly, it has been demonstrated that the hydrophilic linker is essential for the recovery of CoA transferase activity upon dilution of the enzyme from denaturant. This result is not consistent with the observation that an intact hinge region is not required for the folding of mature CoA transferase in *E. coli*. It is proposed that chaperone systems and/or cotranslational folding events may inhibit the aggregation of the hinge-mutant within the bacterial cytosol (Chapter 3). The low refolding yield of the hinge-mutant must also be reconciled with the association of the isolated N- and C-domains to produce active enzyme *in vitro* (Figure 2-18B).

Importantly, following their dilution the domains of the denatured hinge-mutant were found to aggregate at a concentration 500 times less than that of the purified, mixed domains at 22 °C. From these results, it is predicted that the conformers which aggregate during the refolding of the hinge-mutant are distinct from the partially folded, purified domains, and most likely consist of unfolded polypeptides (U_N and U_C) and early folding intermediates (I_N and I_C). An intermediate adduct ($I_{[N_2C_2]}$) may result from the assembly of I_N and I_C, given that the latter are less susceptible to aggregation when they are covalently linked (Figure 2-18B). In contrast, the domains purified from *E. coli* may be altogether distinct intermediates ($I_{N_2}*$ and I_C*) which occur on a separate pathway (Figure 2-18B). Off-pathway conformers of an analogous type have been described for the α- and β-subunits of bacterial luciferase produced individually in *E. coli* (Baldwin et al., 1993; Sinclair et al., 1993; Ziegler et al., 1993; Sinclair et al., 1994). Folding from I_N* and I_C* requires their association to form a second intermediate complex ($I_{[N_2C_2]}*$), which then isomerizes in a rate-limiting manner to $N_{[N_2C_2]}$. Although the data are consistent with this model, other more complex explanations cannot be ruled out. For instance, I_N* and I_C* may not belong to an entirely separate, parallel pathway with respect to that of I_{N1} and I_{C1}, but may instead also proceed through $I_{[N_2C_2]}$. Such a mechanism would be consistent with the general concept of proteins folding according to a framework model in which the number of intermediate states decreases progressively as the native conformation is approached (reviewed in [Jaenicke, 1991]; [Landry & Gierasch, 1994]; [Miranker & Dobson, 1996]). In addition, the unfolded and intermediate forms described above most likely represent an ensemble of states. A more detailed analysis of the structures of the purified N- and C-domains and of kinetic and/or equilibrium intermediates along the folding pathway of CoA transferase will be required to address these questions. It is clear, however, that the N- and C-domains of CoA transferase do not achieve their native folds completely independently of each other, but rather, through productive interactions during their folding and assembly.

ENDNOTES

[1] A portion of this chapter has been published:

> Rochet, J.-C., Oikawa, K., Hicks, L. D., Kay, C. M., Bridger, W. A., & Wolodko, W. T. (1997) *Biochemistry 36*, 8807-8820.

[2] See Appendices 3-6 for further details.

[3] To correct for scatter, the linear portion of a plot of log (absorbance) versus log (wavelength), corresponding to wavelengths between 300 nm and 350 nm, was extrapolated to 278 nm. The amount of scatter at 278 nm, determined as the antilog of the extrapolated value, was subtracted from the observed A_{278} reading.

[4] Samples of wild-type CoA transferase and the hinge-mutant were eluted from the Affi-Gel Blue column in buffer A + 0.5 M KCl (see "Protein purification"). Prior to the measurement of far-UV CD or fluorescence, these samples were dialyzed at 4 °C against 0.5 L of buffer X to remove the KCl, which was absent from preparations of the N- and C-domains. Small-volume samples (< 0.50 mL) and large-volume samples (≥ 0.50 mL) were dialyzed using semi-permeable membranes with MWCO values of 3.5×10^3 (18 mm width) and 1.2×10^4 (32 mm width), respectively. Dialyses was carried out for a minimum of 16 h, with one change of buffer after 8 h.

[5] The reversibility of unfolding of the proteins at 22 °C was not proven rigorously. Accordingly, the values deduced for the various thermodynamic parameters are "apparent" values only.

[6] The term "CoA transferase forms" refers collectively to the wild-type enzyme, hinge-mutant, N- domain, and C-domain.

[7] As will be discussed in Chapter 3, a much higher proportion of soluble CoA transferase was observed in cells of HB-WT or BL-WT grown at 25°C rather than at 37°C. Thus, all the proteins were purified from cultures grown at the lower temperature.

[8] When grown under inducing conditions, this strain of *E. coli* produces a mutant form of the intact CoA transferase, in which glutamate-344 is replaced with an alanine residue (Chapter 6). It is assumed that this substitution does not alter the purification properties of the enzyme, compared to wild-type CoA transferase.

[9] As demonstrated by PAGE under non-denaturing conditions (Figure 2-15), the N- and C-domains assembled to form an N_2C_2-domain complex upon prolonged incubation at 12°C.

[10] The concentrations of wild-type CoA transferase and the N-domain are specified because the $[GuHCl]_{1/2}$ values observed for these two dimeric species reflect association-dissociation equilibria in addition to unfolding.

[11] This argument does not, however, apply to the hinge-mutant, since there is no evidence of efficient crosslinking between the N- and C-domains.

REFERENCES

Babul, J., & Stellwagen, E. (1969) *Anal. Biochem. 28*, 216-221.

Baldwin, T. O., Ziegler, M. M., Chaffotte, A. F., & Goldberg, M. E. (1993) *J. Biol. Chem. 268*, 10766-10772.

Blond, S., & Goldberg, M. E. (1985) *J. Mol. Biol. 182*, 597-606.

Chen, Y. H., Yang, J. T., & Martinez, H. M. (1972) *Biochemistry 11*, 4120-4131.

Chervenka, C. H. (1970) in *A Manual of Methods for the Analytical Ultracentrifuge*. pp. 42-55, Spinco Division of Beckman Instruments, Inc., Palo Alto, CA.

Cohn, E. J., & Edsall, J. T. (1943) in *Proteins, Amino Acids, and Peptides* (Cohn, E. J., & Edsall, J. T., eds.) pp. 370-377, Hafner Publishing Company, Inc., New York.

De Francesco, R., Pastore, A., Vecchio, G., & Cortese, R. (1991) *Biochemistry 30*, 143-147.

Dill, K. A. (1990) *Biochemistry 29*, 7133-7155.

Fenn, J. B., Mann, M., Meng, C. K., Wong, S. F., & Whitehouse, C. M. (1989) *Science 246*, 64-71.

Fersht, A. (1985) *Enzyme Structure and Mechanism*, 2nd ed. W. H. Freeman & Co., New York.

Fredricksen, R. S., & Swenson, C. A. (1996) *Biochemistry 35*, 14012-14026.

Gross, M., Wyss, M., Furter-Graves, E. M., Wallimann, T., & Furter, R. (1996) *Protein Sci. 5*, 320-330.

Howard, J. B., Zieske, L., Clarkson, J., & Rathe, L. (1986) *J. Biol. Chem. 261*, 60-65.

Jaenicke, R. (1987) *Prog. Biophys. Mol. Biol. 49*, 117-237.

Jaenicke, R. (1991) *Biochemistry 30*, 3147-3161.

Jaenicke, R. (1995) *Phil. Trans. R. Soc. Lond.* B *348*, 97-105.

Jaenicke, R., & Rudolph, R. (1986) *Methods Enzymol. 131*, 218-250.

Jasanoff, A., & Fersht, A. R. (1994) *Biochemistry 33*, 2129-2135.

Johnson, M. L., Correia, J. J., Yphantis, D. A., & Halvorson, H. R. (1981) *Biophys. J. 36*, 575-588.

Kippen, A. D., & Fersht, A. R. (1995) *Biochemistry 34*, 1464-1468.

Kippen, A. D., Sancho, J., & Fersht, A. R. (1994) *Biochemistry 33*, 3778-3786.

Kunkel, T. A. (1985) *Proc. Natl. Acad. Sci. U. S. A. 82*, 488-492.

Landry, S. J., & Gierasch, L. M. (1994) *Annu. Rev. Biophys. Biomol. Struct. 23*, 645-669.

Lin, T., & Bridger, W. A. (1992) *J. Biol. Chem. 267*, 975-978.

Mann, M., & Wilm, M. (1995) *Trends Biochem. Sci. 20*, 219-224.

Martin, J., Langer, T., Boteva, R., Schramel, A., Horwich, A. L., & Hartl, F.-U. (1991) *Nature 352*, 36-42.

Marusyk, R., & Sergeant, A. (1980) *Anal. Biochem. 105*, 403-404.

Mayr, E.-M., Jaenicke, R., & Glockshuber, R. (1994) *J. Mol. Biol. 235*, 84-88.

Mihalyi, E. (1968) *J. Chem. Eng. Data 13*, 179-182.

Milla, M. E., Brown, B. M., & Sauer, R. T. (1993) *Protein Sci. 2*, 2198-2205.

Miranker, A. D., & Dobson, C. M. (1996) *Curr. Opin. Struct. Biol. 6*, 31-42.

Missiakas, D., Betton, J. M., Minard, P., & Yon, J. M. (1990) *Biochemistry 29*, 8683-8689.

Mok, Y.-K., Prat Gay, G. de, Butler, P. J., & Bycroft, M. (1996) *Protein Sci. 5*, 310-319.

Morrison, J. F., & Walsh, C. T. (1988) *Adv. Enzymol. 61*, 201-301.

Murray, A. C., Oikawa, K., & Kay, C. M. (1969) *Biochim. Biophys. Acta 175*, 331-338.

Myers, J. K., Pace, C. N., & Scholtz, J. M. (1995) *Protein Sci. 4*, 2138-2148.

Opitz, U., Rudolph, R., Jaenicke, R., Ericsson, L., & Neurath, H. (1987) *Biochemistry 26*, 1399-1406.

Osterman, A. L., Lueder, D. V., Quick, M., Myers, D., Canagarajah, B. J., & Phillips, M. A. (1995) *Biochemistry 34*, 13431-13436.

Pace, C. N. (1975) *Crit. Rev. Biochem. 3*, 1-43.

Pace, C. N. (1986) *Methods Enzymol. 131*, 266-280.

Parales, R. E., & Harwood, C. S. (1992) *J. Bacteriol. 174*, 4657-4666.

Pecorari, F., Minard, P., Desmadril, M., & Yon, J. M. (1993) *Protein Eng. 6*, 313-325.

Prat Gay, G. de, & Fersht, A. R. (1994) *Biochemistry 33*, 7957-7963.

Prat Gay, G. de, Ruiz-Sanz, J., Davis, B., & Fersht, A. R. (1994a) *Proc. Natl. Acad. Sci. U. S. A. 91*, 10943-10946.

Prat Gay, G. de, Ruiz-Sanz, J., & Fersht, A. R. (1994b) *Biochemistry 33*, 7964-7970.

Price, N. C. (1994) in *Mechanisms of Protein Folding* (Pain, R. H., Ed.) pp. 160-193, IRL Press, Oxford, U. K.

Rudolph, R., Heider, I., & Jaenicke, R. (1977) *Biochemistry 16*, 5527-5531.

Rudolph, R., Fuchs, I., & Jaenicke, R. (1986) *Biochemistry 25*, 1662-1667.

Ruiz-Sanz, J., Prat Gay, G. de, Otzen, D. E., & Fersht, A. R. (1995) *Biochemistry 34*, 1695-1701.

Sanger, F., Nicklen, S., & Coulson, A. R. (1977) *Proc. Natl. Acad. Sci. U. S. A. 74*, 5463-5467.

Schellman, J. (1978) *Biopolymers 17*, 1305-1322.

Sharma, A. K., Minke-Gogl, V., Gohl, P., Siebendritt, R., Jaenicke, R., & Rudolph, R. (1990) *Eur. J. Biochem. 194*, 603-609.

Shortle, D. (1989) *J. Biol. Chem. 264*, 5315-5318.

Sinclair, J. F., Waddle, J. J., Waddill, E. F., & Baldwin, T. O. (1993) *Biochemistry 32*, 5036-5044.

Sinclair, J. F., Ziegler, M. M., & Baldwin, T. O. (1994) *Nature Struct. Biol. 1*, 320-326.

Smith, R. D., Loo, J. A., Edmonds, C. G., Baringa, C. J., & Udseth, H. R. (1990) *Anal. Chem. 62*, 882-899.

Stern, J. R., Coon, M. J., del Campillo, A., & Schneider, M. C. (1956) *J. Biol. Chem. 221*, 15-31.

Tasayco, M. L., & Carey, J. (1992) *Science 255*, 594-597.

Taylor, R. P., & Silver, A. (1976) *J. Am. Chem. Soc. 98*, 4650-4651.

Teschke, C. M., & King, J. (1995) *Biochemistry 34*, 6815-6826.

White, H., & Jencks, W. P. (1976) *J. Biol. Chem. 251*, 1708-1711.

Woody, R. W. (1995) *Methods Enzymol. 246*, 34-71.

Wu, L. C., Grandori, G., & Carey, J. (1994) *Protein Sci. 3*, 369-371.

Wyatt, P. J. (1993) *Analytica Chimica Acta 272*, 1-40.

Zettlmeissl, G., Teschner, W., Rudolph, R., Jaenicke, R., & Gäde, G. (1984) *Eur. J. Biochem. 143*, 401-407.

Ziegler, M. M., Goldberg, M. E., Chaffotte, A. F., & Baldwin, T. O. (1993) *J. Biol. Chem. 268*, 10760-10765.

Chapter 3. The Aggregation of CoA Transferase Folding Intermediates[1]

INTRODUCTION

Productive interactions between the N- and C-domains play critical roles at different points along the folding pathway of CoA transferase (Chapter 2). First, the reconstitution of the enzyme from denaturant depends on the presence of the intact hydrophilic linker, which enables the specific interaction of unstructured domains early on the folding pathway. Second, the purified N- and C-domains, which are late intermediates, adopt a native structure by interacting productively as part of an initial N_2C_2-complex. However, under nonideal conditions, the "correct" pairing of the domains of CoA transferase is compromised by side-reactions, which compete kinetically with the main pathway of folding and assembly. For example, only 35% of the initial CoA transferase activity is recovered upon refolding of the enzyme from denaturant. In addition, no enzyme activity accumulates in equimolar mixtures of the purified N- and C-domains incubated at 37 °C under benign conditions. Thus, the early and late folding intermediates of CoA transferase are also susceptible to "wrong" pairing reactions, which decrease the yield of correctly folded enzyme.

The "aggregation" of proteins refers to the nonnative self-association of partially folded or misfolded monomers to yield inactive complexes.[2] This phenomenon results primarily from the transient exposure of nonpolar groups, normally buried within the interior of the protein, to aqueous solvent (reviewed in [Jaenicke & Rudolph, 1986]; [Jaenicke, 1987]; [Jaenicke, 1991]). Unfavorable hydrophobic interactions between these groups lead to the formation of high molecular-weight, filamentous structures which are stabilized at different energy-minima from that of the native enzyme (Zettlmeissl et al., 1979). The rate of aggregation increases with the concentration of susceptible folding intermediates, given that aggregation is an intermolecular process with a reaction order greater than 2 (Zettlmeissl et al., 1979; Goldberg et al., 1991; van der Vies et al., 1992). Thus, the aggregation of proteins is enhanced by conditions which increase the concentration of partially folded intermediates (reviewed in [Jaenicke, 1991]; [Price, 1994]; [Jaenicke, 1995]). *In vitro*, these conditions include elevated temperatures and the presence of denaturants at moderate concentrations. Similarly, the formation of inclusion bodies *in vivo* is favored by elevated temperatures and the accumulation of high levels of nascent polypeptides due to rapid biosynthesis (reviewed in [Jaenicke, 1991]; [Thatcher & Hitchcock, 1994]; [King et al., 1996]; [Mukhopadhyay, 1997]).

In *E. coli*, the concentration of newly-synthesized protein is at least 50 μM, based on the estimated concentration of ribosomes (reviewed in [Rothman, 1989]; [Hlodan & Hartl, 1994]). Nonnative polypeptides are also abundant in eukaryotic organelles such as mitochondria and chloroplasts, which import precursor proteins as unfolded chains from the cytosol (Ostermann et al., 1989; reviewed in [Price, 1994]). *In vitro*, however, much lower concentrations of proteins are susceptible to aggregation during refolding from denaturant (reviewed in [Price, 1994]). As shown in Chapter 2, only one-third of the initial CoA transferase activity is recovered following the refolding of subunits from GuHCl at a concentration of 0.2 μM. Clearly, intracellular mechanisms must exist to reduce the tendency of nascent polypeptides to aggregate at elevated concentrations.

In contrast to the renaturation of proteins *in vitro*, folding *in vivo* is a "vectorial" process (Jaenicke & Rudolph, 1986). Domains which are synthesized early on the ribosomes may assume a partial fold prior to the completion of translation or membrane translocation (reviewed in [Jaenicke, 1987]; [Jaenicke, 1991]; [Hlodan & Hartl, 1994]; [Price, 1994]). Thus, the folding intermediates which are most susceptible to aggregation during refolding *in vitro* may not typically occur *in vivo* due to cotranslational folding (Figure 3-1). Furthermore, protein folding assistants, termed "molecular chaperones" (Ellis, 1987), also inhibit aggregation within the intracellular milieu. These specialized

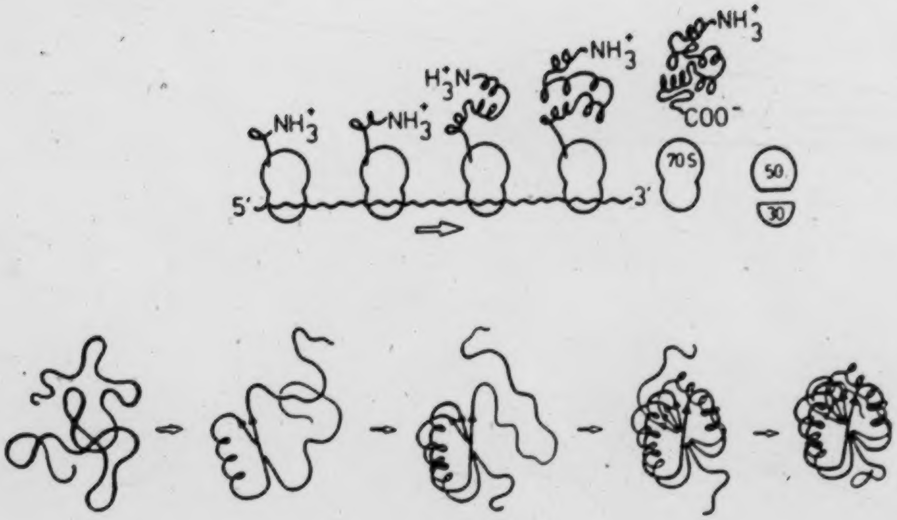

Figure 3-1: Folding *in vivo* versus refolding *in vitro*. Co-translational folding (top) involves the formation of rudimentary structural motifs along portions of the polypeptide chain which have been released from the ribosome (shown here moving in a 5' → 3' direction along the mRNA). In contrast, all portions of the polypeptide chain are exposed simultaneously upon the refolding of a denatured protein (bottom). (Reprinted from [Jaenicke, 1987], with the permission of Elsevier Science).

proteins were originally identified as heat shock proteins (Hsps) due to their abundance in cells subjected to elevated temperatures or other types of stresses (reviewed in [Lindquist, 1986]; [Craig, 1988]; [Craig & Gross, 1991]; [Becker & Craig, 1994]; [Craig et al., 1994]). However, it has been demonstrated that even in the absence of heat shock, chaperones are essential for the folding of polypeptides in the prokaryotic and eukaryotic cytosol, and for the translocation and folding of proteins in eukaryotic organelles (reviewed in [Hlodan & Hartl, 1994]; [Craig et al., 1994]; [Hartl & Martin, 1995]).

As mentioned in Chapter 1, the CoA transferase of eukaryotes is synthesized in the cytosol as an inactive precursor, which is subsequently imported into the mitochondrion. The first 39 residues of the immature protein comprise a presequence with the features predicted for targeting to the mitochondrial matrix; these include: a large number of arginine and serine residues, few acidic residues, and the likelihood of forming a positively charged amphiphilic α-helix (von Heijne, 1986; Lin & Bridger, 1992). The principal constituents of the mitochondrial import pathways of *Saccharomyces cerevisiae* and *Neurospora crassa* (Figure 3-2) have been identified (reviewed in [Lill et al., 1996]; [Schatz, 1996]). Briefly, they consist of: (1) "Tom" receptors and import channels, which interact with the precursor polypeptide at the outer mitochondrial membrane; (2) "Tim" subunits, which are necessary for transport of the precursor across the inner membrane; (3) the matrix-processing peptidase (MPP), which cleaves the signal sequence from the imported precursor; (4) cytosolic chaperones, including Hsp70 and the mitochondrial import stimulating factor (MSF), which maintain the precursor in an unfolded state prior to and during import; and (5) mitochondrial chaperones, including mHsp70, mGrpE, Mdj1, Hsp60, and Cpn10, which assist the folding of the protein once it has been imported. It has been proposed that proteins imported into the mitochondrial matrix adopt correct tertiary and quaternary structures due to the sequential, ATP-dependent activities of the mHsp70 and mHsp60 systems (Manning-Krieg et al., 1991; reviewed in [Gething & Sambrook, 1992]; [Stuart et al.,

Figure 3-2: Major features of the mitochondrial protein import pathway. Prior to translocation across the outer membrane (OM), the precursor protein is maintained in an unfolded conformation by one of two cytosolic chaperones: (1) Hsp70, in an ATP-independent manner; or (2) mitochondrial import stimulating factor (MSF), in an ATP-dependent manner. The positively-charged targeting sequence on the protein precursor is recognized and bound by the Tom receptor complex (including Tom37, Tom70, Tom20, and Tom22), which delivers the precursor to the Tom channel complex (including Tom40, Tom5, Tom6, Tom7, and Tom38 [not shown]) for translocation across the OM. Transport of the precursor across the inner membrane (IM) proceeds through the Tim complex, and depends on the electrochemical gradient ($\Delta\psi$). Once inside the mitochondrial matrix, the precursor folds in an ATP-dependent manner to an initial stage, with the assistance of mHsp70 associated with GrpEp and Tim44. Subsequent folding steps are mediated by $Hsp60_{14}$:$Cpn10_7$ with the hydrolysis of ATP (right), or by other chaperones, including Cpr3p and Mdj1 (left). The presequence is cleaved by the matrix processing peptidase (MPP). (Reprinted from [Schatz, 1996], with the permission of the American Society for Biochemistry and Microbiology).

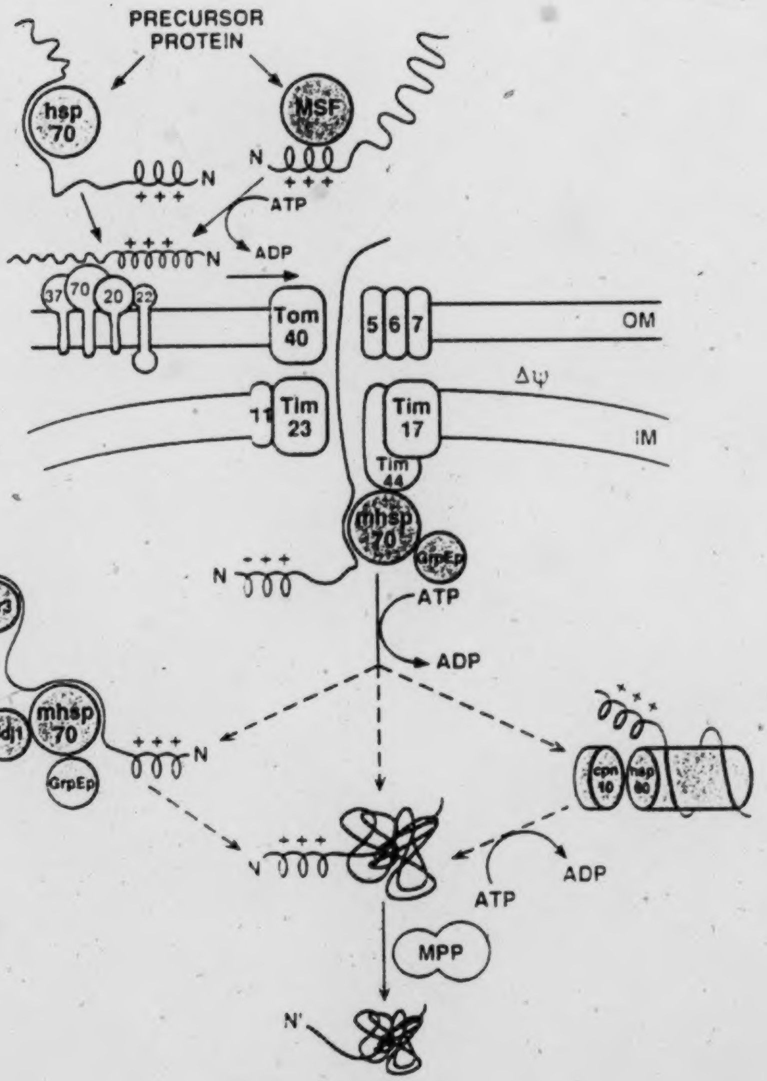
PRECURSOR PROTEIN
hsp 70
MSF
N
+ + +
ATP
ADP
37
70
20
22
Tom 40
5
6
7
OM
Δψ
11
Tim 23
Tim 17
Tim 44
IM
mhsp 70
GrpEp
Cpr3
Mdj1
cpn 10
hsp 60
MPP
N'

1994]). Specifically, monomeric mHsp70 (in association with monomeric mGrpE) binds and stabilizes unfolded polypeptides during their translocation across the inner membrane (Scherer et al., 1990), while a cylindrical complex of fourteen Hsp60 subunits and seven Cpn10 subunits ($Hsp60_{14}$:$Cpn10_7$) is thought to be essential for the folding and assembly of oligomeric enzymes in the matrix (Cheng et al., 1989; Ostermann et al., 1989; Rospert et al., 1993; Höhfeld & Hartl, 1994). In contrast, recent results indicate that some monomeric proteins of the matrix acquire their mature, native fold in the absence of a functional $Hsp60_{14}$:$Cpn10_7$ complex (Rospert et al., 1996). Similarly, in *E. coli*, the folding of only a subset of cytosolic proteins requires a functional $GroEL_{14}$:$GroES_7$ complex, which is evolutionarily related to the $Hsp60_{14}$:$Cpn10_7$ chaperone system of eukaryotic mitochondria (Horwich et al., 1993).

The studies outlined in this chapter have been carried out to assess the degree to which aggregation side-reactions compete with the folding pathway of CoA transferase. The conditions that favor aggregation *in vitro* have been investigated using the purified N- and C-domains in benign buffer or solutions of the refolding wild-type enzyme. In addition, wild-type CoA transferase, the hinge-mutant, and the N- and C-domains have been characterized with respect to their tendencies to form inclusion bodies in *E. coli*. Finally, the ability of the GroEL/GroES system to assist the refolding of the intact enzyme or the hinge-mutant *in vitro* has been examined. The results of these experiments have led to the identification of intermediate forms which occur at different stages of the CoA transferase folding pathway.

EXPERIMENTAL PROCEDURES

Materials. The column matrices Affi-Gel Blue and hydroxyapatite were purchased from Bio-Rad Laboratories, Ltd. DEAE Sephacel, Sephadex G-50, and Sephacryl S-200 were supplied by Pharmacia Biotech. Acrylamide was a Gibco BRL product from Life Technologies. Purified protein preparations were concentrated using

Amicon brand Centriprep-10 concentrators (MWCO = 1.0 x 10^4). Radioactively labeled ^{35}S-methionine (typically 5-10 mCi/mL) was supplied by ICN Biomedicals, Inc. as ^{35}S-TransMet or by Amersham Ltd. The GuHCl was also provided by ICN Biomedicals, Inc. Materials for enzyme activity assays, including acetoacetate, succinyl-CoA, *cis*-oxaloacetate, acetyl-CoA, and DTNB, were obtained from Sigma Chemical Company. The Lumi-Phos 530 and a suspension of citrate synthase (10 mg/mL) were purchased from Boehringer Mannheim. Finally, GroEL and the equimolar mixture of $GroEL_{14}$ and $GroES_7$ were supplied by StressGen Biotechnologies.

Gene expression and protein purification. Gene expression in cultures of *E. coli* BL21(DE3) or HB101, and the subsequent preparation of cell lysates, were carried out as described previously (Chapter 2). Cultures which were subjected to Western blot analysis were grown as described in Table 3-1. In general, the wild-type enzyme, hinge-mutant, and N- and C-domains were purified according to the procedures outlined in Chapter 2. However, the wild-type CoA transferase that was used for refolding experiments with GroEL and/or GroES consisted only of the homodimeric enzyme, whereas the homodimeric and homotetrameric forms were both present in other samples of the intact enzyme. The procedure for purifying the homodimer is given in Chapter 4. Prior to these studies, it was demonstrated that both forms of CoA transferase are identical with respect to their denaturation and refolding in buffers containing GuHCl (Chapter 4).[3]

The homogeneity of all protein preparations was confirmed by SDS-PAGE analysis. The concentrations of the purified protein solutions were determined from measurements of A_{278}, which were corrected for scatter. The following ε_{278} values, in units of $(mg/mL)^{-1}$, were used (Chapter 2): 0.65 for the wild-type enzyme, 0.66 for the hinge-mutant, 0.63 for the N-domain, and 0.69 for the C-domain. The concentrations of solutions of the purified wild-type enzyme or hinge-mutant used for refolding studies

Table 3-1: Growth Times of Bacterial Cultures Analyzed by Immunoblotting

Strain of *E. coli*[a]	Time of growth at 25 °C (h)	Time of growth at 37 °C (h)
BL-pT7-7	N/A[b]	10
BL-WT	12	2
BL-Hng	12	6
HB-pMS119EH	N/A[b]	10
HB-WT	2	2
HB-Hng	10	4
HB-N	N/A[b]	10
HB-C	N/A[b]	10

[a] Cells of BL21(DE3) were induced in the presence of 0.10 mM IPTG. Cells of HB101 were induced in the presence of 1.0 mM IPTG.

[b] N/A: not applicable (i.e. these experiments were not performed in this study).

were determined by measuring A_{278} without correcting for scatter. In such cases, an ε_{278} value of 0.75 $(\text{mg/mL})^{-1}$ was used for both forms of CoA transferase (Chapter 2).

Measurement of enzyme activity. CoA transferase activity was determined spectrophotometrically as described in Chapter 2. In the present study, the assay solutions consisted of 50 mM Tris-HCl, 15 mM $MgCl_2$, 0.060 to 0.30 mM succinyl-CoA, and 13 to 67 mM acetoacetate, at pH 9.1. The extinction coefficient for acetoacetyl-CoA at 310 nm (ε_{310}) was taken to be 7.8×10^3 M^{-1} cm^{-1} under these conditions (Howard et al., 1986). Specific enzyme activities were determined using assay solutions that contained 0.30 mM succinyl-CoA and 67 mM acetoacetate. All assays were carried out at 22 °C.

Citrate synthase activity was determined spectrophotometrically as described by Srere, 1969. The assay solutions consisted of 0.1 M Tris-HCl, 0.25 mM *cis*-oxaloacetate, 50 μM acetyl-CoA, and 0.1 mM DTNB, at pH 8.0. The extinction coefficient for the released thionitrobenzoate product at 412 nm (ε_{412}) was taken to be 1.36×10^4 M^{-1} cm^{-1} under these conditions (Srere, 1969).

Preparation of N- and C-domain mixtures. Appropriate amounts of the two domains were initially mixed at 4 °C in preparation for folding studies at higher temperatures. After transfer of the samples to the appropriate higher temperature, aliquots were removed at specific times, cooled immediately, and stored at 4 °C. After several days, all aliquots were assayed for CoA transferase activity under standard conditions.

The rate of commitment to aggregation of the purified N- and C-domains at 37 °C was evaluated by temperature-shift experiments. Mixtures of the N- and C-domains, in which each polypeptide was present at 0.10 mM, 50 μM, 20 μM, or 10 μM, were incubated at 37 °C for various times before transfer to 22 °C for additionally 2, 4, 9, or 9 h (respectively). The enzyme activity in each mixture was measured with an assay solution of 50 mM Tris-HCl, 15 mM $MgCl_2$, 0.060 mM succinyl-CoA, and 13 mM acetoacetate, at pH 9.1.

Radioactive labeling experiments. To evaluate the proportion of CoA transferase which was soluble in BL-WT or BL-Hng, exclusive labeling experiments were carried out using ^{35}S-methionine (Tabor & Richardson, 1985). Cells were grown at 25 °C or 37 °C in 1.5 mL of LB medium supplemented with ampicillin (final concentration, 0.10 mg/mL) until the OD_{600} of the culture reached 0.5. The cells were then transferred to 1.5 mL of M9 labeling medium (Appendix 6) and allowed to grow for 60 min prior to the induction of gene expression with IPTG (final concentration, 1 mM). After 20 min, each cell culture was treated with rifampicin (final concentration, 0.40 mg/mL) and allowed to grow for additionally 60 min. Subsequently, two aliquots of 0.25 mL were removed from each culture. The first of these was treated with 2.5 µCi of ^{35}S-methionine for 10 min, while the second aliquot was treated with 0.625 µCi of ^{35}S-methionine for 40 min. Following the radioactive labeling period, a portion of the cells (0.20 mL) was removed from each aliquot and lysed with Triton X-100 as described by Horwich et al. (1993). Specifically, cells resuspended in 8.0 µL of ice-cold lysis buffer (50 mM Tris, 25% sucrose, pH 7.4) were treated with 2.0 µL of lysozyme (final concentration, 2.0 mg/mL) for 5 min at 37 °C. The suspension was then supplemented with 30 µL of TENTA buffer (Appendix 6) and incubated for 20 min at 37 °C. The suspension of lysed cells was centrifuged (15 min, 1.0 × 10^4 g), and separate pellet and supernatant fractions were recovered. An aliquot of each, corresponding to 50 µL of the initial culture, was fractionated by SDS-PAGE, and the amount of radioactively labeled protein quantified by phosphorimager analysis.

The stability of CoA transferase proteins in the soluble fraction of *E. coli* BL21(DE3) was assessed at 37 °C by pulse-chase experiments (Tabor & Richardson, 1985). The procedure was similar to that described above, except that the cells were treated with ^{35}S-methionine (10 µCi per 1.0 mL of cell culture) for 7 min prior to a chase with unlabeled methionine. At various time points during the chase, aliquots (0.20 mL) were removed from each culture and the cells lysed with Triton X-100 as described above. A portion of the cell lysate, corresponding to 50 μL of the initial cell culture, was fractionated by SDS-PAGE, and the amount of labeled protein quantified by phosphorimager analysis.

Finally, the stability of CoA transferase proteins in whole cells of *E. coli* BL21(DE3) (as opposed to the soluble fraction; see above) was assessed at 37 °C by pulse-chase experiments similar to those described above. In this case, cells (0.10 mL) were removed from each culture at various times during the chase period and analyzed by SDS-PAGE without prior lysis by Triton X-100.

Refolding studies in vitro. Wild-type CoA transferase (final concentration of the NC monomer, 0.01-0.02 mM) and the hinge-mutant (final concentration of each domain, 0.01 mM) were denatured in unfolding buffer (Chapter 2) at 22 °C for a minimum of 5 h. The solutions of the unfolded proteins were then diluted 1:50 or 1:100 (v/v) in refolding buffer (Chapter 2). Alternatively, the solutions of the unfolded enzymes were placed on a semi-permeable membrane (Millipore VM, pore size 0.05μm) and dialyzed against 600 mL of the same refolding buffer. Solutions of the refolding enzyme, incubated at 22 °C or 37 °C, were assayed for CoA transferase activity at various time points.

For some experiments, unfolded CoA transferase was diluted into refolding buffer containing 12 mM $MgCl_2$ and: (1) 0.2 μM of the GroEL tetradecamer ($GroEL_{14}$); (2) 0.2 μM of $GroEL_{14}$ and 5 mM ATP; or (3) 0.2 μM of an equimolar complex of the GroEL tetradecamer and the GroES heptamer ($GroEL_{14}$:$GroES_7$) and 5 mM ATP. As a control experiment to estimate the non-specific chaperone activity, CoA transferase was diluted into refolding buffer containing 5 mM ATP, 12 mM $MgCl_2$, 0.2-2.0 μM of lysozyme, and the appropriate amount[4] of "GroEL storage buffer" (40 mM Tris-HCl, 80 mM NaCl, 8 mM $MgCl_2$, 4 mM DTT, 0.04% (w/v) NaN_3, and 20% (v/v) glycerol, pH 7.5). The addition of the GroEL storage buffer did not significantly affect the rate or yield of refolding of CoA transferase.

Citrate synthase from pig heart was denatured and refolded by a procedure adapted from Buchner et al. (1991). The enzyme was denatured in a buffer of 6.0 M GuHCl, 0.1 M Tris-HCl, and 20 mM DTT (pH 8.0) at 22 °C for 3.5 h. Solutions of unfolded citrate synthase (final concentration, 40 μM of each subunit) were then diluted 1:100 (v/v) in a buffer of 0.1 M Tris-HCl, 10 mM $MgCl_2$, 10 mM KCl, and 2 mM ATP (pH 8.0), in the presence or absence of $GroEL_{14}$ or $GroEL_{14}$:$GroES_7$ (final concentration, 0.28 μM). In the cases where GroEL was not included, the refolding solutions were supplemented with the appropriate amount of GroEL storage buffer. Solutions of refolding citrate synthase were incubated at 22 °C for 2 h prior to being assayed for enzyme activity.

As a control, the initial activity of CoA transferase or citrate synthase was determined using enzyme solutions with dilutions that reflected the composition of the final refolding mixture.

Kinetic data analysis. Kinetic data (Figures 3-3, 3-4, 3-6, 3-13, 3-15) were fit to single- or double-exponential curves using the program TableCurve 2D (Jandel Scientific, San Rafael, CA). The data and best-fit curves were subsequently plotted using the program SigmaPlot (also from Jandel).

RESULTS

Aggregation of the N- and C-domains in vitro. Partially folded polypeptides display an increased tendency to aggregate compared to proteins with stable tertiary and quaternary structures (reviewed in [Jaenicke, 1991]; [Price, 1994]; [Jaenicke, 1995]). To verify the hypothesis that the individual N- and C-domains lack a native fold (Chapter 2), it was assessed whether or not they are less soluble than the properly assembled hinge-mutant under conditions that favor aggregation.

First, the effect of temperature on the tendency of the two purified domains to aggregate *in vitro* was examined. As mentioned previously, the mixed domains precipitated at 37 °C, and only low levels of enzyme activity were observed (Chapter 2). The kinetics of "commitment" to this aggregation (Goldberg et al., 1991) were evaluated by temperature-shift experiments, in which an equimolar mixture of the N- and C-domains was preincubated at 37 °C for various times before transfer to 22 °C for an additional 2 h. The loss of recoverable enzyme activity with increasing time of preincubation at 37 °C was best described by a double-exponential equation, and was essentially complete at 15 min (Figure 3-3). In contrast, the purified hinge-mutant retained 85% of its initial enzyme activity when incubated at 37 °C for 1 h and subsequently at 22 °C for 3 h (data not shown). When the two protein domains were heated individually, both were found to precipitate at lower temperatures than the purified hinge-mutant; the C-domain aggregated at a lower temperature than the N-domain. From these results, it was concluded that the N- and C-domains are more thermally unstable *in vitro* as separate polypeptides than as components of the correctly folded hinge-mutant, and that the C-domain is more susceptible to heat denaturation than the N-domain.

Second, the effect of protein concentration on the rate of commitment to aggregation of the purified N- and C-domains was investigated. Given that folding intermediates are less soluble at higher concentrations (Zettlmeissl et al., 1979; Goldberg et al., 1991; van der Vies et al., 1992), it was predicted that the recoverable enzyme activity should decrease progressively more slowly from equimolar mixtures of the two domains which were diluted to increasing extents prior to incubation at 37 °C. Mixtures of the N- and C-domains, in which each polypeptide was present at 10 μM, 20 μM, or 50 μM, were incubated at 37 °C for various times before being transferred to 22 °C for additionally 9 h, 9 h, or 4 h (respectively). For each protein solution, the loss of recoverable enzyme activity with increasing time of preincubation at 37 °C was best described as a single-exponential decay (Figure 3-4). The recoverable enzyme activity from mixtures containing 10 μM, 20 μM, or 50 μM of each domain disappeared

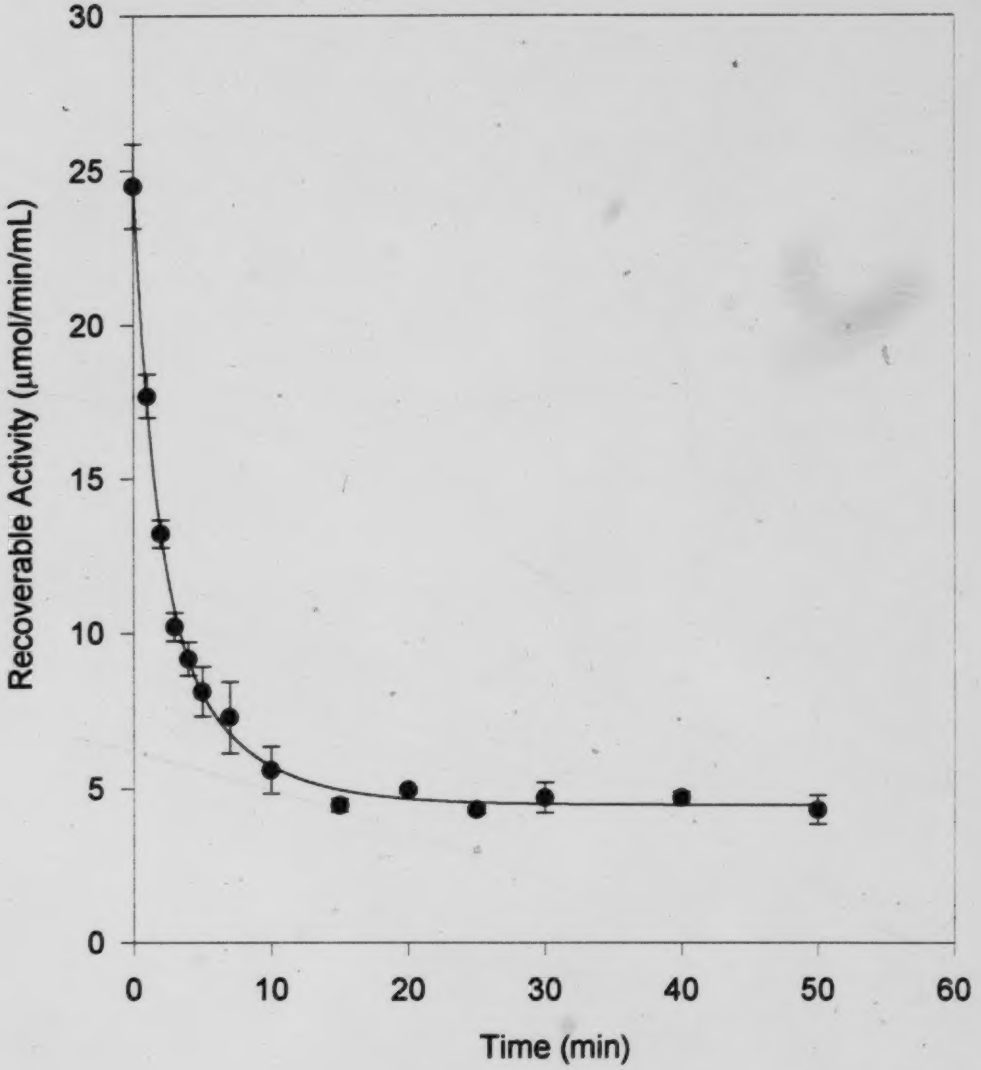

Figure 3-3: Commitment to aggregation *in vitro* of the isolated N- and C-domains. Mixtures of the purified N- and C-domain polypeptides (100 µM each) were preincubated at 37 °C for the times shown. Subsequently, each sample was incubated further at 22 °C for 2 h prior to being assayed for enzyme activity. The data were fit to a double-exponential equation ($A = 4.49 + 12.2e^{-0.65T} + 7.87e^{-0.19T}$; $r^2 = 1.00$), where A = CoA transferase activity (µmol/min/mL) and T = time of preincubation at 37 °C (min). The experiment was performed in duplicate, with an average relative error of ± 7%. Enzyme activities were measured with an assay solution of 50 mM Tris-HCl, 15 mM $MgCl_2$, 0.060 mM succinyl-CoA, and 13 mM acetoacetate, at pH 9.1.

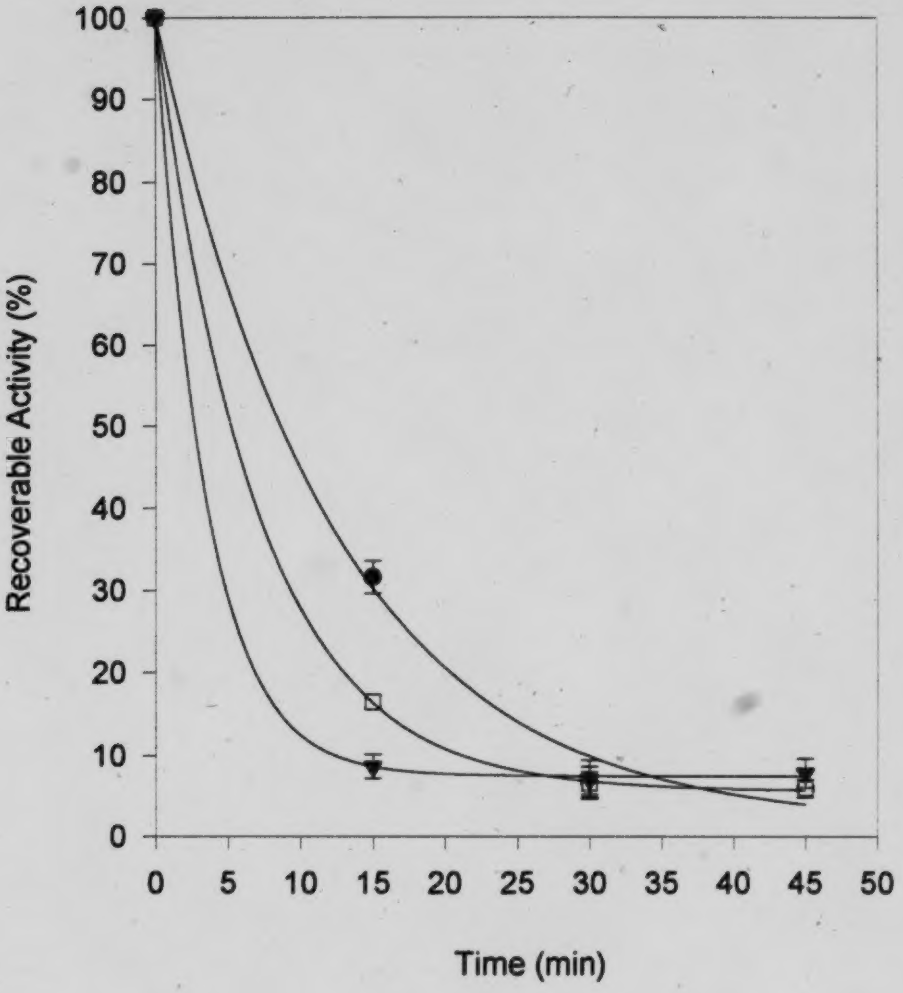

Figure 3-4: Effect of concentration on the rate of commitment to aggregation *in vitro* of the isolated N- and C-domains. Mixtures of the purified N- and C-domain polypeptides were preincubated at 37 °C for the times shown. Subsequently, each sample was incubated further at 22 °C prior to being assayed for enzyme activity. The concentration of each domain in the mixture was 0.010 mM (●), 0.020 mM (❑), or 0.050 mM (▼). The first-order rate constants are: 0.010 mM, $k = 1.4 \times 10^{-3}$ s^{-1} ($r^2 = 1.00$); 0.020 mM, $k = 2.4 \times 10^{-3}$ s^{-1} ($r^2 = 1.00$); 0.050 mM, $k = 4.8 \times 10^{-3}$ s^{-1} ($r^2 = 1.00$). The experiment was performed in duplicate, with an average relative variability of ± 18%. The yield of active enzyme recovered is expressed as a percentage of the activity in the unheated sample.

with half-lives of 8.4, 4.8, or 2.4 min, respectively (Figure 3-4). As a control, it was demonstrated that the three mixtures displayed identical enzyme activities when incubated at 22 °C without preincubation at 37 °C. These results indicated that the rate of commitment to aggregation of the N- and C-domains *in vitro* is directly proportional to the concentration of each domain in the equimolar mixture.

Aggregation of wild-type CoA transferase during refolding in vitro. A maximum of 35% of the initial CoA transferase activity was recovered upon refolding of the wild-type enzyme (0.2 μM) from denaturant at 22 °C (Chapter 2). Most of the initial enzyme activity was presumably lost in the form of aggregates, given that more than half of the CoA transferase protein present in the refolding solution was undetectable by non-denaturing PAGE (Chapter 2). This assumption was verified by examining the decrease in the yield of refolded, wild-type CoA transferase under conditions that favor aggregation. Based on the aggregation properties observed for the purified N- and C-domains, it was predicted that the percentage of active wild-type enzyme recovered upon dilution from denaturant should decrease with increasing protein concentration or temperature. Enzyme which had been denatured in 6.0 M GuHCl for at least 5 h at 22 °C was refolded at 10 μM and 22 °C, or at 0.2 μM and 37 °C. In each case, the yield of correctly refolded wild-type CoA transferase was reduced compared to that observed for enzyme refolded at 0.2 μM and 22 °C (Figure 3-5). Thus, the enzyme is less capable of refolding from denaturant under conditions which promote the aggregation of nonnative polypeptides.

To evaluate the kinetics of commitment to aggregation, solutions of refolding CoA transferase (0.2 μM) were analyzed by temperature-shift experiments. The amount of enzyme activity recovered after refolding for 2 h at 22 °C decreased with increasing time of preincubation at 37 °C (Figure 3-6). This loss of recoverable enzyme activity occurred as a double-exponential decay, and was essentially complete within 5 min (Figure 3-6).

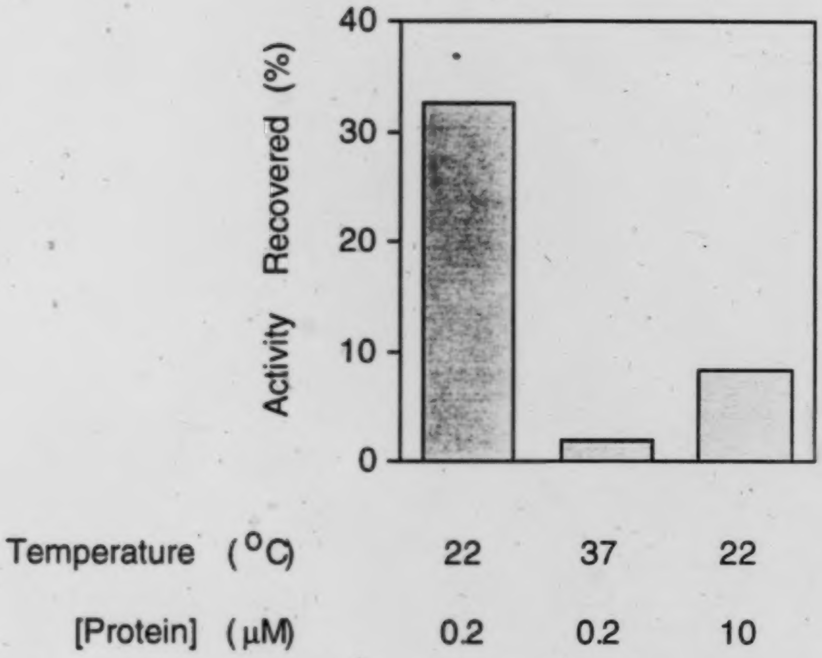

Figure 3-5: Effect of temperature and protein concentration on the refolding of CoA transferase *in vitro*. The wild-type enzyme was denatured in 6.0 M GuHCl at 22 °C for 6 h. Subsequently, the enzyme was diluted 50-fold (v/v; final concentration of the NC monomer, 0.2 μM) with refolding buffer at 22 °C or 37 °C. Alternatively, the unfolded enzyme was dialyzed (final concentration of the NC monomer, 10 μM) against refolding buffer at 22 °C. The yield of active enzyme recovered upon renaturation is expressed as a percentage of the initial activity of non-denatured enzyme.

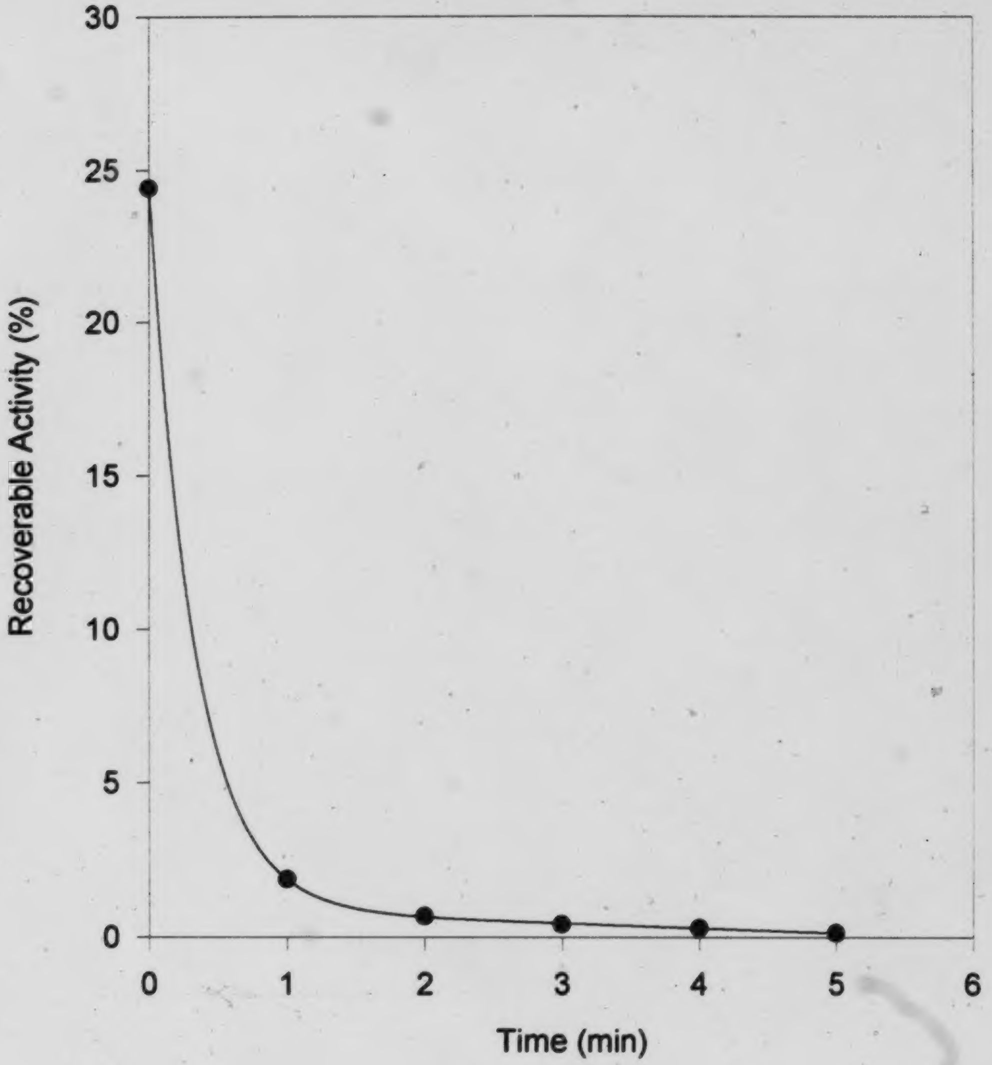

Figure 3-6: Commitment to aggregation *in vitro* of CoA transferase upon refolding. The wild-type enzyme was denatured at 22 °C for 10 h and subsequently diluted 50-fold (v/v; final concentration of the NC monomer, 0.2 μM) with refolding buffer. Immediately after dilution, samples of refolding enzyme were preincubated at 37 °C for the times shown. Subsequently, each sample was incubated further at 22 °C for 12 h prior to being assayed for enzyme activity. The data were best fit to a double-exponential equation ($A = -0.37 + 23.2e^{-3.16T} + 1.56e^{-0.22T}$; $r^2 = 1.00$), where A = CoA transferase activity (expressed as a percentage of the initial activity of non-denatured enzyme) and T = time of preincubation at 37 °C (min).

Effect of temperature on aggregation in vivo. It has been suggested that factors which lead to the aggregation of proteins *in vitro* also promote the formation of insoluble aggregates (or inclusion bodies) in cells of *E. coli* expressing foreign genes (reviewed in [Jaenicke, 1991]; [Thatcher & Hitchcock, 1994]; [King et al., 1996]; [Mukhopadhyay, 1997]). Since the refolding wild-type enzyme and hinge-mutant are susceptible to aggregation at elevated temperatures and protein concentrations *in vitro* (Chapter 2; Figure 3-5), it was predicted that similar effects should be observed *in vivo*. This hypothesis was tested by two experimental approaches, using radioactive labeling and immunoreactivity to monitor the levels of soluble and insoluble protein.

First, the effect of temperature on the level of soluble, recombinant CoA transferase produced in *E. coli* was ascertained by radioactive labeling experiments. Cells of BL-WT or BL-Hng, grown in the presence of 0.10 mM IPTG for 80 min at 25 °C or 37 °C, were treated for an additional 10 or 40 min with ^{35}S-methionine. Radioactively labeled proteins in the cell lysate or insoluble fraction were resolved by SDS-PAGE and quantified by phosphorimager analysis. In this experiment, the proportion of radioactive label in the insoluble fraction of cells treated with ^{35}S-methionine for 10 or 40 min corresponded to the tendency of CoA transferase to aggregate between 80 and 90 min or 80 and 120 min (respectively) after the induction of gene expression. Approximately 95% of the wild-type CoA transferase protein accumulated as inclusion bodies in cells of BL-WT which were grown at 37 °C (Figures 3-7A, 3-8A). In contrast, only about 70% of the wild-type enzyme formed insoluble aggregates in cells of BL-WT grown at 25 °C (Figures 3-7B, 3-8B).

The aggregation properties of the hinge-mutant in *E. coli* were assessed by evaluating the relative amounts of each radioactively labeled domain present in the soluble and insoluble fractions. The total intensity of the bands representing the insoluble and soluble N-domain was 1.5 to 2.0 times greater than the total phosphorimager signal measured for the C-domain (Figure 3-9). Since there are 5.5 times more methionine

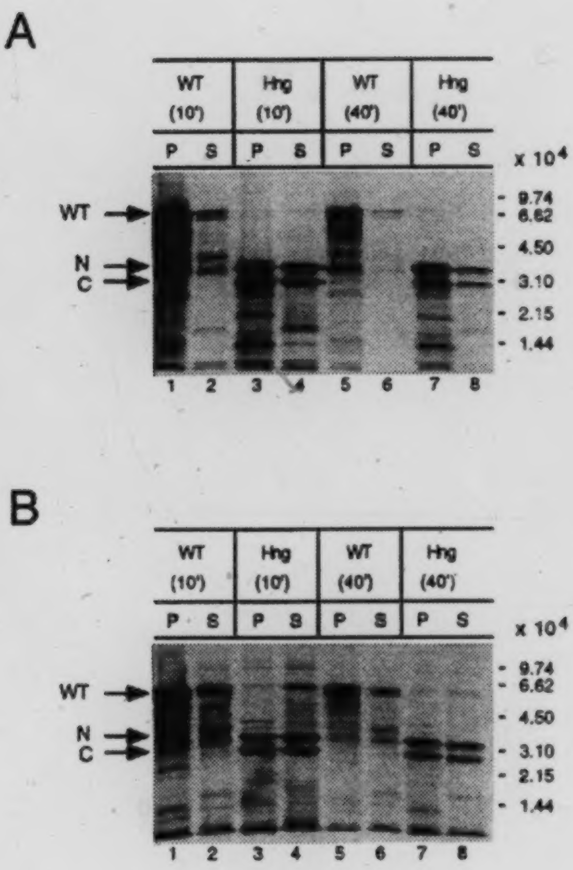
A
WT (10')
Hng (10')
WT (40')
Hng (40')
P S P S P S P S
x 10⁴
9.74
6.62
4.50
3.10
2.15
1.44
WT
N
C
1 2 3 4 5 6 7 8
B
WT (10')
Hng (10')
WT (40')
Hng (40')
P S P S P S P S
x 10⁴
9.74
6.62
4.50
3.10
2.15
1.44
WT
N
C
1 2 3 4 5 6 7 8

Figure 3-7: Aggregation of wild-type CoA transferase and the hinge-mutant *in vivo*, as measured by autoradiography. Cultures of BL21(DE3) were radioactively labeled with ^{35}S-methionine for the indicated times at 37 °C (A) or 25 °C (B). Lanes 1, 2, 5, and 6: wild-type CoA transferase (WT); lanes 3, 4, 7, and 8: hinge-mutant (Hng). Cell pellets (P) and lysates (S) were subsequently analyzed by SDS-PAGE and autoradiography. Bands representing the 5.2 x 10^4 wild-type subunit (WT), 2.8 x 10^4 N-domain (N), and 2.4 x 10^4 C-domain (C) are indicated by appropriately labeled arrows.

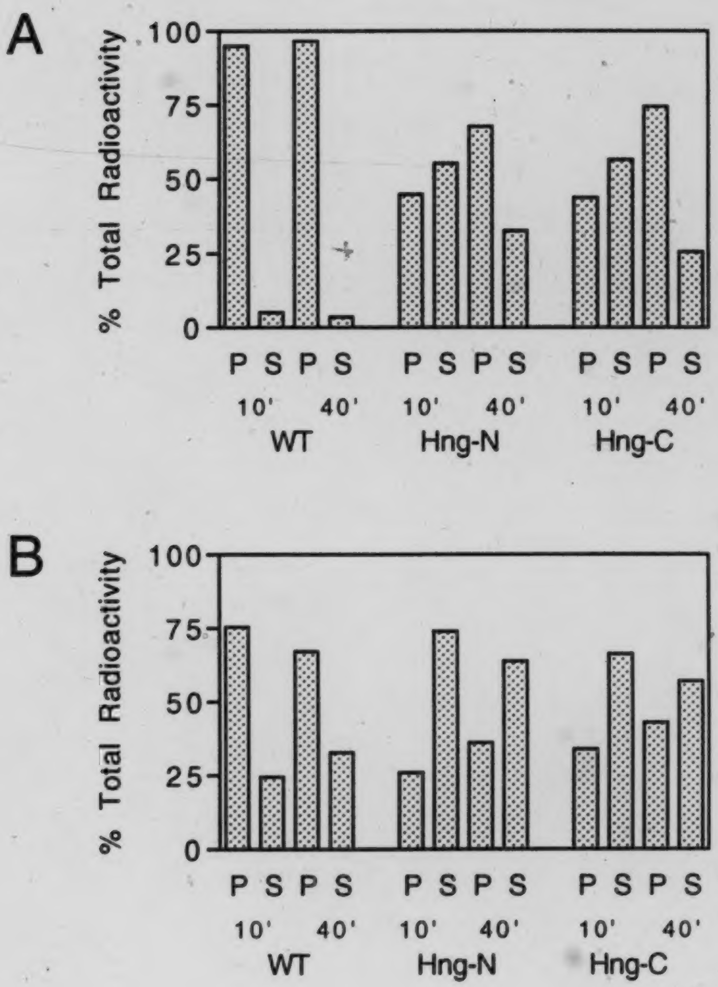

Figure 3-8: Quantification of the results from Figure 3-7 by phosphorimagery. The abbreviations "WT," "Hng-N," and "Hng-C" refer to the wild-type monomer and the N- and C-domains of the hinge-mutant (respectively). All other symbols are as described in the legend to Figure 3-7.

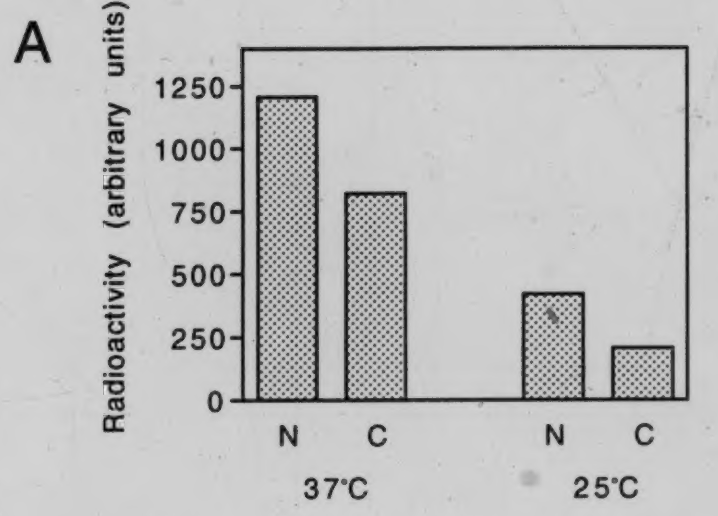

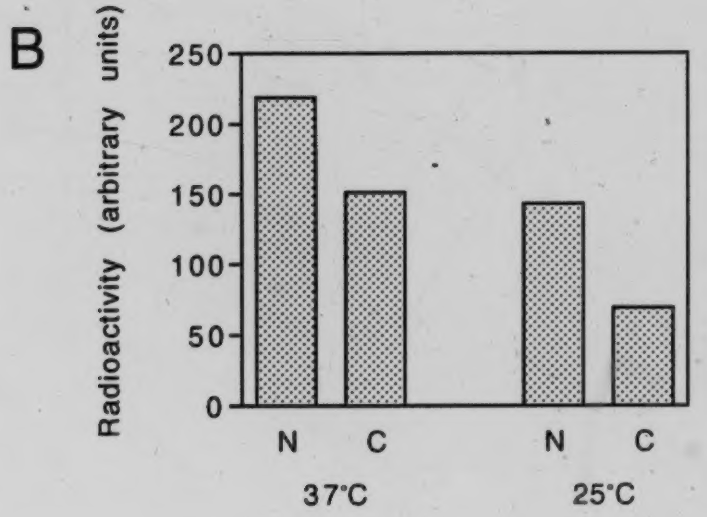

Figure 3-9: Total radioactivity associated with the N- and C-domains in cells of BL-Hng. Cells were radioactively labeled for 10 min (A) or 40 min (B) at the indicated temperatures (see Figure 3-7). The total radioactivity associated with the N-domain (N) or the C-domain (C) in the insoluble and soluble fractions was determined by phosphorimagery. Note that the signal is much weaker in (B) because the cells which were radioactively labeled for 40 min were treated with ^{35}S-methionine at a lower specific activity.

residues in the C-domain than in the N-domain,[5] it was concluded that the N-domain was 8-11 times more abundant than the C-domain in BL-Hng. To account for the imbalance in the levels of the two domains in cells of BL-Hng, it was proposed that the reinitiation of translation on the polycistronic mRNA encoding the hinge-mutant might be inefficient. As a result, the C-domain would be synthesized more slowly than the N-domain in cells of BL-Hng or HB-Hng. Moreover, under these conditions the rate of assembly of the N- and C-domains to the active enzyme form in *E. coli* should be limited by the rate of production of the C-domain. If this hypothesis were true, then the specific enzyme activity should be maximal at later times in lysates of HB-Hng cells compared to lysates of HB-WT cells. At 25 °C, the maximal specific CoA transferase activity in lysates of HB-WT cells and HB-Hng cells occurred after induction periods of 2 h and 10 h, respectively (Figure 3-10). This result was consistent with the hypothesis that the C-domain is synthesized less efficiently than the N-domain in cells of BL-Hng.

Despite the difference in their absolute levels, both proteins were similarly distributed between the soluble and insoluble fractions in *E. coli*. For example, approximately 44% and 30% of each radioactively labeled domain formed aggregates in cells of BL-Hng which were treated with ^{35}S-methionine for 10 min at 37 °C and 25 °C, respectively (Figures 3-7, 3-8). Similarly, 70% and 40% of each radioactively labeled domain formed inclusion bodies in cells of BL-Hng which were treated with ^{35}S-methionine for 40 min at 37 °C and 25 °C, respectively (Figures 3-7, 3-8). Interestingly, at 25 °C and 37 °C, a lower percentage of CoA transferase formed inclusion bodies in cells of BL-Hng than in cells of BL-WT (Figures 3-7, 3-8). This result was consistent with the observation that the maximal specific enzyme activity measured in lysates of HB-Hng cells was two times greater than that measured in lysates of HB-WT cells (Figure 3-10).

Subsequently, the effect of temperature on the level of soluble, recombinant CoA transferase produced in *E. coli* was further investigated by Western blot analysis. Cultures

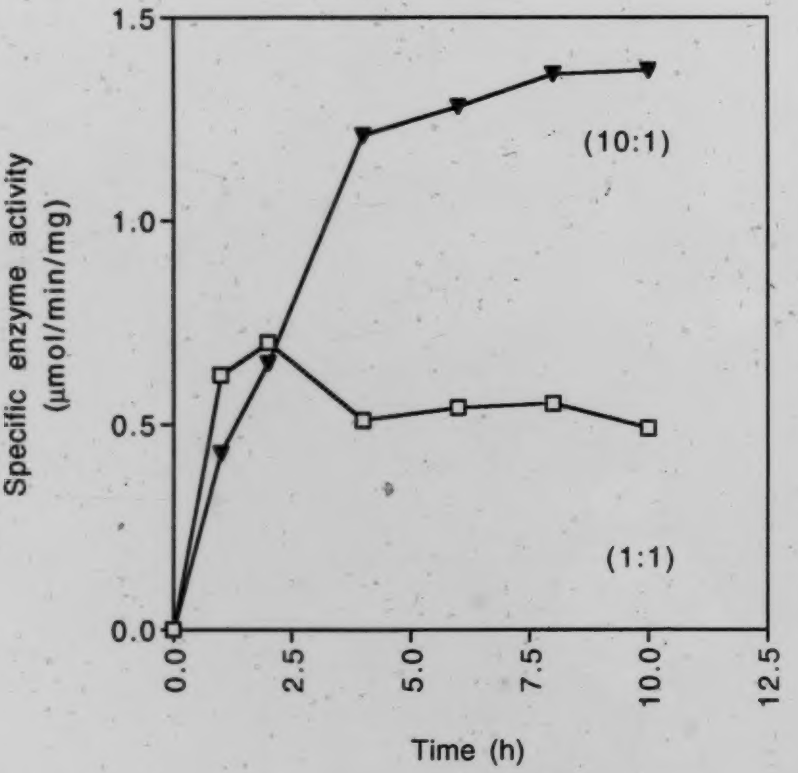

Figure 3-10: Kinetics of the appearance of CoA transferase activity in *E. coli*. Cells from HB-WT (❑) or HB-Hng (▼) were grown in the presence of 1 mM IPTG at 25 °C. Aliquots of these cultures were removed at the indicated times, and the cells were disrupted by sonication. The resulting suspension was clarified of cell debris by centrifugation, and the specific enzyme activity was determined in the soluble fraction. Shown in parentheses beside each curve is the approximate molar ratio of N-domain to C-domain estimated for the corresponding strain of HB-101. CoA transferase activity was measured with an assay solution of 50 mM Tris-HCl, 15 mM $MgCl_2$, 0.30 mM succinyl-CoA, and 67 mM acetoacetate, at pH 9.1.

of BL-WT or BL-Hng were grown in the presence of 0.1 mM IPTG for 12 h at 25 °C, or 2 h at 37 °C. Following disruption of the cells by sonication, proteins in the soluble and insoluble fractions were resolved by SDS-PAGE and transferred to nitrocellulose. In each of these strains of *E. coli*, a greater proportion of immunoreactive CoA transferase accumulated as insoluble aggregates at 37 °C than at 25 °C (Figure 3-11A). At both temperatures, the N- and C-domains of BL-Hng were similarly distributed between the cell lysate and inclusion bodies. Similar results were obtained when the strains HB-WT and HB-Hng were grown in the presence of 1 mM IPTG at 25 °C or 37 °C and subsequently analyzed by Western blot analysis (Figure 3-11B). Finally, at a given temperature, a greater proportion of immunoreactive CoA transferase accumulated as insoluble aggregates in cells of BL-WT or HB-WT than in cells of BL-Hng or HB-Hng, respectively.

In conclusion, results from two independent experiments indicated that: (1) the wild-type enzyme and hinge-mutant are more susceptible to aggregation in cells of *E. coli* grown for various times at 37 °C than at 25 °C; and (2) wild-type CoA transferase is produced in less soluble form *in vivo* than the hinge-mutant at the same temperature.

Aggregation of the individual N- and C-domains in vivo. As mentioned above, the N- and C-domains of CoA transferase displayed similar tendencies to aggregate in BL-Hng or HB-Hng. In each of these strains grown under inducing conditions, the two domains associate to form an enzymatically active N_2C_2-complex (Chapter 2). In the absence of assembly, neither domain is capable of adopting a fully native fold in *E. coli* (Chapter 2). It was considered that the productive interaction between the N- and C-domains may also preclude their aggregation *in vivo*. If this were true, then each domain should be less soluble when synthesized in the absence of the other in *E. coli*.

The solubility of each domain produced separately in *E. coli* was ascertained by Western blot analysis. Cultures of HB-N or HB-C were grown in the presence of 1.0 mM

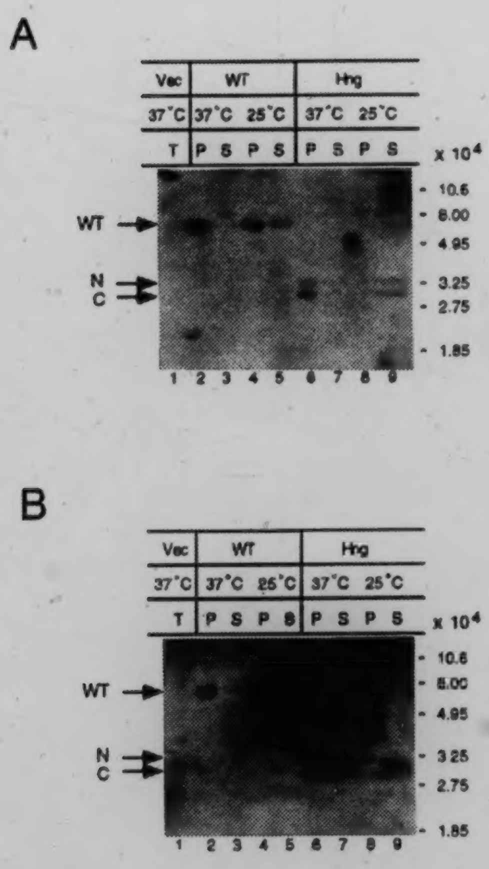
A
Vec
WT
Hng
37°C
37°C 25°C
37°C 25°C
T
P S P S
P S P S
x 10⁴
10.6
6.00
4.95
3.25
2.75
1.85
WT
N
C
1 2 3 4 5 6 7 8 9
B
Vec
WT
Hng
37°C
37°C 25°C
37°C 25°C
T
P S P S
P S P S
x 10⁴
10.6
6.00
4.95
3.25
2.75
1.85
WT
N
C
1 2 3 4 5 6 7 8 9

Figure 3-11: Aggregation of wild-type CoA transferase and the hinge-mutant *in vivo*, as measured by immunoreactivity. Cultures of BL21(DE3) (A) or HB101 (B) were grown under inducing conditions at the indicated temperatures, as described in Table 3-1. Lane 1: vector control (Vec); lanes 2-5: wild-type CoA transferase (WT); lanes 6-9: hinge-mutant (Hng). Unfractionated cells (T), or cell pellets (P) and lysates (S), were analyzed by SDS-PAGE and Western blotting. Each lane was loaded with the equivalent of 50 µL of the initial culture. Bands representing the 5.2 x 10^4 wild-type subunit (WT), 2.8 x 10^4 N-domain (N), and 2.4 x 10^4 C-domain (C) are indicated by appropriately labeled arrows.

IPTG for 10 h at 37 °C. Following disruption of the cells by sonication, proteins in the soluble and insoluble fractions were resolved by SDS-PAGE and transferred to nitrocellulose. The proportion of the C-domain which accumulated as inclusion bodies was greater than that of the N-domain (Figure 3-12), suggesting that the C-domain is more susceptible to aggregation. Interestingly, the solubilities of the individual N- and C-domains in HB-N and HB-C were similar to those of the hinge-mutant and wild-type enzyme in cells of HB-Hng and HB-WT (respectively) grown at 37 °C (Figures 3-11, 3-12).

Depletion of recombinant protein from the cell lysate. The rate of disappearance of recombinant CoA transferase from the soluble fraction of *E. coli* was evaluated by pulse-chase labeling experiments. Cultures of BL-WT, BL-Hng, BL-N, and BL-C, grown at 37 °C, were treated briefly with ^{35}S-methionine, prior to dilution of the label by the addition of excess unlabeled methionine. At different times during the chase period, cell lysates were prepared from aliquots of each culture. Subsequent analysis by SDS-PAGE and autoradiography showed that the exclusively labeled, individual N- and C-domains decayed more rapidly than wild-type CoA transferase or the C-domain of the hinge-mutant (Figure 3-13). Quantitation of these results by phosphorimagery indicated that, for each of the proteins examined, the rate of disappearance of the label was best described by a double-exponential equation — which precluded a simple calculation of the half-life for this process (Figure 3-14). Nevertheless, approximately 50% of the radioactivity associated with wild-type CoA transferase or the C-domain of the hinge-mutant was lost after 5 h, while label disappeared to a similar extent from the individual N- or C-domains within only 2 h or 0.25 h, respectively. The observed disappearance of labeled C-domain from the soluble fraction of BL-C was attributable to the formation of inclusion bodies rather than to proteolysis, given that no significant decrease in label was observed when whole BL-C cells were analyzed in the same manner for 1 h (data not shown).

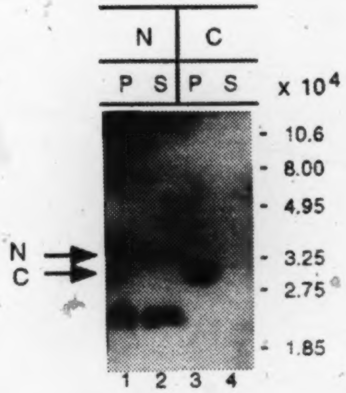

Figure 3-12: Aggregation of the N- and C-domains *in vivo*. Cultures of HB-N or HB-C were grown under inducing conditions at 37 °C, as described in Table 3-1. Lanes 1 and 2, N-domain (N); lanes 3 and 4: C-domain (C). Cell pellets (P) and lysates (S) were analyzed by SDS-PAGE and Western blotting. Each lane was loaded with the equivalent of 80 μL of the initial culture. Bands representing the 2.8 x 10^4 N-domain (N) and 2.4 x 10^4 C-domain (C) are indicated by appropriately labeled arrows.

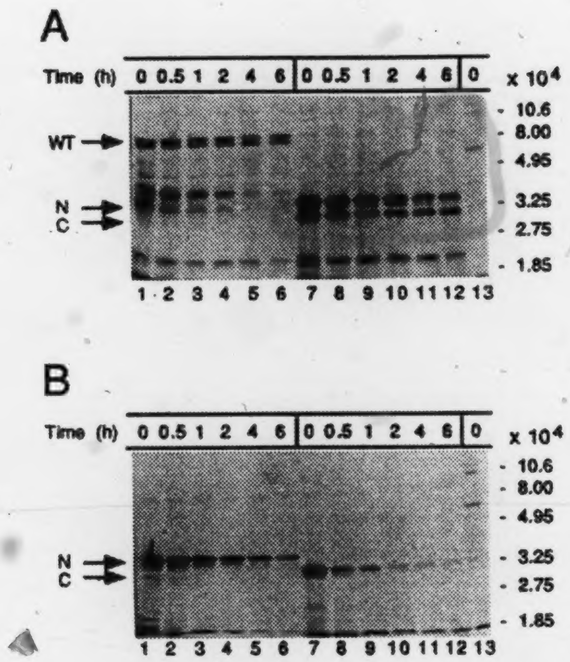
A
Time (h)
0 0.5 1 2 4 6 0 0.5 1 2 4 6 0
x 10⁴
WT
N
C
10.6
8.00
4.95
3.25
2.75
1.85
1 2 3 4 5 6 7 8 9 10 11 12 13
B
Time (h)
0 0.5 1 2 4 6 0 0.5 1 2 4 6 0
x 10⁴
N
C
10.6
8.00
4.95
3.25
2.75
1.85
1 2 3 4 5 6 7 8 9 10 11 12 13

Figure 3-13: Depletion of recombinant protein from *E. coli* cell lysates. (A) Cultures of BL-WT (lanes 1-6), BL-Hng (lanes 7-12), and BL-pT7-7 (lane 13) were pulsed at 37°C with ^{35}S-methionine prior to chase for the indicated times. Cell lysates were subsequently analyzed by SDS-PAGE and autoradiography. Each lane was loaded with 3 μg of total cell lysate protein. Bands representing the 5.2 x 10^4 wild-type subunit (WT), 2.8 x 10^4 N-domain (N), and 2.4 x 10^4 C-domain (C) are indicated by appropriately labeled arrows. (B) Cultures of BL-N (lanes 1-6), BL-C (lanes 7-12), and BL-pT7-7 (lane 13) were treated and evaluated as in (A). Bands representing the 2.8 x 10^4 N-domain (N) and 2.4 x 10^4 C-domain (C) are indicated by appropriately labeled arrows.

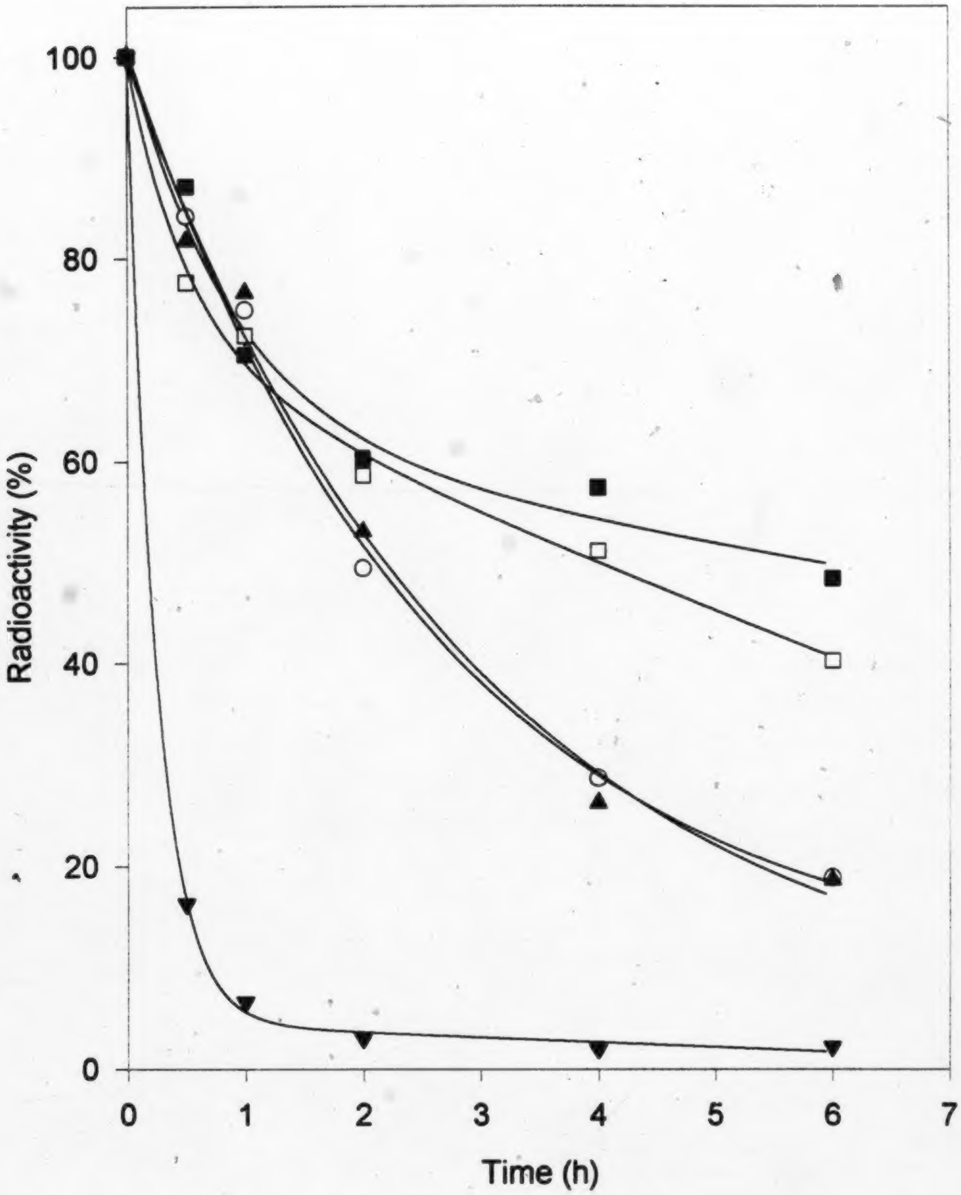

Figure 3-14: Quantification of the results from Figure 3-13 by phosphorimagery. The decay curves represent the disappearance of wild-type CoA transferase (■), the C-domain of the hinge-mutant (❑), the N-domain alone (▲), the N-domain of the hinge-mutant (❍), and the C-domain alone (▼) from the soluble fraction of *E. coli*. In each case, the data were best fit to a double-exponential equation, with r^2 values ranging from 0.98 to 1.00.

Presumably, the depletion of the other three recombinant polypeptides in cells of BL21(DE3) proceeded by the same mechanism (see "Discussion").

It should be noted that the decay of the N-domain apparent with BL-Hng (Figure 3-13A) did not reflect the disappearance of the hinge-mutant, *per se*. Because the N-domain polypeptide has only one fifth of the methionine residues of the C-domain, it follows that the bands of similar intensity in Figure 3-13A (lanes 7 through 12) did not originate from similar amounts of the two proteins; rather, the N-domain was present in large excess over the C-domain in BL-Hng, as discussed above. It was this excess of N-domain that was seen to decrease in a manner parallel to the individual N-domain in BL-N (Figure 3-13B).

In conclusion, the N- and C-domains of CoA transferase are depleted more rapidly than the wild-type enzyme or hinge-mutant from the soluble fraction of *E. coli*. This effect is more pronounced for the C-domain than for the N-domain.

Effects of GroEL and GroES on the refolding of CoA transferase. From the above discussion, it is clear that the folding and assembly of CoA transferase are compromised by aggregation. The aggregation of other oligomeric enzymes of the mitochondrial matrix is decreased *in vivo* due to the action of the eukaryotic Hsp60 (Cheng et al., 1989; Ostermann et al., 1989) and Cpn10 (Rospert et al., 1993; Höhfeld & Hartl, 1994), which are referred to as "chaperonin" and "co-chaperonin," respectively (Hemmingsen et al., 1988). The ability of the chaperonin system to suppress the aggregation of wild-type CoA transferase *in vitro* was tested by investigating the refolding of the enzyme in the presence of GroEL_{14} or GroEL_{14}:GroES_7 from *E. coli*. This experimental approach was considered reasonable, given that: (1) the GroEL/GroES complex of *E. coli* is functionally and structurally homologous to Hsp60_{14}:Cpn10_7, which mediates the folding and assembly of other oligomeric proteins imported into the mitochondrial matrix (Cheng et al., 1989; Ostermann et al., 1989; Rospert et al., 1993; Höhfeld & Hartl, 1994); and (2) unlike GroEL and GroES, purified Hsp60 and Cpn10 were not (until recently) commercially available in purified form. If the bacterial chaperonin system increased the refolding yield of CoA transferase, then it would be predicted (by analogy) that Hsp60_{14}:Cpn10_7 mediates the folding of the enzyme within the more physiological context of the mitochondrial matrix.

Samples of wild-type CoA transferase (final concentration of the NC monomer, 0.01 mM) and the hinge-mutant (final concentration of each domain, 0.01 mM) were denatured in unfolding buffer containing 6 M GuHCl (see "Experimental Procedures"). Subsequently, each protein solution was diluted by a factor of 50 with refolding buffer containing Mg^{2+} and ATP, in the absence or presence of $GroEL_{14}$ (final concentration, 0.2 μM) or $GroEL_{14}$:$GroES_7$ (final concentration, 0.2 μM). No enzyme activity was detected in the refolding hinge-mutant sample up to 24 h after dilution, even in samples which contained $GroEL_{14}$ or $GroEL_{14}$:$GroES_7$. In contrast, enzyme activity appeared with apparent first-order kinetics in all samples of refolding wild-type CoA transferase incubated at 22 °C (Figure 3-15A). The yield of correctly refolded enzyme was 1.5 times greater in the presence of $GroEL_{14}$ or $GroEL_{14}$:$GroES_7$ compared to the spontaneous, unassisted refolding reaction (Figures 3-15A, 3-16A). Furthermore, the apparent first-order rate constant for refolding in the presence of $GroEL_{14}$ or $GroEL_{14}$:$GroES_7$ was 1.5-fold less than that observed for unassisted refolding (Figure 3-15A). In contrast, the enzyme could not be refolded at 37 °C in buffers containing Mg^{2+}, ATP, and $GroEL_{14}$ or $GroEL_{14}$:$GroES_7$. Importantly, the yield and rate of CoA transferase refolding at 22 °C also increased and decreased (respectively) in the presence of increasing concentrations of lysozyme (Figures 3-15B, 3-16A). However, this non-specific effect was less pronounced than the refolding assistance provided by the chaperonin system, since a tenfold molar excess of lysozyme compared to $GroEL_{14}$ was required to achieve a similar increase in the yield and decrease in the rate of refolding of wild-type CoA transferase (Figures 3-15B, 3-16A). Dilution of a solution of the denatured wild-type enzyme (final concentration of the NC monomer, 0.02 mM) by a factor of 100 with refolding buffer

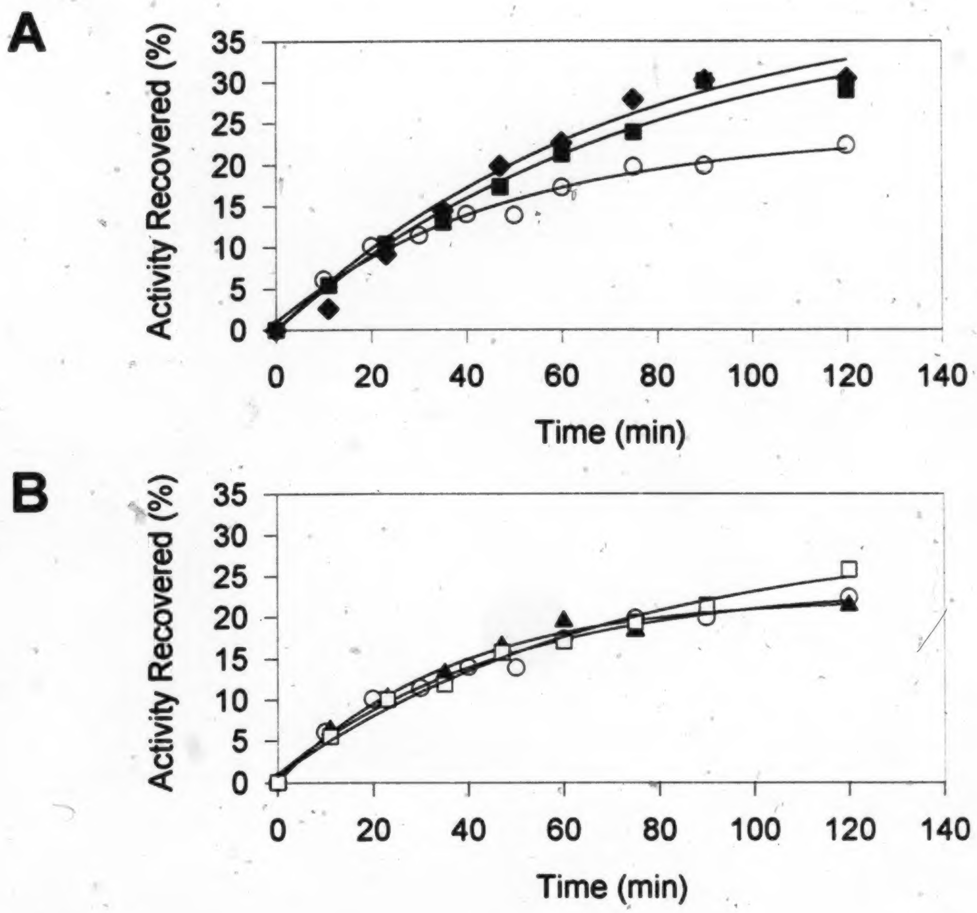

Figure 3-15: Kinetics of refolding of CoA transferase at 22 °C. (A) Effect of GroEL and GroES. Wild-type CoA transferase was denatured in 6.0 M GuHCl at 22 °C for 6 h. The enzyme was then diluted 50-fold (v/v; final concentration of the NC monomer, 0.2 μM) with refolding buffer containing 12 mM $MgCl_2$ and 5 mM ATP. Refolding was in the absence of GroEL and GroES (○), or in the presence of 0.2 μM $GroEL_{14}$ (◆) or 0.2 μM $GroEL_{14}$:$GroES_7$ (■). (B) Effect of lysozyme as a control. The wild-type enzyme was denatured and diluted as described in (A). Refolding was in the absence of lysozyme (○), or in the presence of lysozyme at a final concentration of 0.2 μM (▲) or 2.0 μM (□). Samples which contained lysozyme were also supplemented with GroEL storage buffer (see "Experimental Procedures"). At the indicated times, aliquots were removed from the samples of refolding enzyme and assayed for CoA transferase activity. The apparent first-order rate constants are: no additives, $k = 3.5 \times 10^{-4}\ s^{-1}$ ($r^2 = 0.98$); $GroEL_{14}$, $k = 2.3 \times 10^{-4}\ s^{-1}$ ($r^2 = 0.98$); $GroEL_{14}$:$GroES_7$, $k = 2.2 \times 10^{-4}\ s^{-1}$ ($r^2 = 0.98$); 0.2 μM lysozyme, $4.6 \times 10^{-4}\ s^{-1}$ ($r^2 = 0.99$); 2.0 μM lysozyme, $2.3 \times 10^{-4}\ s^{-1}$ ($r^2 = 0.99$). The yield of active enzyme recovered upon renaturation is expressed as a percentage of the initial activity of non-denatured enzyme.

Figure 3-16: Effect of GroEL and GroES on the yield of refolded CoA transferase or citrate synthase at 22 °C. (A) CoA transferase activity recovered after 2 h of refolding in solutions containing GuHCl at a final concentration of 0.12 M. The samples are described in Figure 3-15. "1×" and "10×" refer to lysozyme concentrations of 0.2 and 2.0 µM, respectively. (B) CoA transferase activity recovered after 2 h of refolding in solutions containing GuHCl at a final concentration of 0.060 M. Wild-type CoA transferase was denatured in 6.0 M GuHCl at 22 °C for 6 h. The enzyme was then diluted 100-fold (v/v; final concentration of NC monomer, 0.2 µM) with refolding buffer containing 12 mM $MgCl_2$ and 5 mM ATP. Refolding was in the absence of GroEL and GroES, or in the presence of 0.2 µM $GroEL_{14}$ or 0.2 µM $GroEL_{14}$:$GroES_7$. (C) Citrate synthase activity recovered after 2 h of refolding in the absence or presence of $GroEL_{14}$ or $GroEL_{14}$:$GroES_7$. The enzyme was denatured and refolded as described in "Experimental Procedures". In (B) and (C), the samples which lacked GroEL and GroES contained an appropriate volume of GroEL storage buffer (see "Experimental Procedures"). The yield of active enzyme recovered upon renaturation is expressed as a percentage of the initial activity of non-denatured enzyme.

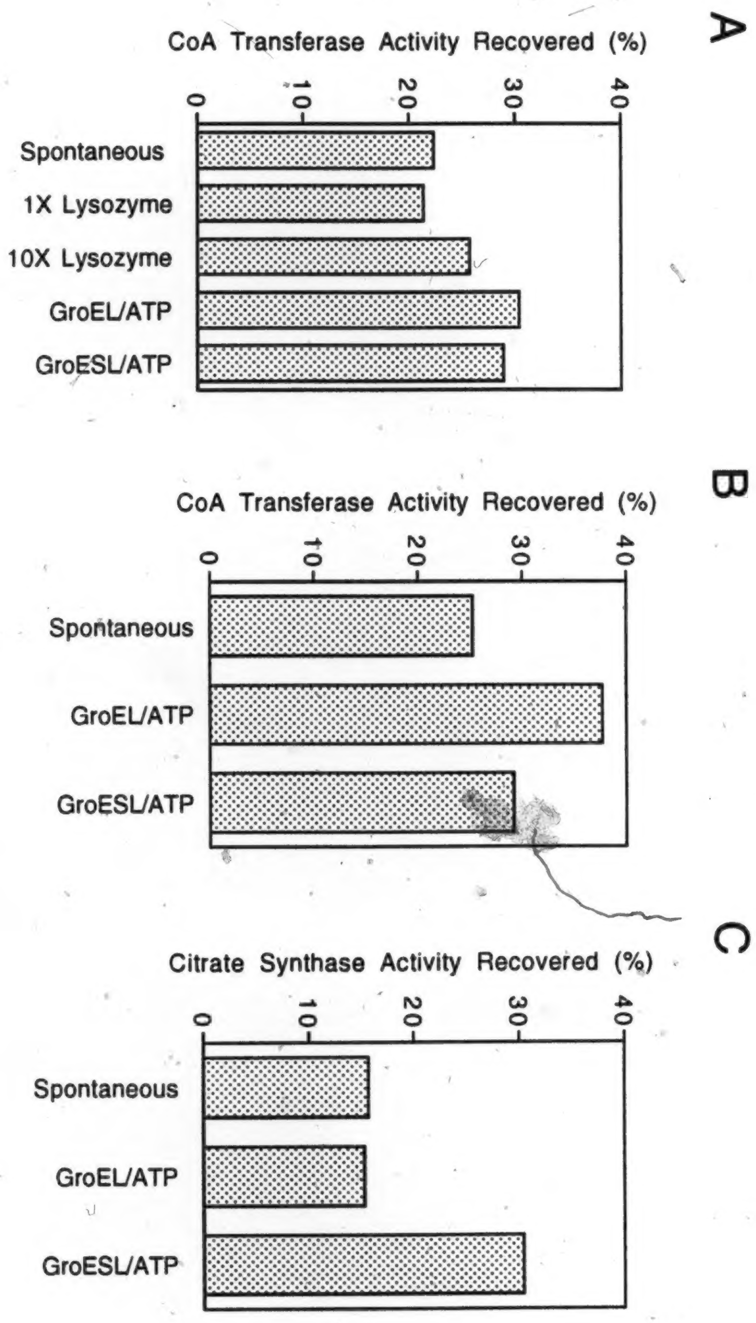
A
CoA Transferase Activity Recovered (%)
0
10
20
30
40
Spontaneous
1X Lysozyme
10X Lysozyme
GroEL/ATP
GroESL/ATP
B
CoA Transferase Activity Recovered (%)
0
10
20
30
40
Spontaneous
GroEL/ATP
GroESL/ATP
C
Citrate Synthase Activity Recovered (%)
0
10
20
30
40
Spontaneous
GroEL/ATP
GroESL/ATP

containing Mg^{2+}, ATP, and $GroEL_{14}$ (final concentration, 0.2 μM) or $GroEL_{14}$:$GroES_7$ (final concentration, 0.2 μM) led to a similar increase in the yield of refolding, compared to the spontaneous reaction (Figure 3-16B). Finally, the refolding of denatured citrate synthase in a buffer containing Mg^{2+}, ATP, and GroEL was much more efficient in the presence than in the absence of GroES (Figure 3-16C), indicating that the preparation of $GroEL_{14}$:$GroES_7$ used in these experiments was functional (Buchner et al., 1991; Zhi et al., 1992). Thus, the yield and rate of refolding of wild-type CoA transferase were increased and decreased, respectively, in the presence of Mg^{2+}, ATP, and GroEL, suggesting that nonnative forms of the enzyme interact with the chaperonin.

Recently, it has been demonstrated that upon binding ATP, the GroEL cylinder undergoes a dramatic conformational change, compatible with the discharge of polypeptide substrates which are bound weakly to the chaperonin (Roseman et al., 1996; Gorovits et al., 1997; reviewed in [Clarke, 1996]; [Martin & Hartl, 1997]). Given the assumption that intermediates of the CoA transferase refolding pathway associate with GroEL, it was predicted that the nonnative enzyme might be trapped on the chaperonin in the absence of nucleotide. Samples of unfolded wild-type CoA transferase (final concentration of the NC monomer, 0.01 mM) were diluted by a factor of 100 with refolding buffer lacking ATP, in the absence or presence of $GroEL_{14}$ (final concentration, 0.2 μM) at 22 °C. While approximately 15% of the initial enzyme activity was recovered in a refolding mixture lacking GroEL, this spontaneous refolding did not occur in the presence of the chaperonin (Figure 3-17). Importantly, the arrest of CoA transferase refolding under these conditions was reversed by the addition of ATP (final concentration, 5 mM) 2 h after the initial dilution of the unfolded enzyme (Figure 3-17). Moreover, a substantial amount of enzyme activity was recovered from a sample of denatured CoA transferase which was: (1) diluted with a buffer containing an equimolar amount of $GroEL_{14}$ but lacking ATP; (2) preincubated at 37 °C for 2 h; and (3) incubated at 22 °C in the presence of ATP (final concentration, 5 mM). Finally, the refolding arrest

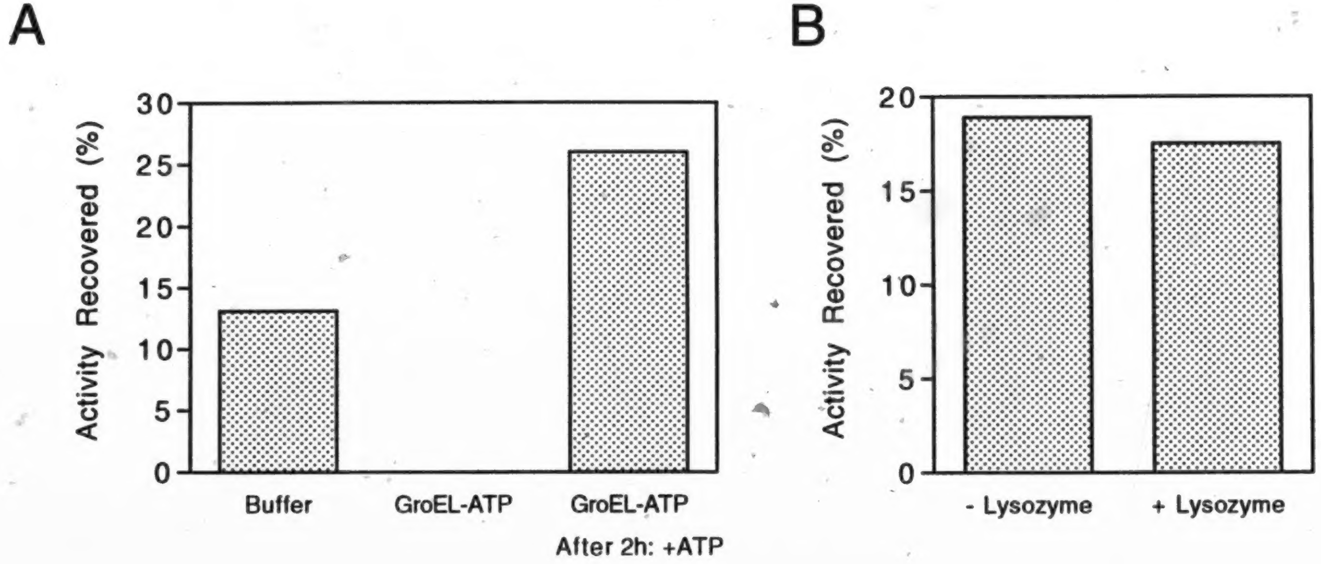

Figure 3-17: Inhibition of CoA transferase refolding by GroEL in the absence of ATP. (A) Wild-type CoA transferase was denatured in 6.0 M GuHCl at 22 °C for 6 h. The enzyme was then diluted 100-fold (v/v; final concentration of NC monomer, 0.1 µM) with refolding buffer lacking ATP. Refolding was carried out for 2 h at 22 °C in the absence or presence of 0.2 µM GroEL_{14}. After 2 h, a portion of the sample containing GroEL was supplemented with ATP (final concentration, 5 mM) and incubated for an additional 4 h at 22 °C. (B) Effect of lysozyme as a control. The wild-type enzyme was denatured and diluted as described in (A). Refolding was carried out for 2 h at 22 °C in the absence (1) or presence (2) of 0.2 µM lysozyme. All samples lacking GroEL contained an appropriate volume of GroEL storage buffer (see "Experimental Procedures"). The yield of active enzyme recovered upon renaturation is expressed as a percentage of the initial activity of non-denatured enzyme.

by the chaperonin in the absence of ATP was specific, since lysozyme did not quench the spontaneous refolding of CoA transferase under the same conditions (Figure 3-17). From these results, it was concluded that intermediates of CoA transferase along the refolding pathway associate with GroEL to form a stable complex.

DISCUSSION

The aggregation of the N- and C-domains in vitro. Preliminary evidence suggested that the purified N- and C-domains of CoA transferase are less susceptible to aggregation during reconstitution under benign conditions than the wild-type enzyme during refolding from denaturant (Chapter 2). It was postulated that the individual domains occur later on the CoA transferase folding pathway than the species which aggregate during refolding from GuHCl. This hypothesis was addressed by identifying conditions which favor the aggregation of the N- and C-domains *in vitro*. An initial temperature-shift experiment (Figure 3-3) indicated that the ability of the domain polypeptides to assemble to the active enzyme form was compromised by their preincubation at 37 °C. The resulting decrease in the yield of active CoA transferase coincided with the appearance of a precipitate, and may therefore be attributed to the aggregation of the domains. The decay in recoverable enzyme activity was best described by a double-exponential equation, which suggests that the rate of aggregation is limited by the unfolding of the individual N- and C-domains in rapid equilibrium with an initial assembled complex (Figure 3-18).

Subsequent temperature-shift experiments (Figure 3-4) indicated that higher levels of enzyme activity were recovered from mixtures diluted prior to their preincubation at 37 °C. This result is consistent with the observation that aggregation occurs more readily in solutions of higher protein concentration (Goldberg et al., 1991; Jaenicke, 1991; van der Vies et al., 1992). It is unclear why the decay in the recoverable enzyme activity from the diluted mixtures was best described by a single-exponential equation, in contrast to

Figure 3-18: Proposed pathways for the aggregation of CoA transferase. The unfolded N- and C-domains (U_N and U_C, respectively) isomerize to early intermediate forms (I_{N_E} and I_{C_E}). These nonnative species, which may resemble the individual, nascent polypeptides in *E. coli* (Netzer & Hartl, 1997), readily undergo aggregation (step 1) to yield "early" aggregates (A_E). Alternatively, I_{N_E} and I_{C_E} isomerize further to yield late intermediate forms (I_{N_L} and I_{C_L}). These conformers, which may resemble the purified N- and C-domains, are less susceptible to aggregation than the early intermediates. The aggregation of I_{N_L} or I_{C_L} yields "late" aggregates (A_L) by a direct reaction (step 2). In addition, I_{N_L} and I_{C_L} may form "early" aggregates via step 1 after first unfolding to I_{N_E} and I_{C_E} (respectively). These aggregation side-reactions compete with the assembly of I_{N_L} and I_{C_L} to form an intermediate adduct ($I_{[N_2C_2]}$), which isomerizes further to the native enzyme form ($N_{[N_2C_2]}$). The early and/or late intermediates associate transiently with GroEL in the presence of ATP, leading to a decrease in the rate of aggregation at steps 1 and/or 2. However, this buffering effect does not allow the refolding of the hinge-mutant, since the rate of aggregation of I_{N_L} and I_{C_L} far exceeds the rate of their assembly if the domains are not covalently linked (Chapter 2).

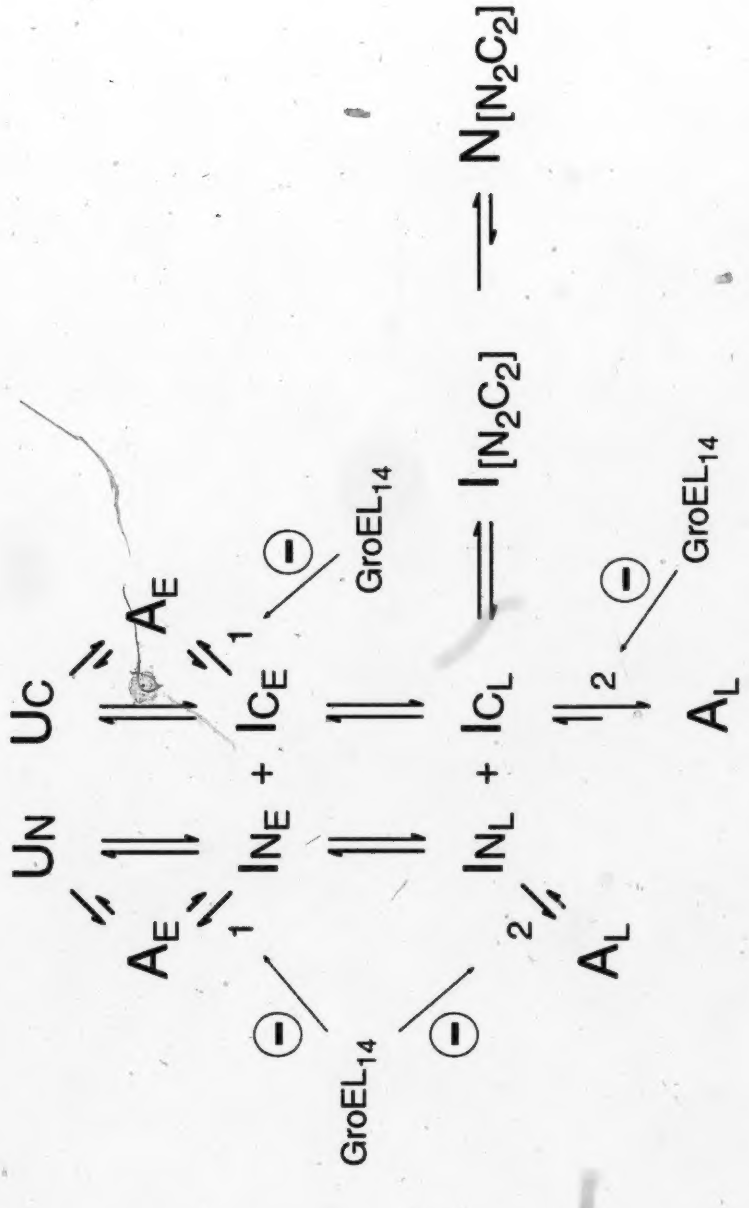
U_N
U_C
A_E
A_E
I_NE
I_CE
I_NL
I_CL
A_L
A_L
I_[N2C2]
N_[N2C2]
GroEL14
GroEL14
GroEL14
1
1
2
2
−
−
−
−
+
+

the first temperature-shift experiment. Presumably, more consistent results with respect to the kinetic order of aggregation of the N- and C-domains could be obtained by analyzing a greater number of data points.

The rate of disappearance of recoverable enzyme activity was directly proportional to the concentration of each domain in the mixture (Figure 3-4). This relation suggests that the aggregation of the N- and C-domains occurs by partially rate-limiting, second-order association steps, which follow the largely rate-determining, first-order unfolding reactions referred to above. Additional temperature-shift experiments with mixtures containing various concentrations of the N- and C-domains may provide further detail with respect to the mechanism of aggregation.

Importantly, the minimal specific enzyme activity recovered even after lengthy preincubation at 37 °C never reached zero (Figures 3-3, 3-4). This observation suggests that a small but significant subpopulation of conformers within the N- and C-domain mixture are capable of associating and adopting a stable native fold immediately (Chapter 2). Moreover, this minimal recoverable activity may reflect the background enzyme observed at 4 °C and detected by non-denaturing PAGE (Figure 2-15, lane 2).

It is proposed that the individual N- and C-domains are most likely in a rapid equilibrium with earlier intermediates of the CoA transferase folding pathway, which are in turn susceptible to aggregation (Figure 3-18). Thus, the increased aggregation of the isolated domains at 37°C compared to 22°C may simply reflect the greater degree of unfolding at the higher temperature. Alternatively, the purified N- and C-domains may aggregate, without prior unfolding, through hydrophobic interactions involving surfaces which are normally buried within the interdomain interface.

The aggregation of CoA transferase refolding intermediates in vitro. The aggregation of intermediates of the CoA transferase refolding pathway was also investigated. First, it was demonstrated that the yield of refolded enzyme decreases with increasing protein concentration or temperature, consistent with the prediction that aggregation side-reactions compete with the refolding of wild-type CoA transferase (Chapter 2). Second, results from a temperature-shift experiment indicated that the commitment to aggregation of the refolding wild-type enzyme is essentially complete within 5 min at 37 °C. Rapid rates of commitment have also been reported for hen egg white lysozyme (Goldberg et al., 1991) and ribulose bisphosphate carboxylase (van der Vies et al., 1992).

Importantly, the disappearance of the recoverable enzyme activity was best described by a double-exponential equation, implying that the rate of aggregation is limited by independent unfolding processes involving each domain of the intact enzyme (Figure 3-18). Presumably, these unfolding events are required to convert relatively compact, late refolding intermediates to relatively disordered, early conformers at 37 °C. The late refolding intermediates were present in excess of the early conformers at the start of the temperature-shift experiment, as suggested by the observation that the kinetics of commitment to aggregation were primarily first-order rather than second-order.

The results of the temperature-shift experiment suggest a model for the refolding of wild-type CoA transferase *in vitro*. Shortly after the dilution of the enzyme from denaturant, the unfolded protein adopts local elements of secondary structure to form early refolding intermediates. At 22 °C, these early conformers partition rapidly between late refolding intermediates and insoluble aggregates. Subsequently, the late conformers undergo irreversible folding and assembly steps that limit the rate of formation of the native enzyme. The late refolding intermediates accumulate during the initial phase of the refolding experiment, since their formation and depletion occur rapidly and slowly (respectively). Importantly, these late conformers are in rapid equilibrium with the early refolding intermediates. Thus, an increase in temperature from 22 °C to 37 °C leads to the partial unfolding of late conformers to early intermediates, which subsequently undergo rapid and quantitative aggregation at the elevated temperature.

The rate of commitment to aggregation at 37 °C was substantially greater for the refolding wild-type enzyme than for the N- and C-domains (Figures 3-3, 3-4, 3-6), despite the fact that the concentration of the refolding CoA transferase monomer was 50 to 500 times less than that of each domain in the equimolar mixture. Thus, the early and late intermediates of the CoA transferase refolding pathway undergo aggregation more readily than the isolated N- and C-domains. This observation is consistent with the prediction that the purified domains possess a more stable, compact fold than the species which aggregate during the refolding of the wild-type enzyme.

In summary, a sample of refolding wild-type CoA transferase was susceptible to aggregation, particularly at elevated temperature and protein concentration. Other proteins which display temperature-sensitive behavior during refolding *in vitro* include ribulosebisphosphate carboxylase (Viitanen et al., 1990), F_{ab} fragment (Buchner & Rudolph, 1991), rhodanese (Mendoza et al., 1991), phage P22 tailspike protein (Mitraki et al., 1991), mitochondrial malate dehydrogenase (Peralta et al., 1994), citrate synthase (Schmidt et al., 1994), and mitochondrial and cytosolic aspartate aminotransferase (Mattingly et al., 1995).

The thermal instability of CoA transferase in vivo. It was demonstrated by radioactive labeling and immunoblotting experiments that the yield of wild-type CoA transferase or the hinge-mutant in soluble form is less in cells of *E. coli* grown at 37 °C compared to 25 °C. These results were independent of the time of induction (minimum, 90 min; maximum, 12 h), the strain of *E. coli* (BL21[DE3] or HB 101), or the method of cell disruption (sonication or lysis by detergent). It should be noted that different proportions of radioactively labeled hinge-mutant accumulated as inclusion bodies in cells of BL-Hng treated with ^{35}S-methionine for 10 min compared to 40 min, both at 25 °C and 37 °C. This difference most likely reflects variability inherent to the experimental method, and does not alter the conclusion that CoA transferase is more susceptible to aggregation *in vivo* at 37 °C than at 25 °C.

In general, proteins synthesized at higher temperatures are expected to aggregate more rapidly. First, the rates of transcription and translation increase with temperature (up to a physiological maximum), which leads in turn to a greater concentration of nascent, incompletely folded polypeptide. Second, the aggregation of proteins typically involves partial unfolding and strong hydrophobic interactions, both of which are enhanced by elevated temperatures. Thus, the tendency of CoA transferase to accumulate as inclusion bodies in *E. coli* cells grown at 37 °C reflects the relative abundance of unstable folding intermediates under these conditions. The increased solubility of CoA transferase in cells of *E. coli* grown at 25 °C has facilitated the purification of the enzyme in large quantities (Chapter 2). A similar strategy has been used to produce other recombinant proteins in the soluble fraction of *E. coli* cells, including: interferon (IFN)-β (Mizukami et al., 1986); IFN-α2 and IFN-γ2 (Schein & Noteborn, 1988); basic fibroblast growth factor (Squires et al., 1988); kanamycin nucleotidyltransferase (Liao, 1991); and isopenicillin N synthase (Durairaj & Jensen, 1996).

The relative solubilities of the N- and C-domains. At 37 °C, a greater proportion of immunoreactive C-domain accumulated as inclusion bodies in cells of HB-C, compared to the N-domain in cells of HB-N. Thus, the C-domain aggregates more readily than the N-domain *in vivo*. Presumably, this difference in solubility accounts for the poor yield of C-domain compared to N-domain purified from equivalent volumes of bacterial cell culture (Chapter 2).[6]

The C-domain was also more susceptible to aggregation than the N-domain *in vitro*. Although a sample of the purified N-domain was resolvable by non-denaturing PAGE, the isolated C-domain accumulated at the interface between the stacking and resolving gels (Chapter 2). Similar results were obtained when the electrophoresis was repeated at 4 °C, or when the samples were analyzed using a continuous rather than a discontinuous system. In addition, the purified C-domain aggregated at a lower temperature than the individual N-domain upon heat treatment. Finally, the C-domain preparation precipitated much earlier than the N-domain sample during prolonged storage at 4 °C.

These differences in solubility observed *in vivo* and *in vitro* cannot be due to the relative hydrophobicities of the N- and C-domains, given that both proteins contain nearly identical proportions of nonpolar residues. Instead, results from far-UV CD, fluorescence, and equilibrium unfolding measurements suggest that the purified C-domain possesses a relatively open, unfolded structure, whereas the fold of the purified N-domain may be more native-like (Chapter 2). Thus, it is proposed that the relative propensity of the C-domain to aggregate in *E. coli* may be due to its lack of a compact, native-like fold. Alternatively, the different solubilities of the N- and C-domains may arise from the fact that the experiments described above were carried out in buffers of pH 7.4, which is much closer to the isoelectric point (pI) of the C-domain (7.2) than that of the N-domain (6.4). Repeating the experiments described above in buffers of higher pH (e.g. pH 8.0) would distinguish between these hypotheses.

The disappearance of recombinant protein from the soluble fraction. Results from the pulse-chase labeling experiments indicated that the individual N- and C-domains are depleted with shorter half-lives than wild-type CoA transferase or the hinge-mutant from cell lysates of BL21(DE3). The loss of radioactive label from the soluble fraction may be due to a combination of proteolysis and aggregation, both of which reflect the partial unfolding of the protein. The rapid decay of the C-domain was due primarily to aggregation, given that the radioactive label observed for whole cells of BL-C was stable during a chase period of 1 h. By analogy with the C-domain, the disappearance of the wild-type enzyme, hinge-mutant, and N-domain from the soluble fraction was also attributed to aggregation, although proteolysis of these polypeptides could not be formally excluded. For each protein, the decrease in label was best described by a double-exponential equation. Thus, the aggregation of CoA transferase and its domain polypeptides *in vivo* may proceed through complex unfolding pathways consisting of more than one first-order, partially rate-limiting component (Figure 3-18). This mechanism is similar to that proposed for the aggregation of CoA transferase folding intermediates *in vitro* (see above).

The apparent, relative solubilities deduced for the recombinant forms of CoA transferase in *E. coli* varied with the experimental protocol. From the 10- and 40-min radioactive labeling experiments and the Western blot analyses, it was inferred that the wild-type enzyme and the individual C-domain accumulate more readily as inclusion bodies than the hinge-mutant or the individual N-domain. In contrast, results from the pulse-chase labeling experiments indicated that the individual N- and C-domains disappear more rapidly than wild-type CoA transferase or the hinge-mutant from the soluble fraction of BL21(DE3). The two methods described above provide information with respect to the aggregation of intermediates at different points along the CoA transferase folding pathway. The proportion of protein which accumulates as inclusion bodies reflects the aggregation of nascent polypeptides and, to a lesser extent, the aggregation of later folding intermediates which have already achieved a soluble, metastable state (Figure 3-18, steps 1 and 2). In contrast, only the second of these aggregation side-reactions (Figure 3-18, step 2) is detected by the pulse-chase experiment.

From the relative solubility of the newly-synthesized N-domain, it is inferred that the latter achieves a native-like, dimeric state at a rate greater than the rate of aggregation. However, despite having adopted a compact fold, the individual N-domain remains more susceptible to aggregation than wild-type CoA transferase or the hinge-mutant. These results imply that nonpolar regions of the N-domain become accessible as a result of partial unfolding (Figure 3-18). Alternatively, the N-domain polypeptide may be susceptible to aggregation — despite maintaining a native-like structure — due to the exposure of hydrophobic patches which are normally sequestered in the interdomain interface of the wild-type enzyme (Figure 3-18, step 2).

Assembly versus aggregation: the role of the C-domain. The pulse-chase experiments indicated that wild-type CoA transferase and the hinge-mutant remain relatively soluble once they have achieved a stable, compact fold. However, the nascent wild-type enzyme accumulated more readily as inclusion bodies in BL-WT or HB-WT than the N- and C-domains in BL-Hng or HB-Hng. This discrepancy can be accounted for by considering the rate of synthesis and the relative solubility of the C-domain in each strain.

The hinge-mutant of CoA transferase was designed by incorporating a stop codon and a reinitiation site in the portion of the cDNA encoding the hydrophilic hinge region (Chapter 2). Although a strong Shine-Dalgarno sequence is properly situated upstream of this reinitiation site (Shine & Dalgarno, 1974; Gold & Stormo, 1987; Gold & Stormo, 1990; Schoner et al., 1990; de Boer & Hui, 1990), synthesis of the C-domain was only 10% as efficient as that of the N-domain encoded by the same operon, based on radioactive labeling experiments. Consistent with this finding, the maximal specific CoA transferase activity detected in lysates of HB-Hng cells only occurred after longer periods of growth compared to HB-WT cells. The low efficiency of translation is reasonable in this case, given that low yields of protein synthesis are commonly observed with reinitiation sites created by site-directed mutagenesis (Gold & Stormo, 1987).

The nascent C-domain is more susceptible to aggregation than the newly-synthesized N-domain in *E. coli*, presumably because the C-domain is less completely folded (see above). It is conceivable that the relatively low concentration of nascent C-domain polypeptide compared to the N-domain in cells which produce the hinge-mutant accounts for the higher proportional yield of soluble enzyme in these cells, compared to cells of BL-WT or HB-WT (Figures 3-8, 3-10). In the presence of excess N-domain, molecules of newly-synthesized C-domain are much less likely to interact with each other than with molecules of the N-domain. This interaction between the N- and C-domains leads preferentially to: (1) correct folding, if the N-domain is at least partially structured;

or (2) aggregation, if a sufficient number of hydrophobic surfaces on the N-domain are exposed. Consequently, in cells of BL-Hng or HB-Hng the probability of aggregation of the C-domain is determined by the frequency of its encounter with incompletely folded N-domain polypeptide. Under these conditions, both domains are equally susceptible to aggregation (Figure 3-8).

As a corollary to the above discussion, the aggregation of the wild-type enzyme is largely determined by unproductive interactions involving the C-domain. During or immediately after translation, each domain initiates its folding independently of the other (Chapter 2). Although the N-domain rapidly achieves a metastable structure, the nascent C-domain to which it is covalently linked remains susceptible to aggregation. As a result, the probability of aggregation *in vivo* of the intact wild-type enzyme is similar to that of the individual C-domain. Consistent with this hypothesis, equal proportions of wild-type CoA transferase and the C-domain were found to accumulate as inclusion bodies in cells of *E. coli* grown at 37 °C (Figures 3-11, 3-12).

Chaperonins and the aggregation of wild-type CoA transferase. The influence of chaperonins on the degree of aggregation of CoA transferase was assessed by examining the effects of $GroEL_{14}$ and $GroEL_{14}$:$GroES_7$ on the renaturation of the wild-type enzyme and hinge-mutant. To test the preparation of $GroEL_{14}$:$GroES_7$ for functional activity, it was verified that the yield of refolded citrate synthase was specifically enhanced in the presence of the complete chaperonin system, under the conditions reported by Buchner et al. (1991). At 22 °C, the refolding yield of wild-type CoA transferase increased nearly twofold in the presence of $MgCl_2$, ATP, and an equimolar amount of $GroEL_{14}$, compared to the unassisted reaction. In addition, the apparent first-order rate constant for the appearance of enzyme activity was significantly lower in the presence than in the absence of $MgCl_2$, ATP, and the chaperonin. However, denatured CoA transferase did not refold upon dilution in a buffer which contained a twofold molar excess of $GroEL_{14}$ but lacked ATP. Together, these results suggest that the refolding enzyme binds to GroEL via interactions that are weakened in the presence of ATP. Presumably, this association involves contacts between the exposed, nonpolar regions of early CoA transferase refolding intermediates and the hydrophobic polypeptide binding sites located on the inner surface of the GroEL toroid (Braig et al., 1994; Fenton et al., 1994; Itzhaki et al., 1995; Lin et al., 1995; Katsumata et al., 1996). Once bound to GroEL, the enzyme is protected from aggregation, as suggested by the observed recovery of activity from a sample of refolding CoA transferase which was first preincubated with GroEL in the absence of ATP at 37 °C for 2 h, and subsequently incubated in the presence of ATP at 22 °C for an additional 4 h (results not shown). Upon binding and hydrolyzing ATP, the chaperonin undergoes conformational changes which alter the affinity of GroEL for its polypeptide substrates (Roseman et al., 1996; Gorovits et al., 1997; reviewed in [Clarke, 1996]; [Martin & Hartl, 1997]). Specifically, the "on" rate of association between nonnative protein and the chaperonin decreases in the presence of ATP (Sparrer et al., 1996). Thus, in buffer containing $MgCl_2$, ATP, and GroEL, CoA transferase most likely refolds while interacting transiently with the chaperonin.

The release from GroEL of folding intermediates which are "committed" to adopt a native structure has been shown to depend on the presence of ATP and GroES (Martin et al., 1991; Schmidt et al., 1994; Mayhew et al., 1996; Weissman et al., 1996; Rye et al., 1997). According to one model, the cochaperonin functions as a "lid" which sequesters polypeptide substrates within the central cavity of one ring of the GroEL cylinder (referred to as the *cis*-ring). Since the enclosed folding intermediates are protected from intermolecular aggregation, this chamber has been referred to as the "Anfinsen cage" (Ellis, 1994). Both the volume of the cage (Chen et al., 1994; Roseman et al., 1996; Xu et al., 1997) and the hydrophilicity of the inner surface (de Crouy-Chanel et al., 1995; Mande et al., 1996; Hunt et al., 1996; Martin & Hartl, 1997; Xu et al., 1997) increase upon the binding of GroES to GroEL. Under these conditions, nonnative species are at least partially released into the central cavity, where they may undergo conformational rearrangements which lead to a committed state of folding. After the hydrolysis of ATP in the *cis*-ring of GroEL, proteins with a committed fold dissociate together with GroES. This release is triggered by the binding of ATP to the opposite (or *trans*-) ring (Rye et al., 1997).

In contrast, the ATP-driven release of CoA transferase from GroEL was unaffected by GroES at 22 °C, suggesting that the enzyme does not dissociate from the chaperonin as a committed folding intermediate. Numerous protein substrates have been shown to require ATP — but not GroES — for their productive release from GroEL, including: β-lactamase precursor (Laminet et al., 1990), lactate dehydrogenase (Badcoe et al., 1991), dihydrofolate reductase (Martin et al., 1991; Viitanen et al., 1991), α-glucosidase (Höll-Neugebauer et al., 1991), glutamine synthetase (Fisher, 1992), trytophanase (Mizobata et al., 1992), phage P22 tailspike protein (Brunschier et al., 1993), phytochrome photoreceptor (Grimm et al., 1993), and enolase (Kubo et al., 1993).[7] It has been argued that for many of these proteins, a requirement for GroES has been overlooked because the experimental conditions were "permissive" for unassisted renaturation; under more stringent conditions, GroEL$_{14}$:GroES$_7$ may be both necessary and sufficient for refolding (Schmidt et al., 1994). However, this reasoning does not apply to CoA transferase, since the enzyme did not refold either in the presence or absence of the complete chaperonin system at the "non-permissive" temperature of 37 °C. Moreover, it is unlikely that the ability of GroEL$_{14}$:GroES$_7$ to release CoA transferase as a committed intermediate was compromised by the denaturant remaining in the refolding buffer, since the concentrations of residual GuHCl in these experiments (0.06 to 0.12 M) were similar to those reported for the successful refolding of other proteins which require the complete chaperonin system (Buchner et al., 1991; Hartman et al., 1992; Zhi et al., 1992; Miller et al., 1993; Zheng et al., 1993; Peralta et al., 1994; Schmidt et al., 1994; Wynn et al., 1994; Mattingly et al., 1995). Instead, it is proposed that transient interactions between nonnative forms of CoA transferase and GroEL decrease the effective, steady-state concentration of conformers which are susceptible to aggregation (Figure 3-18). Rather than refolding within the central cavity of the GroEL complex, the nonnative species merely cycle on and off the chaperonin with little or no change in their structure. This "buffering" effect, recently described for the refolding of β-galactosidase in the presence of GroEL (Ayling & Baneyx, 1996), leads to: (1) an increase in the yield of refolding of CoA transferase under permissive conditions, by suppressing competing aggregation side-reactions; and (2) a decrease in the rate of refolding at 22 °C, by impeding the first-order, rate-determining step(s) which lead to the native structure. Lysozyme was also found to facilitate the refolding of CoA transferase, presumably by the same mechanism. However, this effect was less pronounced than the assistance provided by the chaperonin, most likely because the affinity of the CoA transferase refolding intermediates for the hydrophobic inner surface of the GroEL toroid is greater than for the polar exterior of native lysozyme.

GroEL and GroES have been shown to be necessary and sufficient for the refolding of several oligomeric mitochondrial enzymes under non-permissive conditions. Examples include citrate synthase (Buchner et al., 1991; Zhi et al., 1992), ornithine transcarbamoylase (Hartman et al., 1992; Zheng et al., 1993), malate dehydrogenase (Miller et al., 1993; Peralta et al., 1994; Gietl et al., 1996), the 24-meric E2 inner core domain of branched chain α-keto acid dehydrogenase (Wynn et al., 1994), and aspartate aminotransferase (Mattingly et al., 1995; Widmann & Christen, 1995). In contrast, the complete chaperonin system did not facilitate the renaturation of CoA transferase at a non-permissive temperature. Evidently, intermediates of the enzyme's refolding pathway are not released from $GroEL_{14}$:$GroES_7$ in a form committed to achieving the native state at 37 °C. Thus, CoA transferase must interact differently with the complete chaperonin system compared to other oligomeric enzymes of the mitochondrial matrix during refolding *in vitro*.

From these results alone, the question of whether or not CoA transferase requires the assistance of chaperonins to fold *in vivo* cannot be answered. In general, oligomeric enzymes transported into the mitochondrial matrix are thought to require Hsp60 and Cpn10 to adopt a native fold (Cheng et al., 1989; Ostermann et al., 1989; Rospert et al., 1993; Höhfeld & Hartl, 1994). It is therefore proposed that the refolding of CoA transferase *in vitro* may not accurately represent the folding and assembly of the enzyme *in vivo*. For example, early structural motifs formed along the CoA transferase polypeptide chain during translation in *E. coli* or mitochondrial import in mammalian cells may be necessary for subsequent refolding reactions within the chaperonin's inner chamber. Such motifs may never form during the refolding of the enzyme *in vitro*. In addition, chaperones of the Hsp70 family, which were absent from the CoA transferase refolding mixtures, may bind nonnative forms of the enzyme during translation or translocation *in vivo*, thus influencing the distribution of conformers which are recognized by the chaperonins (Frydman et al., 1994). Given these uncertainties associated with the *in vitro* refolding experiments, the possibility that CoA transferase folds in a chaperonin-dependent manner *in vivo* must be considered.

Chaperonins and the aggregation of the hinge-mutant. Neither GroEL_{14} nor GroEL_{14}:GroES_7 assisted the refolding of the hinge-mutant in buffer containing ATP. This observation implies that any interaction between GroEL and the N- or C-domain precedes their productive assembly, which is slow compared to competing aggregation side-reactions (Figure 3-18). Apparently, the bound N- or C-domain polypeptide is not released as a committed folding intermediate, consistent with results described above for the wild-type enzyme. Alternatively, an initial interaction between the N- and C-domains may be a prerequisite for the binding of nonnative CoA transferase to the chaperonin. In this case, the refolding hinge-mutant could not associate with GroEL_{14}:GroES_7, since domain pairing does not occur in the absence of the hydrophilic linker segment under these conditions (Chapter 2). Importantly, neither hypothesis accounts for the difference between the folding of the hinge-mutant *in vivo* and *in vitro*. This discrepancy cannot be attributed solely to the presence of GroEL and GroES in *E. coli*. Rather, other events specific to the intracellular environment must also be considered, including: (1) co-translational folding; and (2) interactions involving the Hsp70 family of chaperones. The recent report that co-translational folding is less predominant in prokaryotes than in eukaryotes (Netzer & Hartl, 1997) favors the second of these possibilities.

ENDNOTES

[1] A version of this chapter has been published:

> Rochet, J.-C., Oikawa, K., Hicks, L. D., Kay, C. M., Bridger, W. A., & Wolodko, W. T. (1997) *Biochemistry 36*, 8807-8820.

[2] According to this definition, the term "aggregation" does not refer to the assembly of subunits to active, multimeric forms, as described in Chapter 4.

[3] The molecular weights estimated for the homodimer and homotetramer by gel filtration analysis were 1.10×10^5 and 2.45×10^5, respectively (Chapter 4). The preparation of homodimeric CoA transferase was not intended for the GroEL/GroES studies *per se*. Rather, this enzyme was used because it was available and concentrated (12 mg/mL).

[4] The volume of GroEL storage buffer used was equal to the amount of stock GroEL solution added to the refolding mixture containing chaperonin.

[5] The N- and C-domains have 2 and 11 methionine residues, respectively, assuming quantitative removal of the N-terminal methionine of each polypeptide (see Table 1-1).

[6] Alternatively, the N-domain may be less susceptible to proteolysis than the C-domain, given that the N-domain possesses a more compact, stable structure. Such a difference in proteolytic sensitivity could also account for the difference in the overall yields of these two proteins in cells of *E. coli*.

[7] The refolding yields and/or rates of only two of these proteins (trytophanase [Mizobata et al., 1992] and phage P22 tailspike protein [Brunschier et al., 1993] were shown to be unaffected by GroES.

REFERENCES

Ayling, A., & Baneyx, F. (1996) *Protein Sci. 5*, 478-487.

Badcoe, I. G., Smith, C. J., Wood, S., Halsall, D. J., Holbrook, J. J., Lund, P., & Clarke, A. R. (1991) *Biochemistry 30*, 9195-9200.

Becker, J., & Craig, E. A. (1994) *Eur. J. Biochem. 219*, 11-23.

Braig, K., Otwinowski, Z., Hegde, R., Boisvert, D. C., Joachimiak, A., Horwich, A. L., & Sigler, P. B. (1994) *Nature 371*, 578-586.

Brunschier, R., Danner, M., & Seckler, R. (1993) *J. Biol. Chem. 268*, 2767-2772.

Buchner, J., & Rudolph, R. (1991) *Bio/Technology 9*, 157-162.

Buchner, J., Schmidt, M., Fuchs, M., Jaenicke, R., Rudolph, R., Schmid, F. X., & Kiefhaber, T. (1991) *Biochemistry 30*, 1586-1591.

Chen, S., Roseman, A. M., Hunter, A., Wood, S. P., Burston, S. G., Ranson, N., Clarke, A. R., & Saibil, H. R. (1994) *Nature 371*, 261-264.

Cheng, M. Y., Hartl, F.-U., Martin, J., Pollock, R. A., Kalousek, F., Neupert, W., Hallberg, E. M., Hallberg, R. L., & Horwich, A. L. (1989) *Nature 337*, 620-625.

Clarke, A. R. (1996) *Curr. Opin. Struct. Biol. 6*, 43-50.

Craig, E. A. (1988) *Annu. Rev. Genet. 22*, 631-677.

Craig, E. A., & Gross, C. A. (1991) *Trends Biochem. Sci. 16*, 135-140.

Craig, E. A., Weissman, J. S., & Horwich, A. L. (1994) *Cell 78*, 365-372.

de Boer, H. A., & Hui, A. S. (1990) *Methods Enzymol. 185*, 103-114.

de Crouy-Chanel, A., el Yaagoubi, A., Kohiyama, M., & Richarme, G. (1995) *J. Biol. Chem. 270*, 10571-10575.

Durairaj, M., & Jensen, S. E. (1996) *J. Ind. Microbiol. 16*, 197-203.

Ellis, J. (1987) *Nature 328*, 378-379.

Ellis, R. J. (1994) *Curr. Biol. 4*, 633-635.

Fenton, W. A., Kashi, Y., Furtak, K., & Horwich, A. L. (1994) *Nature 371*, 614-619.

Fisher, M. T. (1992) *Biochemistry 31*, 3955-3963.

Frydman, J., Nimmesgern, E., Ohtsuka, K., & Hartl, F.-U. (1994) *Nature 370*, 111-117.

Gething, M.-J., & Sambrook, J. (1992) *Nature 355*, 33-45.

Gietl, C., Seidel, C., & Svendsen, I. (1996) *Biochim. Biophys. Acta 1274*, 48-58.

Gold, L., & Stormo, G. (1987) in *Escherichia coli and Salmonella typhimurium*, Vol. 2 (Neidhardt, F. C., Ed.) pp. 1302-1307, American Society for Microbiology, Washington, D. C.

Gold, L., & Stormo, G. D. (1990) *Methods Enzymol. 185*, 89-93.

Goldberg, M. E., Rudolph, R., & Jaenicke, R. (1991) *Biochemistry 30*, 2790-2797.

Gorovits, B. M., Ybarra, J., & Horowitz, P, M. (1997) *J. Biol. Chem. 272*, 6842-6845.

Grimm, R., Donaldson, G. K., van der Vies, S. M., Schäfer, E., & Gatenby, A. A. (1993) *J. Biol. Chem. 268*, 5220-5226.

Hartl, F. U., & Martin, J. (1995) *Curr. Opin. Struct. Biol. 5*, 92-102.

Hartman, D. J., Hoogenraad, N. J., Condron, R., & Høj, P. B. (1992) *Proc. Natl. Acad. Sci. U. S. A. 89*, 3394-3398.

Hemmingsen, S. M., Woolford, C., van der Vies, S. M., Tilly, K., Dennis, D. T., Georgopoulos, C. P., Hendrix, R. W., & Ellis, R. J. (1988) *Nature 333*, 330-334.

Hlodan, R., & Hartl, F. U. (1994) in *Mechanisms of Protein Folding* (Pain, R. H., Ed.) pp. 194-228, IRL Press, Oxford, U. K.

Höhfeld, J., & Hartl, F. U. (1994) *J. Cell Biol. 126*, 305-315.

Höll-Neugebauer, B., Rudolph, R., Schmidt, M., & Buchner, J. (1991) *Biochemistry 30*, 11609-11614.

Horwich, A. L., Low, K. B., Fenton, W. A., Hirshfield, I. N., & Furtak, K. (1993) *Cell 74*, 909-917.

Howard, J. B., Zieske, L., Clarkson, J., & Rathe, L. (1986) *J. Biol. Chem. 261*, 60-65.

Hunt, J. F., Weaver, A. J., Landry, S. J., Gierasch, L., & Deisenhofer, J. (1996) *Nature 379*, 37-45.

Itzhaki, L. S., Otzen, D. E., & Fersht, A. R. (1995) *Biochemistry 34*, 14581-14587.

Jaenicke, R. (1987) *Prog. Biophys. Mol. Biol. 49*, 117-237.

Jaenicke, R. (1991) *Biochemistry 30*, 3147-3161.

Jaenicke, R. (1995) *Phil. Trans. R. Soc. Lond.* B *348*, 97-105.

Jaenicke, R., & Rudolph, R. (1986) *Methods Enzymol. 131*, 218-250.

Katsumata, K., Okazaki, A., Tsurupa, G. P., & Kuwajima, K. (1996) *J. Mol. Biol. 264*, 643-649.

King, J., Haase-Pettingell, C., Robinson, A. S., Speed, M., & Mitraki, A. (1996) *FASEB J. 10*, 57-66.

Kubo, T., Mizobata, T., & Kawata, Y. (1993) *J. Biol. Chem. 268*, 19346-19351.

Laminet, A. A., Ziegelhoffer, T., Georgopoulos, C., & Plückthun, A. (1990) *EMBO J. 9*, 2315-2319.

Liao, H. H. (1991) *Protein Expression Purif. 2*, 43-50.

Lill, R., Nargang, F. E., & Neupert, W. (1996) *Curr. Opin. Cell Biol. 8*, 505-512.

Lin, T., & Bridger, W. A. (1992) *J. Biol. Chem. 267*, 975-978.

Lin, Z., Schwartz, F. P., & Eisenstein, E. (1995) *J. Biol. Chem. 270*, 1011-1014.

Lindquist, S. (1986) *Annu. Rev. Biochem. 55*, 1151-1191.

Mande, S. C., Mehra, V., Bloom, B. R., & Hol, W. G. J. (1996) *Science 271*, 203-207.

Manning-Krieg, U. C., Scherer, P. E., & Schatz, G. (1991) *EMBO J. 10*, 3273-3280.

Martin, J., & Hartl, F. U. (1997) *Curr. Opin. Struct. Biol. 7*, 41-52.

Martin, J., Langer, T., Boteva, R., Schramel, A., Horwich, A. L., & Hartl, F.-U. (1991) *Nature 352*, 36-42.

Mattingly, J. R., Jr., Iriarte, A., & Martinez-Carrion, M. (1995) *J. Biol. Chem. 270*, 1138-1148.

Mayhew, M., da Silva, A. C. R., Martin, J., Erdjument-Bromage, H., Tempst, P., & Hartl, F. U. (1996) *Nature 379*, 420-426.

Mendoza, J. A., Rogers, E., Lorimer, G. H., & Horowitz, P. M. (1991) *J. Biol. Chem. 266*, 13044-13049.

Miller, A. D., Maghlaoui, K., Albanese, G., Kleinjan, D. A., & Smith, C. (1993) *Biochem. J. 291*, 139-144.

Mitraki, A., Fane, B., Haase-Pettingell, C., Sturtevant, J., & King, J. (1991) *Science 253*, 54-58.

Mizobata, T., Akiyama, Y., Ito, K., Yumoto, N., & Kawata, Y. (1992) *J. Biol. Chem. 267*, 17773-17779.

Mizukami, T., Komatsu, Y., Hosoi, N., Itoh, S., & Oka, T. (1986) *Biotech. Lett. 8*, 605-610.

Mukhopadhyay, A. (1997) *Adv. Bioch. Eng. Biotechnol. 56*, 61-109.

Netzer, W. J., & Hartl, F. U. (1997) *Nature 388*, 343-349.

Ostermann, J., Horwich, A. L., Neupert, W., & Hartl, F.-U. (1989) *Nature 341*, 125-130.

Peralta, D., Hartman, D. J., Hoogenraad, N. J., & Høj, P. B. (1994) *FEBS Lett. 339*, 45-49.

Price, N. C. (1994) in *Mechanisms of Protein Folding* (Pain, R. H., Ed.) pp. 160-193, IRL Press, Oxford, U. K.

Roseman, A. M., Chen, S., White, H., Braig, K., & Saibil, H. R. (1996) *Cell 87*, 241-251.

Rospert, S., Glick, B. S., Jenö, P., Schatz, G., Todd, M. J., Lorimer, G. H., & Viitanen, P. V. (1993) *Proc. Natl. Acad. Sci. U. S. A. 90*, 10967-10971.

Rospert, S., Looser, R., Dubaquié, Y., Matouschek, A., Glick, B. S., & Schatz, G. (1996) *EMBO J. 15*, 764-774.

Rothman, J. E. (1989) *Cell 59*, 591-601.

Rye, H. S., Burston, S. G., Fenton, W. A., Beechem, J. M., Xu, Z., Sigler, P. B., & Horwich, A. L. (1997) *Nature 388*, 792-798.

Schatz, G. (1996) *J. Biol. Chem. 271*, 31763-31766.

Schein, C. H., & Noteborn, M. H. M. (1988) *Bio/Technology 6*, 291-294.

Scherer, P. E., Krieg, U. C., Hwang, S. T., Vestweber, D., & Schatz, G. (1990) *EMBO J. 9*, 4315-4322.

Schmidt, M., Buchner, J. Todd, M. J., Lorimer, G. H., & Viitanen, P. V. (1994) *J. Biol. Chem. 269*, 10304-10311.

Schoner, B. E., Belagaje, R. M., & Schoner, R. G. (1990) *Methods Enzymol. 185*, 94-103.

Shine, J., & Dalgarno, L. (1974) *Proc. Natl. Acad. Sci. U. S. A. 71*, 1342-1346.

Sparrer, H., Lilie, H., & Buchner, J. (1996) *J. Mol. Biol. 258*, 74-87.

Squires, C. H., Childs, J., Eisenberg, S. P., Polverini, P. J., & Sommer, A. (1988) *J. Biol. Chem. 263*, 16297-16302.

Srere, P. (1969) *Methods Enzymol. 13*, 3-11.

Stuart, R. A., Cyr, D. M., Craig, E. A., & Neupert, W. (1994) *Trends Biochem. Sci. 19*, 87-92.

Tabor, S., & Richardson, C. C. (1985) *Proc. Natl. Acad. Sci. U. S. A. 82*, 1074-1078.

Thatcher, D. R., & Hitchcock, A. (1994) in *Mechanisms of Protein Folding* (Pain, R. H., Ed.) pp. 160-193, IRL Press, Oxford, U. K.

van der Vies, S. M., Viitanen, P. V., Gatenby, A. A., Lorimer, G. H., & Jaenicke, R. (1992) *Biochemistry 31*, 3635-3644.

Viitanen, P. V., Lubben, T. H., Reed, J., Goloubinoff, P., O'Keefe, D. P., & Lorimer, G. H. (1990) *Biochemistry 29*, 5665-5671.

Viitanen, P. V., Donaldson, G. K., Lorimer, G. H., Lubben, T. H., & Gatenby, A. A. (1991) *Biochemistry 30*, 9716-9723.

von Heijne, G. (1986) *EMBO J. 5*, 1335-1342.

Weissman, J. S., Rye, H. S., Fenton, W. A., Beechem, J. M., & Horwich, A. L. (1996) *Cell 84*, 481-490.

Widmann, M., & Christen, P. (1995) *FEBS Lett. 377*, 481-484.

Wynn, R. M., Davie, J. R., Zhi, W., Cox, R. P., & Chuang, D. T. (1994) *Biochemistry 33*, 8962-8968.

Xu, Z., Horwich, A. L., & Sigler, P. B. (1997) *Nature 388*, 741-750.

Zettlmeissl, G., Rudolph, R., & Jaenicke, R. (1979) *Biochemistry 18*, 5567-5571.

Zheng, X., Rosenberg, L. E., Kalousek, F., & Fenton, W. A. (1993) *J. Biol. Chem. 268*, 7489-7493.

Zhi, W., Landry, S. J., Gierasch, L. M., & Srere, P. A. (1992) *Protein Sci. 1*, 522-529.

Chapter 4. Alternative Oligomeric Forms of CoA Transferase

INTRODUCTION

In general, proteins can undergo two forms of self-association. First, they may be susceptible to aggregation (Chapter 3), which results from incorrect intermolecular interactions between residues which normally occupy the interior of the protein (reviewed in [Jaenicke & Rudolph, 1986]; [Jaenicke, 1987]; [Jaenicke, 1991]). Aggregation leads to the trapping of folding intermediates as inactive, insoluble complexes, which are thermodynamically stable in the absence of chaotropic agents (Rudolph et al., 1979). Second, the subunits of an oligomeric enzyme may undergo productive assembly to yield an active multimer. Oligomerization occurs near the end of the folding pathway, and may be regulated by salts, cofactors, or ligands (reviewed in [Klotz et al., 1975]; [Jaenicke, 1987]; [Price, 1994]). Thus, aggregation results from the largely irreversible association of incompletely folded polypeptides, while assembly involves "native-like" protomers and is occasionally reversible under benign conditions.

The self-association of CoA transferase can involve "wrong" or "correct" intermolecular interactions. Conformers which occur at different points along the folding pathway show varying tendencies to aggregate (Chapter 3). This effect is especially pronounced at elevated temperatures, due primarily to the thermal instability of the C-domain. The reconstitution of an enzymatically active $\overline{N_2}C_2$-complex in mixtures of the purified N- and C-domains indicates that the intact subunits of CoA transferase undergo oligomerization to yield a homodimer (Chapter 2). The assembly of two CoA transferase monomers depends on the initial association of native-like N-domains, which subsequently interact productively with the partially folded C-domains to produce the active enzyme.

The results from early studies provide more direct support for the homodimeric state of porcine CoA transferase. First, the molecular weights determined for the wild-type enzyme by gel filtration, sedimentation equilibrium, non-denaturing PAGE, or crosslinking followed by SDS-PAGE ranged from 7.8×10^4 to 1.13×10^5, equivalent to 1.5 to 2.2 times the subunit molecular weight of 52 197 (Hersh & Jencks, 1967; Edwards et al., 1973; White & Jencks, 1976; Sharp & Edwards, 1978; Russell & Patel, 1982; Lin & Bridger, 1992). The weight-average molecular weights calculated for the hinge-mutant (Chapter 2) are consistent with the values previously reported for wild-type CoA transferase. Second, the free enzyme is converted stoichiometrically to ECoA upon incubation with two molar equivalents of acyl-CoA substrate, as determined from the maximal extent of inactivation by DTNB (White et al., 1976), by AHA (Pickart & Jencks, 1979; Kindman & Jencks, 1981), or by MMP (Moore & Jencks, 1982). Thus, two moles of active sites are titrated for each mole of CoA transferase, consistent with a homodimeric structure.

Although the smallest active unit of CoA transferase is clearly a homodimer, the existence of a minor population of conformers consisting of more than two subunits cannot be excluded. Recently, two active forms of the recombinant porcine enzyme purified from BL-WT were separated by gel filtration chromatography (E. Brownie, unpublished observations), implying that CoA transferase is capable of adopting more than one quaternary structure. Such heterogeneity is not without precedent. Multiple, coexisting oligomeric states have also been described for recombinant proteins such as human acetylcholinesterase (Velan et al., 1991), glutamate dehydrogenase of *Sulfolobus solfataricus* (Facchiano et al., 1995), and lactate dehydrogenase (LDH) of *Thermotoga maritima* (Dams et al., 1996). In addition, the quaternary structures of many proteins vary due to: (1) the effects of salts, cofactors, or ligands (reviewed in [Klotz et al., 1975] and [Creighton, 1993]); or (2) the "swapping" of domains under conditions which favor partial unfolding (reviewed in [Bennett et al., 1995]; [Schlunegger et al., 1997]).

To understand why CoA transferase exists in more than one multimeric arrangement, the two forms of the enzyme, referred to as the "small" and "large" molecules, have been characterized. Specifically, the following questions have been addressed: (1) What is the subunit composition of each species? (2) Are different specific enzyme activities associated with the two forms? (3) Do the alternative oligomeric states differ with respect to the primary, secondary, or tertiary structure of their subunits? (4) What are the relative stabilities of the small and large molecules? (5) Are the two conformers interconvertible at a significant rate under benign or denaturing conditions? (6) Do specific molecular contacts account for the assembly of a higher-order oligomer of CoA transferase? The existence of multiple quaternary structures presents an additional level of complexity which must be considered during studies of the folding and assembly of CoA transferase.

EXPERIMENTAL PROCEDURES

Materials. The column matrix Affi-Gel Blue was purchased from Bio-Rad Laboratories, Ltd. DEAE Sephacel, Sephadex G-50, Sephadex G-200, Sephacryl S-200, and the gel filtration calibration kits were supplied by Pharmacia Biotech. Acrylamide was a Gibco BRL product from Life Technologies. Lyophilized trypsin and the substrates acetoacetate and succinyl-CoA were obtained from Sigma Chemical Company. Purified protein preparations were concentrated using Millipore brand Ultrafree-15 concentrators (MWCO = 1.0×10^4). Dialyses were carried out using Spectra/Por membranes supplied by Spectrum. Finally, the GuHCl was provided by ICN Biomedicals, Inc.

Reagents used specifically for crystallization experiments were: (1) polyethylene glycol (PEG) 1000 and PEG 2000 from Fluka Chemika; (2) HEPES buffer salt, from Sigma Chemical Company; (3) ultrapure Tris buffer salt, as a Gibco BRL product from Life Technologies; and (4) disodium succinate from Eastman Kodak.

Gene expression and protein purification. Gene expression in cultures of *E. coli* BL21(DE3) and the subsequent preparation of cell lysates were carried out as described previously (Chapter 2). In addition, the hinge-mutant was purified by successive elutions from columns of DEAE-Sephacel, Sephacryl S-200, and Affi-Gel Blue, as outlined in Chapter 2.

Wild-type CoA transferase was isolated from BL-WT in the absence or presence of 2ME (10 mM). The method used was identical to that described in Chapter 2 with two exceptions. First, following elution from a column of DEAE-Sephacel, the enzyme solution was desalted (without additional purification) by gel exclusion chromatography on a column of Sephadex G-50 instead of Sephacryl S-200. Second, after elution from a column of Affi-Gel Blue, the sample of CoA transferase was separated into small and large oligomeric forms by gel filtration through a column of Sephacryl S-200. The column volumes were 0.21 L (diameter 1.5 cm, height 120 cm) or 0.59 L (diameter 2.5 cm, height 120 cm). The protein was eluted from the column using buffer A. Typically, a minor peak corresponding to the large conformer appeared at 0.60 to 0.67 times the column volume, while a major peak corresponding to the small molecule appeared at 0.70 to 0.75 times the column volume. Prior to gel filtration, the enzyme solution was concentrated by precipitation in $(NH_4)_2SO_4$ (final concentration, 50% [w/v]) or by centrifugation (2×10^3 g) using Ultrafree-15 concentrators (MWCO = 1.0×10^4).

The homogeneity of all protein preparations was confirmed by SDS-PAGE analysis. The protein concentration of solutions of the wild-type enzyme used for far-UV CD or fluorescence measurements, ultracentrifugation analyses, and equilibrium unfolding studies was determined from A_{278} readings corrected for scatter. For these measurements, an ε_{278} value of 0.65 $(mg/mL)^{-1}$ was used (Chapter 2). The protein concentration of solutions of the purified wild-type enzyme or hinge-mutant used for other experiments was determined by measuring A_{278} without correcting for scatter. In such cases, an ε_{278} value of 0.75 (mg/mL)$^{-1}$ was used for both forms of CoA transferase (Chapter 2).

Measurement of enzyme activity. CoA transferase activity was determined spectrophotometrically as described in Chapter 2. In the present study, the assay solutions consisted of 50 mM Tris-HCl, 15 mM $MgCl_2$, 0.060 to 0.30 mM succinyl-CoA, and 13 to 67 mM acetoacetate, at pH 9.1. The extinction coefficient for acetoacetyl-CoA at 310 nm (ε_{310}) was taken to be 7.8×10^3 M^{-1} cm^{-1} under these conditions (Howard et al., 1986). Assay solutions used for determining specific enzyme activities contained 0.30 mM succinyl-CoA and 67 mM acetoacetate. All assays were carried out at 22 °C.

Non-denaturing PAGE analysis. Non-denaturing polyacrylamide gels consisted of a 3% (w/v) stacking gel (pH 6.8) and a 6% (w/v) resolving gel (pH 8.8). Electrophoresis was carried out at a constant voltage of 200 V, and was terminated one hour after the disappearance of the tracking dye from the resolving gel. It was determined empirically that these conditions of electrophoresis were optimal for the resolution of bands representing the small and large molecules of wild-type CoA transferase.[1]

Mass spectrometry. Mass analyses were performed as described in Chapter 2. Protein solutions (20 pmol/μL of the NC monomer) were desalted by dialysis against 10 mM Tris-HCl, pH 8.0, using a semi-permeable membrane with a MWCO of 3.5×10^3. The dialysis was carried out for 72 h, and the buffer was changed once every 24 h. Predicted molecular masses were average masses calculated using the program MacProMass.

Circular dichroism and fluorescence studies. Far-UV CD and fluorescence measurements were carried out as described in Chapter 2. Each protein sample was diluted to a final concentration of 0.4 to 0.6 mg/mL for CD or 0.1 to 0.2 mg/mL for fluorescence in buffer X.[2]

Equilibrium unfolding studies. Equilibrium unfolding transitions were analyzed as outlined in Chapter 2. Proteins were denatured overnight at 4 °C in buffer X containing different concentrations of GuHCl. Measurements of far-UV CD and fluorescence were carried out at 15 °C.

Calculation of $[\Delta G_u^{H_2O}]_{app}$. To facilitate the numerical analyses of thermodynamic parameters, a reversible "two-state" transition between folded dimers and unfolded monomers was assumed for both the small and large forms of CoA transferase (Pace, 1975; Pace, 1986; Shortle, 1989).[3] Values of $[\Delta G_u^{H_2O}]_{app}$) were estimated by fitting the data to the following equations (De Francesco et al., 1991; Milla et al., 1993):

$$y = f_u\,(y_u + ds[\mathrm{GuHCl}]) + (1 - f_u)(y_n + ns[\mathrm{GuHCl}])$$

$$f_u = \{-K_{d,app} + ([K_{d,app}]^2 + 8P_t\,K_{d,app})^{0.5}\}/(4P_t)$$

$$K_{d,app} = \exp\{(-[\Delta G_u^{H_2O}]_{app} + m[\mathrm{GuHCl}])/RT\}$$

where y is $[\Theta]_{obs}$ or $\lambda_{max,em}$ at a given concentration of GuHCl; y_n and y_u are the extrapolated ordinate-intercept values of $[\Theta]_{obs}$ or $\lambda_{max,em}$ for the native and unfolded protein, respectively; ns and ds are the slopes of the baselines for the native and denatured protein, respectively; f_u is the molar fraction of unfolded protein; $K_{d,app}$ is the apparent equilibrium dissociation constant; P_t is the total concentration of monomeric protein in mol/L; R is the universal gas constant (8.31 J/mol·K); T is the absolute temperature (K); and m is a constant proportional to the increase in the solvent-accessible surface area of the protein upon denaturation (Schellman, 1978; Myers et al., 1995).[4]

The data were fit to the appropriate equations using the program TableCurve 2D (Jandel Scientific, San Rafael, CA), as described in Chapter 2.

Sedimentation velocity analyses. Sedimentation coefficients were determined using the conventional sedimentation velocity technique (Chervenka, 1970). Prior to centrifugation, solutions of the small conformer (0.30 mL, 7.6 mg/mL) and the large conformer (0.30 mL, 1.6 mg/mL), purified in the absence of 2ME, were dialyzed at 4 °C against 1.0 L of 50 mM K[phosphate], 0.15 M KCl, 1 mM EDTA, pH 7.4, using a semi-permeable membrane with a MWCO of 3.5×10^3. The dialysis was carried out for 36 h, with one change of buffer after 18 h. Sedimentation velocity runs were carried out at 20 °C using a Beckman Model E Analytical Ultracentrifuge equipped with electronic speed control and schlieren optics. Two 2-degree, single-sector KelF sample cells, one equipped with two plane windows and the other equipped with one plane and one wedge window, were used so that two samples could be run simultaneously. The cells were filled with the protein solutions and inserted into a titanium rotor, which was then accelerated to 5.2×10^4 revolutions per minute (rpm). The run timer was started when the rotor reached maximal speed, and photographs of the schlieren peaks were taken at regular time intervals as the proteins sedimented. A Nikon Model 6C microcomparator was used for measurements of the schlieren photographs. A value of s_{obs} was calculated from the slope of a plot of ln (r) versus time, where r is the peak distance measured from the center of the rotor. A value for $s_{20,w}$ was determined by correcting s_{obs} to standard solvent and temperature (i.e. water at 20 °C). The partial specific volume was calculated based on the amino acid composition of wild-type CoA transferase (Cohn & Edsall, 1943).

Sedimentation equilibrium analyses. Molecular weight determinations were made using the conventional sedimentation equilibrium technique, as described in Chapter 2. The protein samples were the same as those analyzed by sedimentation velocity (see above). All sedimentation equilibrium runs were carried out at 20 °C. The sedimentation equilibrium data from each run were analyzed using the program TableCurve 2D (Jandel).

Determination of molecular weights by gel filtration analysis. A mixture of the small and large conformers (final concentration of each, 5 mg/mL) was eluted from a column of Sephadex G-200 using a buffer of 50 mM K[phosphate], 0.1 M KCl, pH 7.5. The column volume was 0.22 L (diameter 2.5 cm, height 45 cm), and the particle size ranged from 40 to 120 μm. The column was calibrated with respect to molecular weight in two separate runs with the following protein standards (2.0 mL, 5-10 mg/mL): (run 1) chymotrypsinogen A (2.50×10^4), albumin (6.70×10^4), and catalase (2.32×10^5); and (run 2) ribonuclease A (1.37×10^4), ovalbumin (4.30×10^4), and aldolase (1.58×10^5). For each standard, the fraction of the stationary gel volume available for diffusion (K_{av}) was calculated using the following formula (Andrews, 1965):

$$K_{av} = (V_e - V_o)/(V_t - V_o),$$

where V_e is the elution volume of the standard, V_o is the column void volume, and V_t is the total bed volume. The elution volume of Blue Dextran 2000 was taken to be the void volume. All elution volumes were calculated by multiplying the number of the "peak" fraction (based on measurements of A_{280}) by the fraction volume (1.9 mL). For each protein standard, the log (molecular weight) was plotted against K_{av} to generate a calibration curve, from which the molecular weights of the small and large forms of CoA transferase were estimated.

Refolding studies in vitro. The small and large forms of wild-type CoA transferase (final concentration of the NC monomer, 7.2 or 12 μM) were denatured in unfolding buffer (Chapter 2) at 22 °C for a minimum of 5 h. The solutions of the unfolded proteins were then diluted 1:50 (v/v) with refolding buffer (Chapter 2). The samples were incubated for 3 h at 22 °C before being assayed for enzyme activity and analyzed by non-denaturing PAGE.

Proteolysis experiments. Limited trypsin digestions were carried out at 37 °C in a buffer of 0.1 M NH_4HCO_3, pH 8.1. Samples of wild-type CoA transferase or the hinge-mutant (final concentration, 2.0 mg/mL) were treated with trypsin (final concentration, 0.050 mg/mL) for various times, before terminating the digestion by cooling to 4 °C. Immediately after proteolysis, the solutions of nicked CoA transferase were assayed for enzyme activity and analyzed by non-denaturing PAGE and SDS-PAGE in parallel.

X-ray crystallography studies. In general, crystals of CoA transferase suitable for x-ray diffraction studies were obtained following methods of microdialysis as described by Wolodko et al. (1984). Prior to use, all dialysis membranes were washed free of metal ion contaminants by thorough heating (without boiling) in 1 L of deionized H_2O containing trace amounts of EDTA. The solutions of purified small and large molecules (2 to 3 mg/mL in buffer A) were concentrated to 10 to 15 mg/mL by one of two methods. In some cases, the protein was precipitated with $(NH_4)_2SO_4$ (final concentration, 50% [w/v]) at 4 °C for at least 12 h. The precipitate was collected from an aliquot (0.30 to 0.40 mL) of the resulting suspension by centrifugation (10 min, 1.0×10^4 g), and the protein was redissolved in a minimal volume of 10 mM Tris-HCl, pH 8.0. Alternatively, the purified protein solutions were concentrated via centrifugation (2×10^3 g) using Ultrafree-15 concentrators (MWCO = 1.0×10^4). The concentrated protein solutions were dialyzed at 4 °C against 10 mM Tris-HCl, pH 8.5, using a semi-permeable membrane with a MWCO of 1.2×10^4. After dialysis for 72 h with one change of buffer every 24 h, the dialyzed protein solutions were cleared of particulate matter by centrifugation (30 min, 3.2×10^4 g), and subsequently assayed for CoA transferase activity and protein concentration as described above. A solution with a specific enzyme activity greater than 20 μmol/min/mg was acceptable. Protein solutions with concentrations greater than 12 mg/mL were diluted with dialysate to give a final protein concentration of 8 to 12 mg/mL. Subsequently, a sample of the solution (10, 20, or 50 μL) was transferred to a well of appropriate volume in a Lucite "button" (McPherson, 1976; Wolodko et al., 1984). A semi-permeable membrane with a MWCO of 3.5×10^3 was placed over the well and secured with a rubber O-ring. Finally, the button was immersed in a vial containing

3.0 mL of precipitant solution, and the vial was stored undisturbed at 22 °C. Generally, the precipitant solution consisted of: (1) 17% to 18% PEG (w/v) 1000, 5 mM succinate, and 0.1 M HEPES, at pH 8.0; or (2) 13% to 14.5% (w/v) PEG 2000, 5 mM succinate, and 0.1 M HEPES, at pH 8.0.

In some cases, crystals of CoA transferase suitable for x-ray diffraction studies were obtained by the hanging drop/vapor diffusion method. Purified enzyme samples were concentrated and dialyzed as described above. Aliquots of the protein solution (4 μL) were mixed with an equivalent volume of the precipitant solution, which generally consisted of 17.5% (w/v) PEG 2000, 5 mM succinate, and 0.1 M HEPES (pH 8.0).

The space group and unit cell dimensions were identified from preliminary diffraction data collected using x-rays of wavelength 1.54 Å and an oscillation camera. The distance from the crystal to the film was 1.2 m. Diffraction intensities were recorded on an area detector.

Diffraction data sets (one native and thirteen potential heavy-atom derivatives) were collected subsequently at beam-line 6A2 of the Photon Factory synchrotron radiation source (Tsukuba, Japan), using x-rays of wavelength 1.0 Å and a screenless Weissenberg camera (Sakabe, 1983; Sakabe, 1991). The distance from the crystal to the film was 430 mm. Diffraction intensities were recorded on Fuji imaging plates and digitized immediately using a Fuji BA-100 scanning system. The crystals (space group $P2_1$) were mounted and aligned with *b** perpendicular to the spindle axis and parallel to the x-ray beam, or parallel to the spindle axis and perpendicular to the x-ray beam for cusp data.

RESULTS[5]

Major and minor forms of wild-type CoA transferase. During routine purifications of recombinant, wild-type CoA transferase by the standard protocol (Chapter 2), two forms of the enzyme were eluted from a gel filtration column (E. Brownie, personal communication). To verify this initial observation from work on crude protein, the enzyme was purified by ion-exchange chromatography through DEAE-Sephacel and Affi-Gel Blue, and subsequently analyzed by gel permeation chromatography. The purified enzyme consistently eluted as two distinct peaks from a column of Sephacryl S-200 (Figure 4-1), based on measurements of protein absorbance (A_{280}) and CoA transferase activity. A much lower amount of protein and enzyme activity were associated with the first peak as compared to the second (Figure 4-1). Thus, the first peak represented a "minor" form of the CoA transferase preparation, while the second peak corresponded to a "major" component. The minor and major forms accounted for 10% and 90% (respectively) of the total enzyme activity eluted from the column of Sephacryl S-200.

Fractions corresponding to each peak were subsequently combined, and the resulting pooled enzyme samples were characterized. The specific activities of these enzyme forms were similar (Table 4-1), suggesting that the minor component does not arise from an incorrect self-association of partially unfolded CoA transferase subunits. However, the sedimentation coefficient ($s_{20,w}$) was substantially less for the major component than for the minor enzyme species (Table 4-1). This observation implied that the major form of CoA transferase is either smaller or less asymmetric than the minor component. In addition, the rate of migration of the minor enzyme species through a non-denaturing polyacrylamide gel was less than that of the major form, which was in turn less than that of the purified hinge-mutant (Figure 4-2). It was confirmed that the bands on this gel corresponding to the major and minor species were authentic forms of CoA transferase by Western blot analysis (results not shown). The average mass of the hinge-mutant (or N_2C_2-domain complex) was predicted to be 1418 Da less than that of the wild-type homodimer, since the hinge-mutant lacks six residues normally present in the linker segment of the wild-type enzyme (Chapter 2). Accordingly, it was postulated that the hinge-mutant and the major form of CoA transferase consist of two N-domains and

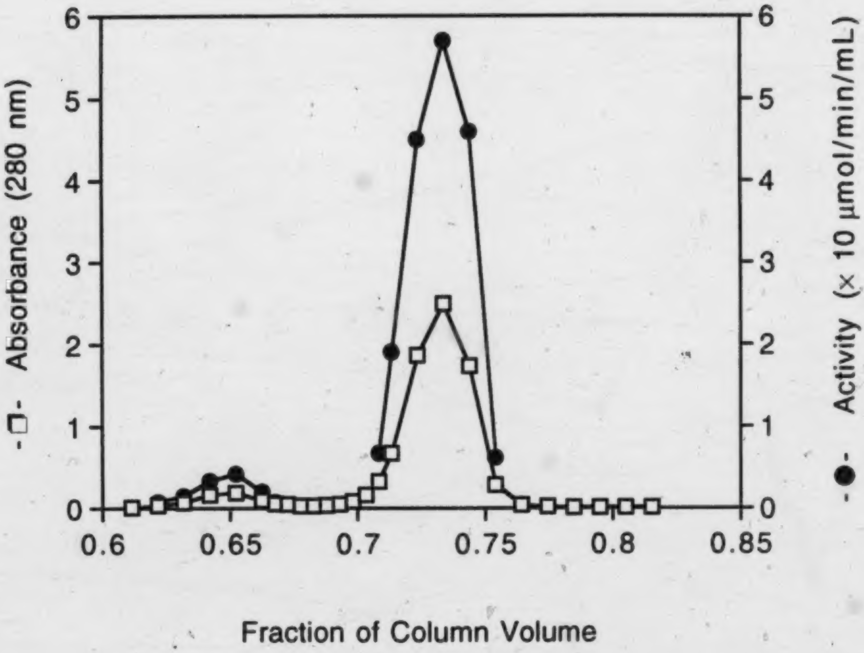

Figure 4-1: Separation of two forms of wild-type CoA transferase. A sample of enzyme (9 mg/mL, or 1.7×10^2 µM of the NC monomer) was fractionated into minor and major components by gel filtration through a column of Sephacryl S-200 (diameter 2.5 cm, height 120 cm, total volume 0.60 L), using buffer A. Aliquots of fractions eluted from the column were assayed spectrophotometrically for protein concentration (□) and CoA transferase activity (●). The pooled fractions of the minor component eluted at 0.62 to 0.67 times the column volume, while the pooled fractions of the major component eluted at 0.71 to 0.75 times the column volume. The minor and major components accounted for 10% and 90% (respectively) of the total activity associated with the unfractionated enzyme sample.

Table 4-1: Preliminary Characterization of the Major and Minor Forms of CoA Transferase[a]

Enzyme species	Specific activity (μmol/min/mg)[b]	$s_{20,w}$ (S)[c]
Major	18.7 ± 2.1	5.45
Minor	17.9 ± 3.0	7.62

[a] The "minor" and "major" forms of CoA transferase correspond to the early and late peaks (respectively) eluted from a column of Sephacryl S-200.

[b] Specific activities are expressed as the average value from three separate calculations, corresponding to two enzyme preparations. The error is the sample standard deviation (σ_{n-1}).

[c] S: Svedberg unit (= 1.0×10^{-13} s).

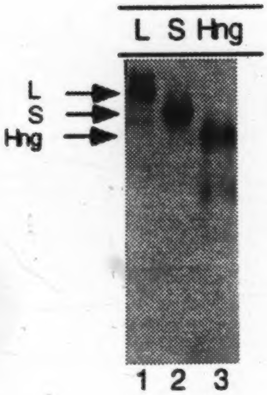

Figure 4-2: Distinct electrophoretic behavior of three forms of CoA transferase under non-denaturing conditions. Lane 1, the minor component of wild-type CoA transferase; lane 2, the major component of wild-type CoA transferase; lane 3, the hinge-mutant. Bands representing the minor component (or large form "L"), the major component (or small form "S"), and the hinge-mutant (Hng) are indicated by appropriately labeled arrows. Each lane was loaded with 5 µg of protein. The gel consisted of a 3% (w/v) stacking gel (pH 6.8) and a 6% (w/v) resolving gel (pH 8.8), and was analyzed by Coomassie Blue staining.

two C-domains, while the minor species is an oligomer of higher order. This preliminary conclusion was subsequently tested by carrying out more rigorous analyses.

Molecular weights of the two forms of CoA transferase. To measure the size and assign the subunit composition of the minor and major components of CoA transferase, the weight-average molecular weights of the two species were determined by sedimentation equilibrium. The plots of ln y vs r^2 were significantly curved (Figure 4-3), suggesting that each enzyme sample consisted of a mixture of multiple forms at equilibrium. The molecular weights measured for the major species ranged from 7.53×10^4 at the meniscus (solute concentration, 0.60 mg/mL) to 9.46×10^4 at the cell bottom (solute concentration, 3.35 mg/mL). In contrast, the molecular weights measured for the minor component ranged from 1.27×10^5 at the meniscus (solute concentration, 0.84 mg/mL) to 1.87×10^5 at the cell bottom (solute concentration, 3.59 mg/mL). The apparent weight-average molecular weights determined for the small and large molecules were $8.48 \pm 0.07 \times 10^4$ and $1.57 \pm 0.02 \times 10^5$, respectively. From these results, it was concluded that: (1) the molecular weight of the minor species is greater than that of the major component; and (2) the dissimilar chromatographic, electrophoretic, and sedimentation properties of the two conformers (see above) are not merely due to differences in molecular shape or charge. Accordingly, the minor and major forms of CoA transferase were renamed the "large" and "small" molecules, respectively.

The sedimentation equilibrium data obtained for the small conformer fit best to a monomer-dimer model (Figure 4-4), suggesting that this sample of CoA transferase consisted of a mixture of monomer and homodimer at equilibrium under the conditions of the ultracentrifugation experiment. In contrast, the data obtained for the large conformer could not be fit satisfactorily to a single-species or a monomer-dimer equation. Nevertheless, given that the maximal molecular weight of the large molecule was approximately double that of the small molecule, it was inferred that the minor component observed by gel filtration and non-denaturing PAGE analyses is most likely a

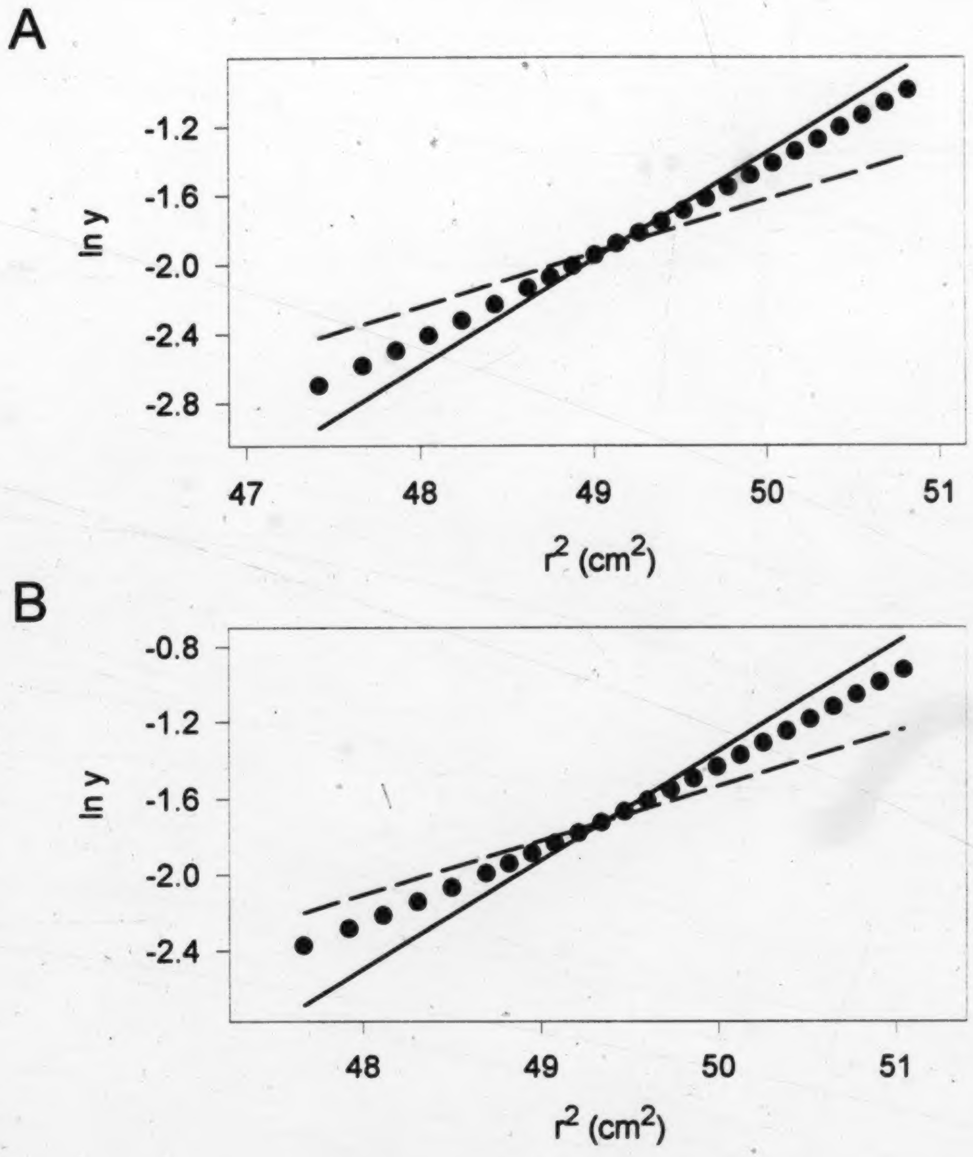

Figure 4-3: Determination of the molecular weights of the two components of wild-type CoA transferase by sedimentation equilibrium. Apparent weight-average molecular weights of $8.48 \pm 0.07 \times 10^4$ ($r^2 = 1.0$) for the small conformer (A) and $1.57 \pm 0.02 \times 10^5$ ($r^2 = 0.99$) for the large conformer (B) were determined as described in "Experimental Procedures." Also shown are the lines predicted for monodisperse solutions of monomer (– – –) and homodimer (——) in (A), or homodimer (– – –) and homotetramer (——) in (B). Note that both ln *y* vs r^2 plots are significantly curved, indicating that the two forms of the enzyme undergo association or dissociation at the protein concentrations examined.

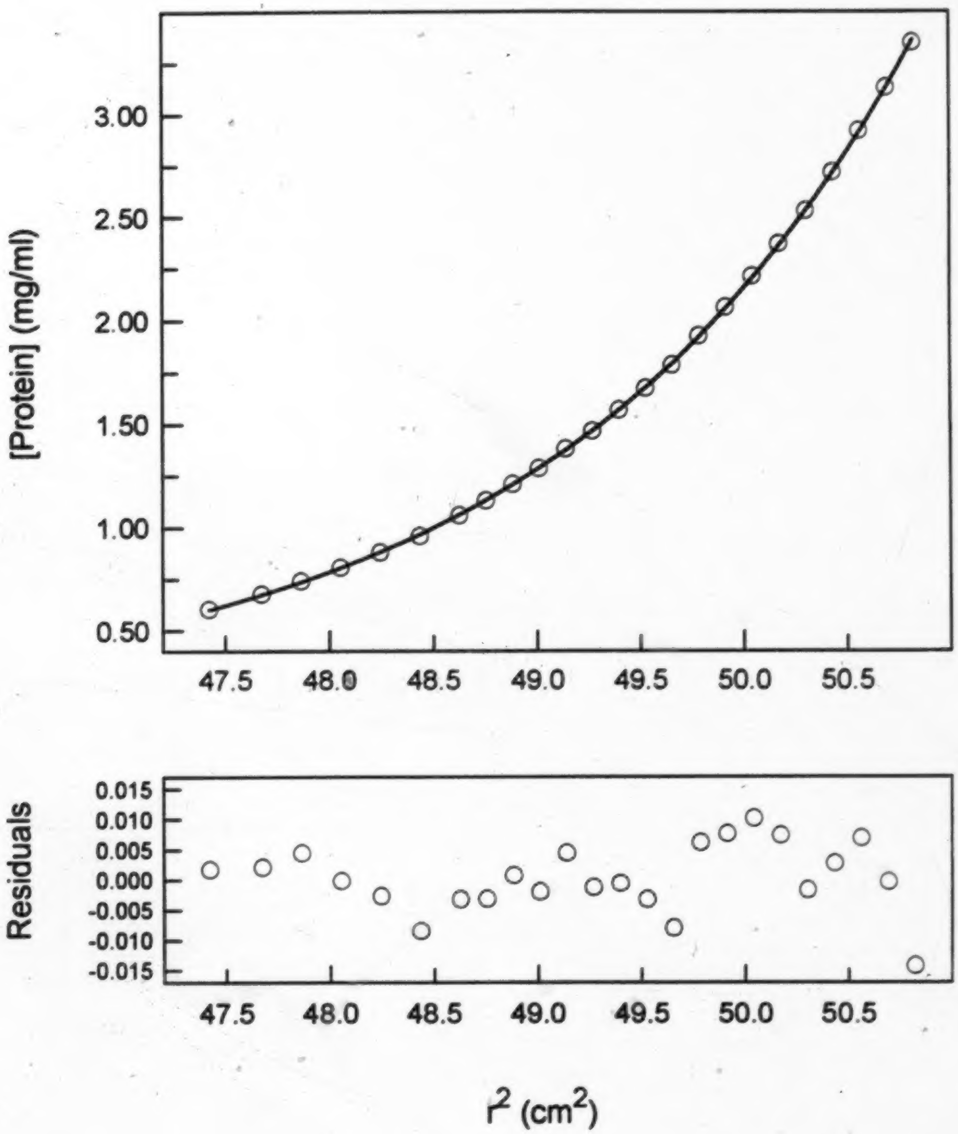

Figure 4-4: Sedimentation equilibrium data of the small conformer fit to a monomer-dimer model. The small enzyme form was analyzed by ultracentrifugation as described in Figure 4-3. Top panel: the data from a single run were fit to a curve consistent with a monomer-dimer equilibrium by the program TableCurve 2D (Jandel). Bottom panel: the goodness of the fit was apparent from the random scatter in the residual plot. Note that a value for the dissociation constant of the homodimer can only be obtained with confidence by repeating this experiment with different initial protein concentrations.

homotetramer. Presumably, some molecules of the total population of minor species undergo dissociation under the conditions used for ultracentrifugation, yielding an equilibrium mixture of several oligomeric forms.

The molecular weights of the small and large forms of CoA transferase were re-evaluated by gel filtration analysis. A mixture of the two conformers (final concentration of each, 5 mg/mL) was fractionated on a column of Sephadex G-200, previously calibrated with protein standards of molecular weights ranging from 1.37×10^4 to 2.32×10^5. Using a calibration curve deduced from the protein standards (Figure 4-5), molecular weights of 1.10×10^5 and 2.45×10^5 were estimated for the major and minor components, respectively. Thus, the oligomeric state inferred for each enzyme species by sedimentation equilibrium analysis was corroborated by gel filtration analysis.

Structural properties of the two forms of CoA transferase. In general, the quaternary structure of a protein is stabilized by hydrophobic, electrostatic, and hydrogen bonding interactions between subunits (Argos, 1988; Janin et al., 1988; Tsai et al., 1996; Tsai et al., 1997). Furthermore, the interfaces of dimeric and tetrameric enzymes often consist of extended β-sheets, closely packed α-helices or β-sheets, and/or interacting loops (Miller, 1989; reviewed in [Jones & Thornton, 1995]). The forces and structural motifs which determine the assembly of a multimeric protein are related to the structure of the individual subunits. Accordingly, the coexistence of distinct oligomeric forms of CoA transferase could be related to differences in primary, secondary, and/or tertiary structure between the subunits of the small and large molecules.

The homodimeric and homotetrameric forms of CoA transferase were indistinguishable by SDS-PAGE analysis (not shown). However, this observation did not exclude the possibility that the small or large molecule was selectively assembled from post-translationally modified protomers. Relatively subtle covalent modifications, including oxidation, phosphorylation, methylation, and acylation (Wold, 1981), could alter the conformation of the subunit without significantly influencing its electrophoretic

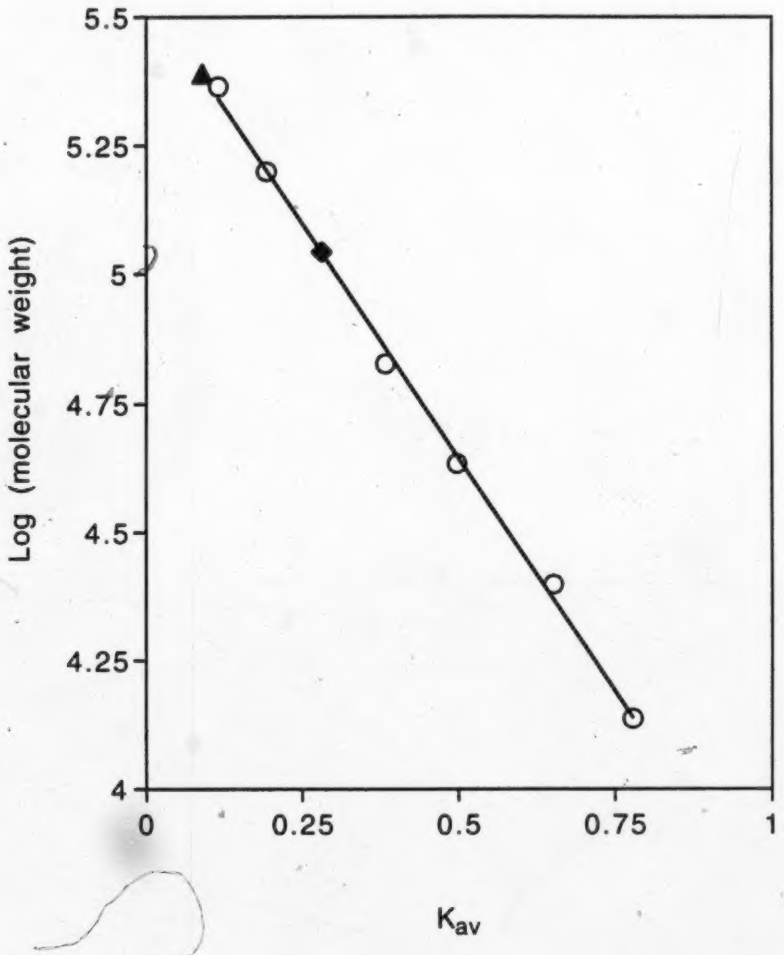

Figure 4-5: Molecular weight determinations for the two components of wild-type CoA transferase by gel filtration. A calibration curve ($r^2 = 1.0$) was generated from a plot of log (molecular weight) against K_{av} (○) for protein standards eluted from a column of Sephadex G-200. A mixture of the small and large conformers was fractionated on the same column, and the molecular weight of each enzyme form was estimated by interpolation (◆) or extrapolation (▲) of the calibration curve. Apparent molecular weights of 1.10×10^5 and 2.45×10^5 were calculated for the small and large conformers, respectively.

behavior. To determine whether or not a change in primary structure was responsible for the coexistence of multiple oligomeric forms of CoA transferase, the small and large molecules were analyzed by ESI-MS. The molecular masses of the subunits comprising both conformers were equal within experimental error to the mass predicted for the wild-type monomer (Figure 4-6; Table 4-2). Thus, the small and large forms of CoA transferase consist of subunits that have not undergone post-translational modifications that are detectable within the limits of the precision of ESI-MS.

A change in the oligomeric state of a protein may reflect a conformational rearrangement of the individual subunits. For example, the unique regulatory properties of allosteric enzymes such as glycogen phosphorylase (Barford & Johnson, 1992) have been attributed to a dynamic coupling between the tertiary and quaternary structures of the protein. To ascertain whether or not a conformational change could account for the coexistence of two multimeric forms of CoA transferase, the small and large molecules were analyzed by measurements of far-UV CD and intrinsic tryptophan fluorescence. The far-UV CD spectra recorded for the homodimer and the homotetramer were each similar to that determined for a sample of wild-type enzyme which had not been separated into its two oligomeric components (compare Figure 4-7 with Figure 2-8B). In addition, the excitation at 295 nm of the small and large conformers produced a $\lambda_{max,em}$ of 335 nm, equal to the maximum determined for the unfractionated wild-type enzyme (Table 2-2). It was therefore concluded that the homodimeric and homotetrameric forms of CoA transferase are nearly identical with respect to their secondary structures and the accessibility of their tryptophan residues to solvent.

Stabilities of the small and large conformers in denaturant. From the measurements of far-UV CD and fluorescence, it was inferred that the subunits of the homodimer and homotetramer adopt similar folds. If this hypothesis were true, then the small and large conformers should display similar stabilities relative to the unfolded state. Measurements of $[\Theta_{obs,222}]$ and $\lambda_{max,em}$ were carried out for each form of CoA

Figure 4-6: Analysis of the two oligomeric forms of CoA transferase by ESI-MS. The homodimer (A) and the homotetramer (B) (approximately 200 pmol of the NC subunit) were analyzed for molecular mass (see "Experimental Procedures"). Shown beside each peak is the number of protons associated with the corresponding ion.

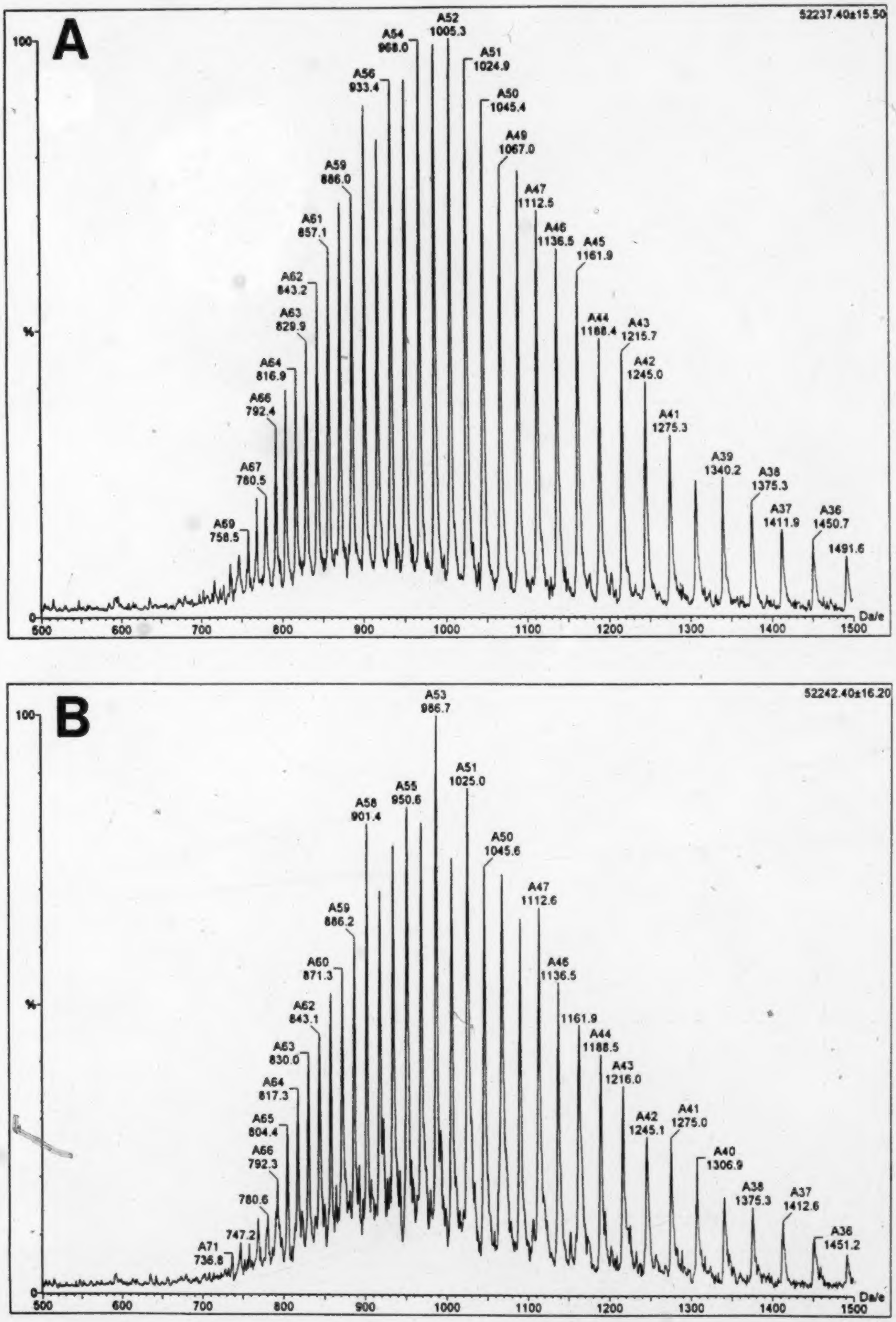
A
52237.40±15.50
100
%
0
A52
1005.3
A54
968.0
A51
1024.9
A56
933.4
A50
1045.4
A49
1067.0
A59
886.0
A47
1112.5
A61
857.1
A46
1136.5
A45
1161.9
A62
843.2
A63
829.9
A44
1188.4
A43
1215.7
A64
816.9
A42
1245.0
A66
792.4
A41
1275.3
A39
1340.2
A67
780.5
A38
1375.3
A37
1411.9
A36
1450.7
A69
758.5
1491.6
500
600
700
800
900
1000
1100
1200
1300
1400
1500
Da/e
B
52242.40±16.20
100
%
0
A53
986.7
A51
1025.0
A55
950.6
A58
901.4
A50
1045.6
A47
1112.6
A59
886.2
A60
871.3
A46
1136.5
A62
843.1
1161.9
A44
1188.5
A63
830.0
A43
1216.0
A64
817.3
A42
1245.1
A41
1275.0
A65
804.4
A66
792.3
A40
1306.9
A38
1375.3
A37
1412.6
780.6
A36
1451.2
747.2
A71
736.8
500
600
700
800
900
1000
1100
1200
1300
1400
1500
Da/e

Table 4-2: Electrospray Mass Spectral Analysis of the Small and Large Forms of CoA Transferase

Enzyme species	Experimental mass[a] (M+H$^+$ [Da])	% Difference[b,c]
Small molecule	52 237 ± 16	0.011
Large molecule	52 242 ± 16	0.021

[a] The error is the standard error of a single measurement.

[b] The average mass predicted for the wild-type subunit (M+H$^+$ = 52 231 Da) was calculated using the program MacProMass, assuming the cleavage of the N-terminal methionine residue from the recombinant polypeptide produced in *E. coli.* The mass of the corresponding unmodified protein is obtained by adding 131 Da.

[c] Percent differences were calculated from the following equation:

$$\{|\text{Predicted Mass} - \text{Experimental Mass}| \div (\text{Predicted Mass})\} \times 100\%.$$

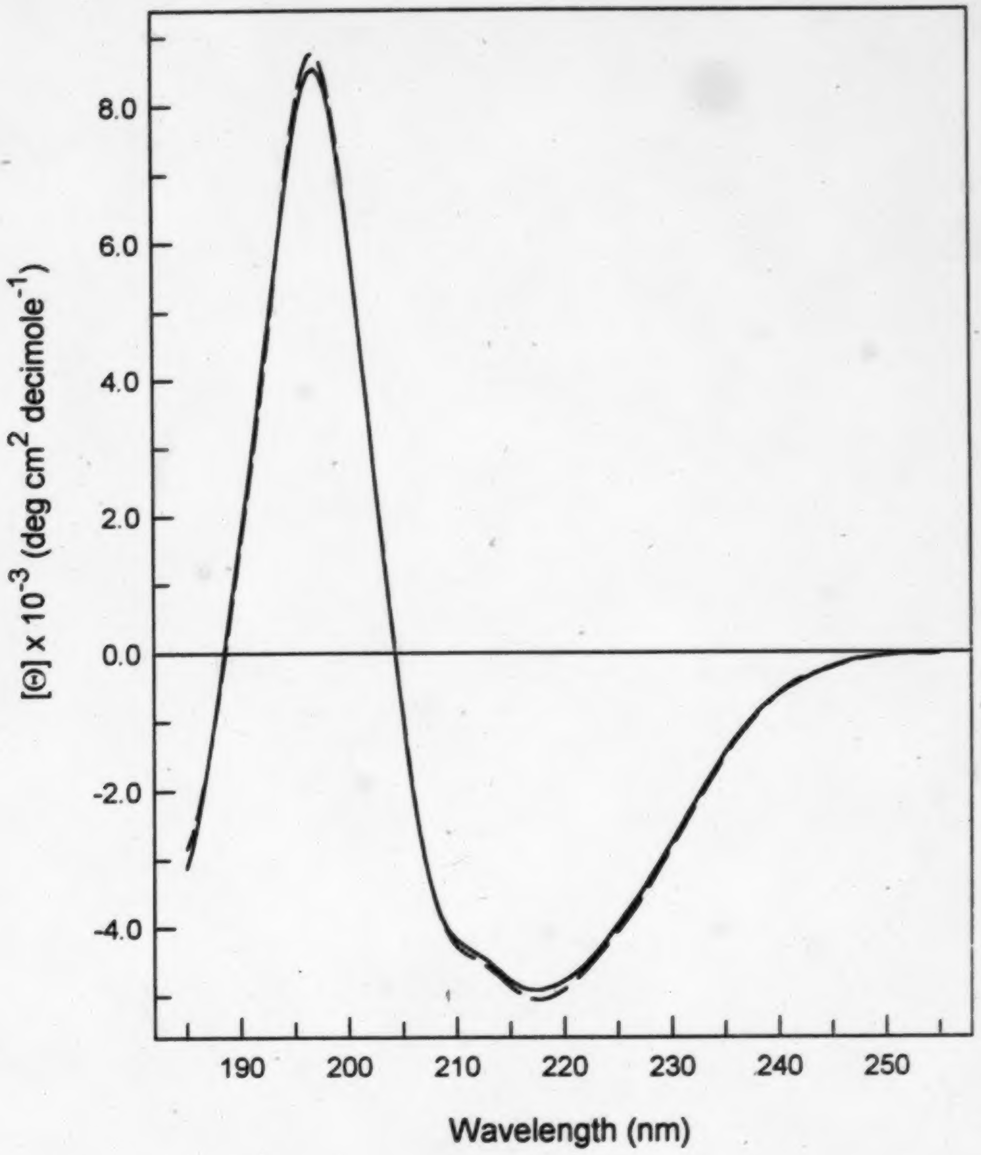

Figure 4-7: Analysis of the two oligomeric forms of CoA transferase by far-UV CD. Spectra were recorded for the small conformer (——) and the large conformer (– – –) as described in "Experimental Procedures".

transferase following incubation with different concentrations of GuHCl. The denaturation profiles of the homodimer and the homotetramer were nearly superimposable (not shown), indicating that both forms undergo a common equilibrium unfolding transition. The values of $[\Delta G_u^{H_2O}]_{app}$ and $[GuHCl]_{1/2}$ calculated for the small and large molecules from measurements of far-UV CD and fluorescence were equal within experimental error (Table 4-3). The assumption of a predominantly "two-state" equilibrium unfolding transition for both the homodimer and homotetramer was reasonable, given the similarity between their denaturation curves. Thus, it was concluded that the conformational stabilities of the small and large forms of CoA transferase are similar.

A kinetic barrier between the homodimer and the homotetramer. The first gel filtration analysis indicated that the homodimer was present in large excess over the homotetramer in a sample of unfractionated, wild-type CoA transferase (Figure 4-1). It was predicted that the relative amounts of the small and large conformers in this sample were dependent on the total concentration of protein. If this were true, then a significant proportion of the large conformer should convert to the small molecule in sufficiently dilute protein solutions, according to Le Châtelier's principle.

To test this hypothesis, a preparation of the large enzyme form (3 mg/mL or 57 µM of the NC monomer) was diluted (1/600) with 50 mM K[phosphate], pH 7.4, and incubated at 4 °C for various times, ranging from 2 to 68 days. Analysis of the diluted samples by non-denaturing PAGE indicated that the large molecule did not dissociate to yield appreciable amounts of homodimer under these conditions (Figure 4-8). Instead, most of the homotetramer was lost after storage at 4 °C for 68 days, presumably due to aggregation and/or proteolytic digestion (Figure 4-8, lane 1). In addition, the diluted large molecule did not convert to the small oligomeric form upon incubation at 22 °C for 48 h, 30 °C for 24 h, or 37 °C for 6 h (Figure 4-9). Thus, even during prolonged storage at

Table 4-3: Denaturation of the Small and Large Molecules of CoA Transferase with GuHCl

Part A: Parameters derived from far-UV CD measurements[a]

Protein[b]	P_t (μM)	$[\Delta G_u^{H_2O}]_{app}$ (kJ/mol)	m (kJ/mol/M)	$[GuHCl]_{1/2}$[c] (M)
Small molecule (-2ME)[d]	9.2	54 ± 0.4	22 ± 0.8	1.2 ± 0.05
Small molecule (+2ME)	11	46 ± 0.0	20 ± 0.4	0.97 ± 0.02
Large molecule (+2ME)	7.7	39 ± 2.9	13 ± 2.5	0.81 ± 0.16

[a] The error shown for each parameter is the standard error due to fitting of the curve, and may therefore be an underestimate. The actual experimental error can be reasonably estimated to be as high as ± 10%.

[b] Purified in the absence (-2ME) or presence (+2ME) of reductant.

[c] Calculated from: $[GuHCl]_{1/2} = \{(RT\ln P_t) + [\Delta G_u^{H_2O}]_{app}\} \div m$ (Mok et al., 1996).

[d] This sample was dialyzed against buffer X without 10 mM 2ME prior to the measurement of CD.

Table 4-3: Denaturation of the Small and Large Molecules of CoA Transferase with GuHCl

Part B: Parameters derived from fluorescence measurements[a]

Protein[b]	P_t (μM)	$[\Delta G_u^{H_2O}]_{app}$ (kJ/mol)	m (kJ/mol/M)	$[GuHCl]_{1/2}$[c] (M)
Small molecule (-2ME)[d]	2.9	38 ± 1.7	14 ± 2.1	0.59 ± 0.09
Small molecule (-2ME)[e]	2.9	41 ± 1.3	13 ± 1.7	0.85 ± 0.12
Large molecule (-2ME)[d]	2.3	39 ± 1.3	12 ± 1.7	0.66 ± 0.09
Small molecule (+2ME)	3.6	41 ± 1.7	18 ± 2.5	0.59 ± 0.08
Large molecule (+2ME)	4.3	40 ± 1.3	15 ± 1.7	0.71 ± 0.08

[a] The error shown for each parameter is the standard error due to fitting of the curve, and may therefore be an underestimate. The actual experimental error can be reasonably estimated to be as high as ± 10%.

[b] Purified in the absence (-2ME) or presence (+2ME) of reductant.

[c] Calculated from: $[GuHCl]_{1/2} = \{(RT \ln P_t) + [\Delta G_u^{H_2O}]_{app}\} \div m$ (Mok et al., 1996).

[d] Although purified in the absence of reductant, these samples were dialyzed against buffer X containing 10 mM 2ME prior to the measurement of fluorescence.

[e] This sample was dialyzed against buffer X without 10 mM 2ME prior to the measurement of fluorescence.

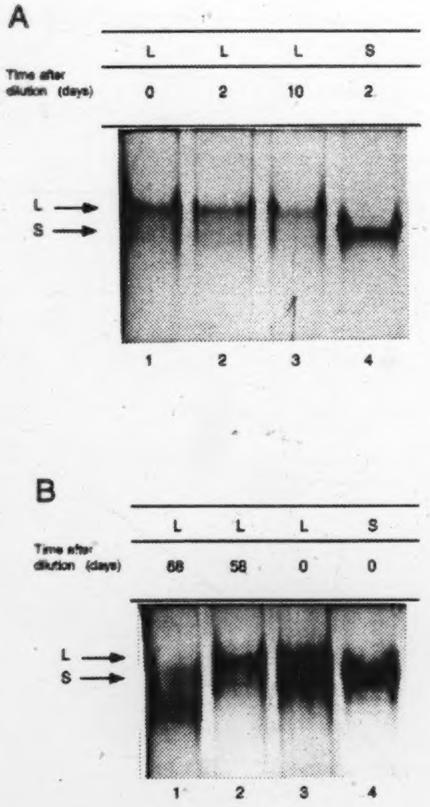
A
L
L
L
S
Time after dilution (days)
0
2
10
2
L
S
1
2
3
4
B
L
L
L
S
Time after dilution (days)
68
58
0
0
L
S
1
2
3
4

Figure 4-8: Lack of detectable dissociation of homotetrameric CoA transferase in dilute protein solutions. The purified enzyme forms (5 µg/mL, or 0.1 mM of the NC monomer) were incubated in 50 mM K[phosphate] (pH 7.4) at 4 °C for the indicated times prior to analysis by non-denaturing PAGE. The incubation times ranged from 0 to 10 days (A) or 0 to 68 days (B). Bands representing the homotetramer (L; lanes 1-3) and the homodimer (S; lane 4) are indicated by appropriately labeled arrows. Each lane was loaded with 0.38 µg of protein. The gel consisted of a 3% (w/v) stacking gel (pH 6.8) and a 6% (w/v) resolving gel (pH 8.8), and was analyzed by staining with $AgNO_3$.

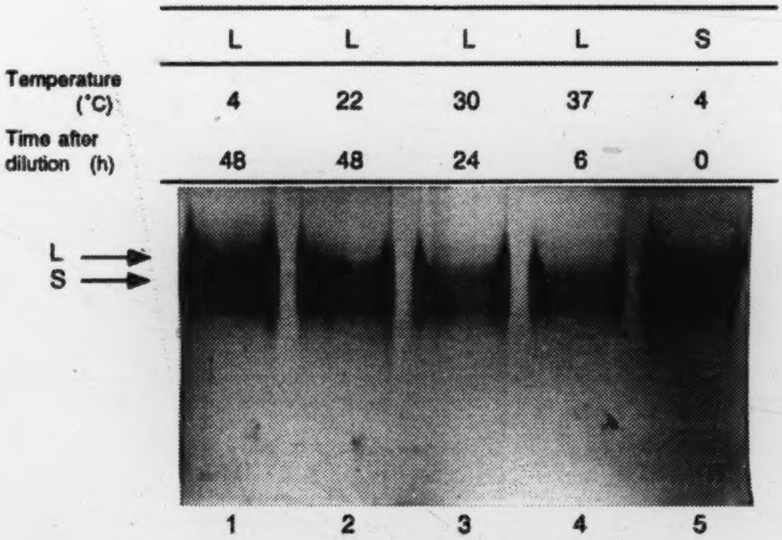

Figure 4-9: Lack of detectable dissociation of homotetrameric CoA transferase in dilute protein solutions at elevated temperatures. The purified enzyme forms (5 µg/mL, or 0.1 µM of the NC monomer) were incubated in 50 mM K[phosphate] (pH 7.4) for the indicated times prior to analysis by non-denaturing PAGE. The incubation temperatures were 4 °C (lanes 1 and 5), 22 °C (lane 2), 30 °C (lane 3), and 37 °C (lane 4). Bands representing the homotetramer (L; lanes 1-4) and the homodimer (S; lane 5) are indicated by appropriately labeled arrows. Each lane was loaded with 0.38 µg of protein. The gel consisted of a 3% (w/v) stacking gel (pH 6.8) and a 6% (w/v) resolving gel (pH 8.8), and was analyzed by staining with $AgNO_3$.

relatively low protein concentrations, the homotetramer does not dissociate to the homodimer at an appreciable rate.

From these observations, it was inferred that a substantial kinetic barrier separates the two multimeric states of CoA transferase under benign conditions. To estimate the magnitude of this barrier, the Gibbs free energy of activation ($\Delta G^{\ddagger}$) was calculated from the following equation (Segel, 1975):

$$\Delta G^{\ddagger} = -2.3RT\log(k_1 h/k_B T),$$

where k_1 is the maximal first-order rate constant for the conversion of the large molecule to the small form, h is Planck's constant (6.62608×10^{-34} J·s), and k_B is the Boltzmann constant (1.38066×10^{-23} J/K).[6] A limiting value of $\Delta G^{\ddagger} \geq 1.0 \times 10^2$ kJ/mol was determined for the dissociation of the large molecule to the small oligomeric form at 22 °C or 30 °C, assuming that a conversion of at least 10% of the initial homotetramer was detectable by non-denaturing PAGE analysis.

Finally, it was predicted that the distribution of CoA transferase between the homodimer and the homotetramer is dependent on the total protein concentration in the absence of a kinetic barrier. If this were true, then a proportion of the large conformer unfolded in the presence of denaturant should refold to the small multimeric form upon dilution. The homodimer and homotetramer were denatured and refolded as described in "Experimental Procedures," so that the final concentration of protein in the refolding buffer was 7.2 to 12 μg/mL (or 14 to 23 μM of the NC monomer). For each species, the yield and kinetics of refolding were similar to those measured for unfractionated wild-type CoA transferase (Chapter 2), consistent with the hypothesis that both multimeric forms are assembled from identical subunits. Importantly, non-denaturing PAGE analysis revealed that only the homodimer was present in solutions of the refolded large and small molecules (Figure 4-10). Thus, the denatured homotetramer is converted to the homodimer during refolding at low protein concentrations.

Role of the hinge region in the formation of the homotetramer. The linker segment which joins the N- and C-domains of CoA transferase contains a large number of polar residues, and is most likely organized as an amphipathic helix-turn-helix motif (Chapter 1). In general, loop regions contribute to the stabilization of oligomeric proteins through charged hydrogen bonds at the relatively hydrophilic periphery of the subunit interface (Miller, 1989; reviewed in [Jones & Thornton, 1995]). It was predicted that an intact hinge region may be necessary for the stability of the homotetramer.

This hypothesis was addressed by examining the effect of mild proteolysis of the linker segment on the distribution of CoA transferase between the small and large oligomeric forms. If the hinge region were necessary to stabilize the large conformer, then the latter should be converted directly to the N_2C_2-domain complex upon proteolysis, without the accumulation of a nicked form consisting of four of each domain (N_4C_4). Samples of pure homodimer and homotetramer were treated with trypsin (1/40, w/w) at 37 °C for various times. After 15 min, both forms of CoA transferase were converted to a common molecular species which migrated more rapidly than the untreated hinge-mutant through a non-denaturing polyacrylamide gel (Figure 4-11, top panel). It was confirmed by SDS-PAGE analysis that this species was a nicked form of CoA transferase, consisting of two polypeptide fragments with apparent molecular weights of 2.8×10^4 and 2.4×10^4 (Figure 4-11, bottom panel). This nicked enzyme was also the major species observed in samples of the small and large conformers treated with trypsin for 30 or 60 min (Figure 4-11). Importantly, a complex of intermediate molecular weight, greater than that of the untreated hinge-mutant but less than that of the intact homotetramer, was not detected by non-denaturing PAGE analysis of the nicked homotetramer (Figure 4-11, top panel). The hinge-mutant migrated through the non-denaturing polyacrylamide gel as a single band (Figure 4-11, top panel), which was

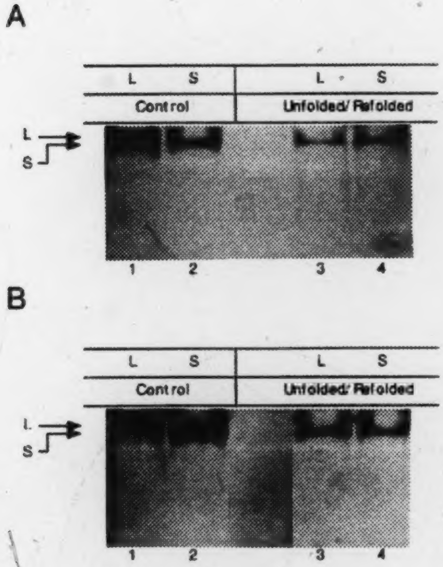

Figure 4-10: Non-denaturing PAGE analysis of the homotetramer and the homodimer after unfolding and renaturation. (A) Samples of the small and large conformers purified in the presence of 2ME. Lanes 1 and 2, control samples diluted without prior denaturation; lanes 3 and 4, samples diluted to a final concentration of 12 µg/mL (or 0.24 µM of the NC monomer) after unfolding in 6.0 M GuHCl. (B) Samples of the small and large conformers purified in the absence of 2ME. Lanes 1 and 2, control samples diluted without prior denaturation; lanes 3 and 4, samples diluted to a final concentration of 7.5 µg/mL (or 0.14 µM of the NC monomer) after unfolding in 6.0 M GuHCl. Bands representing the homotetramer (L) and the homodimer (S) are indicated by appropriately labeled arrows. Each lane was loaded with 1.7 µg (A) or 0.5 µg (B) of protein. The gels consisted of a 3% (w/v) stacking gel (pH 6.8) and a 6% (w/v) resolving gel (pH 8.8), and were analyzed by staining with $AgNO_3$.

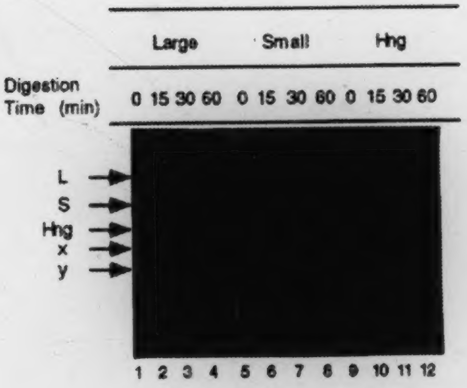
Large
Small
Hng
Digestion Time (min)
0 15 30 60 0 15 30 60 0 15 30 60
L
S
Hng
x
y
1 2 3 4 5 6 7 8 9 10 11 12

x 10⁴
9.74
6.62
4.50
3.10
2.15
WT
N
C
1 2 3 4 5 6 7 8 9 10 11 12

Figure 4-11: Effect of limited tryptic digestion on the stability of homotetrameric CoA transferase. Samples of the large conformer (lanes 1-4), small conformer (lanes 5-8), and hinge-mutant (lanes 9-12) were treated with trypsin (1/40, w/w) at 37 °C for the indicated times, prior to analysis by non-denaturing PAGE (top panel) or SDS-PAGE (bottom panel). Bands representing the homotetramer (L), homodimer (S), hinge-mutant (Hng), 5.2×10^4 wild-type subunit (WT), 2.7×10^4 N-domain (N), and 2.4×10^4 C-domain (C) are indicated by appropriately labeled arrows. Bands representing low-molecular weight species (x and y) formed by mild proteolysis of the hinge-mutant and the two wild-type conformers (respectively) are also indicated. Each lane was loaded with 9 μg of protein, and the gels were analyzed with Coomassie Blue staining. The native gel consisted of a 3% (w/v) stacking gel (pH 6.8) and a 6% (w/v) resolving gel (pH 8.8).

previously shown to correspond to the N_2C_2-domain complex (Chapter 2). Similarly, the purified hinge-mutant eluted as a single, homogeneous species from a column of Sephacryl S-200 (Figure 4-12), and did not display the minor peak characteristic of the gel filtration elution profile observed for the wild-type enzyme (Figure 4-1). From these results, it was suggested that the homotetramer is unstable in the absence of the intact hydrophilic linker segment.

It should be noted that 50% of the initial CoA transferase activity associated with the homodimer or homotetramer was lost during the first 15 min of incubation with trypsin, while the subsequent disappearance of enzyme activity was much more gradual. As mentioned, the electrophoretic mobility of the nicked homodimer or homotetramer was greater than that of the untreated hinge-mutant under non-denaturing conditions (Figure 4-11, top panel). From these observations, it was inferred that the tryptic digestion of the small and large conformers was more extensive than the mild nicking previously reported for the CoA transferase of sheep kidney (Sharp & Edwards, 1978) or pig heart (Moore & Jencks, 1982; Lin & Bridger, 1992) isolated in the absence of proteinase inhibitors. Consistent with this hypothesis, the hinge-mutant itself was degraded to a smaller, partially active enzyme species when treated with trypsin as described above (Figure 4-11). Thus, the proteolytic digestion observed in these experiments was most likely not limited to the hydrophilic linker region. It could therefore not be excluded that a short peptide segment, located at the N- or C-terminus of either domain, is also required for the stability of the homotetramer.[7]

Crystallization of CoA transferase. It was of considerable interest to determine the structure of CoA transferase by x-ray crystallography, as this information would provide insight as to the molecular details accounting for the enzyme's function. Prior to the studies outlined in this chapter, crystals of wild-type CoA transferase were grown using samples of the enzyme that were not fractionated into the small and large conformers. Following the identification of two oligomeric forms of CoA transferase, it was suggested

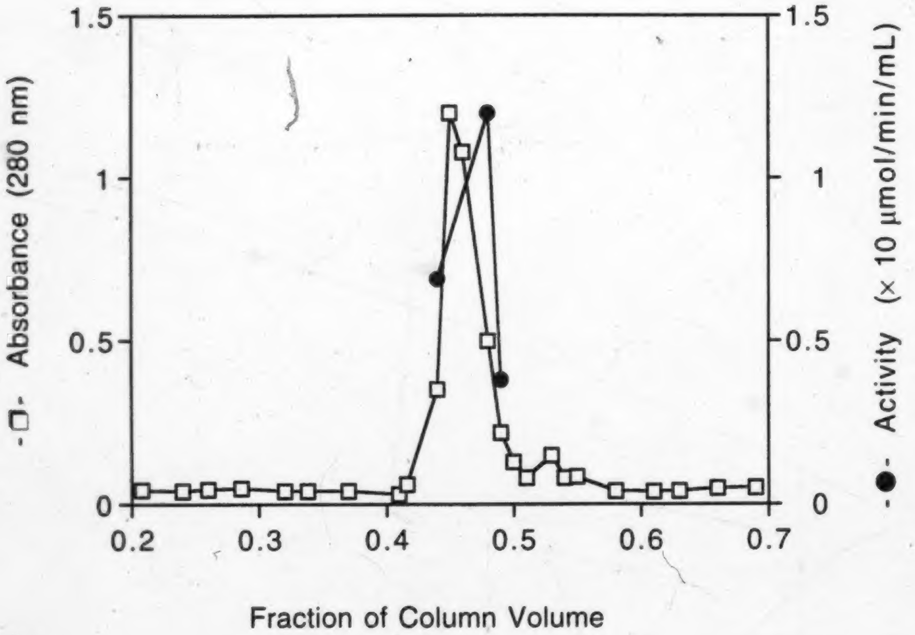

Figure 4-12: Analysis of the hinge-mutant by gel filtration chromatography. A sample of the hinge-mutant (16 mg/mL, or 3.1 × 10^2 µM of each domain) eluted as a single peak from a column of Sephacryl S-200 (diameter 1.5 cm, height 120 cm, total volume 0.21 L), using 10 mM K[phosphate], 0.1 mM EDTA, 2.0 mM 2ME (pH 7.4). Aliquots of fractions eluted from the column were assayed spectrophotometrically for protein concentration (❑) and CoA transferase activity (●). The fractions of the hinge-mutant that were pooled eluted at 0.44 to 0.50 times the column volume.

that these preliminary crystals were obtained preferentially from one of the two oligomeric forms in the enzyme mixture. If this hypothesis were true, then the purified homodimer and homotetramer should display different tendencies to crystallize under the same experimental conditions.

Various concentrations of the small and large forms of the enzyme were tested, with systematic variation of the precipitant, buffer, and salt additives (Table 4-4). Examples of salts used included succinate, SCN^-, or I^-, each of which binds to the active site of CoA transferase (Hersh & Jencks, 1967) and may stabilize a conformation of the enzyme compatible with crystallization. Crystals suitable for x-ray diffraction grew within 2 to 3 days in solutions of the homodimer (8 to 12 mg/mL) containing 17 to 18% (w/v) PEG 1000, 5 mM succinate, and 0.1 M HEPES, at pH 8.0. These crystals were shaped as elongated "blades" or "planks," similar to the crystals obtained from unfractionated samples of CoA transferase. In contrast, the homotetramer formed amorphous precipitates or stacks of thin, crystalline plates under these conditions. Thus, it was inferred that the crystals obtained prior to this study were grown preferentially from the homodimeric form of CoA transferase within the unfractionated enzyme preparations.

Subsequently, crystals were grown in solutions of the homodimer (8 to 12 mg/mL) containing 13 to 17.5% (w/v) PEG 2000, 5 mM succinate, and 0.1 M HEPES, at pH 8.0. The morphology of these crystals (Figure 4-13) was similar to that of crystals of the small conformer grown in solutions containing PEG 1000. The dimensions of the largest crystals were 0.1 × 0.2 × 5.0 mm.

Preliminary x-ray diffraction data were obtained using single crystals of the homodimer (Table 4-5). The largest crystals from solutions containing PEG 1000 or PEG 2000 diffracted to 1.9 Å or 2.3 Å, respectively. The space group was identified as $P2_1$, based on the twofold symmetry of oscillation data and the systematic absence of reflections along the principal (b*) axis (Figure 4-14). The number of molecules in the unit cell ($Z = 8$) was inferred from the most likely value of V_M (2.4) (Matthews, 1968).

Table 4-4: Conditions Tested for the Growth of Crystals of Wild-Type CoA Transferase by Microdialysis

[Protein] (mg/mL)	Buffer (pH)	Precipitant[a]	Salt additive
8.0-24 mg/mL	0.1 M HEPES (8.0)	PEG 1000 (15-20%)	KSCN (5.0 mM)
	0.1 M Tris-HCl (8.5)	PEG 2000 (13-16%)	NaI (5.0 mM)
	0.1 M MOPS (7.5)	$(NH_4)_2SO_4$ (1.6-2.2 M)	Na[succinate] (0.0050-0.10 M)
	0.1 M Bicine (9.3)		Li[acetoacetate] (5.0 mM)
			CoA (0.50 mM)

[a] Precipitant solutions in which crystals of CoA transferase were successfully grown are underlined.

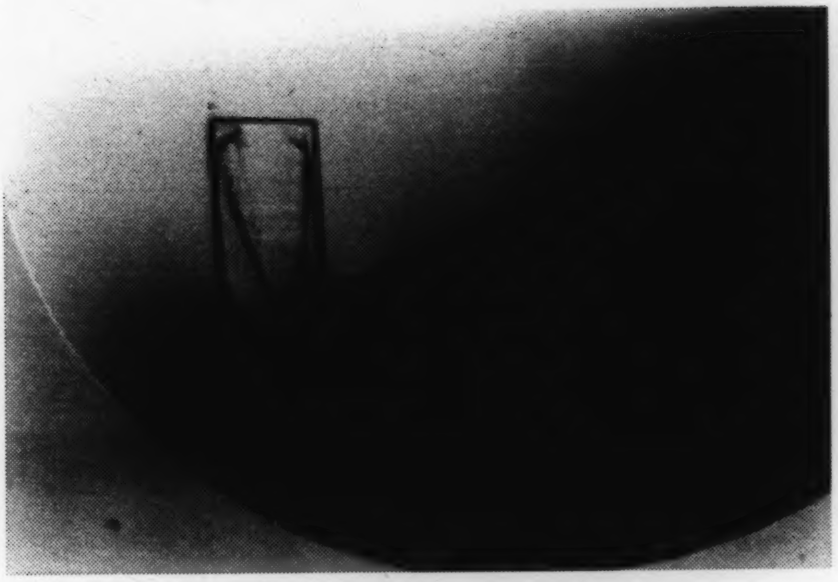

Figure 4-13: Crystals of wild-type CoA transferase. The dimensions of the crystal that is vertical in the figure are 0.1 × 0.2 × 0.6 mm. The crystals were grown by the hanging drop method, using 4 μL of a solution of homodimeric enzyme (final concentration, 7.5 mg/mL, or 1.4×10^2 μM of the NC monomer) and 4 μL of the precipitant solution (17.5% [w/v] PEG 2000, 5 mM succinate, and 0.1 M HEPES, at pH 8.0).

Table 4-5: Crystallographic Data for Crystals of CoA Transferase

Crystal system	Monoclinic
Unit cell dimensions	a = 62.97 Å b = 262.01Å c = 60.81 Å
Interaxial angles	$\alpha = \gamma = 90°$ $\beta = 112.31°$
Unit cell volume	1.00×10^6 Å^3
Space group	$P2_1$
Molecules/unit cell[a]	8
V_M[b]	2.39
Molecules/asymmetric unit[a]	4

[a] "Molecules" refer to monomer subunits.

[b] Assuming a value of 5.22×10^4 for the molecular weight of the CoA transferase monomer.

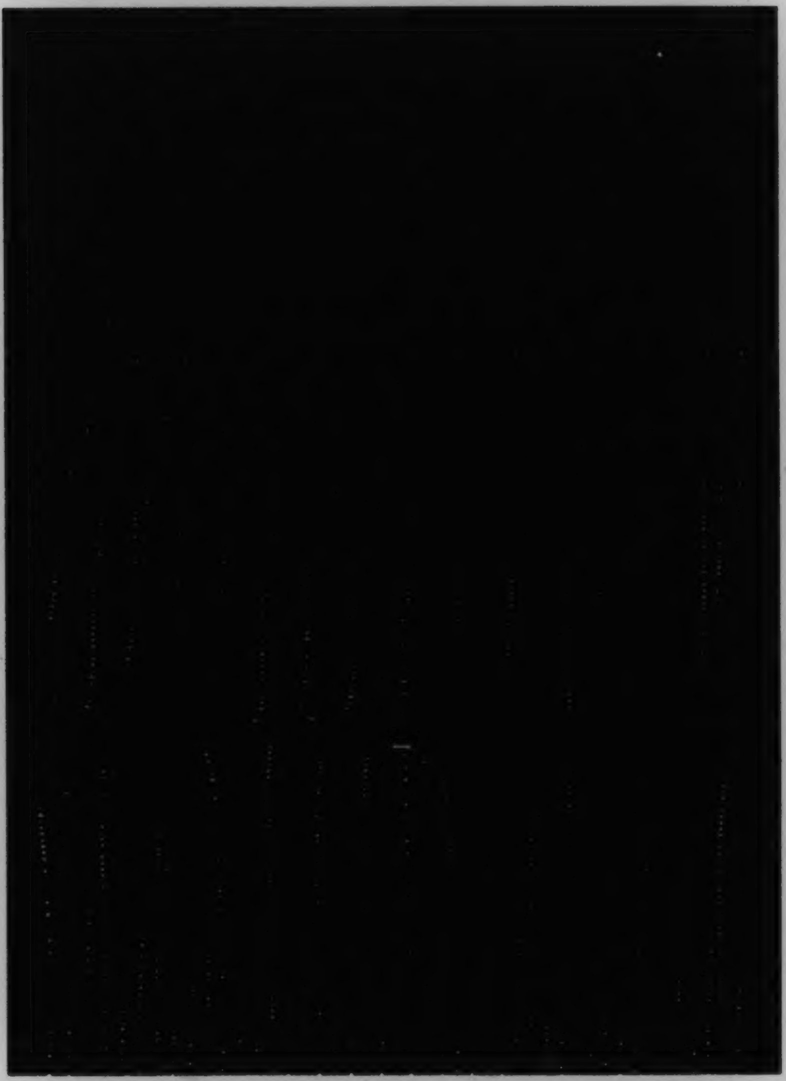

Figure 4-14: X-ray diffraction by crystals of CoA transferase. Diffraction data were obtained with x-rays of wavelength 1.0 Å and a screenless Weissenberg camera. The oscillation ranged from $\omega_1 = 84.5°$ to $\omega_2 = 92°$, and the coupling constant was 1.4° per mm. The distance from the crystal to the film was 430 mm. Prior to x-ray irradiation, the crystals were treated with di-μ-iodobis(ethylenediamine)diplatinum(II) nitrate (PIP) at a final concentration of 0.1 mM for 24 h. The crystals, which belong to the space group $P2_1$ (a = 62.97 Å, b = 262.01Å, c = 60.81 Å; $\alpha = \gamma = 90°$, $\beta = 112.31°$), were mounted and aligned with *b** perpendicular to the spindle axis and parallel to the x-ray beam. The systematic absences along the twofold screw axis (*b**) are evident.

DISCUSSION

Two oligomeric forms of wild-type CoA transferase. By gel filtration, sedimentation, and non-denaturing PAGE analyses, it was confirmed that the purified, recombinant CoA transferase adopts two different quaternary structures, referred to as "small" and "large". Each of these molecular species is compatible with the native enzyme fold, given that both forms display equivalent specific activities. Thus, the small and large conformers are assembled as a result of correct rather than incorrect intermolecular interactions.

The small conformer constituted 95% of the enzyme species in a sample of CoA transferase which had not been fractionated by gel filtration.[8] The $s_{20,w}$ determined for this conformer (5.45 S) was consistent with values reported for the single enzyme species observed in early preparations of the enzyme (Hersh & Jencks, 1967; Sharp & Edwards, 1978). In addition, the apparent molecular weight of the small conformer, determined by sedimentation equilibrium or gel filtration analyses, was 8.48×10^4 or 1.10×10^5 (respectively). These values were consistent with previously published molecular weights, which ranged from 7.8×10^4 to 1.13×10^5 (Hersh & Jencks, 1967; Edwards et al., 1973; White & Jencks, 1976; Sharp & Edwards, 1978; Russell & Patel, 1982). Together, these results suggested that the major component of the CoA transferase preparation is homodimeric.

The $s_{20,w}$ determined for the minor component of CoA transferase was 1.4 times greater than that of the small form. Given this difference, it is surprising that the large molecule was not detected by previous sedimentation velocity experiments, which were carried out using enzyme samples which had not been fractionated by gel filtration (Hersh & Jencks, 1967; Sharp & Edwards, 1978). However, in one of these studies, the principal peak of sedimenting material reportedly accounted for only 85% of the total protein (Hersh & Jencks, 1967). Given that the large conformer comprised only 5% of the enzyme species in a preparation of recombinant CoA transferase, it is conceivable that this minor component was dismissed as aggregated or contaminating material during early sedimentation velocity analyses. The apparent molecular weight of the large molecule, determined by sedimentation equilibrium and gel filtration experiments, was 1.57×10^5 or 2.45×10^5, respectively. These values were approximately two times greater than those determined for the small conformer, implying that the minor component exists predominantly as a homotetramer.

Attempts to evaluate the molecular weights of the small and large enzyme forms by sedimentation equilibrium were complicated by the curvature of the corresponding ln y vs r^2 plots. This non-linearity presumably resulted from the dissociation of both macromolecular complexes during the ultracentrifugation run. Sedimentation equilibrium data corresponding to the small species best fit to a monomer-dimer model, suggesting that this sample consists of an equilibrium mixture of homodimeric and monomeric forms under the conditions of the ultracentrifugation. In contrast, the association-dissociation equilibrium observed for the large molecule was much more complex, implying that this sample consists of a mixture of homotetrameric, homodimeric, and monomeric species. The ln y vs r^2 plots derived from previous sedimentation equilibrium analyses of pig heart CoA transferase were reportedly linear (White & Jencks, 1976), in contrast to the results reported here. Whereas the buffer used in our procedure contained 0.15 M KCl (see "Experimental Procedures," Chapter 2), the early studies were performed using a 50 mM K[phosphate] buffer (pH 7.4) which lacked salt (White & Jencks, 1976). Thus, the extent of dissociation of the homodimeric and homotetrameric forms of CoA transferase may depend in part on the ionic strength of the protein solution (discussed further below).

Structural features of the homodimer and homotetramer. Initially, it was predicted that the primary structures of the subunits which constitute the small and large oligomeric forms of CoA transferase might be different. Specifically, it was conceivable that a post-translational change could influence the assembly of the enzyme subunits to the small or large oligomeric state. The substitution or covalent modification of a single amino acid residue has been shown to affect the quaternary structure of other proteins, including: hemoglobin (Sasaki et al., 1978; Ishimori et al., 1992; Ishimori et al., 1994); *Eco*RI endonuclease (Geiger et al., 1989); lactose repressor (Chakerian & Matthews, 1991); glycogen phosphorylase (Barford & Johnson, 1992; Lin et al., 1995); spectrin (Sahr et al., 1993); aldolase (Beernink & Tolan, 1994); triosephosphate isomerase (Borchert et al., 1995); and fructose 6-phosphate, 2-kinase:fructose 2, 6-bisphosphatase (Tsujikawa et al., 1995). However, the primary structures of the subunits comprising the large and small forms of CoA transferase were shown to be identical by ESI-MS analysis.

The homodimer and homotetramer also displayed equivalent spectral properties. The far-UV CD spectra recorded for both oligomeric forms were similar to that observed for the unfractionated wild-type enzyme, reflecting significant β-sheet and/or β-turn components (Chapter 2). In addition, measurements of intrinsic tryptophan fluorescence revealed identical values of $\lambda_{max,em}$ for the homodimer and homotetramer. These results indicated that: (1) the overall secondary structure of the subunits is similar in both multimeric states; and (2) tryptophan residues are not implicated in intermolecular contacts which stabilize the tetramer. Multiple, coexisting oligomeric forms of LDH from *Thermotoga maritima* (Dams et al., 1996) have also been shown to consist of structurally equivalent protomers. In contrast, the subunits of the hexameric glutamate dehydrogenase of *Sulfolobus solfataricus* possess a less random secondary structure and a more compact tertiary structure than the dissociated monomer (Facchiano et al., 1995).

Thermodynamic stabilities of the small and large conformers. From the similar specific enzyme activities and spectral properties of the homodimer and homotetramer, it was suggested that the subunits of both oligomeric forms adopt a common protein fold. This hypothesis was tested by examining the equilibrium unfolding transitions of the small and large molecular forms. The homodimer and homotetramer displayed similar susceptibilities to denaturation, implying that the large molecule dissociated to the small species at a relatively low concentration of GuHCl. Accordingly, the major equilibrium unfolding transition observed for both conformers reflected the dissociation of the native-like homodimer to the unfolded monomer (Chapter 2), consistent with the two-state mechanism assumed throughout these studies. The values of $[\Delta G_u^{H_2O}]_{app}$ calculated for the small and large molecules were similar, suggesting that the conformational stabilities of both oligomeric forms were equivalent. It is unclear why the values determined for $[\Delta G_u^{H_2O}]_{app}$ or m by far-UV CD and fluorescence measurements were not significantly different, in contrast to previous data (Chapter 2). Presumably, consistent results with respect to the relationship between far-UV CD and fluorescence data could be obtained by carrying out additional experiments.[9]

Interconversion of the homodimer and homotetramer. From the similar conformational stabilities of the two multimeric forms of CoA transferase, it was concluded that the uneven distribution of CoA transferase between the homodimer and the homotetramer is not driven thermodynamically. Instead, it was postulated that the relative amounts of the two species in the unfractionated mixture varies with the total concentration of enzyme subunits.

To test this prediction, the effect of protein concentration on the distribution of CoA transferase between its two oligomeric forms was examined. Samples of the homotetramer (5 μg/mL, or 0.096 μM of the NC monomer) did not dissociate to the homodimer upon storage at 4 °C for up to 68 days. Instead, most of the large molecule was lost under these conditions, presumably due to aggregation and/or proteolysis. From these observations, it was concluded that a large kinetic barrier prevents the rapid interconversion of the small and large oligomers. The $\Delta G^{\ddagger}$ associated with this energy barrier was estimated to be at least 1.0×10^2 kJ/mol, which is similar to the $\Delta G^{\ddagger}$ of 112 kJ/mol determined for a slow conformational change in the folding of α-lytic protease (Baker et al., 1992), and for the dissociation of domain-swapped dimers to the corresponding monomers (reviewed in [Bennett et al., 1995]; [Schlunegger et al., 1997]; see below).

The results of experiments to address whether or not the homodimer converts to the homotetramer at elevated protein concentrations were inconclusive (not shown). Briefly, samples of the small conformer incubated for extended periods at a relatively low protein concentration (3 mg/mL, or 57 μM of the NC monomer) did not convert to the large molecule. In contrast, prolonged incubation of the CoA transferase homodimer at a relatively high protein concentration (23 mg/mL, or 4.4×10^2 μM of the NC monomer) led to the formation of complexes which could not be resolved by non-denaturing PAGE. The formation of these species of high molecular weight may have involved the preliminary conversion of the homodimer to the homotetramer. This inference can be verified by assessing the distribution of oligomeric forms in a highly concentrated sample of the small conformer after short incubation times.

After unfolding and subsequent renaturation, the homotetramer was converted to the homodimer. It is proposed that the homotetramer refolded to the homodimeric species due to the dilute conditions of the renaturation. Thus, in the absence of a kinetic barrier, the distribution of CoA transferase between the small and large oligomeric forms is dependent on the protein concentration, with high protein concentrations favoring the homotetramer. Similar results were recently reported for LDH from *Thermotoga maritima* (Dams et al., 1996). Under benign conditions, tetrameric and octameric forms of the enzyme resist interconversion. However, after denaturation of either conformer in 5 M GuHCl, the proportion of large and small molecules recovered during refolding is dependent on the protein concentration and the temperature.

During ultracentrifugation, a sample of the purified large molecule in a buffer containing 0.15 M KCl was heterogeneous, most likely consisting of a mixture of homotetrameric, homodimeric, and monomeric species. However, in a buffer lacking salt the dissociation of the large molecule to the small conformer was undetectable, even at a relatively low protein concentration. This discrepancy may be due to the difference in ionic strength of the two protein samples. In the presence of salt, the exchange between the two oligomeric forms may occur readily, so that the relative amounts of homodimer and homotetramer are dependent on the protein concentration. In contrast, at low ionic strength, the exchange between the small and large conformers may occur slowly due to a large kinetic barrier. Based on this mechanism, it is proposed that the relative amounts of the homodimer and homotetramer are determined by the total concentration of CoA transferase at stages of the purification which involve transient increases in the concentration of $(NH_4)_2SO_4$ or KCl. After the removal of these salts by gel filtration, the distribution of the enzyme between the small and large conformers does not vary with the protein concentration. This hypothesis can be tested by measuring the relative amounts of the homodimer and homotetramer in a dilute solution of the large conformer containing various amounts of salt. The dimerization of other monomeric proteins, including *Eco*RI endonuclease (Geiger et al., 1989) and lysozyme (Wilson et al., 1996), has also been shown to be favored by high ionic strength.

Intermolecular interactions involving the hydrophilic linker segment. Mild proteolysis of the small and large conformers led to the formation of identical molecular species, with electrophoretic properties similar to those of the hinge-mutant. Furthermore, an N_4C_4-domain complex was not detected by gel filtration analysis of a sample of the purified hinge-mutant. Thus, although not required for the formation of the small form of CoA transferase (Chapter 2), the intact hydrophilic linker segment is necessary for the stability of the homotetramer. Alternatively, residues 249 to 254 of the hinge region, which are deleted in the hinge-mutant (Chapter 2), may stabilize the large conformer. It should be noted that the glutaconate CoA-transferase of *Acidaminococcus fermentans* exists as an $\alpha_4\beta_4$ heterooctamer (Buckel et al., 1981; Mack et al., 1994), which is structurally analogous to the hypothetical N_4C_4-domain complex that was not observable by non-denaturing PAGE or gel filtration analyses. However, the interface between the

$\alpha_2\beta_2$ heterodimers of the prokaryotic enzyme is formed from the α-helical C-terminal segments of the α-subunits (Jacob et al., 1997), and is therefore distinct from the contact region between the two homodimers of the pig heart CoA transferase homotetramer.

The native folds of other enzymes, including β-galactosidase (Ullmann et al., 1968; Edwards et al., 1988) and hexokinase (Okazaki et al., 1992), have also been probed by limited proteolysis. For each of these enzymes, the activities of the intact and nicked forms were identical. It was predicted that the same should be true of the uncleaved and nicked forms of CoA transferase, assuming that proteolysis was restricted to the hydrophilic linker segment. However, much of the initial enzyme activity associated with wild-type CoA transferase or the hinge-mutant was lost following tryptic digestion under the conditions described here. Thus, it could not be excluded that a short N- or C-terminal segment of either domain was also cleaved, and that the removal of this segment contributed to the dissociation of the homotetramer. Future efforts will be aimed at identifying optimal levels of trypsin which permit the specific proteolysis of the hinge region without loss of enzyme activity.

Previously, the analysis of a sample of intact CoA transferase by non-denaturing PAGE revealed three closely spaced bands (White & Jencks, 1976). Since these bands could be separated by isoelectric focusing through a sucrose gradient, it was concluded that the enzyme consists of several forms with different pI values. Interestingly, only a single band was observed by non-denaturing PAGE analysis of a sample of nicked CoA transferase (Moore & Jencks, 1982). By analogy, the heterogeneity associated with early preparations of the uncleaved enzyme may have been due to the presence of small and large oligomeric forms. This hypothesis can be verified by comparing the pI values of the homodimer and homotetramer to those of the isoenzymes described by White & Jencks (1976).

Models for the formation of the homotetramer. Two quaternary structural arrangements can be proposed to account for the observation that the hinge region is necessary for the stability of the large molecule. First, a pair of CoA transferase homodimers may associate by interactions which directly involve the hydrophilic linker segment (Figure 4-15A). Such contacts, which may be mediated by the helical and/or turn elements of the hinge region, are not without precedent. From a survey of the x-ray crystallographic structures of 18 dimeric and tetrameric proteins, Miller (1989) estimated that loop regions constitute an average of approximately 40% of the contact surface between subunits.[10] Second, the hydrophilic linker segment may be required for a conformational change which leads to the swapping of domains between two homodimers (Figure 4-15B). Three dimensional domain swapping, which involves the exchange of identical domains between subunits, has been described for numerous proteins (reviewed in [Bennett et al., 1995]; [Schlunegger et al., 1997]); recent examples include diphtheria toxin (Bennett et al., 1994), RNase (Di Donato et al., 1995; Adinolfi et al., 1996), the cell cycle-regulatory protein suc1 (Bourne et al., 1995; Khazanovich et al., 1996), and odorant binding protein (Tegoni et al., 1996). Interestingly, the activation energy separating the small and large forms of CoA transferase is similar to values of $\Delta G^{\ddagger}$ typically observed for the dissociation of a domain-swapped dimer to the corresponding monomer (reviewed in [Bennett et al., 1995]; [Schlunegger et al., 1997]). This similarity of $\Delta G^{\ddagger}$ can be taken as circumstantial evidence that the homotetrameric species of CoA transferase is formed by a domain-swapping mechanism.

The two models proposed above are not mutually exclusive. For example, in the presence of salt two homodimers associate reversibly through direct contacts involving their respective hinge regions (Figure 4-15A). This initial assembly is favored at high ionic strength, presumably due to the neutralization of like charges on the surfaces of opposing hydrophilic linker segments. Removal of the salt by gel filtration reverses this shielding effect, leading to the destabilization of the hinge regions. This destabilization

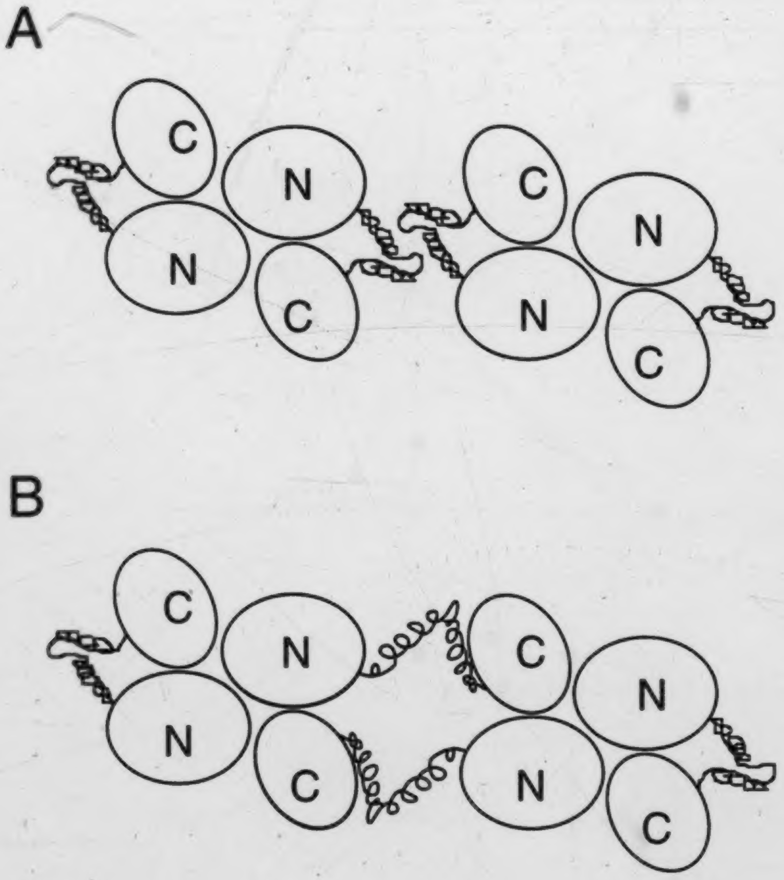

Figure 4-15: Models for the assembly of two homodimers to the homotetrameric form. (A) Association of two homodimers via direct contacts involving the hydrophilic linker segments. This interaction may be favored at high ionic strength. (B) Association by a domain-swapping mechanism. The exchange of domains may require a conformational change that is favored by the flexibility of the hinge region.

may in turn provide the driving force for the irreversible swapping of two C-domains (Figure 4-15B). Importantly, both models account for two conclusions of this report: (1) the homodimer and homotetramer adopt a common fold; and (2) the large conformer does not assemble in the absence of the hydrophilic linker.

Crystallization studies. Following the identification of the homodimeric and homotetrameric forms of CoA transferase, it was necessary to determine whether or not the two multimeric species differ with respect to their ability to form crystals under a defined set of conditions. This information was initially considered essential to optimize the crystallization protocol, which was carried out using unfractionated enzyme samples prior to the studies outlined in this chapter. Currently, it is also of interest to obtain crystals of the homodimer and homotetramer as a first step towards determining the structure of each oligomeric form.

Crystals of the small conformer have been grown, and x-ray diffraction data from these crystals are currently being processed (Chapter 7). In contrast, despite numerous efforts, crystals of the homotetramer suitable for x-ray diffraction studies have not been obtained under the same conditions. Presumably, the interactions which determine the packing of the small molecules into a regular, crystalline array are prevented by intermolecular contacts inherent to the large conformer. Accordingly, it is predicted that eventual crystals of the homotetramer will be of a morphology distinct from that of the crystals of homodimeric CoA transferase. This argument is supported by the observation that the preliminary crystalline forms of the homotetramer are stacks of thin plates, while crystals of the homodimer are "planks" or "blades". Multiple crystal forms, obtained under identical conditions, have recently been described for the alternative oligomeric states of other proteins, including ADP-ribosylation factor-1 (Greasley et al., 1995) and monocyte chemoattractant protein (Lubkowski et al., 1997).

ENDNOTES

[1] If the electrophoresis was terminated immediately after the disappearance of the tracking dye from the resolving gel, then the proteins migrated only a short distance (as shown, for example, in Figure 4-10).

[2] Samples of the wild-type enzyme which were previously analyzed by measurements of far-UV CD or fluorescence were diluted in buffer X (Chapter 2). However, the large and small forms of wild-type CoA transferase were eluted from the Sephacryl S-200 column in buffer A (see "Protein purification"). Therefore, to be consistent with the earlier measurements, it was necessary to dialyze these samples at 4 °C against 0.5 L of buffer X prior to the measurement of far-UV CD or fluorescence. The choice of dialysis membrane was determined by the volume of the dialyzed sample, as outlined in Chapter 2.

[3] The unfolding of unfractionated, wild-type CoA transferase at 15 °C was shown to be 60-70% reversible. Accordingly, the values deduced for the various thermodynamic parameters are "apparent" values only.

[4] For most of the denaturation curves derived from measurements of intrinsic tryptophan fluorescence, ds was taken to be equal to zero. This assumption was reasonable, given that the values of y in the post-transition region did not differ greatly from y_u.

[5] The experiments described in this chapter were carried out using preparations of wild-type CoA transferase purified in the absence or presence of 2ME, with similar results. Unless otherwise specified, the observations reported here are from studies of the wild-type enzyme purified in buffers lacking the reductant.

[6] Note that the "Gibbs free energy of activation" ($\Delta G^\ddagger$) and the "activation energy" (E_a) (Chapter 2) are fundamentally different parameters. As discussed by Segel (1975), $\Delta G^\ddagger$ is related to the enthalpy ($\Delta H^\ddagger$) and entropy ($\Delta S^\ddagger$) of activation by the following expression:

$$\Delta G^\ddagger = \Delta H^\ddagger - T\Delta S^\ddagger.$$

In contrast, E_a and $\Delta H^\ddagger$ are related by the following equation (Segel, 1975):

$$E_a = \Delta H^\ddagger + RT.$$

[7] It is reasonable to predict that the removal of such a short peptide segment might affect the migration of the N_2C_2-domain complex under non-denaturing conditions, without being detectable within the limits of resolution of SDS-PAGE.

[8] As mentioned in the "Results" section, the small molecule accounted for 90% of the total enzyme activity associated with the unfractionated sample of CoA transferase. This is approximately equal to 95% of the molecular species, assuming equivalent specific activities for the homodimer and the homotetramer.

[9] For example, the effect of temperature on the value of each thermodynamic parameter should be investigated, since the equilibrium unfolding experiments described in Chapter 2 and in this chapter were carried out at 22 °C and 15 °C, respectively.

[10] Similarly, from a recent survey of the x-ray crystallographic structures of 32 dimeric proteins, it has been estimated that approximately 50% of the residues located at the subunit interface belong to an α-helical or a turn motif (reviewed in [Jones & Thornton, 1995]).

REFERENCES

Adinolfi, S., Piccoli, R., Sica, F., & Mazzarella, L. (1996) *FEBS Lett. 398*, 326-332.

Andrews, P. (1965) *Biochem. J. 96*, 595-606.

Argos, P. (1988) *Protein Eng. 2*, 101-113.

Baker, D., Sohl, J. L., & Agard, D. A. (1992) *Nature 356*, 263-265.

Barford, D., & Johnson, L. N. (1992) *Protein Sci. 1*, 472-493.

Beernink, P. T., & Tolan, D. R. (1994) *Protein Sci. 3*, 1383-1391.

Bennett, M. J., Choe, S., & Eisenberg, D. (1994) *Proc. Natl. Acad. U. S. A. 91*, 3127-3131.

Bennett, M. J., Schlunegger, M. P., & Eisenberg, D. (1995) *Protein Sci. 4*, 2455-2468.

Borchert, T. V., Zeelen, J. P., Schliebs, W., Callens, M., Minke, W., Jaenicke, R., & Wierenga, R. K. (1995) *FEBS Lett. 367*, 315-318.

Bourne, Y., Arvai, A. S., Bernstein, S. L., Watson, M. H., Reed, S. I., Endicott, J. E., Noble, M. E., Johnson, L. N., & Tainer, J. A. (1995) *Proc. Natl. Acad. U. S. A. 92*, 10232-10236.

Buckel, W., Dorn, U., & Semmler, R. (1981) *Eur. J. Biochem. 118*, 315-321.

Chakerian, A. E., & Matthews, K. S. (1991) *J. Biol. Chem. 266*, 22206-22214.

Chervenka, C. H. (1970) in *A Manual of Methods for the Analytical Ultracentrifuge*. pp. 23-33, Spinco Division of Beckman Instruments, Inc., Palo Alto, CA.

Cohn, E. J., & Edsall, J. T. (1943) in *Proteins, Amino Acids, and Peptides* (Cohn, E. J., & Edsall, J. T., eds.) pp. 370-377, Hafner Publishing Company, Inc., New York.

Creighton, T. (1993) *Proteins: Structures & Molecular Properties*, 2nd ed. W. H. Freeman & Co., New York.

Dams, T., Ostendorp, R., Ott, M., Rutkat, K., & Jaenicke, R. (1996) *Eur. J. Biochem. 240*, 274-279.

De Francesco, R., Pastore, A., Vecchio, G., & Cortese, R. (1991) *Biochemistry 30*, 143-147.

Di Donato, A., Cafaro, V., Romeo, I., & D'Alessio, G. (1995) *Protein Sci. 4*, 1470-1477.

Edwards, L. A., Tian, M. R., Huber, R. E., & Fowler, A. V. (1988) *J. Biol. Chem. 263*, 1848-1854.

Edwards, M. R., Singh, M., & Tubbs, P. K. (1973) *FEBS Lett. 37*, 155-158.

Facchiano, A. M., Ragone, R., Consalvi, V., Scandurra, R., De Rosa, M., & Colonna, G. (1995) *Biochim. Biophys. Acta 1251*, 170-176.

Geiger, R., Rüter, T., Alves, J., Fliess, A., Wolfes, H., Pingoud, V., Urbanke, C., Maass, G., Pingoud, A., Düsterhoft, A., & Kröger, M. (1989) *Biochemistry 28*, 2667-2677.

Greasley, S. E., Jhoti, H., Teahan, C., Solari, R., Fensome, A., Thomas, G. M., Cockcroft, S., & Bax, B. (1995) *Nature Struct. Biol. 2*, 797-806.

Hersh, L. B., & Jencks, W. P. (1967) *J. Biol. Chem. 242*, 3468-3480.

Howard, J. B., Zieske, L., Clarkson, J., & Rathe, L. (1986) *J. Biol. Chem. 261*, 60-65.

Ishimori, K., Imai, K., Miyazaki, G., Kitagawa, T., Wada, Y., Morimoto, H., & Morishima, I. (1992) *Biochemistry 31*, 3256-3264.

Ishimori, K., Hashimoto, M., Imai, K., Fushitani, K., Miyazaki, G., Morimoto, H., Wada, Y., & Morishima, I. (1994) *Biochemistry 33*, 2546-2553.

Jacob, U., Mack, M., Clausen, T., Huber, R., Buckel, W., & Messerschmidt, A. (1997) *Structure 5*, 415-426.

Jaenicke, R. (1987) *Prog. Biophys. Mol. Biol. 49*, 117-237.

Jaenicke, R. (1991) *Biochemistry 30*, 3147-3161.

Jaenicke, R., & Rudolph, R. (1986) *Methods Enzymol. 131*, 218-250.

Janin, J., Miller, S., & Chothia, C. (1988) *J. Mol. Biol. 204*, 155-164.

Jones, S., & Thornton, J. M. (1995) *Prog. Biophys. Molec. Biol. 63*, 31-65.

Kindman, L. A., & Jencks, W. P. (1981) *Biochemistry 20*, 5183-5187.

Khazanovich, N., Bateman, K., Chernaia, M., Michalak, M., & James, M. (1996) *Structure 4*, 299-309.

Klotz, I. M., Darnall, D. W., & Langerman, N. R. (1975) in *The Proteins*, 3rd ed. (Neurath, H., & Hill, R. L., Eds) Vol. I, pp. 293-411, Academic Press, Inc., New York.

Lin, K., Hwang, P. K., & Fletterick, R. J. (1995) *J. Biol. Chem. 270*, 26833-26839.

Lin, T., & Bridger, W. A. (1992) *J. Biol. Chem. 267*, 975-978.

Lubkowski, J., Bujacz, G., Boqué, L., Domaille, P. J., Handel, T. M., & Wlodawer, A. (1997) *Nature Struct. Biol. 4*, 64-69.

Mack, M., Bendrat, K., Zelder, O., Eckel, E., Linder, D., & Buckel, W. (1994) *Eur. J. Biochem. 226*, 41-51.

McPherson, A., Jr. (1976) *Methods Biochem. Anal. 23*, 249-345.

Matthews, B. W. (1968) *J. Mol. Biol. 33*, 491-497.

Milla, M. E., Brown, B. M., & Sauer, R. T. (1993) *Protein Sci. 2*, 2198-2205.

Miller, S. (1989) *Protein Eng. 3*, 77-83.

Mok, Y.-K., Prat Gay, G. de, Butler, P. J., & Bycroft, M. (1996) *Protein Sci. 5*, 310-319.

Moore, S. A., & Jencks, W. P. (1982) *J. Biol. Chem. 257*, 10893-10907.

Myers, J. K., Pace, C. N., & Scholtz, J. M. (1995) *Protein Sci. 4*, 2138-2148.

Okazaki, H., Takebayashi, Y., Ando, M., Date, S., Tokuda, H., & Ishibashi, S. (1992) *Mol. Cell. Biochem. 117*, 87-92.

Pace, C. N. (1975) *Crit. Rev. Biochem. 3*, 1-43.

Pace, C. N. (1986) *Methods Enzymol. 131*, 266-280.

Pickart, C. M., & Jencks, W. P. (1979) *J. Biol. Chem. 254*, 9120-9129.

Price, N. C. (1994) in *Mechanisms of Protein Folding* (Pain, R. H., Ed.) pp. 160-193, IRL Press, Oxford, U. K.

Rudolph, R., Zettlmeissl, G., & Jaenicke, R. (1979) *Biochemistry 18*, 5572-5575.

Russell, J. J., & Patel, M. S. (1982) *J. Neurochem. 38*, 1446-1452.

Sahr, K. E., Coetzer, T. L., Moy, L. S., Derick, L. H., Chishti, A. H., Jarolim, P., Lorenzo, F., Miraglia del Giudice, E., Iolascon, A., Gallanello, R., Cao, A., Delaunay, J., Liu, S.-C., & Palek, J. (1993) *J. Biol. Chem. 268*, 22656-22662.

Sakabe, N. (1983) *J. Appl. Cryst. 16*, 542-547.

Sakabe, N. (1991) *Nucl. Instr. and Meth. A303*, 448-463.

Sasaki, J., Imamura, T., Yanase, T., Atha, D. H., Riggs, A., Bonaventura, J., & Bonaventura, C. (1978) *J. Biol. Chem. 253*, 87-94.

Schellman, J. (1978) *Biopolymers 17*, 1305-1322.

Schlunegger, M. P., Bennett, M. J., & Eisenberg, D. (1997) *Adv. Prot. Chem. 50*, 61-122.

Segel, I. H. (1975) *Enzyme Kinetics*. John Wiley & Sons, Inc., New York.

Sharp, J. A., & Edwards, M. R. (1978) *Biochem. J. 173*, 759-765.

Shortle, D. (1989) *J. Biol. Chem. 264*, 5315-5318.

Tegoni, M., Ramoni, R., Bignetti, E., Spinelli, S., & Cambillau, C. (1996) *Nature Struct. Biol. 3*, 863-867.

Tsai, C.-J., Lin, S. L., Wolfson, H., & Nussinov, R. (1996) *CRC Crit. Rev. Biochem. Mol. Biol. 31*, 127-152.

Tsai, C.-J., Lin, S. L., Wolfson, H. J., & Nussinov, R. (1997) *Protein Sci. 6*, 53-64.

Tsujikawa, T., Watanabe, F., & Uyeda, K. (1995) *Biochemistry 34*, 6389-6393.

Ullmann, A., Jacob, F., & Monod, J. (1968) *J. Mol. Biol. 32*, 1-13.

Velan, B., Kronman, C., Grosfeld, H., Leitner, M., Gozes, Y., Flashner, Y., Sery, T., Cohen, S., Ben-Aziz, R., Seidman, S., Shafferman, A., & Soreq, H. (1991) *Cell. Molec. Neurobiol. 11*, 143-156.

White, H., & Jencks, W. P. (1976) *J. Biol. Chem. 251*, 1708-1711.

White, H., Solomon, F., & Jencks, W. P. (1976) *J. Biol. Chem. 251*, 1700-1707.

Wilson, L. J., Adcock-Downey, L., & Pusey, M. L. (1996) *Biophys. J. 71*, 2123-2129.

Wold, F. (1981) *Annu. Rev. Biochem. 50*, 783-814.

Wolodko, W. T., James, M. N. G., & Bridger, W. A. (1984) *J. Biol. Chem. 259*, 5316-5320.

Chapter 5. Identification of Glutamate 344 as the Catalytic Nucleophile in the Active Site of CoA Transferase[1]

INTRODUCTION

From results of radioactive labeling experiments using tritiated borohydride, Solomon & Jencks (1969) concluded that the catalytic nucleophile in the active site of CoA transferase is a glutamate residue (Chapter 1). Subsequently, the isolation of a cDNA encoding the enzyme (Lin & Bridger, 1992) made possible the identification of this residue within the context of the deduced amino acid sequence.

In general, a functionally important amino acid sidechain in the active site of an enzyme can be identified by various methods, including amino acid sequence alignment, three-dimensional structure analysis, site-directed mutagenesis, and chemical labeling. Frequently, the success of the latter approach has been limited due to the indiscriminate modification of enzyme residues. However, recent technological advances have facilitated the development of a protocol for the specific labeling of acid nucleophiles critical to catalysis (Tull et al., 1995). This method, applied most successfully to the glycosyl hydrolases (reviewed in [Withers & Aebersold, 1995]), requires the preliminary inactivation of the enzyme with a mechanism-based inhibitor. After proteolysis, the covalently modified peptide is identified by reversed-phase high performance liquid chromatography (RP-HPLC) in conjunction with electrospray ionization tandem mass spectrometry (ESI-MS/MS). This peptide is then sequenced by further ESI-MS/MS or conventional Edman degradation chemistry (Tull et al., 1995). Not only is this approach rapid, sensitive, and selective, but it also lacks the inconvenience associated with the handling of radioactive isotopes.

To probe the active site of CoA transferase by a similar method, conditions under which the enzyme is specifically modified at the active site glutamate residue must be identified. The autolytic fragmentation of CoA transferase (Chapter 1) has been shown to require the covalent attachment of CoA to the catalytic nucleophile (Howard et al., 1986). In addition, the autolysis of several plasma proteins involves a glutamate residue which is joined by an internal linkage to a cysteine residue; examples include the complement components C3 and C4 (Gorski & Howard, 1980; Howard, 1980; Janatova et al., 1980; Janatova & Tack, 1981; Sim & Sim, 1981) and the plasma proteinase inhibitor α2-macroglobulin (Harpel et al., 1979; Howard et al., 1980; Howard, 1981). Based on this evidence, Howard et al. (1986) proposed that the autolytic fragmentation proceeds through the cyclization of an activated glutamate residue. By virtue of this chemical mechanism (Figure 1-13), the autolysis of ECoA is predicted to target the catalytic nucleophile with the same degree of selectivity as a mechanism-based inactivator.

Preliminary studies of the autolytic fragmentation of CoA transferase indicated that the active site glutamate residue is approximately two-thirds of the distance from the N-terminus of the enzyme (Howard et al., 1986). The deduced amino acid sequence revealed three such residues (Glu 344, Glu 358, and Glu 369) in this vicinity of the CoA transferase primary structure (Figure 5-1). The site of autolysis could not be identified more precisely by Edman sequencing of the C-terminal fragment since the latter was blocked at its N-terminus by a pyroglutamate moiety (Khan & Erickson, 1984; Howard et al., 1986). This group was resistant to enzymatic cleavage with pyroglutaminase (Howard et al., 1986). In addition, recent attempts to remove the pyroglutamate moiety by methanolysis (Kawasaki & Itano, 1971) have proved unsuccessful (unpublished results).

In this study, the autolytic nature of the heat-dependent fragmentation of CoA transferase has been verified by carrying out the reaction in the presence of proteinase inhibitors. Moreover, the susceptibility to autolysis of the proteolytically nicked form of the enzyme has been investigated. Finally, the catalytic glutamate residue has been identified by determining the molecular mass of a small peptide generated by the autolytic fragmentation of nicked CoA transferase.

VKT$\overset{293}{\text{R}}\overset{294}{\text{S}}\overset{295}{\text{G}}\overset{296}{\text{K}}$LGDNVRERIIKRA

ALEFEDGMYANLGIGIPLLA

SNFISPNMTVHLQS$\overset{344}{\text{E}}$NGILG

LGPYPLQN$\overset{358}{\text{E}}$VDADLINAGK$\overset{369}{\text{E}}$T

Figure 5-1: Primary structure of pig heart CoA transferase in the vicinity of the active site glutamate residue. Numbers which are based on the sequence of the precursor form of the enzyme (Lin & Bridger, 1992) indicate amino acids referred to in the text.

EXPERIMENTAL PROCEDURES

Materials. Acrylamide was obtained as a Gibco BRL products from Life Technologies. DEAE Sephacel, Sephadex G-50, and Sephacryl S-200 were purchased from Pharmacia Biotech. The column matrix Affi-Gel Blue and the protein assay dye were purchased from Bio-Rad Laboratories, Ltd. The proteinase inhibitors (pepstatin A, antipain, PMSF), tricine, trifluoroacetic acid, and substrates (acetoacetate and succinyl-CoA) were obtained from Sigma Chemical Company. The acetonitrile was provided by BDH, Canada. Purified protein preparations were concentrated using Millipore brand Immersible concentrators (MWCO = 3.0×10^4). Dialyses were carried out using Spectra/Por membranes supplied by Spectrum.

Protein purification. Pig heart CoA transferase was extracted from fresh myocardium as described by Hersh & Jencks (1969). The fractionation by $(NH_4)_2SO_4$ and the subsequent chromatographic procedures were carried out as outlined in Chapter 2. Intact enzyme was purified in the presence of 0.1 mM PMSF, whereas the nicked form of CoA transferase was obtained by the omission of this serine proteinase inhibitor from all purification buffers. The homogeneity of all protein preparations was confirmed by SDS-PAGE analysis. The concentrations of the purified protein solutions were determined by the assay method of Bradford (1976).

Measurement of enzyme activity. CoA transferase activity was determined spectrophotometrically as described in Chapter 2. In the present study, the assay solutions consisted of 50 mM Tris-HCl, 15 mM $MgCl_2$, 0.30 mM succinyl-CoA, and 67 mM acetoacetate, at pH 9.1. The extinction coefficient for acetoacetyl-CoA at 310 nm (ε_{310}) was taken to be 7.8×10^3 M^{-1} cm^{-1} under these conditions (Howard et al., 1986). All assays were carried out at 22 °C. The specific activities of the intact and nicked CoA transferase preparations ranged typically from 3.5 to 11.7 µmol/min/mg.

Autolytic fragmentation. Microgram quantities of intact or nicked CoA transferase were subjected to autolysis as described by Howard et al. (1986). Briefly, the enzyme was diluted with 3 to 4 volumes of 50 mM Na[phosphate] buffer (pH 8.0) containing 3 mM or 10 µM succinyl-CoA (see "Results" for details). Where applicable, a proteinase inhibitor cocktail was included consisting of pepstatin A (1 µg/mL), antipain (1-2 µg/mL), PMSF (100 µg/mL), and EDTA (1 mM). Samples were incubated at 25 °C for 15 min and then additionally at 70 °C for 60 min. The reaction was terminated by adding TFA or formic acid to 0.5% (v/v) before analysis by RP-HPLC. Alternatively, an equivalent volume of SDS-PAGE loading buffer (Appendix 6) was added prior to analysis via denaturing PAGE.

Tricine SDS-PAGE. Peptides of low molecular weight were resolved by tricine SDS-PAGE, as described by Schägger & von Jagow (1987). The overall assembly consisted of a 16.5% T, 3% C separating gel (23 mL), a 10% T, 3% C spacer gel (6 mL), and a 4% T, 3% C stacking gel (4 mL).[2] The anode buffer consisted of 0.2 M Tris-HCl (pH 8.9), while the cathode buffer consisted of 0.1 M Tris and 0.1 M tricine at a pH of about 8.25 (without adjustment). Electrophoresis was carried out at a constant voltage of 85 V for a period of 20-24 hours.

RP-HPLC. Liquid chromatography was performed on a Vydac 218TP C18 column (50 mm x 2.1 mm ID, 5-µm particle size, 300-Å pore size) purchased from The Sep/a/ra/tions Group (Hesperia, California). A gradient defined by a 1% (v/v) per min increase in solvent B (where A is 0.1% [v/v] TFA in water and B is 0.1% [v/v] TFA in acetonitrile) was used to elute peptides at a flow rate of 0.2 mL/min. Elution was monitored by measuring absorbance at 206 nm, and one fraction was collected per min. Beckman System Gold (IBM) was used for the analysis and printing of data.

Mass spectrometry. Mass analyses were performed on a Fisons VG Quattro triple quadrupole mass spectrometer (Manchester, UK) fitted with an electrospray ionization source operating in positive ion mode (Fenn et al., 1989; Smith et al., 1990; Mann & Wilm, 1995). Protein samples (10 μL of monomer, 1 to 10 pmol/μL) were injected into the electrospray source at a rate of 10 μL/min via a carrier solution of: (1) water:acetonitrile (1:1, v/v) containing 0.5% (v/v) formic acid; or (2) isopropanol containing 0.05% (v/v) TFA. The quadrupoles were scanned at 2 s per scan for mass over charge ratios ranging from 400 to 2400. Data were acquired in the MCA mode, and 5 to 10 scans were summed to produce the final spectrum. Each molecular mass was determined as the mean value calculated for several multiply charged ions within a coherent series. The instrument was calibrated using the series of ion peaks from either bovine ubiquitin or a synthetic peptide of known mass. Predicted molecular masses were average masses, calculated using the program MacProMass.

RESULTS

SDS-PAGE analysis of autolytically fragmented CoA transferase. The extent of autolysis of CoA transferase under different conditions was monitored by SDS-PAGE analysis. In an initial experiment, a preparation of pure, unnicked enzyme isolated from pig myocardium was incubated, with or without succinyl-CoA (3 mM), for 75 min at 25 °C, or for 15 min at 25 °C and subsequently for 60 min at 70 °C. Samples were then diluted in an appropriate volume of sample buffer and analyzed by SDS-PAGE (Figure 5-2A). Two bands representing fragments of molecular weights approximately equal to 4.0 × 10^4 and 2.0 × 10^4 were diagnostic of the autolytic fragmentation of CoA transferase. These fragments were only produced by samples in which ECoA was formed (Figure 5-2A, lanes 1 and 3). In addition, incubation of the covalent intermediate at 70 °C resulted in about 50% of the enzyme being fragmented, an efficiency much greater than that achieved by incubating at a lower temperature (Figure 5-2A, lane 1 versus lane 3).

Although this fragmentation clearly depended on the exposure of ECoA to an elevated temperature, the involvement of a proteinase had not been ruled out prior to this

Figure 5-2: SDS-PAGE analysis of autolytically fragmented CoA transferase. (A) Standard autolytic fragmentation of CoA transferase. Unnicked enzyme (90 µg, or 1.7 nmol of the NC monomer) was incubated at 25 °C for 15 min and then at 70 °C for 60 min in the presence (lane 1) or absence (lane 2) of 3 mM succinyl-CoA. The same amount of enzyme was incubated at 25 °C for 75 min in the presence of 3 mM succinyl-CoA (lane 3). Samples were fractionated by electrophoresis on a 12% (w/v) polyacrylamide gel, which was subsequently stained with Coomassie Blue. (B) Effect of proteinase inhibitors on the autolytic fragmentation of CoA transferase. Unnicked enzyme (50 µg, or 1.0 nmol of the NC monomer) was subjected to autolysis in the presence (lane 1) or absence (lane 2) of a proteinase inhibitor cocktail consisting of pepstatin A, antipain, PMSF, and EDTA. The same amount of enzyme was left unfragmented and included as a control (lane 3). For both gels, the top arrow identifies the band corresponding to the intact enzyme (WT), while the lower two arrows indicate bands corresponding to the fragments generated by autolysis. Samples were fractionated by electrophoresis on a 7-15% (w/v) gradient polyacrylamide gel, which was subsequently stained with Coomassie Blue.

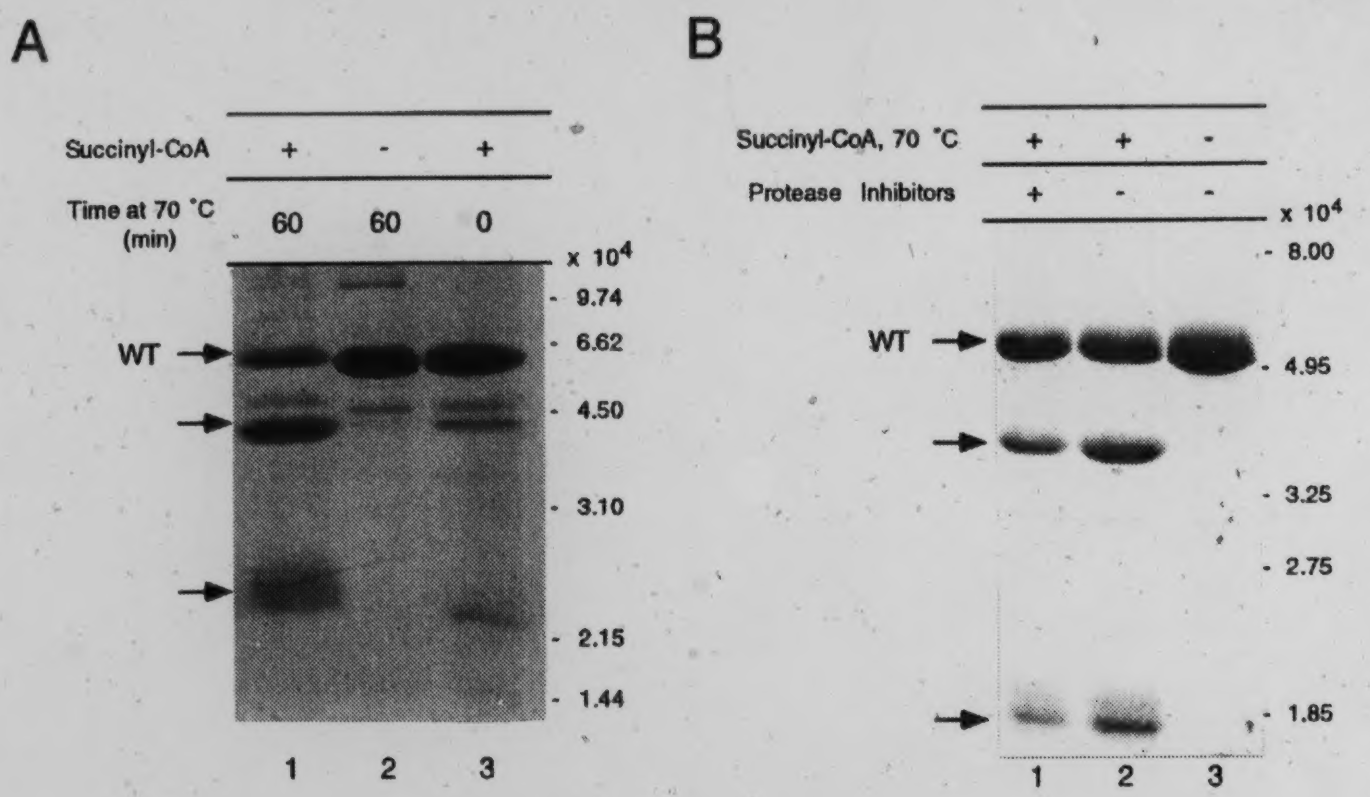
A
Succinyl-CoA
+
-
+
Time at 70 °C (min)
60
60
0
x 10^4
9.74
6.62
4.50
3.10
2.15
1.44
WT
1
2
3
B
Succinyl-CoA, 70 °C
+
+
-
Protease Inhibitors
+
-
-
x 10^4
8.00
4.95
3.25
2.75
1.85
WT
1
2
3

study. CoA transferase is known to undergo a conformational change upon forming the thiolester intermediate (White et al., 1976), and could therefore become more susceptible to the effects of a heat-insensitive proteolytic activity. However, the autolytic fragmentation occurred to similar yield in the presence and absence of a proteinase inhibitor cocktail consisting of Pepstatin A, Antipain, PMSF, and EDTA (Figure 5-2B, lane 1 versus lane 2). This result, along with the temperature optimum of the cleavage reaction, confirmed that the fragmentation is not the result of a proteolytic event.

The initial autolysis protocol suggested a range of 1 to 3 mM as the optimal concentration of succinyl-CoA (Howard et al., 1986). However, the ultraviolet absorbance due to the thiolester bond of the excess substrate produced an unacceptable background which interfered with the detection of peptides eluted by RP-HPLC (see "Experimental Procedures"). Furthermore, it was desirable to lower the salt concentration within the autolytically fragmented sample to preclude interference with subsequent mass spectrometry measurements. Therefore, the fragmentation protocol described above was repeated using a range of succinyl-CoA concentrations, and the samples were analyzed by SDS-PAGE as before. A concentration of succinyl-CoA as low as 0.5 μM, or 2000-fold lower than the minimum amount previously recommended (Howard et al., 1986), was sufficient for heat-induced autolysis (Figure 5-3).

Autolysis of proteolytically nicked CoA transferase. From the above results, it was predicted that the proteolytically cleaved form of CoA transferase should also be autolytically fragmented when heated in the presence of micromolar concentrations of succinyl-CoA. This reaction was expected to generate a peptide bordered at its N-terminus by the nicking site and at its C-terminus by the site of autolysis (Figure 5-4, fragment P). The ultimate goal was to obtain a value for the molecular mass of this fragment. As listed in Table 5-1, accurate determination of the mass of peptide P should lead to the identification of the active site glutamate residue, since the location of the proteolytic cleavage in the sequence of CoA transferase was known (Lin & Bridger,

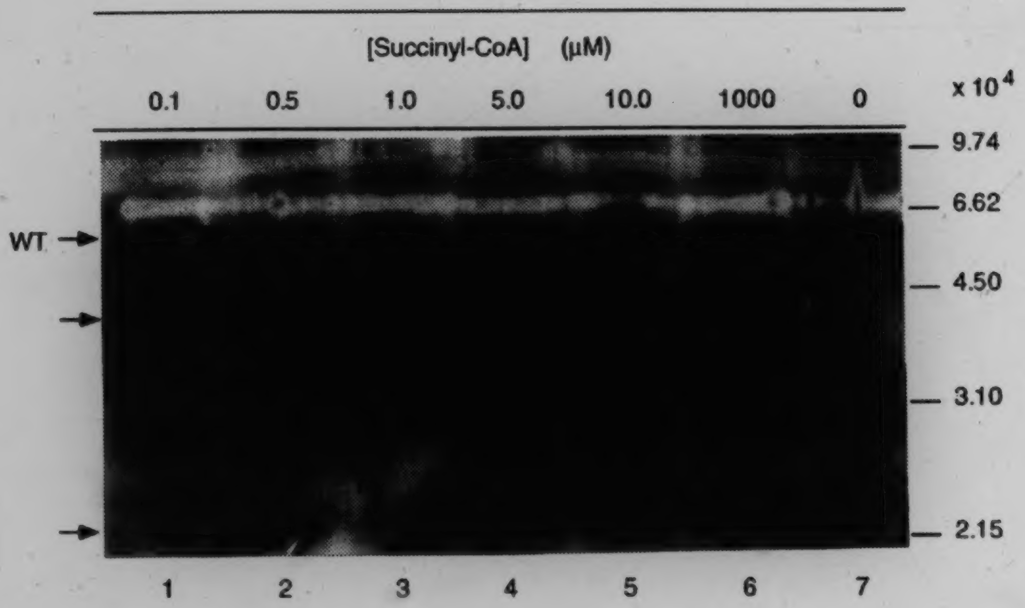
[Succinyl-CoA] (µM)
0.1
0.5
1.0
5.0
10.0
1000
0
x 10⁴
9.74
6.62
4.50
3.10
2.15
WT
1
2
3
4
5
6
7

Figure 5-3: Effect of succinyl-CoA concentration on the autolysis of CoA transferase. Unnicked enzyme (30 µg, or 0.6 nmol of the NC monomer) was autolytically fragmented in the presence of the indicated amounts of succinyl-CoA. Samples were fractionated by electrophoresis on a 12% (w/v) polyacrylamide gel, which was subsequently stained with $AgNO_3$. The top arrow identifies the band corresponding to the intact enzyme (WT), while the lower two arrows indicate bands corresponding to the fragments generated by autolysis.

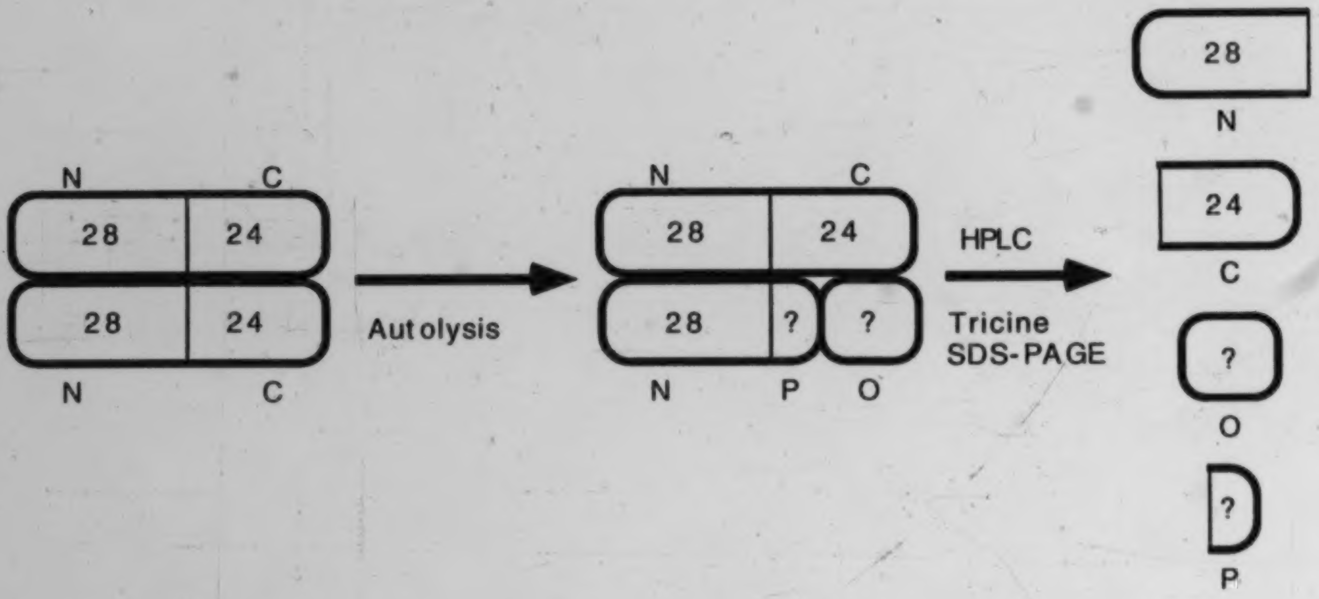

Figure 5-4: Schematic representation of the nicked form of CoA transferase, both prior and subsequent to autolysis. Proteolysis alone generates the N- and C-domains, while the autolytic fragmentation releases peptides O and P. Numbers refer to previously determined molecular weight values (× 10^3) (Lin & Bridger, 1992). Fragments O and P are shown to be released from only one of the two subunits to reflect the observed 50% efficiency of the autolytic fragmentation. Peptide P is bordered at its N-terminus by the previously identified proteolytic cleavage site, and at its C-terminus by the site of autolysis (i.e. the site of thiolesterification).

Table 5-1. Predicted Molecular Masses[a] for Fragment P

Potential active site residue	Fragment[b]	Predicted mass M+H$^+$ (Da)[c]
E344	S294 — S343	5491.3
	G295 — S343	5404.2
	K296 — S343	5347.2
E358	S294 — N357	6958.0
	G295 — N357	6870.9
	K296 — N357	6813.8
E369	S294 — K368	8084.2
	G295 — K368	7997.1
	K296 — K368	7940.1

[a] The size of this peptide is related to the site of autolysis, which could be located at one of the three glutamate residues listed. Average masses for the corresponding, hypothetical fragments were calculated using the program MacProMass.

[b] Three alternative peptides are listed in each case because protease and/or aminopeptidase activities apparently generate N-terminal heterogeneity in the fragment of molecular weight 2.4×10^4 (see text for further discussion).

[c] Calculation of predicted average mass assumes the oxidation of both methionine residues to methionine sulfoxide. The mass of the corresponding unoxidized fragments is obtained by subtracting 32.0 Da.

1992). Prior to developing this approach, attempts to purify the C-terminal autolytic fragment (Figure 5-4, fragment O) by RP-HPLC were unsuccessful. This difficulty was likely due to the poor solubility of the autolytically fragmented sample prior to application to the HPLC column, although it could not be ruled out that sufficiently injected fragment O precipitated on the column. It was predicted that the much smaller fragment P, by virtue of its lower hydrophobicity, might be more easily isolated prior to analysis by electrospray mass spectrometry.

In order to verify that fragment P could be generated, nicked CoA transferase was incubated in the presence or absence of 10 μM succinyl CoA and subsequently heated as described above. The reaction was then terminated by dilution in an appropriate volume of sample buffer and analyzed by tricine SDS-PAGE (Figure 5-5). Two bands representing fragments of molecular weights approximately equal to 2.0×10^4 and 5.0×10^3 were associated only with the sample in which the nicked ECoA was formed (Figure 5-5, lane 1). The deduced molecular weight of the smaller fragment (possibly fragment P) was 5.9×10^3, implying that Glu 344 or possibly Glu 358 could be the site of autolysis. However, the apparent molecular weights of CoA transferase and its proteolytic fragments, estimated by SDS-PAGE analysis, were generally greater than the values calculated from the amino acid sequence. For this reason, a more accurate value for the mass of the smaller peptide was desirable.

RP-HPLC and electrospray mass spectrometry. Nicked CoA transferase was autolytically fragmented as described above and analyzed by RP-HPLC. Nicked but unfragmented enzyme was similarly analyzed as a control. A comparison of their corresponding elution profiles (Figure 5-6) indicated that three peptides, represented by peaks X, Y, and Z, were specifically associated with the autolytically fragmented sample. Conversely, peaks labeled 1 through 5 were present in both plots, and were therefore not likely to represent the peptide of interest, fragment P.

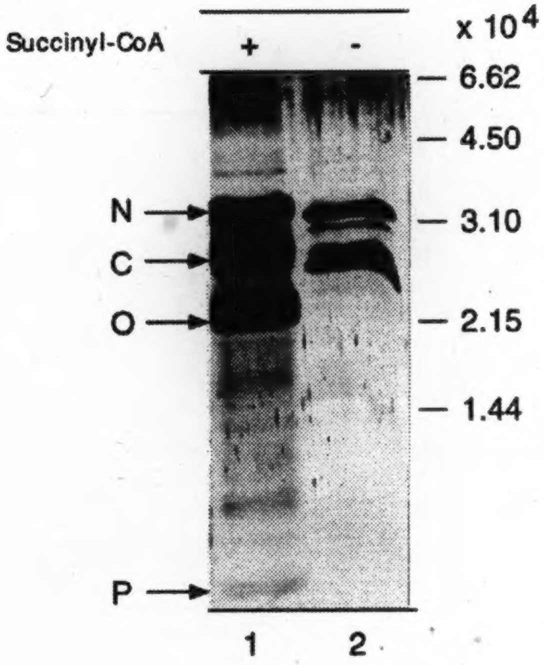

Figure 5-5: Analysis of nicked, autolytically fragmented CoA transferase by tricine SDS-PAGE. Nicked enzyme (30 µg, or 0.6 nmol of the NC monomer) was incubated at 25 °C for 15 min and then at 70 °C for 60 min in the presence (lane 1) or absence (lane 2) of 10 µM succinyl-CoA. Samples were subjected to electrophoresis on a 16.5% T, 3% C polyacrylamide gel, which was subsequently stained with AgNO$_3$. Bands corresponding to the peptides N, C, O, and P are indicated by appropriately labeled arrows.

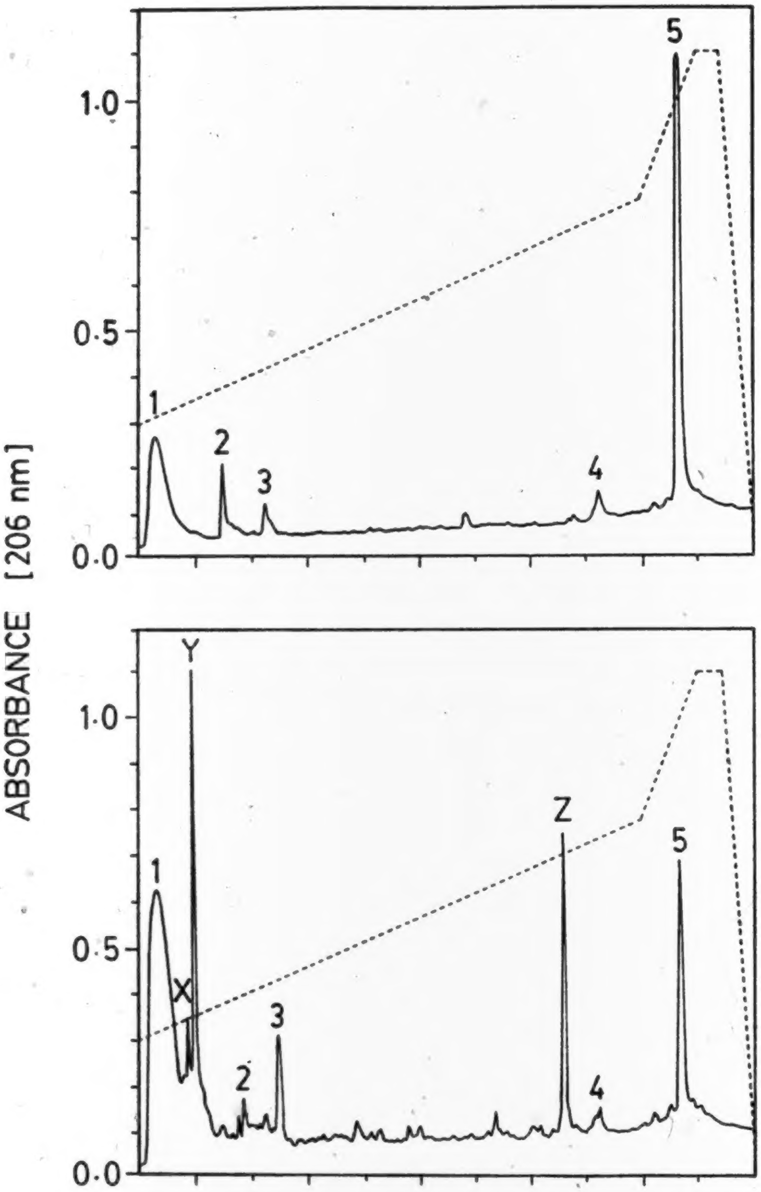

Figure 5-6: Elution profiles for RP-HPLC of CoA transferase, either nicked (top) or nicked/autolytically fragmented (bottom). Separations were performed as described in "Experimental Procedures". The gradient curve indicates 25% (v/v) B → 70% (v/v) B → 100% (v/v) B → 100% (v/v) A, where A is 0.1% (v/v) TFA in H_2O, and B is 0.1% (v/v) TFA in CH_3CN. Peaks appearing in both plots are labeled 1 through 5, whereas those unique to the lower plot are labeled X, Y, and Z.

Electrospray mass spectrometry of a pool of HPLC fractions representing peaks X and Y indicated the presence of a single peptide of molecular mass 2510.0 Da (data not shown). This value did not match any of the three masses predicted for fragment P (Table 5-1). A similar analysis of a pool of fractions representing peak Z revealed that the mass of its major component was 5404.3 Da (Figure 5-7, peak A1). This value was equal to the mass predicted for fragment P (with N-terminal Gly 295) if the site of autolysis were Glu 344 (Table 5-1). The minor component of mass 5347.0 Da (Figure 5-7, peak B1) most likely corresponded to the main peptide without the N-terminal glycine. Similarly, the minor species of mass 5491.0 Da (Figure 5-7, peak C1) consisted of the major component with an additional serine at its N-terminus. Thus, although Lin & Bridger (1992) had shown Lys 296 to be the N-terminal residue of the 2.4×10^4 fragment, the results suggested that this sample of nicked CoA transferase may contain a population of C-terminal proteolytic segments that are heterogeneous in their N-terminal extensions. The major component A1, then, had Gly 295 at its N-terminus, while the minor components B1 and C1 had Lys 296 and Ser 294 at their N-termini, respectively. Furthermore, the measured masses were equal to those calculated with the assumption that both methionine residues are oxidized to methionine sulfoxide. The oxidation of methionine to methionine sulfoxide on peptide P is a likely outcome of the elevated temperature used in the autolytic fragmentation reaction.

Table 5-2 summarizes the identification of these fragments and other more minor components predicted to be sodium or potassium adducts. Clearly, the molecular masses obtained by electrospray mass spectrometry point to Ser 343 as the C-terminus of peptide D, and therefore to Glu 344 as the site of the autolytic fragmentation.

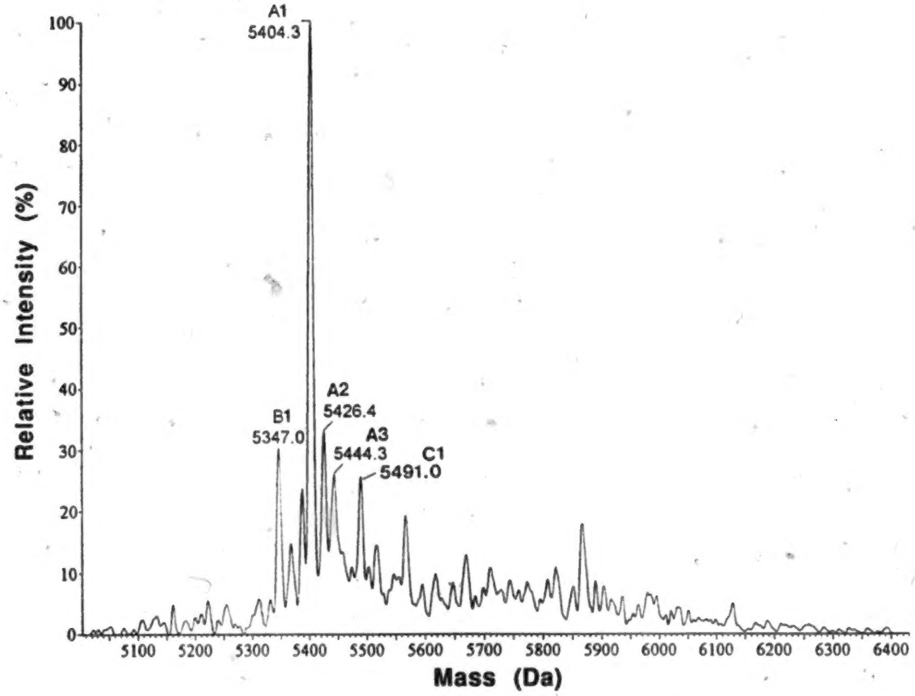

Figure 5-7: Electrospray mass spectrum of peptide Z (approximately 10 pmol). The symbols A1, A2, A3, B1, and C1 indicate peaks referred to in the text. See also Table 5-2 for a summary of relevant peaks.

Table 5-2: Summary of Significant Components Detected by Electrospray Mass Spectrometry

Peak label[a]	M+H$^+$ (Da)	Predicted peptide[b]	Associated ion(s)
A1	5404.3	G295-S343	—
A2	5426.4	G295-S343	1 Na$^+$
A3	5444.3	G295-S343	1 K$^+$
B1	5347.0	K296-S343	—
C1	5491.0	S294-S343	—

[a] Peaks are labeled according to the lettering scheme used in Figure 5-7.

[b] The single-letter amino acid code is used to indicate the N-terminal and C-terminal residues of each peptide. Numbering is based on the sequence of the precursor form of the enzyme (Lin & Bridger, 1992). Note that the two methionine residues in each of the three peptides listed are predicted to be oxidized to methionine sulfoxide.

DISCUSSION

Conditions suitable for autolysis. The fragmentation of CoA transferase at 70 °C was proposed to be autolytic in nature because it only occurs under conditions suitable for the formation of the enzyme-CoA intermediate. Furthermore, the release of an N-terminally blocked C-terminal fragment supported the predicted mechanism of autolysis (Howard et al., 1986). This mechanism was further substantiated by the demonstration that the degree of fragmentation is not altered by the presence of a mixture of proteinase inhibitors. A similar autolytic process, also involving nucleophilic attack by a main-chain nitrogen group, has recently been described for the biosynthesis of the green fluorescent protein chromophore (Cubbitt et al., 1995).

The site of the fragmentation in the CoA transferase sequence was determined by RP-HPLC in combination with ESI-MS, techniques which are generally susceptible to interference by high concentrations of salt. For this reason, the finding that micromolar amounts of succinyl-CoA are sufficient for obtaining a high yield of autolysis contributed significantly to the success of the approach.

Identification of Glu 344 as the catalytic nucleophile by ESI-MS. A peptide (fragment P) bordered N-terminally by the previously identified proteolytic cleavage site (Lin & Bridger, 1992) and C-terminally by the autolytic fragmentation site was released upon subjecting the nicked form of CoA transferase to autolysis. Analysis of a sample of nicked, fragmented enzyme by RP-HPLC revealed two species absent from the control. The first of these, represented by two peaks eluting at very similar retention times, was assigned a molecular mass of 2510.0 Da by electrospray mass spectrometry. This species may have been a degradation product of fragment C, given that: (1) its mass was significantly less than the minimum predicted for peptide P; and (2) attempts to determine its N-terminal sequence by the Edman degradation method were unsuccessful, indicating a blocked N-terminus. The second eluted species, similarly analyzed by electrospray mass spectrometry, consisted predominantly of a 5404.3 Da peptide. This mass value was equivalent to that predicted for fragment P (with N-terminal Gly 295) if Glu 344 is the site of autolysis. Thus, it was concluded that Glu 344 is the catalytic nucleophile of CoA transferase.

The electrospray mass spectrum also revealed peaks at 5491.0 Da and 5347.0 Da (i.e. respectively, 86.7 Da greater than and 57.3 Da less than the mass of the 5404.3 Da species). These mass increments most likely represented the addition of a serine and the loss of a glycine (respectively) at the N-terminus of the 5404.3 Da species, assuming that the C-terminus of all peptides in this fraction was strictly defined by the autolytic fragmentation. Based on the knowledge of the sequence of CoA transferase, it was predicted that this identification of terminal Ser-Gly- and Gly- reflected the N-terminal sequence of the 2.4 × 10^4 fragment. Thus, the species represented by peak Z was identified as peptide P, both by its mass and its N-terminal sequence.

The identification of three components with an N-terminal Ser 294, Gly 295, or Lys 296 in the electrospray mass spectrum of fragment P suggested that the 2.4 × 10^4 C-terminal proteolytic segment of nicked CoA transferase may consist of a population of polypeptides differing in length at their N-termini. Given that the enzyme is not nicked when purified in the presence of PMSF, a serine proteinase such as trypsin or thrombin is likely responsible for the cleavage when the inhibitor is omitted. The susceptible of the native CoA transferase to limited tryptic digestion has also been observed directly (Chapter 4). This proteolysis generates two fragments equivalent in size to those present in a preparation of nicked enzyme (2.8 × 10^4 and 2.4 × 10^4). It is conceivable that CoA transferase purified in the absence of PMSF is cut in its hydrophilic linker between Arg 293 and Ser 294, which corresponds to a trypsin cleavage site. Contaminating aminopeptidases (e.g. cathepsin C) may subsequently remove one or two amino acids from the N-termini of some of the resulting proteolytic fragments. Significant N-terminal heterogeneity was not detected previously (Lin and Bridger, 1992) because the sequence of the 2.4 × 10^4 fragment was obtained by the Edman degradation method, which, when applied to a protein of unknown sequence, is normally used to identify the most abundant amino acid released at each cycle. In addition, the predominant species present in two different preparations of the proteolytically nicked enzyme may not be identical.

Finally, the enzyme was exposed to potassium phosphate during the purification and to sodium phosphate and sodium succinyl-CoA during autolysis. Thus, the identification of Na^+ and K^+ adducts present as minor components in the electrospray mass spectrum is reasonable.

Related studies and applications. Mass spectrometry has been successfully applied to the characterization of other mechanism-based enzyme modifications, including the transient formation of a covalent bond between α-glucosyltransferase and its substrate (Mooser et al., 1991) and the autolytic fragmentation of myeloperoxidase (Taylor et al., 1992). In addition, the catalytic nucleophiles of several glycosyl hydrolases have been identified by HPLC coupled with ESI-MS/MS, following enzyme inactivation by a mechanism-based inhibitor. Recent examples include: glucocerebrosidase (Miao et al., 1994a), xylanase (Miao et al., 1994b), glycogen debranching enzyme (Braun et al., 1996), α-glucosidase (McCarter & Withers, 1996), and lysosomal β-galactosidase (McCarter et al., 1997). In this report, it has been demonstrated that the mass spectrometric analysis of autolytic fragments can be used to identify the catalytic nucleophile in an enzyme whose mechanism involves an activated glutamate residue. Other enzymes potentially sharing this mechanistic feature, and therefore amenable to this approach, include CoA transferases from different species, tryptophanyl-tRNA synthetase (Kisselev et al., 1979; Kovaleva et al., 1983), long-chain fatty acyl-CoA synthetase (Spector, 1982), and β-galactosidase (Cupples et al., 1990).

The identification of glutamate 344 as the catalytic nucleophile of CoA transferase corroborates the observations of Williams (1990), who isolated and sequenced peptides containing the thiolesterified glutamate residue.[3] The results presented in this chapter reveal an active site element suitable for modification by site-directed mutagenesis, thus effectively permitting a more thorough exploration of the structure-function relationships governing the mechanism of this enzyme.

A conserved sequence motif. The nucleophilic glutamate residue is part of a larger motif (consisting of residues 343-346) which is conserved among the $\alpha_2\beta_2$-type prokaryotic and the eukaryotic CoA transferases (Parales & Harwood, 1992; see Figure 5-8). This segment, referred to as the "ENG" motif, is identical to the "ENG" consensus region of the "family 1" glycosyl hydrolases (Davies & Henrissat, 1995; Moracci et al., 1996; see Figure 5-8). For both the CoA transferases and the glycosyl hydrolases, the glutamate residue within this motif fulfills the role of nucleophile, suggesting that the sequence Glu-Asn-Gly encodes structural information which is optimal for this catalytic function.

The three-dimensional structures of two "family 1" glycosyl hydrolases, cyanogenic β-glucosidase (Barrett et al., 1995) and 6-phospho-β-galactosidase (Wiesmann et al., 1995), were recently solved to 2.15 and 2.3 Å, respectively. The overall fold of each enzyme is a $(\beta\alpha)_8$ barrel. As has been observed for other enzymes which share this fold, the residues of the active site are located at the C-terminal end of the barrel (reviewed in [Farber & Petsko, 1990]). Specifically, the nucleophilic glutamate residue is located at the C-terminal end of β-strand 7, a property shared by a "superfamily" of glycosyl hydrolases consisting of families 2, 5, 10, and 17 (Barrett et al., 1995; Jenkins et al., 1995; Wiesmann et al., 1995). It has been proposed that substitution of the asparagine and glycine residues of the "ENG" motif disrupts the structural integrity of β-strand 7 and/or the catalytic geometry of the nucleophilic glutamate residue (Barrett et al., 1995). It is possible that the active sites of the "family 1" glycosyl hydrolases and the $\alpha_2\beta_2$-type prokaryotic and the eukaryotic CoA transferases are characterized by similar structural properties, which may have evolved convergently. Interestingly, there is precedence for a $(\beta\alpha)_8$ barrel structure among the CoA-binding proteins. Namely, CoA is

A

CoA transferases

Pig	341	L Q S	**E N G**	I L G L	350
Human	341	L Q S	**E N G**	V L G L	350
C. eleg.	339	L Q S	**E N G**	I I G V	348
C. acet. (Ctf B)	48	F Q S	**E N G**	I V G M	57
A. calc. (Cat J)	47	L H S	**E N G**	L L A F	56
P. puti. (Pca J)	47	L H S	**E N G**	L L G M	56
A. tume. (Pca J)	48	H T	**E N G**	I L N F	56
B. subt. (Pca J)	44	L Q S	**E N G**	L L G I	53
M. tube. (Pca J?)	47	L H S	**E N G**	I L G V	56
H. infl. (Ato A)	43	L Q S	**E N G**	F L G L	52
E. coli. (Ato A)	41	L Q S	**E N G**	F L G L	50

B

Glycosyl hydrolases
(family 1)

S. solf. (glyc.)	384	Y V T	**E N G**	I A - -	391
S. solf. (galac.)	386	Y V M	**E N G**	I A - -	393
P. furi. (gluc.)	369	I I T	**E N G**	M A - -	376
T. mari (gluc. A)	348	Y I T	**E N G**	- A A F	356
C. ther. (gluc. A)	352	V I S	**E N G**	- A A F	360
Agrobac. sp. (gluc.)	356	Y I T	**E N G**	- A C Y	364
B. poly. (gluc. A)	349	Y I T	**E N G**	- A C I	357
B. poly. (gluc. B)	353	L I T	**E N G**	- A A M	361
C. sacc. (gluc. A)	360	Y I T	**E N G**	- A A Y	368
B. circ. (gluc.)	352	Y I T	**E N G**	- A C Y	360
T. repe. (gluc.)	394	Y I T	**E N G**	R N E F	403

Figure 5-8: Conservation of the "ENG" sequence motif (shown in bold lettering within a box). (A) Amino acid sequence alignment of the eukaryotic and $\alpha_2\beta_2$-type prokaryotic CoA transferases in the region of the nucleophilic glutamate residue. The numbering and abbreviations are as described in the legend to Figure 1-9. (B) Amino acid sequence alignment of the "family 1" glycosyl hydrolases in the region of the nucleophilic glutamate residue. The abbreviations are: "*glyc.*", β-glycosidase; "*galac.*", β-galactosidase; "*gluc.*", β-glucosidase; "*S. solf.*", *Sulfolobus solfataricus*; "*P. furi.*", *Pyrococcus furiosus*; "*T. mari.*", *Thermotoga maritima*; "*C. ther.*", *Clostridium thermocellum*; "*Agrobac.*", *Agrobacterium*; "*B. poly.*", *Bacillus polymixa*; "*C. sacc.*", *Caldocellum saccharolyticum*; "*B. circ.*", *Bacillus circulans*; "*T. repe.*", *Trifolium repens*. (Adapted from [Moracci et al., 1996]).

bound as an extended molecule in the $(\beta\alpha)_8$ barrel of the methylmalonyl-CoA mutase α-subunit (Engel & Wierenga, 1996).

Alternatively, the conservation of the "ENG" motif of the CoA transferases may have been necessary to maintain a local conformation unrelated to that of the glycosyl hydrolase active site. Consistent with this hypothesis, it has been recently proposed that the three-dimensional structures of all CoA transferases resemble that of the glutaconate CoA-transferase of *Acidaminococcus fermentans*, which adopts an open α/β-protein fold (Jacob et al., 1997). The x-ray structure of pig heart CoA transferase will provide insight as to the structure of the enzyme's catalytic center.

ENDNOTES

[1] A version of this chapter has been published:

Rochet, J.-C., & Bridger, W. A. (1994) *Protein Sci. 3*, 975-981.

[2] The letter T refers to the total percentage concentration (w/v) of acrylamide and bisacrylamide, while C denotes the percentage concentration (w/v) of bisacrylamide relative to T (Hjertén & Mosbach, 1962).

[3] The results of Williams (1990) were first cited during the course of the studies outlined in this chapter, by Parales and Harwood (1992).

REFERENCES

Barrett, T., Suresh, C. G., Tolley, S. P., Dodson, E. J., & Hughes, M. A. (1995) *Structure 3*, 951-960.

Bradford, M. M. (1976) *Anal. Biochem. 72*, 248-254.

Braun, C., Lindhorst, T., Madsen, N. B., & Withers, S. G. (1996) *Biochemistry 35*, 5458-5463.

Cubitt, A. B., Heim, R., Adams, S. R., Boyd, A. E., Gross, L. A., & Tsien, R. Y. (1995) *Trends Biochem. Sci. 20*, 448-455.

Cupples, C. G., Miller, J. H., & Huber, R. E. (1990) *J. Biol. Chem. 265*, 5512-5518.

Davies, G., & Henrissat, B. (1995) *Structure 3*, 853-859.

Engel, C., & Wierenga, R. (1996) *Curr. Opin. Struct. Biol. 6*, 790-797.

Farber, G. K., & Petsko, G. A. (1990) *Trends Biochem. Sci. 15*, 228-234.

Fenn, J. B., Mann, M., Meng, C. K., Wong, S. F., & Whitehouse, C. M. (1989) *Science 246*, 64-71.

Gorski, J. P., & Howard, J. B. (1980) *J. Biol. Chem. 255*, 10025-10028.

Harpel, P. C., Hayes, M. B., & Hugli, T. E. (1979) *J. Biol. Chem. 254*, 8669-8678.

Hersh, L. B., & Jencks, W. P. (1969) *Methods Enzymol. 13*, 75-81.

Hjertén, S., & Mosbach, R. (1962) *Anal. Biochem. 3*, 109-118.

Howard, J. B. (1980) *J. Biol. Chem. 255*, 7082-7084.

Howard, J. B. (1981) *Proc. Natl. Acad. Sci. U. S. A. 78*, 2235-2239.

Howard, J. B., Vermuelen, M., & Swenson, R. P. (1980) *J. Biol. Chem. 255*, 3820-3823.

Howard, J. B., Zieske, L., Clarkson, J., & Rathe, L. (1986) *J. Biol. Chem. 261*, 60-65.

Jacob, U., Mack, M., Clausen, T., Huber, R., Buckel, W., & Messerschmidt, A. (1997) *Structure 5*, 415-426.

Janatova, J., & Tack, B. F. (1981) *Biochemistry 20*, 2394-2402.

Janatova, J., Tack, B. F., & Prahl, J. W. (1980) *Biochemistry 19*, 4479-4485.

Jenkins, J., Lo Leggio, L., Harris, G., & Pickersgill, R. (1995) *FEBS Lett. 362*, 281-285.

Kawasaki, I., & Itano, H. A. (1971) *Anal. Biochem. 48*, 546-556.

Khan, S. A., & Erickson, B. W. (1984) *J. Am. Chem. Soc. 106*, 799-801.

Kisselev, L. L., Favorova, O. O., & Kovaleva, G. K. (1979) in *Transfer RNA: Structure, Properties, and Recognition* (Schimmel, P. R., Söll, D., & Abelson, J. N., Eds.) pp. 235-246, Cold Spring Harbor Laboratory, Cold Spring Harbor, NY.

Kovaleva, G. K., Holmuratov, E. G., & Kisselev, L. L. (1983) *FEBS Lett. 151*, 79-82.

Lin, T., & Bridger, W. A. (1992) *J. Biol. Chem. 267*, 975-978.

McCarter, J. D., & Withers, S. G. (1996) *J. Biol. Chem. 271*, 6889-6894.

McCarter, J. D., Burgoyne, D. L., Miao, S., Zhang, S., Callahan, J. W., & Withers, S. G. (1997) *J. Biol. Chem. 272*, 396-400.

Mann, M., & Wilm, M. (1995) *Trends Biochem. Sci. 20*, 219-224.

Miao, S., McCarter, J. D., Grace, M. E., Grabowski, G. A., Aebersold, R., & Withers, S. G. (1994a) *J. Biol. Chem. 269*, 10975-10978.

Miao, S., Ziser, L., Aebersold, R., & Withers, S. G. (1994b) *Biochemistry 33*, 7027-7032.

Mooser, G., Hefta, S. A., Paxton, R. J., Shively, J. E., & Lee, T. D. (1991) *J. Biol. Chem. 266*, 8916-8922.

Moracci, M., Capalbo, L., Ciaramella, M., & Rossi, M. (1996) *Protein Eng. 9*, 1191-1195.

Parales, R. E., & Harwood, C. S. (1992) *J. Bacteriol. 174*, 4657-4666.

Schägger, H., & von Jagow, G. (1987) *Anal. Biochem. 166*, 368-379.

Sim, R. B., & Sim, E. (1981) *Biochem. J. 193*, 129-141.

Smith, R. D., Loo, J. A., Edmonds, C. G., Baringa, C. J., & Udseth, H. R. (1990) *Anal. Chem. 62*, 882-899.

Solomon, F., & Jencks, W. P. (1969) *J. Biol. Chem. 244*, 1079-1081.

Spector, L. B. (1982) in *Covalent Catalysis by Enzymes*, pp. 212-214, Springer-Verlag, New York.

Taylor, K. L., Pohl, J., & Kinkade, J. M. Jr. (1992) *J. Biol. Chem. 267*, 25282-25288.

Tull, D., Miao, S., Withers, S. G., & Aebersold, R. (1995) *Anal. Biochem. 224*, 509-514.

White, H., Solomon, F., & Jencks, W. P. (1976) *J. Biol. Chem. 251*, 1700-1707.

Wiesmann, C., Beste, G., Hengstenberg, W., & Schulz, G. E. (1995) *Structure 3*, 961-968.

Williams, W. A. (1990) Ph. D. thesis, University of Minnesota, Minneapolis.

Withers, S. G., & Aebersold, R. (1995) *Protein Sci. 4*, 361-372.

Chapter 6. Site-Directed Mutagenesis at the Active Site of CoA Transferase

INTRODUCTION

A detailed description of the fold of the pig heart CoA transferase subunit awaits the solution of a three-dimensional model of the enzyme by x-ray crystallography. In the absence of such a model, two tertiary structural motifs have been proposed for the porcine monomer. First, as discussed in Chapter 5, the conservation of the "ENG" motif suggests that the active site of the $\alpha_2\beta_2$-type prokaryotic and the eukaryotic CoA transferases is located at the C-terminal end of a $(\beta\alpha)_8$ barrel, as has been observed for the family 1 glycosyl hydrolases (Barrett et al., 1995; Wiesmann et al., 1995). Second, Jacob et al. (1997) have postulated that all CoA transferases, regardless of whether or not they display significant amino acid sequence similarity, possess the open α/β-protein fold adopted by the glutaconate CoA-transferase of *Acidaminococcus fermentans*. The active sites of enzymes which adopt this fold are generally defined by "topological switch points" located at the C-terminal end of the β-strands (Brändén & Tooze, 1991).

The catalytic residues of enzymes with $(\beta\alpha)_8$-barrel or open α/β-sheet structures are generally provided by non-adjacent segments in the amino acid sequence (Brändén & Tooze, 1991). The active site of pig heart CoA transferase may also be organized in this manner. First, a cDNA isolated from a human patient with low levels of CoA transferase activity was found to encode a version of the enzyme truncated at serine 283 (Kassovska-Bratinova et al., 1996). This result indicated that removal of the 237 C-terminal amino acid residues abolishes the catalytic function of the mammalian CoA transferase. Second, it was demonstrated that enzyme activity is only produced in an equimolar mixture of the N- and C-domains following their assembly to form an N_2C_2-domain complex (Chapter 2). Thus, both domains of CoA transferase are essential for catalytic activity, consistent with the hypothesis that the enzyme is organized as an α/β-barrel or an open α/β-sheet.

To understand the "layout" of the active site of CoA transferase, it is necessary to identify key catalytic residues associated with the N- or C-domain. Glutamate 344, identified as the active site nucleophile of the mammalian CoA transferase (Chapter 5), is located in the C-domain, which accounts for the inactivity of a C-terminally truncated form of the enzyme (Kassovska-Bratinova et al., 1996). In addition, peptide sequencing techniques have demonstrated that cysteine 67 and cysteine 235 (both located in the N-domain of pig heart CoA transferase) are the predominant cysteine residues modified upon prolonged treatment of the enzyme with [^{14}C]-NEM, specifically in the presence of acetoacetyl-CoA (Williams, 1990). The modification of these cysteine residues inactivates ECoA, suggesting that cysteine 67 or cysteine 235 is the essential sulfhydryl residue previously described by White et al. (1976).

The inactivation of ECoA in the presence of DTNB involves rapid and slow phases (White et al., 1976). The rapid loss of enzyme activity, which is due to the modification of a single, essential cysteine residue, is reversible in the presence of DTT and sensitive to the formation of a stable Michaelis complex (White et al., 1976). From these observations, it is suggested that covalent modification of the reactive cysteine residue by bulky thiol reagents leads to steric hindrance at the active site, without significant unfolding of the enzyme (White et al., 1976; Kindman & Jencks, 1981). In contrast, the slow phase of inactivation, presumably due to the nonspecific modification of all five cysteine residues (Williams, 1990), involves the unfolding and dissociation of the CoA transferase subunits (White et al., 1976). Conceivably, one of the two cysteine residues identified by Williams (1990) was modified by the rapid pathway, while the other reacted more slowly during the prolonged incubation of ECoA in a solution containing [^{14}C]-NEM (see above). Although the ECoA complex is inactivated by a combination of the rapid (reversible) and slow (irreversible) reactions, the free form of CoA transferase is only modified by the gradual, irreversible process (White et al., 1976).

The smallest form of active CoA transferase is the $(NC)_2$-homodimer (Chapters 2 and 4), indicating that the individual monomer is incapable of enzyme function. Furthermore, catalytic residues are contributed by both the N- and C-domains, as outlined above. Given these observations, the disposition of the active sites between the subunits of the homodimer can be described by two models. As one possibility, a complete set of catalytic residues may be contained within an individual monomer. In this case, each subunit can only adopt a catalytically competent conformation upon association with the second monomer. Alternatively, a single active site may be "shared" between the N- and C-domains of opposing subunits in a reciprocal manner, by a twofold axis of symmetry.

Evidence for shared active sites in a homodimeric enzyme can be provided by a method referred to as "subunit hybridization" or "active site complementation" (Wente & Schachman, 1987; Tobias & Kahana, 1993). This experimental approach requires the identification and isolation of two types of inactive monomers (referred to as "X" and "Y"), which carry amino acid substitutions on opposing faces of the active site (Figure 6-1). The two monomers, mixed in an equimolar ratio, are unfolded in denaturant and subsequently refolded. The random association of subunits during refolding leads to a binomial distribution of dimeric species, consisting of "XX" homodimers, "XY" heterodimers, and "YY" homodimers in a 1:2:1 ratio (Figure 6-1). If the catalytic residues are located at the interface between subunits, then one of the two active sites of the reconstituted "XY" hybrid is fully functional (Figure 6-1). Alternatively, if the catalytic residues are not located at the interface between subunits, then both active sites of the "XY" heterodimer are defective. Thus, the arrangement of the active sites between the subunits of the homodimer can be determined by measuring the specific activity of the refolded, equimolar mixture of the two mutant enzymes, and comparing this level of activity to that of the wild-type enzyme.

The experiments described below were carried out to investigate the layout of the CoA transferase active site. First, mutants in which glutamate 344 was replaced with an

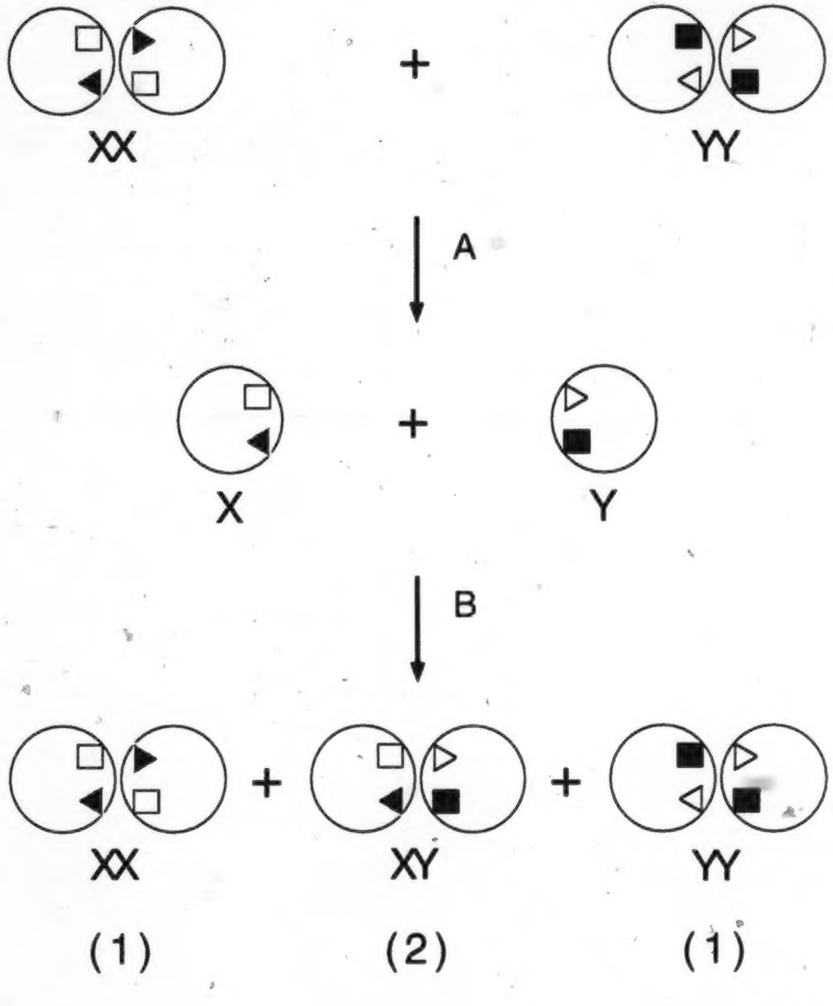

Figure 6-1: The identification of shared active sites of a homodimeric enzyme by subunit hybridization. The mutants XX and YY, each of which carries an inactivating substitution (white square or white triangle) at a different position of the amino acid sequence, are mixed and unfolded (A) and subsequently refolded (B). The random association of X and Y subunits during renaturation leads to a binomial distribution of dimeric species, consisting of XX homodimers, XY heterodimers, and YY homodimers in a 1:2:1 ratio. One of the two active sites of the XY hybrid is fully functional (black square together with black triangle), so that the specific activity of the reconstituted enzyme mixture is 0.25 times that of the wild-type enzyme.

alanine (E344A), aspartate (E344D), or glutamine (E344Q) residue were characterized with respect to their specific enzyme activities.[1] Second, mutants in which a serine residue replaced cysteine 67 (C67S) or cysteine 235 (C235S) were examined for their susceptibility to inactivation by DTNB in the presence or absence of acetoacetyl-CoA. Finally, subunit hybridization studies were performed to determine whether or not the active sites of the CoA transferase homodimer are shared between the two monomers.

EXPERIMENTAL PROCEDURES[2]

Materials. The restriction endonucleases and T4 DNA ligase were purchased from New England Biolabs, Inc. or as Gibco BRL products from Life Technologies, with no obvious differences. Acrylamide and *Taq* DNA polymerase were also obtained as Gibco BRL products from Life Technologies. The deoxynucleotide triphosphates, DEAE Sephacel, Sephadex G-50, and Sephacryl S-200 were purchased from Pharmacia Biotech. The Sequenase was supplied by the United States Biochemical Corporation. The T4 DNA polymerase was obtained from Boehringer Mannheim. The column matrices Affi-Gel Blue and hydroxyapatite were purchased from Bio-Rad Laboratories, Ltd. Acetohydroxamic acid (AHA), DTNB, β-hydroxyacyl-CoA dehydrogenase, NADH, and the substrates acetoacetate succinyl-CoA were obtained from Sigma Chemical Company. Purified protein preparations were concentrated using Millipore brand Ultrafree-15 (MWCO = 1.0×10^4). Dialyses were carried out using Spectra/Por membranes supplied by Spectrum. Finally, the GuHCl was provided by ICN Biomedicals, Inc.

Site-directed mutagenesis. A gene encoding the E344A mutant was synthesized in three steps using standard protocols for the PCR and overlap extension (Higuchi et al., 1988; Ho et al., 1989; see Figure 6-2). First, a cDNA corresponding to residues 342-520 of CoA transferase was amplified from pT7-Hng using the primers E344A (which encoded alanine at position 344 of the amino acid sequence) and HIND (Appendix 3). Second, a PCR product corresponding to residues 1-348 of CoA transferase was

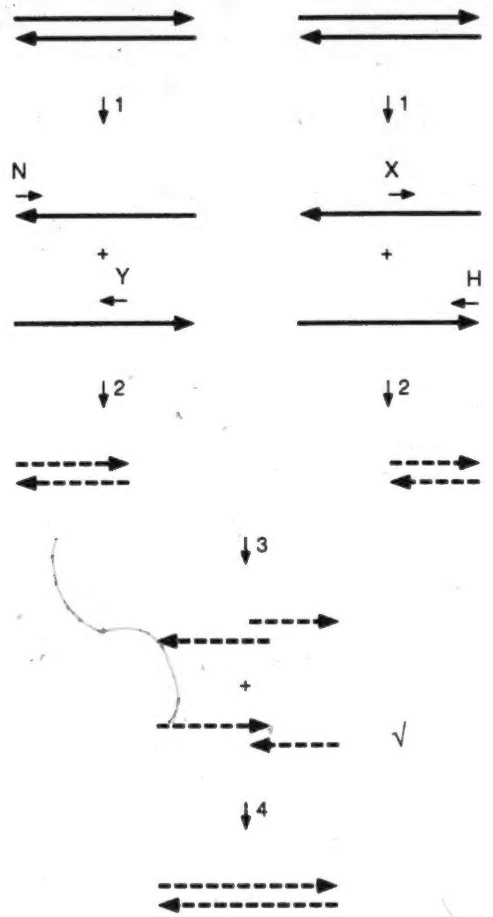

Figure 6-2: Mutagenesis at position 344 of CoA transferase by overlap extension. (1) A full-length, double-stranded DNA encoding the wild-type enzyme is heat-denatured and annealed to the primer NDE (N) and the mutagenic primer Y (left panel), or the primer HIND (H) and the mutagenic primer X (right panel). Primer X encodes an amino acid other than glutamate at position 344, while primer Y is complementary to primer X. (2) The annealed products are extended and amplified by the PCR to generate two double-stranded DNA fragments. (3) The fragments are mixed, heat-denatured, and cooled to form two annealed products. (4) One of the annealed products (labeled "√") can be extended and amplified by the PCR to generate a full-length, double-stranded DNA encoding a mutant form of CoA transferase. The solid and broken arrows correspond to unaltered or mutated DNA fragments, respectively. All arrows point in the 5' to 3' direction.

amplified from pT7-WT using the primers E344A(C) (which was complementary to E344A) and NDE (Appendix 3). Finally, the overlapping products of the first two reactions were annealed to form a full-length template (Figure 6-2), from which a cDNA encoding the E344A mutant was amplified using the primers NDE and HIND. The amplified cDNA was subcloned as a 0.3 kb *Msc*I-*Nco*I fragment into pT7-WT, generating pT7-E344A.

Genes encoding E344D and E344Q were also produced by overlap extension, using E344D/E344D(C) and E344Q/E344Q(C), respectively as the "internal", mutagenic primer pairs (Appendix 3), and pT7-Hng as the initial template. The two overlapping PCR products corresponded to residues 1-347 and 341-520 of the amino acid sequence.

An M13 vector containing a gene to encode the C67S mutant (M13-C67S) was generated by site-directed mutagenesis according to previously described methods (Kunkel, 1985). The single-stranded DNA template and the mutagenic primer were M13-WT and C67S, respectively. The primer C67S encoded serine at position 67 of the amino acid sequence (Appendix 3). The expression plasmid pT7-C67S was created in two steps. First, the 1.5 kb *Xba*I-*Hin*dIII segment cleaved from M13-C67S RF DNA was subcloned into pT7-WT. Second, to ensure that most of the cDNA insert from this initial recombinant plasmid was free of mutations due to misincorporation by Taq polymerase, the 1.2 kb *Bam*HI-*Hin*dIII segment was cleaved and replaced with the equivalent region excised from pT7-WT.

An M13 vector containing a gene to encode the C235S mutant (M13-C235S) was generated by site-directed mutagenesis as described for M13-C67S (Kunkel, 1985). The single-stranded DNA template and the mutagenic primer were M13-WT and C235S, respectively. The primer C235S encoded serine at position 235 of the amino acid sequence (Appendix 3). The expression plasmid pT7-C235S was created in two steps. First, the 1.5 kb *Xba*I-*Hin*dIII segment cleaved from M13-C235S RF DNA was subcloned into pT7-WT. Second, to ensure that much of the cDNA insert from this initial recombinant plasmid was free of mutations due to misincorporation by Taq polymerase, the 0.6 kb *Msc*I-*Hin*dIII segment was cleaved and replaced with the equivalent region excised from pT7-WT.

The absence of possible mutations due to misincorporation by *Taq* DNA polymerase or Sequenase during the *in vitro* DNA synthesis reactions was confirmed by automated sequence determinations using previously described methods (Sanger et al., 1977) and an Applied Biosystems (ABI) 373A DNA sequencer.

Electrocompetent BL21(DE3) cells (*hsdS gal* [*λc*I*ts*857 *ind*1 *S*am7 *nin*5 *lac*UV5-T7 gene*1*]) were electroporated with the pT7-7 vectors described above, yielding the new strains BL-E344A, BL-E344D, BL-E344Q, BL-C67S, and BL-C235S.

Gene expression and protein purification. The CoA transferase mutants E344A and C235S were purified from cultures of *E. coli* BL21(DE3) (2 to 4 L) by the procedure described previously for the wild-type enzyme (Chapter 2). The mutant E344D was isolated in an identical manner, except that 2ME was omitted from the purification buffers.

The mutants C67S and E344Q were prepared from 10 L cultures of *E. coli* BL21(DE3) incubated in a fermenter unit with vigorous aeration. Following growth under inducing conditions at 25 °C for 8 to 12 h, the cells were harvested by centrifugation (10 min, 4.2×10^3 g, 4 °C), and the cell pellet was resuspended in 0.5 L of buffer S. The resuspended cells were then partially cracked by freezing at -70 °C and thawing at 4 °C. The protein suspension was sonicated at 4 °C with three three-minute pulses using a large-sized (green-coded) probe attached to a BioSonik IV sonicator (Bronwill Scientific), set at high intensity. The cell debris were separated from the cell lysate by centrifugation (10 min, 4.2×10^3 g). Generally, the protein concentration of the cell lysate prepared in this manner was 2 to 4 mg/mL.

The fraction of the cell lysate which was soluble at 18% (w/v) $(NH_4)_2SO_4$ but insoluble at 50% (w/v) $(NH_4)_2SO_4$ (Chapter 2) was dissolved in buffer D. The protein solution (3 to 5 mg/mL) was desalted by gel exclusion chromatography on a Sephadex G-50 column (diameter 5 cm, height 60 cm, total volume 1.2 L) prior to further purification. Typically, elution of the protein mixture from this column occurred at 0.32-0.56 L. The mutant enzyme was then eluted from a column of DEAE-Sephacel (diameter 5 cm, height 30 cm, total volume 0.59 L) at 0.10 to 0.19 M KCl, using a gradient of 0 to 0.50 M KCl in 1.8 L buffer D. The partially pure protein sample was concentrated by precipitation in $(NH_4)_2SO_4$ (final concentration, 50% [w/v]), prior to gel filtration chromatography on Sephacryl S-200 and ion exchange on a column of Affi-Gel Blue (Chapter 2). Optimally, a 10 L culture of BL-C67S or BL-E344Q yielded 50 mg of the corresponding mutant protein in pure form.

The homogeneity of all protein preparations was confirmed by SDS-PAGE analysis. The protein concentration of enzyme solutions used for far-UV CD or fluorescence measurements and unfolding studies was determined from readings of A_{278} which were corrected for scatter. For these measurements, an ε_{278} value of 0.65 $(mg/mL)^{-1}$ was used (Chapter 2). The protein concentration of enzyme solutions used for other experiments was determined by measuring A_{278} without correcting for scatter. In such cases, an ε_{278} value of 0.75 $(mg/mL)^{-1}$ was used for both forms of CoA transferase (Chapter 2).

Measurement of enzyme activity. For all the work other than the kinetic analyses, CoA transferase activity was determined spectrophotometrically as described in Chapter 2. In the present study, the assay solutions consisted of 50 mM Tris-HCl (pH 9.1), 15 mM $MgCl_2$, 0.060 to 0.30 mM succinyl-CoA, and 13 to 67 mM acetoacetate. The extinction coefficient for acetoacetyl-CoA at 310 nm (ε_{310}) was taken to be 7.8×10^3 M^{-1} cm^{-1} under these conditions (Howard et al., 1986). Assay solutions used for determining specific enzyme activities contained 0.30 mM succinyl-CoA and 67 mM acetoacetate. All assays were carried out at 22 °C.

Enzyme kinetics. Kinetics measurements were performed at 22 °C using previously published procedures (Hersh & Jencks, 1967; White & Jencks, 1976). Enzyme samples were dialyzed as described in Chapter 2 against 0.5 L of 10 mM Tris-HCl (pH 8.0) or 20 mM K[phosphate] (pH 7.4) prior to kinetic analysis.

The formation of succinyl-CoA from acetoacetyl-CoA (0.045 to 0.135 μM) and succinate (4.0 to 40 mM) was monitored by the decrease in A_{310} in an assay solution of 0.067 M Tris-SO_4 buffer (pH 8.1). The ionic strength of the reaction mixture was adjusted to 1.0 M by the addition of the appropriate amount of Na_2SO_4. An ε_{310} value of 5.20×10^3 M^{-1} cm^{-1}, identical to that reported by Whitty et al. (1995), was measured for acetoacetyl-CoA under these conditions. The accuracy of this assay was compromised by two factors. First, reaction mixtures lacking enzyme consistently showed a spontaneous decrease in A_{310} with time of incubation. This spontaneous decrease occurred at a progressively slower rate, which eventually reached a minimum after approximately 5 min. Accordingly, the enzyme was added after the spontaneous decrease in A_{310} occurred at a constant rate, which was then subtracted from the rate of the catalyzed reaction. From separate measurements, it was demonstrated that less than 3% of the initial acetoacetyl-CoA was hydrolyzed during this period. Second, the observed CoA transferase activity decreased with first-order kinetics during the time of the assay. To correct for this decrease, the initial rate was estimated from a plot of "log (enzyme activity) versus time" by extrapolating to zero time. The enzyme activity was shown to be proportional to the concentration of enzyme up to 0.32 μg of C67S or 4.0 μg of E344Q.

The formation of acetoacetyl-CoA from succinyl-CoA (0.284 to 1.14 mM) and acetoacetate (0.018 to 0.18 mM) could not be measured directly by the increase in A_{310} due to product inhibition (Hersh & Jencks, 1967). Instead, this reaction was coupled to the reduction of acetoacetyl-CoA by β-hydroxyacyl-CoA dehydrogenase. This reduction was monitored by the decrease in A_{340}, which reflects the disappearance of NADH. The assay solution consisted of 0.061 M Tris-SO_4 buffer, 0.14 mM NADH, 0.29 M Na_2SO_4, and 10 μg of β-hydroxyacyl-CoA dehydrogenase, at pH 8.1.[3] An ε_{340} value of 6.22×10^3 M^{-1} cm^{-1} was used for NADH under these conditions (Horecker & Kornberg, 1948; Hersh & Jencks, 1967). The rate of the catalyzed reaction was corrected for a spontaneous decrease in A_{340}, observed in reaction mixtures lacking CoA transferase. The CoA transferase activity was shown to be linear with respect to the concentration of enzyme up to 4.0 μg of C67S or 0.10 mg of E344Q.

The concentration of acetoacetyl-CoA was determined spectrophotometrically, using an ε_{310} value of 9.30×10^3 M^{-1} cm^{-1} for a solution of the substrate prepared in 0.067 M Tris-SO_4 and 5 mM $MgCl_2$, at pH 8.1 (White & Jencks, 1976). In addition, the concentration of succinyl-CoA was determined using an ε_{232} value of 4.50×10^3 M^{-1} cm^{-1} for a solution of the substrate prepared in 0.10 M Tris-HCl, 10 mM $MgCl_2$, 0.1 M KCl, and 10 mM Na_2[succinate], at pH 7.5 (Bridger et al., 1969). Finally, the concentration of NADH in a stock solution prepared with distilled water was determined using an ε_{340} value of 6.22×10^3 M^{-1} cm^{-1} (Horecker & Kornberg, 1948).

Kinetic data were evaluated as described by Segel (1975). Briefly, the reciprocal of the enzyme velocity was plotted against the inverse of the concentration of one substrate (A), for each fixed concentration of the second substrate (B). The ordinate-intercepts were replotted against the reciprocal of the concentration of substrate B to verify the kinetic mechanism. Values for K_M [B] and $V_{\max}$ (or k_{cat}) were calculated directly from this replot, while K_M [A] was determined from $V_{\max}$ and the average slope of the parallel lines of the original double-reciprocal plot.

Kinetic parameters for the E344Q-catalyzed reaction between succinyl-CoA and acetoacetate were evaluated differently. In this case, the abcissa-intercepts from a plot of (1/V) versus (1/[acetoacetate]) were replotted against (1/[succinyl-CoA]). Values for K_M [acetoacetate] and K_M [succinyl-CoA] were calculated directly from this replot, while $V_{\max}$ (or k_{cat}) was determined from K_M [acetoacetate] and the average slope of the parallel lines of the original double-reciprocal plot.

Finally, all standard errors were calculated using accepted formulae for the propagation of error (Parratt, 1961).

Autolytic fragmentation. Microgram quantities of the wild-type or mutant forms of CoA transferase were subjected to autolysis essentially as described in Chapter 5. Briefly, the enzyme was treated with 0.018 to 0.3 mM succinyl-CoA or 4 μM acetoacetyl-CoA in 0.10 M K[phosphate] (pH 7.4). Samples were incubated at 25 °C for 5 to 10 min and then additionally at 70 °C for 60 min. The reaction was terminated by adding an equivalent volume of SDS-PAGE loading buffer (Appendix 6), prior to analysis of the samples via denaturing PAGE.

Activation of E344Q. Samples of E344Q (final concentration, 3.7 to 5.1 mg/mL, or 71 to 98 μM of the NC monomer) were diluted with 0.072-0.10 M Tris-SO_4 (pH 8.1) and treated with acetoacetyl-CoA (final concentration, 0.73 to 1.0 mM) or succinyl-CoA (final concentration, 0.73 to 9.3 mM). Alternatively, the samples of mutant enzyme were diluted with 0.10 M K[phosphate] at pH 7.4. In some cases, acetoacetate (final concentration, 0.74 mM to 0.10 M) or succinate (final concentration, 0.10 mM to 0.10 M) was included in the reaction mixture. For experiments in which the concentration of succinate was varied, the ionic strength of the reaction mixture was maintained constant by the addition of the appropriate amount of Na_2SO_4.

To generate a sample of "activated" E344Q for subsequent autolysis, the mutant enzyme was diluted with 0.10 M K[phosphate] (pH 7.4) to a final concentration of 5.1 mg/mL (or 98 μM of the NC monomer), and subsequently treated with acetoacetyl-CoA (final concentration, 1.0 mM) for 3 h at 37 °C.

Active site titration experiments. The concentration of functional active sites in a sample of enzyme was estimated as described previously (Pickart & Jencks, 1979; Kindman & Jencks, 1981). Specifically, wild-type CoA transferase (5.8 μM of NC monomer) was treated with acetoacetyl-CoA (0.058 to 12 μM) in the presence of AHA

(0.4 mM). Alternatively, E344Q (26 μM of NC monomer) was treated with acetoacetyl-CoA (0.13 to 51 μM) in the presence of AHA (0.4 mM). In each case, the percentage of the initial enzyme activity was determined after incubation of the reaction mixture for 10 min at 22 °C. The activity of a sample of wild-type CoA transferase treated with AHA in the absence of acetoacetyl-CoA remained unchanged after 50 min at 22 °C.

Circular dichroism and fluorescence studies. Far-UV CD and fluorescence measurements were carried out as described in Chapter 2. Each protein sample was diluted to a final concentration of 0.5 to 0.6 mg/mL for CD) or 0.06 to 0.1 mg/mL for fluorescence in buffer X.[4]

Equilibrium unfolding studies. Equilibrium unfolding transitions were analyzed as outlined in Chapter 2. Proteins were denatured overnight at 4 °C in buffer X containing different concentrations of GuHCl. Measurements of far-UV CD and fluorescence were carried out at 15 °C.

Calculation of $[\Delta G_u^{\mathrm{H_2O}}]_{\mathrm{app}}$. To facilitate the numerical analyses of thermodynamic parameters, a reversible "two-state" transition between folded dimers and unfolded monomers was assumed for the wild-type and mutant forms of CoA transferase (Pace, 1975; Pace, 1986; Shortle, 1989).[5] Values of $[\Delta G_u^{\mathrm{H_2O}}]_{\mathrm{app}}$) were estimated by fitting the data to the following equations (De Francesco et al., 1991; Milla et al., 1993):

$$y = f_u\,(y_u + \mathrm{ds}[\mathrm{GuHCl}]) + (1-f_u)(y_n + \mathrm{ns}[\mathrm{GuHCl}])$$

$$f_u = \{-K_{\mathrm{d,app}} + ([K_{\mathrm{d,app}}]^2 + 8\mathrm{P}_t\,K_{\mathrm{d,app}})^{0.5}\}/(4\mathrm{P}_t)$$

$$K_{\mathrm{d,app}} = \exp\{(-[\Delta G_u^{\mathrm{H_2O}}]_{\mathrm{app}} + m[\mathrm{GuHCl}])/RT\}$$

where y is $[\Theta]_{\mathrm{obs}}$ or $\lambda_{\mathrm{max,em}}$ at a given concentration of GuHCl; y_n and y_u are the extrapolated ordinate-intercept values of $[\Theta]_{\mathrm{obs}}$ or $\lambda_{\mathrm{max,em}}$ for the native and unfolded protein, respectively; ns and ds are the slopes of the baselines for the native and denatured protein, respectively; f_u is the molar fraction of unfolded protein; $K_{d,app}$ is the apparent equilibrium dissociation constant; P_t is the total concentration of monomeric protein in mol/L; R is the universal gas constant (8.31 J/mol·K); T is the absolute temperature (K): and m is a constant proportional to the increase in the solvent-accessible surface area of the protein upon denaturation (Schellman, 1978; Myers et al., 1995).[6]

The data were fit to the appropriate equations using the program TableCurve 2D (Jandel), as described in Chapter 2.

Inactivation of CoA transferase by DTNB. Inactivation experiments were carried out as described by White et al. (1976). Preparations of C67S, C235S, or wild-type CoA transferase were dialyzed as described in Chapter 2 against 0.5 L of 10 mM Tris-HCl (pH 8.0) prior to inactivation. Each enzyme sample (final concentration, 40 µg/mL, or 0.77 µM of NC monomer) was treated with 0.4 mM DTNB in a buffer containing 0.2 M Tris-HCl and 0.8 mM EDTA, at pH 8.0. Treated samples were incubated at 22 °C in the presence or absence of acetoacetyl-CoA (final concentration, 0.40 to 4.0 µM) or succinyl-CoA (0.40 to 48 µM). Aliquots were removed from the reaction mixture at various times and assayed for enzyme activity.

The reversibility of the inactivation by DTNB was assessed by adding DTT (final concentration, 2 mM) to aliquots which were removed from the reaction mixture. These aliquots were then incubated under an atmosphere enriched in nitrogen for 3 h at 22 °C prior to being assayed for CoA transferase activity. The nitrogen was included to decrease the frequency of inactivating oxidation reactions.

The sample of wild-type CoA transferase used in these studies consisted of pure homodimer, isolated as described in Chapter 4. In contrast, the samples of C67S and C235S consisted of homodimeric and homotetrameric forms. This difference in the enzyme preparations was inconsequential, since results from separate experiments indicated that the large and small forms of CoA transferase are inactivated by DTNB at similar rates in the presence or absence of acetoacetyl-CoA.

In general, the CoA transferase activity decreased to approximately 80% of the initial value upon incubation of the enzyme in a solution containing acetoacetyl-CoA but lacking DTNB. This decrease in activity, which was apparently complete within 5 min, was presumably due to a slow acylation of the enzyme under these conditions (Chapter 1). Thus, the amount of CoA transferase activity remaining in solutions containing 0.4 mM DTNB was calculated as the percentage of the "corrected" initial enzyme activity, which is equal to 80% of the true enzyme activity.

Active site complementation. To prepare a hybrid of C67S and E344A subunits, an equimolar mixture of the C67S and E344A mutants (final concentration of each NC monomer, 4.8 or 9.6 μM) was denatured in unfolding buffer (Chapter 2) at 22 °C for 6 h. As a control, both mutants (final concentration of NC monomer, 9.6 or 19.2 μM) were denatured individually under the same conditions. The solutions of the unfolded proteins were then diluted 1:50 (v/v) with refolding buffer (Chapter 2) and incubated for 4 h at 22 °C before being assayed for enzyme activity.

Kinetic data analysis. Kinetic data (Figures 6-6 and 6-14) were fit to single-exponential curves using the program TableCurve 2D (Jandel Scientific, San Rafael, CA). The data and best-fit curves were subsequently plotted using the program SigmaPlot (also from Jandel).

RESULTS

Effects of replacing glutamate 344 with alanine or aspartate. The results of mass spectral analyses (Chapter 5) and the strict conservation of the "ENG" motif indicated that glutamate 344 is the catalytic nucleophile of pig heart CoA transferase. Furthermore, given the specificity of the enzyme for acetoacetate and succinate (Chapter 1), it was postulated that a very precise fit between the substrates and the catalytic groups of the active site is required for optimal CoA transferase activity. If this hypothesis were true, then a mutant form of the enzyme in which glutamate 344 is replaced with an alanine or aspartate residue should be much less active than wild-type CoA transferase.

The E344A and E344D mutants were constructed by site-directed mutagenesis (see "Experimental Procedures"). Each enzyme form was isolated from a recombinant strain of *E. coli* BL21(DE3) and subsequently characterized. The specific activity of E344A was more than 3 orders of magnitude lower than that of the wild-type enzyme (Table 6-1). In addition, E344D did not display a detectable level of activity. Based on the sensitivity of the enzyme assay method, it was estimated that E344D is at least 10^5 times less active than wild-type CoA transferase (Table 6-1). Neither enzyme form was susceptible to autolytic fragmentation upon heating in the presence of succinyl-CoA (Figure 6-3), demonstrating that both mutants are incapable of forming a covalent intermediate with CoA. These results confirmed that the sidechain of glutamate 344 is required for catalysis by CoA transferase.

To ensure that the replacement of glutamate 344 did not markedly alter the conformation of the enzyme, the spectrophotometric properties of E344A were investigated. The far-UV CD spectrum recorded for the mutant enzyme was similar to that determined for wild-type CoA transferase (Figure 6-4). In addition, the excitation of E344A at 295 nm produced a $\lambda_{max,em}$ of 335.0 nm, equal to the maximum observed for the wild-type enzyme (Table 6-2). It was therefore concluded that E344A and wild-type CoA transferase are similar with respect to their secondary structures and the accessibility of their tryptophan residues to solvent.

The E344A mutant was also examined with respect to its stability in GuHCl. Measurements of $[\Theta_{obs,222}]$ and $\lambda_{max,em}$ were carried out following incubation of the enzyme with different concentrations of GuHCl. The values of $[\Delta G_u^{H_2O}]_{app}$ and $[GuHCl]_{1/2}$ calculated for E344A by far-UV CD and fluorescence analyses (Table 6-3)

Table 6-1: Specific Enzyme Activities of Wild-Type and Mutant Forms of CoA Transferase

Enzyme	Specific activity[a] (μmol/min/mg)	% of wild-type specific activity[b]
Wild-type	25.2 ± 1.2[c]	100
E344A	0.015[d]	0.059
E344D	$\leq 2.4 \times 10^{-4}$[d]	$\leq 9.5 \times 10^{-4}$
E344Q	0.35 ± 0.02[e]	1.4
C67S	7.1 ± 0.2[f]	28
C235S	22.4 ± 1.0[f]	89

[a] Specific enzyme activities were calculated as described in "Experimental Procedures".

[b] Percentages refer to the mean specific activity divided by 0.252.

[c] The specific activity is expressed as the average of six calculations, corresponding to preparations of the homodimeric and homotetrameric forms of the enzyme. The error is the sample standard deviation (σ_{n-1}).

[d] Data for E344A and E344D are from single measurements only.

[e] The specific activity is expressed as the average of three calculations, corresponding to a single preparation of enzyme. The error is the sample standard deviation (σ_{n-1}).

[f] The specific activity is expressed as the average of two calculations, corresponding to a single preparation of enzyme. The error is the deviation from the mean.

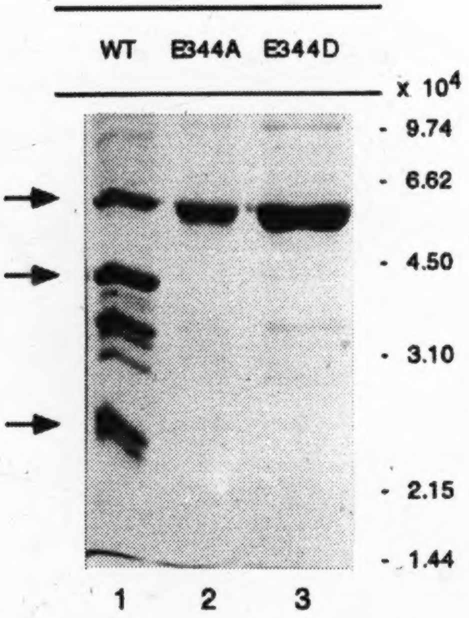

Figure 6-3: Inability of E344A and E344D to undergo autolysis. Enzyme samples (20 μg, or 0.38 nmol of the NC monomer) were incubated at 25 °C for 15 min and then at 70 °C for 60 min in the presence of 18 μM succinyl-CoA. The samples were then analyzed by SDS-PAGE. Lane 1, wild-type CoA transferase; lane 2, E344A; lane 3, E344D. The top arrow identifies the band corresponding to the intact enzyme, while the lower two arrows indicate bands corresponding to the fragments generated by autolysis. The gel was stained with Coomassie Blue.

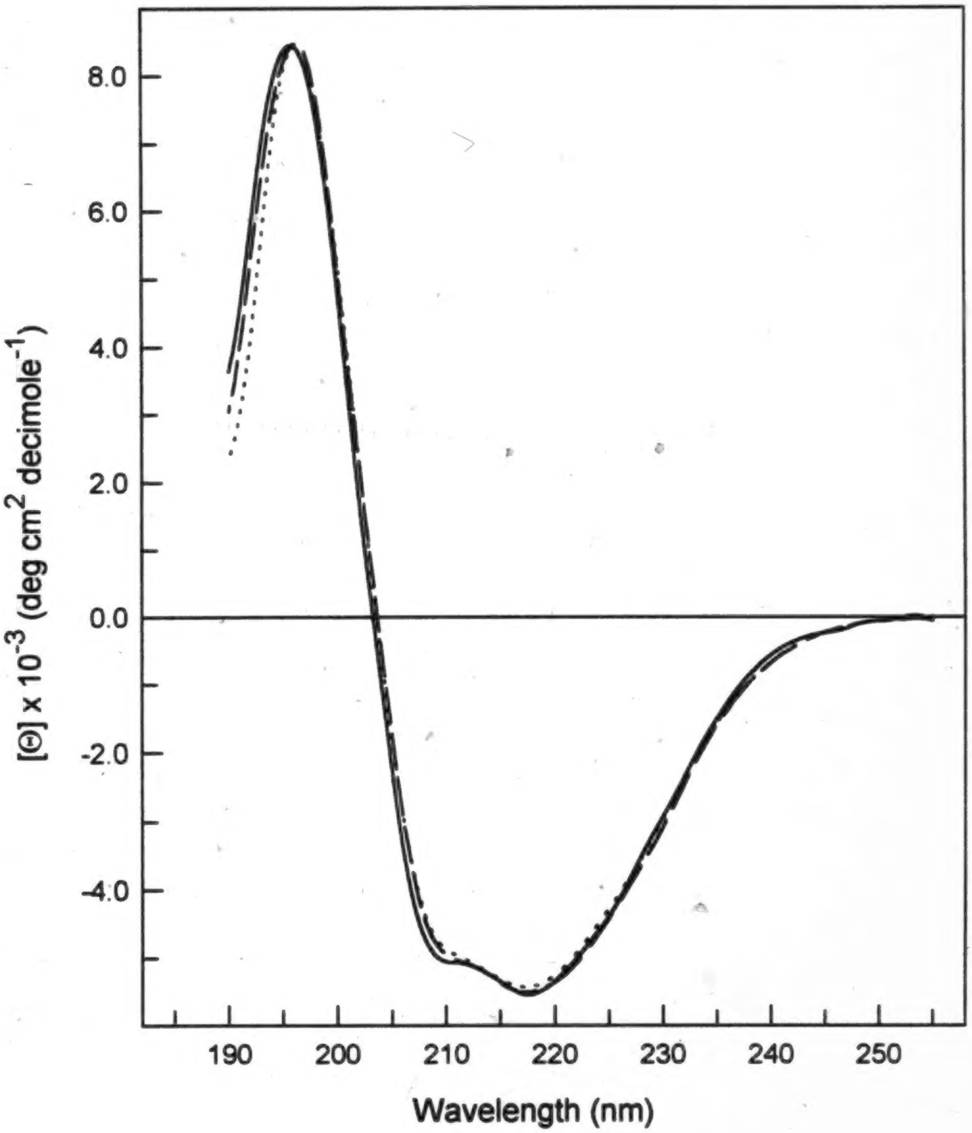

Figure 6-4: Analysis of mutant forms of CoA transferase by far-UV CD (part 1). Spectra were recorded for the wild-type enzyme (——), E344A (– – –), and E344Q (· · · ·) as described in "Experimental Procedures".

Table 6-2: Fluorescence Properties of Wild-Type and Mutant Forms of CoA Transferase

Sample[a]	$\lambda_{max,em}$[b] (nm)
Wild-type[c]	335.1
E344A	335.0
E344Q	335.5
C67S	334.3
Tryptophan	348.1

[a] Enzyme samples were purified in the presence of 2ME, without fractionation into homodimeric and homotetrameric species by gel filtration.

[b] Wavelength of maximal tryptophan fluorescence; excitation at 295 nm.

[c] Data were taken from Table 2-2.

Table 6-3: Denaturation of Wild-Type and Mutant Forms of CoA Transferase with GuHCl

Part A: Parameters derived from far-UV CD measurements[a]

Protein	P_t (μM)	$[\Delta G_u^{H_2O}]_{app}$ (kJ/mol)	m (kJ/mol/M)	$[GuHCl]_{1/2}$[b] (M)
Wild-type[c]	11	46 ± 0.0	20 ± 0.4	0.97 ± 0.02
E344A[d]	9.1	46 ± 2.1	17 ± 2.1	0.97 ± 0.13
E344Q[d]	11	46 ± 0.4	18 ± 0.0	1.0 ± 0.01
C67S[d]	12	40 ± 1.7	13 ± 1.3	1.0 ± 0.11

Part B: Parameters derived from fluorescence measurements[a]

Protein	P_t (μM)	$[\Delta G_u^{H_2O}]_{app}$ (kJ/mol)	m (kJ/mol/M)	$[GuHCl]_{1/2}$[b] (M)
Wild-type[c]	3.6	41 ± 1.7	18 ± 2.5	0.59 ± 0.08
E344A[d]	2.7	37 ± 0.8	10 ± 0.8	0.66 ± 0.06
E344Q[d]	2.1	40 ± 0.8	11 ± 1.3	0.81 ± 0.10
C67S[d]	2.0	38 ± 0.8	8.4 ± 1.3	0.82 ± 0.12

[a] The error shown for each parameter is the standard error due to fitting of the curve, and may therefore be an underestimate. The actual experimental error can be reasonably estimated to be as high as ± 10%.

[b] Calculated from: $[GuHCl]_{1/2} = \{(RT \ln P_t) + [\Delta G_u^{H_2O}]_{app}\} \div m$ (Mok et al., 1996).

[c] The wild-type enzyme sample consisted of the homodimeric form, purified in the presence of 2ME. Data were taken from Table 4-3.

[d] Mutant enzyme samples were purified in the presence of 2ME, without fractionation into homodimeric and homotetrameric species by gel filtration.

were similar to those determined for the purified, wild-type homodimer (Table 4-3; Table 6-3) and homotetramer (Table 4-3) at 15 °C. Thus, the conformational stabilities of E344A and wild-type CoA transferase are equal within experimental error.

Effects of replacement of glutamate 344 with glutamine. Since no significant enzyme activity was associated with E344D, it was concluded that the length of the acidic sidechain at position 344 is critical to the catalytic function of CoA transferase. Subsequently, it was also predicted that the activity of the wild-type enzyme depends on the nucleophilicity of the glutamate 344 γ-carboxylate group. If this hypothesis were true, then a mutant form of CoA transferase in which glutamate 344 is replaced with a glutamine residue should be less active than the wild-type enzyme, given that the amide moiety of glutamine is less basic (or nucleophilic) than the γ-carboxylate group of glutamate (Homer & Johnson, 1970).

The E344Q mutant of CoA transferase was produced and isolated as described above. The specific activity of E344Q was almost 2 orders of magnitude less than that of the wild-type enzyme (Table 6-1), implying that the nucleophilicity of the glutamate 344 sidechain contributes substantially to the activity of wild-type CoA transferase. A double-reciprocal plot of data from kinetic analyses of E344Q gave a series of parallel lines, consistent with a "ping-pong" kinetic mechanism for the mutant. Most of the decrease in specific activity of E344Q compared to wild-type CoA transferase was due to a lower k_{cat} for the reaction between succinyl-CoA and acetoacetate, with little change in the K_M values for these substrates (Table 6-4). Similar results were obtained when the kinetic analysis of E344Q was repeated for the reaction between acetoacetyl-CoA and succinate (Table 6-4).

To verify that the reduced catalytic function of the mutant enzyme was not merely due to a pronounced conformational change, the spectrophotometric and equilibrium unfolding properties of E344Q were analyzed. The far-UV CD spectrum recorded for

Table 6-4: Kinetic Constants of Wild-Type and Mutant Forms of Pig Heart CoA Transferase

Kinetic parameter	Wild-type enzyme[a]	E344Q	C67S
$k_{cat[forward]}$[b] ($\times 10^4$ min^{-1})	7.5 ± 0.4[d]	0.22 ± 0.12 (0.088 ± 0.048)[c]	4.9 ± 0.4
K_M [acetoacetyl-CoA] (mM)	0.20 ± 0.04	0.20 ± 0.11	0.097 ± 0.010
K_M [succinate] (mM)	20 ± 4	25 ± 13	39 ± 4
$k_{cat[reverse]}$[d] ($\times 10^3$ min^{-1})	5.9 ± 0.4	0.030 ± 0.002 (0.012 ± 0.001)[c]	0.55 ± 0.08
K_M [succinyl-CoA] (mM)	6.5 ± 0.5	1.9 ± 0.1	1.7± 0.3
K_M [acetoacetate] (mM)	0.10 ± 0.03	0.094 ± 0.004	0.049± 0.008

[a] Data taken from Moore & Jencks (1982). See Table 1-4.

[b] Forward direction: [acetoacetyl-CoA + succinate → succinyl-CoA + acetoacetate].

[c] Values in parentheses are corrected values, assuming that the mutant and wild-type enzymes account for 40% and 60% (respectively) of the total activity associated with the preparation of E344Q (Appendix 7).

[d] Reverse direction: [succinyl-CoA + acetoacetate → acetoacetyl-CoA + succinate].

E344Q was similar to that observed for the wild-type enzyme (Figure 6-4). In addition, the excitation of E344Q at 295 nm produced a $\lambda_{\mathrm{max,em}}$ of 335.5 nm, which is only marginally red-shifted compared to the maximum determined for wild-type CoA transferase (Table 6-2). Finally, the values of $[\Delta G_u^{\mathrm{H_2O}}]_{\mathrm{app}}$ and $[\mathrm{GuHCl}]_{1/2}$ calculated for E344Q by measurements of $[\Theta_{\mathrm{obs,222}}]$ and $\lambda_{\mathrm{max,em}}$ (Table 6-3) were similar to those determined for the purified, wild-type homodimer (Table 4-3; Table 6-3) and homotetramer (Table 4-3) at 15 °C. Thus, E344Q and wild-type CoA transferase are identical (within experimental error) with respect to their secondary structures, the exposure of their tryptophan residues to solvent, and their conformational stabilities.

Activation of E344Q — effects of acyl-CoA substrates. Interestingly, a slow increase in the activity of purified E344Q was detected during prolonged incubation of the enzyme in the CoA transferase assay solution. In contrast, the activity of E344Q was unchanged after treatment of the enzyme with acetoacetate or succinate in the absence of acyl-CoA substrates. To account for these preliminary observations, it postulated that the active site glutamine residue of E344Q is deamidated to produce glutamate and thus wild-type CoA transferase by a reaction which depends on the participation of an "energy-rich" thiolester. This hypothesis was addressed by incubating the mutant enzyme in the absence or presence of acetoacetyl-CoA or succinyl-CoA (final concentration of each, 1.0 mM) for 4 h at 22 °C prior to the measurement of CoA transferase activity. Although the activity of E344Q increased 3-fold in a solution containing acetoacetyl-CoA, a similar effect was not observed for the enzyme sample treated with succinyl-CoA (Figure 6-5A). In addition, E344Q was not activated in a solution containing succinyl-CoA at a concentration of 9.3 mM, well above the K_M for this substrate (Table 6-4). The increase in the activity of E344Q in the presence of acetoacetyl-CoA was inhibited by free CoA (Figure 6-5B), indicating that the thiolester linkage of acetoacetyl-CoA is essential for activation. In addition, the activation of E344Q occurred with apparent first-order

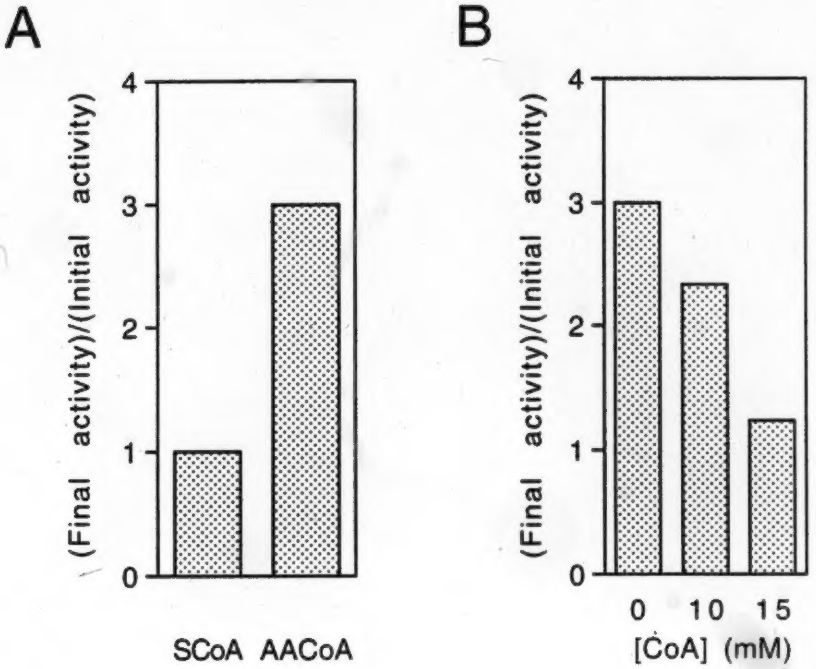

Figure 6-5: Activation of E344Q in the presence of acetoacetyl-CoA. A sample of the mutant enzyme was diluted with 0.10 M Tris-SO_4 (pH 8.1) to a final concentration of 5.1 mg/mL (or 98 μM of the NC monomer). (A) The sample of E344Q was incubated in a solution containing succinyl-CoA (SCoA) or acetoacetyl-CoA (AACoA) (final concentration of each, 1.0 mM) for 4 h at 22 °C. (B) The sample of E344Q was incubated in a solution containing acetoacetyl-CoA (final concentration, 1.0 mM) for 4 h at 22 °C, in the absence or presence of CoA (final concentration, 10 or 15 mM). "(Final activity)/(Initial activity)" refers to the ratio of the enzyme activities associated with the treated and untreated samples of E344Q.

kinetics. Both the yield of enzyme activity and the apparent first-order rate constant increased with increasing temperature between 22 °C and 37 °C (Figure 6-6). In contrast, E344Q was not activated upon incubation in the presence of acetoacetyl-CoA at 4 °C (not shown). Finally, the susceptibility of E344Q to autolysis increased dramatically following the preincubation of the enzyme with acetoacetyl-CoA (final concentration, 1 mM) for 3 h at 37 °C (Figure 6-7). From these observations, it was concluded that: (1) E344Q is activated (presumably by the deamidation of glutamine 344) upon incubation of the enzyme with acetoacetyl-CoA, but not with succinyl-CoA; and (2) prior to activation, ECoA is formed very inefficiently from E344Q in the presence of acyl-CoA substrate.

Activation of E344Q — effect of carboxylate substrates. The experiments described above indicated that the energy-rich thiolester linkage of acetoacetyl-CoA is necessary for the activation of E344Q. Accordingly, it was predicted that one possible route for the deamidation of glutamine 344 involves the transient formation of ECoA, in which CoA is covalently linked to a glutamate residue at position 344. If the release of CoA from this intermediate were rate-limiting, then both carboxylate substrates should enhance the activation of E344Q by facilitating the breakdown of ECoA, as per the normal catalytic cycle.

The mutant enzyme was treated with acetoacetyl-CoA (final concentration, 0.73 mM) and acetoacetate (final concentration, 0.74 or 74 mM) for 8 h at 22 °C. At the lower concentration of the carboxylate substrate, the activation of E344Q was unchanged compared to a reaction which lacked acetoacetate (Figure 6-8A). In contrast, the deamidation of glutamine 344 was partially inhibited by acetoacetate at a concentration of 74 mM, which is 7.9×10^2 times the K_M of E344Q for the carboxylate substrate (Table 6-4). From these observations, it was inferred that the rate of activation of E344Q decreases as the concentration of acetoacetate becomes saturating, presumably due to the weak binding of acetoacetyl-CoA to the enzyme under these conditions.

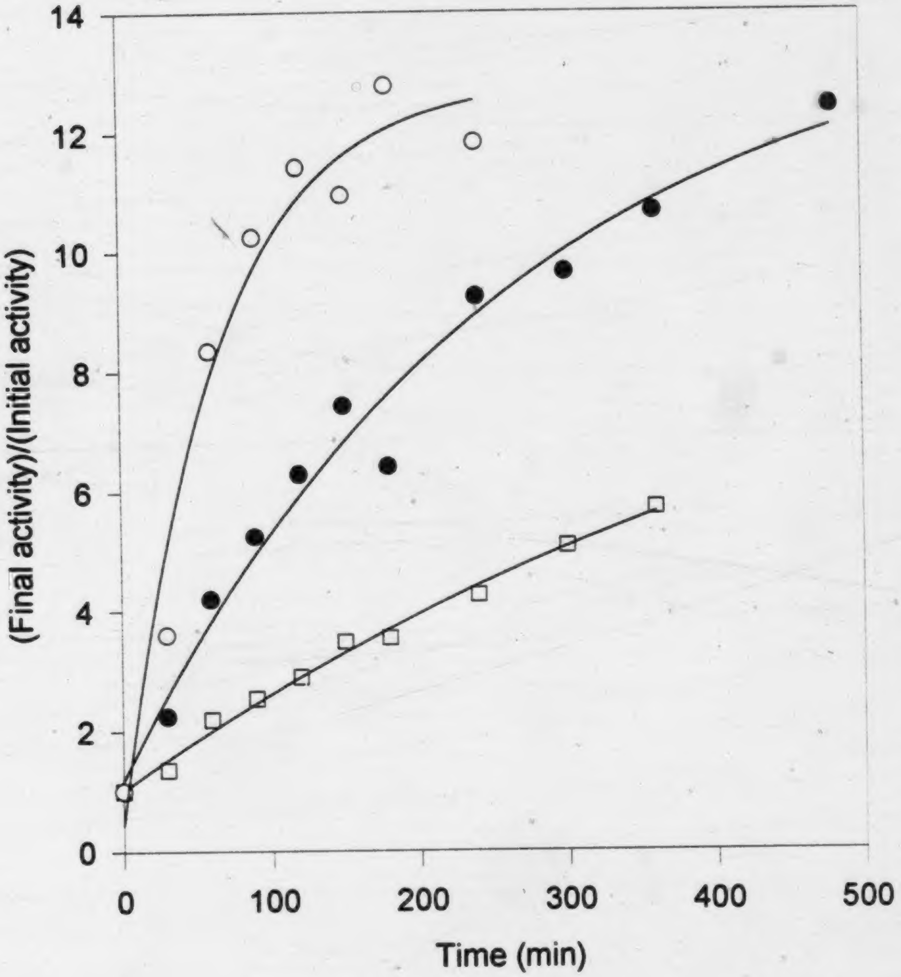

Figure 6-6: Kinetics of activation of E344Q at various temperatures. A sample of the mutant enzyme was diluted with 0.10 M K[phosphate] (pH 7.4) to a final concentration of 5.1 mg/mL (or 98 μM of the NC monomer). The sample was incubated in the presence of acetoacetyl-CoA (final concentration, 1.0 mM) for various times at 22 °C (☐), 30 °C (●), or 37 °C (○). The apparent first-order rate constants are: 22 °C, $k = 2.9 \pm 1.1 \times 10^{-5}$ s^{-1} ($r^2 = 0.99$); 30 °C, $k = 6.3 \pm 1.4 \times 10^{-5}$ s^{-1} ($r^2 = 0.98$); and 37 °C, $k = 2.6 \pm 0.6 \times 10^{-4}$ s^{-1} ($r^2 = 0.96$). "(Final activity)/(Initial activity)" refers to the ratio of the enzyme activities associated with the treated and untreated samples of E344Q.

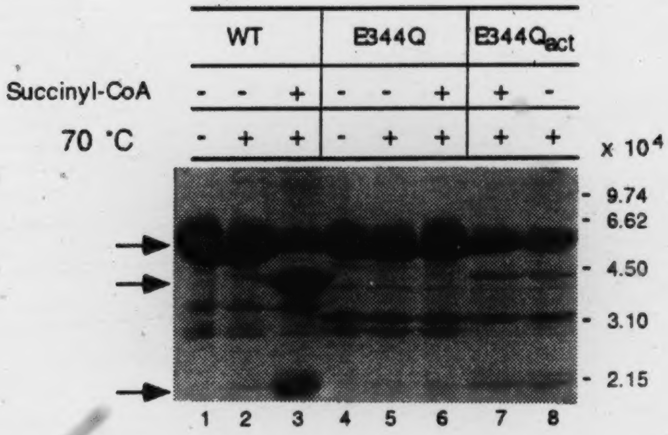

Figure 6-7: Autolytic fragmentation of E344Q. Enzyme samples (95 µg, or 1.8 nmol of the NC monomer) were incubated at 22 °C for 5 min and then at 70 °C for 60 min in the absence (lanes 2, 5, and 8) or presence (lanes 3, 6, and 7) of 0.3 mM succinyl-CoA. As controls, two samples were incubated at 22 °C for 65 min in the absence of succinyl-CoA (lanes 1 and 4). The samples were then analyzed by SDS-PAGE. Lanes 1 to 3, wild-type CoA transferase; lanes 4 to 6, E344Q, not previously activated; lanes 7 and 8, E344Q, previously activated. The top arrow identifies the band corresponding to the intact enzyme, while the lower two arrows indicate bands corresponding to the fragments generated by autolysis. The gel was stained with Coomassie Blue.

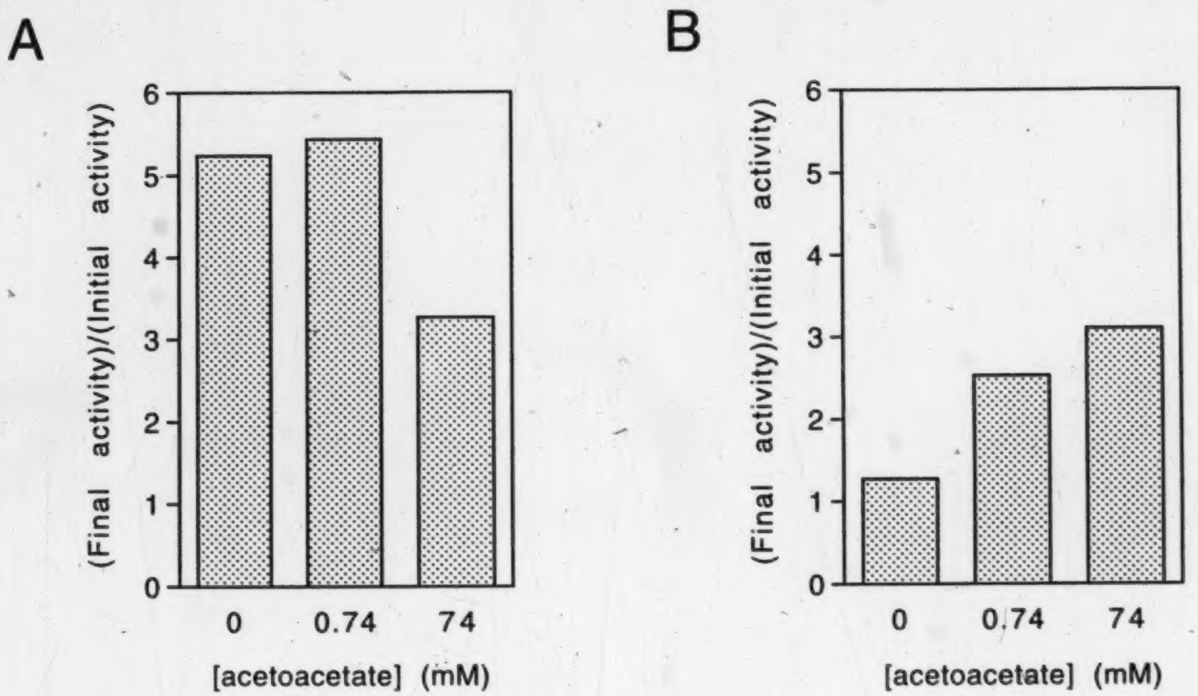

Figure 6-8: Effect of acetoacetate on the activation of E344Q. A sample of the mutant enzyme was diluted with 0.072 M Tris-SO_4 (pH 8.1) to a final concentration of 3.7 mg/mL (or 71 μM of the NC monomer). The sample of E344Q was incubated in the presence of acetoacetyl-CoA (A) or succinyl-CoA (B) (final concentration of each, 0.73 mM) for 8 h at 22 °C. Some reaction mixtures also contained acetoacetate (final concentration, 0.74 or 74 mM). "(Final activity)/(Initial activity)" refers to the ratio of the enzyme activities associated with the treated and untreated samples of E344Q.

The yield of activation of E344Q in the presence of succinyl-CoA (final concentration, 0.73 mM) increased with the concentration of acetoacetate (Figure 6-8B). The incubation of E344Q in the presence of 74 mM acetoacetate and succinyl-CoA or acetoacetyl-CoA led to equivalent extents of deamidation (Figure 6-8). Thus, the activation of E344Q by succinyl-CoA was markedly stimulated by acetoacetate, even under conditions which weaken the binding of the acyl-CoA substrate to the enzyme.

Subsequently, it was examined whether or not E344Q is activated by succinyl-CoA in the presence of succinate rather than acetoacetate. The mutant enzyme was incubated with succinyl-CoA (final concentration, 1.0 mM) and succinate (final concentration, 0.10 mM to 0.10 M) for 4 h at 22 °C. Under all conditions examined, the initial and final enzyme activities of E344Q were equivalent (Figure 6-9A). Thus, in contrast to acetoacetate, succinate did not facilitate the deamidation of glutamine 344 by succinyl-CoA.

Finally, the effect of succinate on the activation of E344Q by acetoacetyl-CoA was investigated. The mutant enzyme was incubated with acetoacetyl-CoA (final concentration, 1.0 mM) and succinate (final concentration, 0.10 mM to 0.10 M) for 4 h at 22 °C. An increase in the concentration of the carboxylate substrate led to a progressive decrease in the degree of activation of E344Q, such that the extent of deamidation was only half-maximal in a solution containing 1 mM succinate (Figure 6-9B). From these observations, we concluded that the binding of succinate at the active site of E344Q inhibits the deamidation of glutamine 344.

Importantly, the inhibitory effect of succinate was much more pronounced than that displayed by acetoacetate (compare Figures 6-8A and 6-9B). However, the results of kinetic analyses indicated that succinate binds E344Q with much lower affinity than acetoacetate (Table 6-4). Thus, the decrease in the extent of activation of E344Q with increasing succinate concentration could not be due simply to the diminished binding of acetoacetyl-CoA to the active site under these conditions. Instead, it was proposed that

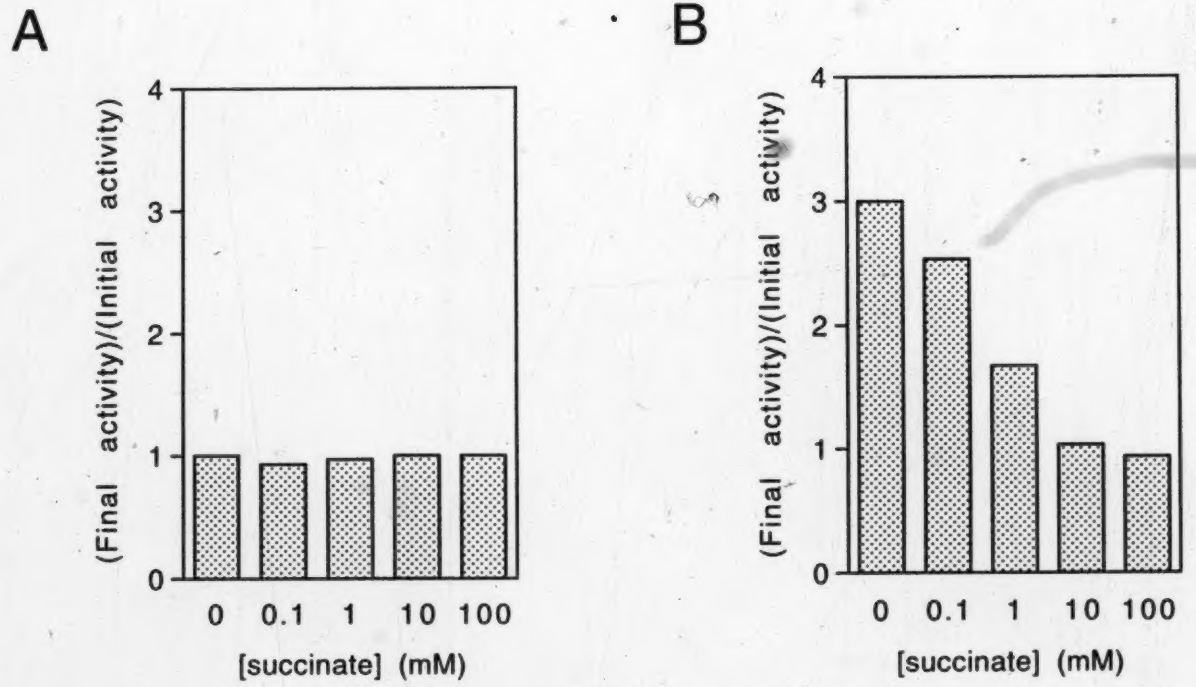

Figure 6-9: Effect of succinate on the activation of E344Q. A sample of the mutant enzyme was diluted with 0.10 M Tris-SO_4 (pH 8.1) to a final concentration of 5.1 mg/mL (or 98 µM of the NC monomer). The sample of E344Q was incubated in the presence of succinyl-CoA (A) or acetoacetyl-CoA (B) (final concentration of each, 1.0 mM) for 4 h at 22 °C. Some reaction mixtures also contained succinate (final concentration, 0.10 mM to 0.10 M). "(Final activity)/(Initial activity)" refers to the ratio of the enzyme activities associated with the treated and untreated samples of E344Q.

succinate inhibits the deamidation of glutamine 344 by interfering with a step which follows the binding of acetoacetyl-CoA to the enzyme. Acetoacetate does not prevent this reaction, and is therefore not inhibitory to the same extent as succinate. If this hypothesis were true, then the activation of E344Q in the presence of succinate should be partially restored by increasing the concentration of acetoacetate in the reaction mixture. The mutant enzyme was incubated with acetoacetyl-CoA (final concentration, 1.0 mM), acetoacetate (final concentration, 1.0 mM or 0.10 M), and succinate (final concentration, 10 μM to 10 mM), for 8 h at 22 °C. In the presence of 1.0 mM acetoacetate, the degree of activation of E344Q decreased markedly as the concentration of succinate was raised above 0.10 mM (Figure 6-10). However, in the presence of 0.10 M acetoacetate, a significant decrease in the extent of activation of E344Q only occurred as the concentration of succinate was raised above 1.0 mM (Figure 6-10). In the absence of succinate, the degree of activation of E344Q was greater at the lower concentration of acetoacetate (Figure 6-10), presumably due to the more efficient binding of acetoacetyl-CoA to the enzyme under these conditions.

In conclusion, the varying effects of the carboxylate substrates on the activation of E344Q were complex, and did not prove whether or not the breakdown of ECoA limits the rate of deamidation of glutamine 344. Acetoacetate was found to stimulate the activation of E344Q by succinyl-CoA, while succinate inhibited the acetoacetyl-CoA-dependent reaction. The inhibition by succinate was partially offset by acetoacetate, suggesting that succinate disrupts the deamidation of glutamine 344 by associating with the enzyme after acetoacetyl-CoA has reacted at the active site.

Active site titration of E344Q. Since E344Q could be activated in the presence of acetoacetyl-CoA, it was postulated that the mutant enzyme might also be partially converted to wild-type CoA transferase *in vivo* prior to protein purification. Thus, it was conceivable that the sample of E344Q isolated from BL21(DE3) contained a background level of contaminating wild-type enzyme.

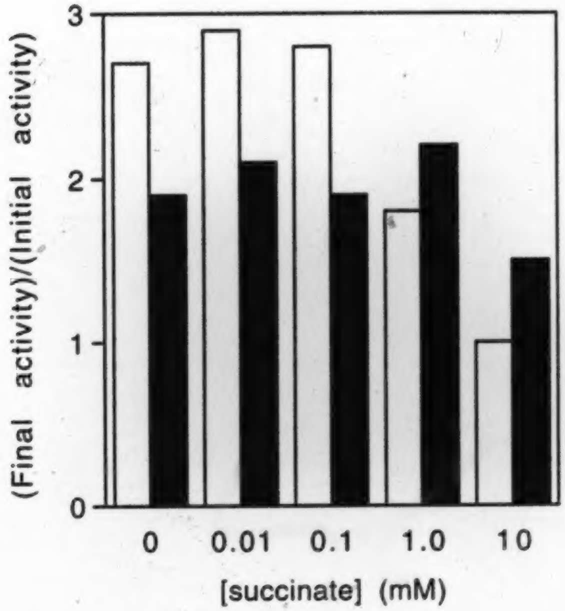

Figure 6-10: Effect of acetoacetate on the succinate-dependent inhibition of the activation of E344Q. A sample of the mutant enzyme was diluted with 0.10 M Tris-SO_4 (pH 8.1) to a final concentration of 5.1 mg/mL (or 98 μM of the NC monomer). The sample was incubated for 8 h at 22 °C in the presence of acetoacetyl-CoA (final concentration, 1.0 mM) and acetoacetate at a final concentration of 1.0 mM (white bars) or 0.10 M (black bars). Some reaction mixtures also contained succinate (final concentration, 10 μM to 10 mM). "(Final activity)/(Initial activity)" refers to the ratio of the enzyme activities associated with the treated and untreated samples of E344Q.

The purity of the E344Q sample was assessed by active site titration. Previously, Kindman & Jencks (1981) showed that the proportional amount of fully active species in a sample of CoA transferase can be determined by treating the enzyme with various concentrations of acyl-CoA in the presence of excess AHA. Since ECoA reacts with AHA to form an inactive, mixed anhydride (Pickart & Jencks, 1979), the number of functional active sites can be calculated from the concentration of acetoacetyl-CoA at which the enzyme is maximally inhibited.

It was predicted that the purified sample of E344Q consisted of a mixture of wild-type and mutant enzymes. If this were true, then the fractional enzyme activity of this mixture associated with wild-type CoA transferase should decrease with increasing concentrations of acetoacetyl-CoA. In contrast, the proportional activity due to the mutant enzyme should be relatively resistant to inactivation, given that E344Q is not readily converted to ECoA during short incubations with acyl-CoA substrate (see above). Aliquots of the E344Q preparation were treated with AHA (0.4 mM) and acetoacetyl-CoA (at concentrations ranging from 0.005 to 2 times that of the NC monomer). The total enzyme activity associated with the E344Q sample decreased sharply to a minimum of 58% of the initial value as the concentration of acetoacetyl-CoA was increased up to 0.01 times that of the NC monomer (Figure 6-11). In the presence of higher concentrations of acetoacetyl-CoA, the total enzyme activity associated with the E344Q sample decreased much more gradually. From these observations, it was concluded that the preparation of E344Q contained subpopulations of wild-type CoA transferase and mutant enzyme.

To evaluate the proportional amounts of the wild-type and mutant enzymes in the E344Q sample, it was first necessary to determine the maximal degree of inactivation of pure, wild-type CoA transferase under the conditions of the experiment described above. The active site titration curve determined for the wild-type enzyme consisted of two linear portions (Figure 6-11): (1) a region of relatively large, negative slope, for concentrations of acetoacetyl-CoA less than or equal to the concentration of NC

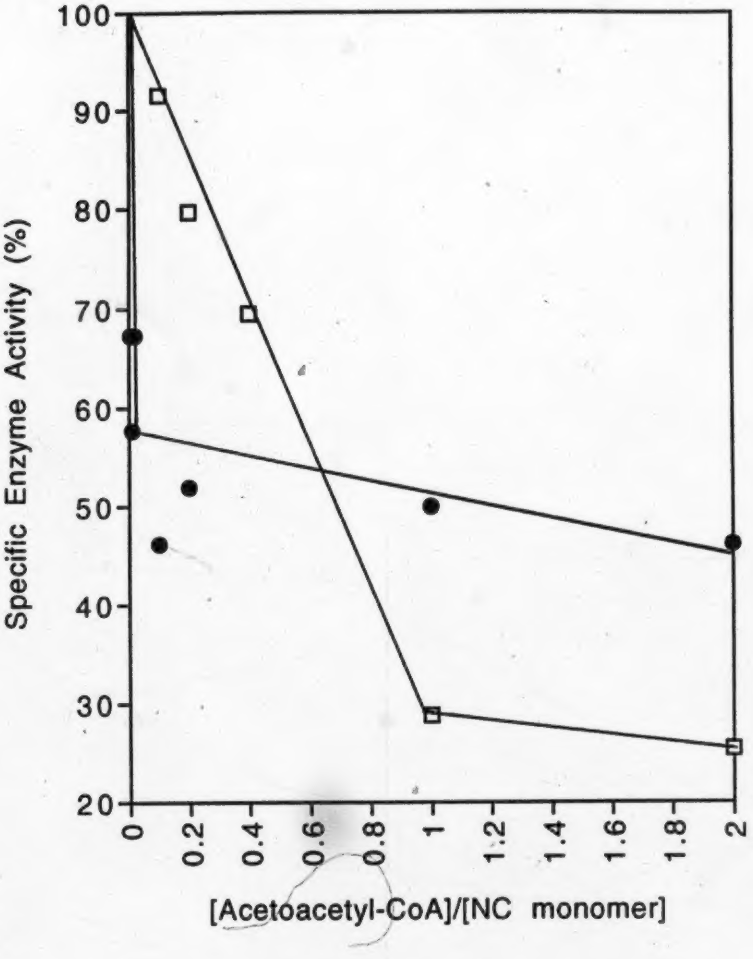

Figure 6-11: Titration of functional active sites within the sample of E344Q. Preparations of wild-type CoA transferase (❑) and the mutant enzyme (●) were treated with different molar ratios of acetoacetyl-CoA in the presence of AHA (0.4 mM). Following incubation for 10 min at 22 °C, the reaction mixtures were assayed for CoA transferase activity.

monomer; and (2) a region of relatively small, negative slope, for concentrations of acetoacetyl-CoA greater than the concentration of NC monomer. The two linear portions were intersected to form a discontinuity or "break-point," at which the concentration of acetoacetyl-CoA was equal to that of the NC monomer. It was assumed from this control experiment that 30% of the initial activity remains in a sample of wild-type CoA transferase treated with an equimolar amount of acetoacetyl-CoA and 0.4 mM AHA. Based on this assumption, the wild-type enzyme accounted for approximately 60% of the total enzyme activity (or 0.8% of the total protein) associated with the E344Q sample (Appendix 7).

Given that the sample of E344Q contained a background level of wild-type enzyme, the previously reported values of k_{cat} for the mutant were overestimated. Corrected values of k_{cat}, calculated by multiplying the initial values by a factor of 0.4, are shown in Table 6-4.

Thiol inactivation of C67S and C235S. From previous studies, it was demonstrated that the prolonged treatment of ECoA with thiol reagents leads to the specific modification of cysteine 67 and cysteine 235, resulting in the inactivation of the enzyme by the reversible and irreversible pathways (White et al., 1976; Williams, 1990; see "Introduction"). However, the modification of only one of these residues could account for the rapid, reversible inactivation of CoA transferase due to steric hindrance at the active site (White et al. (1976). To determine which cysteine residue was responsible for the rapid, reversible loss of enzyme activity, the C67S and C235S mutants were constructed by site-directed mutagenesis (see "Experimental Procedures"). Each enzyme form was purified from a recombinant strain of *E. coli* BL21(DE3) and subsequently characterized.

It was predicted that the single-atom replacement of sulfur by oxygen in the sidechain of amino acid residue 67 or 235 should not alter the catalytic function of CoA transferase. As expected, the specific activity of C235S was similar to that of wild-type

CoA transferase (Table 6-1). Surprisingly, however, the specific activity of C67S was 3.6 times lower than that of the wild-type enzyme (Table 6-1). A double-reciprocal plot of data from kinetic analyses of C67S gave a series of parallel lines, consistent with a "ping-pong" kinetic mechanism for the mutant. The decrease in specific activity of C67S compared to wild-type CoA transferase was due to a lower k_{cat} for the reaction between succinyl-CoA and acetoacetate, which was partially offset by lower K_M values for these substrates compared to the wild-type enzyme (Table 6-4). A kinetic analysis of the C67S-catalyzed reaction between acetoacetyl-CoA and succinate indicated that the K_M for succinate and the k_{cat} were increased and decreased (respectively) compared to the wild-type enzyme (Table 6-4). Both C67S and C235S were susceptible to autolytic fragmentation upon heating in the presence of acetoacetyl-CoA or succinyl-CoA (Figure 6-12), indicating that the mutants were capable of forming the ECoA thiolester intermediate. From these results, it was concluded that cysteine 67 fulfills a structural or functional role necessary for optimal catalysis by CoA transferase.

To ensure that the reduced specific activity of C67S was not merely due to incorrect protein folding, the spectrophotometric and equilibrium denaturation properties of the enzyme were analyzed. The far-UV CD spectrum recorded for C67S was similar to that observed for the wild-type enzyme (Figure 6-13). In addition, the excitation of C67S at 295 nm produced a $\lambda_{max,em}$ of 334.3 nm, which is only slightly blue-shifted compared to the maximum determined for wild-type CoA transferase (Table 6-2). Finally, the values of $[\Delta G_u^{H_2O}]_{app}$ and $[GuHCl]_{1/2}$ calculated for C67S by measurements of $[\Theta_{obs,222}]$ and $\lambda_{max,em}$ (Table 6-3) were similar to those determined for the purified, wild-type homodimer (Table 4-3; Table 6-3) and homotetramer (Table 4-3) at 15 °C. Thus, C67S and wild-type CoA transferase are equivalent with respect to their secondary structures, the solvent-accessibility of their tryptophan residues, and their conformational stabilities.

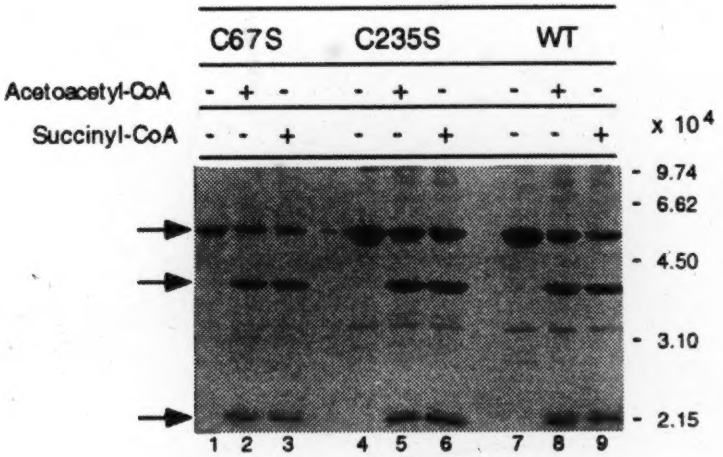
C67S
C235S
WT
Acetoacetyl-CoA
- + - - + - - + -
Succinyl-CoA
- - + - - + - - +
x 10^4
- 9.74
- 6.62
- 4.50
- 3.10
- 2.15
1 2 3 4 5 6 7 8 9

Figure 6-12: Autolytic fragmentation of C67S and C235S. Enzyme samples (10 μg, or 0.19 nmol of the NC monomer) were incubated at 22 °C for 10 min and then at 70 °C for 60 min in the absence (lanes 1, 4, and 7) or presence of 4 μM acetoacetyl-CoA (lanes 2, 5, or 8) or 48 μM succinyl-CoA (lanes 3, 6, and 9). The samples were then analyzed by SDS-PAGE. Lanes 1 to 3, C67S; lanes 4 to 6, C235S; lanes 7 to 9, wild-type CoA transferase. The top arrow identifies the band corresponding to the intact enzyme, while the lower two arrows indicate bands corresponding to the fragments generated by autolysis. The gel was stained with Coomassie Blue.

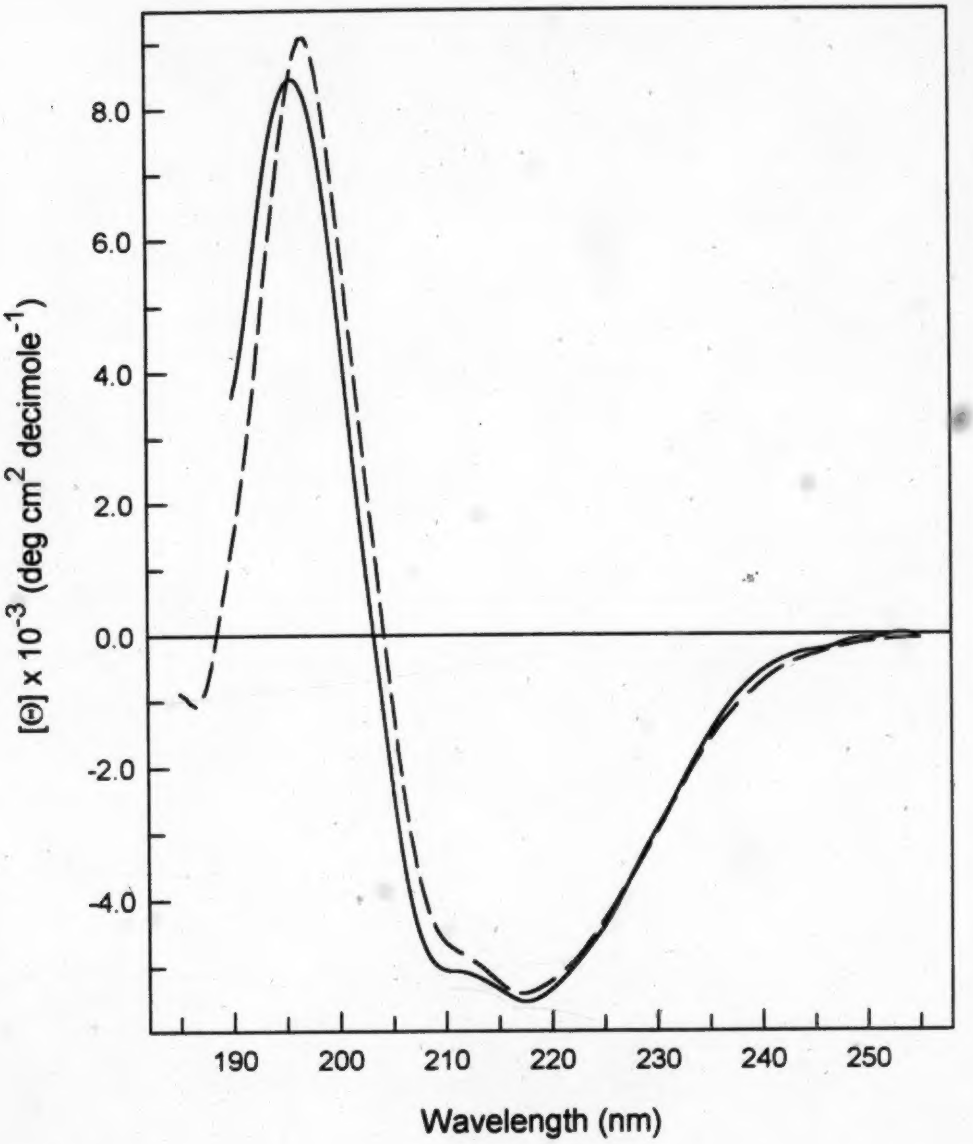

Figure 6-13: Analysis of mutant forms of CoA transferase by far-UV CD (part 2). Spectra were recorded for the wild-type enzyme (——) and C67S (– – –) as described in "Experimental Procedures".

Since the relatively low specific activity of C67S was not due to a disruption of the protein fold, it was inferred that cysteine 67 is located at or near the active site of the enzyme. Accordingly, it was predicted that the modification of this amino acid residue by thiol reagents was responsible for the rapid, reversible, and acyl-CoA-dependent inactivation of wild-type CoA transferase described previously (White et al., 1976; Kindman & Jencks, 1981; Williams, 1990). If this hypothesis were true, then the inactivation of C67S by DTNB should be relatively slow, irreversible, and independent of the formation of ECoA.

Samples of purified mutant or wild-type enzyme (final concentration, 0.77 μM of the NC monomer) were treated with DTNB as described in "Experimental Procedures," in the absence or presence of acetoacetyl-CoA (0.40 to 4.0 mM) or succinyl-CoA (0.40 to 48 μM). The C67S mutant was inactivated by the thiol reagent more slowly than the wild-type enzyme or C235S (Figure 6-14). Furthermore, C67S was inactivated somewhat less rapidly in solutions containing acyl-CoA substrate than in solutions lacking acyl-CoA substrate (Figure 6-14A). In contrast, wild-type CoA transferase and C235S were both inactivated more rapidly in the presence than in the absence of acetoacetyl-CoA or succinyl-CoA (Figure 6-14B,C). Significantly, results from autolysis experiments (Figure 6-12) indicated that the relatively slow inactivation of C67S in solutions containing acyl-CoA substrate was not due to the inability of the enzyme to form ECoA. Finally, samples of wild-type CoA transferase or C235S which were partially inactivated by DTNB in solutions containing acetoacetyl-CoA were substantially reactivated upon treatment with DTT (Figure 6-15A,B). For instance, although less than 30% of the initial activity of wild-type CoA transferase or C235S remained after incubation of the enzyme for 10 min with acetoacetyl-CoA and DTNB, 80 to 90% of the initial activity was recovered after the addition of DTT to the sample. In contrast, the inactivation of C67S by DTNB in the presence or absence of acetoacetyl-CoA was irreversible, even under reducing conditions (Figure 6-16A,B). Similarly, a sample of wild-type CoA transferase which was slowly

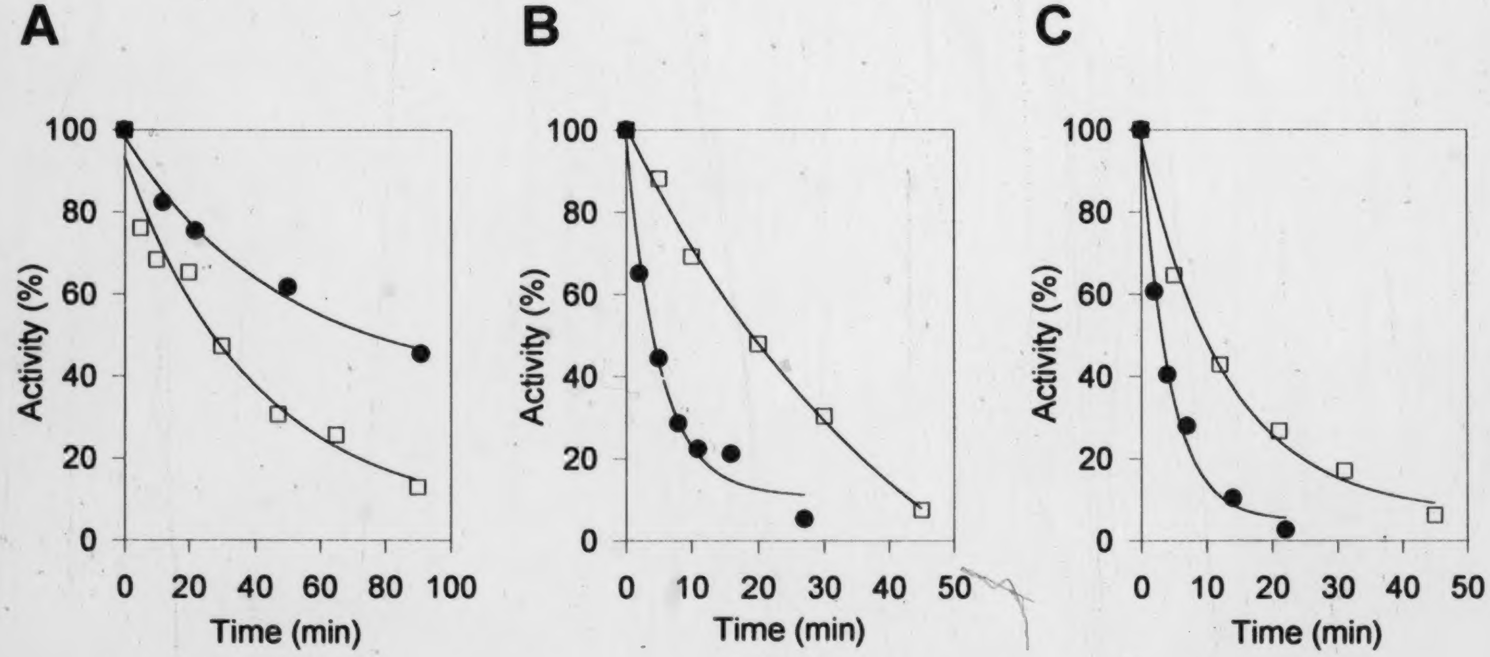

Figure 6-14: Kinetics of inactivation by DTNB. Samples of C67S (A), wild-type CoA transferase (B), and C235S (C) (final concentration, 0.77 μM of each NC monomer) were treated with DTNB in the absence (❑) or presence (●) of a 1.5-fold molar excess of acetoacetyl-CoA. Aliquots were removed at different times from the reaction mixture and assayed for CoA transferase activity. The apparent first-order rate constants are: C67S (❑), $4.1 \pm 1.3 \times 10^{-4}$ s^{-1} ($r^2 = 0.97$); C67S (●), $3.4 \pm 1.1 \times 10^{-4}$ s^{-1} ($r^2 = 0.99$); wild-type (❑), $3.7 \pm 0.8 \times 10^{-4}$ s^{-1} ($r^2 = 1.00$); wild-type (●), $3.2 \pm 0.6 \times 10^{-3}$ s^{-1} ($r^2 = 0.98$); C235S (❑), $1.3 \pm 0.2 \times 10^{-3}$ s^{-1} ($r^2 = 0.99$); C67S (●), $3.8 \pm 0.5 \times 10^{-3}$ s^{-1} ($r^2 = 0.99$). The activity is expressed as a percentage of the initial activity associated with the sample.

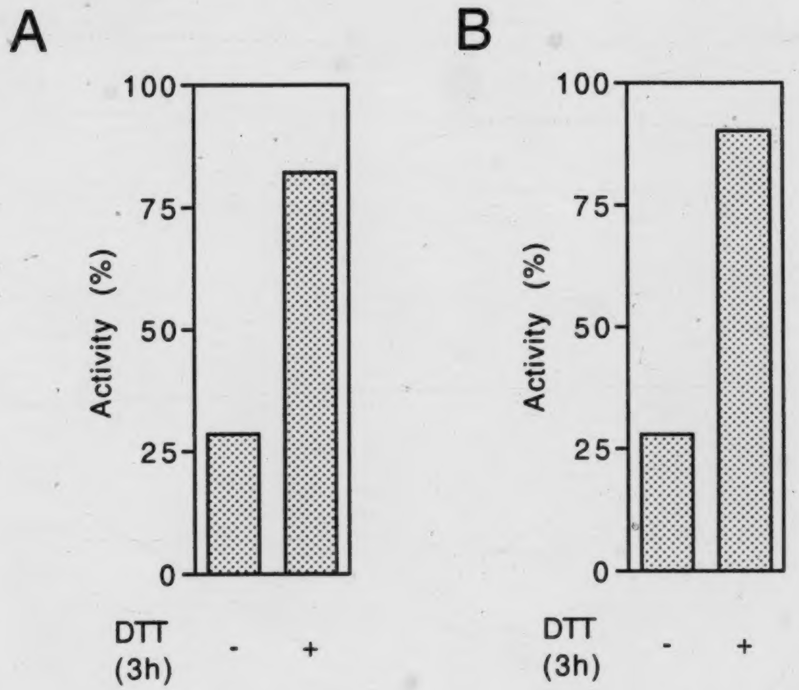

Figure 6-15: Effect of DTT on the rapid inactivation of ECoA by DTNB. Samples of wild-type CoA transferase (A) and C235S (B) were treated for 10 min with DTNB and a 1.5-fold molar excess of acetoacetyl-CoA. The reaction mixtures were subsequently incubated in the absence or presence of DTT for 3 h, prior to being assayed for CoA transferase activity.

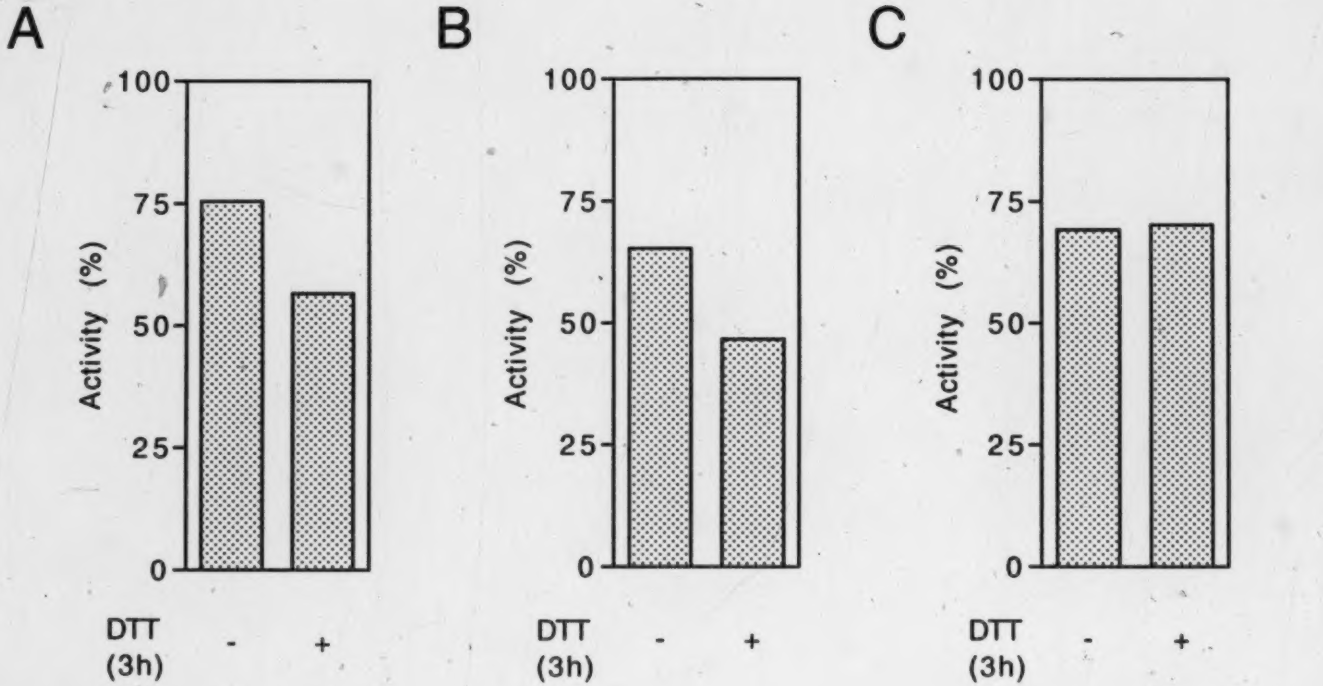

Figure 6-16: Effect of DTT on the inactivation of C67S by DTNB. Samples of C67S were incubated for 20 min in solutions containing DTNB, in the presence (A) or absence (B) of a 1.5-fold molar excess of acetoacetyl-CoA. As a control, a sample of wild-type CoA transferase (C) was incubated for 10 min in a solution lacking acetoacetyl-CoA but containing DTNB. The reaction mixtures were treated additionally with DTT for 3 h or left untreated, prior to being assayed for CoA transferase activity.

inactivated by DTNB in a solution lacking acetoacetyl-CoA was not significantly reactivated by the addition of DTT (Figure 6-16C).

In summary, the inactivation of C67S by DTNB was independent of the formation of ECoA, and similar to that observed for the wild-type enzyme or C235S treated without acyl-CoA substrate. Thus, it was concluded that cysteine 67 is a thiol-sensitive residue located at or near the active site of CoA transferase.

Subunit hybridization of E344A and C67S. To identify whether or not each active site is shared between the two subunits of the CoA transferase homodimer, *in vitro* hybridization (Wente & Schachman, 1987; Tobias & Kahana, 1993) was carried out with C67S and E344A. These mutant enzymes were considered suitable for active site complementation since cysteine 67 and glutamate 344 are located on separate domains of CoA transferase. The hybridization method was complicated by the residual enzyme activity of C67S, which was approximately 0.3 times that of wild-type CoA transferase. Nevertheless, the absence or presence of shared active sites could be determined by carefully measuring the specific enzyme activity of an equimolar mixture of C67S and E344A refolded from denaturant. If cysteine 67 and glutamate 344 were not located at the interface between the two subunits, then the total specific enzyme activity of the refolded, equimolar mixture of C67S and E344A should be 1.2/8.0 or 0.15 times that of wild-type CoA transferase (Figure 6-17A). In contrast, if cysteine 67 and glutamate 344 were located in the intersubunit contact region, then the total specific enzyme activity of the refolded, equimolar mixture of C67S and E344A should be 2.6/8.0 or 0.32 times that of wild-type CoA transferase, due to the reconstitution of one fully functional active site per heterodimer (Figure 6-17B). Based on this reasoning, it was predicted that the total specific activity of the refolded, equimolar mixture of C67S and E344A should be either: (1) equal to that of an equimolar mixture of the two mutant enzymes prepared under non-denaturing conditions, assuming independent active sites; or (2) twice that of an

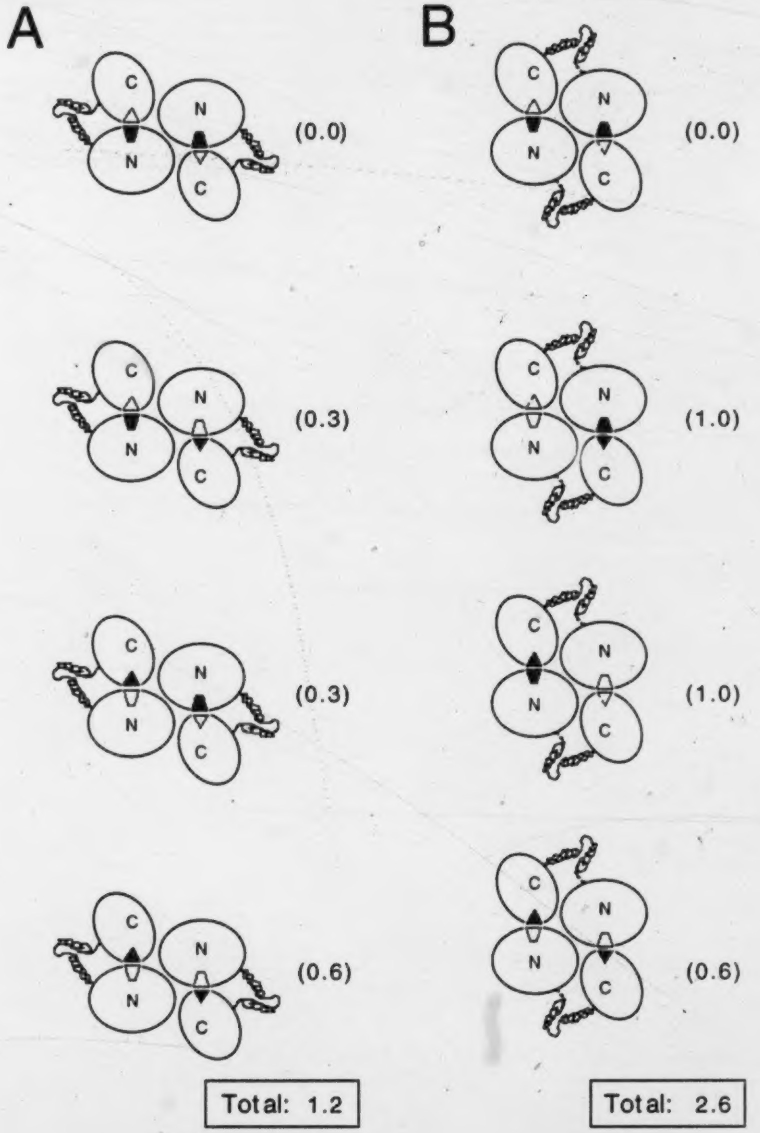

Figure 6-17: Models for the hybridization of CoA transferase subunits. The unfolding and refolding of an equimolar mixture of C67S and E344A leads to the formation of one of two sets of dimeric species, depending on whether the active sites are unshared (A) or shared (B). The predicted number of functional active sites is indicated beside each conformer, assuming that the active site of C67S is 0.3 times as efficient as that of wild-type CoA transferase. The total number of functional active sites for each set of dimeric species is shown enclosed within a box. The black and white trapezoids represent cysteine 67 and serine 67 (respectively), while the black and white triangles symbolize glutamate 344 and alanine 344 (respectively). The N- and C-domains are indicated appropriately.

equimolar mixture of the two mutant enzymes prepared in the absence of denaturant, assuming shared active sites.

Equal amounts of the C67S and E344A mutant enzymes were combined, either before or after unfolding and subsequent renaturation (see "Experimental Procedures"). Two final protein concentrations were used in these experiments. First, approximately 20% of the initial CoA transferase activity was detected in equimolar mixtures (final concentration of each NC monomer, 96 nM) prepared prior to or following denaturation and subsequent refolding (Figure 6-18A). Second, approximately 13% of the initial CoA transferase activity was detected in equimolar mixtures (final concentration of each NC monomer, 0.19 μM) prepared prior to or following denaturation and subsequent refolding (Figure 6-18B). Furthermore, non-denaturing PAGE analysis of the diluted enzyme samples confirmed that C67S and E344A were refolded in a soluble form to similar yields (Figure 6-19). Importantly, the major species in the refolded, equimolar mixture of the two mutant enzymes displayed an electrophoretic mobility greater than that of pure C67S but less than that of pure E344A (Figure 6-19, lane 5). Presumably, this molecule corresponded to the C67S/E344A hybrid, indicating that the two mutant enzymes are capable of associating in an equimolar mixture during refolding. From these results, it was concluded that the active sites of homodimeric CoA transferase are not shared between the two subunits.

DISCUSSION

The E344A and E344D mutants. The replacement of glutamate 344 with an alanine or aspartate residue led to a severe reduction in the specific activity of pig heart CoA transferase. Surprisingly, the residual activity of E344A was at least 60 times greater than that of E344D. Since E344A lacks a catalytic nucleophile, it is incapable of catalyzing the transfer of CoA from succinyl-CoA to acetoacetate by the "ping-pong" kinetic mechanism proven for the wild-type enzyme (Chapter 1). Instead, it is likely that

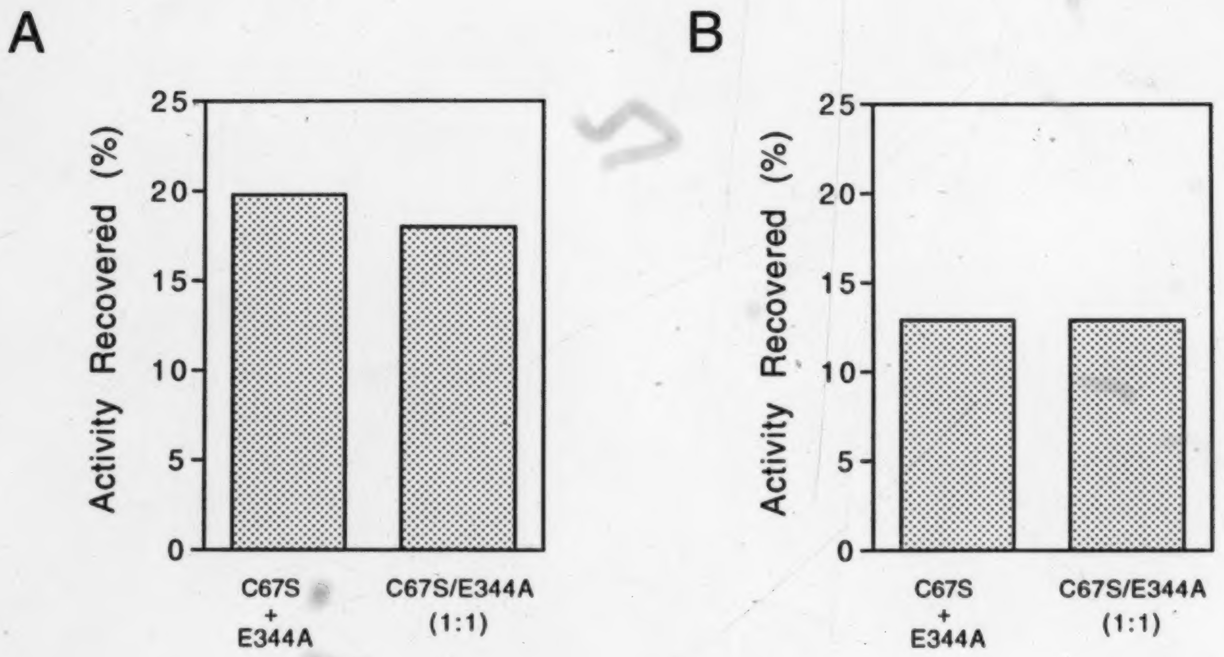

Figure 6-18: Active site complementation analyses of CoA transferase. Samples of C67S and E344A were mixed in an equimolar ratio to give a final concentration of 96 nM (A) or 0.19 μM (B) of each NC monomer. The equimolar mixtures were prepared either before or after denaturation and subsequent refolding (right or left bar, respectively).

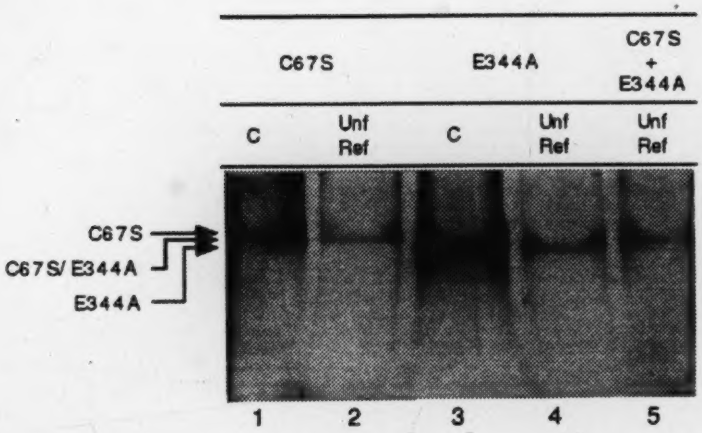

Figure 6-19: Non-denaturing PAGE analysis of C67S and E344A after unfolding and renaturation. Lanes 1 and 3, control samples of C67S and E344A (respectively), diluted without prior denaturation; lanes 2 and 4, samples of C67S and E344A (respectively), diluted after unfolding in 6.0 M GuHCl (final concentration, 0.19 μM of the NC monomer); lanes 5, samples of C67S and E344A mixed in an equimolar ratio prior to unfolding and subsequent refolding (final concentration of each NC monomer, 96 nM). Bands representing C67S, E344A, and a hybrid of the two mutant subunits (C67S/E344A) are indicated by appropriately labeled arrows. Each lane was loaded with 1.5 μg of protein. The gel consisted of a 3% (w/v) stacking gel (pH 6.8) and a 6% (w/v) resolving gel (pH 8.8), and was analyzed by staining with $AgNO_3$.

the preparation of E344A contained trace amounts of contaminating wild-type CoA transferase, perhaps resulting from errors of protein synthesis in BL-E344A. The relative specific activity of E344A compared to the wild-type enzyme (5.9×10^{-4}) is consistent with the frequency of translational misincorporation *in vivo*, which ranges from 10^{-3} to 10^{-4} (Schimmel, 1990). In contrast, the preparation of E344D lacked significant levels of background wild-type CoA transferase. Assuming that the frequency of translational misreading varies with the identity of the codon, it is conceivable that the correct amino acid was incorporated at position 344 with greater efficiency in the strain BL-E344D than in BL-E344A. Finally, although the enzyme mutants were purified with new chromatographic resins where possible, it cannot be ruled out that a column used to purify E344A was contaminated with wild-type CoA transferase. To address this possibility, it will be necessary to measure the specific activities of several independent preparations of E344A. Despite uncertainties with respect to the absolute catalytic efficiencies of E344A and E344D, the low specific activities of these mutants clearly confirmed that glutamate 344 is the active site nucleophile of pig heart CoA transferase. Similarly, replacement of the active site glutamate residue (βE54) of glutaconate CoA-transferase with an alanine (βE54A) or an aspartate (βE54D) residue also led to a substantial loss of enzyme activity (Mack & Buckel, 1995; Mack & Buckel, 1997). The residual enzyme activity of the βE54A mutant of glutaconate CoA-transferase was 0.02% of the specific activity of the wild-type enzyme (Mack & Buckel, 1995), similar to that reported here for the E344A mutant of pig heart CoA transferase.

The inability of E344D to catalyze the transfer of CoA from succinyl-CoA to acetoacetate indicated that the length of the acidic sidechain at position 344 is critical for catalysis. This conclusion implies, in turn, that the active site of pig heart CoA transferase is inflexible with respect to the manner in which substrates are bound. Presumably, the tight binding of the acyl-CoA substrate to the active site of E344D renders the thiolester bond relatively inaccessible to nucleophilic attack by the sidechain of aspartate 344, which is shorter than that of a glutamate residue by the length of one methylene group. Recently, it has been demonstrated that the βE54D mutant of glutaconate CoA-transferase displays substantial acyl-CoA hydrolase activity (Mack & Buckel, 1997). A space in the active site of this mutant, created by shortening the acidic sidechain at position 344, may be occupied by a water molecule. Once activated by the aspartate sidechain acting as a general base, this water molecule may carry out a nucleophilic attack on the thiolester bond of the acyl-CoA substrate, leading to the release of free CoA. Future studies of the E344D mutant of pig heart CoA transferase will address whether or not this enzyme also possesses an acyl-CoA hydrolase activity.

Site-directed mutagenesis has led to the identification of a glutamate residue as the catalytic nucleophile of a number of glycosyl transferases or glycosyl hydrolases. Recent examples include: glucocerebrosidase (Miao et al., 1994); nucleoside 2-deoxyribosyltransferase (Porter et al., 1995); mannanase A (Bolam et al., 1996); xylanase (Lawson et al., 1996); β-1,4-glycanase (MacLeod et al., 1996); and β-glycosidase (Moracci et al., 1996). The replacement of the nucleophilic glutamate residue of each of these enzymes with a glycine, alanine, aspartate, glutamine, or cysteine residue leads to a reduction in specific activity by at least three orders of magnitude.

The E344Q mutant. The replacement of glutamate 344 by a glutamine residue led to a 1.8×10^2-fold decrease in the specific activity of pig heart CoA transferase, assuming from active site titration experiments that the wild-type enzyme constituted 0.8% of the preparation of E344Q (Appendix 7). This decrease in the value of the specific enzyme activity was due to a decrease in k_{cat} for the two CoA transferase reactions, indicating that the amino acid substitution affected the chemistry of enzymatic turnover rather than the binding of the substrates. Since the amide moiety of glutamine is less nucleophilic than the γ-carboxylate group of glutamate (Homer & Johnson, 1970), it was concluded that optimal catalysis by CoA transferase depends largely on the nucleophilicity of glutamate 344. Nevertheless, despite the relative nucleophilicity of the aspartate β-carboxylate group compared to the glutamine amide moiety, E344D was at least 5.9 × 10^2-fold less active than E344Q. Apparently, a β-carboxylate moiety at position 344 is incapable of approaching the precisely bound acyl-CoA thiolester to carry out a nucleophilic attack. Thus, the length of the glutamate 344 sidechain is much more critical to catalysis than the anionic charge on the γ-carboxylate group, implying that substrates are bound rather inflexibly in the active site of CoA transferase.

The specific activity and degree of autolysis of E344Q increased dramatically after prolonged incubation of the enzyme in buffer containing acetoacetyl-CoA. Presumably, the mutant was deamidated at position 344 under these conditions, leading to the formation of wild-type CoA transferase. In addition, the mutant may have been activated by substrates following its synthesis in *E. coli*, since the proportion of wild-type enzyme in the E344Q preparation was much greater than that predicted for translational misreading alone (Schimmel, 1990). The yield and apparent first-order rate constant of activation of E344Q *in vitro* increased with temperature between 22 °C and 37 °C. In contrast, no increase in CoA transferase activity was observed for a sample of E344Q incubated in the presence of acetoacetyl-CoA at 4 °C. Thus, the activation of the mutant requires a minimum of kinetic energy, most likely because a substantial kinetic barrier is associated with the proposed deamidation of glutamine 344.

The activation of E344Q was blocked by CoA, which inhibits the binding of acetoacetyl-CoA to the wild-type enzyme competitively with a K_I of 1.7 ± 0.5 mM (Whitty et al., 1995). Hence, an intact thiolester linkage is essential for the deamidation of glutamine 344. In addition, E344Q was not activated by succinyl-CoA unless acetoacetate was also present in the reaction mixture. The deamidation of glutamine 344 requires specific binding interactions between acetoacetate and the E344Q active site. These interactions may also facilitate the activation of the mutant in the presence of acetoacetyl-CoA, from which acetoacetate is released by hydrolysis or enzymatic turnover. Increasing the concentration of acetoacetate to saturating levels led to a decrease in the efficiency of glutamine 344 deamidation, likely because the binding of acetoacetyl-CoA to the active site of E344Q was diminished under these conditions. Finally, succinate inhibited the activation of E344Q by acetoacetyl-CoA. This inhibitory effect was alleviated by the addition of acetoacetate to the reaction mixture, demonstrating that succinate does not merely inhibit by occluding acetoacetyl-CoA from the active site. Instead, succinate may prevent the deamidation of glutamine 344 by binding to the active site after acetoacetyl-CoA has reacted with the enzyme. Reversal of the succinate-dependent inhibition by acetoacetate was incomplete, presumably due to the poor binding of acetoacetyl-CoA to E344Q in the presence of excess carboxylate substrate (see above).

To account for these observations, the following reaction mechanism is proposed. First, a nucleophilic attack by the amide oxygen atom of glutamine 344 displaces CoA from the carbonyl moiety of acetoacetyl-CoA to generate a "type I" mixed anhydride intermediate (Figure 6-20, reaction 1). The latter readily undergoes an O-to-N rearrangement to yield a "type II" mixed anhydride (Figure 6-20, reaction 2), due to the relative instability of the *O*-acylimidate compared to the *N*-acylamide (Challis & Challis, 1970). Presumably, the type II mixed anhydride is not formed by a direct nucleophilic attack on acetoacetyl-CoA by the glutamine 344 amide nitrogen atom, since the latter carries a much weaker partial negative charge than the amide oxygen atom (Challis & Challis, 1970). A subsequent nucleophilic attack by CoA on the carboximidic carbonyl group of the type II mixed anhydride yields ECoA and acetoacetamide as products (Figure 6-20, reaction 3). Finally, the reaction of ECoA with acetoacetate or succinate generates unliganded, wild-type CoA transferase.

The O to N rearrangement and the subsequent nucleophilic attack by CoA are the most likely targets for inhibition by succinate. These steps may be favored by a conformation of the E344Q active site which is stabilized by the covalent binding of acetoacetate to the enzyme as part of a type I or type II mixed anhydride. However, the

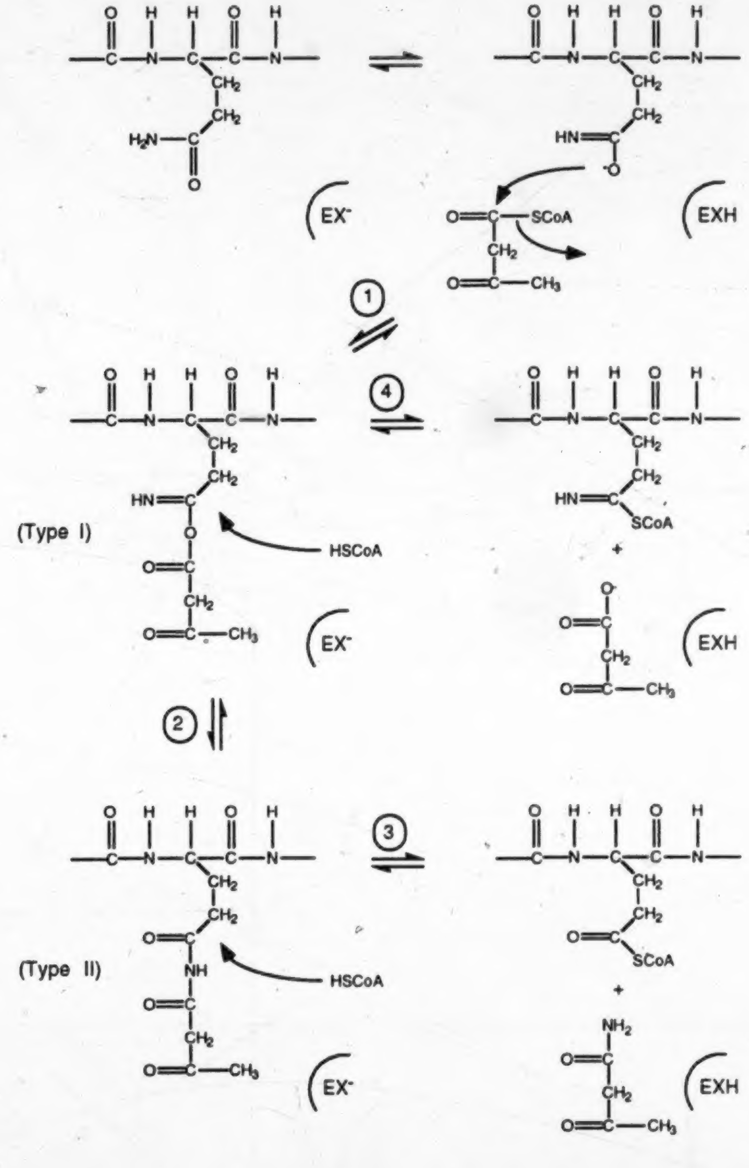

Figure 6-20: Mechanism for the activation of E344Q to wild-type CoA transferase via the formation of ECoA. (1) Nucleophilic attack by the amide oxygen atom of glutamine 344 on the carbonyl moiety of acetoacetyl-CoA, yielding a type I mixed anhydride. (2) O-to-N rearrangement of the type I mixed anhydride to a type II mixed anhydride. (3) Nucleophilic attack by CoA on the carboximidic carbonyl group of the type II mixed anhydride, yielding ECoA and acetoacetamide. (4) Competing nucleophilic attack by CoA on the carboximidic nitrogen atom of the type I mixed anhydride, to form a thiolimidic ECoA intermediate and acetoacetate. "EX" represents a general acid/base group in the active site.

presence of succinate in the reaction mixture may lead to the disruption of this high-energy intermediate. For example, a nucleophilic attack by CoA on the carboximidic nitrogen atom of a "productive" type I mixed anhydride, formed by the reaction of acetoacetyl-CoA at the E344Q active site, releases a thiolimidic ECoA intermediate and acetoacetate (Figure 6-20, reaction 4). The regeneration of the productive type I mixed anhydride by the reverse reaction could be prevented by the exchange of succinate for acetoacetate in the active site. This exchange, and the resulting inhibition of glutamine 344 deamidation, would then be partially reversed by the presence of excess acetoacetate in the reaction mixture.

The activation of E344Q may also occur by a cyclization mechanism (Figure 6-21). This pathway, similar to that proposed for the autolytic fragmentation of CoA transferase, involves the conversion of a type II mixed anhydride to an oxyproline derivative, followed by hydrolysis at the newly-formed amide bond to generate the wild-type enzyme. Interestingly, the nonenzymatic deamidation of asparagine residues has been shown to proceed by the formation of a succinimide intermediate (Geiger & Clarke, 1987; Capasso et al., 1989; Patel & Borchardt, 1990).

A mutant of glutaconate CoA-transferase in which the nucleophilic glutamate residue is replaced by glutamine (βE54Q) also undergoes activation (Mack & Buckel, 1995). The substrates glutaconate and acetyl-CoA are both strictly required for the deamidation, in contrast to results obtained for the E344Q mutant of pig heart CoA transferase. Mack & Buckel (1995) propose that the mutant is activated by a mechanism involving: (1) the formation of a mixed anhydride and the concomitant release of NH_2^-; and (2) a lowering of the activation energy for deamidation due to binding interactions between the enzyme and acetyl-CoA. Such a mechanism appears unlikely on chemical and enzymological grounds. First, NH_2^-, a very strong base, is predicted to be a much poorer leaving group than the incoming glutaconate molecule. Second, the proposed simultaneous binding of glutaconate and acetyl-CoA to the active site contradicts the

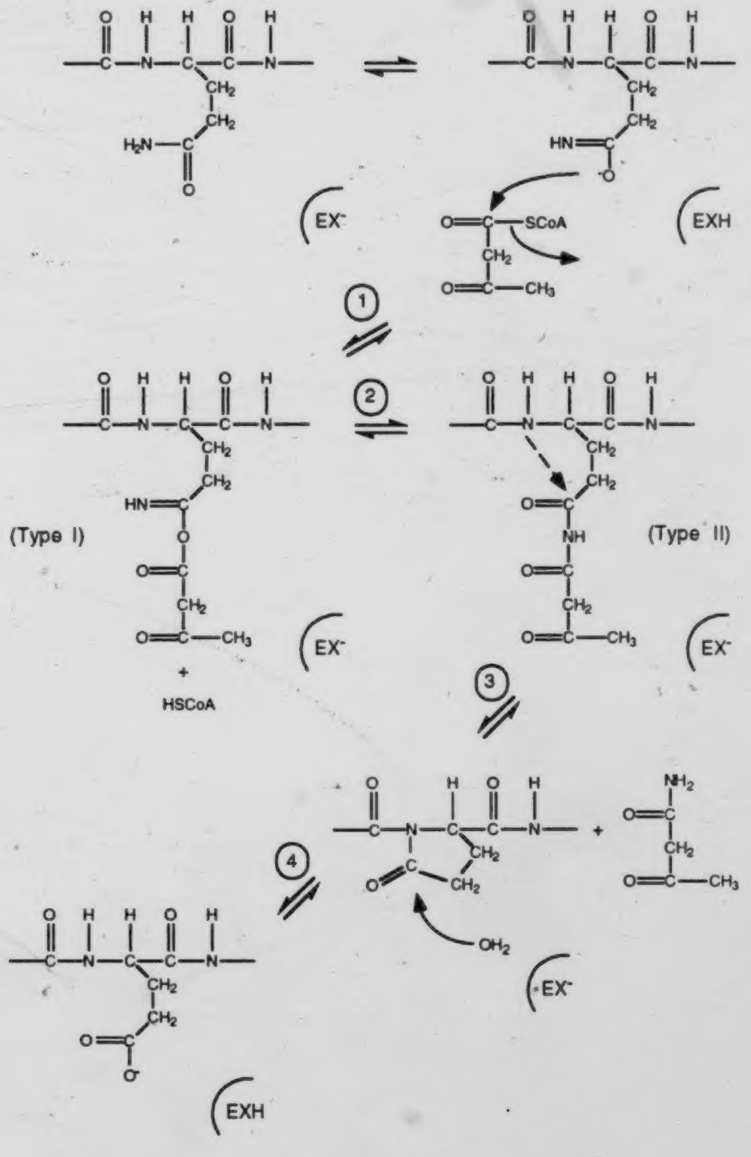

Figure 6-21: Mechanism for the activation of E344Q to wild-type CoA transferase via cyclization. Steps (1) and (2) are as described in the legend to Figure 6-20. (3) Nucleophilic attack by the α-amino nitrogen atom of glutamine 344 on the carboximidic carbonyl group of the type II mixed anhydride, yielding an oxyproline intermediate. (4) Hydrolysis of the newly-formed amide bond to produce glutamate at position 344. "EX" represents a general acid/base group in the active site.

"ping-pong" kinetic mechanism proven for the bacterial and mammalian CoA transferases. As an alternative, it is proposed that the βE54 mutant of glutaconate CoA-transferase is activated by one of the two pathways described above for the E344Q mutant of succinyl-CoA:3-ketoacid CoA transferase.

The two mechanisms proposed for the activation of E344Q require an initial nucleophilic attack by the glutamine 344 sidechain on acetoacetyl-CoA. It is predicted that this reaction must be facilitated by catalytic groups in the active site of CoA transferase, since the amide moiety is only weakly basic (Homer & Johnson, 1970). For instance, a nucleophilic attack by glutamine 344 on acetoacetyl-CoA may be favored by an oxyanion hole near the substrate's thiolester carbonyl moiety. In addition, a general acid-base group in the active site of E344Q may increase the nucleophilicity of glutamine 344 by deprotonation of the sidechain nitrogen atom. It has been argued that the pH optimum of 7.7 observed for wild-type CoA transferase reflects the deprotonation of the nucleophilic glutamate residue (Hersh & Jencks, 1967; Jencks, 1973). The pK_a of the γ-carboxylate group of glutamate 344 is likely increased from the norm by the exposure of the sidechain to a relatively non-polar environment (Jencks, 1973). Thus, the general acid-based group proposed for E344Q may also ensure that glutamate 344 of the wild-type enzyme is negatively-charged at physiological pH, and thus poised for nucleophilic attack on the acyl-CoA substrates. The nucleophilic glutamate residues of other enzymes have been shown to be maintained in a deprotonated state by hydrogen bonding interactions. Recently described examples include: β-1,4-glycanase (White et al., 1994), β-glucosidase (Gebler et al., 1995), and glutaconate CoA-transferase (Jacob et al., 1997). Further insight into the mechanism of activation of E344Q may therefore prove instructive with respect to key structural features of the active site of wild-type CoA transferase.

The identification of an essential cysteine residue. The C67S and C235S mutants of CoA transferase were investigated with respect to susceptibility to inactivation by

DTNB and enzyme activity. The inactivation of C67S by DTNB was relatively slow, even under conditions which led to the formation of ECoA. Moreover, this gradual loss of enzyme activity could not be reversed by the addition of DTT. In contrast, the inactivation of wild-type CoA transferase or C235S by thiol reagent was rapid and reversible in the presence of acetoacetyl-CoA, and slow and irreversible in the absence of the substrate. From these observations, it was inferred that: (1) cysteine 67 is the essential, reactive cysteine residue of wild-type CoA transferase; and (2) cysteine 235 is not necessary for optimal CoA transferase activity, although it too reacts rapidly with thiol reagents when the enzyme is treated with acetoacetyl-CoA (Williams, 1990).

The results described above provide insight as to the mechanism of inactivation of CoA transferase by DTNB. The change in conformation of the enzyme upon the formation of ECoA leads to the exposure of cysteine 67, which then reacts rapidly with a bulky thiol reagent such as DTNB. This covalent modification, which results in the inactivation of CoA transferase due to steric hindrance at the active site, is reversed by the addition of a reducing agent such as DTT. However, a slower reaction between DTNB and other cysteine residues, including cysteine 235, eventually causes the irreversible denaturation of the enzyme. Given the extended time of incubation of ECoA with [^{14}C]-NEM (Williams, 1990; see "Introduction"), it is reasonable that both cysteine 67 and cysteine 235 were originally identified as targets for the thiol inactivation of CoA transferase.

Upon the formation of ECoA, the C67S mutant of CoA transferase presumably undergoes a conformational change which leads to the exposure of a serine residue in place of cysteine 67. Accordingly, C67S is protected from rapid inactivation by DTNB, since serine does not react with the bulky thiol reagent. However, the mutant is slowly and irreversibly inactivated by DTNB, in the presence or absence of acetoacetyl-CoA, due to the covalent modification of other cysteine residues in C67S.

The identification of cysteine 67 as an essential residue of the active site was consistent with the observation that C67S was 0.3 times as active as wild-type CoA transferase. The relatively low value for the specific enzyme activity of C67S was due in part to a decrease in k_{cat} for the two CoA transferase reactions, as well as to an increase in the K_M for succinate. Given that the essential cysteine residue of CoA transferase does not fulfill a direct mechanistic role (Kindman & Jencks, 1981), cysteine 67 may be required to ensure a conformation of the active site optimal for catalysis and/or the binding of succinate. Alternatively, interactions between cysteine 67 and the nucleotide portion of CoA may be necessary to ensure a conformation of the acyl-CoA substrates suitable for catalysis. The latter possibility is implied by the location of cysteine 67 in the conserved sequence motif [Gly-Gly-Phe-(Xxx)-(Xxx)-(Xxx)-Gly], which is similar to a sequence associated with the ADP-binding βαβ fold of other proteins (Wierenga et al., 1986; Williams, 1990; Parales & Harwood, 1992). Finally, it is unclear why the single-atom replacement of sulfur by oxygen in the sidechain of amino acid residue 67 led to a decrease in CoA transferase activity, while the covalent attachment of a cyanide group to cysteine 67 did not alter the enzyme's catalytic function (Kindman & Jencks, 1981). It is conceivable that electrostatic and/or hydrogen bonding properties specific to the serine hydroxyl moiety account for this discrepancy.

The combination of chemical modification and site-directed mutagenesis used in these studies has proven to be a powerful method for the mapping of essential cysteine residues in the active sites of other enzymes. Recent examples include: fructose 6-phosphate, 2-kinase:fructose 2,6-bisphosphatase (Kitamura et al., 1989; Tsujikawa et al., 1995); 3-hydroxyisobutyrate dehydrogenase (Hawes et al., 1995); pyruvate phosphate dikinase (Xu et al., 1995); type I inositol-1,4,5-trisphosphate 5-phosphatase (Communi & Erneux, 1996); yeast invertase (Reddy & Maley, 1996); and class II *E. coli* prolyl-tRNA synthetase (Stehlin et al., 1997). Given the reliability of this experimental approach, the results obtained from the studies of C67S and C235S are considered reasonable.

Active site complementation. The disposition of the active sites between the subunits of the CoA transferase homodimer was assessed by *in vitro* hybridization studies, using the mutants E344A and C67S. By a similar experimental approach, it has been demonstrated that the active sites of other oligomeric enzymes are shared between two or more subunits. Examples of such enzymes include: aspartate transcarbamoylase (Robey & Schachman, 1985; Wente & Schachman, 1987); phosphofructokinase (Lau & Fersht, 1989); mercuric reductase (Distefano et al., 1990); thymidylate synthase (Pookanjanatavip et al., 1992; Carreras et al., 1994; Maley et al., 1995); ornithine decarboxylase (Tobias & Kahana, 1993; Coleman et al., 1994); orotate phosphoribosyltransferase (Ozturk et al., 1995); adenylosuccinate synthetase (Kang et al., 1996); and ornithine transcarbamoylase (Murata & Schachman, 1996).

The specific enzyme activity associated with a hybrid of C67S and E344A was identical to that of an equimolar mixture of C67S and E344A prepared in benign buffer. The formation of this hybrid during the refolding of the two mutants in an equimolar mixture was confirmed by non-denaturing PAGE analysis. Finally, the assumption that both mutants are capable of refolding to a soluble form with similar efficiencies was verified. From these observations, it was inferred that: (1) a C67S/E344A heterodimer was formed in the sample of reconstituted enzyme, with a yield equivalent to that predicted for a binomial distribution of dimeric species; and (2) the C67S/E344A hybrid did not contain a fully functional active site. Thus, the catalytic residues of homodimeric CoA transferase are not shared between the two subunits.

Ideally, active site complementation experiments should be performed using two types of inactive monomers that carry amino acid substitutions on opposing faces of the active site. Although the work described here was complicated by the partial enzyme activity of C67S, the difference in the specific activities predicted for shared versus individual active sites in CoA transferase was large enough to be detected. Future efforts will be aimed at repeating these experiments using a mutant of CoA transferase which carries a fully inactivating amino acid replacement at position 67.

Recently, it was proposed that oligomeric enzymes with shared active sites may have evolved by domain swapping (reviewed in [Bennett et al., 1995]; [Schlunegger et al., 1997]). This mechanism stipulates that the fusion of two genes encoding single-domain proteins led to the evolution of a monomer with an active site located at the interface between two domains (Figure 6-22A). The exchange of these domains between two monomers produced a homodimer with two active sites shared between the subunits (Figure 6-22A). The mammalian CoA transferases could not have evolved by domain swapping, however, given that gene fusion only occurred after two N-domains and two C-domains had assembled to form a primitive oligomer (Figure 6-22B; Parales & Harwood, 1992; see also Chapter 1). Thus, the finding that the active sites of CoA transferase are not shared is reasonable on evolutionary grounds.

In conclusion, the results of *in vitro* hybridization studies suggested that the catalytic residues of CoA transferase are located at the interface between the N- and C-domains of a given subunit. Given that the individual monomer is incapable of enzyme function (Chapters 2 and 4), interactions between the two subunits must determine the final conformation of the active sites. A full characterization of the structural and functional consequences of these interactions will require the solution of the structure of CoA transferase by x-ray crystallographic methods.

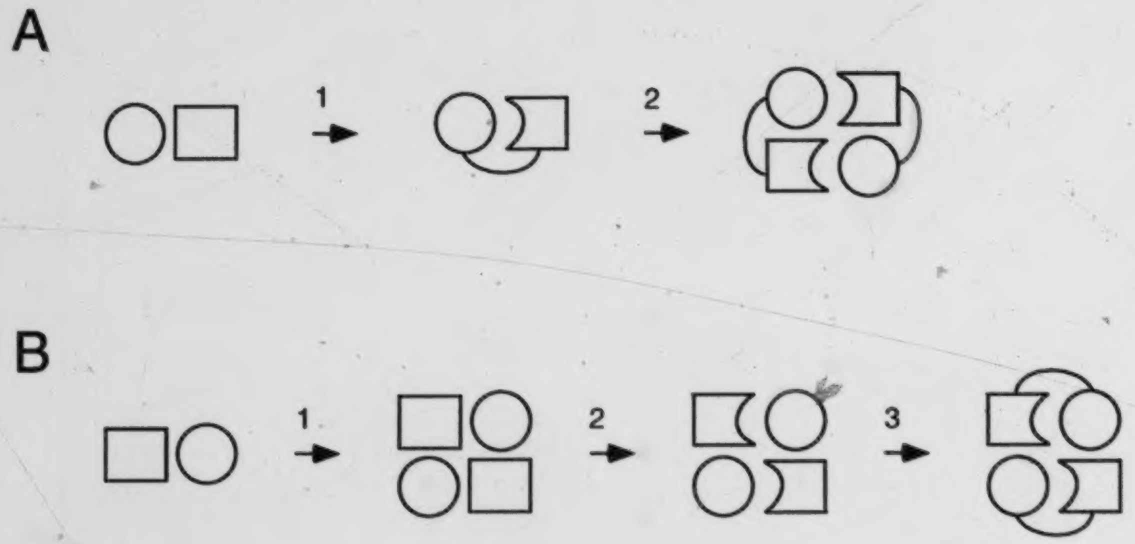

Figure 6-22: Models proposed for the evolution of homodimeric enzymes with two-domain subunits. (A) Evolution of dimers with shared active sites. (1) The fusion of two genes encoding single-domain proteins yields a monomer with its active site located at the interface between two domains. (2) The swapping of domains between two monomers produces a homodimer with its active sites shared between the two subunits. (Adapted from [Bennett et al., 1995]). (B) Evolution of dimers with unshared active sites. (1) Two pairs of single-domain proteins (e.g. N and C) assemble to form a heterotetramer (e.g. N_2C_2). (2) Two active sites evolve at the interdomain interfaces (e.g. the N-C interfaces). (3) The fusion of the genes encoding the two single-domain proteins yields a homodimer with each active site located at the interface between two domains.

ENDNOTES

[1] CoA transferase mutants are identified by the corresponding substitution, using the one-letter code for the natural amino acids. For example, the mutant termed "E344A" contains an alanine rather than a glutamate residue at position 344. The numbering is based on the precursor form of the enzyme (Lin & Bridger, 1992).

[2] See Appendices 3-6 for further details.

[3] The β-hydroxyacyl-CoA dehydrogenase, supplied as a suspension in a saturated $(NH_4)_2SO_4$ solution, was dialyzed against 0.5 L of 10 mM Tris-HCl, 1 mM EDTA, and 2 mM 2ME (pH 8.0) prior to use.

[4] Samples of the wild-type enzyme which were previously analyzed by measurements of far-UV CD or fluorescence were diluted in buffer X (Chapter 2). However, the mutants of CoA transferase were eluted from the Affi-Gel Blue column in buffer A + 0.5 M KCl (see "Protein purification"). Therefore, to be consistent with the earlier measurements, it was necessary to dialyze these samples at 4 °C against 0.5 L of buffer X prior to the measurement of far-UV CD or fluorescence. The choice of dialysis membrane was determined by the volume of the dialyzed sample, as outlined in Chapter 2.

[5] The unfolding of unfractionated, wild-type CoA transferase at 15 °C was shown to be 60-70% reversible. Accordingly, the values deduced for the various thermodynamic parameters are "apparent" values only.

[6] For most of the denaturation curves derived from measurements of intrinsic tryptophan fluorescence, ds was taken to be equal to zero. This assumption was reasonable, given that the values of y in the post-transition region did not differ greatly from y_u.

REFERENCES

Barrett, T., Suresh, C. G., Tolley, S. P., Dodson, E. J., & Hughes, M. A. (1995) *Structure 3*, 951-960.

Bennett, M. J., Schlunegger, M. P., & Eisenberg, D. (1995) *Protein Sci. 4*, 2455-2468.

Bolam, D. N., Hughes, N., Virden, R., Lakey, J. H., Hazlewood, G. P., Henrissat, B., Braithwaite, K. L., & Gilbert, H. J. (1996) *Biochemistry 35*, 16195-16204.

Brändén, C., & Tooze, J. (1991) in *Introduction to Protein Structure*, pp. 47-51, Garland Publishing, Inc., New York.

Bridger, W. A., Ramaley, R. F., & Boyer, P. D. (1969) *Methods Enzymol. 13*, 70-75.

Capasso, S., Mazzarella, L., Sica, F., & Zagari, A. (1989) *Pept. Res. 2*, 195-200.

Carreras, C. W., Costi, P. M., & Santi, D. V. (1994) *J. Biol. Chem. 269*, 12444-12446.

Challis, B. C., & Challis, J. (1970) in *The Chemistry of Amides* (Zabicky, J., Ed.), pp. 731-857, Interscience Publishers, New York.

Coleman, C. S., Stanley, B. A., Viswanath, R., & Pegg, A. E. (1994) *J. Biol. Chem. 269*, 3155-3158.

Communi, D., & Erneux, C. (1996) *Biochem. J. 320*, 181-186.

De Francesco, R., Pastore, A., Vecchio, G., & Cortese, R. (1991) *Biochemistry 30*, 143-147.

Distefano, M. D., Moore, M. J., & Walsh, C. T. (1990) *Biochemistry 29*, 2703-2713.

Gebler, J. C., Trimbur, D. E., Warren, A. J., Aebersold, R., Namchuk, M., & Withers, S. G. (1995) *Biochemistry 34*, 14547-14553.

Geiger, T., & Clarke, S. (1987) *J. Biol. Chem. 262*, 785-794.

Hawes, J. W., Crabb, D. W., Chan, R. M., Rougraff, P. M., & Harris, R. A. (1995) *Biochemistry 34*, 4231-4237.

Hersh, L. B., & Jencks, W. P. (1967) *J. Biol. Chem. 242*, 3468-3480.

Higuchi, R., Krummel, B., & Saiki, R. K. (1988) *Nucl. Acids Res. 16*, 7351-7367.

Ho, S. N., Hunt, H. D., Horton, R. M., Pullen, J. K., & Pease, L. R. (1989) *Gene 77*, 51-59.

Homer, R. B., & Johnson, C. D. (1970) in *The Chemistry of Amides* (Zabicky, J., Ed.), pp. 187-243, Interscience Publishers, New York.

Horecker, B. L., & Kornberg, A. (1948) *J. Biol. Chem. 175*, 385-390.

Howard, J. B., Zieske, L., Clarkson, J., & Rathe, L. (1986) *J. Biol. Chem. 261*, 60-65.

Jacob, U., Mack, M., Clausen, T., Huber, R., Buckel, W., & Messerschmidt, A. (1997) *Structure 5*, 415-426.

Jencks, W. P. (1973) in *The Enzymes*, 3rd ed. (Boyer, P. D., Ed.) Vol. IX, pp. 483-496, Academic Press, Inc., New York.

Kang, C., Kim, S., & Fromm, H. J. (1996) *J. Biol. Chem. 271*, 29722-29728.

Kassovska-Bratinova, S., Fukao, T., Song, X.-Q., Duncan, A. M. V., Chen, H. S., Robert, M.-F., Pérez-Cerdá, C., Ugarte, M., Chartrand, C., Vobecky, S., Kondo, N., & Mitchell, G. A. (1996) *Am. J. Hum. Genet. 59*, 519-528.

Kindman, L. A., & Jencks, W. P. (1981) *Biochemistry 20*, 5183-5187.

Kitamura, K., Uyeda, K., Hartman, F. C., Kangawa, K., & Matsuo, H. (1989) *J. Biol. Chem. 264*, 6344-6348.

Kunkel, T. A. (1985) *Proc. Natl. Acad. Sci. U. S. A. 82*, 488-492.

Lau, F. T.-K., & Fersht, A. R. (1989) *Biochemistry 28*, 6841-6847.

Lawson, S. L., Wakarchuk, W. W., & Withers, S. G. (1996) *Biochemistry 35*, 10110-10118.

Lin, T., & Bridger, W. A. (1992) *J. Biol. Chem. 267*, 975-978.

MacLeod, A. M., Tull, D., Rupitz, K., Warren, R. A., & Withers, S. G. (1996) *Biochemistry 35*, 13165-13172.

Mack, M., & Buckel, W. (1995) *FEBS Lett. 357*, 145-148.

Mack, M., & Buckel, W. (1997) *FEBS Lett. 405*, 209-212.

Maley, F., Pedersen-Lane, J., & Changchien, L. (1995) *Biochemistry 34*, 1469-1474.

Miao, S., McCarter, J. D., Grace, M. E., Grabowski, G. A., Aebersold, R., & Withers, S. G. (1994) *J. Biol. Chem. 269*, 10975-10978.

Milla, M. E., Brown, B. M., & Sauer, R. T. (1993) *Protein Sci. 2*, 2198-2205.

Mok, Y.-K., Prat Gay, G. d., Butler, P. J., & Bycroft, M. (1996) *Protein Sci. 5*, 310-319.

Moore, S. A., & Jencks, W. P. (1982) *J. Biol. Chem. 257*, 10893-10907.

Moracci, M., Capalbo, L., Ciaramella, M., & Rossi, M. (1996) *Protein Eng. 9*, 1191-1195.

Murata, L. B., & Schachman, H. K. (1996) *Protein Sci. 5*, 709-718.

Myers, J. K., Pace, C. N., & Scholtz, J. M. (1995) *Protein Sci. 4*, 2138-2148.

Ozturk, D. H., Dorfman, R. H., Scapin, G., Sacchettini, J. C., & Grubmeyer, C. (1995) *Biochemistry 34*, 10764-10770.

Pace, C. N. (1975) *Crit. Rev. Biochem. 3*, 1-43.

Pace, C. N. (1986) *Methods Enzymol. 131*, 266-280.

Parales, R. E., & Harwood, C. S. (1992) *J. Bacteriol. 174*, 4657-4666.

Parratt, L. G. (1961) *Probability and Experimental Errors in Science*. John Wiley & Sons, Inc., New York.

Patel, K., & Borchardt, R. T. (1990) *Pharm. Res. 7*, 703-711.

Pickart, C. M., & Jencks, W. P. (1979) *J. Biol. Chem. 254*, 9120-9129.

Pookanjanatavip, M., Yuthavong, Y., Greene, P. J., & Santi, D. V. (1992) *Biochemistry 31*, 10303-10309.

Porter, D. J., Merrill, B. M., & Short, S. A. (1995) *J. Biol. Chem. 270*, 15551-15556.

Reddy, A., & Maley, F. (1996) *J. Biol. Chem. 271*, 13953-13957.

Robey, E. A., & Schachman, H. K. (1985) *Proc. Natl. Acad. Sci. U. S. A. 82*, 361-365.

Sanger, F., Nicklen, S., & Coulson, A. R. (1977) *Proc. Natl. Acad. Sci. U. S. A. 74*, 5463-5467.

Schellman, J. (1978) *Biopolymers 17*, 1305-1322.

Schimmel, P. (1990) *Biochemistry 29*, 9495-9502.

Schlunegger, M. P., Bennett, M. J., & Eisenberg, D. (1997) *Adv. Prot. Chem. 50*, 61-122.

Segel, I. H. (1975) *Enzyme Kinetics*. John Wiley & Sons, Inc., New York.

Shortle, D. (1989) *J. Biol. Chem. 264*, 5315-5318.

Stehlin, C., Heacock, D. H. 2nd., Liu, H., & Musier-Forsyth, K. (1997) *Biochemistry 36*, 2932-2938.

Tobias, K. E., & Kahana, C. (1993) *Biochemistry 32*, 5842-5847.

Tsujikawa, T., Watanabe, F., & Uyeda, K. (1995) *Biochemistry 34*, 6389-6393.

Wente, S. R., & Schachman, H. K. (1987) *Proc. Natl. Acad. Sci. U. S. A. 84*, 31-35.

White, A., Withers, S. G., Gilkes, N. R., & Rose, D. R. (1994) *Biochemistry 33*, 12546-12552.

White, H., & Jencks, W. P. (1976) *J. Biol. Chem. 251*, 1688-1699.

White, H., Solomon, F., & Jencks, W. P. (1976) *J. Biol. Chem. 251*, 1700-1707.

Whitty, A., Fierke, C. A., & Jencks, W. P. (1995) *Biochemistry 34*, 11678-11689.

Wierenga, R. K., Terpstra, P., & Hol, W. G. J. (1986) *J. Mol. Biol. 187*, 101-107.

Wiesmann, C., Beste, G., Hengstenberg, W., & Schulz, G. E. (1995) *Structure 3*, 961-968.

Williams, W. A. (1990) Ph. D. thesis, University of Minnesota, Minneapolis.

Xu, Y., Yankie, L., Shen, L., Jung, Y. S., Mariano, P. S., Dunaway-Mariano, D., & Martin, B. M. (1995) *Biochemistry 34*, 2181-2187.

Chapter 7. Conclusions and Final Discussion

Part A: Summary

The studies described in this thesis were designed to address how succinyl-CoA:3-ketoacid CoA transferase of porcine heart adopts a native fold, and how the enzyme achieves catalysis. The relative importance of assembly versus aggregation at early and late points along the CoA transferase folding pathway was investigated. Two oligomeric forms of the enzyme were isolated and characterized. In addition, two residues of the active site were identified, and the effects of amino acid substitutions at these positions were studied. Finally, the disposition of the active sites between the two subunits of the CoA transferase homodimer was examined by subunit hybridization experiments.

To summarize and illustrate the results of these investigations, a comprehensive model for the formation of active, wild-type CoA transferase is proposed (Figure 7-1). During or immediately after protein synthesis, the N- and C-domains of each monomer initiate folding independently of each other. The N-domain adopts a native-like fold, while the C-domain assumes an open, random-coil structure. An initial, homodimeric complex is formed upon the association of two monomers via their N-domains. Subsequently, productive interactions between the N- and C-domains involving a substantial rearrangement of secondary and tertiary structure enable the enzyme to achieve its final, native fold.

Early folding intermediates of CoA transferase may be trapped by aggregation, which results mainly from unproductive interactions involving the disordered C-domains. This tendency to undergo aggregation decreases as the nonnative species achieve a more stable, compact fold. However, the steps which precede the association of the N- and C-domains are reversible, so that late intermediates may undergo limited aggregation by

Figure 7-1: Model describing the folding and assembly of wild-type CoA transferase to the active enzyme form. (1) Folding of the N-domain to a native-like structure. (2) Assembly of two primitive monomers via productive interactions involving the native-like N-domains. (3) Association of two C-domains with two native-like N-domains to form the native CoA transferase homodimer. (4) Association of two native homodimers via direct interactions involving the hinge region to form the CoA transferase homotetramer. (5) Formation of the homotetramer by a domain-swapping mechanism. (6) and (8) Aggregation of early and late folding intermediates (respectively) via incorrect interactions involving the unstructured C-domains. (7) Aggregation of early intermediates via incorrect interactions involving the unstructured N-domains. (Note that steps 6 through 8 may be slowed by the action of chaperonins). (9) Incorrect pairing of the native-like N-domains (perhaps similar to the interactions within the individual N_2-dimer). Unstructured domains are depicted as square shapes, while native-like or native domains are represented by ellipsoid figures. The productive folding and assembly pathway of the CoA transferase homodimer is shown enclosed within a dashed box. Cysteine 67 and glutamate 344 are represented by the black trapezoids and triangles, respectively. The N- and C-domains are indicated appropriately.

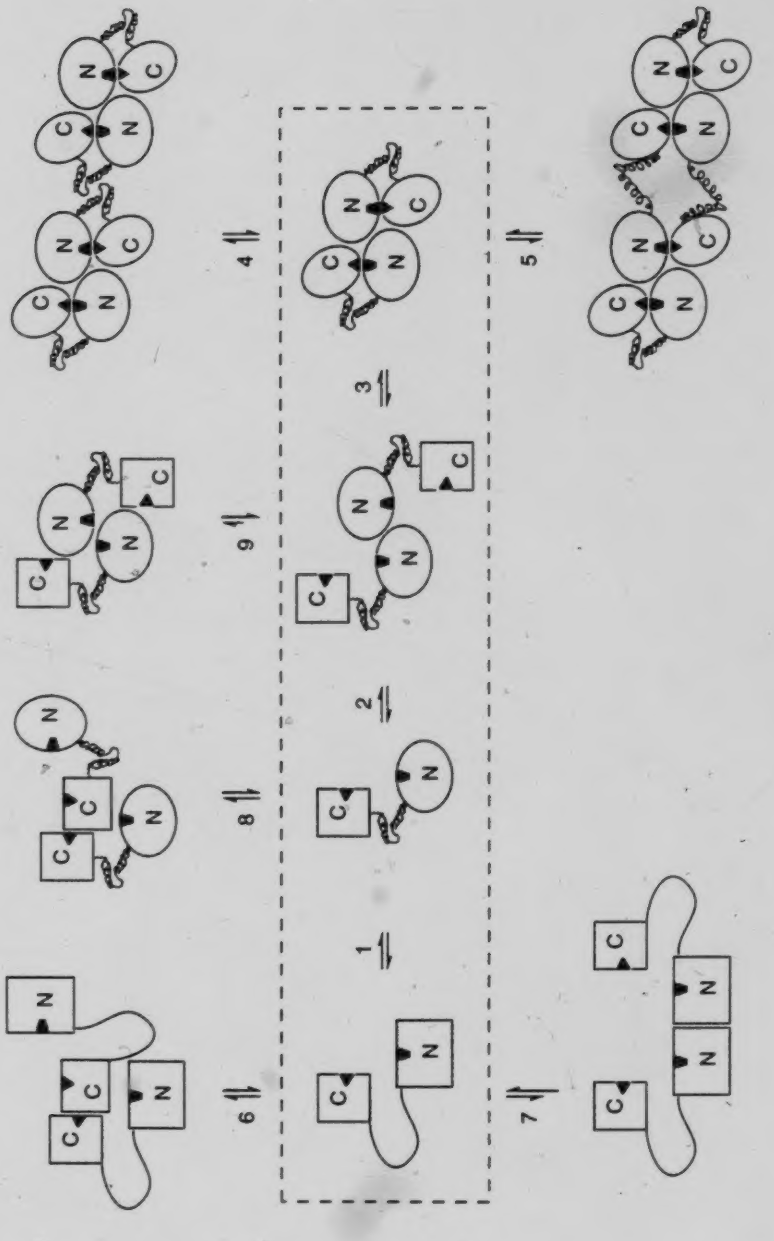
N
C

partially unfolding to yield early conformers. Under conditions that would favor aggregation, the hydrophilic linker segment can facilitate the folding of CoA transferase by enhancing the rate of assembly of the N- and C-domains. In addition, the chaperonin complex $GroEL_{14}$:$GroES_7$ prevents aggregation by binding early folding intermediates, presumably through hydrophobic contacts involving the incompletely folded C-domain.

The correct folding of homodimeric CoA transferase creates two functional active sites, each of which is shared between the N- and C-domains of a given subunit. Cysteine 67 may contribute to catalysis by interacting with succinate and/or the nucleotide portion of CoA. Glutamate 344 is the active site nucleophile responsible for the formation of ECoA. The length of the glutamate 344 sidechain is more critical to catalysis than the nucleophilicity of the γ-carboxyl group, presumably because acyl-CoA substrates are bound inflexibly in the active site.

Finally, two CoA transferase homodimers may assemble to form an enzymatically active homotetramer under conditions of high ionic strength. The hydrophilic linker segment is essential for this association, suggesting that the large conformer is stabilized by direct interactions between the hinge regions of adjacent homodimers. Alternatively, the tetramer may be formed by a domain swapping mechanism.

Part B: Significance and Future Perspectives

Assembly of the N- and C-domains of CoA transferase. A conformational rearrangement associated with the assembly of the N- and C-domains to the active enzyme form only occurred after the domain polypeptides were mixed at a permissive temperature (Chapter 2). Thus, the N- and C-domains require a productive interaction to achieve a native structure. In addition, the spectrophotometric, sedimentation, and equilibrium unfolding properties of the individual domains implied that the monomeric C-domain remains relatively disordered until after the formation of an initial N_2C_2-domain complex (Chapter 2). Finally, the C-domain was much more susceptible to aggregation than the N-domain, even at late stages of the folding pathway (Chapter 3). These results suggest that the C-domain of wild-type CoA transferase achieves a stable, native fold only after the initial association of two monomers through their native-like N-domains.

The mechanism of folding and assembly of CoA transferase extends the current understanding of how oligomeric enzymes fold in general. It has been argued that a dimeric protein adopts its native structure by a "sequential" pathway, involving: (1) the folding of monomeric intermediates; (2) the assembly of structured monomers to yield an initial dimer; and (3) additional folding of the immature dimer to form the native protein (reviewed in [Jaenicke, 1987]; [Jaenicke, 1991]; [Jaenicke, 1995]). Importantly, monomeric intermediates require well-defined tertiary structures to undergo specific dimerization instead of incorrect aggregation (reviewed in [Jaenicke & Rudolph, 1986]). Thus, for many dimeric proteins, the folding or subsequent assembly of the structured monomers is rate-limiting, while conformational rearrangements subsequent to dimerization are relatively minor (reviewed in [Jaenicke, 1987]). In contrast to this general mechanism, the β_2 subunit of tryptophan synthase (Blond & Goldberg, 1985), bacterial luciferase (Ziegler et al., 1993), and wild-type CoA transferase (above) are examples of dimeric proteins which undergo substantial structural reorganization *after* the formation of an initial complex. Indeed, the activation energy associated with the reconstitution of CoA transferase from its individual domains ($2.9 \pm 0.4 \times 10^2$ kJ/mol) is greater than values previously reported for other oligomeric enzymes (Rudolph et al., 1977; Zettlmeissl et al., 1984). It is therefore concluded that the degree of folding which precedes or follows subunit assembly varies with the protein and cannot be predicted *a priori*.

A dimeric protein which adopts much of its native structure after the pairing of incompletely folded subunits is predicted to be relatively susceptible to aggregation side-reactions (reviewed in [Jaenicke & Rudolph, 1986]). Consistent with this prediction, the efficiency of folding of wild-type CoA transferase in *E. coli* is compromised by aggregation, due mainly to unproductive interactions involving the disordered C-domain (Chapter 3). Why do some dimeric proteins remain sensitive to aggregation until late in the folding pathway, while others achieve relatively compact, soluble structures prior to subunit assembly? The extent to which folding steps precede the association of monomeric intermediates may be determined in part by the final quaternary structure of the dimeric protein. For example, if each C-domain of native, homodimeric CoA transferase is in simultaneous contact with the two N-domains, then the C-domain may be incapable of folding in the absence of a "scaffold" formed by the association of two protomers. To verify whether or not such quaternary structural constraints can limit the ability of the C-domain to fold autonomously, it will be necessary to determine the structure of the homodimeric enzyme by x-ray crystallography.

The mechanism proposed for the folding and assembly of CoA transferase also suggests intriguing possibilities regarding the evolution of oligomeric enzymes. It has been suggested that a gene encoding a multidomain protein could be created by the fusion of exons which code for single-domain polypeptides (Gilbert, 1978; reviewed in [Bennett et al., 1995]). Initially, each domain of the new protein would behave as an independent folding unit. However, the ability of a given domain to complete its folding in the absence of the other domain(s) might be compromised during evolution, due to the accumulation of amino acid substitutions at the interdomain interface. Although these mutations would presumably stabilize the native fold of the multidomain protein, they would also increase the susceptibility to aggregation of folding intermediates.

During the evolution of the mammalian CoA transferases from $\alpha_2\beta_2$-type precursors, the C-domain may have lost its ability to fold independently of the N-domain due to the accumulation of selected amino acid substitutions. As a result, folding intermediates would have become more susceptible to aggregation through interactions involving the incompletely folded C-domain. Speculating further, the hydrophilic linker segment of the mammalian CoA transferases may have evolved to increase the rate of assembly of the N- and C-domains compared to the rate of aggregation, thus improving the folding efficiency of the C-domain. This hypothesis is supported by the demonstration that the hinge region of CoA transferase is necessary for the refolding of enzyme *in vitro* (Chapter 2), and by preliminary results which suggest that the N_2C_2-domain complex is produced more slowly than wild-type CoA transferase in *E. coli* (not shown). Although the kinetic advantage provided by the hydrophilic linker segment was shown to be inessential to the production of active enzyme in *E. coli* (Chapter 2), the same may not be true in the mitochondrial matrix, which contains elevated concentrations of nascent, unfolded polypeptides (Ostermann et al., 1989; reviewed in [Price, 1994]). In short, the mechanism of folding of pig heart CoA transferase implies that the final, native structure of a protein may be stabilized during evolution at the expense of the ability of one or more domains to fold independently. The efficiency of folding of such a protein might in turn be improved by covalently tethering the domains to facilitate their mutual, productive interaction.

A more thorough understanding of the folding pathway of CoA transferase will require further structural analyses. For instance, the kinetics of assembly of the N- and C-domains could be evaluated from measurements of far-UV CD and intrinsic tryptophan fluorescence (reviewed in [Jaenicke & Rudolph, 1986]; [Price, 1994]). From these studies, it may be deduced whether or not the secondary and tertiary structural changes resulting from the interaction between the domains occur prior to or in concert with the formation of active enzyme. More specific conformational rearrangements may be monitored by repeating the kinetic analysis with carefully designed mutants. For instance, the single tryptophan residue (W213) of the purified N-domain may be selectively used as a probe by creating a double mutant of the C-domain in which both of its tryptophan residues (W413 and W490) are replaced with phenylalanine. From measurements of the intrinsic tryptophan fluorescence associated with an equimolar mixture of the wild-type

N-domain and the mutant C-domain, the rate at which tryptophan 213 is sequestered from solvent may be evaluated. The results of these studies would best be rationalized in consideration of a model for the three-dimensional structure of CoA transferase.

Additional experiments must also be carried out to address whether or not the individual N- and C-domains are true intermediates of the CoA transferase folding pathway. The evidence presented in Chapter 2 does not exclude the possibility that the individual domain polypeptides are off-pathway conformers, similar to the α- and β-subunits of bacterial luciferase produced individually in *E. coli* (Baldwin et al., 1993; Sinclair et al., 1993; Ziegler et al., 1993; Sinclair et al., 1994). In particular, the native-like fold of the homodimeric N-domain may represent an energy minimum distinct from that of the paired N-domains of wild-type CoA transferase. Consistent with this prediction, the two N-domains of the hinge-mutant or wild-type enzyme were crosslinked less efficiently than those of the N_2 dimer (Chapter 2). Accordingly, the conformational change associated with the assembly of the N- and C-domains may be due in part to reshuffling of the N_2 interface. If this possibility were confirmed, then the initial hypothesis that folding occurs largely *after* the formation of an initial CoA transferase homodimer would require re-evaluation. However, the conclusion that the individual domains do not complete their folding independently of each other (Chapter 2) would remain unchallenged.

To determine whether or not the individual N-domain is a true folding intermediate, the conformational properties of this polypeptide must be compared with those of the N-domain within the context of the intact enzyme. This comparison is currently not feasible, since the spectrophotometric and equilibrium unfolding data obtained for the wild-type enzyme (Chapter 2) represent contributions from both the N- and C-domains. However, from studies of a double mutant of CoA transferase in which both tryptophan residues of the C-domain (W413 and W490) are replaced with phenylalanine, the tertiary structure of the N-terminal half of the intact enzyme may be probed selectively. If the $\lambda_{max,em}$ of this double-mutant were similar to that of the individual N-domain, in the absence or presence or varying concentrations of GuHCl, then it could be inferred that the isolated domain polypeptide and the N-domain of the intact enzyme share a similar folding pathway. In addition, solution of the three-dimensional structures of wild-type CoA transferase and the purified N-domain by x-ray crystallography would permit a detailed comparison of the N_2 interfaces of both molecules at atomic resolution. The progress of such studies will be limited by the ability to identify appropriate conditions under which the N-domain crystallizes, given that this protein aggregates more readily than wild-type CoA transferase (Chapter 3).

The mechanism of aggregation of CoA transferase folding intermediates also warrants further investigation. These efforts may lead in turn to a more precise description of the degree of compactness of the enzyme domains at various stages of folding. From studies of gene expression in HB-WT and HB-Hng (Chapter 3), it was inferred that the aggregation of wild-type CoA transferase in *E. coli* is due primarily to unproductive interactions between the C-domains, and that the C-domain therefore adopts a native fold less efficiently than the N-domain. These inferences could be tested by monitoring the appearance of enzyme activity at 22 °C in mixtures containing the purified domains at different molar ratios. If the mechanism proposed for the aggregation of wild-type CoA transferase is correct (Figure 7-1), then greater yields of enzyme activity should be associated with mixtures containing higher relative concentrations of the N-domain. In addition, from detailed kinetic analyses of the loss of recoverable activity in these mixtures at 37 °C, the sequence of rate-limiting first- and/or second-order steps leading to aggregation may be identified. To determine whether or not the aggregation properties of the C-domain are due to random-coil structure independent of significant charge effects, or due to folded protein in an isoelectric situation, the solubility of the polypeptide must also be examined using various buffers. If it were demonstrated that the insolubility of the C-domain at pH 7.4 is due to isoelectric precipitation, then the model depicted in Figure

7-1 should be modified to account for differences in the balance between folding and aggregation in solutions of different pH. However, regardless of the mechanism for the aggregation of the C-domain, the current hypothesis must still be relevant to the folding of CoA transferase *in vivo*, since studies of the individual domain polypeptides were carried out at physiological pH (Chapters 2 and 3). The three-dimensional structure of wild-type CoA transferase will provide a basis for a detailed analysis of the complementary, intermolecular contacts which constitute the interface between the N- and C-domains. By identifying interactions which appear necessary to stabilize the native structure of the C-domain, it may be possible to predict which regions of the isolated polypeptide are responsible for its inability to fold autonomously (see above). These predictions may then be verified by examining the folding and aggregation properties of relevant C-domain mutants.

Future studies will also be aimed at assessing the effect of the hinge region on the folding and assembly of pig heart CoA transferase. The hydrophilic linker segment may facilitate an essential interaction between the N- and C-domains, thus enhancing the efficiency of folding under conditions that favor aggregation. Does this presumed kinetic advantage depend on the hypothetical helix-loop-helix structure of the hinge region? This question could be addressed by designing a mutant of CoA transferase with a sequence of glycine residues replacing the hydrophilic linker segment. If this mutant were capable of folding *in vivo* and refolding *in vitro* to soluble enzyme with the same yield and rate as wild-type CoA transferase, then it could be concluded that a flexible, covalent tether lacking significant secondary structure is sufficient to facilitate the association of the incompletely folded N- and C-domains. In addition, the ability of the $\alpha_2\beta_2$-type prokaryotic CoA transferases to refold from denaturant must be examined. If, in contrast to the hinge-mutant, the bacterial enzyme were capable of refolding *in vitro*, then it would be inferred that the individual α- and β-subunits of the prokaryotic CoA transferase are less susceptible to aggregation than the N- and C-domains of the pig heart enzyme. This conclusion would indirectly support the hypothesis that the hinge region evolved to offset the relative insolubility of the mammalian C-domain (see above). Alternatively, the bacterial enzyme might not be capable of refolding *in vitro*, demonstrating that the separate α- and β-subunits of the prokaryotic CoA transferase are prone to aggregation. In this case, the role of the hydrophilic linker segment could be tested by creating a mutant of the bacterial enzyme with the α- and β-subunits linked by a flexible hinge-region.[1] The successful refolding of this mutant from denaturant would provide direct evidence that the hydrophilic linker segment facilitates the correct association of the domains to which it is attached. Finally, the extent to which the role of the covalent tether depends on the folding environment may be assessed by comparing the reconstitution of wild-type CoA transferase and the hinge-mutant in a eukaryotic system such as *Saccharomyces cerevisiae*. If only the mature wild-type enzyme adopted a native fold after the import of the precursor into the mitochondrial matrix, then it would be inferred that the evolution of the hinge region enabled the mammalian CoA transferases to adapt to the harsh folding environment of the eukaryotic organelle (Ostermann et al., 1989; reviewed in [Price, 1994]). This experimental approach may be technically very challenging, as it requires that a mitochondrial presequence be appended to the C-domain, and that a gene expression system also be developed for the coordinate synthesis of the N- and C-domains in *Saccharomyces cerevisiae*.

Refolding versus aggregation in vitro. The yield of refolded wild-type CoA transferase was markedly compromised by aggregation, particularly at elevated temperature and protein concentration (Chapters 2 and 3). Similar results have been reported for the renaturation of other oligomeric enzymes (reviewed in [Jaenicke, 1991]; [Price, 1994]; [Jaenicke, 1995]). In general, multimeric enzymes refold less efficiently *in vitro* than monomeric enzymes (reviewed in [Jaenicke & Rudolph, 1986]; [Price, 1994]). The refolding of monomeric enzymes involves a series of first-order conformational changes, while the reconstitution of oligomeric enzymes consists of first- and second-order steps. Accordingly, the refolding of a monomeric enzyme should be substantially favored over aggregation at a sufficiently low protein concentration, given that the rates of first-order reactions are unaffected by dilution. Aggregation, which is of kinetic order greater than two, occurs more slowly with decreasing protein concentration (reviewed in [Price, 1994]). The refolding of an oligomeric enzyme does not compete effectively with aggregation below a minimal protein concentration, since the rate of second-order association decreases with decreasing protein concentration. Under sufficiently dilute conditions, the nonnative subunits of the oligomeric enzyme can undergo inactivating, first-order structural changes to form molecular species which are incapable of productive assembly (Ziegler et al., 1993; reviewed in [Price, 1994]). Given these arguments, the inability to identifying conditions suitable for the quantitative renaturation of CoA transferase is reasonable.

From the results of the temperature-shift experiments, it was inferred that the refolding pathway of the wild-type enzyme consists of early and late intermediates in a rapid equilibrium (Chapter 3). The early conformers are relatively susceptible to aggregation, likely due to the exposure of a substantial proportion of their hydrophobic residues to the aqueous solvent. In contrast, the late intermediates aggregate less readily, presumably because they possess a relatively stable tertiary structure. At 22 °C, the late conformers undergo a slow, nearly irreversible conversion to the native enzyme. However, under conditions which promote unfolding, the late intermediates revert rapidly to early molecular species, which subsequently aggregate.

This model for the reconstitution of CoA transferase supports currently held views of how proteins partition between correct and incorrect pathways during refolding. Previously, "double-mixing experiments" were used to investigate the rates of commitment to aggregation and renaturation of hen and turkey lysozyme (Goldberg et al., 1991). From the results of these studies, it was concluded that the refolding process consists of three phases: (1) the rapid, reversible conversion of the unfolded protein to early intermediates which are susceptible to aggregation; (2) the rapid, reversible conversion of early intermediates to late intermediates, which resist aggregation; and (3) the slow, irreversible conversion of late intermediates to the native structure. The similarity between this scheme and that proposed for the renaturation of CoA transferase suggests that monomeric and oligomeric proteins refold and aggregate by common pathways.

The kinetics of reconstitution and aggregation of CoA transferase *in vitro* merit further investigation. For example, the enzyme's rate of commitment to achieve the native state at 22 °C could be assessed by incubating a solution of refolding enzyme at 37 °C for 5 to 10 min, after preincubation for various times at 22 °C. If the rate of commitment to refold coincided with the rate of appearance of enzyme activity, then it could be inferred that nonnative forms which do not unfold at 37 °C are absent from the CoA transferase refolding pathway. In addition, the enzyme's rate of commitment to aggregation at 22 °C could be evaluated by refolding a solution of CoA transferase at high concentration for various times before diluting to a final, low protein concentration. This approach is similar to that described by Goldberg et al. (1991). From the results of this experiment, the rate of aggregation of early CoA transferase refolding intermediates may be determined. Since this rate is very rapid (Chapter 3), it may be necessary to carry out the two-step dilution using stopped-flow techniques.

The final yield of refolded, soluble CoA transferase depends on the kinetic partitioning of the early intermediates between late conformers and insoluble aggregates. Accordingly, once the rate of aggregation of the early conformers has been estimated, appropriate strategies may be devised to slow this process. For example, the optimal protein concentration for the reconstitution of CoA transferase *in vitro* should be evaluated by measuring the activity recovered upon diluting the unfolded enzyme to various extents. In addition, the enzyme's rate of commitment to aggregation should be measured at temperatures lower than 22 °C by using variations of the two-step dilution procedure described above. Finally, the effects of low molecular-weight additives on the enzyme's rate of commitment to aggregation should be examined. One such additive which has been used with success to increase protein refolding yields is L-arginine (Buchner & Rudolph, 1991; reviewed in [Guise et al., 1996]; [Mukhopadhyay, 1997]). Based on the results of these studies, methods may be developed for the recovery of large amounts of recombinant, wild-type CoA transferase from inclusion bodies produced in cells of *E. coli*. Conceivably, such an approach could lead to improved yields of protein and simplified protocols of enzyme purification.

Effects of chaperonins on folding and refolding. Intermediates of the CoA transferase refolding pathway formed a stable complex with GroEL in the absence of ATP (Chapter 3). The yield and rate of refolding of the wild-type enzyme were increased and decreased, respectively, in solutions containing GroEL and ATP. Importantly, the conformers released from the chaperonin were not committed to adopt a native fold, even in the presence of GroES. It was concluded that GroEL can decrease the rate of aggregation of CoA transferase refolding intermediates by a "buffering" mechanism, involving transient interactions between nonnative forms of the enzyme and the hydrophobic interior of the GroEL toroid. (Chapter 3).

These results provide insight with respect to the mechanisms by which chaperonins facilitate the refolding of enzymes *in vitro*. First, GroEL can increase the yield of refolded, functional protein without releasing conformers that are committed to achieve the native state. This passive process, referred to as the "buffering" effect (Buchner et al., 1991; Ayling & Baneyx, 1996), accounts for the increased yield of reconstitution of enzyme to the active form in the presence of GroEL and ATP but in the absence of GroES. Under these conditions, proteins that refold to the native form with enhanced yields are normally reconstituted by first-order, rate-limiting structural changes. Nonnative forms of these proteins cycle on and off the chaperonin, leading to a decrease in the effective concentration of conformers susceptible to aggregation. Second, GroEL can assist the renaturation of an enzyme by releasing intermediates that are more committed to fold than the species which were initially bound to the chaperonin (Martin et al., 1991; Schmidt et al., 1994; Mayhew et al., 1996; Weissman et al., 1996; Fedorov & Baldwin, 1997; Rye et al., 1997). Proteins which require GroEL, GroES, and ATP to refold under non-permissive conditions (Schmidt et al., 1994) are reconstituted by this active process.

Results obtained from studies of the refolding of CoA transferase in the presence of GroEL also address the current model for the folding and assembly of oligomeric proteins in mammalian mitochondria. It has been argued that multimeric enzymes transported into the mitochondrial matrix require Hsp60 and Cpn10 to achieve the native state (Cheng et al., 1989; Ostermann et al., 1989; Rospert et al., 1993; Höhfeld & Hartl, 1994). As discussed in Chapter 3, GroEL and GroES are necessary and sufficient for the refolding of oligomeric mitochondrial enzymes under non-permissive conditions *in vitro*. In contrast, the complete chaperonin system does not assist the reconstitution of wild-type CoA transferase *in vitro* (Chapter 3), indicating that this enzyme interacts with GroEL$_{14}$:GroES$_7$ in a manner distinct from other multimeric mitochondrial proteins. Based on the evidence presented in this thesis, it is not possible to predict whether or not the folding and assembly of CoA transferase in the mitochondrial matrix are independent of Hsp60 and Cpn10. As one possibility, the enzyme may require the complete chaperonin system to refold *in vivo*. If this hypothesis were true, then it could be inferred that pig heart CoA transferase evolved to interact specifically with Hsp60$_{14}$:Cpn10$_7$ but not with GroEL$_{14}$:GroES$_7$. In turn, this important conclusion could be the first step towards identifying structural features of the mammalian enzymes which discriminate between the two homologous chaperonin systems (see below). As a second possibility, Hsp60 and Cpn10 may not be necessary for the folding and assembly of CoA transferase *in vivo*. Accordingly, it could be inferred that the enzyme is relatively insusceptible to aggregation in the mitochondrial matrix due to its own molecular properties rather than the participation of the chaperonin system. This conclusion could suggest further research aimed at identifying the molecular features of CoA transferase necessary for its autonomous folding *in vivo*. Interestingly, recent studies indicate that some monomeric enzymes of the mitochondrial matrix (including the cyclophilin Cpr3p) adopt a native fold in an $Hsp60_{14}$:$Cpn10_7$-independent manner (Rospert et al., 1996). However, similar findings have not been reported for oligomeric mitochondrial proteins.

Future experiments must be performed to thoroughly assess the role played by the prokaryotic and eukaryotic chaperonins in the (re)folding of CoA transferase. The formation of a complex between the refolding wild-type enzyme and GroEL in the absence of ATP should be verified by immunoprecipitation, using a commercially available monoclonal antibody that recognizes the chaperonin. If such a complex is detectable by this method, then immunoprecipitation experiments could also be performed to probe possible interactions between the individual N- and C-domains and GroEL. The results of this analysis might confirm the hypothesis that the C-domain exposes a greater proportion of its hydrophobic residues than the N-domain (see above). In addition, it is uncertain whether or not a complex is formed between the hinge-mutant and GroEL upon dilution of the unfolded enzyme in a solution containing the chaperonin. This question could also be addressed by immunoprecipitation of the hinge-mutant in the absence of ATP. If the N- and C-domains were found to associate with GroEL, then it could be concluded that the complete chaperonin system also binds the hinge-mutant. In this case, the inability of the hinge-mutant to refold in the presence of GroEL and GroES would be attributed not to the inability of the separate domains to bind the chaperonin, but to the release of the domains as intermediate species not committed to fold (Chapter 3).

Recently it was suggested that the prokaryotic and eukaryotic chaperonins release different nonnative forms of the same polypeptide (Tian et al., 1995). In addition, Rospert et al. (1996) have demonstrated that GroEL and Hsp60 influence the refolding of a given protein substrate to markedly different extents. Accordingly, the effect of Hsp60 on the reconstitution of CoA transferase cannot be inferred from the results of refolding studies using GroEL, but must be tested directly. Specifically, the yield and kinetics of CoA transferase renaturation should be evaluated in the presence of Hsp60, or Hsp60 and ATP, or Hsp60, ATP, and Cpn10, as described by Rospert et al. (1996). In addition, a similar experiment can be carried out to determine if the hinge-mutant is capable of refolding in the presence of the mitochondrial chaperonin. Assuming that the hydrophilic linker segment evolved to fulfill a role that is essential for the folding of wild-type CoA transferase in the mitochondrial matrix, it is predicted that Hsp60 will not facilitate the refolding of the hinge-mutant *in vitro*. The possible formation of a complex between Hsp60 and wild-type CoA transferase or Hsp60 and the individual domains can be assessed by immunoprecipitation using a commercially available monoclonal antibody that recognizes the mitochondrial chaperonin.

If it were demonstrated that Hsp60 facilitates the refolding of wild-type CoA transferase, then it would be inferred that the enzyme interacts specifically with the mitochondrial chaperonin system, but not with $GroEL_{14}$:$GroES_7$ (see above). In turn, this conclusion would imply that the $\alpha_2\beta_2$-type prokaryotic CoA transferases associate specifically with the bacterial chaperonin system, but not with $Hsp60_{14}$:$Cpn10_7$. This hypothesis could be tested by repeating the refolding and immunoprecipitation experiments described above with appropriate combinations of the prokaryotic CoA transferase, $GroEL_{14}$:$GroES_7$, and $Hsp60_{14}$:$Cpn10_7$. By analyzing how the two homologous enzymes interact differently with Hsp60 and GroEL, it may be possible to predict which molecular features are specifically recognized by each chaperonin. These predictions can then be tested by extensive mutagenesis studies.

The results of refolding and immunoprecipitation experiments will provide insight with respect to interactions between the CoA transferases and the chaperonins *in vitro*. Ultimately, the physiological relevance of these interactions must be confirmed by examining the effect of the chaperonins on the folding and assembly of the CoA transferases *in vivo*. First, the yield of active pig heart CoA transferase in a strain of *E. coli* that lacks a functional GroEL complex should be determined. For example, the mutant strain NRK117 contains a form of the chaperonin which is inactivated at 43 °C (Kusukawa et al., 1989). However, preliminary studies of the folding and assembly of CoA transferase in NRK117 have been unsuccessful, since the enzyme is not produced in soluble form even in the control, wild-type strain at the non-permissive temperature. As an alternative, this experiment should be repeated using the "ts2R" strain of *E. coli*, which contains a mutant of GroEL that is inactivated at a lower temperature of 37 °C (Horwich et al., 1993). In addition, it has been reported that the synthesis of high levels of a C-terminal deletion mutant of GroEL interferes with the assembly of the wild-type chaperonin in *E. coli* (McLennan et al., 1994). Accordingly, the effect of GroEL on the folding and assembly of CoA transferase *in vivo* may be assessed by measuring the yield of enzyme activity in cells containing large amounts of the C-terminally truncated chaperonin. Since this experiment can be carried out at 22 °C, the effect of the inactivation of GroEL on the yield of native CoA transferase *in vivo* can be assessed under conditions suitable for the production of high levels of soluble enzyme. As well, the yield of active pig heart CoA transferase in a strain of *S. cerevisiae* that lacks a functional Hsp60 complex should be determined. The mutant strain *mif4*, which contains a form of the chaperonin that is inactivated at 37 °C (Cheng et al., 1989), may be used for this purpose. For all of these studies, the production of active CoA transferase must be measured shortly after the inactivation of GroEL or Hsp60, since the disruption of chaperonin function is lethal to the host cell (Cheng et al., 1989; Horwich et al., 1993).

Finally, the results of this thesis do not explain why the hinge-mutant fails to refold *in vitro* despite being correctly folded and assembled *in vivo*. This question may be addressed by measuring the yield of soluble, active hinge-mutant in cells of *E. coli* that lack a functional GroEL complex. If the folding and assembly of the hinge-mutant *in vivo* were dependent on GroEL, then it would be concluded that the chaperonin is necessary — but not sufficient — for the reconstitution of the hinge-mutant *in vitro* (Chapter 3). Subsequent efforts could be aimed at identifying additional cellular components required for the renaturation of the hinge-mutant. For example, it could be determined that the bacterial Hsp70 or cyclophilin is necessary by including either chaperone in the reaction mixture. Perhaps this approach of "trial-and-error" could lead to the development of an *in vitro* system for the complete refolding of the hinge-mutant.

Two multimeric forms of CoA transferase. The recombinant pig heart CoA transferase isolated from cells of *E. coli* was shown to consist of homodimeric and homotetrameric species in a molar ratio of 18 to 1 (Chapter 4). The two oligomeric forms were indistinguishable with respect to specific enzyme activity, subunit mass, far-UV CD, intrinsic tryptophan fluorescence, and equilibrium unfolding.

These results extend the current understanding of the structure of the mammalian CoA transferases. From previous studies, it was accepted that the enzyme exists as a homodimer in solution (Chapter 4). However, it is proposed here for the first time that CoA transferase can adopt at least two quaternary structures under certain conditions. Accordingly, the homodimeric form of the enzyme should not be considered the obligatory end-product of the folding pathway. Rather, the small molecule possesses structural features that enable it to engage in additional intermolecular interactions, thus forming the large conformer.

The hydrophilic linker segment was shown to be necessary for the formation of the large molecule, implying that two homodimers interact through the hinge region to form the homotetramer. This finding may facilitate the interpretation of a model for the three-dimensional structure of CoA transferase. As mentioned in Chapter 4, there are four monomers present in each asymmetric unit of the crystals obtained to date from a sample of the small conformer. These may be organized as one homotetramer, equivalent to the large molecule which exists in solution, or as two homodimers that interact via protein-

protein crystal-packing contacts (Carugo & Argos, 1997). To distinguish between these possibilities, crystals of CoA transferase should be dissolved in a small volume of buffer, and the resulting protein solution analyzed by non-denaturing PAGE.

Under benign conditions, a substantial energy barrier prevented the rapid interconversion of the homodimer and homotetramer. However, under denaturing conditions the relative amounts of the two conformers were apparently dependent on the total concentration of monomer. This result provides further evidence that protein folding and assembly pathways may be kinetically determined (reviewed in [Creighton, 1994]). Consequently, the native fold of a polypeptide is the most kinetically accessible of all possible conformations, and not necessarily the most stable. Examples of proteins that adopt their native structures by kinetically determined pathways include influenza hemagglutinin (Gething et al., 1986), α-lytic protease (Baker et al., 1992), plasminogen activator inhibitor-1 (Mottonen et al., 1992), subtilisin BPN' (Eder et al., 1993), and bacterial luciferase (Sinclair et al., 1994). Pig heart CoA transferase and the LDH of *Thermotoga maritima* (Dams et al., 1996) are examples of proteins that adopt multiple quaternary structures by the kinetically-controlled assembly of identical subunits.

Further studies are required to identify the conditions that lead to the formation of the CoA transferase homotetramer. For example, it was suggested that this oligomerization occurs readily at high ionic strength (Chapter 4). To test this hypothesis, the relative amounts of the homodimer and homotetramer in solutions of varying salt concentration should be determined by non-denaturing PAGE analysis. In addition, the effect of pH on the oligomerization of CoA transferase should be assessed by carrying out similar studies using different buffers. For both experiments, the concentration of CoA transferase should be relatively high, given that the assembly of the small molecules to the large form is dependent on the monomer concentration in the absence of a kinetic barrier. Moreover, it should be verified by non-denaturing PAGE analysis that the small conformer does not convert rapidly to the large molecule in solutions prepared for the crystallization of CoA transferase. Such equilibration would be detrimental to the growth of the crystals described in this thesis, given that the homotetramer does not crystallize under the same conditions as the homodimer (Chapter 4). If it were demonstrated that the small molecule does convert to the large form under these conditions, then subsequent efforts would be aimed at slowing this exchange by appropriate modification of the crystallization protocol. For example, the crystallization temperature could be decreased from 22 °C to 4 °C.

The structural properties of the CoA transferase homotetramer also warrant further investigation. It was proposed that the large conformer consists of two homodimers that associate via direct interactions between their respective hinge-regions, or the swapping of identical domains (Chapter 4). These possibilities can be distinguished by constructing deletion mutants of CoA transferase which lack several amino acid residues in the hinge-region. If the first model were correct, then the deletion mutant should be less capable of tetramerization than the wild-type subunit due to a decrease in the number of contacts between the interacting homodimers. In contrast, if the second model were correct, then the deletion mutant should be more capable of tetramerization than the wild-type enzyme, since a shortening of the covalent tether would prevent the swapped domain from folding back and interacting with the opposite domain of the same subunit (reviewed in [Bennett et al., 1995]; [Schlunegger et al., 1997]). Active site complementation experiments may be used to investigate the structure of the large form of CoA transferase. If the domain-swapping model were correct, then a tetramer assembled from two different, inactive homodimers should contain a pair of functional, reconstituted active sites (Figure 7-1). In contrast, a hybrid tetramer formed without the exchange of domains would contain no functional active sites (Figure 7-1). The subunit hybridization experiment could not be carried out as described in Chapter 6, since the large conformer is not produced upon refolding wild-type CoA transferase *in vitro* (Chapter 4). Instead, a hybrid tetramer could potentially be isolated from cells of *E. coli* in which the genes encoding the two inactive mutants were co-expressed. A substantial amount of enzyme activity associated with this recovered hybrid tetramer would be taken as evidence for a domain-swapped structure. However, a lack of enzyme activity would be much less meaningful, given the large number of assumptions inherent to the experimental approach. Ultimately, a complete understanding of the interactions that stabilize the homotetramer will require that a model of its three-dimensional structure be solved by x-ray crystallography. To this end, current efforts are aimed at identifying conditions suitable for the crystallization of the large conformer.

Finally, it is unknown whether or not the homotetrameric enzyme exists *in vivo*. To address this question, the quaternary structure(s) of CoA transferase in lysates of *E. coli* cells should be determined by non-denaturing PAGE analysis combined with immunoblotting. Moreover, if the conversion of the small molecule to the large conformer does occur *in vivo*, then this process may confer some advantage upon the enzyme (Chapter 4). Thus, physiological relevance can also be attributed to the large molecule by proving that this form of the enzyme displays catalytic or regulatory properties distinct from those of the small conformer. For example, a thorough kinetic analysis of the homotetramer should be carried out to determine if this form of CoA transferase is subject to allosteric modulation, as was demonstrated for the domain-swapped dimer of bovine seminal RNase (Piccoli et al., 1988). In addition, the question of whether or not the homotetramer exists *in vivo* may be addressed more easily once the solution conditions favoring the formation of the large conformer are identified (see above). These conditions may be incompatible with the intracellular milieu, suggesting that the homotetramer represents an artifact of protein purification. Regardless of the answer, knowledge of the molecular properties of the large molecule may provide insight with respect to the conformational flexibility of the CoA transferase homodimer.

The active site of CoA transferase. From the mass of a peptide released by the autolytic fragmentation, it was inferred that glutamate 344 is the catalytic nucleophile of pig heart CoA transferase (Chapter 5). This conclusion was confirmed by demonstrating that the E344A and E344D mutants are at least 1.7×10^3 and 1.1×10^5 fold less active than the wild-type enzyme, respectively (Chapter 6). Furthermore, the C67S mutant was resistant to rapid inactivation by DTNB, indicating that cysteine 67 is located near the substrate binding pocket (Chapter 6). The mapping of glutamate 344 and cysteine 67 to the active site represents a significant contribution to the study of pig heart CoA transferase. As mentioned in Chapter 1, previous analyses led to a thorough characterization of the enzyme's "ping-pong" kinetic mechanism (Hersh & Jencks, 1967a,b; Benson & Boyer, 1969; Solomon & Jencks, 1969; Jencks, 1973; White & Jencks, 1976; Howard et al., 1986; Williams, 1990) and sensitivity to thiol reagents (White et al., 1976; Kindman & Jencks, 1981; Williams, 1990). Each of these functional properties of CoA transferase can now be rationalized with reference to a specific amino acid residue. In turn, this knowledge will facilitate efforts to interpret the structure of the enzyme with respect to the function of CoA transferase. Furthermore, the identification of cysteine 67 and glutamate 344 underscores the functional importance of the glycine cluster and the "ENG" motif, both of which are conserved among the eukaryotic and $\alpha_2\beta_2$-type prokaryotic CoA transferases. Notably, the "ENG" sequence was recognized as being similar to the conserved "ENG" motif of the "family 1" glycosyl hydrolases. This similarity of amino acid sequence led to the suggestion that both classes of enzymes, which catalyze similar chemical reactions, acquired a common structural motif through convergent evolution (Chapter 5).

The specific enzyme activity of the E344Q mutant was at least 6.0×10^2 times greater than that of the E344D mutant, indicating that the length of the glutamate 344 sidechain is more crucial for catalysis than the negative charge on the γ-carboxylate group (Chapter 6). The loss of enzymatic activity associated with the E344D mutation was remarkable, given that the sidechain of an aspartate residue is shorter than that of a glutamate residue by the size of only one methylene group. Apparently, movements of the E344D polypeptide chain to place the β-carboxylate group of aspartate 344 in proximity with the acyl-CoA thiolester were prohibited. These results extend the current understanding of how CoA transferase achieves large rate accelerations. Namely, the significance attributed to the length of the glutamate 344 sidechain suggests that the acyl-CoA substrates are bound precisely in the active site. As mentioned in Chapter 1, this rigid binding is necessary to ensure the loss of entropy of the substrates in the Michaelis complex (Moore & Jencks, 1982a,b,c; Jencks, 1987).

Upon incubation in buffer containing acetoacetyl-CoA, the E344Q mutant was slowly converted to the wild-type enzyme. It was proposed that this activation of the mutant involves a nucleophilic attack by glutamine 344 on the acyl-CoA thiolester, leading to the formation of a mixed anhydride intermediate. These results provide insight with respect to the catalytic function of wild-type CoA transferase. For example, the ability of glutamine 344 of the mutant to carry out a nucleophilic attack suggests that a general acid-base group may be necessary for catalysis of the normal reaction by the wild-type enzyme (Chapter 6). A role for such a group in the active site of CoA transferase has not been proposed prior to this study. In addition, the nucleophilicity of glutamine 344 of the mutant may be facilitated by electrostatic and hydrogen-bonding interactions between the substrate's thiolester carbonyl moiety and the residues of a nearby oxyanion hole. These interactions may also facilitate the reaction between glutamate 344 of the wild-type enzyme and succinyl-CoA or acetoacetyl-CoA. In a similar way, two main-chain amide nitrogens of glutaconate CoA-transferase are proposed to stabilize a developing negative charge on the thiolester carbonyl moiety of the acyl-CoA substrate (Jacob et al., 1997). Finally, the mechanism proposed for the deamidation of glutamine 344 of the mutant involves the formation of a mixed anhydride intermediate (Chapter 6). This hypothesis supports the stepwise chemistry proposed for the wild-type CoA transferase half-reaction (White & Jencks, 1976; Pickart & Jencks, 1979; Moore & Jencks, 1982a,b).

The results of the subunit hybridization studies suggested that the active sites of the homodimeric wild-type enzyme are not located at the interface between the two monomers (Chapter 6). This conclusion is consistent with the view (Chapter 6) that a primitive N_2C_2-domain complex was assembled during the evolution of the CoA transferases prior to the gene-fusion event proposed by Parales & Harwood (1992). Moreover, the fact that the active sites are not shared between the subunits implies that an alternative rationale must be considered to account for the homodimeric structure of pig heart CoA transferase. For example, it has been proposed that the oligomerization of proteins leads to a decrease in the osmotic pressure of the cell (Goodsell & Olson, 1993). Presumably, this argument also applies to eukaryotic organelles such as the mitochondria. In addition, it has been suggested that the degree of hydrophobicity at the interface between the subunits of oligomeric proteins is relatively intermediate between the solvent-accessible surface and the interior of folded monomers (Argos, 1988; Janin et al., 1988; Miller, 1989; Tsai et al., 1996; Tsai et al., 1997). Accordingly, the homodimeric form of pig heart CoA transferase may be less susceptible to aggregation than two separate monomers. Finally, an understanding of how the active sites are arranged in the homodimer may facilitate the fitting of a structural model of CoA transferase into an initial electron density map. For example, ambiguities in tracing the polypeptide chain through the electron density corresponding to the active site region may be resolved using the knowledge that cysteine 67 and glutamate 344 must belong to the same subunit.

Numerous questions with respect to the layout of the active site of CoA transferase remain unanswered. For instance, the precise role of cysteine 67 is unclear. From the results of studies of C67S, it was concluded that even a subtle change at position 67 such as the replacement of a sulfur atom with an oxygen atom leads to a substantial decrease in enzyme activity (Chapter 6). The effects of charge and/or size of the sidechain of residue 67 on the enzyme's catalytic function could be studied further by measuring the specific activities of mutants containing residues other than cysteine or serine at this position of the active site. For example, it is predicted that the replacement of cysteine 67 with a bulky hydrophobic or aromatic residue should abolish the activity of CoA transferase, due to steric hindrance at the active site (Kindman & Jencks, 1981). Once identified, such a mutant could be used along with E344A or E344D for further subunit hybridization experiments, carried out *in vitro* or *in vivo*. In addition, it should be demonstrated that a double-mutant subunit, which carries both inactivating amino acid replacements, does not negatively complement the subunit of the wild-type enzyme (Wente & Schachman, 1987). Conceivably, the results of such studies would further support the inference that the active sites of the CoA transferase homodimer are not shared between the two subunits (Chapter 6). Finally, the kinetic parameters of all mutants containing an amino acid substitution at position 67 should be assessed to confirm the preliminary conclusion that cysteine 67 of wild-type CoA transferase participates in the binding of succinate (Chapter 6).

The mechanism of activation of E344Q should also be studied further. The deamidation of glutamine 344 may be confirmed by demonstrating a correlation between the activation of E344Q and the appearance of a new site for proteolysis by endoproteinase Glu-C. This experimental approach is reasonable, given that endoproteinase Glu-C is extremely specific for peptide cleavage at glutamate residues compared to glutamine residues (Staedtler et al., 1995). In addition, it is predicted that succinate inhibits the deamidation of glutamine 344 only *after* the formation of a covalent intermediate between E344Q and CoA (Figure 6-20). Accordingly, the inhibition by succinate should be uncompetitive with respect to acetoacetyl-CoA (Segel, 1975). This hypothesis could be verified by measuring the rate of activation of E344Q in solutions containing various amounts of acetoacetyl-CoA and succinate. Finally, the formation and subsequent breakdown of a type II mixed anhydride should lead to the release of acetoacetamide from the active site (Figure 6-20). To test this prediction, one-dimensional NMR or HPLC can be used to analyze the reaction mixture after the activation of E344Q.

Additional site-directed mutagenesis studies should be carried out to address the functional importance of the "ENG" motif of CoA transferase (Chapter 5). Interestingly, asparagine residues within a similar "NG" motif of other proteins are highly susceptible to deamidation via the formation of a succinimide intermediate (Geiger & Clarke, 1987; Capasso et al., 1989; Patel & Borchardt, 1990; Tyler-Cross & Schirch, 1991). It has been argued that the flexibility of the polypeptide chain within the region containing the "NG" sequence is critical to the rate of deamidation (Kossiakoff, 1988; Capasso et al., 1996). By analogy, a similar local conformation may facilitate the deamidation of E344Q and the autolytic fragmentation of wild-type CoA transferase, both of which may also involve a cyclization mechanism (Chapters 1, 5 and 6). This intriguing hypothesis could be addressed by analyzing the effects of amino acid substitutions at positions 345 and 346 on the rates of deamidation of glutamine 344 or autolysis of the mutant enzymes. Ultimately, the local conformation of the polypeptide chain in the region of the "ENG" motif may be confirmed by inspecting a model for the three-dimensional structure of CoA transferase. This structural information may provide insight with respect to the conformations of proteins which enhance the reactivity of amide groups in general. The current understanding in this area is largely due to studies of the stereochemical properties which favor the N-glycosylation of asparagine residues (Imperiali & Shannon, 1991; Imperiali et al., 1992a,b).

The importance of x-ray crystallography. From the above discussion, it is clear that numerous important questions concerning the folding and catalytic properties of succinyl-CoA:3-ketoacid CoA transferase remain unanswered. In many cases, these problems would best be addressed by examining a model for the three-dimensional structure of the enzyme. As mentioned, crystals of CoA transferase have been obtained, and attempts are ongoing to solve the structure of the enzyme by using the multiple isomorphous replacement (MIR) method (reviewed in [Drenth, 1994]) to obtain phase information. To date, however, crystals that are optimal for x-ray analysis have not been obtained reproducibly. In addition, crystals soaked in solutions containing heavy atoms have not proven to be isomorphous compared to the unsoaked (or "native") crystal forms. Thus, both the crystallization protocol and the screening of heavy atom derivatives must be refined before the solution of the structure of this enzyme may be achieved.

Ultimately, knowledge of the three-dimensional structures of several CoA transferases would be extremely useful. For example, a comparison of the structures of pig heart CoA transferase and acetate/succinate CoA-transferase of *Trichomonas vaginalis* might provide a rationale for the subtle difference in substrate specificities between these two enzymes (Chapter 1). In addition, a detailed characterization of the active sites of the CoA transferases of *T. vaginalis* and *Mycobacterium tuberculosis* might facilitate the rational design of drugs specific for the enzymes of these pathogens. Finally, the evolutionary relationships between the $\alpha_2\beta_2$-type prokaryotic and the eukaryotic CoA transferases would be understood more clearly if the structures of these enzymes were known at atomic resolution.

Final remarks. In summary, the results of the investigations described in this thesis provide insight with respect to the structural properties of CoA transferase responsible for folding, assembly, and catalysis. This information will likely be crucial to the eventual interpretation of a model for the enzyme's three-dimensional structure. Moreover, the conclusions drawn from this work have suggested additional questions that may be tested by careful experimentation. Finally, many of the observations described in this thesis are relevant to the general understanding of how oligomeric proteins adopt a native fold, and how enzymes achieve large rate accelerations.

ENDNOTES

[1] Such a mutant of the glutaconate CoA-transferase of *Acidaminococcus fermentans* was recently shown to display partial enzyme activity (Mack & Buckel, 1997). However, the refolding properties of this mutant were not investigated.

REFERENCES

Argos, P. (1988) *Protein Eng. 2*, 101-113.

Ayling, A., & Baneyx, F. (1996) *Protein Sci. 5*, 478-487.

Baker, D., Sohl, J. L., & Agard, D. A. (1992) *Nature 356*, 263-265.

Baldwin, T. O., Ziegler, M. M., Chaffotte, A. F., & Goldberg, M. E. (1993) *J. Biol. Chem. 268*, 10766-10772.

Bennett, M. J., Schlunegger, M. P., & Eisenberg, D. (1995) *Protein Sci. 4*, 2455-2468.

Benson, R. W., & Boyer, P. D. (1969) *J. Biol. Chem. 244*, 2366-2371.

Blond, S., & Goldberg, M. E. (1985) *J. Mol. Biol. 182*, 597-606.

Buchner, J., & Rudolph, R. (1991) *Bio/Technology 9*, 157-162.

Buchner, J., Schmidt, M., Fuchs, M., Jaenicke, R., Rudolph, R., Schmid, F. X., & Kiefhaber, T. (1991) *Biochemistry 30*, 1586-1591.

Capasso, S., Mazzarella, L., Sica, F., & Zagari, A. (1989) *Pept. Res. 2*, 195-200.

Capasso, S., Di Donato, A., Esposito, L., Sica, F., Sorrentino, G., Vitagliano, L., Zagari, A., & Mazzarella, L. (1996) *J. Mol. Biol. 257*, 492-496.

Carugo, O., & Argos, P. (1997) *Protein Sci. 6*, 2261-2263.

Cheng, M. Y., Hartl, F.-U., Martin, J., Pollock, R. A., Kalousek, F., Neupert, W., Hallberg, E. M., Hallberg, R. L., & Horwich, A. L. (1989) *Nature 337*, 620-625.

Creighton, T. E. (1994) in *Mechanisms of Protein Folding* (Pain, R. H., Ed.) pp. 1-25, IRL Press, Oxford, U. K.

Dams, T., Ostendorp, R., Ott, M., Rutkat, K., & Jaenicke, R. (1996) *Eur. J. Biochem. 240*, 274-279.

Drenth, J. (1994) in *Principles of Protein X-ray Crystallography*, pp. 129-182, Springer-Verlag, Inc., New York.

Eder, J., Rheinnecker, M., & Fersht, A. R. (1993) *Biochemistry* 32, 18-26.

Fedorov, A. N., & Baldwin, T. O. (1997) *J. Mol. Biol. 268*, 712-723.

Geiger, T., & Clarke, S. (1987) *J. Biol. Chem. 262*, 785-794.

Gething, M.-J., McCammon, K., & Sambrook, J. (1986) *Cell 46*, 939-950.

Gilbert, W. (1978) *Nature 271*, 501.

Goldberg, M. E., Rudolph, R., & Jaenicke, R. (1991) *Biochemistry 30*, 2790-2797.

Goodsell, D. S., & Olson, A. J. (1993) *Trends Biochem. Sci. 18*, 65-68.

Guise, A. D., West, S. M., & Chaudhuri, J. B. (1996) *Mol. Biotechnol. 6*, 53-64.

Hersh, L. B., & Jencks, W. P. (1967a) *J. Biol. Chem. 242*, 3468-3480.

Hersh, L. B., & Jencks, W. P. (1967b) *J. Biol. Chem. 242*, 3481-3486.

Höhfeld, J., & Hartl, F. U. (1994) *J. Cell Biol. 126*, 305-315.

Horwich, A. L., Low, K. B., Fenton, W. A., Hirshfield, I. N., & Furtak, K. (1993) *Cell 74*, 909-917.

Howard, J. B., Zieske, L., Clarkson, J., & Rathe, L. (1986) *J. Biol. Chem. 261*, 60-65.

Imperiali, B., & Shannon, K. L. (1991) *Biochemistry 30*, 4374-4380.

Imperiali, B., Shannon, K. L., & Rickert, K. W. (1992a) *J. Am. Chem. Soc. 114*, 7942-7944.

Imperiali, B., Shannon, K. L., Unno, M., & Rickert, K. W. (1992b) *J. Am. Chem. Soc. 114*, 7944-7945.

Jacob, U., Mack, M., Clausen, T., Huber, R., Buckel, W., & Messerschmidt, A. (1997) *Structure 5*, 415-426.

Jaenicke, R. (1987) *Prog. Biophys. Mol. Biol. 49*, 117-237.

Jaenicke, R. (1991) *Biochemistry 30*, 3147-3161.

Jaenicke, R. (1995) *Phil. Trans. R. Soc. Lond.* B *348*, 97-105.

Jaenicke, R., & Rudolph, R. (1986) *Methods Enzymol. 131*, 218-250.

Janin, J., Miller, S., & Chothia, C. (1988) *J. Mol. Biol. 204*, 155-164.

Jencks, W. P. (1973) in *The Enzymes*, 3rd ed. (Boyer, P. D., Ed.) Vol. IX, pp. 483-496, Academic Press, Inc., New York.

Jencks, W. P. (1987) *Cold Spring Harbor Symp. Quant. Biol. 52*, 65-73.

Kindman, L. A., & Jencks, W. P. (1981) *Biochemistry 20*, 5183-5187.

Kossiakoff, A. A. (1988) *Science 240*, 191-194.

Kusukawa, N., Yura, T., Ueguchi, C., Akiyama, Y., & Ito, K. (1989) *EMBO J. 8*, 3517-3521.

Mack, M., & Buckel, W. (1997) *FEBS Lett. 405*, 209-212.

McLennan, N. F., McAteer, S., & Masters, M. (1994) *Mol. Microbiol. 14*, 309-321.

Martin, J., Langer, T., Boteva, R., Schramel, A., Horwich, A. L., & Hartl, F.-U. (1991) *Nature 352*, 36-42.

Mayhew, M., da Silva, A. C. R., Martin, J., Erdjument-Bromage, H., Tempst, P., & Hartl, F. U. (1996) *Nature 379*, 420-426.

Miller, S. (1989) *Protein Eng. 3*, 77-83.

Moore, S. A., & Jencks, W. P. (1982a) *J. Biol. Chem. 257*, 10874-10881.

Moore, S. A., & Jencks, W. P. (1982b) *J. Biol. Chem. 257*, 10882-10892.

Moore, S. A., & Jencks, W. P. (1982c) *J. Biol. Chem. 257*, 10893-10907.

Mottonen, J., Strand, A., Symersky, J., Sweet, R. M., Danley, D. E., Geoghegan, K. F., Gerard, R. D., & Goldsmith, E. J. (1992) *Nature 355*, 270-273.

Mukhopadhyay, A. (1997) *Adv. Bioch. Eng. Biotechnol. 56*, 61-109.

Ostermann, J., Horwich, A. L., Neupert, W., & Hartl, F.-U. (1989) *Nature 341*, 125-130.

Parales, R. E., & Harwood, C. S. (1992) *J. Bacteriol. 174*, 4657-4666.

Patel, K., & Borchardt, R. T. (1990) *Pharm. Res. 7*, 787-793.

Piccoli, R., Di Donato, A., & D'Alessio, G. (1988) *Biochem. J. 253*, 329-336.

Pickart, C. M., & Jencks, W. P. (1979) *J. Biol. Chem. 254*, 9120-9129.

Price, N. C. (1994) in *Mechanisms of Protein Folding* (Pain, R. H., Ed.) pp. 160-193, IRL Press, Oxford, U. K.

Rospert, S., Glick, B. S., Jenö, P., Schatz, G., Todd, M. J., Lorimer, G. H., & Viitanen, P. V. (1993) *Proc. Natl. Acad. Sci. U. S. A. 90*, 10967-10971.

Rospert, S., Looser, R., Dubaquié, Y., Matouschek, A., Glick, B. S., & Schatz, G. (1996) *EMBO J. 15*, 764-774.

Rudolph, R., Heider, I., & Jaenicke, R. (1977) *Biochemistry 16*, 5527-5531.

Rye, H. S., Burston, S. G., Fenton, W. A., Beechem, J. M., Xu, Z., Sigler, P. B., & Horwich, A. L. (1997) *Nature 388*, 792-798.

Schlunegger, M. P., Bennett, M. J., & Eisenberg, D. (1997) *Adv. Prot. Chem. 50*, 61-122.

Schmidt, M., Buchner, J. Todd, M. J., Lorimer, G. H., & Viitanen, P. V. (1994) *J. Biol. Chem. 269*, 10304-10311.

Segel, I. H. (1975) *Enzyme Kinetics*. John Wiley & Sons, Inc., New York.

Sinclair, J. F., Waddle, J. J., Waddill, E. F., & Baldwin, T. O. (1993) *Biochemistry 32*, 5036-5044.

Sinclair, J. F., Ziegler, M. M., & Baldwin, T. O. (1994) *Nature Struct. Biol. 1*, 320-326.

Solomon, F., & Jencks, W. P. (1969) *J. Biol. Chem. 244*, 1079-1081.

Staedtler, P., Hoenig, S., Frank, R., Withers, S. G., & Hengstenberg, W. (1995) *Eur. J. Biochem. 232*, 658-663.

Tian, G., Vainberg, I. E., Tap, W. D., Lewis, S. A., & Cowan, N. J. (1995) *Nature 375*, 250-253.

Tsai, C.-J., Lin, S. L., Wolfson, H., & Nussinov, R. (1996) *CRC Crit. Rev. Biochem. Mol. Biol. 31*, 127-152.

Tsai, C.-J., Lin, S. L., Wolfson, H. J., & Nussinov, R. (1997) *Protein Sci. 6*, 53-64.

Tyler-Cross, R., & Schirch, V. (1991) *J. Biol. Chem. 266*, 22549-22556.

Weissman, J. S., Rye, H. S., Fenton, W. A., Beechem, J. M., & Horwich, A. L. (1996) *Cell 84*, 481-490.

Wente, S. R., & Schachman, H. K. (1987) *Proc. Natl. Acad. Sci. U. S. A. 84*, 31-35.

White, H., & Jencks, W. P. (1976) *J. Biol. Chem. 251*, 1688-1699.

White, H., Solomon, F., & Jencks, W. P. (1976) *J. Biol. Chem. 251*, 1700-1707.

Williams, W. A. (1990) Ph. D. thesis, University of Minnesota, Minneapolis.

Zettlmeissl, G., Teschner, W., Rudolph, R., Jaenicke, R., & Gäde, G. (1984) *Eur. J. Biochem. 143*, 401-407.

Ziegler, M. M., Goldberg, M. E., Chaffotte, A. F., & Baldwin, T. O. (1993) *J. Biol. Chem. 268*, 10760-10765.

APPENDICES

Appendix 1. Enzyme Commission Numbers for some CoA Transferases[a]

Propionate CoA transferase	E.C. 2.8.3.1
Oxalate CoA transferase	E.C. 2.8.3.2
Succinyl-CoA:3-ketoacid CoA transferase	E.C. 2.8.3.5
β-Ketoadipate:succinyl-CoA transferase	E.C. 2.8.3.6
Acetyl-CoA:acetoacetate CoA transferase	E.C. 2.8.3.8
Butyrate-acetoacetate CoA transferase	E.C. 2.8.3.9
Glutaconate CoA transferase	E.C. 2.8.3.12

---

[a] Adapted from: *Enzyme Nomenclature* (1992) 2nd ed. Academic Press, Inc. San Diego, CA.

Appendix 2. Fundamental Constants and Conversion Factors

Part A: Fundamental Constants

Constant	Symbol	SI value
Universal gas constant	R	8.3145 J/mol·K
Planck constant	h	6.62608×10^{-34} J·s
Boltzmann constant	k_B	1.38066×10^{-23} J/K

Part B: Conversion Factors

0 °C = 273.15 K

1 cal = 4.184 J

Adapted from: Levine, I. N. (1988) in *Physical Chemistry*, 3rd ed., McGraw-Hill Book Co., New York.

Appendix 3: Oligonucleotides used for PCR and/or Mutagenesis

NDE
5'-CGCGGCATATGACCAAATTTTATACGGATGC-3'

HIND
5'-GCACAAAGCTTGGGACAAATATCTGTTCC-3'

INT-1
5'-TTATCAGTCCGGAAGGAGTAAAATCATATGTCTGGTAAACTTGGA-3

INT-2
5'-CAGACATATAAGCTTACTCCTTCCGGACTGATAA-3'

E344A
5'-TGCAAAGTGCAAATGGAA-3'

E344A(C)
5'-CCAGGATTCCATTTGCACTTTGCA-3'

E344D
5'-ACCTGCAAAGTGACAATGGAATCC-3'

E344D(C)
5'-GGATTCCATTGTCACTTTGCAGGT-3'

E344Q
5'-ACCTGCAAAGTCA(G/T)AATGGAATCC-3'

E344Q(C)
5'-GGATTCCATT(A/C)TGACTTTGCAGGT-3'

C67S
5'-GTTTTGGGTTATCTGGAATTCCGG-3'

C235S
5'-ACCTGCCGATGTCCAAAGCTGCAG-3'

Appendix 4: Plasmids and RF-DNA

pT7-7 series

pT7-7
pT7-WT pT7-E344A pT7-E344D pT7-E344Q pT7-C67S pT7-C235S
pT7-Hng
pT7-N
pT7-C

pMS119EH series

pMS119EH
pMS-WT
pMS-Hng
pMS-N
pMK119EH
pMK-C
pMS-C/N

M13-mp19 series

M13-mp19
M13-WT M13-C67S M13-C235S
M13-Hng

Appendix 5: Strains of *E. coli*

BL21(DE3) (*hsdS gal* [λ*cIts*857 *ind*1 *S*am7 *nin*5 *lac*UV5-T7 gene*1*])[a]

BL-pT7-7
BL-WT BL-E344A BL-E344D BL-E344Q BL-C67S BL-C235S
BL-Hng
BL-N
BL-C

HB101 (*supE*44 *hsdS*20[$r_B^- m_B^-$] *recA*13 *ara*-14 *proA*2 *lacY*1 *galK*2 *rpsL*20 *xyl*-5 *mtl*-1)[b]

HB-pMS119EH
HB-WT
HB-Hng
HB-N
HB-pMK119EH
HB-C
HB-C/N

JM103 (*endA*1, *hsdR*, *supE*, *sbcBC*, *thi*-1, *strA*, Δ(*lac-pro*),F'[*traD*36, *lacI*^{q}ZΔM15, *pro*AB$^+$])[c]

JM-WT JM-C67S JM-C235S

JM-Hng

CJ236 (*dut*1, *ung*1, *thi*-1, *relA*1/pCJ105[*cam*^{r}F'])[d]

CJ-WT

---

[a] Used for the expression of cDNA inserts cloned into pT7-7.
[Studier, F. W., & Moffatt, B. A. (1986) *J. Mol. Biol. 189*, 113-130]

[b] Used for the expression of cDNA inserts cloned into pMS119EH.
[Boyer, H. W., & Roulland-Dussoix, D. (1969) *J. Mol. Biol. 41*, 459-472; Bolivar, F., & Backman, K. (1979) *Methods Enzymol. 68*, 245-267]

[c] Used for the propagation of M13-mp19 DNA.
[Hanahan, D. (1983) *J. Mol. Biol. 166*, 557-580]

[d] Used for the preparation of uracil-containing, single-stranded DNA for site-directed mutagenesis.
[Kunkel, T. A., Roberts, J. D., & Zakour, R. A. (1987) *Methods Enzymol. 154*, 367-82]

Appendix 6: Buffers and Media

Polymerase chain reaction

PCR buffer	15 mM Tris-HCl, 40 mM KCl, 1.5 mM $MgCl_2$, 0.10 mg/mL gelatin, pH 8.35

DNA manipulations

TE	10 mM Tris-HCl, 1 mM EDTA, pH 8.0
TAE	40 mM Tris-acetate, 1 mM EDTA

Bacterial cell culture

LB	1% (w/v) bacto-tryptone, 0.5% (w/v) bacto-yeast extract, 1% (w/v) NaCl, pH 7.0

Pulse-chase analyses

M9 labeling medium	0.4% (w/v) glucose, 50 mM Na_2HPO_4, 22 mM KH_2PO_4, 8.6 mM NaCl, 19 mM NH_4Cl, 0.1 mM $CaCl_2$, 1.0 mM $MgSO_4$

Cell lysis by detergent

TENTA buffer	20 mM Tris-HCl, 1% (v/v) Triton X-100, 5 mM EDTA, 150 mM NaCl, pH 7.5

SDS-PAGE

sample loading buffer	50 mM Tris-Cl, 2.5% (w/v) SDS, 1% (v/v) 2ME, 35% (v/v) glycerol, and 0.01% (w/v) bromophenol blue, pH 6.6.
gel running buffer	25 mM Tris, 0.19 M glycine

Western blotting

transfer buffer	25 mM Tris, 0.19 M glycine, 20% (v/v) methanol
blocking buffer	5% (w/v) skim milk powder, 0.15 M NaCl, 20 mM Tris-HCl, pH 7.5
PBS[a]	0.14 M NaCl, 2.7 mM KCl, 10 mM Na_2HPO_4, 1.8 mM KH_2PO_4, pH 7.4

---

[a] "PBS" is an abbreviation for phosphate buffered saline.

Appendix 7: Calculation of the Percentage of Activity in E344Q Attributable to Wild-Type CoA Transferase

Consider that a sample of E344Q consists of two subpopulations: a minor pool of wild-type molecules and a major pool of mutant conformers.

Let x = the fraction of the total enzyme activity associated with the subpopulation of wild-type enzyme.

Let y = the fraction of the total enzyme activity associated with the subpopulation of mutant enzyme.

Then, for uninhibited enzymes the total activity would be given by

$$x + y = 1 \qquad (1)$$

Now assuming that:

> (1) 70% of the wild-type CoA transferase active sites are inhibited in the presence of an equimolar amount of acetoacetyl-CoA and 0.4 mM AHA (Figure 6-11); and (2) the mutant enzyme is not readily converted to ECoA (and thus not significantly inhibited by AHA) under the conditions of the experiment;

then the total enzyme activity at the "break-point" of the E344Q titration curve should consist of 30% of the activity associated with the wild-type subpopulation and 100% of the activity associated with the mutant subpopulation.

Since the total enzyme activity of E344Q at the "break-point" is 0.58 times that of the initial activity of E344Q, then:

$$0.3x + y = 0.58 \qquad (2)$$

Solving the system of equations by subtracting (2) from (1):

$$0.7x = 0.42$$
$$\therefore\ x = 0.6 \text{ and } y = 0.4$$

Thus, 60% of the total enzyme activity of E344Q is due to the wild-type subpopulation, while 40% is due to the mutant subpopulation.

Given that: (1) the specific, total enzyme activity of E344Q is 0.35 μmol/min/mg; and (2) the specific enzyme activity of pure, wild-type CoA transferase is 25.2 μmol/min/mg, then the percentage (W) of the E344Q sample which consists of wild-type protein is calculated to be:

$$\begin{aligned} W &= [(0.6)(0.35)/(25.2)](100) \\ &= 0.83\% \end{aligned}$$

Thus, 0.83% of the E344Q protein may be attributed to wild-type CoA transferase, while the remaining 99.17% consists of the mutant enzyme.